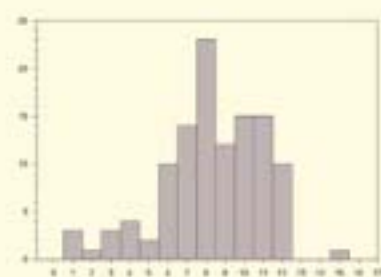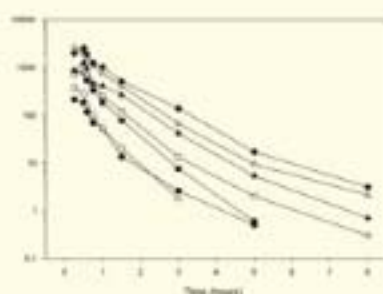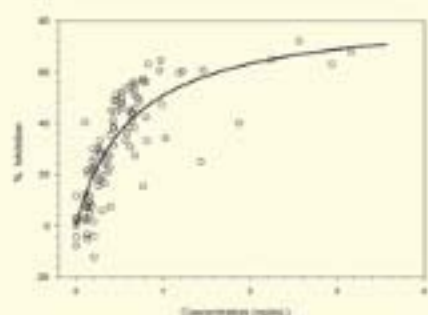# Pharmacokinetics in Drug Development: Advances and Applications

## Volume 3



*Edited by*
Peter L. Bonate, Ph. D.
Danny R. Howard, Ph. D.

aapspress

Springer

# Pharmacokinetics in Drug Development

Peter L. Bonate • Danny R. Howard
Editors

# Pharmacokinetics in Drug Development

Volume 3: Advances and Applications

aapspress

Springer

*Editors*
Peter L. Bonate, Ph.D.
Clinical Pharmacology,
Modeling, and Simulation
GlaxoSmithKline
Research Triangle Park, NC, USA
peter.l.bonate@gsk.com

Danny R. Howard, Ph.D.
Translational Sciences
Novartis
East Hanover, NJ, USA
dan.howard@novartis.com

# Preface

The primary objective of this book series is to provide readers with practical guidance on the application of pharmacokinetics as a drug development science. Our goal has been, and continues to be, to provide the link between the theoretical and the applied. We ask every author to write their chapter with this question in the back of their mind: "If you were training someone new to industry, what about this topic should they know?" In the first two volumes, topics were chosen specifically for their relative "stability" and they represented the core what we do as a profession. Though the approaches and technologies may have advanced, the practical considerations for topics like bioavailability study designs, analysis procedures for absorption data or dose-proportionality, or the role of pharmacokinetics in early development have remained relatively consistent over time. Some of the topics, however, have changed and some become more prominent over time. With this volume, we begin to address the more "adaptable" issues facing pharmacokineticists and pharmacologists supporting new compound development.

The topics chosen for this volume were selected because they are some of the current development or technological issues facing drug development project teams. They regard the practical considerations for the assessment of selected special development populations. For example, they include characterization of drug disposition in pregnant subjects, for measuring arrhythmic potential, for analysis of tumor growth modeling, and for disease progression modeling. Practical considerations for metabolite safety testing, transporter assessments, Phase 0 testing, and development and execution of drug interaction programs reflect current regulatory topics meant to address enhancement of both safety assessment and early decision-making during new candidate selection. Important technologies like whole body autoradiography, digital imaging and dried blood spot sample collection methods are introduced, as both have begun to take a more visible role in pharmacokinetic departments throughout the industry.

We are very pleased to extend the goals of the series to this newest volume. We remain committed to the aim of publishing material to fill the gap between the academic sciences and the practical application of that knowledge in drug development. Our grateful thanks goes out to the authors who contributed their time (and more importantly) their opinions, thoughts, authorship, and most of all, *patience* to this project. Without their hard work, expertise, and keen knowledge of the subjects presented, it would not be possible to have reached our shared goal.

We would like to dedicate this book to the editors and authors' families – whose love for us and understanding for our obsession make it possible for us to happily wander through the maze of our scientific dreams.

Research Triangle Park, NC                                              Peter L. Bonate
East Hanover, NJ                                                          Danny R. Howard

## About the Editors

**Peter Bonate** has 16 years industrial experience, 13 years as a clinical pharmacologist/pharmacokineticist and three years in drug metabolism and bioanalysis. He is currently a Director in the Clinical Pharmacology, Modeling, and Simulation department at GlaxoSmithKline in the oncology therapeutic area. He has also worked at Genzyme, Hoechst Marion Roussel, Eli Lilly, and Quintiles. He received his PhD in 1996 from Indiana University in Medical Neurobiology with an emphasis on the pharmacokinetics of drugs of abuse. He received an MS in Statistics from the University of Idaho and an MS in Pharmacology from Washington State University both in 1990. In 2003, he was elected a Fellow of the American College of Clinical Pharmacology and in 2007 was elected a Fellow of the American Association of Pharmaceutical Scientists (AAPS). He was founder of the Modeling and Simulation focus group, has served as chair of the population pharmacokinetics focus group, and was section leader for the Clinical Pharmacology and Translational Research Section within AAPS. He has served or currently serves on the editorial boards for the *Journal of Clinical Pharmacology*, *Pharmaceutical Research, Journal of Pharmacokinetics and Pharmacodynamics*, and *the AAPS Journal*. He has more than 40 publications in the field of pharmacokinetics and clinical pharmacology, is co-editor of the series *Pharmacokinetics in Drug Development* published by AAPS Press in 2004, and is author of the book *Pharmacokinetic–Pharmacodynamic Modeling and Simulation* published by Springer in 2006.

**Danny Howard** received his Bachelor of Science degree in Pharmacy, and PhD from the University of Missouri in Kansas City. He began working in the pharmaceutical industry in 1991, first as a biopharmaceutics consultant and then as pharmaceutical scientist for Marion Merrell Dow, Hoechst Marion Roussel, Aventis, and Quintiles. He is currently the Vice President of Global Pharmacokinetics and Pharmacodynamics for Novartis. His career has included responsibilities in both clinical and nonclinical pharmacokinetics and pharmacodynamics, bioanalytics, and pharmaceutical business operations. He has worked with numerous drug submissions supporting both large and small molecules worldwide. He was a charter member of the Missouri Biotech Association and served as its first Board Chairman. With Peter Bonate, he is the co-editor of the series *Pharmacokinetics in Drug Development* published by AAPS Press in 2004.

# Contents

# Contributors

**Robyn P. Araujo**  Center for Applied Proteomics and Molecular Medicine, George Mason University, Manassas, VA, USA

**Carlo L. Bello**  Pfizer, Oncology, Clinical Pharmacology, La Jolla, CA, USA

**Peter L. Bonate**  GlaxoSmithKline, Clinical Pharmacology, Modeling, and Simulation, Research Triangle Park, NC, USA

**Jack Cook**  Pfizer, Clinical Pharmacology, Specialty Care Business Unit New London, CT, USA

**Stephen B. Duffull**  School of Pharmacy, University of Otago, Dunedin, New Zealand

**Joseph C. Fleishaker**  Pfizer, St. Louis Laboratories, Clinical Research, St. Louis, MO, USA

**Lee-Kien Foo**  School of Pharmacy, University of Otago, Dunedin, New Zealand

**David M. Haas**  Indiana University School of Medicine, Indianapolis, IN, USA

**Brett E. Houk**  Pfizer, Oncology, Clinical Pharmacology, La Jolla, CA, USA

**Danny R. Howard**  Novartis, Drug Metabolism and Pharmacokinetics Translational Sciences, East Hanover, NJ, USA

**J. Matthew Hutzler**  Boehringer Ingelheim, Ridgefield, CT, USA

**Caroline H. Johnson**  Laboratory of Metabolism, Center for Cancer Research, National Institutes of Health, National Cancer Institute, Bethesda, MD, USA

**David J. Kazierad**  Cardiovascular, Metabolic & Endocrine Disease Research Unit, Pfizer, Groton, CT, USA

**Graham Lappin**  Xceleron, The BioCentre, York, UK

**John C. Lindon**  Department of Biomolecular Medicine, Faculty of Medicine, Imperial College London, South Kensington Campus, London, UK

**Tapan K. Majumdar**  Novartis, Drug Metabolism and Pharmacokinetics, Translational Sciences, East Hanover, NJ, USA

**Majid Y. Moridani**  Department of Pharmaceutical Sciences, School of Pharmacy, Texas Tech University HSC, Amarillo, TX, USA; Department of Pediatrics, School of Medicine, Texas Tech University HSC, Amarillo, TX, USA

**Diane R. Mould**  Projections Research Inc., Phoenixville, PA, USA

**Angus N.R. Nedderman**  Pfizer, Department of Pharmacokinetics, Dynamics and Metabolism, Sandwich, Kent, UK

**Jamie L. Renbarger**  Indiana University School of Medicine, Indianapolis, IN, USA

**Tanya Russell**  Pfizer, Oncology Clinical Pharmacology, San Diego, CA, USA

**Alain Schweitzer**  Novartis, Drug Metabolism and Pharmacokinetics, Translational Sciences, Basel, Switzerland

**Daniel S. Stein**  Novartis, Translational Medicine, Translational Sciences, East Hanover, NJ, USA

**Thomas N. Thompson**  R&D Services Pharma Consulting, Omaha, NE, USA

**Don K. Walker**  Pfizer, Department of Pharmacokinetics, Dynamics and Metabolism, Sandwich, Kent, UK

Peter L. Bonate

**Abstract**

In cancer drug development, measurement of tumor growth is necessary for preclinical assessment of anticancer activity and clinical assessment of efficacy. This chapter reviews mathematical models of preclinical and clinical tumor growth. Issues and models with regards to mouse xenograft data will be highlighted.

## 1.1 Introduction

Cancer is one of the leading causes of death worldwide. It is expected that in 2010, 1.5 MM new cases of cancer will be diagnosed in the USA and more than a half-million people will die from their illness (1,500 persons each day), with prostate, breast, lung, and colon having the greatest incidence (American Cancer Society 2010). Vast amounts of money, time, and effort are spent every year to develop new drugs to treat cancer. Unfortunately, the approval rating for new cancer drugs is dismal; around 5% of drugs that enter the clinic will be approved for use by doctors and patients (Kola and Landis 2004). Certainly, one way companies can improve their success rates for achieving new drugs is to better leverage their preclinical and clinical data and reduce

attrition via application of mathematical models of disease. Prospective modeling of tumor growth is an example of how pharmaceutical companies are working to reach this goal.

As part of the drug development process for cancer drugs, particularly with regards to solid tumors, measurement of tumor burden and size, both before and after therapy, is common at different points in the development process to assess the effectiveness of a drug. Preclinically, mice are injected with tumor fragments that are allowed to grow and are then administered the new chemical entity (NCE) to determine whether the NCE can retard or shrink tumor growth. Tumor size or volume are later assessed in humans to determine whether the NCE is effective and can prolong survival. Recent attention has focused on modeling tumor growth to better understand the exposure–response relationship for NCEs. This chapter will review tumor growth kinetics in both preclinical and clinical models used to characterize the growth of tumors over time. Tumor growth models are also described by Mould in the chapter on Modeling the Progression of Disease elsewhere in this book.

P.L. Bonate
Clinical Pharmacology, Modeling, and Simulation, GlaxoSmithKline, 5 Moore Drive, 17.2259, Research Triangle Park, Durham, NC 27709, USA
e-mail: Peter.l.bonate@gsk.com

## 1.2 Xenograft Models

The preclinical models for measuring antitumor activity are relatively straightforward. As part of the drug discovery process, researchers will subcutaneously implant human tumor fragments into the flank of nude or severe combined immunodeficient (SCID) mice and allow the tumors to grow. Once the tumors have reached a predefined size (usually 100–300 mm$^3$), the mice are randomized to different treatment groups: these usually include a placebo, some dose of the NCE, and a positive control of a drug already known to have an antitumor effect at the given dose. The doses are given and tumor size is measured over a period of time defined by the protocol, usually weeks. The effect of the NCE relative to the placebo and active control is determined. Effective cancer agents are assumed to be those that will reduce or shrink tumors. Such models are referred to as xenograft models and are meant as a model for human tumor growth. Most every drug approved in cancer was first tested in a xenograft model to determine its anticancer activity.

There are often two types of measurements reported in these studies, tumor volume and tumor weight, both of which are derived from the same set of measurements. Because the volume or weight of the tumors cannot be actually measured, their length (the longest axis) and width (in mm) is measured using calipers and then weight or volume is estimated using one of several formulas based on these values. Assuming the tumor is a prolate ellipsoid (which has a shape like a monolithic dome or an egg cut along its shortest axis at the middle, see http://www.monolithic.com/stories/shapes-prolate-ellipsoid-vertical for example, accessed July 2010), tumor volume (in mm$^3$) is estimated as $0.5 \times \text{length} \times \text{width}^2$. If it is assumed that the tumor has unit volume, then tumor weight (in mg) is equal to tumor volume assuming a density of 1 mg/mm$^3$ for tumor tissue. For nonspherical tumors other equations are used to estimate the volume. The reader is referred to Clarke (1997) and Rygaard and Spang-Thomsen (1997) for details. Plots of tumor weight or volume over time are often used to show the effect of the drugs on the tumors.

Figure 1.1 presents an example of a xenograft study for ABT-263, a small molecule inhibitor of Bcl-2, which has shown activity in cell-cultured tumors. ABT-263 showed activity in a variety of tumors under a once-daily dosing schedule (Shoemaker et al. 2008). Figure 1.1 shows that ABT-263 has similar or better activity than etoposide, cyclophosphamide, and carboplatin in SCLC H146 xenografts and had activity in paclitaxel-resistant H146 xenografts. AVT-263 also did not exhibit resistance with multiple cycles of therapy. ABT-263 is now currently in Phase 1/2a under a daily dosing schedule (14 days on/7 days off or continuous dosing) in patients with SCLC and non-hematologic malignancies.

Although xenografts are relatively easy to perform, there are problems (Kelland 2004). First, these are human tumors grown in mice and so the mice must be immunocompromised for the tumors to grow in order to prevent a severe transplant reaction from occurring in the host animal. Second, since these tumors are implanted in the flank, they do not mimic tumors of other origins, e.g., a lung cancer tumor grown in the flank of mice may not be representative of a lung cancer tumor in the lung. Recent interest has focused on so-called orthotopic models, wherein tumors of particular origin are grown at the origin of interest (Garber 2010), and in transgenic mice, which are thought to more faithfully mimic the human cancer process (Sharpless and DePinho 2006). There are problems and criticisms associated with these models as well, the foremost being that there is no proof that these models perform any better at predicting human activity than conventional approaches. There is also the question of the relevance of the xenograft models with targeted therapeutics. Last, xenograft models never metastasize.

Xenografts have been criticized for their low predictive value. A retrospective analysis done by the National Cancer Institute showed that only 15 of 33 compounds that were in Phase 2 of drug development had activity in more than one-third of the xenograft models tested ($p = 0.04$). Also, activity in a particular tumor line did not generally predict human activity in that cancer, e.g., activity in breast cancer xenograft models
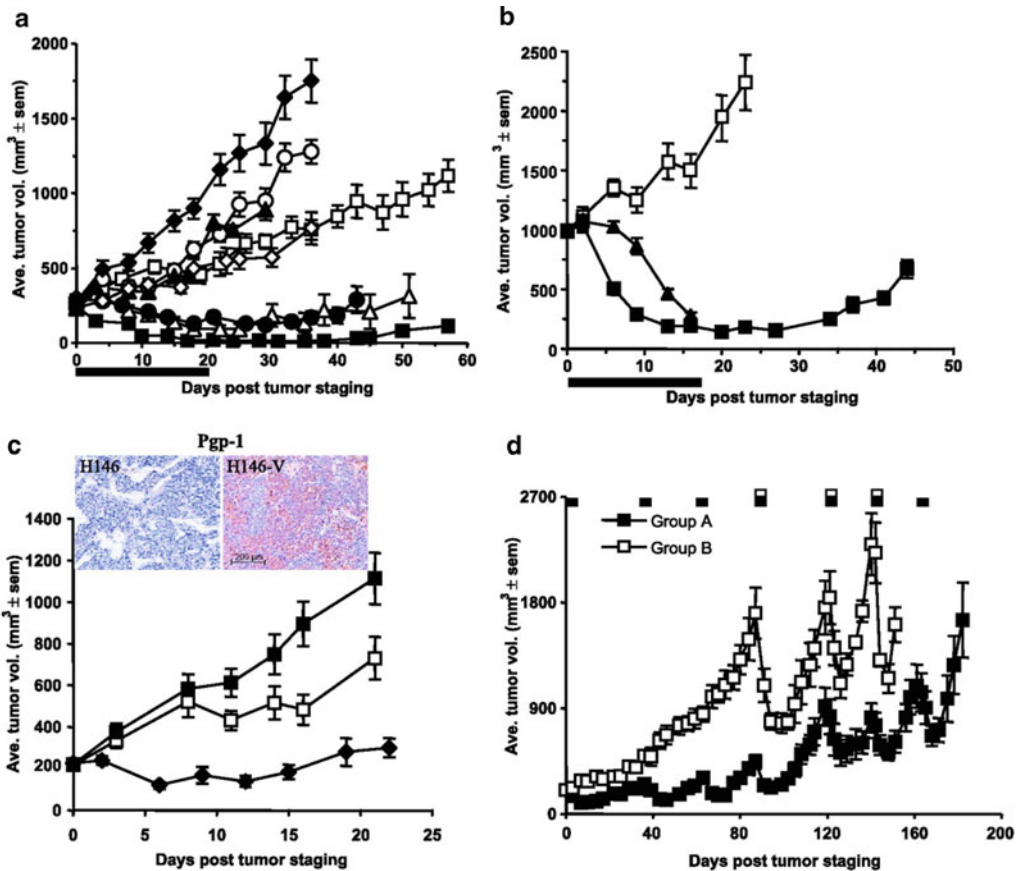
**Fig. 1.1** Example of a xenograft study. (**a**) Efficacy of ABT-263 in the H146 SCLC xenograft model relative to several standard cytotoxic agents. Shown is data compiled from seven independent experiments. In each trial, tumors were size matched to 240–300 mm³ (day 0) and therapy was initiated the following day. *Open circles*, cisplatin given at 3 mg/kg, IP, thrice every 4 days; *closed triangles*, etoposide given at 25 mg/kg, IP, q4d × 3; *open squares*, carboplatin given at 50 mg/kg, IP, q4d × 4; *open diamonds*, cyclophosphamide given at 100 mg/kg, IP, q4d × 3; *closed circles*, vincristine given at 0.5 mg/kg, IV, q7d × 4; *open triangles*, paclitaxel given at 30 mg/kg, IP, q4d × 3; *closed squares*, ABT-263 given at 100 mg/kg, po, 21 doses daily (*black bar*); *closed diamonds*, cisplatin vehicle. For simplicity, only one vehicle group has been plotted. However, all statistics and analyses of efficacy were conducted by comparing to the vehicle control specific for each agent. All cytotoxic agents were given at or near their maximum tolerated doses. All drugs exhibited a statistically significant inhibition of tumor growth throughout the study except for cyclophosphamide, which was significant only on days 4, 8, and 16 postdose initiation ($p < 0.05$, Wilcoxon rank sum test). (**b**) Treatment with ABT-263 causes regression of large, established H146 xenograft tumors. Tumors were allowed to reach an average tumor volume of ~1,000 mm³ before initiation of therapy. *Closed squares*, ABT-263 was given at 100 mg/kg, po, 17 doses daily (*black bar*); *closed triangles*, docetaxel given at 30 mg/kg, IV, q7d × 2; *open squares*, vehicle. ABT-263 treatment resulted in 92% TGI at the end of therapy with all tumors showing at least an 80% reduction in tumor volume relative to starting size ($n = 10$ mice per group). (**c**) Analysis of paclitaxel-resistant variant of H146. Parental H146 tumors were initially treated with four doses of paclitaxel at 30 mg/kg/day. Tumors that relapsed after treatment were propagated into new hosts and expanded into new lines. The H146 variant line (H146-V) shown here was significantly more resistant to paclitaxel treatment of 30 mg/kg/day compared with the parental line. *Closed diamonds*, ABT-263 given at 100 mg/kg, po, 21 doses daily; *open squares*, paclitaxel given at 30 mg/kg, IP, q4d × 3; *closed squares*, paclitaxel vehicle. Immunohistochemical analysis of parental H146 and H146-V tumors showed that the variant line expresses significantly higher levels of Pgp-1 (*inset*; magnification, ×100). ABT-263 given at 100 mg/kg/day still showed significant efficacy in the H146-V line ($p < 0.01$, Wilcoxon rank sum test). (**d**) Efficacy of ABT-263 in the H146 xenograft model after multiple cycles of therapy. Tumors were randomized into groups of equal tumor volume (~200 mm³) on day 0 with group A receiving ABT-263 at 100 mg/kg/day, po, from day 0 to day 4 and group B receiving vehicle. Additional 5-day cycles of treatment with ABT-263 at 100 mg/kg/day were administered as follows: group A, days 36–40, 63–67, 87–91, 119–123, 140–145, and 161–165; group B, days 87–91,

did not predict activity in breast cancer in humans, the exception being non-small cell lung cancer which had a 45% predictive rate (Johnson et al. 2001). What is interesting about this argument about the predictive value of xenografts is the perceived need for a high prediction rate. In toxicology, the overall concordance rate between toxicity in man and similar toxicity in animals is only 70%, with 30% of human toxicities not predicted at all by animal studies (Greaves et al. 2004), and yet few would suggest we should not do toxicology studies prior to first time in man. Although xenograft are not completely predictive of activity, they are much better at weeding out failures, as drugs that fail to show efficacy in xenograft models very likely will not be active clinically.

It has been argued that the predictive value of xenograft models can be significantly improved when the doses administered to mice produce exposures similar to the exposures seen in the clinic (Kerbel 2003; Inaba et al. 1988) since often the doses given to mice are four- to fivefold higher than the maximum tolerated dose (MTD) seen in humans (Maruo et al. 1990; Inaba et al. 1989; Tashiro et al. 1989). The difficulty with this approach is that prior to first time in man, the MTD in humans is not known so the doses studied in mice are often the MTD in mice. Later, after the MTD has been established in man, the dose in mice can be adjusted to produce pharmacokinetically equivalent exposures. Further testing of this hypothesis needs to be performed.

## 1.3 Preclinical Models for Tumor Growth

Modeling of tumor growth kinetics began in the 1960s with Anna Kane Laird (1964) who showed that unperturbed tumor growth in a test tube followed Gompertzian kinetics, which look similar to the profiles produced by the sigmoid $E_{max}$ model familiar to most pharmacokineticists. The proposed equation for cell growth was

$$Y(t) = Y(0) \exp\left[\frac{A}{\alpha}\left(1 - \exp(-\alpha t)\right)\right] \quad (1.1)$$

where, $Y(t)$ is tumor size at time $t$, $Y(0)$ is the baseline tumor size, and $A$ and $\alpha$ are constants. For small values of $\alpha t$ or when $\alpha = 0$, tumor growth becomes exponential. Since Laird's initial report, Gompertzian growth has been shown for a variety of tumors in different unperturbed situations both in vitro and in vivo. The first paper to show that a Gompertz equation best described tumor growth in animals was by Simpson-Herren and Lloyd (1976) in a C3H mouse mammary tumor and L1210 ascites tumor (often used as a model for leukemia). The first paper to show that a Gompertz equation applies to human tumor growth was Sullivan and Salmon (1972).

It was a series of papers by Norton and Simon (1976a,b) that really called attention to the use of the Gompertz equation in describing tumor growth (Norton 1988). Based on their studies, they predicted that for chemotherapy, one could increase cell kill by delivering treatments at higher doses (increased dose intensity) through minimization of tumor regrowth between cycles. This hypothesis, referred to as the Norton–Simon hypothesis, was confirmed in clinical trials (Citron et al. 2003). Norton et al. (2005) later showed how a Gompertz equation could be modified to account for perturbation in the presence of an active treatment and how to optimize chemotherapeutic dose regimens under Gompertzian growth. In the unperturbed state, tumor volume could be modeled by

$$\frac{dY}{dt} = \alpha Y(t) - \alpha \times Ln(Y(t)) \times Y(t) \quad (1.2)$$

**Fig. 1.1** (continued) 119–123, and 140–144. Group B was also treated with vehicle on days 36–40 and 63–67. *Black boxes*, dosing periods for group A; *white boxes*, dosing periods for group B. ABT-263 treatment resulted in significant tumor regression, even after six previous cycles of therapy. Regression of large (>2,000 mm³) tumors was also seen after multiple therapy cycles. Reprinted with permission from Shoemaker et al. (2008). Copyright American Association of Cancer Research, 2008

but in the presence of drug effect the equation is modified to

$$\frac{dY}{dt} = \alpha Y(t) - \alpha \times Ln(Y(t)) \times Y(t) \times (1 - DE)$$
(1.3)

where, DE is a drug effect function whose domain is on the interval (0, 1). When the model was applied to capecitabine, the point of maximal drug effect was approximately 7 days of treatment. The model predicts that dosing after 7 days diminishes anticancer benefit but increases the risk of toxicity. Preclinical studies in xenograft models confirmed that a 7 day-on/7 day-off regimen achieved a maximum tolerated dose 1.5 times higher than the conventional schedule (Traina et al. 2006). Based on these preclinical results, a clinical trial was started testing the safety of a 7 day-on/7 day-off schedule for capecitabine and was found to be safe and well tolerated (Traina et al. 2008). A Phase 2 study to determine the efficacy under this dosing schedule is on-going.

Miklavcic et al. (1995) modeled the effects of bleomycin and electrotherapy in xenografts. Four different models were tested: exponential, Gompertz, Bertalanffy, and logisitic. Untreated mice were modeled as

$$\frac{dY}{dt} = \lambda Y \qquad \text{Exponential}$$
$$\frac{dY}{dt} = Y\left(\alpha - \beta Ln\left(\frac{Y}{Y_0}\right)\right) \quad \text{Gompertz}$$
$$\frac{dY}{dt} = \alpha Y^{2/3} - \beta Y \qquad \text{Bertalanffy}$$
$$\frac{dY}{dt} = \alpha Y - \beta Y^2 \qquad \text{Logistic}$$
(1.4)

with initial conditions $Y(0) = Y_0$. Based on goodness of fit measures, the Gompertz model was chosen as best. Mice treated with bleomycin were modeled as

$$\frac{dY}{dt} = Y\left(\alpha - \beta Ln\left(\frac{Y}{Y_0}\right) - \gamma C_t\right) \qquad (1.5)$$

where $\gamma$ was a measure of drug effect and $C_t$ was the predicted tissue concentration based on a three-compartment model.

Jackson et al. (2010) used a Gompertz model to describe the tumor growth rate for A2780 mice xenografts and the interaction between a targeted therapeutic and cytotoxic chemotherapeutic agent. Since only concentration data were available for the targeted therapeutic, a kinetic–dynamic model was used to model the temporal relationship with the cytotoxic agent. The authors also included a biomarker model linking the pharmacokinetic model for the targeted therapeutic and its effect on tumor growth. The model was able to discriminate between the effects of the two agents and showed that the two agents had an additive effect on tumor growth inhibition.

Although there has been some debate as to whether Gompertz or logistic growth rates have a biological basis (Xu 1987), their original use was purely empirical. Marusic (1995) showed that Gompertz, logistic, and Bertalanffy models are in fact special cases of the generalized two parameter model

$$\frac{dY}{dt} = aY^{\alpha} - bY^{\beta}. \qquad (1.6)$$

For example, in a logistic equation $\alpha = 1$ and $\beta = 2$. Other types of empirical models to explain tumor growth include the nonlinear mixed effects model proposed by Liang and Sha (2004) wherein tumor growth was modeled using a biexponential equation

$$Y_i(t_{ij}) = \exp(p_{i1} - d_{i1}t_{ij}) - \exp(p_{i2} - d_{i2}t_{ij}) + \varepsilon_{ij} \qquad (1.7)$$

where, the subscript $i$ refers to the $i$th subject at the $j$th timepoint. While useful to explain a particular set of data, such empirical models are difficult to extrapolate beyond the conditions originally studied. Gompertzian models also suffer from the fact that the plateau is difficult to estimate because the mice are often killed for ethical reasons when tumor sizes exceed

a certain size (usually $>1,000$ mm$^3$), which often occurs prior to the plateau occurring.

More recent models attempt to account for treatment effects through the use of mechanistic or semi-mechanistic models. Yamazaki et al. (2008) used a modified indirect response model where tumor growth was described by

$$\frac{dY}{dt} = K_{in}\left(1 - \frac{Y(t)}{TG_{50} + Y(t)}\right) \times \left(1 - \frac{E_{\max} \times C^n}{EC_{50}^n + C^n}\right)Y(t) - K_{out}Y(t) \quad (1.8)$$

where, the additional $Y(t)$ on Kin-side of the equation allows for tumor growth and the term $\left(1 - \frac{Y(t)}{TG_{50} + Y(t)}\right)$ allows tumor growth to plateau. Using this model, the authors predicted the tumor growth profiles for GTL16 gastric carcinoma and U87MG glioblastoma xenografts following treatment at five different dose levels with PF-02341066, a cMET tyrosine kinase inhibitor. Interestingly, although they modeled cMET phosphorylation levels in tumors, they did not test whether cMET phosphorylation could be a driver of (1.8) instead of plasma concentrations. Also, such a model implies that the drug inhibits tumor growth with no effect on cell death. It may be that in such a case, the model needs to be modified to

$$\frac{dY}{dt} = K_{in}\left(1 - \frac{E_{\max} \times C^n}{EC_{50}^n + C^n}\right)Y(t)$$
$$- K_{out}\left(1 + \frac{E_{\max death} \times C^n}{EC_{50,death}^n + C^n}\right)Y(t) \quad (1.9)$$

where a term is added to the Kout-side of the equation to account for cell death.

A model that has seen rapid acceptance within the pharmacometrics community is the Simeoni tumor growth model. Using paclitaxel and 5-flurouracil (5-FU) as probes, Simeoni et al. (2004a) reported on a semi-mechanistic model of tumor growth. In the unperturbed state, tumor growth is expected to occur exponentially, at least initially, followed by a linear growth phase that eventually

plateaus. Such tumor growth can be modeled using a Gompertz or logistic model. In their data, a plateau phase was never achieved and to account for this detail, a model was developed to explain the exponential and linear growth components. The authors used a change point differential equation to account for the two different phases. In terms of differential equations, tumor size $Y$ was modeled as

$$\frac{dY}{dt} = \lambda_0 Y(t), Y(t) \le Y_t$$
$$\frac{dY}{dt} = \lambda_1, Y(t) > Y_t \quad (1.10)$$
$$Y(0) = Y_0$$

where $\lambda_0$ and $\lambda_1$ are the parameters characterizing the exponential and linear rate of growth, and $Y_t$ is the tumor size at which growth changes from exponential to linear. $Y_t$ can be expressed as a function of $\lambda_0$ and $\lambda_1$ where $\lambda_0 Y_t = \lambda_1$. The parameters $\lambda_0$ and $\lambda_1$ are considered an indication of the aggressiveness of the tumor. The change point model in (1.10) can be simplified to

$$\frac{dY}{dt} = \frac{\lambda_0 Y(t)}{\left[1 + \left(\frac{\lambda_0}{\lambda_1}Y(t)\right)^{\Psi}\right]^{1/\Psi}}, Y(0) = Y_0 \quad (1.11)$$

For large values of $\Psi$, (1.11) is a good representation of (1.10) and for this reason $\Psi$ is fixed to 20. When $Y(t) < Y_t$, the system behaves exponentially because the term $(\lambda_0/\lambda_1)Y(t)^{\Psi}$ is negligible. On the other hand, when $Y(t) > Y_t$, the term of 1 in the denominator becomes negligible and the system switches to linear growth.

In the perturbed state when animals are treated with cancer drugs, the model needs to account for the cells that are killed by the drug. To do this, the proliferating cells are modeled as a set of damaged cells and dead cells in a transit compartment manner (top of Fig. 1.2). This represents the semi-mechanistic part of the model. Three transit compartments are used to account for the damaged cells, representing the
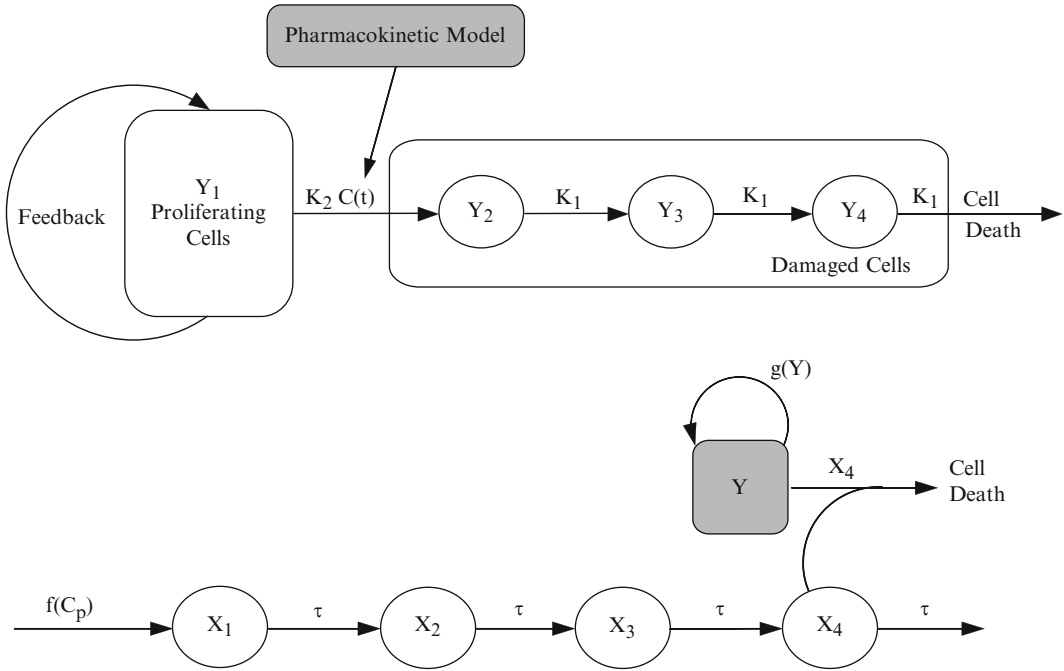
**Fig. 1.2** Schematic of the semi-mechanistic tumor growth model proposed by Simeoni et al. (2004a) (*top*) and the cell transit model proposed by Lobo and Balthasar (2010) (*bottom*)

three degrees of damage. Mathematically, the differential equations for the model become

$$\frac{dY_1}{dt} = \frac{\lambda_0 Y_1(t)}{\left[1 + \left(\frac{\lambda_0}{\lambda_1} Y_1(t)\right)^\Psi\right]^{1/\Psi}} - K_2 C(t) Y_1(t)$$

$$\frac{dY_2}{dt} = K_2 C(t) Y_1(t) - K_1 Y_2(t)$$

$$\frac{dY_3}{dt} = K_1 Y_2(t) - K_1 Y_3(t)$$

$$\frac{dY_4}{dt} = K_1 Y_3(t) - K_1 Y_4(t)$$

$$w(t) = Y_1(t) + Y_2(t) + Y_3(t) + Y_4(t)$$

$$Y_1(0) = w(0), Y_2(0) = Y_3(0) = Y_4(0) = 0$$

$$C(t) = 0, t \leq t_0$$

$$(1.12)$$

where $K_2$ is a parameter that represents the efficacy of the drug at killing the tumor, $K_1$ is the rate of death of the drug, $w(t)$ is the total tumor weight and $C(t)$ is the drug concentration at time $t$, and $t_0$ is the start of drug administration.

The number of transit compartments between cell proliferation and cell death is empirical and can in fact be changed depending on the tumor type. The top of Fig. 1.3 shows a theoretical tumor growth curve assuming a single intravenous bolus of drug on day 9. Depending of the value of $K_2$, the drug can transiently retard growth or completely shrink the tumor.

A number of secondary parameters can be defined from the primary model parameters. The average time to cell death is equal to $n/K_1$. A Time Efficacy Index (TEI), which can be interpreted as the time interval required to achieve a predefined tumor weight animals during linear growth, can be defined as

$$TEI = \frac{K_2 \times AUC}{\lambda_0} \qquad (1.13)$$

where, AUC is the total area under the curve following a single dose administration. If animals are exposed to a constant drug concentration $C_{ss}$, the threshold concentration for tumor eradication ($C_{TE}$) can be estimated as $\lambda_0/K_2$ such
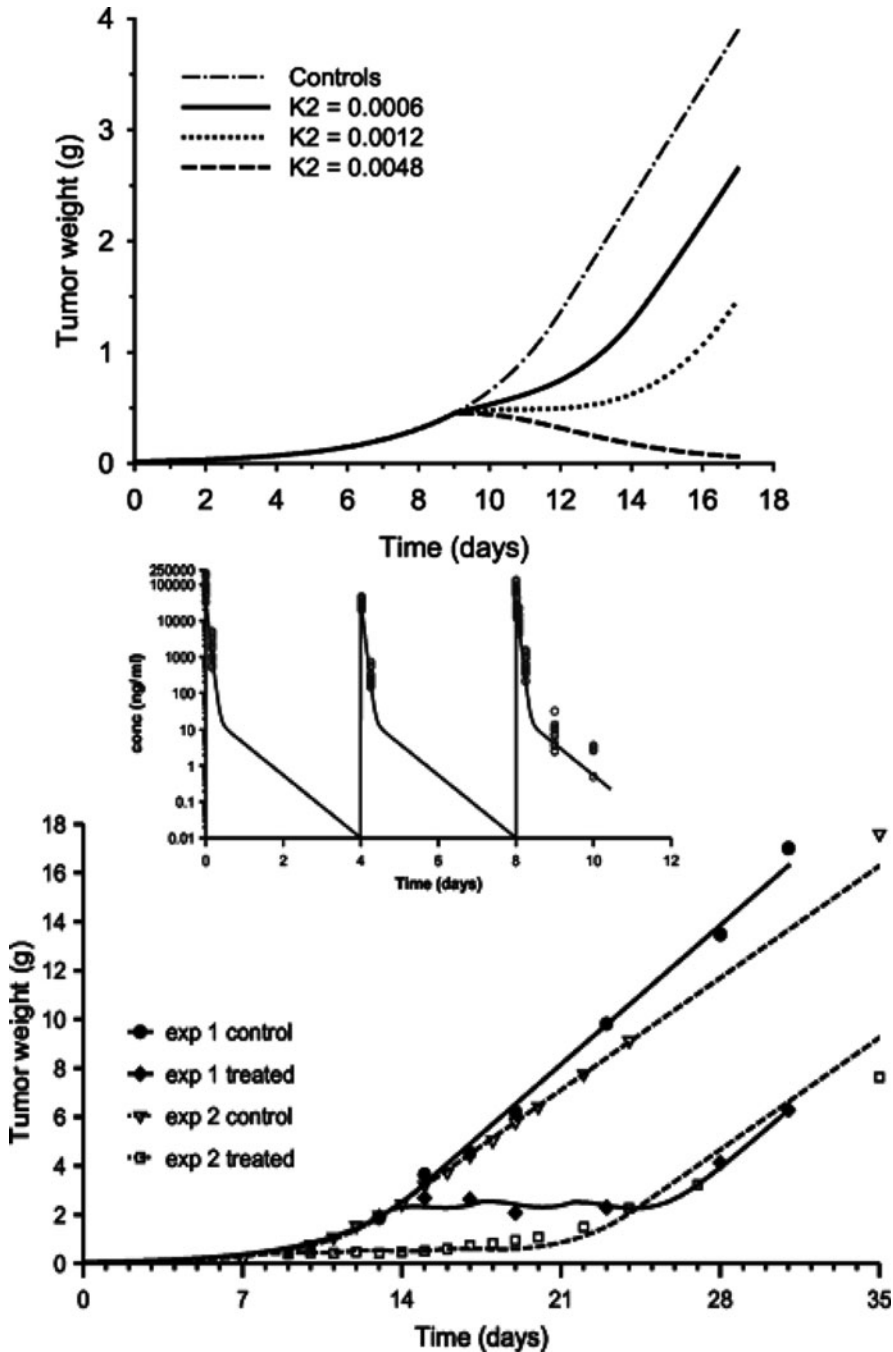
**Fig. 1.3** Top plot shows the theoretical effect of $K_2$ on simulated tumor growth curves: the simulations were performed assuming a single intravenous bolus given on day 9; $\lambda_0 = 0.0154$/day; $\lambda_1 = 0.0211$ g/day; $w(0) = 0.0162$ g; $K_1 = 0.0265$/day. $\lambda_0$, first-order rate constant of tumor growth; $\lambda_0$, zero-order rate constant of tumor growth; $w(0)$, tumor weight at the inoculation time; $K_1$, first-order rate constant of transit; $K_2$, measure of drug potency. Bottom two plots show the observed and model-fitted tumor growth curves obtained in two different experiments in nude mice given intravenously either the vehicle or paclitaxel [experiment 1 (*exp* 1), 30 mg/kg every 4 days for 3 days from day 8; experiment 2 (*exp* 2), 30 mg/kg every 4 days for 3 days from day 13]. Middle plot shows the fitting of the pharmacokinetic data of paclitaxel given as repeated intravenous bolus doses at 30 mg/kg dose level; *Conc.*, concentration. Reprinted with permission from Simeoni et al. (2004a). Copyright American Association of Cancer Research, 2004

that if $C_{ss} < C_{TE}$ then the tumor will grow to the asymptotic weight of $\lambda_1/(K_2 \times C_{ss})$. If $C_{ss} > C_{TE}$, then the tumor size will decrease. In examining the product of CTE and human total systemic clearance, a linear relationship on a log–log scale was noted for ten different drugs and further when $K_2$ was plotted against the maximum tolerated dose, a linear log–log relationship was again seen (Rochetti et al. 2007).

Using this model, Simeoni et al. modeled a variety of tumor growth curves for paclitaxel, 5-FU, and a NCE. The bottom of Fig. 1.3 shows the observed and predicted growth curves for two different experiments in mice bearing A2780 tumors following paclitaxel administration. From this initial report, a number of further examinations of the usefulness of the model have been reported by the authors (Magni et al. 2006; Rocchetti et al. 2005; Simeoni et al. 2004b; Poggesi et al. 2004), and by others outside the group (Goteti et al. 2010).

It should be pointed out, however, that the Simeoni model is not without its flaws. First, unlike the Gompertz model, the Simeoni model has no plateau and continues linear growth to infinity. In reality, tumors have a self-limiting size and when the animal does not die before that limit is reached, a plateau is evident in tumor size and/or weight. The Simeoni model cannot account for a plateau. Second, although the model is touted as a semi-mechanistic model, the actual growth function is empirical based on observation. Also, the model is new to pharmacologists who perform the xenograft studies. Gompertzian growth has 40 years of experience behind it; pharmacologists are comfortable with it. The Simeoni model is new and untested and the comfort level is not the same when it is used. Despite these, however, the model still has its advantages and good modeling practice would be to compare a variety of models (Simeoni, Gompertz, logistic, etc.) before choosing an appropriate form.

Since these initial reports, the basic Simeoni model has been expanded to other situations. Stuyckens et al. (2007) extend the basic model by allowing for drug resistance to occur either through an empirical resistance function or through a semi-mechanistic approach and further

show how the model can be expanded in a kinetic–dynamic model through which concentration measurements are not necessary.

Koch et al. (2009) modified the Simeoni model to allow a smooth transition between exponential and linear growth by changing $dY_1/dt$ in (1.12) to

$$\frac{dY_1}{dt} = \frac{2\lambda_0\lambda_1 Y_1(t)^2}{(\lambda_1 + 2\lambda_0 Y_1(t))w(t)} - K_2 C(t) Y_1(t) \quad (1.14)$$

All other equations remain the same. In the studies is reported by Simeoni, none the drugs examined were given in combination. Koch et al. extend their model to account for combination therapy when two drugs are getting together. They replace $K_2$ in (1.14) with a term they refer to as the "total influence" function and change the first two differential equations in the model to

$$\frac{dY_1}{dt} = \frac{2\lambda_0\lambda_1 Y_1(t)^2}{(\lambda_1 + 2\lambda_0 Y_1(t))w(t)}$$
$$\qquad - \left(K_2^a C_a(t) + K_2^b C_b(t)\Phi\right)Y_1(t)$$
$$\frac{dY_2}{dt} = \left(K_2^a C_a(t) + K_2^b C_b(t)\right)Y_1(t) - K_1 Y_2(t)$$
$$(1.15)$$

where, $K_2^a$ and $K_2^b$ are the $K_2$ values for Drug A and Drug B and $\Phi$ is a synergy term such that $\Phi > 1$ implies synergy, $\Phi = 1$ implies additive, and $\Phi < 1$ implies antagonism. It should be noted that unless many different dose combinations of Drug A and Drug B are given, $\Phi$ may be unestimable.

Bueno et al. (2008) reported a model which characterized the pharmacokinetics of LY2157299, a novel Type I receptor TGF-β kinase antagonist, and tumor growth kinetics in Calu6 and MX1 tumor types. The pharmacokinetic model consisted of a two compartment model with first-order absorption and first-order elimination. Since tumor size did not plateau, the tumor model used was the Simeoni growth model where the change in tumor size $(dY/dt)$ was characterized by

$$\frac{dY}{dt} = \frac{\lambda_0(1 - INH2)Y(t)}{\left[1 + \left(\frac{\lambda_0}{\lambda_1}Y(t)\right)^\psi\right]^{1/\psi}}. \quad (1.16)$$

INH2 was a zero to one time-delayed, normalized inhibition effect related to the degree of phosphorylated Smad, proteins that modulate the activity of TGF-β agonists (Fig. 1.4). The authors then used simulation to understand the relationship of tumor growth inhibition and tumor growth delay with steady-state concentrations of LY2157299 and different dosing schedule.

A competing model to the Simeoni model is the proposed transit model approach by Lobo and Balthasar (2010), which they developed to account for the delay in tumor growth inhibition versus methotrexate plasma concentrations. The transit model they proposed is shown in the bottom of Fig. 1.2. Mathematically, the model proposed was

$$\frac{dY}{dt} = g(Y) - K_4 Y(t), Y(0) = w(0)$$

$$\frac{dX_1}{dt} = \tau \left( \frac{K_{max} C_p}{IC_{50} + C_p} - X_1(t) \right)$$

$$\frac{dX_2}{dt} = \tau (X_1 - X_2)$$

$$\frac{dX_3}{dt} = \tau (X_2 - X_3) \tag{1.17}$$

$$\frac{dX_4}{dt} = \tau (X_3 - X_4)$$

$$X_1(0) = X_2(0) = X_3(0) = X_4(0) = 0$$

where $Y$ is the tumor size, $\tau$ is the transit rate constant (similar to $K_1$ in the Simeoni model), and $g(.)$ is a tumor growth function. Sample growth functions include a exponential growth
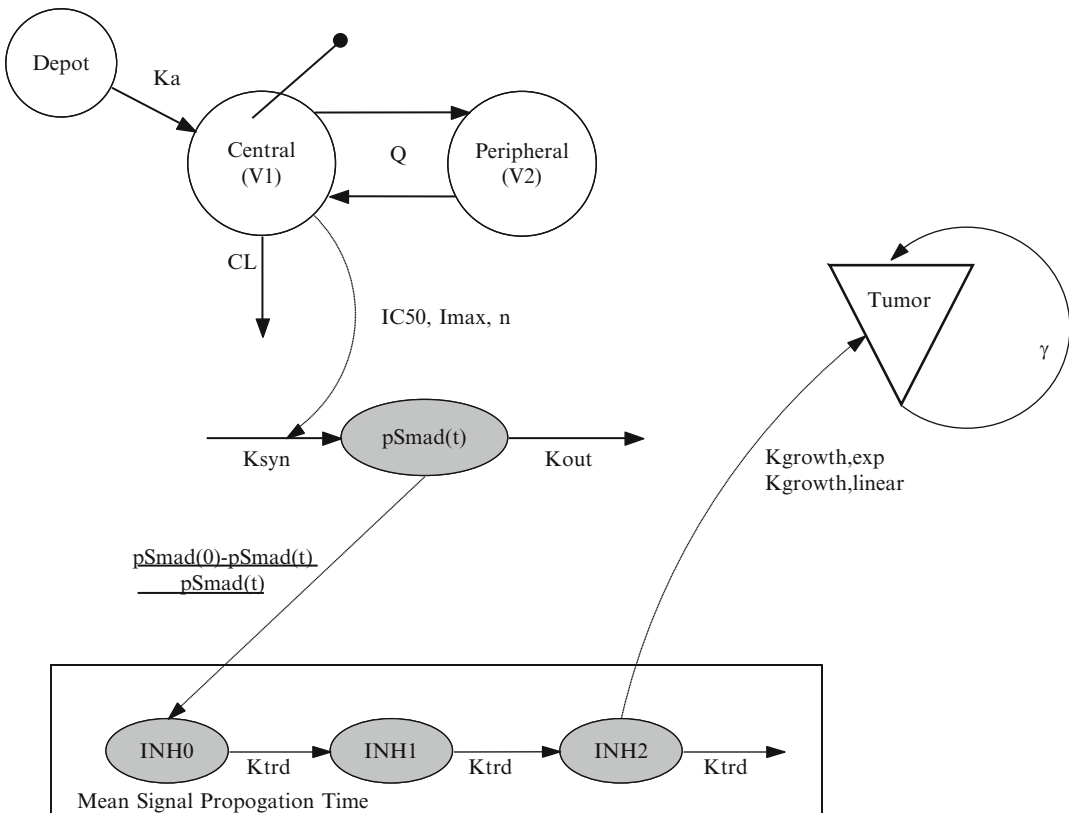


**Fig. 1.4** Schematic model for the tumor growth kinetics following treatment with LY2157299 as presented by Bueno et al. (2008). *Gray circles* denote biomarkers. Best lines denote negative influence functions, e.g., plasma concentrations of LY2157299 inhibit phosphory-lation of pSmad

$$g(.) = K_g Y(t),  \qquad (1.18)$$

exponential growth that plateaus

$$g(.) = K_g Y(t) \left( 1 - \frac{Y(t)}{Y_{\max}} \right), \qquad (1.19)$$

or even a Simeoni type function

$$g(.) = \left[ 1 + \left( \frac{\lambda_0}{\lambda_1} Y(t) \right)^{\Psi} \right]^{1/\Psi}. \qquad (1.20)$$

Lobo and Balthasar compared the transit model to two established models for chemotherapeutic effects, a phase-specific and phase-nonspecific model. The transit model was found to provide a superior goodness of fit compared to the established models. Yang et al. (2010) simulated data from the Simeoni model (which they call the cell distribution model) and the transit model (which they call the signal distribution model) and compared the simulated data using the alternative model. Their analysis revealed that the signal distribution model was more flexible in fitting data derived from the cell distribution model than vice versa. They concluded that although the models appear similar, they are in fact mechanistically distinct, are not interchangeable, and that the cell transit model is more robust, particularly when data are sparse.

Jumbe et al. (2010) recently reported a modified transit compartment model wherein tumor cells were divided into two groups, those that were insensitive to the drug and grow a constant rate and those that were sensitive to the drug and eventually die. The sensitive cells were modeled as a progressive process of cell damage whereby the cells stop replicating and then eventually die. The total volume of the tumor was the sum of the insensitive cells and sensitive cells at the progressive stages of death. Using this model, the authors were able to characterize the effects of trastuzumab-DM1, an antibody–drug conjugate under development for the treatment of breast cancer, in two different mice xenograft models of HER2-positive breast cancer specifically designed to be trastuzumab resistant.

The effect of trastuzumab was shown to be cell-cycle-phase nonspecific in its mechanism of action.

A new model has recently been reported to model the antitumor effect of antiangiogenic agents. Ribba et al. (2010) used four ordinary differential equations to describe the temporal changes of non-hypoxic (P), hypoxic (Q), and necrotic (N) tissue within a tumor. A latent variable K, which they call the carrying capacity, accounts for the process of angiogenesis. Using sunitinib as a probe, the authors modeled the tumor growth kinetics of HT29 lung and HCT116 colon xenografts in mice using a kinetic–dynamic model to account for temporal changes in sunitinib concentrations. It is too early at this point to determine the value of the model in drug development but its mechanistic nature holds promise.

## 1.4   Measuring Tumor Size in Cancer Patients

There are many different ways to measure tumor size, the most common being radiologic measurement. Usually, the cross product measurement of the two longest perpendicular diameters seen on a cross-sectional image, like an X-ray, ultrasound, CT, or MRI scan, is taken as the size of the tumor. With new imaging techniques, actual tumor volume can now be assessed, but this is not often done (yet). For X-ray measurement, diameter may be measured manually with a caliper, but for imaging and digital X-rays, computerized measurements can be made. The difficulty with measuring perpendicular diameters is when the legion of interest is not well defined or is asymmetrical. For this reason, measurment of tumor size in many pivotal trials is done by a standardized review, sometimes using just a single reviewer, to reduce intersubject variability and increase reproducibility.

Being able to accurately measure tumor size is important for many reasons. A patient's initial tumor size is used to stage the patient for many types of cancers. For example, breast cancer patients having a tumor size of 2–5 cm are classified as T-2. Tumors >5 cm are classified as T-3.

How a patient is treated depends upon their staging. Once a patient initiates therapy, treatment is dependent on how the tumor shrinks in response to a therapy. A tumor may show initial shrinkage with a drug but then may start to grow again, a process known as disease progression, at which point the physician may change the course of treatment. Without an accurate tumor size measurement physicians are treating blind. Tumor size is also an important indicator for survival. For example, patients with lung tumors <2 cm in size have a higher survival rate than patients with larger sized tumors.

In most cases, multiple lesions are measured and the sum of these lesions is returned as a composite measure of tumor burden; this is often called the sum of longest diameters. Nearly 30 years ago, the World Health Organization (WHO) (Miller et al. 1981) reported on guidelines to standardized tumor measurements across studies. Under the WHO criteria, patients can be defined into one of five response types: "complete response" (CR), "partial response" (PR), "stable disease" (SD), "progressive disease" (PD), or "not evaluable."

While a huge step forward there were still problems with the WHO guidelines, like lack of specification of the number of lesions to be reviewed, definitions for what constitutes progressive disease, and how to handle new imaging modalities. In 2000, several research groups updated the WHO guidelines and created the Response Evaluation Criteria in Solid Tumors (RECIST) guidelines (Therasse et al. 2000). The core of RECIST is standardized tumor size measurement. In 2009, RECIST Version 1.1 was released as a means to further improve consistency and standardization across clinical trials (Eisenhauer et al. 2009). RECIST 1.1 has a few changes to version 1. These include reducing the number of measured lesions to be assessed from a maximum of ten to five, reducing the number of measured lesions from a maximum of five to two in a particular organ, new guidelines for assessment of measuring the lymph nodes, guidelines on defining disease progression, and new guidelines on imaging (interestingly, in the first version of RECIST no radiologists were included in developing the guidelines). Table 1.1 presents definitions for the response criteria under RECIST 1.1.

The overall response rate (ORR) for a trial is the proportion of patients that achieve a specified reduction in tumor size for a predefined period of time (at least 4 weeks) that includes both CR and PR (McKee et al. 2010). Stable disease is not included in ORR, but is included in the Disease Control Rate, which is the proportion of patients achieving a PR, CR, or SD. Response duration is defined as the time from initial response to the time of documented disease progression. In considering a drug's ORR, the FDA considers magnitude, percent of CRs, and duration of response.

**Table 1.1** Summary of response criteria under RECIST 1.1

| Response | Definition |
|---|---|
| Complete response | Complete disappearance of all lesions lasting at least 4 weeks; lymph nodes must be non-pathological in size |
| Partial response | A 30% decrease in sum of longest diameters lasting at least 4 weeks taking as a reference the baseline tumor size |
| Stable disease | Neither partial response or progressive disease criteria met taking as a reference the smallest sum of diameters as the reference |
| Progressive disease | 20% increase in tumor size using the smallest sum of diameters as the reference (which may be the baseline) with no complete response, partial response, or stable disease documented before increased disease and a minimum increase of at least 5 mm or appearance of new lesions |
| Not evaluable | When no measurement is available or incomplete measurements are done |

Tumor measurements are often made every few weeks, usually 4–8 weeks, depending on the cancer type. From these, the best overall response is determined (which in itself is complicated, see Eisenhauer et al. (2009) Tables 1–3 for details) and then based on when, and if, progression occurs, time to progression (TTP) is determined, which is formally defined as the time from randomization to documented, objective disease progression (McKee et al. 2010). TTP is related to progression-free survival (PFS), which is defined as the time from randomization to disease progression or death. Should a patient die during study, TTP is censored. TTP can be used as a primary endpoint in a clinical trial in which the majority of patients who die on the study are not expected to be to the cancer itself, although PFS is preferred since it is expected to better correlate with overall survival, the gold standard of primary endpoints in oncology.

While standardized criteria certainly have their advantages, there are still unresolved issues with regards to standardization. Examples include when there are more than five lesions, radiologists do not consistently choose the same five lesions to assess. Reproducibility is still an issue, with interobserver and intraobserver variabilities of 15% and 6% for measurements of tumor size in three dimensions using CT (Schwartz et al. 2000). And, there are some questions as to whether RECIST applies to pediatric oncology (McHugh and Kao 2003).

## 1.5 Clinical Models for Tumor Growth

There have been few published models that have examined the relationship between exposure and tumor growth over time in humans. The goals of these studies have been to relate short-term changes in tumor size to long-term changes in outcome or to confirm the presence of a concentration-effect relationship. Both of these goals have utility. The success rate in Phase 3 oncology studies is not as large as one would think, about

50%. Being able to leverage the information from Phase 2 may increase the probability of success in Phase 3. Being able to establish a concentration-tumor size relationship may be useful as supporting data in a registration dossier with only a single well-controlled study.

Tham et al. (2008) presented a model for tumor growth in non-small cell lung cancer (NSCLC) patients using a kinetic–dynamic model. Under this empirical model, an effect compartment was used to transduce dose into an "effect concentration" which was then used as an input into an indirect response type-model. Using this model, the authors were able to predict tumor size following treatment with gemcitabine.

Wang et al. (2009) modeled four randomized clinical trials for NSCLC. Tumor size $Y$ was modeled using a mixed exponential decay and linear growth function

$$Y(t) = Y(0)\exp(-St) + kt \qquad (1.21)$$

where, $Y(0)$ is the baseline tumor size, $S$ is the exponential tumor rate shrinkage constant, and $k$ is the linear growth rate constant. The exponential portion of the model explains the rate of tumor shrinkage, while the linear growth function explains the rate of tumor growth after tumors have ceased shrinking. Random effects were added to the model by allowing the baseline, $S$, and $k$ to be log normally distributed. An exponential error model was used to account for unexplained residual variability. Figure 1.5 presents a goodness of fit plots for six representative patients. The model appears to capture the general tendencies of the observed data.

Simply modeling tumor size was not the goal of the Wang et al. paper. The goal was to incorporate changes in tumor size as a predictor of survival and to determine whether short-term changes in tumor size could be used to predict long-term overall survival. The authors found that overall survival could be modeled using a parametric lognormal survival model in which the mean survival time was a function of ECOG (Eastern Cooperative Oncology Group) performance status, baseline tumor size, and percent
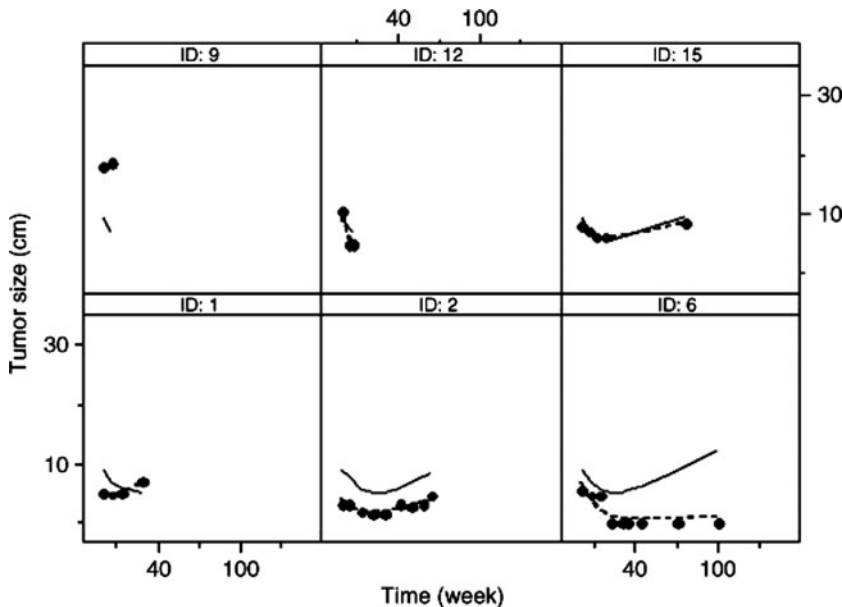
**Fig. 1.5** The time course of NSCLC tumor size change for representative individual patients. The *symbols* represent the observed tumor sizes, the *solid line* represents the mean tumor size for the overall population, and the *broken line* represents the individual predicted tumor size. Figure reprinted from Wang et al. (2009). Reprinted by permission from Nature Publishing Group [Clinical Pharmacology and Therapeutics, 2004]

change from baseline 8 weeks after initiating therapy. Wang et al. did not link the tumor size model to a particular pharmacokinetic model because the studies used to develop the model were different drugs. But future analyses could link a pharmacokinetic model with a tumor model. Similarly, for NCEs being developed for NSCLC, a model could be developed explaining change in tumor size as a function of that drug's pharmacokinetics, which could then be linked to the Wang et al. survival model to predict overall survival based on short-term efficacy studies, thus leveraging information.

Claret et al. (2009) developed a kinetic–pharmacodynamic model linking capecitabine exposure to tumor growth inhibition in patients with colorectal cancer. Using data from Phase II and Phase III data, the authors modeled tumor size $Y$ at time $t$ using the equation

$$\frac{dY}{dt} = K_{growth} \times Y(t) - K_{death} \times \text{Dose}$$
$$\times \exp(-\lambda t) \times Y(t) \quad (1.22)$$

where, $K_{growth}$ is the tumor growth rate, $K_{death}$ is the tumor death rate, Dose is the daily dose administered, and $\exp(-\lambda t)$ is the progression rate at time $t$, where $\lambda$ is the estimated progression appearance factor. Because no pharmacokinetic data were available, dose was used as the exposure measure affecting tumor death. Between-subject variability was accounted for by allowing $K_{growth}$, $K_{death}$, and $\lambda$ to be treated as log normally distributed random effects. Similar to the Wang et al. paper, the authors then developed a survival model linking percent change in tumor size 7 weeks after treatment to overall survival but with a twist. The twist was that they did not have a survival data with capecitabine, but they did have survival data with 5-FU so they developed their survival model using the 5-FU data and then piggybacked the models together (Fig. 1.6). Hence, one part of their model was drug-specific while the other part of their model was disease-specific. Using simulation, the authors validated their model using an independent Phase 3 study. Based on these

**Fig. 1.6** Schematic of the kinetic–dynamic-survival model of Claret et al. (2009). *Gray boxes* are model outputs
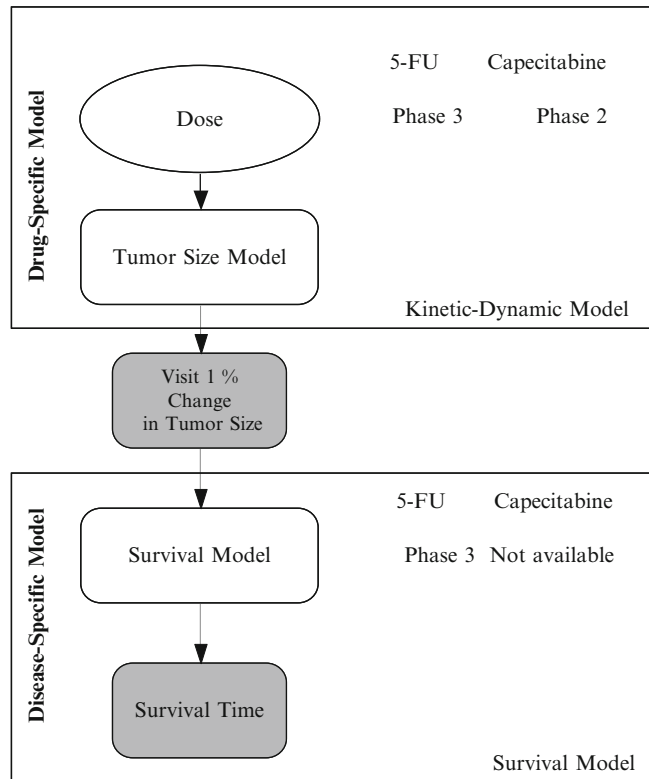
results the authors have developed a framework for predicting the Phase 3 survival based on Phase 2 data which might be useful when deciding whether to pursue further development of the compound.

Houk et al. (2009) expanded on the Claret et al. model and reported on the tumor growth kinetics in patients with metastatic renal cell cancer (mRCC) and gastrointestinal stromal tumors (GIST) following treatment with sunitinib.[1] Tumor growth kinetics ($dY/dt$), as measured by the sum of longest diameters, for each tumor type was described by

$$\frac{dY}{dt} = K_{growth} \times Y(t) - K_{death} \times C(t)$$
$$\times \exp(-\lambda t) \times Y(t) \quad (1.23)$$

where, $C(t)$ is the plasma concentration of sunitinib. This time, exposure was modeled as a function of drug concentration. Their models showed a different rate of growth and death for mRCC and GIST. Patients with mRCC had a $K_{growth}$ twofold higher than patients with GIST and threefold higher $K_{death}$. The rate of progression was 1.5-times faster in mRCC than in GIST. Simulations showed that 38% more of mRCC patients and 23% more of GIST patients would show a partial response (at the least a 30% decrease from baseline in tumor size) when sunitinib was administered 50 mg once-daily compared to 25 mg once-daily. Combining this efficacy model with a variety of different adverse event models, the authors generated a composite efficacy – adverse event profile for sunitinib. It should be noted that one difficulty with this model is the estimation of $K_{growth}$. Since most patients, once they start to show signs of disease progression, are taken off the study drug, an estimate of $K_{growth}$ is often unavailable or imprecisely estimated.

---

[1]Houk et al. discussed this model in another chapter in this book.

## 1.6 Modeling Response in Humans

Under RECIST criteria, patients are assigned a best overall response. It is often of interest to model best overall tumor response as a function of exposure. The usual method is to treat the responses as an ordinal variable such that CR > PR > SD > PD and then use ordinal logistic regression to model response as a function of exposure. An example of this approach is the exposure–response analysis reported for sunitinib in mRCC patients as reported by Houk et al. (2009) in which there was a significant relationship between sunitinib exposure and the probability of either a CR or PR ($p < 0.0001$). In GIST patients a trend toward significance was observed but did not reach statistical significance. In both cases there was a trend towards decreasing tumor size with increasing sunitinib exposure.

There are pros and cons to this approach. The pros are that the results have direct interpretation and is relevant, e.g., increasing exposure increases the probability of a complete response. The con is that RECIST collapses a dynamic measure (tumor growth) into a single endpoint, which always results in loss of information and decreased statistical power at detecting covariate effects. Further research is needed in the link between dynamic models of tumor growth and logistic regression of best overall response.

## 1.7 Mathematical Models of Cancer

A handful of reports have been published on theoretical models of cancer growth and progression, some of which were reviewed in Sanga et al. (2006). Araujo and McElwain (2004) present a history of these type of mathematical models. These models do not use the traditional ordinary differential equation framework familiar to most pharmacokineticists and instead use partial differential equations, which take into account both time and space. For example, Sinek et al. (2009) reported on the effect of doxorubicin and cisplatin using a partial differential multicompartment model of concentrations in the extracellular, cytosolic, and nuclear compartments. From this they were able to predict DNA-bound drug concentrations, drug concentrations at various cell depths, cell inhibition, and cell survival. Sanga et al. argue that "*the multifaceted nature of cancer requires sophisticated, nonlinear mathematical models to capture more realistic growth dynamics and morphologies*". Although none of these models have yet to show utility in drug development, with the rise of systems biology it is only a matter of time before these nonlinear time- and space-models of cellular dynamics link with pharmacokinetic–pharmacodynamic models to lead to an integrative holistic model of drug response and effect.

### Conclusions

The difficulties and challenges associated with understanding the dynamics of cancer may benefit from mathematical modeling. Indeed, the role of mathematical modeling in drug development is becoming more mainstream and accepted. In the March 2010 issue of Forbes magazine, there was a cover item that said "Can Math Cure Cancer?" and inside was a story called "The Mathematics of Cancer". The main focus of the article was on Larry Norton, of the Norton–Simon hypothesis, and how he thinks that "*adding more mathematics to the crude science of cancer therapy will help*". Forbes is not a scientific magazine, it is not even oriented towards professional economists. The target audience for Forbes is the everyday investor and yet here is a story discussing the role of modeling in drug development and how it could help cure cancer.

Modeling tumor growth may prove to be an advantageous tool in cancer drug development since modeling allows for greater understanding of mechanisms and allow for predictions outside the domain of the studies used to develop the model. And yet, there are still many limitations to the models we use. The linear ordinary differential equations used to characterize tumor growth are a gross simplification and have only a small face validity in their use. True tumor growth is nonlinear

and stochastic and requires much more complex models involving partial differential equations. Still, modeling provides a means to understand data from a variety of complex sources and across many different data types. Early leveraging of preclinical information (even if the model is a simplification of the true underlying data generating process) and later application of modeling in drug development will allow companies make better decisions, hopefully earlier. The use of mathematical modeling in oncology is relatively new and is ripe for research with a need for new innovative modeling methods, techniques, and applications.

## References

American Cancer Society. Cancer Facts and Figures: 2010. 2010.

Araujo RP and McElwain LS (2004) A history of the study of solid tumor growth: the contribution of mathematical modeling. *Bulletin of Mathematical Biology* **66**:1039–1091.

Bueno L, de Alwis DP, Pitou C, Yingling J, Lahn M, Glatt S and Troconiz IF (2008) Semi-mechanistic modelling of the tumour growth inhibitory effects of LY2157299, a new type I receptor TGF-beta kinase antagonist, in mice. *European Journal of Cancer* **44**:142–150.

Citron ML, Berry DA, Cirrincione C, Hudis C, Winer EP, Gradishar WJ, Davidson NE, Martino S, Livingston R, Ingle JN, Perez EA, Carpenter J, Hurd D, Holland JF, Smith BL, Sartor CI, Leung EH, Abrams J, Schilsky RL, Muss HB and Norton L (2003) Randomized trial of dose-dense versus conventionally scheduled and sequential versus concurrent combination chemotherapy as postoperative adjuvant treatment of node-positive primary breast cancer: first report of Intergroup Trial C9741/Cancer and Leukemia Group B Trial C9741. *Journal of Clinical Oncology* **21**:1431–1439.

Claret L, Girard P, Hoff PM, Van Custem E, Zuideveld KP, Jorga K, Fagerberg J and Bruno R (2009) Model-based prediction of Phase III overall survival in colorectal cancer on the basis of Phase II tumor dynamics. *Journal of Clinical Oncology* **27**:4103–4108.

Clarke R (1997) Issues in the experimental design and endpoint analysis in the study of experimental cytotoxic agents in vivo in breast cancer and other models. *Breast Cancer Research Treatment* **46**:225–278.

Eisenhauer EA, Therasse P, Bogaerts J, Schwartz LH, Sargent D, Ford R, Dancey J, Arbuck S, Gwyther S, Mooney M, Rubinstein L, Shankar L, Dodd L, Kaplan R, Lacombe D and Verweij J (2009) New response evaluation criteria in solid tumours: revised RECIST guideline (version 1.1). *European Journal of Cancer* **45**:228–247.

Garber K (2010) Debate grows over mouse models of cancer. *Journal of the National Cancer Institute* **98**:1176–1178.

Goteti K, Garner CE, Utley L, Dai J, Ashwell S, Moustakas DT, Gonen M, Schwartz GK, Kern SE, Zabludoff S and Brassil PJ (2010) Preclinical pharmacokinetics/pharmacodynamic models to predict synergistic effects of co-administered anti-cancer agents. *Cancer Chemotherapy and Pharmacology* **66**:245–254.

Greaves P, Williams A and Eve M (2004) First dose of potential new medicine to humans: how animals help. *Nature Reviews Drug Discovery* **3**:226–236.

Houk BE, Bello CL, Poland B, Rosen LS, Demetri GD and Motzer RJ (2009) Relationship between exposure to sunitinib and efficacy and tolerability endpoints in patients with cancer: results of a pharmacokinetic–pharmacodynamic meta-analysis. *Cancer Chemotherapy and Pharmacology* **66**:357–371.

Inaba M, Kobayashi T, Tashiro T and Sakurai Y (1988) Pharmacokinetic approach to rational therapeutic doses for human tumor-bearing nude mice. *Japanese Journal of Cancer Research* **79**:509–516.

Inaba M, Kobayashi T, Tashiro T, Sakurai Y, Maruo K, Ohnishi Y, Ueyama Y and Nomura T (1989) Evaluation of antitumor activity in a human breast tumor/nude mouse model with a special emphasis on treatment dose. *Cancer* **64**:1577–1582.

Jackson K, Chedid M, Evans R and Troconiz IF (2010) A novel PKPD model to describe the interaction of drug response of combination therapy: an application in preclinical oncology. Presented at the Population Analysis Group in Europe, Berlin.

Johnson JI, Decker S, Zaharevitz D, Rubinstein LV, Venditti JM, Schepartz S, Kalyandrug S, Christian M, Arbuck S, Hollingshead M and Sausville EA (2001) Relationships between drug activity in NCI preclinical in vitro and in vivo models and early clinical trials. *British Journal of Cancer* **84**:1424–1431.

Jumbe NL, Xin Y, Leipold D, Crocker L, Dugger D, Mai E, Slikowski MX, Fielder PJ and Tibbitts J (2010) Modeling the efficacy of trastuzumab-DM1, an antibody drug conjugate, in mice. *Journal of Pharmacokinetics and Pharmacodynamics* **37**:221–242.

Kelland LR (2004) "Of mice and men": values and liabilities of the athymic nude mouse model in anticancer drug development. *European Journal of Cancer* **40**:827–836.

Kerbel RS (2003) Human tumor xenografts as predictive preclinical models for anticancer drug activity in humans: better than commonly perceived – but they can be improved. *Cancern Biology and Therapy* **4**, **Suppl 1**:S134–S139.

Koch G, Walz A, Lahu G and Schropp J (2009) Modeling of tumor growth and anticancer effects of combination therapy. *Journal of Pharmacokinetics and Pharmacodynamics* **36**:179–197.

Kola I and Landis J (2004) Can the pharmaceutical industry reduce attrition rates? *Nature Reviews. Drug Discovery* **3**:711–715.

Laird AK (1964) Dynamics of tumor growth. *British Journal of Cancer* **18**:490–502.

Liang H and Sha N (2004) Modeling antitumor activity by using a nonlinear mixed effects model. *Mathematical Biosciences* **189**:61–73.

Lobo E and Balthasar J (2010) Pharmacodynamic modeling of chemotherapeutic effects: application of a transit compartment model to characterize methotrexate effects in vitro. *AAPS PharmSci* **4**:Article 42.

Magni P, Simeoni M, Poggesi I, Rochetti M and De Nicolao G (2006) A mathematical model to study the effects of drug administration on tumor growth dynamics. *Mathematical Biosciences* **200**:127–151.

Maruo K, Ueyama Y, Inaba M, Emura R, Ohnishi Y, Nakamura O, Sato O and Nomura T (1990) Responsiveness of subcutaneous human glioma xenografts to various antitumor agents. *Anticancer Research* **10**:209–212.

Marusic M (1995) Mathematical models of tumor growth. Lecture presented at the Mathematical Colloquium in Osijek organized by the Croatian Mathematical Society.

McHugh K and Kao S (2003) Response evaluation criteria in solid tumours (RECIST): problems and need for modifications in paediatric oncology? *The British Journal of Radiology* **76**:433–436.

McKee AE, Farrell AT, Pazdur R and Woodcock J (2010) The role of the U.S. Food and Drug Administration review process: clinical trial endpoints in oncology. *Oncologist* **15**, **Suppl 1**:13–18.

Miklavcic D, Jarm T, Karba R and Sersa G (1995) Mathematical modeling of tumor growth in mice following electrotherapy and bleomycin treatment. *Mathematics and Computers in Simulation* **39**:597–602.

Miller AB, Hoogstraten B, Staquet M and Winkler A (1981) Reporting results of cancer treatment. *Cancer* **47**:207–214.

Norton L (1988) A Gompertzian model of the human breast cancer growth. *Cancer Research* **48**:7067–7081.

Norton L and Simon R (1976a) The growth curve of an experimental solid tumor following radiotherapy. *Journal of the National Cancer Institute* **58**:1735–1741.

Norton L and Simon R (1976b) Tumor size, sensitivity to therapy in the design of treatment protocols. *Cancer Treatment Reports* **61**:1307–1317.

Norton L, Dugan U, Hudis C, Young D, Farrell C, Tanaka Y, Theodoulou M and Traina T (2005) Optimizing chemotherapeutic dose-scheduling (CDS) by Norton–Simon modeling: capecitabine (Xeloda). *Proceeding of the American Association of Cancer Research* **46**:1182-Abstract 5007.

Poggesi I, Simeoni M, Germani M, De Nicolao G and Rocchetti M (2004) Population modeling of tumor growth in untreated mice. Presented at Population Approach Group in Europe (PAGE), Uppsala, Sweden.

Ribba B, Watkin E, Tod M, Girard P, Grenier E, You B, Wei M, Giraudo E and Freyer G (2010) Combined analysis of tumor size and histological markers. Presented at the Population Analysis Group in Europe Meeting, Berlin.

Rocchetti M, Poggesi I, Massimiliano G, Fiorentini F, Pellizzoni C, Zugoni P, Pesenti E, Simeoni M and De Nicolao G (2005) A pharmacokinetic–pharmacodynamic model for predicting tumour growth inhibition in mice: a useful tool in oncology drug development. *Basic and Clinical Pharmacology and Toxicology* **96**:265–268.

Rochetti M, Simeoni M, Pesenti E, De Nicolao G and Poggesi I (2007) Predicting the active doses in humans from animal studies: a novel approach in oncology. *European Journal of Cancer* **1862**:1868.

Rygaard K and Spang-Thomsen M (1997) Quantitation and Gompertzian analysis of tumor growth. *Breast Cancer Research Treatment* **46**:303–312.

Sanga S, Sinek JP, Frieboes HB, Ferrari M, Fruehauf JP and Cristini V (2006) Mathematical modeling of cancer progression and response to chemotherapy. *Expert Review of Anticancer Therapy* **6**:1361–1765.

Schwartz LH, Ginsberg MS, DeCorato D, Rothenberg LN, Einstein S, Kijewski P and Panicek DM (2000) Evaluation of tumor measurements in oncology: use of file based and electronic techniques. *Journal of Clinical Oncology* **18**:2179–2184.

Sharpless NE and DePinho RA (2006) The mighty mouse: genetically engineered mouse models in cancer drug development. *Nature Reviews. Drug Discovery* **5**:741–754.

Shoemaker AR, Mitten MJ, Adickes J, Ackler S, Refici M, Ferguson D, Oleksijew A, O'Connor JM, Wang B, Frost DJ, Bauch J, Marsh K, Tahir SK, Yang X, Tse C, Fesik SW, Rosenberg SH and Elmore SW (2008) Activity of the Bcl-2 family inhibitor ABT-263 in a panel of small cell lung cancer xenograft models. *Clinical Cancer Research* **14**:3268–3277.

Simeoni M, Magni P, Cammia C, De Nicolao G, Croci V, Pesenti E, Germani M, Poggesi I and Rochetti M (2004a) Predictive pharmacokinetic–pharmacodynamic modeling of tumor growth kinetics in xenograft models after administration of anticancer agents. *Cancer Research* **64**:1094–1101.

Simeoni M, Poggesi I, Germani M, De Nicolao G and Rocchetti M (2004b) Population modeling of tumor growth inhibition in vivo: application to anticancer drug development. Presented at Population Approach Group in Europe (PAGE), Uppsala, Sweden.

Simpson-Herren L and Lloyd HH (1976) Kinetic parameter and growth curves for experimental tumor systems. *Cancer Chemotherapy Reports* **54**:143–174.

Sinek JP, Sanga S, Zheng X, Frieboes HB, Ferrari M and Cristini V (2009) Predicting drug pharmacokinetics and effect in vascularized tumors using computer simulation. *Journal of Mathematical Biology* **58**:484–510.

Stuyckens K, Perez Ruixo JJ, Vermeulen A and Cox E (2007) Modeling drug effects and resistance development on tumor growth dynamics. Presented at Population Approach Group in Europe (PAGE), Kobenhavn, Denmark.

Sullivan PW and Salmon S (1972) Kinetics of tumor growth and regression in IgG multiple myeloma. *Journal of Clinical Investigation* **51**:1697–1708.

Tanaka C, O'Reilly T, Kovarik JM, Shand N, Hazell K, Judson I, Raymond E, Zumstein-Mecker S, Stephan C, Boulay A, Hattenberger M, Thomas G and Lane HA (2008) Identifying optimal biologic doses of everolimus (RAD001) in patients with cancer based on the modeling of preclinical and clinical pharmacokinetic and pharmacodynamic data. *Journal of Clinical Oncology* **26**:1596–1602.

Tashiro N, Inaba M, Kobayashi T, Sakurai Y, Maruo K, Ohnishi Y, Ueyama Y and Nomura T (1989) Responsiveness of human lung cancer/nude mouse to antitumor agents in a model using clinically equivalent doses. *Cancer Chemotherapy and Pharmacology* **24**:187–192.

Tham LS, Wang L, Soo RA, Lee SC, Lee HS, Yong WP, Goh BC and Holford NHG (2008) A pharmacodynamic model for the time course of tumor shrinkage by gemcitabine + carboplatin in non-small cell lung cancer patients. *Clinical Cancer Research* **14**:4213–4218.

Therasse P, Arbuck S, Eisenhauer EA, Wanders J, Kaplan EL, Rubinstein L, Verweij J, Van Glabbeke M, van Oosterom A, Christian MC and Gwyther S (2000) New guidelines to evaluate the response to treatment to solid tumors. *Journal of the National Cancer Institute* **92**:205–216.

Traina T, Theodoulou M, Higgins B, Kolinsky K, Packman K, Dugan U, Hudis C and Norton L (2006) In vivo activity of a novel regimen of capecitabine in a breast cancer xenograft model. *Breast Cancer Research Treatment* **100**, **Suppl 1**:S2709-Abstract 6071.

Traina T, Theodoulou M, Feigin K, Patil S, Tan KL, Edwards C, Dugan U, Norton L and Hudis C (2008) Phase I study of a novel capecitabine schedule based on the Norton–Simon mathematical model in patients with metastatic breast cancer. *Journal of Clinical Oncology* **26**:1797–1802.

Wang Y, Sung C, Dartois C, Ramchandani R, Booth BP, Rock E and Gobburu J (2009) Elucidation of relationship between tumor size and survival in non-small-cell lung cancer patients can aid early decision making in clinical drug development. *Clinical Pharmacology and Therapeutics* **86**:167–174.

Xu X (1987) The biological foundation of the Gompertz Model. *International Journal of Bio-Medical Computing* **20**:35–39.

Yamakazi S, Skaptason J, Romero D, Lee JH, Zou HY, Christensen JG, Koup JR, Smith BJ and Koudriakova T (2008) Pharmacokinetic–pharmacodynamic modeling of biomarker response and tumor growth inhibition to an orally available cMet kinase inhibitor in human tumor xenograft mouse models. *Drug Metabolism and Disposition* **36**:1267–1274.

Yang J, Mager D and Straubinger RM (2010) Comparison of two pharmacodynamic transduction models for the analysis of tumor therapeutic responses in model systems. *The AAPS Journal* **12**:1–10.

# Drug–Drug Interactions: Designing Development Programs and Appropriate Product Labeling

**2**

J. Matthew Hutzler, Jack Cook, and Joseph C. Fleishaker

## Abstract

Drug–drug interactions can represent a major public health issue. Drug metabolism science has evolved to the point where interactions with cytochrome P-450 isozymes can be predicted and potentially avoided or managed, but much work remains to allow accurate prediction of non-P-450 mediated interactions. Based on preclinical data, rational clinical plans can be developed to study potential drug–drug interactions in humans and develop labeling that allows optimal usage of new drugs.

## 2.1 Introduction

Adverse drug reactions are a major public health concern. It has been estimated that approximately 5% of hospital admissions are related to adverse drug reactions (Kongkaew et al. 2008), although other estimates have placed this value between 3% and 28% (McDonnell and Jacobs 2002). Hospital admissions for adverse drug reactions are highest in elderly subjects who are taking multiple medications (Kongkaew et al. 2008), suggesting drug–drug interactions (DDIs) may contribute to this observation. Indeed, in the elderly, 4.8% of hospital admissions were due to DDIs (Becker et al. 2007). These data suggest DDIs contribute to hospital admissions and health care costs.

On an individual basis, DDIs can have catastrophic and life-threatening consequences. Several high profile drugs have been removed from the market due to DDIs. The antihistamine terfenadine caused QT prolongation, torsades de pointes, and sudden cardiac death in patients who were also receiving CYP3A4 inhibitors. Astemizole and cisapride were removed from the market for similar reasons (Smith and Schmid 2006). The calcium channel blocker mibefradil caused significant DDI's with a number of agents and was removed from the market (Krayenbühl et al. 1999). Most notable were rhabdomyolysis when combined with simvastatin or lovastatin and nephrotoxicity in combination with cyclosporine or tacrolimus. In all of these cases, changes in the product labeling were ineffective in avoiding DDIs in clinical use and thus precluded the continued safe prescribing of these agents.

Given the potential societal and individual impact of drug interactions, assessment of drug interaction potential has been an important aspect

J.C. Fleishaker (✉)

Pfizer, St. Louis Laboratories, Clinical Research, Cortex Building, 4320 Forest Park Boulevard, Suit 320, St. Louis, MO 63108, USA

e-mail: joseph.c.fleishaker@pfizer.com

of drug development for decades. Initially- decisions on which drug interactions were studied were based on the likelihood two drugs would be co-administered in the targeted patient population. This philosophy resulted in a large number of drug interaction studies conducted to support marketing and medical practice, many of which were redundant and may not have been truly necessary or scientifically informative. With increased understanding of the mechanisms of drug transport, metabolism, and elimination, in vitro data have been increasingly used to assess potential risk for drug interaction. The Food and Drug Administration's 2006 draft guidance (Drug Interaction Studies – Study Design, Data Analysis, and Implications for Dosing and Labeling) helped codify this concept and laid out strategies for how in vitro data can be used to screen for potential metabolic interactions and on how to use in vitro data to decide which clinical interaction studies should be run.

## 2.2   Why Use Preclinical Data to Guide Clinical Drug Development

Using in vitro methods to guide a drug interaction program for a new chemical entity (NCE) has a number of advantages. First, in vitro studies can be used to identify drug combinations that may result in large changes in exposure, either for one drug or for both. The observation of a substantial in vitro interaction can be a strong signal indicating an in vivo investigation is warranted. In addition, in vitro data allows the results of in vivo studies to be readily generalized based on the mechanism of interaction. An example of this is evident in the labeling for ZYFLO CR® tablets, which contain zileuton as the active ingredient. A number of drug interaction studies were performed (theophylline, warfarin, propranolol, prednisone, ethinyl estradiol, digoxin, phenytoin, sulfasalazine, and naproxen), with clinically significant interactions noted for theophylline, propranolol, and warfarin. The increase in theophylline and propranolol AUC was approximately twofold, while the increase

in R-warfarin AUC was about 22%. Subsequent in vitro work has shown zileuton is an inhibitor of CYP1A2, with minimal effects on other CYP isozymes (Lu et al. 2003). These in vitro data could have been generalized to predict interactions with other CYP1A2 substrates, rather than having discussions in the labeling concerning drugs in the same therapeutic class.

Additional benefits can be gained by limiting the conduct of in vivo drug interaction studies to those where interactions are likely to occur. The decreased cost of drug development is accompanied by a reduction in the generation of data that does not provide additional information beyond that obtained in vitro. In the zileuton example, the in vitro data showing lack of effect on CYP isozymes other than CYP1A2 could have been used to avoid conducting drug interaction studies with drugs that are substrates of other isozymes, most notably CYP3A4 and CYP2C9 (terfenadine, prednisone, ethinyl estradiol, phenytoin, and naproxen).

A recent evaluation of the use of in vitro data on p-glycoprotein inhibition to predict drug interactions with digoxin illustrates this point on a broader basis (Fenner et al. 2009). Clinical drug interaction studies with digoxin were routinely conducted in drug development programs, both before and after the main mechanism for this interaction was elucidated (p-glycoprotein inhibition in the gut and kidney). The primary reason for the routine conduct of this study was digoxin's narrow therapeutic window and the potentially serious consequences of digoxin toxicity. As described by Fenner et al. 93% of 123 digoxin DDI studies examined showed changes in digoxin area under the curve <25%. Thus in the vast majority of studies, the magnitude of change was less than the upper limit typically used for bioequivalence trials and therefore the interaction is not considered clinically relevant. Fenner et al. argue that appropriate in vitro studies of p-glycoprotein inhibition by new drugs, with appropriate cutoff criteria, will substantially lower the number of times DDIs with digoxin would need to be studied clinically. They also argue, for NCEs that are p-glycoprotein substrates and have reasonable therapeutic ranges, drug interactions with p-glycoprotein

would rarely, if ever, require substantial dose adjustment and that these interactions may not require detailed in vivo investigation. Hence, the use of in vitro models makes sense scientifically and financially.

## 2.3   Preclinical Assessment of DDI Potential in Drug Development

In order to reduce the risks associated with clinical DDIs, and meet the mutual goal of providing safe and effective medicines to the public, health authorities and pharmaceutical companies have focused on the development of in vitro strategies for characterizing metabolism early in the drug discovery process. Evaluation of inhibition and induction of cytochrome P450 enzymes by NCEs is now common practice for clinical candidate selection. With the ready availability of recombinant DNA expressed P450 isozymes, commercially available human hepatocytes and microsomes, known substrates and inhibitors for P450 isozymes, and rapid liquid chromatography/mass spectrometry (LC-MS) techniques, early assessment enables an understanding of the structural features leading to inhibition (e.g. structure-activity relationships, SAR). This section of the

chapter will focus on the most recent in vitro methods for assessing DDIs, as it pertains to cytochrome P450 inhibition, induction of cytochrome P450, and transporter DDI (e.g. p-glycoprotein). In addition, methods for predicting clinical DDI using in vitro data, as well as the future direction of screening strategies for assessing clinical DDI risk, will be discussed.

## 2.4   Inhibition of Cytochrome P450 and Other Drug-Metabolizing Enzymes

In humans, the biotransformation of xenobiotics is most often catalyzed by the cytochrome P450 family of drug-metabolizing enzymes. It is well understood that the P450 isozymes 3A4, 2D6, 2C9, 2C19, and 1A2 contribute to some degree to the metabolism of >90% of marketed drugs (Fig. 2.1, Wienkers and Heath 2005; Guengerich 2008). Consequently, most labs supporting preclinical pharmacokinetics and metabolism in drug discovery (so-called ADME groups) screen synthesized test compounds against these enzymes in high throughput inhibition assays. The format of these assays has evolved substantially over the years, as the balance between
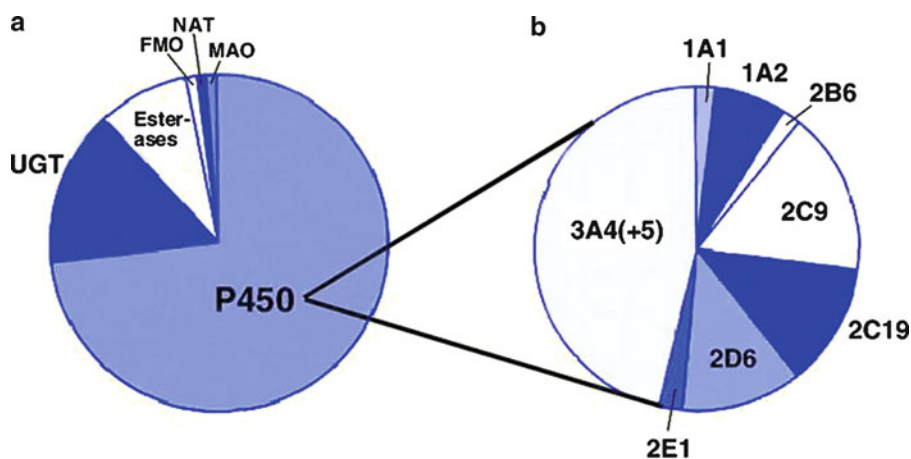


**Fig. 2.1** Contributions of enzymes to the metabolism of top 200 prescribed drugs. The results are from a study of Pfizer drugs (Williams et al. 2004). (**a**) Fraction of metabolic clearance catalyzed by various human drug-metabolizing enzymes. *UGT* uridine glucuronosyltransferase,

*FMO* flavin-containing monoxygenase, *NAT* N-acetyltransferase, and *MAO* monoamine oxidase. (**b**) Fractions of P450 oxidations on drugs catalyzed by individual P450 enzymes. Reprinted with permission from review in *Chemical Research in Toxicology* (Guengerich 2008)

generation of robust predictive data and high throughput to support rapid cycle times for discovery chemistry has been a continuous challenge. Traditional academic methods for testing inhibition of cytochrome P450 enzymes using HPLC with UV or fluorescence detection were simply unable to accommodate the high-throughput screening (HTS) requirements of drug discovery to evaluate hundreds or even thousands of drug molecules on a weekly basis. Instead, assay technologies that enable improved throughput at a low cost have been developed over the years, including the use of nonselective fluorogenic P450 probe substrates (resorufins, coumarins, quinolines, etc.) and 96 or 384 plate-reading techniques (Crespi and Stresser 2000; Miller et al. 2000). Despite the clear advantage of ultra-high throughput, the fluorogenic probe approach is fraught with issues such as the potential for test compounds to interfere with or quench the fluorescence signal (unpublished observations), and the fact that fluorogenic probes are not "drug-like," in that they are not used in DDI trials, making it more challenging to extrapolate this type of in vitro data to the clinical setting. In addition, studies comparing the use of fluorogenic

probes with traditional LC/MS methods have found poor correlations, especially for CYP3A4 (Cohen et al. 2003, Fig. 2.2; Bell et al. 2008), raising concerns about the predictability of these methods. Despite the aforementioned issues with using fluorogenic probes, some pharmaceutical/ biotechnology companies are still willing to accept this risk in an early screening environment to take advantage of throughput capabilities. Alternatively, another approach, developed to circumvent the potential for interference with fluorescence signal while maintaining high throughput, is the use of luminogenic cytochrome P450 inhibition assays (Cali et al. 2006).

With substantial advances in bioanalytical technology in recent years, ADME groups within the pharmaceutical industry have moved toward the use of clinically relevant and selective probe substrates of the P450 enzymes, according to guidelines generated by the FDA (Table 2.1), using LC-MS. Assay incubations are typically conducted in human liver microsomes (HLMs) pooled from at least 50 donors. This HLM system better represents of the intact liver compared to recombinantly expressed P450 enzymes (e.g. Supersomes® from BD-Biosciences or
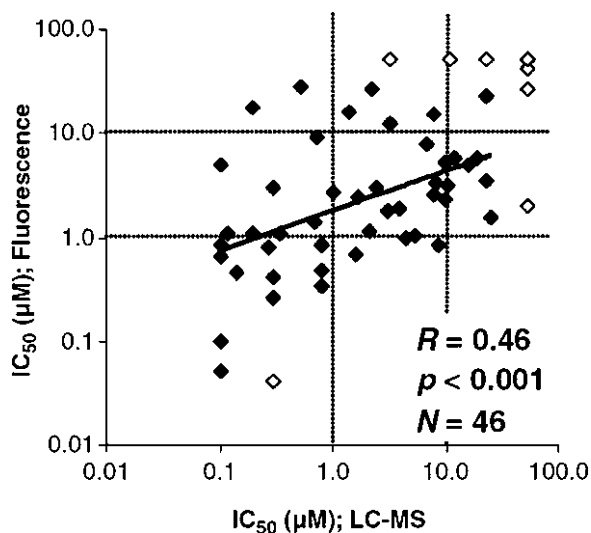


**Fig. 2.2** Comparison of $IC_{50}$s generated using recombinant CYPs with fluorescent probe (dibenzylfluorescein, DBF) to HLM with LC/MS detection with traditional probe substrate (midazolam). *Dotted lines* define the $IC_{50}$ limits used for DDI risk binning (<1 μM, high risk;

1–10 μM, moderate risk; >10 μM, low risk). *Shaded areas* represent concordance in binning between the two assays approaches. Reprinted with permission from *Journal of Biomolecular Screening* (Bell et al. 2008)

**Table 2.1** Substrates and positive controls for assessing DDI in vitro

| Enzyme | Activity | Positive control inhibitor (recommended concentration) | Positive control time-dependent inactivator (TDI) |
|---|---|---|---|
| CYP1A2* | Phenacetin O-deethylase | Furafylline (10 μM) | Furafylline |
| CYP2B6 | Bupropion hydroxylase | PPP (2-phenyl-2-(1-piperidinyl) propane) | PPP (2-phenyl-2-(1-piperidinyl)propane) |
| CYP2C8* | Amodiaquine N-deethylase | Montelukast (0.1 μM) | thioTEPA |
| CYP2C9 | Diclofenac 4′-hydroxylase (S)-warfarin 7-hydroxylase | Sulfaphenazole (10 μM) | Tienilic acid |
| CYP2C19 | (S)-Mephenytoin 4′-hydroxylase | (+)N-Benzylnirvanol (10 μM) | Ticlopidine |
| CYP2D6* | Dextromethorphan O-demethylase | Quinidine (1.0 μM) | Paroxetine |
| CYP2E1 | Chlorzoxazone 6-hydroxylase | Diethyldithiocarbamate (10 μM) | Diethyldithiocarbamate |
| CYP3A4 | Midazolam 1′-hydroxylase Testosterone 6β-hydroxylase Felodipine dehydrogenase | Ketoconazole (1.0 μM) | Verapamil, erythromycin, TAO |

Baculosomes® from Invitrogen), which are coexpressed with the electron-shuttling co-proteins oxidoreductase and cytochrome b5 at nonphysiological ratios. To meet the demands of higher throughput in a drug discovery environment, a critical development has been ultraperformance liquid chromatography/tandem mass spectrometry (UPLC-MS-MS), where the use of sub-2 μm porous particle LC coupled to high flow rates results in sufficient resolution for fast separation methods (Fig. 2.3, Plumb et al. 2008). In addition, the bioanalysis and/or the incubation itself may be conducted in a cocktail assay format (Testino and Patonay 2003; Kim et al. 2005; Dixit et al. 2007), and early "tier 1" ADME screening assays may be performed at one or two concentrations of test compound, with data reported as percent (%) inhibition. Algorithms for estimating an $IC_{50}$ based on a single-point inhibition assessment have also been employed as a screening approach to P450 inhibition (Gao et al. 2002).

One concern with conducting P450 inhibition assays with a "cocktail" of substrates, is "crosstalk" or nonselective interactions of the probe substrates with other P450 enzymes, potentially compromising the fidelity of the data. To address this concern, multiple studies have been conducted recently comparing $IC_{50}$ values generated from both singlet and cocktail assays (Zientek et al. 2008; Youdim et al. 2008). In methods reported by Youdim et al. a 384-well cocktail assay evaluating inhibition of CYP1A2 (tacrine), 2C9 (diclofenac), 2C19 (S-mephenytoin), 2D6 (dextromethorphan), and 3A4 (midazolam) was developed with an LC/MS method run time on the order of 1 min. Interestingly, comparison of $IC_{50}$ values (geometric mean) generated with this miniaturized cocktail method closely resembled those generated in the individual P450 inhibition assays tested, with a slight upward bias in the cocktail results. In further studies by Zientek et al. the enzyme kinetics ($K_{m,app}$ and $V_{max}$) of the selective probe substrate reactions were compared and while it was found there was minimal shift in $K_{m,app}$ values between singlet and cocktail formats, the velocities measured in the cocktail probe substrate format were consistently lower than those measured in the single substrate format (Fig. 2.4, Zientek et al. 2008). Causes for this observation are unclear at this time, but the authors speculate it may be the result of P450 isoform competition for oxidoreductase, as reported by Cawley et al. (1995). Despite these velocity differences, the accuracy of the $IC_{50}$ values compared to those generated in the singlet assay format did not appear to impact decisions made based on their results. One strategy that seems to be the result of some of the difficulties just described is the elimination of CYP2C19 from early screening. Despite being a selective probe for CYP2C19, (S)-mephenytoin is the most problematic probe substrate within the
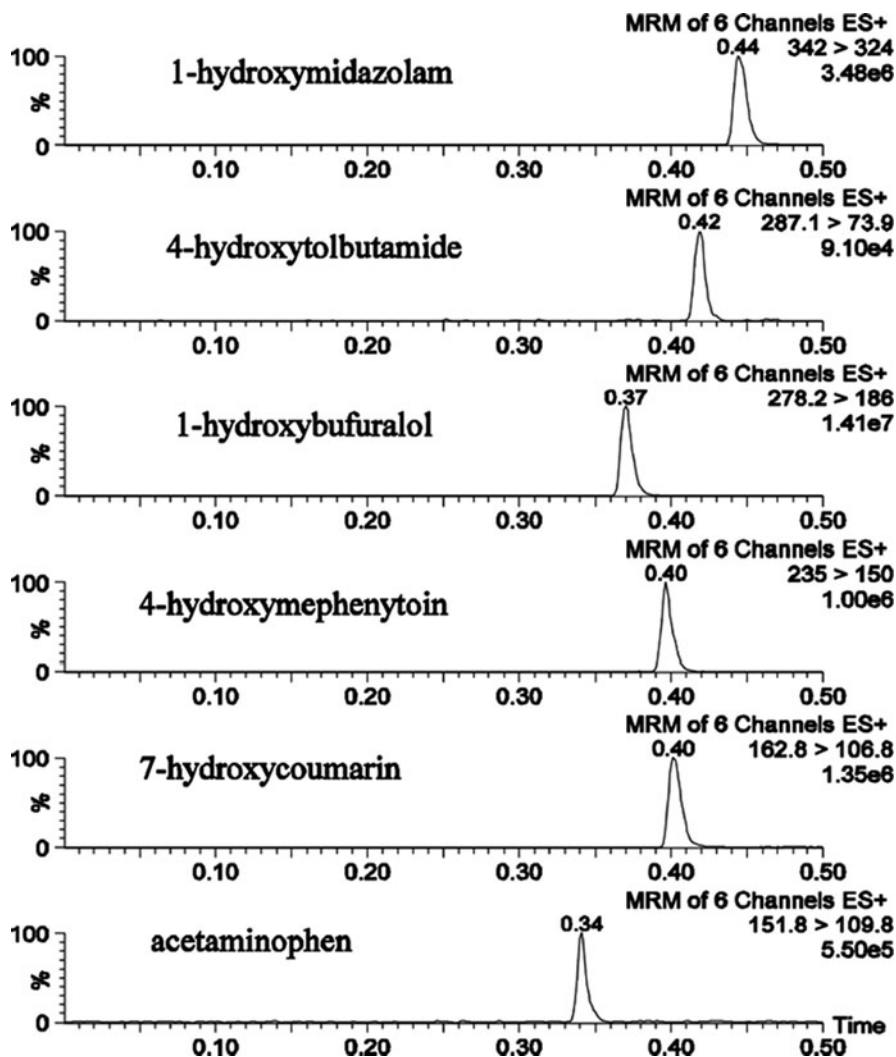
**Fig. 2.3** LC/MS/MS analysis of six analytes commonly used in cytochrome P450 inhibition screens in a cocktail format. Use of UPLC/MS/MS methods with a 2.1 × 50 mm ACQUITY BEH C18 1.7 μm column enables ultra-high throughput (0.5 min/sample), while maintaining analyte resolution. Reprinted with permission from *Rapid Communications in Mass Spectrometry* (Plumb et al. 2008)

cocktail of substrates, as it is metabolized slowly, and the metabolite monitored (4-hydroxymephenytoin) does not ionize well by mass spectrometry, resulting in an insensitive assay. Identification of a more optimal selective probe substrate for CYP2C19 would be of great benefit. Nonetheless, from these reports, it is clear that cocktail inhibition assays are sufficiently reliable for identifying potent inhibitors of P450 in early stage drug discovery, which is ultimately the intent of ADME screening. However, at this time, with some of the uncertainties about the cause of the minor differences between cocktail and singlet $IC_{50}$ inhibition assays, it is not recommended to use cocktail $IC_{50}$ data for labeling purposes until additional work is performed to validate the accuracy and use of in vitro cocktail assays beyond screening. Validated singlet $IC_{50}$ assays are recommended for drug labeling, in which the assay conditions have been optimized
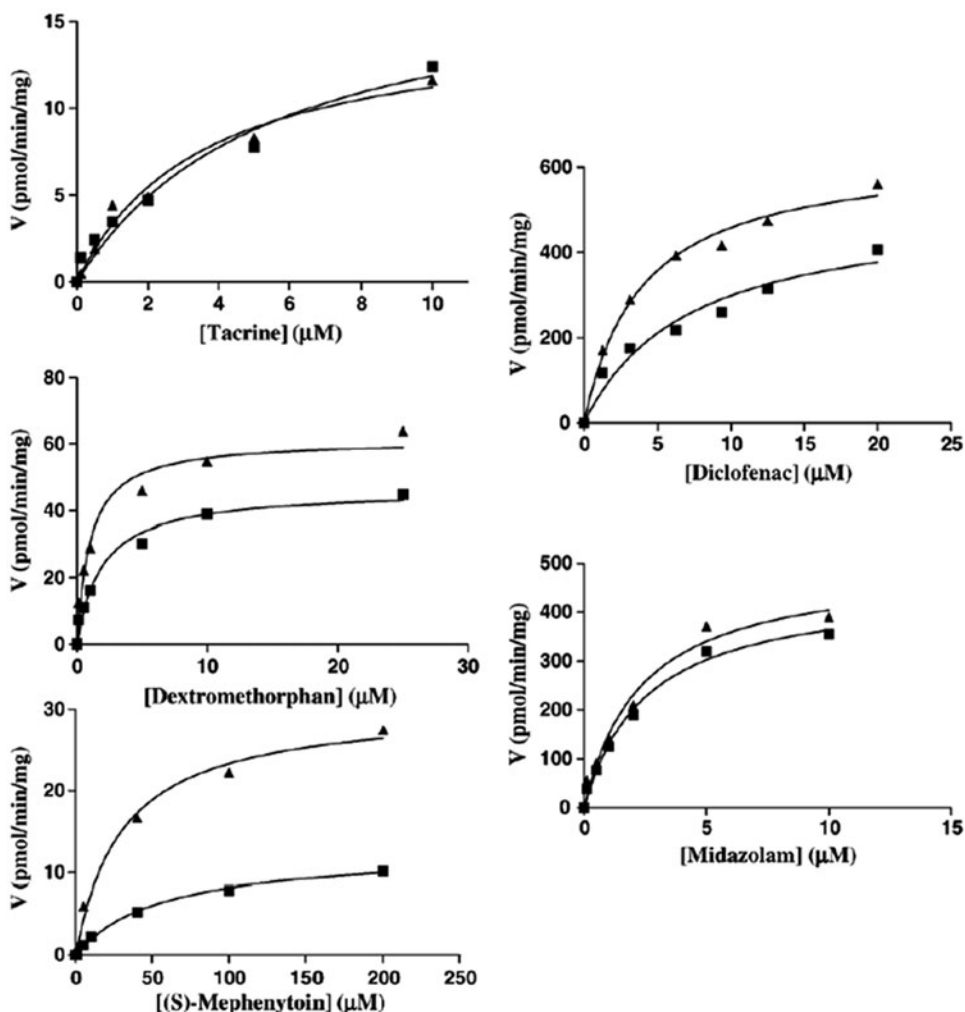
**Fig. 2.4** Direct comparison of velocity (pmol/min/mg) versus substrate (μM) enzyme kinetic plots for five traditional P450 probe substrates (tacrine, CYP1A2; dextromethorphan, CYP2D6; (S)-mephenytoin, CYP2C19; diclofenac, CYP2C9; and midazolam, CYP3A4) in a cocktail incubation (*filled square*) and singlet substrate/P450 incubations (*filled triangle*). Rates are generally lower when incubations are conducted in the cocktail format. Reprinted with permission from *Journal of Pharmacological and Toxicological Methods* (Zientek et al. 2008)

for low protein concentrations to minimize non-specific protein binding (where unbound drug concentration approximates total drug in the incubation) and incubation times are set to maintain linear Michaelis-Menten steady-state kinetics (<10% consumption of substrate) (Walsky and Obach 2004). It is much more challenging to optimize cocktail assays to maintain these critical conditions, with the selective probe substrates demonstrating such drastic differences in metabolic rates. In addition, multiple probe substrates

for complex P450 enzymes such as CYP3A4 (midazolam, testosterone, and felodipine), where inhibition has been demonstrated to be substrate-dependent in some cases (Wang et al. 2000), must be used for a comprehensive assessment of inhibition of this important drug-metabolizing enzyme.

In addition to screening for inhibition of the major P450 enzymes, Walsky et al. (2005, 2006) have concluded that CYP2C8 and CYP2B6 may also be of potential risk of being inhibited by new

NCEs. Screening efforts discovered a hit rate against CYP2C8 (>50% inhibition at 30 μM) of ~23% when testing >200 compounds in one discovery program. In particular, montelukast, a leukotriene receptor antagonist used in the treatment of asthma, was found to be an especially potent inhibitor of CYP2C8 ($IC_{50} = 0.02$ μM). In similar efforts, 30 compounds were found to inhibit CYP2B6 by greater than 50% at 30 μM, most notably clopidogrel and ticlopidine, with an $IC_{50}$ of 0.02 and 0.15 μM, respectively (Walsky et al. 2006). While CYP2C8 does not metabolize a large percentage of drugs on the market, testing for inhibition of this enzyme may become of higher importance, especially for discovery programs working in a chemical space outside the Lipinski Rule of 5 guideline for molecular weight (>500 amu), as the size of the CYP2C8 active site rivals that of CYP3A4 (Schoch et al. 2004), metabolizing large molecules such as the chemotherapeutic agent TAXOL® (Rahman et al. 1994). These findings suggest compounds should be tested for inhibition of CYP2C8 and CYP2B6 at some time prior to dosing patients who may be taking medications metabolized by these enzymes.

An intense area of research within the pharmaceutical industry in recent years is time-dependent inhibition (TDI) of cytochrome P450 enzymes, where an increase in the extent of inhibition is observed following pre-incubation with the test inhibitor. This phenomenon may be the result of generation of inhibitory metabolites generated in situ, or mechanism-based inactivation (MBI), where the metabolism of a substrate to a reactive electrophilic species (e.g. bioactivation) leads to either covalent modification of a nucleophilic amino acid residue in the P450 active site or to the heme moiety itself (Ortiz de Montellano 2005). MBI was originally described by Silverman and George (1988) and there are many mechanistic studies that must be performed for a compound to qualify as a MBI. An alternative mechanism of inactivation is formation of what is termed a metabolite-inhibitory complex (MIC), where an intermediate species such as nitroso or carbene noncovalently complexed with the heme iron, also referred to as a pseudoirreversible mechanism because of the tight nature of this complex (Ortiz de Montellano 2005). Whether or not MIC formation is the operable mechanism of TDI can easily be determined by monitoring an increase in absorbance 448–455 nm on a spectrophotometer (Jones et al. 1999; Hutzler et al. 2006). For example, Fig. 2.5 demonstrates a typical MI complex formed when troleandomycin (TAO) is incubated with recombinant CYP3A4 Supersomes®, with a pronounced time-dependent increase in absorbance at ~455 nm. Regardless of mechanism, the end
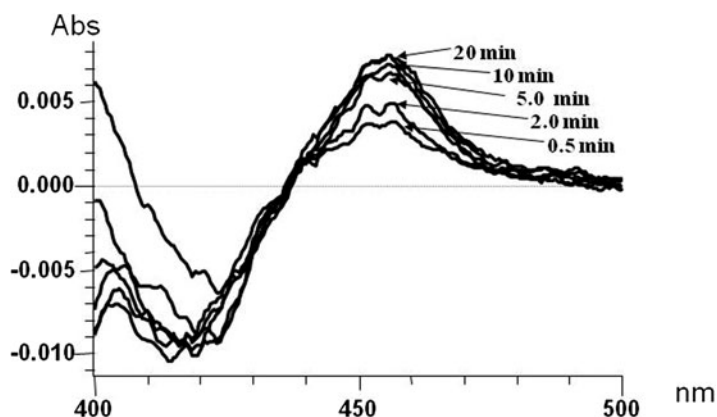


**Fig. 2.5** Formation of metabolite-inhibitory complex (MIC) with troleandomycin, a known time-dependent inhibitor of CYP3A4, when incubated with 0.1 pmol/μL of CYP3A4 Supersomes®. There is a clear time-dependent increase in absorbance at 455 nm, indicative of MIC formation, in this case due to nitroso intermediate complexing with heme iron. Spectra were collected using a Hitachi U3300 dual-beam spectrophotometer

result from a pharmacokinetic perspective is likely similar: potential increase in exposure of a co-administered substrate of the impacted metabolic pathway. Failure to consider this mechanism may lead to drastic underestimation of the magnitude of a clinical DDI.

The mechanism of inactivation may also be relevant as it pertains to drug toxicity. It is known, for example, that inactivation of CYP2C9 by tienilic acid results in covalent modification of the 2C9 apoprotein (Lopez-Garcia et al. 1994), which is proposed to result in an immunogenic response, providing a strong link to observed hepatotoxicity (Lecoeur et al. 1994). There are numerous reviews on the subject of clinical drugs that behave as mechanism-based inactivators of CYP3A4 (Zhou et al. 2004; Hollenberg et al. 2008), as well as comprehensive reviews that summarize the functional groups typically susceptible to bioactivation (Fontana et al. 2005; Kalgutkar et al. 2007). In addition to reviews in the literature, many pharmaceutical companies have also developed their own database of "structural alerts," summarizing functional groups that may undergo metabolic activation. These alerts can be used by drug metabolism scientists and medicinal chemists as a guide for avoiding or engineering out the risk of TDI of P450 when designing small molecules for therapeutic targets.

The in vitro assay design for assessing the kinetics of TDI is quite complex. Briefly, a primary incubation, containing the enzyme system of choice (typically recombinantly expressed P450s or human liver microsomes), test inactivator at various concentrations, and NADPH (or NADPH regeneration system) is initiated, and aliquots from this incubation are subsequently taken at various times (typically up to 30 min) and diluted into a secondary incubation containing a probe substrate at a concentration $\geq$4-fold $K_m$ to measure residual enzyme activity. It is imperative that if HLMs are used as the enzyme source in the primary assay, a low protein concentration (mg/ml) be used to minimize nonspecific binding of the test inactivator, which may lead to false negative results for highly bound drugs (unpublished observations). From

these kinetic studies, the ability to use in vitro time-dependent inhibition (TDI) data to predict the magnitude of a clinical DDI requires the estimation of kinetic parameters $k_{inact}$ (the maximal rate of inactivation) and $K_I$ (the concentration of inactivator resulting in half the maximal rate of inactivation), described in the following equation:

$$k_{obs} = k_{inact} \cdot [I]/K_I + [I].$$

As a result of this complex assay design, the pharmaceutical industry has sought alternative screening approaches to enable higher throughput assessment of TDI earlier in the drug discovery process, such as abbreviated inactivation studies with one or two concentrations of test compound and a single pre-incubation time to assess percent loss in activity over a fixed period of time relative to a solvent control (Watanabe et al. 2007). Interpreting data from TDI screening studies is often challenging, but the general consensus is if a NCE causes more than 20–25% loss of activity following a 30 min pre-incubation, then follow-up studies to characterize the kinetics of inactivation may be warranted (Grimm et al. 2009). In addition, $IC_{50}$-shift studies, where probe substrate is added after a pre-incubation with multiple concentrations of test compound, may be conducted to assess the risk for TDI. While the debate about the predictive ability of $IC_{50}$-shift data is on-going, reports have shown a good relationship between shifted $IC_{50}$ (measured after pre-incubation) and the $k_{inact}/K_I$ ratio (Obach et al. 2007; Berry and Zhao 2008; Grim et al. 2009), which suggests $IC_{50}$-shift assays may be useful not only for identifying potential TDI, but also for estimating the kinetics of inactivation.

As previously mentioned, accurate estimation of the kinetics of inactivation ($k_{inact}$ and $K_I$) is critical to predicting the magnitude of any potential clinical DDI. As demonstrated by Ghanbari et al. (2006), following an exhaustive effort to assemble and compare incubation conditions from literature reports of mechanism-based inactivators, the in vitro assay design and subsequent data analysis varies considerably between labs. In particular, protein concentration in the

primary assay, dilution factor into the secondary activity assay, pre-incubation times, correction for decreased enzyme activity in the absence of inhibitor, and probe substrate concentration relative to $K_m$ in the secondary activity assay, all critical to the accurate estimation of $k_{inact}$ and $K_I$, were identified as being variable. An additional report also focused on assay design for TDI (Van et al. 2006), and should be referred to when questioning the impact on estimation of inactivation kinetics for the purpose of predicting clinical DDIs (discussed in Sect. 2.4). An important point worth mentioning is that on occasion, biphasic inactivation plots may be observed, as was shown by Hutzler et al. with PH-302, an inactivator of CYP3A4 (Hutzler et al. 2006, Fig. 2.6). When biphasicity is observed, it is the initial linear kinetic phase that should be considered and modeled, similar to metabolic stability data from substrate depletion studies for estimating intrinsic clearance ($Cl_{int}$), so that one is not at risk for underpredicting the magnitude of a DDI. Thus, it is critical to include sufficiently early time points (<5 min) when conducting in vitro TDI studies to enable characterization of the initial inactivation kinetic phase. Additional studies that may be conducted in order to understand the mechanism of time-dependent inhibition include the following (but are not required from a regulatory perspective), which

were discussed in a recent article describing results of an industry-wide PhRMA survey on assessment of time-dependent inhibition of drug metabolizing enzymes (Grimm et al. 2009):

1. Estimation of partition ratio (a measure of biochemical efficiency);
2. Dialysis or microsome washing to establish reversibility;
3. Ferricyanide treatment or spectral studies to diagnose metabolite inhibitory complex (MIC) formation; and
4. Protection of inactivation by addition of competing substrate/inhibitor, reduced glutathione (GSH), and reactive oxygen scavengers such as catalase and superoxide dismutase.

When a compound has advanced to the point of clinical candidate nomination, yet still carries with it the apparent risk of P450 TDI, it is critical to consider all of the clearance pathways of the time-dependent inhibitor, particularly metabolic. Raloxifene serves as a classic example of how this may be critical to a comprehensive risk assessment of time-dependent inactivation of P450. In vitro systems where metabolism is essentially forced to proceed via P450 (e.g. recombinant P450 or human liver microsomes), represent the most sensitive system for evaluating TDI, especially in recombinant systems such as CYP3A4 Supersomes®, where the catalytic activity is known to be markedly higher than
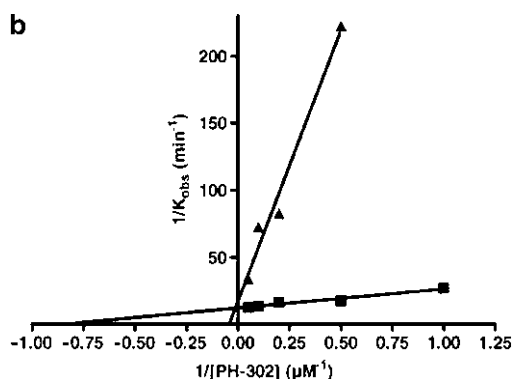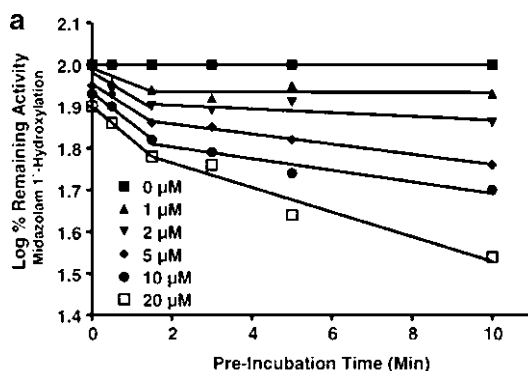


**Fig. 2.6** Demonstration of biphasic time-dependent inhibition (TDI) data. (**a**) Log % remaining activity versus pre-incubation time (0–10 min), illustrating time-dependent inhibition (TDI) of CYP3A4 by PH-302 (0–20 μM). (**b**) Data from both the initial and terminal phases were subsequently subjected to a Kitz–Wilson analysis and shown to produce distinct inactivation kinetic parameters (initial phase $k_{inact}$ = 0.08 min$^{-1}$, $K_I$ = 1.2 μM, terminal phase $k_{inact}$ = 0.06 min$^{-1}$, $K_I$ = 23.8 μM). Reprinted with permission from *Chemical Research in Toxicology* (Hutzler et al. 2006)

human liver microsomes. Raloxifene is reported to cause time-dependent inhibition of CYP3A4, and is also bioactivated to reactive metabolite species in vitro (Chen et al. 2002; Pearson et al. 2007), yet remains a relatively safe drug. Raloxifene is predominantly cleared by glucuronidation in the gut (Dalvie et al. 2008), and this metabolic clearance is proposed to protect the liver from high exposure to raloxifene. While this may serve as an extreme case, it points to the importance of careful consideration of the complete distributional properties of any drug that shows time-dependent inhibition in early screens. In an effort to account for the complete metabolic pathways of compounds that appear to be time-dependent inhibitors of CYP3A4, inactivation assays in hepatocytes have been conducted and reported (Zhao et al. 2005; McGinnity et al. 2006; Zhao 2008).

## 2.5  Reaction Phenotyping and Victim DDIs

Reaction phenotyping is the experimental procedure by which one attempts to identify which human enzymes contribute to the metabolism of a NCE, including estimation of relative contributions (e.g. fraction metabolized, $f_m$) of enzymes to the overall metabolic clearance (Williams et al. 2003). A thorough understanding of the metabolic pathways of a drug molecule is critical to the prediction of pharmacokinetic DDIs, where inhibition of a metabolic pathway by a co-administered inhibitor (called the perpetrator) results in increased exposure of the victim drug (e.g. "victim" drug–drug interaction). Two drugs withdrawn from the market due to DDIs and subsequent unacceptable safety profiles are terfenadine and cerivastatin. Reaction phenotyping information is also useful for the prediction of interindividual variability in drug exposure in the clinic, especially relevant when polymorphic enzymes such as CYP2C9, 2C19, 2D6, and 3A5 contribute significantly to overall clearance, shown to impact the clinical exposure of drugs such as celecoxib (Tang et al. 2001), sertraline (Wang et al. 2001), and metoprolol (Ismail and

Teh 2006) in poor metabolizers. CYP2B6 has also been recently described as the most polymorphic P450 in humans (Zanger et al. 2007), and metabolizes many relevant therapeutics such as efavirenz, nevirapine, and bupropion. Other non-P450 drug metabolizing enzymes shown to be polymorphically expressed include UGT1A1 and N-acetyl transferase 2 (NAT2) (Tomalik-Scharte et al. 2008), however, the science behind non-CYP DDIs generally lags behind the P450 enzymes. As a result of the aforementioned examples, there is a clear need to understand the potential variability in efficacy and toxicity of all new drugs, and thus, it is a requirement from global regulatory agencies that the metabolic pathways of an NCE be characterized prior to submission of any new drug application (NDA).

As indicated in a recent review by Zhang et al. (2007), it is the fraction of total clearance (CL) by metabolism ($f_m$) and contribution of each individual CYP to total CYP-mediated metabolism ($f_{m,CYP}$) that determines the magnitude of a drug interaction, whether it is by chemical inhibition or compromised metabolism due to polymorphic expression of the drug-metabolizing enzyme.

$$Cl_{total} = CL_{hepatic} + CL_{renal} + CL_{nonhepatic}$$

Typically, the likelihood of a victim DDI is reduced when an NCE is cleared <60% by any one metabolic pathway, especially a polymorphically expressed drug metabolizing enzyme. As shown in Fig. 2.7, the magnitude of DDI ($AUC_I/AUC$) increases substantially as the fraction metabolized ($f_{m,CYP}$) exceeds 0.6.

"Definitive" reaction phenotyping can only be performed with a radiolabeled human ADME study, which often is not performed until late in drug development after a drug candidate has demonstrated some measure of safety and effectiveness in patients (e.g. after "proof-of-concept"). As a result, reaction phenotyping studies to support early clinical plans must be done using non-labeled (e.g. cold) test drug, and often without the advantage of having authentic metabolite standards. A traditional approach in discovery would include substrate depletion methods in the in vitro system of choice (e.g. human liver
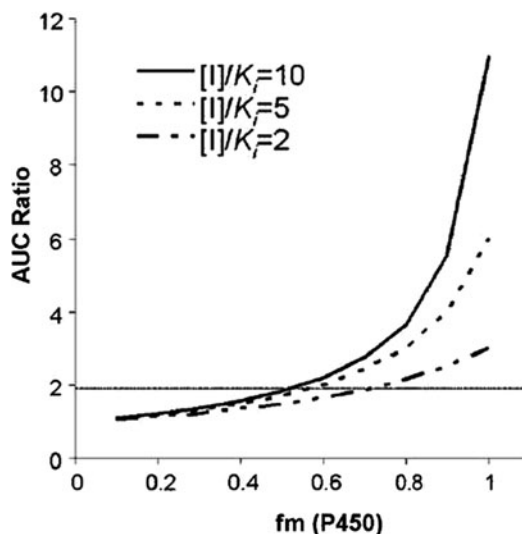
**Fig. 2.7** Simulated effect of fraction metabolized ($f_m$) on the change in AUC ratio (AUC of victim drug in presence of co-administered inhibitor/AUC minus inhibitor). The AUC ratio begins to drastically increase with increase in $f_m$ of victim drug, especially when the $[I]/K_i$ ratio exceeds 2 (e.g. when in vivo inhibitor concentration $> K_i$). Reprinted with permission from *Drug Metabolism and Disposition* (Rock et al. 2008)

microsomes with 1 μM test compound), where selective chemical inhibitors or antibodies of the individual P450s would be coincubated to determine the effect on the in vitro intrinsic clearance ($Cl_{int}$). Table 2.1 includes recommended P450 inhibitors to use in reaction phenotyping studies, as well as recommended concentrations to optimize selectivity. Complete inhibition by chemical inhibitors while maintaining selectivity has proven to be challenging, which complicates interpretation of reaction phenotyping data. Rock et al. (2008) report that typically, maximal inhibition of CYP3A activity with a chemical inhibitor such as ketoconazole is only ~80%. They showed inhibition >99% could be achieved by including both CYP3A chemical inhibitor and antibody, leading to improved accuracy in estimating fraction metabolized. Along those same lines, the use of 1-aminobenzotriazole (1-ABT) as a nonselective P450 inhibitor in phenotyping studies to decipher P450 from non-P450 mediated metabolism has recently been called into question. Linder et al. (2009) demonstrated

that while 1-ABT does inhibit all P450 enzymes, it is only somewhat selective and is especially weak against CYP2C9.

In order to effectively use the substrate depletion approach, there should be sufficient depletion of substrate to measure a difference in $Cl_{int}$ in the presence of an inhibitor. Often, drug molecules are slowly metabolized in HLMs (half-life > 60 min), and thus, alternative methods must be employed, such as the use of recombinant P450 enzymes (rCYPs) with the appropriate scaling factors included for predicting $f_{m,CYP}$. For example, use of an intersystem extrapolation factor (ISEF), which accounts for differences in enzymatic activity between the recombinant system and human liver microsomes, as well as the liver abundance of the CYP in question, has been recommended (Proctor et al. 2004).

Monitoring for metabolite formation may also be a valuable approach, as this is often easier to observe than depletion of substrate. Figure 2.8 demonstrates how use of rCYPs and metabolite formation in a single experiment for slow-turnover compounds may be complementary, as formation of metabolites M1 and M2 were both inhibited by coincubation with 1 μM ketoconazole, and were also shown to be formed with rCYP3A4. If predictions of $f_{m,CYP}$ using data from chemical and/or antibody inhibitors and rCYPs leads to conflicting results, then a third approach such as correlation analysis is recommended. A more detailed description of reaction phenotyping methods has been provided by Wienkers and Stevens (2003).

## 2.6 Induction of Cytochrome P450 and DDIs

Induction of cytochrome P450 enzymes is also of concern for new molecular entities in drug development, as inducers of P450 enzymes are known to increase drug elimination and cause decreased exposure, resulting in the potential for altered pharmacodynamic profile, and eventual therapeutic failures. For example, acute transplant rejection with cyclosporine and failure of oral contraceptives when co-administered with
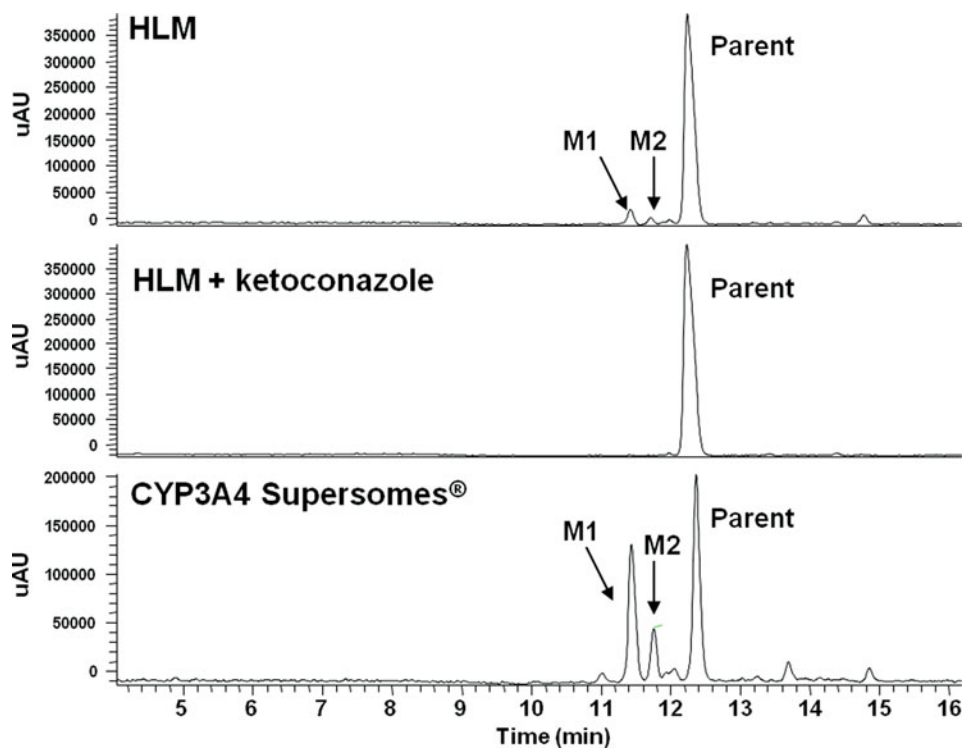
**Fig. 2.8** Chromatogram illustrating the value of metabolite formation approach when conducting in vitro reaction phenotyping studies with low-turnover drug molecules, which precludes the use of traditional approaches such as coincubation with specific chemical/antibody inhibitors (unpublished internal data). This figure demonstrates formation of *M1* and *M2* metabolites in both HLMs and recombinant CYP3A4 Supersomes®, and also inhibition of metabolite formation in HLMs by coincubation with ketoconazole, a known potent inhibitor of CYP3A4

rifampicin has been reported (Hebert et al. 1992; LeBel et al. 1998). In addition, the potential for toxicity due to increase in reactive metabolite formation exists when induction of an enzyme involved in a bioactivation metabolic pathway occurs (e.g. acetaminophen and hepatotoxicity). Notable inducers of cytochrome P450 include rifampin, phenobarbital, phenytoin, ritonavir, carbamezepine, and St. John's Wort, an herbal treatment for mild to moderate depression (Luo et al. 2004). During the past decade, substantial advances have been made in the technology for investigating induction of cytochrome P450 enzymes. Thus, a broader understanding of the mechanisms regulating expression of drug metabolizing enzymes (and transporters) is now in place. It is now widely accepted that induction of CYP3A4 expression is initiated by binding and transactivation of the nuclear receptor human pregnane X receptor (hPXR) (Lehmann et al. 1998; Bertilsson et al. 1998). In addition, CYP3A7, CYP2B6, CYP2C8, CYP2C9, UGT1A1, MDR1 (p-glycoprotein), BSEP, and MRP2 appear to be inducible by the transactivation of hPXR (Sinz et al. 2006; Olinga et al. 2008). Constitutive androstane receptor (CAR), glucocorticoid receptor (GR), and aryl hydrocarbon receptor (AhR) have all been shown to play a role in the induction of CYP enzymes (Lin 2006).

Due to the prevailing role of CYP3A4 in elimination of drug molecules, there is increased potential for clinically significant DDIs when expression of this DME is modulated. Thus, the drug industry has devoted much attention to implementation of in vitro assays to evaluate the potential for NCEs to induce CYP3A4, despite the fact that the number of drugs causing metabolic induction in patients appears to be

small (Smith 2000). The gold standard approach for investigating induction potential is the use of primary cultures of human hepatocytes (Lin 2006), while cryopreserved hepatocytes have also been shown to produce similar induction response (Roymans et al. 2005). However, the difficulty in acquiring quality hepatocytes on a routine basis is extremely challenging. To address this, binding and reporter gene assays, which are amenable to higher throughput, have been developed for use in early drug discovery (Jones et al. 2002; El-Sankary et al. 2001). Despite rapid throughput, the disadvantage of the PXR binding assay is that it cannot distinguish between agonists and antagonists, while reporter gene assays only test one mechanism of induction. Nonetheless, comparison of activation of human PXR in a reporter gene assay to induction observed in human hepatocytes resulted in a reasonable correlation (Luo et al. 2002). In a separate study, activation of PXR was shown to be indicative of induction signal in the clinic (Cui et al. 2008), suggesting reporter gene assays may be suitable in an early drug discovery screening paradigm. Lastly, Sinz et al. conducted an extensive study with 170 xenobiotics in a hPXR transactivation assay, and were able to take a hit rate of 54% and conclude only 5% the compounds tested were likely to induce CYP3A4 clinically after consideration of therapeutic $C_{max}$, distribution, route of administration, dosing regimen, liver exposure, and potential to inhibit CYP3A4 (Sinz et al. 2006), pointing to the risk of overinterpreting results from reporter gene assays.

With the known complexities of screening for induction using reporter gene assays, and the poor availability of primary human hepatocytes, the search for an intermediate, yet relevant in vitro model for P450 induction is ongoing. In 2004, the use of an immortalized human hepatocyte cell line (Fa2N-4) was introduced (Mills et al. 2004) with the advantage of easier culturing and higher throughput potential relative to primary human hepatoctyes. Ripp et al. (2006) went on to test 24 compounds (18 positive, and 6 negative for induction based on previous data from human

hepatocytes) in the Fa2N-4 cells and found all 18 positive controls caused a >2-fold maximal induction, while the six negative controls caused <1.5-fold induction, suggesting these immortalized cells could be used reliably to assess risk of induction. However, reports since have clearly shown limitations to the Fa2N-4 cells, namely low expression of CAR, a mechanism of both CYP3A4 and CYP2B6 induction, as well as hepatic uptake transporters (e.g. OATP1B1), concluding Fa2N-4 cells cannot replace primary human hepatocytes as an in vitro model system for induction (Hariparsad et al. 2008; Kenny et al. 2008). Most recently, HepaRG cells have been shown to respond to PXR, CAR, and AhR activators, resulting in induction of CYPs 1A1, 1A2, 2B6, 2C8, 2C9, 2C19, and 3A4 (Kanebratt and Andersson 2008). The apparent success of HepaRG cells in the prediction of induction potential was further supported by a recent study where many of the aforementioned methods for assessing induction were compared (McGinnity et al. 2009). Similar to CYP3A4 time-dependent inhibition, a recent PhRMA survey of current practices for assessment of induction was published (Chu et al. 2009). From this collection of information from 14 PhRMA member companies, some recommendations were made as to how to conduct in vitro and in vivo studies evaluating induction. Worth noting, recommendations for assessment of induction included use of fresh or plateable cryopreserved hepatocytes, treatment with NCE for 2–3 days, measurement of catalytic activity, and at least three donor hepatocytes. For more information and guidance on this subject, see Chu et al. (2009).

Obviously, advantages and disadvantages of each in vitro induction assay (see Table 2.2) need to be weighed against the needs of the particular company. As we continue to explore new chemical space in the drug industry, it would be prudent to assess the risk of enzyme induction in an in vitro system containing the full complement of nuclear receptors, DMEs and transporters prior to clinical development, in order to gain a comprehensive view of induction risk and enable

**Table 2.2** Advantages and disadvantages of current in vitro assays used to evaluate induction of drug metabolizing enzymes/transporters

| In vitro assay | Advantages | Disadvantages | Reported to be predictive of clinical response? | References |
|---|---|---|---|---|
| Binding assays | High throughput<br>Low cost | Does not differentiate between agonists and antagonists (e.g. potential for false positive) | No | Jones et al. (2002) |
| Reporter gene assay (hPXR, AhR, etc.) | Medium-to-high throughput; SAR | Unable to assess other induction mechanisms | Yes | El-Sankary et al. (2001), Luo et al. (2002), Cui et al. (2008) |
| Primary human hepatocytes | Gold standard for evaluation of induction; full complement of DMEs, nuclear receptors, and transporters | Routine access to high quality cells a challenge; low throughput; variability between donors; cost | Yes | Chu et al. (2009) |
| Cryopreserved human hepatocytes | Availability | Cost; variable response | No | Roymans et al. (2005) |
| Human liver slices | Full complement of DMEs, nuclear receptors, and transporters | Availability | No | Olinga et al. (2008) |
| HepG2 cells | Robust induction response to CYP1A inducers | mRNA levels of most CYPs lower than primary hepatocytes; unresponsive to some CYP3A4 inducers | No | Harmsen et al. (2008) |
| Immortalized hepatocytes (Fa2N-4) | Ease of culture and handling; good response to CYP3A4 and 1A2 inducers; apparently able to relate data to clinic | Utility limited by very low expression of CAR and several other drug transporters | Yes | Ripp et al. (2006), Hariparsad et al. (2008), Kenny et al. (2008) |
| HepaRG cells | Functionally resemble primary cultured human hepatocytes | Expression of enzymes and nuclear receptors, and response to enzyme inducers varies depending on media and culture conditions; cost | Yes | Aninat et al. (2006), Kanebratt and Andersson (2008), McGinnity et al. (2009) |

identification of novel origins of clinically relevant induction DDIs.

## 2.7 Predicting and Simulating Clinical DDIs

### 2.7.1 Perpetrator DDI (Competitive and Time-Dependent Inhibition)

The early, reliable prediction of DDIs using in vitro and in silico methodologies are important in drug discovery and development for candidate design and prediction of the human in vivo situation. Understanding the mechanisms of potential DDIs is critical to the successful advancement of drug candidates, as patient safety and labeling restrictions from a commercial standpoint are of the utmost importance in the pharmaceutical industry. The science of using in vitro inhibition data (e.g. $K_i$ or $IC_{50}$) to predict clinical DDI risk has advanced considerably in recent years, and thus has become more widely accepted, particularly by regulatory agencies such as the FDA, who have issued a regulatory guidance on in vitro drug interaction studies (www.fda.

gov/cder/guidance/6695dft.htm). The underlying mechanisms of DDIs are typically either competitive inhibition of drug clearance, time-dependent inhibition (TDI) or inactivation of drug clearance, and induction, which may result in increased drug clearance and loss of efficacy. Since the cytochrome P450 family of drug-metabolizing enzymes remain the most important enzymes that are involved in the clearance of drug molecules, they will be the focus of this discussion, although the concepts may be applicable to any enzyme involved in drug clearance.

The initial step in conducting a DDI prediction is the generation of the in vitro inhibition parameter $K_i$ or $IC_{50}$. Typically, $IC_{50}$ data is generated early in the discovery continuum due to the ease of conducting this assay, relative to generating a $K_i$ in vitro. An approach often utilized is conversion of the $IC_{50}$ to an estimated $K_i$ using the Cheng-Prusoff equation (Equation 1 in Table 2.3), assuming a competitive inhibition mechanism (Cheng and Prusoff 1973). This in vitro derived inhibition constant is then used along with the projected in vivo inhibitor concentration ($[I]_{in\ vivo}$) in basic equations such as Equation 2. The general relationship of $[I]_{in\ vivo}$ to $K_i$ is shown in Fig. 2.9, and while useful for initial assessment of clinical DDI risk, more sophisticated methodologies with additional input parameters may be used such as the Rowland-Matin equation (Equation 3). Equation 3 incorporates the fraction of the probe substrate (e.g. victim drug) metabolized by CYP ($f_{m(cyp)}$), a key factor to the magnitude of any clinical drug–drug interaction.

A topic of much discussion and debate is what concentration to use for $[I]_{in\ vivo}$, or the in vivo inhibitor concentration (e.g. total systemic $C_{max}$, free systemic $C_{max}$, $C_{average}$, hepatic portal inlet, etc.). While it is impossible to measure the actual concentration that the enzyme is exposed to within the liver, the best estimates that exist are either the systemic drug level, which is directly measurable, or the hepatic portal inlet, which makes sense conceptually given that for an oral drug absorbed via the portal vein, the liver will be exposed to higher drug concentrations than

the systemic circulation. Additional uncertainty is brought into the discussion as the question of the role of protein binding is on-going (e.g. the "free-drug" hypothesis). The most extensive work to understand and compare the differences associated with using systemic vs. estimated hepatic portal inlet concentrations (and free vs. total) has been reported by Obach et al. (2006). The conclusion from this work was that for competitive (e.g. reversible) inhibitors, the use of estimated free-portal-vein $C_{max}$ for $[I]_{in\ vivo}$ yielded the best predictions of clinical DDI. Equation 4, originally proposed by Kanamitsu et al. (2000), may be used to estimate the free-portal-vein $C_{max}$ for a given dose. Interestingly, work by the same group (Obach et al. 2007; Obach 2009) evaluating mechanism-based inactivation (e.g. time-dependent inhibition) found that the use of free systemic $C_{max}$ for $[I]_{in\ vivo}$ yielded the most accurate overall DDI predictions. The reasons why different surrogate values for $[I]_{in\ vivo}$ appear to work best for competitive and time-dependent inhibition are not clear. Regarding mechanism-based inactivators, it is important to characterize this phenomenon so as to not underpredict the magnitude of the clinical interaction. Accurate estimates of inactivation kinetic parameters $k_{inact}$ and $K_I$ (discussed earlier in this chapter) are key to predicting the clinical DDI. Equation 5, a variation of the Rowland-Matin equation (Equation 4), is reported to yield accurate predictions of clinical DDI (Mayhew et al. 2000; Obach et al. 2007; Foti and Wahlstrom 2008). Yet another important parameter of uncertainty is the $k_{deg}$, the normal first-order degradation rate of the affected enzyme. This uncertainty is due to the fact that no accurate method for determining $k_{deg}$ in humans exists. The impact of using different $k_{deg}$ values has been reviewed by Yang et al. (2008).

An additional component to accurate DDI predictions is the contribution of the gut to the overall first-pass clearance of drug, particularly for CYP3A4 substrates. For some substrates, the contribution of the gut to first-pass clearance is significant (Galetin et al. 2006, 2007, 2008), despite the fact that there is ~100-fold less

**Table 2.3** Summary of equations that may be used for prediction of clinical drug–drug interaction risk using in vitro data

| Name | Equation | Descriptors | References |
|---|---|---|---|
| Equation 1 (Cheng-Prusoff) | $K_i = \dfrac{IC_{50}}{1 + \frac{[S]}{K_m}}$ | $K_i$ = Inhibition constant | Cheng and Prusoff (1973) |
| | | $IC_{50}$ = Concentration at which 50% inhibition is observed in vitro | |
| | | $K_m$ = Michaelis–Menten constant and the concentration of probe substrate $[S]$ used in in vitro $IC_{50}$ experiment (e.g. $[S] = K_m$) | |
| Equation 2 | $1 + \dfrac{[I]_{\text{in vivo}}}{K_i}$ | $K_i$ = Inhibition constant | Wienkers and Heath (2005) |
| | | $[I]_{\text{in vivo}}$ = Concentration of inhibitor in vivo | |
| Equation 3 (Rowland-Matin) | $\dfrac{AUC_i}{AUC} = \dfrac{1}{\frac{f_{m(cyp)}}{1 + \frac{[I]_{\text{in vivo}}}{K_i}} + (1 - f_{m(cyp)})}$ | $AUC_i$ = Exposure of victim drug when co-administered with inhibitor | Rowland and Martin (1973) |
| | | $AUC$ = Exposure of victim drug when given without inhibitor | |
| | | $f_{m(cyp)}$ = Fraction of substrate metabolized by CYP | |
| | | $[I]_{\text{in vivo}}$ = Concentration of inhibitor in vivo | |
| | | $K_i$ = Inhibition constant | |
| Equation 4 | $[I]_{u,portal} = f_u \cdot \left( C_{max} + \dfrac{K_a \cdot F_a \cdot Dose}{Q_h} \right)$ | $f_u$ = Fraction unbound | Kanamitsu et al. (2000), Obach et al. (2006) |
| | | $C_{max}$ = Maximal systemic concentration | |
| | | $K_a$ = Absorption rate constant | |
| | | $F_a$ = Fraction of dose absorbed | |
| | | $Q_h$ = Hepatic blood flow (21 ml/min/kg) | |
| Equation 5 | $\dfrac{AUC_i}{AUC} = \dfrac{1}{\frac{f_{m(cyp)}}{1 + \frac{k_{inact} \cdot [I]_{\text{in vivo}}}{K_I \cdot k_{deg}}} + (1 - f_{m(cyp)})}$ | $AUC_i$ = Exposure of victim drug when co-administered with inhibitor | Obach et al. (2007) |
| | | $AUC$ = Exposure of victim drug when given without inhibitor | |
| | | $f_{m(cyp)}$ = Fraction of substrate metabolized by CYP | |
| | | $[I]_{\text{in vivo}}$ = Concentration of inhibitor in vivo | |
| | | $k_{inact}$ = Maximal rate of inactivation determined from in vitro study (units are $\text{min}^{-1}$) | |
| | | $K_I$ = Concentration of inactivator that yield one-half the maximal rate of inactivation (μM) | |
| | | $k_{deg}$ = Normal rate of enzyme degradation (for CYP3A4, a value of 0.00032 $\text{min}^{-1}$ is typically used) | |
| Equation 6 | $\dfrac{F'_g}{F_g} = \dfrac{1}{F_g + (1 - F_g) \cdot \left( \frac{1}{1 + \left( \frac{k_{inact} \cdot [I]_{gut}}{k_{deg} \cdot (K_I + [I]_{gut})} \right)} \right)}$ | $F'_g$ = The fraction of the drug that remains intact following oral dose | Wang et al. (2004), Obach et al. (2007) |
| | | $k_{inact}$ = Maximal rate of inactivation determined from in vitro study (units are $\text{min}^{-1}$) | |
| | | $K_I$ = Concentration of inactivator that yield one-half the maximal rate of inactivation (μM) | |

(*continued*)

**Table 2.3** (continued)

| Name | Equation | Descriptors | References |
|------|----------|-------------|------------|
| | | $k_{deg}$ = Normal rate of enzyme degradation (for CYP3A4, a value of 0.00048 min$^{-1}$ is typically used) | |
| | | $[I]_{gut}$ = Concentration of drug in the intestine | |
| Equation 7 | $[I]_{gut} = \dfrac{k_a \cdot F_a \cdot \text{Dose}}{Q_g}$ | $k_a$ = Absorption rate constant | Obach (2009) |
| | | $F_a$ = Fraction of dose absorbed | |
| | | $Q_g$ = Villous blood flow (3.5 ml/min/kg) | |
| Equation 8 | $\text{RIS} = \dfrac{C_u \cdot E_{max}}{C_u + EC_{50}}$ | $C_u$ = Unbound efficacious concentration | Ripp et al. (2006), Fahmi et al. (2008) |
| | | $E_{max}$ = Maximal observed induction in vitro | |
| | | $EC_{50}$ = concentration of drug that yield 50% induction in vitro | |
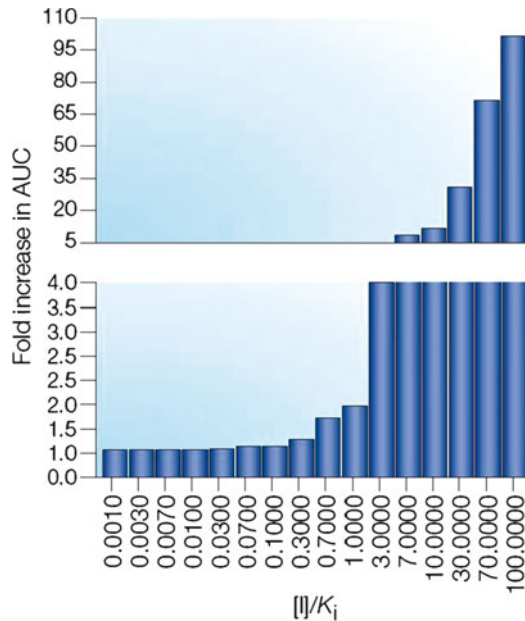


**Fig. 2.9** The relationship between the in vivo inhibitor concentration ($[I]_{in\ vivo}$) to the in vitro inhibition constant ($K_i$) as it relates to fold-increase in AUC of a victim drug. As the $[I]/K_i$ ratio increases, the fold-increase in AUC increases. Reprinted with permission from *Nature Reviews* (Wienkers and Heath 2005)

CYP3A4 in the gut relative to the liver (Shen et al. 1997). For consideration of the gut in DDI, Equation 6 was proposed by Wang et al. (2004). Within this equation, the component $[I]_{gut}$ is equally important, and may be estimated using Equation 7.

## 2.7.2 DDI Predictions for Induction

Prediction of DDIs due to induction of cytochrome P450 enzymes is equally important, yet has proven difficult, primarily due to multitude of in vitro models of induction, and extrapolation
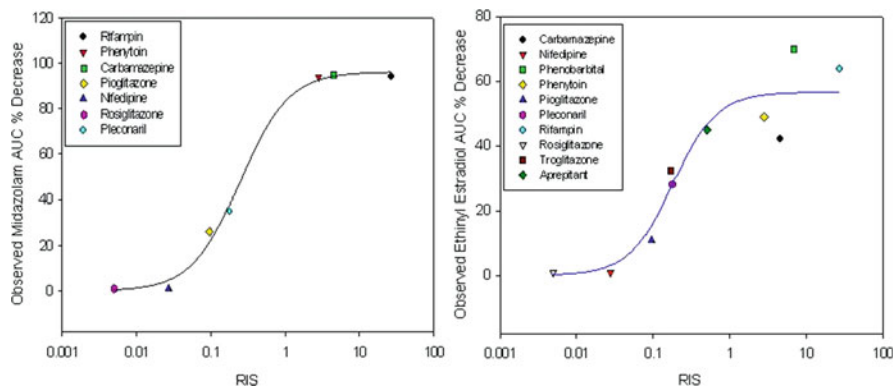
**Fig. 2.10** Relationship between the calculated Relative Induction Score (RIS) and clinical observations with co-administered midazolam and ethinyl estradiol with numerous known CYP3A inducers using human cryopre-served hepatocytes. Observed correlations were $r^2 = 0.96$ and 0.82, respectively. Reprinted with permission from Drug *Metabolism and Disposition* (Fahmi et al. 2008)

of in vitro induction data to the clinic. Lately, however, several reports have been published which have shown progress in predicting DDI resulting from induction. A novel technique for predicting the magnitude of clinical interaction due to induction of CYP3A was developed using the Fa2N-4 immortalized human hepatocyte line (Ripp et al. 2006). This approach is based on combining in vitro induction parameters ($EC_{50}$ and $E_{max}$) with the efficacious free plasma concentrations to calculate a relative induction score (RIS) (Equation 8), which was then correlated to the magnitude of clinical DDI for midazolam or ethinyl estradiol, with $r^2$ values of 0.92 and 0.93, respectively (Ripp et al. 2006). This RIS method has since been assessed using human cryopre-served hepatocytes with comparable success, as shown in Fig. 2.10 (Fahmi et al. 2008).

## 2.7.3 SimCYP

SimCYP© (SimCYP© Limited, Sheffield, UK) is a computer simulation program developed for the prediction of metabolic DDIs that applies fundamental scaling concepts (Houston 1994) for the prediction of in vivo clearance from in vitro metabolism data (Rostami-Hodjegan and Tucker 2007; Jamei et al. 2009). The SimCYP model requires a number of inputs including molecular weight and physicochemical properties of the molecule (LogP, $pK_a$ and acid/base/neutral character together with measured $f_{u(plasma)}$ and blood:plasma ratio), as well as predicted clearance pathways and pharmacokinetic properties in humans, if available. SimCYP uses a physiologically based pharmacokinetic model that enables modeling of the dynamic nature of in vivo inhibitor and substrate concentrations, as well as the interindividual variability among the population.

The effects of perpetrator DDIs are predicted using the relationship between the inhibitor concentration in vivo and the $K_i$ determined in vitro. From the $IC_{50}$ values generated in the relevant in vitro system, $K_i$ values are determined assuming competitive inhibition (e.g. Cheng-Prusoff Equation), unless a $K_i$ value has been estimated experimentally. The values determined for the appropriate CYPs are used together with an estimate of its in vivo clearance and absorption characteristics. SimCYP© incorporates the population variability in each parameter (e.g. CYP abundance) by applying a Monte Carlo approach. Using appropriate clinical probes (Table 2.4), the potential for NCE compounds to be involved in a DDI are then predicted. Physiological variability is calculated automatically using databases within SimCYP©, while pharmacokinetic variability can be incorporated by the user in the form of a coefficient of variation. Clinical trials of

**Table 2.4** Recommended clinically used probes and inhibitors for perpetrator and victim SimCYP® simulation studies

| CYP | Perpetrator studies (clinical probe studied) | Victim studies (clinical inhibitor studied) |
|---|---|---|
| 1A2 | Theophylline | Fluvoxamine |
| 2C9 | S-warfarin | Fluconazole |
| 2C19 | Omeprazole | Omeprazole |
| 2D6 | Desipramine | Paroxetine |
| | Dextromethorphan | |
| 3A4 | Midazolam | Ketoconazole (potent) |
| | | Erythromycin (moderate) |

various sizes can be simulated to determine the effects of trial size on variability.

For victim drugs (substrates), $CL_{int}$ values for the individual CYP enzymes are used as inputs for DDI prediction using numbers from HLM incubations or from recombinant human CYPs with appropriate Intersystem Extrapolation Factors (ISEF) correction (Proctor et al. 2004). These data can also be entered using $V_{max}$ and $K_m$ information for the individual CYPs if these are available, allowing saturation of metabolic clearance to be simulated. Since data for clearance and inhibition (inhibition constants for reversible ($K_i$) or time dependent ($K_I$, $k_{inact}$) inhibitors or induction ($Ind_{50}$, $Ind_{max}$, Ind slope) are also incorporated in the model, cumulative effects may be modeled simultaneously for complex drugs like ritonavir. Activities for enzymes catalyzing non-CYP mediated metabolism are also inputs in the SimCYP© model so that $f_{m(CYP)}$ (the fraction of metabolism mediated by a particular CYP), is calculated appropriately. In addition, undefined HLM $CL_{int}$ (e.g. for FMO mediated metabolism) and other enzymes can be used and incorporated as a component of the overall clearance using appropriate scaling factors. In this way, all known pathways of metabolic clearance can be incorporated in a SimCYP© model.

## 2.8 Transporters and DDIs

While alteration of drug metabolizing enzymes is most often the cause of DDIs, there is increasing evidence this may not entirely explain the pharmacokinetic variability observed with some drug

molecules (Zhang et al. 2008). For example, the mechanism of the digoxin–quinidine interaction (Hager et al. 1979) was not truly understood until relatively recently (Fromm et al. 1999). Thus, as the science behind drug transporters continues to evolve, their role in absorption, distribution, and elimination of drugs is becoming one of the topics of highest interest in the ADME discipline. Figure 2.11 demonstrates the numerous uptake and efflux transporters expressed in the hepatocyte, which can complicate the distribution of drug molecules. The FDA has issued a guidance (September 2006) that includes a decision tree to determine if clinical in vivo interaction studies are warranted based on in vitro data. P-glycoprotein (P-gp) is able to transport a diverse range of compound structures, similar to CYP3A4, and is thus the most studied and understood efflux transporter. The expression of P-gp in the body is high in tissues such as the gut, blood–brain barrier and in organs of drug clearance such as the liver and kidney, making it of significance in the distribution and elimination of drugs.

Interestingly, a recent publication has suggested DDIs solely related to P-gp are generally not clinically relevant, as changes in pharmacokinetics were modest, with only moderate changes in drug exposure (Fenner et al. 2009). For example, valspodar (PSC 833) is one of the most potent inhibitors of P-gp known ($IC_{50} = 0.02$ µM) (Kawahara et al. 2000), yet in a clinical DDI study, only a 76–211% increase in digoxin AUC was observed (Kovarik et al. 1999), typically considered insignificant. However, if digoxin or any P-gp substrate with a narrow therapeutic index (TI) is the potential victim drug, then a even a 25% change in drug exposure
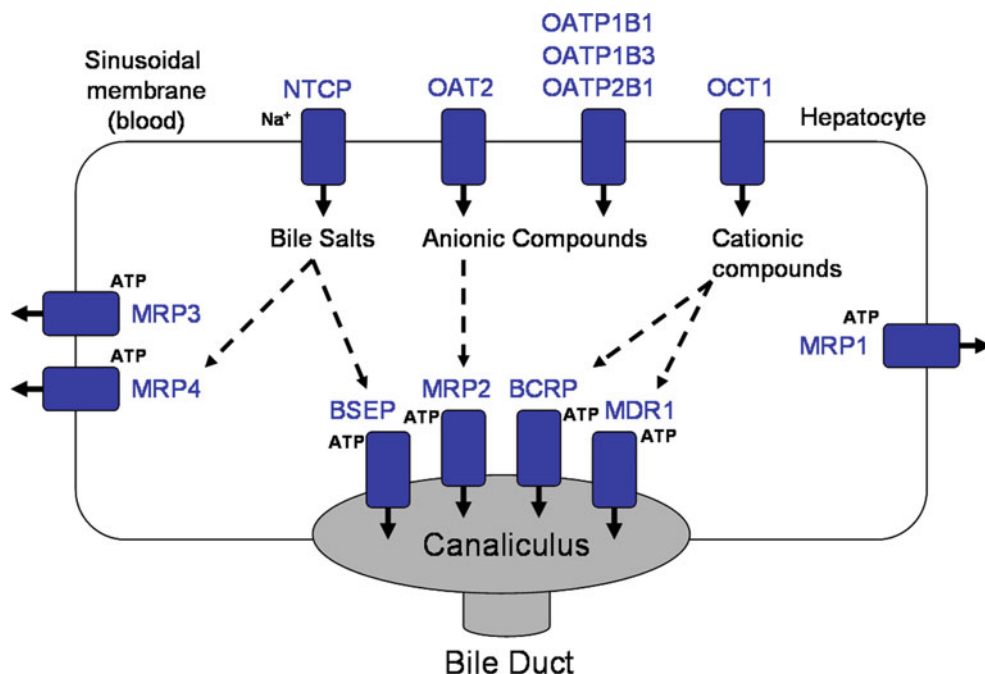
**Fig. 2.11** Schematic showing the numerous uptake and efflux transporters that contribute to the distribution of drug molecules within the hepatocyte. Currently, P-gp (MDR1) is the most studied and understood efflux transporter with respect to DDIs. However, the science of transporters is rapidly evolving, evidenced by the recent reports of DDI with statin drugs, reportedly due to inhibition of uptake transporter OATP1B1

due to inhibition of P-gp may lead to unwanted toxicities (e.g. digitalis for digoxin). As digoxin is a commonly prescribed heart medication, in vitro assessment of the potential for a drug interaction specifically with digoxin is warranted for compounds progressing toward first-in-patient (FIP) or proof-of-concept (POC) in clinical development.

In vitro evaluation of whether an NCE is a substrate or inhibitor of P-gp is relatively straightforward, yet there are numerous assay formats that may be utilized. It is recommended in the FDA guidance document to use bidirectional transport studies with either Caco-2 cells or recombinant epithelial cell lines (MDCK_MDR1 or LLC-PK1_MDR1). In general, if the efflux ratio (B → A)/(A → B) is ≥2 and addition of a specific P-gp inhibitor decreases this efflux ratio then the NCE is categorized as a potential P-gp substrate. Use of a specific P-gp inhibitor is especially critical when Caco-2 cells are used, since it is known other efflux transporters (e.g. BCRP

and MRP2) are expressed in this human cell line (Taipalensuu et al. 2001). Follow-up studies may then need to be performed to evaluate the actual risk for a drug–drug interaction. A simple decision tree adopted from Zhang et al. (2008) is shown in Fig. 2.12. For early evaluation of an NCE as a potential inhibitor of P-gp, the calcein-AM assay, where inhibition of the P-gp-mediated efflux of the fluorescent substrate (calcein) is determined, has been useful in the discovery setting (Tiberghien and Loor 1996; Feng et al. 2008). This assay should be used on an "as needed" basis since, as previously mentioned, most P-gp-mediated DDIs are not significant. The gold-standard assay for assessing P-gp inhibition includes the use of MDCK_MDR1 cells and $^3$H-digoxin, and should be a conducted where that results would be available prior to the first study where digoxin may be as a possible concomitant medication. To aid in use of in vitro derived inhibition data with transporters, a decision tree for evaluation of NCEs as potential
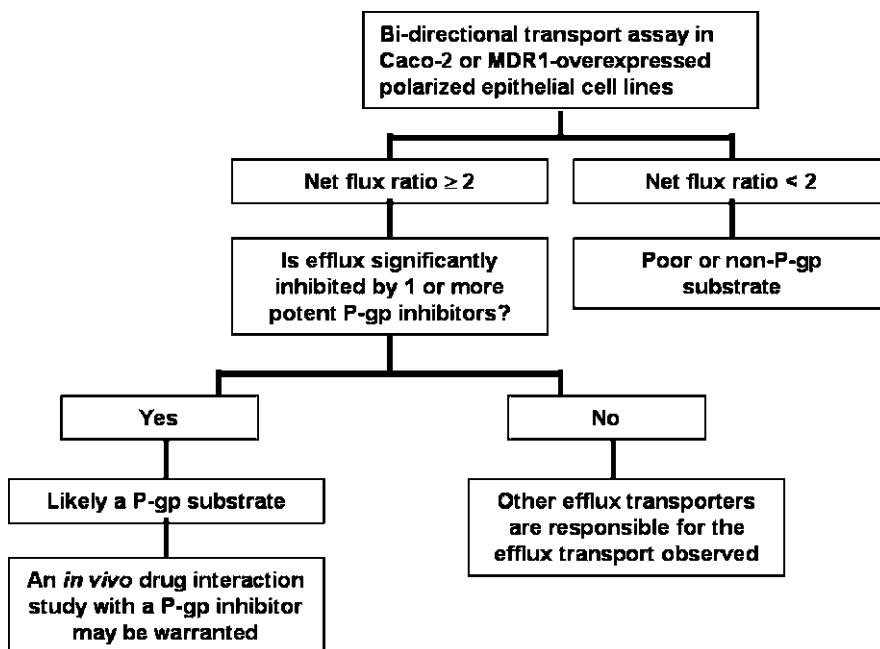
**Fig. 2.12** Decision tree for use as a guide in determining if an NCE is a substrate for P-glycoprotein (P-gp). Net flux ratio is calculated as $F_{B-A}/F_{A-B}$. A net flux ratio of $\geq 2$ is considered to be a positive signal for P-gp substrate interaction. Use of a P-gp inhibitor is also recommended in diagnosing P-gp substrate, and reduction of net flux >50% or to unity is further evidence for P-gp interactions. Additional data may be needed to decipher the clinical relevance of in vitro data, including the potential contribution from other efflux transporters (e.g. BCRP and MRP2)

inhibitors of P-gp has also been proposed by the FDA in a recent report (Zhang et al. 2008), and is shown in Fig. 2.13.

While P-gp clearly remains the most studied transporter, several reports of transporter-mediated DDI with transporters other than P-gp have been published (Simonson et al. 2004; Treiber et al. 2007; Seithel et al. 2007). Regarding uptake transporters, OATP1B1 is of most interest at this time due to the observed DDIs with HMG-CoA-reductase inhibitors (e.g. statin drugs). For an extensive review of OATP and OCT-mediated DDIs, the reader is referred to a recent review on this subject (Kindla et al. 2009). Despite these clinical observations, at this point there has been no consensus established for in vitro methods, probe substrates or tool inhibitors to use for transporters such as OATP1B1, BCRP, OATs and OCTs, although an international working group consisting of members from academia, industry,

and the FDA has been formed to establish some guidelines in this area. It is likely that the knowledge and understanding of transporter-mediated DDI will progress significantly in the next few years.

Lastly, it is worth mentioning, even though not considered DDIs, inhibition of efflux transporters multidrug resistance protein 2 (MRP2) and bile salt export pump (BSEP) have been shown to lead to certain toxicities. Specifically, inhibition of MRP2 can lead to hyperbilirubinemia, while evidence exists that inhibition of BSEP leads to increases in bile salts, and subsequent cholestasis and hepatotoxicity, as observed with nefazodone (Kostrubsky et al. 2006), and more recently with CP-724,714 (Feng et al. 2009). As a result, drug discovery DMPK and toxicology programs have begun to test compounds for their potential to inhibit these hepatobiliary transporters.
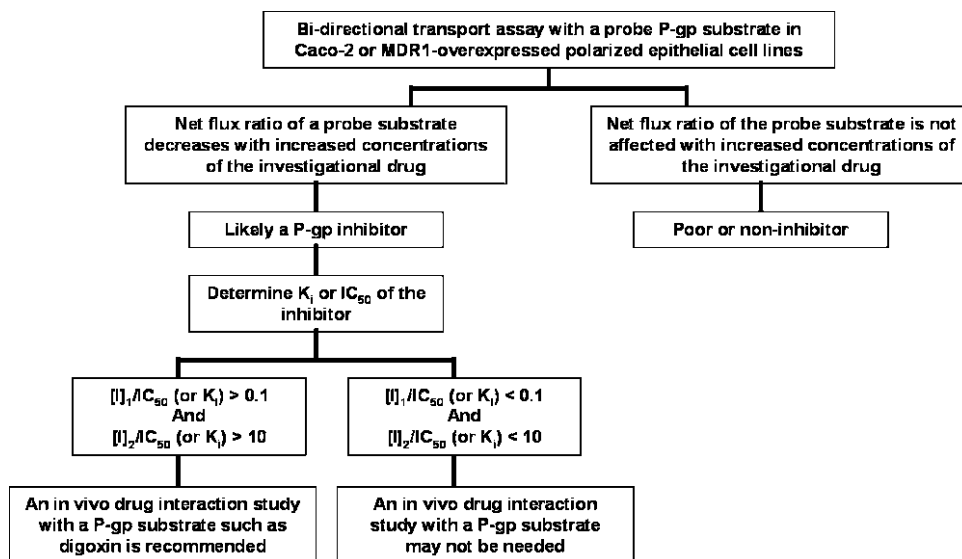
**Fig. 2.13** Decision tree for use as a guide in determining if an NCE is an inhibitor of P-glycoprotein (P-gp), and whether a clinical DDI study with digoxin needs to be conducted. Net flux ratio is calculated as $F_{B-A}/F_{A-B}$. $[I]_1$ represents mean steady-state $C_{max}$ values for total drug following administration at the highest proposed clinical dose; $[I]_2$ = dose of inhibitor (mol)/250 ml

## 2.9  The Future of DDI Investigations

### 2.9.1  Polymorphic Metabolism and DDI

Several of the human cytochrome P450 enzymes (e.g. CYP2B6, 2C9, 2C19, 2D6, and 3A5) are known to be polymorphically expressed to different degrees in the human population. The primary impact of these polymorphisms includes reduced oral clearance for certain medications, and subsequent increase in exposure, resulting in potential for pharmacokinetic variability and increased incidence of adverse events. A relevant question clinically is whether individuals with polymorphic expression are more or less susceptible to a clinical DDI when an inhibitor is co-administered. Understanding this relationship is clearly important as dose adjustments in individuals with particular genotypes (e.g. poor metabolizer or PM) may be different from a normal "extensive" metabolizer (EM). It has been reported that individuals possessing polymorphisms resulting in expression of inactive protein (e.g. CYP2C19 and 2D6) are less susceptible to DDI (Hamelin et al. 2000; Lessard et al. 2001; Uno et al. 2006). In vitro experiments evaluating this effect are not possible due to the lack of enzymatic activity. However, for polymorphically expressed P450 enzymes or allelic variants (e.g. CYP2C9*2 and *3) that still possess some activity, the same question of susceptibility to DDI is applicable. Kumar et al. (2006) reported that inhibition of CYP2C9 was genotype-dependent, which triggered a clinical study using flurbiprofen to show that individuals homozygous for the *3 allele of CYP2C9 did not have a significant decrease in oral clearance when co-administered with fluconazole (Kumar et al. 2008). This finding is reasonable, as the baseline pharmacokinetics in the *3/*3 individuals were different, suggesting that fraction metabolized by CYP2C9, which contributes to the magnitude of the interaction, is clearly different in PM compared to EM individuals. This finding warrants further investigation, and argues in vitro assays

evaluating inhibition of CYP2C9 allelic variant enzymes should be considered for clinical candidates with a risk of CYP2C9-mediated DDI.

## 2.9.2    The Role of CYP3A5

While CYP3A4 has been estimated to play a significant role in the metabolism of >50% of all drugs on the market (Guengerich 2002), the contribution of CYP3A5 to the overall metabolism of NCE's has received increased attention due to its polymorphic expression (3A5*3, *6, *7). Interestingly, only ~15% of Caucasians express high levels of CYP3A5, compared to 75% of African-Americans (Xie et al. 2004). Despite 84% amino acid sequence similarity between CYP3A4 and 3A5, several drugs, including midazolam and lidocaine have been reported to be more efficiently metabolized by CYP3A5 compared to 3A4 (Wrighton and Stevens 1992), which suggests CYP3A5 may play a significant role in the overall clearance of some drugs. However, this assessment is complicated by conflicting reports comparing CYP3A4 to 3A5 activity. Some of the differences can be attributed to the different expression systems used, where some enzyme preps were coexpressed with coenzymes (e.g. P450 oxidoreductase and cytochrome b5), and others only supplemented with these coenzymes (Huang et al. 2004). Nonetheless, several examples of pharmacokinetic variability in the clinic for CYP3A5 substrates have been reported. Most notably, reduced oral clearance of tacrolimus was reported in subjects homozygous for the CYP3A5*3 genotype compared to those with 3A5*1 genotype (Hesselink et al. 2003, 2008). Other drugs reported to have substantial clinical pharmacokinetic variability thought to be attributed to CYP3A5 genotype, include cyclosporine (Anglicheau et al. 2007), vincristine, where exposure varied up to 19-fold (Van den Berg et al. 1982), and the PDE5 inhibitor vardenafil, with 14-fold variability observed across subjects given a 20 mg dose (Klotz et al. 2001; Rajagopalan et al. 2003; Ku et al. 2008). Not only has the potential impact of CYP3A5 ex-

pression on pharmacokinetic variability been of concern, it has also been observed that CYP3A5 may in fact produce a distinct metabolite profile compared to 3A4, as observed with quetiapine (Bakken et al. 2009). This may have ramifications not only for pharmacological, but also the toxicological profile of impacted drugs.

Currently, estimating the contribution of CYP3A5 in overall metabolism is challenging, as there are no completely specific inhibitors or substrates used as in vitro tools to differentiate 3A5 from 3A4 activity. A reasonable approach has been a direct comparison of CYP3A4 and 3A5 in vitro intrinsic activity using recombinantly expressed enzymes with the same ratio of reductase and cytochrome b5 (e.g. Supersomes®). However, scaling of this in vitro intrinsic clearance is challenging, as abundances of CYP3A5 in liver are variable. There are now genotyped human liver microsomes available where both CYP3A4 and 3A5 expression levels are known (www.bdbiosciences.com), which may be useful in comparing intrinsic metabolic capacity in vitro in CYP3A5 expressers vs. non-expressers. This approach was taken by Huang et al. with numerous substrates of CYP3A4 and 3A5 (Huang et al. 2004). Another approach with potential for estimating of the contribution of CYP3A5 to overall metabolism of NCEs may be use of raloxifene, which has been reported to be a selective mechanism-based inhibitor (MBI) of CYP3A4 (Pearson et al. 2007), even though it is a competitive inhibitor of both CYP3A4 and 3A5.

## 2.9.3    Non-P450 Enzymes and DDI

While the cytochrome P450 family of drug-metabolizing enzymes are the clear origin of most clinically relevant DDIs, other enzymes such as UDP-glucuronosyltransferases (UGT), sulfotransferases (ST), monoamine oxidases (MAO-A and MAO-B), aldehyde oxidase (AO), and flavin monooxygenase (FMO) are of interest from a DDI perspective due to their potential role in metabolic clearance. Of these non-P450 enzymes, the UGTs have received the most attention of late, due in part to a report in 2004

by Williams et al. who demonstrated that glucuronidation is a clearance mechanism for 1 in 10 of the top 200 prescribed drugs in 2002 (Williams et al. 2004). While a primary conclusion from this report was that inhibition of UGT enzymes rarely lead to any clinically significant DDI (AUC Ratio >2), recent advances in the understanding of UGT enzymes and in vitro characterization of activity have triggered a re-evaluation of this subject. For example, it has generally been thought UGT enzymes are low-affinity (e.g. high $K_m$) enzymes. However, recently it has been shown that addition of albumin to HLM and recombinant UGT incubations significantly reduces the $K_m$ for AZT glucuronidation by UGT2B7 (Rowland et al. 2007), a result of albumin sequestering inhibitory fatty acids liberated during microsomal incubations. This realization may lead to more attention being paid to UGT-mediated metabolism, particularly to UGT1A1 since this represents the predominant clearance pathway for bilirubin, and polymorphic expression leads to hyperbilirubinemia, a condition known as Gilbert's Syndrome (Burchell et al. 2000). The other non-P450 drug metabolizing enzymes are currently less understood as it relates to DDIs, probably because they rarely contribute 100% to the clearance of drug molecules. This may change in the future as NCEs continue to be profiled, especially as chemistry and drug metabolism scientists work to reduce P450-mediated metabolism in optimization efforts.

## 2.10  Design and Execution of a Clinical Assessment of DDI Potential in a Drug Development Program

The major determinant of drug interaction studies is no longer the list of approved drugs most likely to be co-administered, rather than determination is based on likely mechanisms for a drug interaction. Thus, the first step in determining which drug interactions studies should be performed in a clinical program is to utilize in vitro and preclinical data to judge the likely risk of interactions. Typical interactions to be considered are those where one drug might alter the pharmacokinetics of another, such as inhibiting clearance. Additional consideration must also be given to pharmacodynamic interactions, which can alter the drug's pharmacology, as has been observed with the sedative effects of compounds with inhibitory central nervous system activity.

For pharmacokinetic interactions, equal consideration should be given to circumstances where a drug is an object, or victim, of the interaction and where the drug is the perpetrator (precipitant, inhibitor, or inducer). When the drug is the victim, the projected metabolic pathways are potential sites of interactions and the more predominate a pathway, the higher the risk of a clinically relevant interaction. Thus for drugs predominately cleared by a single pathway, there will almost always be interactions of clinical relevance. Conversely, if a molecule is cleared by multiple mechanisms, then the risk of a clinically relevant interaction is lower. Additionally clinically relevant interactions due to transporters have been observed. For instance inhibitors of liver uptake transporters resulted in 2 to 25-fold increases in systemic statin concentrations (Neuvonen et al. 2006).

Other distribution phenomena are generally less important. For example, alterations in plasma protein binding typically do not necessitate a dose adjustment, as they do not affect the clearance of free drug, the presumed active form. Thus, while plasma total drug concentrations may be altered, free drug concentrations will return to the same steady-state levels as observed prior to administration of the perpetrator. The exceptions to the above generalization are except in two instances. The first is when a drug has the attributes of a high extraction ratio, a narrow therapeutic index, and is parentally given (e.g. lidocaine). The second case is for a drug that has a narrow therapeutic index, is orally administered and has a very rapid pharmacokinetic–pharmacodynamic equilibration time. In these rare cases, DDIs causing protein binding changes can have clinical consequences (Benet and Hoener 2002).

Studies typically involve sensitive probe substrates or potent specific inhibitors to elicit the

maximum magnitude of an interaction. Thus if no interaction is observed, one can be reasonably assured there will not be a relevant interaction with the investigational drug and other drugs acting through the same pathway. Further, if there is an interaction, other interactions with the investigation drug involving the same pathway will be of a similar or lesser magnitude. Thus, if an enzyme or transporter is identified as potentially important, a single probe substrate and/or inhibitor study is conducted and the results extrapolated. Less potent inhibitors may be considered for study, however, where an interaction has been shown and the results require contraindication or dose adjustment. In these cases, the resulting smaller magnitude of the interaction could result in different dosing recommendations based on inhibitor potency. A list of probe substrates and inhibitors can be found in the FDA draft drug interaction guidance (Drug Interaction Studies – Study Design, Data Analysis, and Implications for Dosing and Labeling. September 11, 2006, http://www.fda.gov/downloads/Drugs/Guidance ComplianceRegulatoryInformation/Guidances/ucm072101.pdf).

### 2.10.1 Metabolism Based Drug Interactions

The FDA has published guidance on drug interaction strategies for cytochrome P450 (CYP) based interaction studies (previously cited). The guidance suggests interactions with CYP1A2, 2C8, 2C9, 2C19, 2D6, and 3A be considered. Clinical studies should be performed when the drug is a substrate of an isozyme and when the isozyme is a major elimination pathway or it is unclear as to if it is a major elimination pathway. The guidance does not provide explicitly state to what constitutes a major pathway. However, the guidance does show that human in vivo data indicate CYP enzymes contribute more than 25% of a drug's overall clearance, investigations to identify responsible CYP isozymes should be conducted. A theoretical maximal change in systemic drug concentrations can be estimated as:

$$\% \text{ Increase in systemic exposure} = \frac{100\%}{(1 - \text{faction of overall clearance due to pathway})} - 100\%$$

Thus if a particular isozyme is responsible for 25% of a drugs clearance, maximal inhibition of the pathway would cause a 33% increase in systemic drug concentrations.

The same CYP isozymes are to be evaluated when considering a drug's potential to be an inhibitor or inducer. Only those instances where preclinical data suggest a drug is an inhibitor or inducer of that isozyme need to be considered for clinical study. To evaluate the potential for reversible inhibition, the likelihood of an interaction is determined by the $[I]/K_i$ ratio where $[I]$ represents the mean steady-state $C_{max}$ value following administration of the highest proposed clinical dose. As the ratio increases, the likelihood of an interaction increases. An estimated $[I]/K_i$ ratio of greater than 0.1 is considered positive and the guidance recommends a clinical study. Further, it is suggested that the most sensitive isozymes (i.e. where the drug has the lowest inhibitor 50 or induction 50 concentration) should be studied first. If no clinical interaction is observed for these most sensitive pathways, other less sensitive pathways do not need to be studied in clinical studies. For mechanism-based inhibition, the guidance recommends clinical evaluation if any time dependent inhibition is detected. Finally for induction potential, no guidance is given as to what the threshold for clinical evaluations is, however the guidance does note that if induction studies with a compound confirm that it is not an inducer of CYP3A4 then it can be concluded the drug is not an inducer of CYP2C8, CYP2C9, or CYP2C19.

Strategies for non-CYP metabolic pathways are less well established. However, a similar philosophy of using a sensitive probe substrate or potent inhibitor can be applied.

## 2.10.2 Transporter Based Drug Interactions

Strategies for transporter based interaction studies are less well defined as transporters are less well understood. The FDA does offer a guidance for P-glycoprotein based drug interactions (cited above). A drug is considered a substrate if the net flux ratio is greater than 2, where net flux ratio is the ratio of basal-apical permeability to apical-basal permeability in preclinical models. Evaluation in clinical studies is recommended for substrates where preclinical models show inhibition of transport by 1 or more known P-glycoprotein inhibitors. To assess the potential for P-glycoprotein inhibition, the $[I]/IC_{50}$ value is considered, where $IC_{50}$ is the concentration causing half the maximal drug related inhibition. The guidance suggests $[I]/IC_{50}$ values greater than 0.1 warrant clinical investigations. Recent work by Cook et al. (submitted) suggest this threshold may result in an unacceptable false-negative rate (i.e. indication a lack of potential to inhibit P-glycoprotein when clinically relevant interaction does occur) and suggest cut-off values for $[I]/IC_{50} < 0.1$ and $[I_2]/IC_{50} < 5$ ($I_2$ is the dose/250 ml) were identified to minimize the error rate which resulted in a reduction of false negatives to 9%. Finally for induction potential, the guidance notes a lack of predictable preclinical models but does state if a drug is not an inducer of CYP3A4, then it can be concluded the drug does not induce P-glycoprotein.

Specific criteria for transporters other than P-glycoprotein have not been established. However, Wu and Benet (2005) have utilized the Biopharmaceutics Classification System to assess the potential importance of transporters. For Class 1 compounds (highly soluble, highly permeable), transporters are expected to have minimal impact on drug disposition and thus drug interactions are not expected. For Class 2 compounds (low solubility, highly permeable), efflux transporter effects will predominate. For Class 3 compounds (highly soluble, low permeability), absorptive transporter effects will predominate. For Class 4 compounds (low solubility, low permeability) absorptive or efflux transporters could be important.

Once transporters important to a drugs disposition have been identified, a preclinical assessment as to their importance can be estimated using a model proposed by Shirasaka et al. (2008):

$$V_{app} = V_{passive} \pm V_{transporter}$$
$$= P_{passive} \cdot S \cdot C \pm \frac{V_{max} \cdot C}{K_m + C}$$

where $V$ is the flux and app, passive and transporter subscripts denote whether the flux is apparent, passive or due to the transporter respectively; $S$ is the surface area of the membrane, $P$ is the permeability, $V_{max}$ and $K_m$ are the maximum velocity and concentration producing half-maximal velocity, and $C$ is the concentration at the membrane. The sign in front of the transporter term depends on whether the transporter is an absorptive transporter $(+)$ or efflux transporter $(-)$ with respect to the driving concentration, $C$. $V_{passive}$ can be determined in preclinical experiments through the use of inhibitor. The difference between the apparent flux without and with an inhibitor will yield the flux due to the transporter. If passive permeability predominates $(V_{passive} \gg V_{transpoter})$ then drug interactions are not expected. Similarly the impact of a drug's inhibition potential may be considered using the following model (Tamai 2009):

$$P_{app} = P_{passive} \pm \frac{P_{max}, \text{transporter}}{(1 + [I]/K_i)}$$

where, $P_{max}$ is the maximum change in permeability of the substrate due to the transporter, $[I]$ is the concentration of the inhibitor and $K_i$ is the inhibitory constant. Again if passive permeability predominates, no clinically relevant interaction is expected.

## 2.10.3 Pharmacodynamically Based Drug Interactions

In general there are only two typical cases where pharmacodynamic interactions are considered. The first is for drugs with activity in the central

nervous system. Generally if a drug is centrally acting and sedation a frequent side-effect, evaluation of co-administration of other CNS active agents is warranted using a pharmacodynamic endpoint. The other typical case is drug interaction studies involving warfarin. S-Warfarin in a substrate probe for CYP 2C9 based interaction studies. Because of the relatively low therapeutic window, warfarin pharmacodynamics are often evaluated using prothrombin time and the international normalized ratio (INR). There are certain instances where drugs are co-administered because they have beneficial additive or synergistic pharmacodynamic effects. These are not considered further in this chapter as the interaction is typically evaluated in clinical efficacy trials.

## 2.10.4  Other Interaction Studies

There may be instances where it is beneficial to conduct clinical drug interaction studies even though there is no basis for an interaction. One instance may be to facilitate recruitment into Phase II or III trials. There are some instances where a background therapy may be given while patients are given the investigational drug. In some instances the drug given as background therapy may have a narrow therapeutic index. Another example might be interactions with oral contraceptives (OCs). Patients in clinical trials may be required to use barrier forms of contraception while enrolled and for a period thereafter. Showing the absence of an interaction with OCs may allow this restriction to be lifted. In these cases, these studies are conducted to show the absence of a clinical significant interaction, and thus assure investigators that the compounds can be given concomitantly. A second reason for conducting a drug interaction when there is no basis for an interaction is to demonstrate a competitive treatment advantage. Both patient and prescriber benefit from knowledge that a new medicine does not carry the same drug interaction liabilities as other available treatments. For example clinical evaluations for pregabalin were undertaken to show a lack of interaction

with a number of antiepileptic drugs (carbamazepine, valproic acid, lamotrigine, phenytoin, phenobarbital, and topiramate), when most of other antiepileptic drugs have clinically relevant drug interactions. Thus, pregabalin could be added to a patient's regimen for seizure control without fear of altering the pharmacokinetics, and potentially the efficacy and safety of the therapy.

## 2.10.5  Determination of When to Do Drug Interaction Studies

Once it is determined what clinical drug interaction studies need to be done in a drug development program, the timing of these studies should be determined. Considering only one in nine compounds entering human drug development are eventually marketed and clinical safety (of which drug interactions contribute some fraction) accounts for approximately 12% of the failures, it would seem drug interactions are not typically go/no-go studies once a drug development program starts with clinical studies. (Presumably preclinical assessments have caused the attrition of most compounds with major drug interaction liabilities). Consequently it is economically prudent not to spend too many resources early in clinical development to assess drug interactions. It is therefore recommended that prior to initial studies in patients, two types of drug interaction studies are performed. The first are those where definitive "go/no-go" development decisions can be made based on the interaction: where there is an unacceptably high risk of a major drug interaction that would preclude further development. If the interaction study does not need to be conducted (e.g. the efficacy trial can be run without the need for concomitant medication), the level of risk of a relevant interaction [P(DDI)] and cost of the drug interaction study (DDI$) should be considered against the risk of lack of efficacy [P(LOE)] and the cost of the initial efficacy trial (EFF$). The drug interaction study should be done first if:

$$(1 - P(DDI)) \cdot P(LOE) \cdot Eff\$ + DDI\$$$
$$< (1 - P(LOE)) \cdot P(DDI) \cdot DDI\$ + Eff\$$$

And the estimates of probability can be based on historical rates or efficacy trials and past performance of preclinical models used to estimate the magnitude of clinical interactions.

The second type of drug interaction study that should be conducted are those where concomitant medications need to be given in the initial efficacy trials, and the pharmacokinetics or pharmacodynamics involve pathways identified as likely to be affected by or likely to alter the pharmacokinetics of the investigational drug. For example, if the investigational drug is predominately metabolized by CYP 3A4 and a typical concomitant medication is likely to be a CYP 3A4 inhibitor, a drug interaction study investigating the effect of CYP 3A4 inhibition of the investigational drug is likely needed prior to the study so that dosing recommendations can be made. After the initial efficacy trial, it may be necessary to perform similar enabling studies (those necessary to allow dosing recommendations for other possible concomitant medications as well as those required by investigators to facilitate recruitment) prior to larger clinical trials in order to expand enrollment criteria to encompass a more diverse patient population.

During Phase II and III, sparse pharmacokinetic sampling is now routinely included to evaluate exposure and/or effect relationships in the population pharmacokinetics of patients. These same data can be used to evaluate the influence of concomitant medications on the pharmacokinetics of the investigational drug. Commonly, these data are used to confirm the lack of an interaction when preclinical data suggest that no interaction is expected or to confirm the clinical importance of an interaction previously observed in healthy volunteers. Regulatory agencies have label statements describing the findings (Duan 2007). They are typically not used to confirm the lack of an interaction when preclinical data suggest an interaction is likely, for safety reasons. These analyses may also be useful in detecting unsuspected DDIs. Before such analyses are conducted, simulations are recommended to optimize study design elements (e.g. sample collection) and to assess the study's ability to characterize an interaction if one were to occur.

Frequently, drug interaction studies are conducted near the end of the development plan to provide labeling information. Many of these studies are conducted to confirm a lack of interaction with commonly co-administered medications in the target treatment population. For instance the FDA guidance on drug interactions (previously sited) suggests conducting at least one drug interaction study with a concomitant inducing or inhibiting drug. The concomitant drug is chosen based on its interaction with the CYP isozyme most sensitive to the investigational drug (e.g. the one for which the investigational drug has the lowest $K_i$). If the clinical study results in no important interaction, no further studies involving CYP isozymes are warranted. If an interaction does occur, another drug interaction study should be considered with the probe substrate selected based on the next most sensitive CYP isozyme.

## 2.11 Labeling Considerations

As previously mentioned, the results of drug interaction studies with probe substrates or potent inhibitors are generally extrapolated to other drugs where the interaction would occur through the same pathway. For example if a clinical study indicated no interaction, the drug interaction section of the label might look like the following example suggested by the FDA draft guidance on In Vivo Drug Metabolism/Drug Interaction Studies – Study Design, Data Analysis, and Recommendations for Dosing and Labeling 11/24/1999. (http://www.fda.gov/downloads/Drugs/Guidance ComplianceRegulatoryInformation/Guidances/ ucm072119.pdf last accessed 7/14/2009.):

*Data from a drug–drug interaction study involving (drug) and (probe drug) in _____ patients/healthy individuals indicate that the PK disposition of (probe drug) is not altered when the drugs are co-administered. This indicates*

*that (drug) does not inhibit CYP3A4 and will not alter the metabolism of drugs metabolized by this enzyme.*

Similarly, if a significant interaction did occur, the following is an example of a possible portion of the drug interaction section of the label.

*The effect of (drug) on the pharmacokinetics of (probe drug) has been studied in _____ patients/healthy subjects. The $C_{max}$, AUC, half-life and clearances of (probe drug) increased/ decreased by ____% (90% Confidence Interval: ____ to ____%) in the presence of (drug). This indicates that (drug) can inhibit the metabolism of drugs metabolized by CYP3A4 and can increase blood concentrations of such drugs. (See PRECAUTIONS, WARNINGS, DOSAGE AND ADMINISTRATION, or CONTRAINDICA-TIONS sections.)*

Declaration of a clinically relevant effect or lack thereof is based on a statistical comparison of pharmacokinetic (or pharmacodynamic) parameters, typically $C_{max}$ and AUC for metabolic based interactions. Proof of a lack of interaction is based on the 90% confidence interval limits for the ratio of pharmacokinetic parameter values (substrate + inhibitor as numerator, substrate only as denominator) and whether or not the 90% confidence intervals lies between no effect boundaries. Two approaches can be used to set no effect boundaries. The first is to use boundary limits that are used for bioequivalence: 80% and 125%. This is the most conservative approach in that lack of interaction is accepted without question. A second approach is to consider exposure-response relationships for both safety and efficacy and to set boundary limits where changes in exposure will not lead to clinical consequences. Thus a large therapeutic window and/or a shallow exposure-efficacy relationship can lead to no effect boundaries that are wider than the 80% and 125% limits used in the first approach. Choice of the approach, the expected magnitude of the interaction and the variability of the substrate can all be used to size the clinical study.

In cases where a clinically relevant interaction is expected, the size of the study should be based on the expected magnitude of the interaction, the variability of the substrate and the precision required to provide appropriate dosing recommendations. For example, if a very large interaction is expected that is likely to result in a contraindication, few subjects are typically needed than for a study that might result in a dosage adjustment or declaration of no interaction. In general the study design should reflect the expected labeling by either demonstrating that there is no clinically relevant interaction (e.g. powered to rule out a interaction) or resulting in recommendation for dosage adjustment or contraindication (e.g. sized to yield a sufficiently precise estimate of effect).

## Conclusions

DDIs can represent a major public health issue. The science has evolved to the point where the risk interactions occurring at various cytochrome-P450 isozymes in humans can be reliably predicted from in vitro data. The science in the area of drug interactions with other enzymes will continue to evolve, hopefully to the point where the likelihood of clinically significant interactions may be more accurately predicted. Clinical drug development scientists and regulators will use these data to assure that the most critical information on drug interactions are obtained in the clinic and to provide appropriate information to physicians and patients to guide the safe and effective use of new and existing medications.

## References

Anglicheau D, Legendre C, Beaune P, and Thervet E. Cytochrome P450 3A polymorphisms and immuno-suppressive drugs: an update. Pharmacogenomics 2007; 8: 835–849.

Aninat C, Piton A, Glaise D, Le CT, Langouet S, Morel F, Guguen-Guillouzo C, and Guillouzo A. Expression of cytochromes P450, conjugating enzymes and nuclear receptors in human hepatoma HepaRG cells. Drug Metab Dispos 2006; 34: 75–83.

Bakken GV, Rudberg I, Christensen H, Molden E, Refsum H, and Hermann M. Metabolism of quetiapine by CYP3A4 and CYP3A5 in presence or absence of cytochrome B5. Drug Metab Dispos 2009; 37: 254–258.

Becker ML, Kallewaard M, Caspers PWJ, Visser LE, Leufkens HGM, and Strick BHC. Hospitalisations

and emergency department visits dues to drug–drug interactions: a literature review. Pharmacoepidemiol Drug Saf 2007; 16: 641–651.

Bell L, Bickford S, Nguye PH, Wang J, He T, Zhang B, Friche Y, Zimmerlin A, Urban L, and Bojanic D. Evaluation of fluorescence- and mass spectrometry-based CYP inhibition assays for use in drug discovery. J Biomol Screen 2008; 13: 343–353.

Benet LZ and Hoener BA. Changes in plasma protein binding have little clinical relevance. Clin Pharmacol Ther 2002; 71: 115–121.

Berry LM and Zhao Z. An examination of IC50 and IC50-shift experiments in assessing time-dependent inhibition of CYP3A4, CYP2D6 and CYP2C9 in human liver microsomes. Drug Metab Lett 2008; 2: 51–59.

Bertilsson G, Heidrich J, Svensson K, Asman M, Jendeberg L, Sydow-Backman M, Ohlsson R, Postlind H, Blomquist P, and Berkenstam A. Identification of a human nuclear receptor defines a new signaling pathway for CYP3A induction. Proc Natl Acad Sci U S A 1998; 5: 12208–12213.

Burchell B, Soars M, Monaghan G, Cassidy A, Smith D, and Ethell B. Drug-mediated toxicity caused by genetic deficiency of UDP-glucuronosyltransferases. Toxicol Lett 2000; 112–113: 333–340.

Cali JJ, Ma D, Sobol M, Simpson DJ, Frackman S, Good TD, Daily WJ, and Liu D. Luminogenic cytochrome P450 assays. Expert Opin Drug Metab Toxicol 2006; 2: 629–645.

Cawley GF, Batie CJ, and Backes WL. Substrate-dependent competition of different P450 isozymes for limiting NADPH-cytochrome P450 reductase. Biochemistry 1995; 34: 1244–1247.

Chen Q, Ngui JS, Doss GA, Wang RW, Cai X, DiNinno FP, Blizzard TA, Hammond ML, Stearns RA, Evans DC, Baillie TA, and Tang W. Cytochrome P450 3A4-mediated bioactivation of raloxifene: irreversible enzyme inhibition and thiol adduct formation. Chem Res Toxicol 2002; 15: 907–914.

Cheng Y-C and Prusoff WH. Relationship between the inhibition constant ($K_I$) and the concentration of inhibitor which causes 50 per cent inhibition ($I_{50}$) of an enzymatic reaction. Biochem Pharmacol 1973; 23: 3099–3108.

Chu V, Einolf HJ, Evers R, Kumar G, Moore D, Ripp S, Silva J, Sinha V, Sinz M, and Skerjanec A. In vitro and in vivo induction of cytochrome p450: a survey of the current practices and recommendations: a pharmaceutical research and manufacturers of America perspective. Drug Metab Dispos 2009; 37: 1339–1354.

Cohen LH, Remley MJ, Raunig D, and Vaz ADN. In vitro drug interactions of cytochrome P450: an evaluation of fluorogenic to conventional substrates. Drug Metab Dispos 2003; 31: 1005–1015.

Cook JA, Feng B, Fenner KS, Kempshall S, Liu R, Rotter C, Smith DA, Troutman MD, Ullah M, and Lee CA. Refining the in vitro and in vivo critical parameters for P-glycoprotein, [I]/IC$_{50}$ and [I2]/IC$_{50}$, that allow for the exclusion of drug candidates from clinical digoxin interaction studies. Mol Pharm 2010; Apr 5;7(2): 398–411.

Crespi CL and Stresser DM. Flurometric screening for metabolism-based drug–drug interactions. J Pharmacol Toxicol Methods 2000; 44: 325–331.

Cui X, Thomas A, Gerlach V, White RE, Morrison RA, and Cheng KC. Application and interpretation of hPXR screening data: validation of reporter signal requirements for prediction of clinically relevant CYP3A4 inducers. Biochem Pharmacol 2008; 76: 680–689.

Dalvie D, Kang P, Zientek M, Xiang C, Zhou S, and Obach RS. Effect of intestinal glucuronidation in limiting hepatic exposure and bioactivation of raloxifene in humans and rats. Chem Res Toxicol 2008; 21: 2260–2271.

Dixit V, Haraparsad N, Desai P, and Unadkat JD. In vitro LC–MS cocktail assays to simultaneously determine human cytochrome P450 activities. Biopharm Drug Dispos 2007; 28: 257–262.

Duan JZ. Applications of population pharmacokinetics in current drug labelling. J Clin Pharm Ther 2007; 32: 57–79.

El-Sankary W, Gibson GG, Ayrton A, and Plant N. Use of a reporter gene assay to predict and rank the potency and efficacy of CYP3A4 inducers. Drug Metab Dispos 2001; 29: 1499–1504.

Fahmi OA, Maurer TS, Kish M, Cardenas E, Boldt S, and Nettleton D. A combined model for predicting CYP3A4 clinical net drug–drug interaction based on CYP3A4 inhibition, inactivation, and induction determined in vitro. Drug Metab Dispos 2008; 36: 1698–1708.

Feng B, Mills JB, Davidson RE, Mireles RJ, Janiszewski JS, Troutman MD, and de Morais SM. In vitro P-glycoprotein assays to predict the in vivo interactions of P-glycoprotein with drugs in the central nervous system. Drug Metab Dispos 2008; 36: 268–275.

Feng B, Xu JJ, Bi YA, Mireles R, Davidson R, Duignan DB, Campbell S, Kostrubsky VE, Dunn MC, Smith AR, and Wang HF. Role of hepatic transporters in the disposition and hepatotoxicity of a HER2 tyrosine kinase inhibitor CP-724,714. Toxicol Sci 2009; 108: 492–500.

Fenner KS, Troutman MD, Kempshall S, Cook JA, Ware JA, Smith DA, and Lee CA. Drug–drug mediated interactions mediated through p-glycoprotein: clinical relevance and in vitro–in vivo correlation using digoxin as a probe drug. Clin Pharmacol Ther 2009; 85: 173–181.

Fontana E, Dansette PM, and Poli SM. Cytochrome p450 enzymes mechanism based inhibitors: common substructures and reactivity. Curr Drug Metab 2005; 6: 413–454.

Foti RS and Wahlstrom JL. Prediction of CYP-mediated drug interactions in vivo using in vitro data. IDrugs 2008; 11: 900–905.

Fromm MF, Kim RB, Stein CM, Wilkinson GR, and Roden DM. Inhibition of P-glycoprotein-mediated drug transport: a unifying mechanism to explain

the interaction between digoxin and quinidine [see comments]. Circulation 1999; 99: 552–557.

Galetin A, Burt H, Gibbons L, and Houston JB. Prediction of time-dependent CYP3A4 drug–drug interactions: impact of enzyme degradation, parallel elimination pathways, and intestinal inhibition. Drug Metab Dispos 2006; 34: 166–175.

Galetin A, Hinton LK, Burt H, Obach RS, and Houston JB. Maximal inhibition of intestinal first-pass metabolism as a pragmatic indicator of intestinal contribution to the drug–drug interactions for CYP3A4 cleared drugs. Curr Drug Metab 2007; 8: 685–693.

Galetin A, Gertz M, and Houston JB. Potential role of intestinal first-pass metabolism in the prediction of drug–drug interactions. Expert Opin Drug Metab Toxicol 2008; 4: 909–922.

Gao F, Johnson DL, Ekins S, Janiszewski J, Kelly KG, Meyer RD, and West M. Optimizing higher through-put methods to assess drug–drug interactions for CYP1A2, CYP2C9, CYP2C19, CYP2D6, rCYP2D6, and CYP3A4 in vitro using a single point IC(50). J Biomol Screen 2002; 7: 373–382.

Ghanbari F, Rowland-Yeo K, Bloomer JC, Clarke SE, Lennard MS, Tucker GT, and Rostami-Hodjegan A. A critical evaluation of the experimental design of studies of mechanism based enzyme inhibition, with implications for in vitro–in vivo extrapolation. Curr Drug Metab 2006; 7: 315–334.

Grim KH, Bird J, Ferguson D, and Riley RJ. Mechanism-based inhibition of cytochrome P450 enzymes: an evaluation of early decision making in vitro approaches and drug–drug interaction prediction methods. Eur J Pharm Sci 2009; 36: 175–191.

Grimm SW, Einolf HJ, Hall SD, He K, Lim HK, Ling KH, Lu C, Nomeir AA, Seibert E, Skordos KW, Tonn GR, Van HR, Wang RW, Wong YN, Yang TJ, and Obach RS. The conduct of in vitro studies to address time-dependent inhibition of drug-metabolizing enzymes: a perspective of the pharmaceutical research and manufacturers of America. Drug Metab Dispos 2009; 37: 1355–1370.

Guengerich FP. Update information on human P550s. Drug Metab Rev 2002; 34: 7–15.

Guengerich FP. Cytochrome P450 and chemical toxicity. Chem Res Toxicol 2008; 21: 70–83.

Hager WD, Fenster P, Mayersohn M, Perrier D, Graves P, Marcus FI, and Goldman S. Digoxin–quinidine inter-action pharmacokinetic evaluation. N Engl J Med 1979; 300(22): 1238–1241.

Hamelin BA, Bouayad A, Methot J, Jobin J, Desgagnes P, Poirier P, Allaire J, Dumesnil J, and Turgeon J. Significant interaction between the nonprescription antihistamine diphenhydramine and the CYP2D6 substrate metoprolol in healthy men with high or low CYP2D6 activity. Clin Pharmacol Ther 2000; 67: 466–477.

Hariparsad N, Carr BA, Evers R, and Chu X. Comparison of immortalized Fa2N-4 cells and human hepatocytes as in vitro models for cytochrome P450 induction. Drug Metab Dispos 2008; 36: 1046–1055.

Harmsen S, Koster AS, Beijnen JH, Schellens JH, and Meijerman I. Comparison of two immortalized human cell lines to study nuclear receptor-mediated CYP3A4 induction. Drug Metab Dispos 2008; 36: 1166–1171.

Hebert MF, Roberts JP, Prueksaritanont T, and Benet LZ. Bioavailability of cyclosporine with concomitant rifampin administration is markedly less than pre-dicted by hepatic enzyme induction. Clin Pharmacol Ther 1992; 52: 453–457.

Hesselink DA, van Schaik RH, van der Heiden IP, van der Werf M, Gregoor PJ, Lindemans J, Weimar W, and van Gelder T. Genetic polymorphisms of the CYP3A4, CYP3A5, and MDR-1 genes and pharmacokinetics of the calcineurin inhibitors cyclosporine and tacrolimus. Clin Pharmacol Ther 2003; 74: 245–254.

Hesselink DA, van Schaik RHN, van Agteren M, de Fijter JW, Hartmann A, Zeier M, Budde K, Kuypers DR, Pisarski P, Meur YL, Mamelok RD, and van Gelder T. CYP3A5 genotype is not associated with a higher risk of acute rejection in tacrolimus-treated renal trans-plant recipients. Pharmacogenet Genomics 2008; 18: 339–348.

Hollenberg PF, Kent UM, and Bumpus NN. Mechanism-based inactivation of human cytochromes p450s: experimental characterization, reactive intermediates, and clinical implications. Chem Res Toxicol 2008; 21: 189–205.

Houston JB. Utility of in vitro drug metabolism data in predicting in vivo metabolic clearance. Biochem Pharmacol 1994; 47: 1469–1479.

Huang W, Lin YS, McConn DJ, Calamia JC, Totah RA, Isoherranen N, Glodowski M, and Thummel KE. Evi-dence of significant contribution from CYP3A5 to hepatic drug metabolism. Drug Metab Dispos 2004; 32: 1434–1445.

Hutzler JM, Melton RJ, Rumsey JM, Schnute ME, Locuson CW, and Wienkers LC. Inhibition of cyto-chrome P450 3A4 by a pyrimidineimidazole: evidence for complex heme interactions. Chem Res Toxicol 2006; 19: 1650–1659.

Ismail R and Teh LK. The relevance of CYP2D6 genetic polymorphism on chronic metoprolol therapy in cardio-vascular patients. J Clin Pharm Ther 2006; 31: 99–109.

Jamei M, Marciniak S, Feng K, Barnett A, Tucker G, and Rostami-Hodjegan A. The Simcyp® population-based ADME simulator. Expert Opin Drug Metab Toxicol 2009; 5: 211–223.

Jones DR, Gorski JC, Hamman MA, Mayhew BS, Rider S, and Hall SD. Diltiazem inhibition of cytochrome P-450 3A activity is due to metabolite intermediate complex formation. J Pharmacol Exp Ther 1999; 290: 1116–1125.

Jones SA, Moore LB, Wisely GB, and Kliewer SA. Use of in vitro pregnane X receptor assays to assess CYP3A4 induction potential of drug candidates. Methods Enzymol 2002; 357: 161–170.

Kalgutkar AS, Obach RS, and Maurer TS. Mechanism-based inactivation of cytochrome P450 enzymes: chemical mechanisms, structure–activity relationships and relationship to clinical drug–drug interactions and idiosyncratic adverse drug reactions. Curr Drug Metab 2007; 8: 407–447.

Kanamitsu S, Ito K, and Sugiyama Y. Quantitative prediction of in vivo drug–drug interactions from in vitro data based on physiological pharmacokinetics: use of maximum unbound concentration of inhibitor at the inlet to the liver. Pharm Res 2000; 17: 336–343.

Kanebratt KP and Andersson TB. HepaRG cells as an in vitro model for evaluation of cytochrome P450 induction in humans. Drug Metab Dispos 2008; 36: 137–145.

Kawahara I, Kato Y, Suzuki H, Achira M, Ito K, Crespi CL, and Sugiyama Y. Selective inhibition of human cytochrome P450 3A4 by N-[2(R)-hydroxy-1(S)-indanyl]-5-[2(S)-(1, 1-dimethylethylaminocarbonyl)-4-[(furo[2, 3-b]pyridin-5-yl)methyl]piperazin-1-yl]-4 (S)-hydroxy-2(R)-phenylmethy lpentanamide and P-glycoprotein by valspodar in gene transfectant systems. Drug Metab Dispos 2000; 28: 1238–1243.

Kenny JR, Chen L, McGinnity DF, Grime K, Shakesheff KM, Thomson B, and Riley R. Efficient assessment of the utility of immortalized Fa2N-4 cells for cytochrome P450 (CYP) induction studies using multiplex quantitative reverse transcriptase-polymerase chain reaction (qRT-PCR) and substrate cassette methodologies. Xenobiotica 2008; 38: 1500–1517.

Kim M-J, Kim H, Cha I-J, Park J-S, Shon J-H, Liu K-H, and Shin J-G. High-throughput screening of inhibitory potential of nine cytochrome P450 enzymes in vitro using liquid chromatography/tandem mass spectrometry. Rapid Commun Mass Spectrom 2005; 19: 2651–2658.

Kindla J, Fromm MF, and Konig J. In vitro evidence for the role of OATP and OCT uptake transporters in drug–drug interactions. Expert Opin Drug Metab Toxicol 2009; 5: 489–500.

Klotz T, Sachse R, Heidrich A, Jockenhovel F, Rohde G, Wensing G, Horstmann R, and Engelmann R. Vardenafil increases penile rigidity and tumescence in erectile dysfunction patients: a RigiScan and pharmacokinetic study. World J Urol 2001; 19: 32–39.

Kongkaew C, Noyce PR, and Ashcroft DM. Hospital admissions associated with adverse drug reactions: a systematic review of prospective observational studies. Ann Pharmacother 2008; 42: 1017–1025.

Kostrubsky SE, Strom SC, Kalgutkar AS, Kulkarni S, Atherton J, Mireles R, Feng B, Kubik R, Hanson J, Urda E, and Mutlib AE. Inhibition of hepatobiliary transport as a predictive method for clinical hepatotoxicity of nefazodone. Toxicol Sci 2006; 90: 451–459.

Kovarik JM, Rigaudy L, Guerret M, Gerbeau C, and Rost KL. Longitudinal assessment of a P-glycoprotein-mediated drug interaction of valspodar on digoxin. Clin Pharmacol Ther 1999; 66: 391–400.

Krayenbühl JC, Vozeh S, Kondo-Oestreicher M, and Dayer P. Drug–drug interactions of the new active substances: mibefradil example. Eur J Clin Pharmacol 1999; 55: 559–565.

Ku HY, Ahn HJ, Seo KA, Kim H, Oh M, Bae SK, Shin JG, Shon JH, and Liu KH. The contributions of cytochromes P450 3A4 and 3A5 to the metabolism of the phosphodiesterase type 5 inhibitors sildenafil, udenafil, and vardenafil. Drug Metab Dispos 2008; 36: 986–990.

Kumar V, Wahlstrom JL, Rock DA, Warren CJ, Gorman LA, and Tracy TS. CYP2C9 inhibition: impact of probe selection and pharmacogenetics on in vitro inhibition profiles. Drug Metab Dispos 2006; 34: 1966–1975.

Kumar V, Brundage RC, Oetting WS, Leppik IE, and Tracy TS. Differential genotype dependent inhibition of CYP2C9 in humans. Drug Metab Dispos 2008; 36: 1242–1248.

LeBel M, Masson E, Guilbert E, Colborn D, Paquet F, Allard S, Vallee F, and Narang PK. Effects of rifabutin and rifampicin on the pharmacokinetics of ethinylestradiol and norethindrone. J Clin Pharmacol 1998; 38: 1042–1050.

Lecoeur S, Bonierbale E, Challine D, Gautier JC, Valadon P, Dansette PM, Catinot R, Ballet F, Mansuy D, and Beaune PH. Specificity of in vitro covalent binding of tienilic acid metabolites to human liver microsomes in relationship to the type of hepatotoxicity: comparison with two directly hepatotoxic drugs. Chem Res Toxicol 1994; 7: 434–442.

Lehmann JM, McKee DD, Watson MA, Willson TM, Moore JT, and Kliewer SA. The human orphan nuclear receptor PXR is activated by compounds that regulate CYP3A4 gene expression and cause drug interactions. J Clin Invest 1998; 102: 1016–1023.

Lessard E, Yessine MA, Hamelin BA, Gauvin C, Labbe L, O'Hara G, LeBlanc J, and Turgeon J. Diphenhydramine alters the disposition of venlafaxine through inhibition of CYP2D6 activity in humans. J Clin Psychopharmacol 2001; 21: 175–184.

Lin JH. CYP induction-mediated drug interactions: in vitro assessment and clinical implications. Pharm Res 2006; 23: 1089–1116.

Linder CD, Renaud NA, and Hutzler JM. Is 1-aminobenzotriazole an appropriate in vitro tool as a nonspecific cytochrome P450 inactivator? Drug Metab Dispos 2009; 37: 10–13.

Lopez-Garcia MP, Dansette PM, and Mansuy D. Thiophene derivatives as new mechanism-based inhibitors of cytochromes P-450: inactivation of yeast-expressed human liver cytochrome P-450 2C9 by tienilic acid. Biochemistry 1994; 33: 166–175.

Lu P, Schrag ML, Slaughter DE, Raab CE, Shou M, and Rodrigues AD. Mechanism-based inhibition of human liver microsomal cytochrome P450 1A2 by zileuton, a 5-lipoxygenase inhibitor. Drug Metab Dispos 2003; 31: 1352–1360.

Luo G, Cunningham M, Kim S, Burn T, Lin J, Sinz M, Hamilton G, Rizzo C, Jolley S, Gilbert D, Downey A, Mudra D, Graham R, Carroll K, Xie J, Madan A, Parkinson A, Christ D, Selling B, LeCluyse E, and Gan LS. CYP3A4 induction by drugs: correlation

between a pregnane X receptor reporter gene assay and CYP3A4 expression in human hepatocytes. Drug Metab Dispos 2002; 30: 795–804.

Luo G, Guenthner T, Gan LS, and Humphreys WG. CYP3A4 induction by xenobiotics: biochemistry, experimental methods and impact on drug discovery and development. Curr Drug Metab 2004; 5: 483–505.

Mayhew BS, Jones DR, and Hall SD. An in vitro model for predicting in vivo inhibition of cytochrome P450 3A4 by metabolic intermediate complex formation. Drug Metab Dispos 2000; 28: 1031–1037.

McDonnell PJ and Jacobs MR. Hospital admissions resulting from preventable adverse drug reactions. Ann Pharmacother 2002; 36: 1331–1336.

McGinnity DF, Berry AJ, Kenny JR, Grime K, and Riley RJ. Evaluation of time-dependent cytochrome P450 inhibition using cultured human hepatocytes. Drug Metab Dispos 2006; 34: 1291–1300.

McGinnity DF, Zhang G, Kenny JR, Hamilton GA, Otmani S, Stams KR, Haney S, Brassil P, Stresser DM, and Riley RJ. Evaluation of multiple in vitro systems for assessment of CYP3A4 induction in drug discovery: human hepatocytes, pregnane X receptor reporter gene, and Fa2N-4 and HepaRG cells. Drug Metab Dispos 2009; 37: 1259–1268.

Miller VP, Stresser DM, Blanchard AP, Turner S, and Crespi CL. Fluorometric high-throughput screening for inhibitors of cytochrome P450. Ann NY Acad Sci 2000; 919: 26–32.

Mills JB, Rose KA, Sadagopan N, Sahi J, and de Morais SM. Induction of drug metabolism enzymes and MDR1 using a novel human hepatocyte cell line. J Pharmacol Exp Ther 2004; 309: 303–309.

Neuvonen PJ, Niemi M, and Backman JT. Drug interactions with lipid-lowering drugs: mechanisms and clinical relevance. Clin Pharmacol Ther 2006; 80: 565–581.

Obach RS. Predicting drug–drug interactions from in vitro drug metabolism data: challenges and recent advances. Curr Opin Drug Discov Devel 2009; 12: 81–89.

Obach RS, Walsky RL, Venkatakrishnan K, Gaman EA, Houston JB, and Tremaine LM. The utility of in vitro cytochrome P450 inhibition data in the prediction of drug–drug interactions. J Pharmacol Exp Ther 2006; 316: 336–348.

Obach RS, Walsky RL, and Venkatakrishnan K. Mechanism-based inactivation of human cytochrome p450 enzymes and the prediction of drug–drug interactions. Drug Metab Dispos 2007; 35: 246–255.

Olinga P, Elferink MG, Draaisma AL, Merema MT, Castell JV, Perez G, and Groothuis GM. Coordinated induction of drug transporters and phase I and II metabolism in human liver slices. Eur J Pharm Sci 2008; 33: 380–389.

Ortiz de Montellano PR, ed. Cytochrome P450: Structure, metabolism, and biochemistry, 3rd ed. Klower Academic/Plenum Publishers, New York, 2005.

Pearson JT, Wahlstrom JL, Dickmann LJ, Kumar S, Halpert JR, Wienkers LC, Foti RS, and Rock DA. Differential time-dependent inactivation of P450 3A4 and P450 3A5 by raloxifene: a key role for C239 in quenching reactive intermediates. Chem Res Toxicol 2007; 20: 1778–1786.

Plumb RS, Potts WB, III, Rainville PD, Alden PG, Shave DH, Baynham G, and Mazzeo JR. Addressing the analytical throughput challenges in ADME screening using rapid ultra-performance liquid chromatography/tandem mass spectrometry methodologies. Rapid Commun Mass Spectrom 2008; 22: 2139–2152.

Proctor NJ, Tucker GT, and Rostami-Hodjegan A. Predicting drug clearance from recombinantly expressed CYPs: intersystem extrapolation factors. Xenobiotica 2004; 34: 151–178.

Rahman A, Korzekwa KR, Grogan J, Gonzalez FJ, and Harris JW. Selective biotransformation of taxol to 6-hydroxytaxol by human cytochrome P450 2C8. Cancer Res 1994; 54: 5543–5546.

Rajagopalan P, Mazzu A, Xia C, Dawkins R, and Sundaresan P. Effect of high-fat breakfast and moderate-fat evening meal on the pharmacokinetics of vardenafil, an oral phosphodiesterase-5 inhibitor for the treatment of erectile dysfunction. J Clin Pharmacol 2003; 43(3): 260–267.

Ripp SL, Mills JB, Fahmi OA, Trevena KA, Liras JL, Maurer TS, and de Morais SM. Use of immortalized human hepatocytes to predict the magnitude of clinical drug–drug interactions caused by CYP3A4 induction. Drug Metab Dispos 2006; 34: 1742–1748.

Rock DA, Foti RS, and Pearson JT. The combination of chemical and antibody inhibitors for superior P450 3A inhibition in reaction phenotyping studies. Drug Metab Dispos 2008; 36: 2410–2413.

Rostami-Hodjegan A and Tucker GT. Simulation and prediction of in vivo drug metabolism in human populations from in vitro data. Nat Rev Drug Discov 2007; 6: 140–148.

Rowland M and Martin SB. Kinetics of drug–drug interactions. J Pharmacokinet Biopharm 1973; 1: 553–567.

Rowland A, Gaganis P, Elliot DJ, Mackenzie PI, Knights KM, and Miners JO. Binding of inhibitory fatty acids is responsible for the enhancement of UDP-glucuronosyltransferase 2B7 activity by albumin: implications for in vitro–in vivo extrapolation. J Pharmacol Exp Ther 2007; 321: 137–147.

Roymans D, Annaert P, Van HJ, Weygers A, Noukens J, Sensenhauser C, Silva J, Van LC, Hendrickx J, Mannens G, and Meuldermans W. Expression and induction potential of cytochromes P450 in human cryopreserved hepatocytes. Drug Metab Dispos 2005; 33: 1004–1016.

Schoch GA, Yano JK, Wester MR, Griffin KJ, Stout CD, and Johnson EF. Structure of human microsomal cytochrome P450 2C8. J Biol Chem 2004; 279: 9497–9503.

Seithel A, Eberl S, Singer K, Auge D, Heinkele G, Wolf NB, Dorje F, Fromm MF, and Konig J. The influence of macrolide antibiotics on the uptake of organic anions and drugs mediated by OATP1B1 and OATP1B3. Drug Metab Dispos 2007; 35: 779–786.

Shen DD, Kunze KL, and Thummel KE. Enzyme-catalyzed processes of first-pass hepatic and intestinal

drug extraction. Adv Drug Deliv Rev 1997; 27: 99–127.

Shirasaka Y, Sakane T, and Yamashita S. Effect of P-glycoprotein expression levels on the concentration-dependent permeability of drugs to the cell membrane. J Pharm Sci 2008; 97: 553–565.

Silverman RB and George C. Mechanism of inactivation of gamma-aminobutyric acid aminotransferase by (S, E)-4-amino-5-fluoropent-2-enoic acid. Biochem Biophys Res Commun 1988; 150(3): 942–946.

Simonson SG, Raza A, Martin PD, Mitchell PD, Jarcho JA, Brown CD, Windass AS, and Schneck DW. Rosuvastatin pharmacokinetics in heart transplant recipients administered an antirejection regimen including cyclosporine. Clin Pharmacol Ther 2004; 76: 167–177.

Sinz M, Kim S, Zhu Z, Chen T, Anthony M, Dickinson K, and Rodrigues AD. Evaluation of 170 xenobiotics as transactivators of human pregnane X receptor (hPXR) and correlation to known CYP3A4 drug interactions. Curr Drug Metab 2006; 7: 375–388.

Smith DA. Induction and drug development. Eur J Pharm Sci 2000; 11: 185–189.

Smith DA and Schmid EF. Drug withdrawals and the lessons within. Curr Opin Drug Discov Devel 2006; 9: 38–46.

Taipalensuu J, Tornblom H, Lindberg G, Einarsson C, Sjoqvist F, Melhus H, Garberg P, Sjostrom B, Lundgren B, and Artursson P. Correlation of gene expression of ten drug efflux proteins of the ATP-binding cassette transporter family in normal human jejunum and in human intestinal epithelial Caco-2 cell monolayers. J Pharmacol Exp Ther 2001; 299: 164–170.

Tamai I. Intestinal and Hepatic Transport and Metabolism: Role of Transporters in Drug Absorption. Presentation at Strategies in Oral Drug Delivery 2009. Garmisch, Germany, March 8–13, 2009.

Tang C, Shou M, Rushmore TH, Mei Q, Sandhu P, Woolf EJ, Rose MJ, Gelmann A, Greenberg HE, De Lepeleire I, Van Hecken A, De Schepper PJ, Ebel DL, Schwartz JI, and Rodrigues AD. In-vitro metabolism of celecoxib, a cyclooxygenase-2 inhibitor, by allelic variant forms of human liver microsomal cytochrome P450 2C9: correlation with CYP2C9 genotype and in-vivo pharmacokinetics. Pharmacogenetics 2001; 11: 223–235.

Testino SA and Patonay G. High-throughput inhibition screening of major human cytochrome P450 enzymes using an in vitro cocktail and liquid chromatography–tandem mass spectrometry. J Pharm Biomed Anal 2003; 30: 1459–1467.

Tiberghien F and Loor F. Ranking of P-glycoprotein substrates and inhibitors by a calcein-AM fluorometry screening assay. Anticancer Drugs 1996; 7: 568–578.

Tomalik-Scharte D, Lazar A, Fuhr U, and Kirchheiner J. The clinical role of genetic polymorphisms in drug-metabolizing enzymes. Pharmacogenomics J 2008; 8: 4–15.

Treiber A, Schneiter R, Hausler S, and Stieger B. Bosentan is a substrate of human OATP1B1 and OATP1B3: inhibition of hepatic uptake as a common mechanism of its interactions with cyclosporin A, rifampicin and sildenafil. Drug Metab Dispos 2007; 35: 1400–1407.

Uno T, Shimizu M, Yasui-Furukori N, Sugawara K, and Tateishi T. Different effects of fluvoxamine on rabeprazole pharmacokinetics in relation to CYP2C19 genotype status. Br J Clin Pharmacol 2006; 61: 309–314.

Van den Berg HW, Desai ZR, Wilson R, Kennedy G, Bridges JM, and Shanks RG. The pharmacokinetics of vincristine in man: reduced drug clearance associated with raised serum alkaline phosphatase and dose-limited elimination. Cancer Chemother Pharmacol 1982; 8: 215–219.

Van LM, Heydari A, Yang J, Hargreaves J, Rowland-Yeo K, Lennard MS, Tucker GT, and Rostami-Hodjegan A. The impact of experimental design on assessing mechanism-based inactivation of CYP2D6 by MDMA (Ecstasy). J Psychopharmacol 2006; 20: 834–841.

Venkatakrishnan K, von Moltke LL, Court MH, Harmatz JS, Crespi CL, and Greenblatt DJ. Comparison between cytochrome P450 (CYP) content and relative activity approaches to scaling from cDNA-expressed CYPs to human liver microsomes: ratios of accessory proteins as sources of discrepancies between the approaches. Drug Metab Dispos 2000; 28: 1493–1504.

Walsky RL and Obach RS. Validated assays for human cytochrome P450 activities. Drug Metab Dispos 2004; 32: 647–660.

Walsky RL, Gaman EA, and Obach RS. Examination of 209 drugs for inhibition of cytochrome P450 2C8. J Clin Pharmacol 2005; 45: 68–78.

Walsky RL, Astuccio AV, and Obach RS. Evaluation of 227 drugs for in vitro inhibition of cytochrome P450 2B6. J Clin Pharmacol 2006; 46: 1426–1438.

Wang RW, Newton DJ, Liu N, Atkins WM, and Lu AY. Human cytochrome P-450 3A4: in vitro drug–drug interaction patterns are substrate-dependent. Drug Metab Dispos 2000; 28: 360–366.

Wang JH, Liu ZQ, Wang W, Chen XP, Shu Y, He N, and Zhou HH. Pharmacokinetics of sertraline in relation to genetic polymorphism of CYP2C19. Clin Pharmacol Ther 2001; 70: 42–47.

Wang YH, Jones DR, and Hall SD. Prediction of cytochrome P450 3A inhibition by verapamil enantiomers and their metabolites. Drug Metab Dispos 2004; 32: 259–266.

Watanabe A, Nakamura K, Okudaira N, Okazaki O, and Sudo K. Risk assessment for drug–drug interaction caused by metabolism-based inhibition of CYP3A using automated in vitro assay systems and its application in the early drug discovery process. Drug Metab Dispos 2007; 35: 1232–1238.

Wienkers LC and Heath TG. Predicting in vivo drug interactions from in vitro discovery data. Nat Rev Drug Discov 2005; 4: 825–833.

Wienkers LC and Stevens JC. Cytochrome P450 reaction phenotyping. *In: Drug metabolizing enzymes: Cytochrome P450 and other enzymes in drug discovery and*

*development*. Edited by Lee JA, Obach RS, and Fisher MB. CRC Press, Boca Raton, 2003, pp. 255–310.

Williams JA, Hurst SI, Bauman J, Jones BC, Hyland R, Gibbs JP, Obach RS, and Ball SE. Reaction phenotyping in drug discovery: moving forward with confidence? Curr Drug Metab 2003; 4: 527–534.

Williams JA, Hyland R, Jones BC, Smith DA, Hurst S, Goosen TC, Peterkin V, Koup JR, and Ball SE. Drug–drug interactions for UDP-glucuronosyltransferase substrates: a pharmacokinetic explanation for typically observed low exposure (AUCi/AUC) ratios. Drug Metab Dispos 2004; 32: 1201–1208.

Wrighton SA and Stevens JC. The human hepatic cytochromes P450 involved in drug metabolism. Crit Rev Toxicol 1992; 22: 1–21.

Wu CY and Benet LZ. Predicting drug disposition via application of BCS: transport/absorption/elimination interplay and development of a biopharmaceutics drug disposition classification system. Pharm Res 2005; 22: 11–23.

Xie HG, Wood AJ, Kim RB, Stein CM, and Wilkinson GR. Genetic variability in CYP3A5 and its possible consequences. Pharmacogenomics 2004; 5: 243–272.

Yang J, Liao M, Shou M, Jamei M, Yeo KR, Tucker GT, and Rostami-Hodjegan A. Cytochrome p450 turnover: regulation of synthesis and degradation, methods for determining rates, and implications for the prediction of drug interactions. Curr Drug Metab 2008; 9: 384–394.

Youdim KA, Lyons R, Payne L, Jones BC, and Saunders K. An automated, high-throughput, 384 well Cytochrome P450 cocktail IC50 assay using a rapid reso-lution LC–MS/MS end-point. J Pharm Biomed Anal 2008; 48: 92–99.

Zanger UM, Klein K, Saussele T, Blievernicht J, Hofmann MH, and Schwab M. Polymorphic CYP2B6: molecular mechanisms and emerging clinical significance. Pharmacogenomics 2007; 8: 743–759.

Zhang H, Davis CD, Sinz MW, and Rodrigues AD. Cytochrome P450 reaction-phenotyping: an industrial perspective. Expert Opin Drug Metab Toxicol 2007; 3: 667–687.

Zhang L, Zhang YD, Strong JM, Reynolds KS, and Huang SM. A regulatory viewpoint on transporter-based drug interactions. Xenobiotica 2008; 38: 709–724.

Zhao P. The use of hepatocytes in evaluating time-dependent inactivation of P450 in vivo. Expert Opin Drug Metab Toxicol 2008; 4: 151–164.

Zhao P, Kunze KL, and Lee CA. Evaluation of time-dependent inactivation of CYP3A in cryopreserved human hepatocytes. Drug Metab Dispos 2005; 33: 853–861.

Zhou S, Chan E, Lim LY, Boelsterli UA, Li SC, Wang J, Zhang Q, Huang M, and Xu A. Therapeutic drugs that behave as mechanism-based inhibitors of cytochrome P450 3A4. Curr Drug Metab 2004; 5: 415–442.

Zientek M, Miller H, Smith D, Dunklee MB, Heinle L, Thurston A, Lee C, Hyland R, Fahmi O, and Burdette D. Development of an in vitro drug–drug interaction assay to simultaneously monitor five cytochrome P450 isoforms and performance assessment using drug library compounds. J Pharmacol Toxicol Methods 2008; 58: 206–214.

# Modeling the Progression of Disease

**3**

Diane R. Mould

**Abstract**

Clinical pharmacology is the science of understanding drugs as applied to their use in the treatment of disease. It is underpinned by the basic science of pharmacology, focusing on the application of pharmacological principles and methods in clinical practice. One of the primary objectives in any drug development process if to determine if a new drug treatment provides therapeutic benefit to patients, and if so, what is the best dose to use for an individual patient. Disease progression modeling can be a useful tool to investigate the effects of new drugs on disease and can provide insight into the activity of the drug on disease progression. Models can be developed to incorporate the effects of changing disease status over time, the effects of placebo or concomitant therapy and can therefore increase the amount of information obtained from a clinical trial. Furthermore, these models can be used to explore alternative dose regimens and provide information on dose adjustments.

## 3.1    Introduction

In 1995, Sheiner and Rubin pointed out that evaluations for significance levels of clinical trial outcomes and their associated estimates were generally conducted using the intention-to-treat principle. In that paper, the authors noted that the intention-to-treat estimator estimates "use-effectiveness", which is the causal effect on outcome after prescribing the drug, regardless of whether

the patient takes the drug or not, rather than the medically more relevant "method-effectiveness", which represents the causal effect on outcome after actually taking the drug. Several arguments have been made against using an as-treated or "method-effectiveness" approach. Lee et al. (1991) argued that using an as-treated approach would potentially disturb the prognostic balance brought about by randomization, reduce the sample size, and undermine the validity of statistical test procedures.

While many statistical methods can provide an unbiased comparison of treatment effects when all missing observations are ignorable, in many cases missing data are not ignorable (Little and Rubin 2000). Consequently, the use of as-treated

D.R. Mould
Projections Research, Inc., 535 Springview Lane,
Phoenixville, PA 19460, USA
e-mail: drmould@pri-home.net

evaluation methods have gained in popularity because they provide a conceptual framework for dealing with the problems posed by deviations from the planned protocol, particularly those arising from noncompliance and drop-out (Sheiner 2000; Sheiner and Rubin 1995). Drop-out in particular has been an issue that is difficult to deal with during the evaluation of clinical trial data. For example, the last observation carried forward (LOCF) is a commonly employed strategy that imputes a missing observation at the end of the study for an individual that has dropped out as the last observed value for that subject, i.e. the patient's last observed value is used for all subsequent missing values. However, most diseases and the associated biomarkers that evolve over time follow a smooth trajectory, so that the last observed biomarker response is usually a biased estimate of the true last value. If the response being evaluated were a measurement for a progressive chronic disease, then application of LOCF would imply that once a patient drops out, the disease status stays fixed at the last observed value despite the fact that the biomarker would ordinarily be expected to change in accordance with the natural history of the disease. Other methods such as incomplete-data methods based on models that assume random dropout, have serious drawbacks as well (Little and Yau 1996). Imputing the missing data using a model that describes the expected trajectory of the disease should therefore provide a less biased estimate of missing data (Diggle and Kenward 1994; Little and Rubin 1987).

In a clinical trial, the available information is dependent on the ratio of signal to noise in the data. Information is the total variation in the data, the signal is the variation due to identifiable causes such as differences in dose or other treatment, and noise is the unexplained variation. Jonsson and Sheiner (2002) and others (Sheiner and Rubin 1995; Little and Rubin 2000) have suggested that greater statistical power for the determination of drug effect can be achieved through model-based evaluations rather than through traditional evaluations because models increase the amount of information by providing a basis for explaining the

variation in the data, thereby improving the signal to noise ratio. Furthermore, with repeated measures assessment, random error on clinical observations can be appropriately accounted for in the model. Ultimately, if controlling or modifying the trajectory of the disease over time is the goal of treatment, then an endpoint defined on the observed disease trajectory with and without treatment may yield a more powerful test than one based on observing a less informative binary outcome, such as response rate. However, the ability to develop a model that appropriately describes the disease trajectory involves an understanding of the underlying pharmacology of both the disease and the drug effect, and sometimes an understanding of the physiology and biochemistry of the system.

Clinical pharmacology is the science of understanding drugs as applied to their use in the treatment of disease. It is underpinned by the basic science of pharmacology, focusing on the application of pharmacological principles and methods in clinical practice. The science of clinical pharmacology covers a broad range of topics, from the discovery of new target molecules to the understanding and quantifying the effects of drug usage in patient populations. However, in the context of drug development, clinical pharmacology can also be perceived as a model itself – specifically, the combination of disease progression and drug action (Holford and Sheiner 1981; Holford et al. 2006):

$$\begin{aligned} &\text{Clinical pharmacology} \\ &= \text{disease progress} + \text{drug action.} \end{aligned} \tag{3.1}$$

In this equation, "disease progress" refers to the evolution or trajectory of a disease over time. Specifically, this implies that a function or model, either empirical or mechanistic, can be used to describe the time course of a biomarker or clinical outcome reflecting the status of a disease, which is a reflection of the state of the disease at any given point in time. In an untreated state, disease status may improve or worsen over time, or may exhibit periodic behavior, improving and worsening over time. Therefore, a model of disease progress, which is a special class of pharmacodynamic model, is a

**Fig. 3.1** Response surface for a drug. The shaded area represents the response surface. The dot is the expected response of a patient given his covariates and present dose regimen. Altering the dose in the direction of the *arrow* would result in an anticipated improvement in benefit
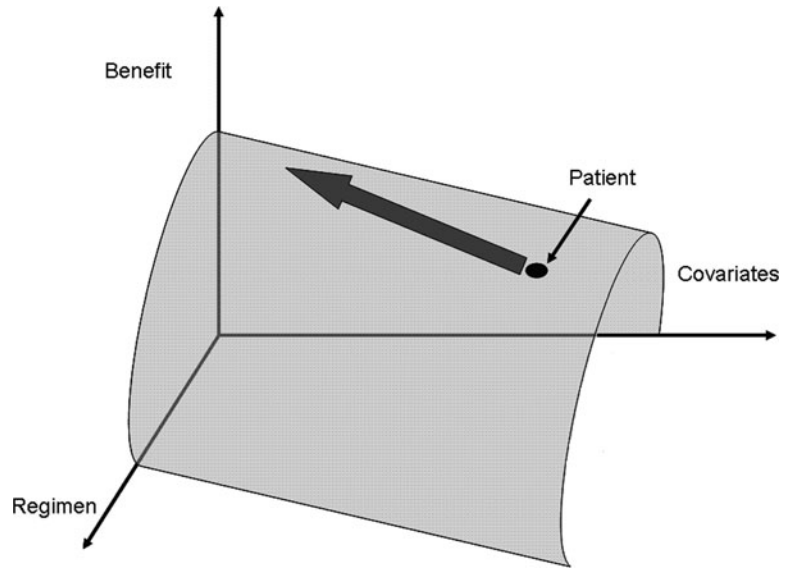


mathematical function or expression that describes the expected trajectory of a disease, as measured by specific biomarkers, over time.

The term "drug action" involves the pharmacokinetic and pharmacodynamic processes involved in producing a beneficial effect on the disease. The drug effect is assumed to influence the disease status either by providing transient improvement (e.g. symptomatic drug action) or by altering the trajectory of the disease (e.g. disease modifying drug action). Pharmacokinetic and pharmacodynamic characteristics determine the drug exposure, action and its subsequent effect on the progression of the disease. In the equation above, drug action would also include the effect of placebo on disease progression. Placebo effects, as will be discussed later in this chapter, can constitute a substantial component of disease trajectory in a clinical trial.

Because of demographic and other patient factors, together with patient compliance with scheduled treatment, not all patients will exhibit the same response to a selected dose of a test drug. Furthermore, not all patients will progress in their disease at the same rate. In addition, dose adjustments due to adverse events, compliance and drop-out will increase the overall noise in the data collected.

During the drug development process, it is not feasible to investigate all potential treatment modalities. However, evaluation of the pharmacokinetic and pharmacodynamic behavior of the drug in various patient populations can be used to develop a response surface (Fig. 3.1), which can be used to estimate the expected response in a subset of patients at a given dose given their covariate factors.

The response surface, as described by Sheiner (1997) as a part of the learning and confirming process in drug development, is a function of the models for drug action and disease progression the shape of which is influenced by patient factors, such as demographics, and disease that may make a patient more or less sensitive to drug effect or may result in higher or lower drug exposure. Used in this context, disease progression models can be valuable to facilitate the visualization of underlying disease changes both for the reference treatment and the treatment being evaluated.

An additional benefit of developing disease progression models is that such models provide a basis for learning from prior clinical experience and summarizing the knowledge in a quantitative fashion. Employing disease progression models to

design clinical trials and overall drug development strategies can help streamline investigation and strengthen "Go/No-Go" decisions. As models of disease progression are largely independent of therapeutic intervention, this knowledge can be retained, used for other therapeutics, and refined over time. Furthermore, the United States FDA supports and also develops models of disease progression as a means to evaluate drug effects (Gobburu and Lesko 2009).

## 3.2 Overview of Basic Disease Progression Models

Evaluating disease progression through model-based evaluations was first proposed by Holford and Sheiner (1981). In this paper, the authors proposed a new interpretation of an old model:

$$E(t) = E_0 + \frac{E_{\max} C_{\mathrm{p}}(t)}{EC_{50} + C_{\mathrm{p}}(t)}. \qquad (3.2)$$

In this equation, $E(t)$ is the measure of disease status at some time $t$. $E_0$ represents the disease status at baseline. $E_{\max}$ and $EC_{50}$ are the largest effect that can be achieved by the drug and the drug concentration that achieves half maximal response, respectively. $C_{\mathrm{p}}(t)$ is the drug concentration at the time $t$.

This function represents a "zero progression" model for disease status where, over the course of evaluation, the observed untreated disease status does not change except through therapeutic drug intervention. In this sense, the zero progression model is analogous to the LOCF approach, in that when drug is discontinued, the disease status will remain fixed.

However as noted previously, disease status generally does not remain stable, but instead follows a smoothly changing trajectory. In order to account for the change in status over time, the "zero progression" model was expanded to allow for disease status to change over time using a linear function:

$$S(t) = S_0 + \alpha t. \qquad (3.3)$$

In this equation, $S(t)$ is the disease status at time $t$, $S_0$ represents the baseline disease status and $\alpha$ represents the rate of change of the status over time. The effect of drug on disease progression generally is not instantaneous. Therefore, the use of a lag time or an "effect compartment" (Holford and Sheiner 1982) is commonly employed to allow for a delay between the initiation of treatment and observable response.

Drug effect can provide symptomatic benefit resulting in a transient improvement in the disease status during treatment, but which rapidly reverses to the untreated status after treatment is discontinued. In this type of model, the drug effect is added (or subtracted) from the overall disease status.

$$S(t) = S_0 + E_{\mathrm{symptom}}(\mathrm{Ce_A}) + \alpha t. \qquad (3.4)$$

In this equation, $E_{\mathrm{symptom}}(\mathrm{Ce_A})$ represents a drug effect that provides symptomatic benefit, shifting the status $S(t)$ above its untreated trajectory.

Conversely, the effect of treatment can be described as altering the progression of disease. For a protective or disease modifying drug, the disease status would not return to the pretreatment course when therapy is discontinued, but would be expected to result in a permanent improvement. In this case, the drug effect is applied directly to the disease progression parameter $\alpha$.

$$S(t) = S_0 + (E_{\mathrm{progression}}(t) + \alpha))t. \qquad (3.5)$$

In this equation $E_{\mathrm{progression}}(t)$ is the effect of treatment on the disease progress. Again, if a long delay between initiation of treatment and onset of effect is observed, an effect compartment can be implemented.

The time course of both symptomatic and disease modifying activity are presented in Fig. 3.2. In this figure, the light black dashed lines are the drug concentration over time, the
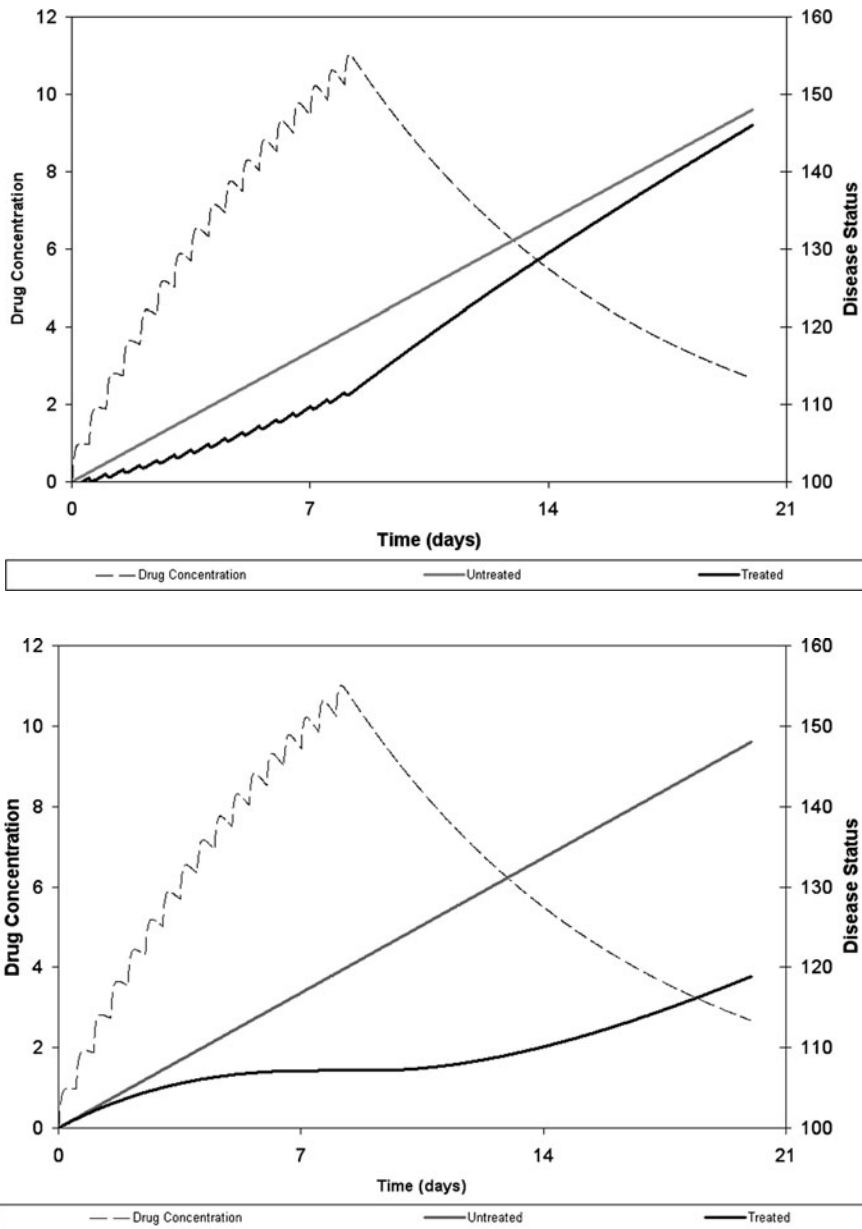
**Fig. 3.2** Symptomatic and disease modifying drug effect on the progression of disease. The *dashed lines* are drug concentration. *Heavy solid line* is the natural time course of untreated drug. The light line is the progression following symptomatic treatment (panel A) or disease modifying treatment (panel B). Note that the cessation of treatment in panel A results in the patient disease rapidly returns to pretreatment status; this is not the case in panel B

heavy solid black line is the natural (untreated) progression of the disease and the wide light gray solid line is the disease trajectory in the presence of drug. There are numerous other functions that have been developed in addition to the simple linear function and there are several good

publications that review various structural disease progression models and associated parameterizations for describing the effect of treatment on disease progression (Holford and Sheiner 1981; Mould 2007).

## 3.3 Examples of Disease Progression Models

In the following sections, several examples of disease progression models for different therapeutic areas will be discussed. These examples represent a sampling of published work. A wide variety of structural models have been used to describe both disease progression and drug response. Each model must be tailored to the specific disease and treatment being studied. In developing models of disease progression, the analyst should realize that one of the most important aspects of the disease progression model is the characterization of the relationships between the biomarker(s) being collected and the clinical outcome of that therapeutic intervention. Thus, whenever possible, these models should replicate physiological aspects of the disease being modeled. However, in many diseases the mechanistic basis of disease is not well understood, necessitating the use of empirical models.

### 3.3.1 Models for CNS Diseases

#### 3.3.1.1 Clinical Depression

Designing clinical trials to evaluate treatment for major depression is challenging in part because of the pronounced placebo response that may be significantly affected by the trial design [http://www.wired.com/medtech/drugs/magazine/17-09/ff_placebo_effect?currentPage=all]. In fact, more than half of all recent clinical trials of commonly used antidepressants failed to show statistical superiority for the drug over placebo, primarily due to placebo response (Khan and Schwartz 2005; Dworkin

et al. 2005). Khan et al. evaluated the results from 52 randomized, double-blind, placebo-controlled clinical trials obtained from the FDA in an attempt to correlate placebo response as the percentage mean change from baseline in the Hamilton depression rating scale (HAMD) with trial outcome (Khan et al. 2003). In trials with a large mean placebo response (e.g. a greater than 30% mean change from baseline), only 21% of these trials found active treatment superior over placebo. However, in trials with a low placebo response, a greater proportion of the trials (74%) showed superiority of the active treatment. Review of existing controlled trials demonstrates a wide variety in study methodology. Factors such as small sample sizes, inclusion/exclusion criteria, study design, the study location, methods of patient recruitment, and choice of outcome measures all influence the ability of a study to detect differences between an antidepressant and placebo (Emslie et al. 2005). The magnitude of placebo response is variable and has an important impact on the power of antidepressant trials to detect the effect of active treatment, but that care should be taken in the evaluation of placebo effect (Kienle and Kiene 1997).

Ernst and Resch (1995) differentiated between a true placebo effect and a perceived placebo effect. The authors indicated that a perceived placebo effect is a function of several factors including the natural time course of the disease, a natural tendency for individuals to regress to the mean state, and unidentified parallel interventions. This distinction between true and perceived placebo effects is consistent with the approach taken with disease progression modeling, which attempts to describe the natural time course of the disease as well as the effect of placebo (Holford and Sheiner 1981). For example, Holford and Peace (1992a, b) used a placebo function to describe the transient improvement observed in patients with Alzheimer's disease (AD) after randomization to placebo in clinical trials.

The primary measure to assess a drug's antidepressive effect clinically is the HAMD, which is multiple choice questionnaire administered by

a health professional, usually a nurse (Hedlung and Vieweg 1979). Although the original test, developed in 1960 on patients in an asylum, had 17 questions, there are currently different versions of the test available with the most common version having 21 items that assess mood, insomnia, suicide, somatic symptoms, etc. With the 21 item version, scores can range from 0 to 66 with increasing score indicating increasing disease severity.

Several models used to describe the time course of depression have been reported in the literature, most of which all use HAMD scores as the dependent variable. Schematic diagrams of these models are provided in Fig. 3.3. All these models assume that HAMD scores can be adequately modeled as a continuous random variable having a normal or log-normal distribution, despite the variable actually being a bounded one. The impact of this distributional assumption has yet to be examined. The physiological basis for depression is not well understood and all functions are largely empirical in application. The first such model used to describe the time course of depression was the inverse Bateman function (Holford et al. 2002). The equation for the inverse Bateman function, which describes a smooth decrease of HAMD scores over time, is given below:

$$
\begin{aligned}
\text{HAMD} = S_0 - D_{\text{rec}} &\left( \frac{K_{\text{rec}}}{K_{\text{rec}} - K_{\text{ons}}} \right) \\
&\times \left( e^{(-K_{\text{ons}}t)} - e^{(-K_{\text{rec}}t)} \right) \\
&+ \varepsilon_{\text{additive}}.
\end{aligned}
\tag{3.6}
$$

In this equation, $S_0$ is the baseline HAMD score. $K_{\text{rec}}$ is the apparent rate constant of spontaneous recovery from depression. $K_{\text{ons}}$ is the apparent rate constant of spontaneous worsening of depression. $\varepsilon_{\text{additive}}$ is the residual error. $D_{\text{rec}}$ is a scaling function for the maximum decrease from baseline.

The second type of model that has been proposed for describing the time course of depression is an indirect effect type model after the work proposed by Dayneka et al. (1993). There have been several modifications of the indirect effect model used to describe depression data. Gruwez et al. (2005) proposed a modified version in which antidepressants exert their effect by increasing the transduction set-point or by increasing the rate of feedback mechanisms. A second variant of the indirect effect model used to describe the time course of clinical depression was the Kinetic-PD (KPD) model (Jacqmin et al. 2001; Pillai et al. 2004) which uses a dose based forcing function (e.g. a virtual dose driving rate)
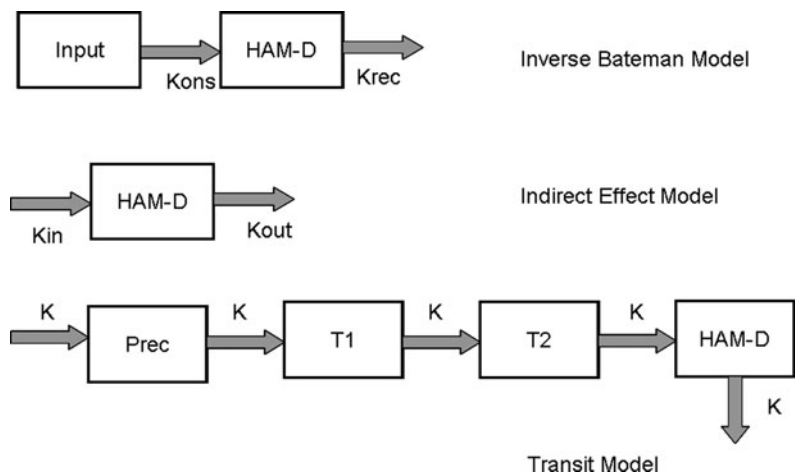


**Fig. 3.3** Schematic diagrams for structural models evaluated for depression. Three commonly used depression models are provided above

instead of measured concentrations to affect a change in the observed HAMD score. The model was successfully applied to placebo data from clinical trials of major depression (Cosson and Gomeni 2005). The equation for the indirect effect model is given below:

$$\frac{dHAMD}{dt} = (K_{in} - K_{out}HAMD(1 + Slope\, C_{placebo})) + \varepsilon_{additive}. \quad (3.7)$$

In this equation, $K_{in}$ is the rate of spontaneous worsening of depression and $K_{out}$ is the rate of spontaneous improvement. Prior to the initiation of treatment this function assumes that there is no change in HAMD and that the baseline HAMD score is equal to $K_{in}/K_{out}$. Consequently, this function requires an external function to cause a decrease in HAMD score, which can be accomplished by assuming that the placebo effect is described by a "placebo concentration–time model" or by use of a more standard KPD type function. The effect of "placebo concentration" ($C_{placebo}$) in the equation above was described using a linear function applied as a stimulatory effect on $K_{out}$ using a scale factor (Slope) to adjust for different degrees of individual response.

Shang et al. (2006, 2009) evaluated the inverse Bateman and the indirect effect models, and also tested a two-transit-compartment model (Friberg et al. 2000) for the ability to describe the time course of placebo response in depression. The equations for a two-transit-compartment model are presented below:

$$\frac{dP_{rec}}{dt} = KS_0(1 - Slope\, C_{placebo}) - KP_{rec}$$
$$\frac{dT1}{dt} = KP_{rec} - KT1$$
$$\frac{dT2}{dt} = KT1 - KT2$$
$$\frac{dHAMD}{dt} = KT2 - K\, HAMD$$
$$HAMD = HAMD(t) + \varepsilon_{additive}$$
$$(3.8)$$

In these equations, $S_0$ is the baseline HAMD score, $P_{rec}$ is the amount in a precursor pool compartment, T1 and T2 are transit compartments and

HAMD is the observation compartment. Rate constants of transfer between compartments ($K$) are assumed to be equal and reflect the rate of spontaneous improvement. The value for $K$ is determined based on the mean transit time (MTT) between compartments where $K = $ MTT/3.

The results obtained from an evaluation of data pooled from four clinical trials of major depression using the inverse Bateman function were presented in 2005 (Holford et al. 2002) and the associated parameter values for that evaluation are presented in Table 3.1. A visual predictive check for one of the four studies is shown in Fig. 3.4. Notably, the half life of recovery (THR) is approximately 60 days and the half life of onset (THO) is approximately 280 days, although the duration of the studies included in the database appear to have been no longer than approximately 84 days (12 weeks), suggesting that the inverse Bateman function is not well informed when used to describe placebo response to depression. Shang et al. (2009) found the indirect effect and transit-type models preformed adequately to describe depression, providing parameter estimates that were reasonable and robust.

Further complicating the interpretation of data obtained from studies of clinical depression is the fact that the time course of depression in humans is known to be cyclical with episodes of depression and typically spontaneous remission (see Fig. 3.5). Despite the definition of a specific cyclical syndrome, seasonal affective disorder (Magnusson 2000), there is almost no quantitative description of the pattern of depression within an episode and from episode to episode in patients with clinical depression. The largest

**Table 3.1** Reported (Holford et al. 2002) parameter values for placebo model using inverse Bateman function

| Parameter (units) | Population value |
| --- | --- |
| $S_0$ (HAMD) | 24 |
| $T_{lag}$[a] (days) | 4.7 |
| $D_{rec}$ (HAMD) | 20.6 |
| THR (days) | 60 |
| THO (days) | 280 |

[a]$T_{lag}$ was included in the model to account for the run in interval prior to administration of placebo or active drug which was approximately 7 days
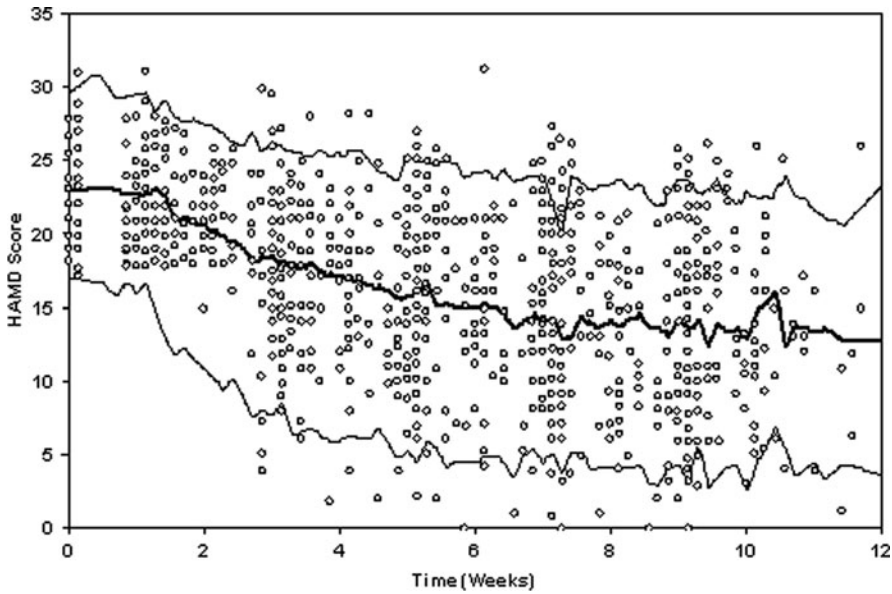
**Fig. 3.4** Simulated 95% prediction intervals and observed HAMD versus time – derived from Holford et al. (2002). Observed HAMD scores over time overlaid on a prediction interval. The central *solid line* is the median simulated value, the upper and lower lines are the upper and lower 95% prediction intervals

**Fig. 3.5** Theoretic cyclical pattern of Hamilton depression scores (HAMD) over time. The time course of depression is generally cyclical with periodic worsening and improvement
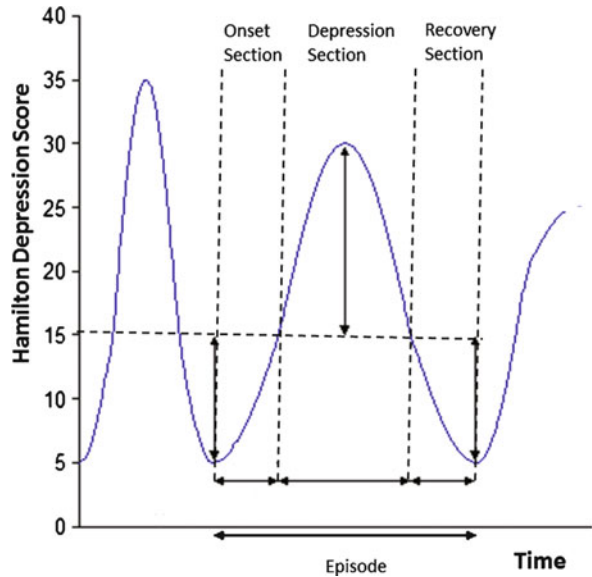


collections of data in depressed individuals arise in the setting of clinical trials of antidepressants, but these trials are typically short (approximately 6–8 weeks) and span less than half of a typical episode of depression. Consequently, the cyclical trends in HAMD scores over time can be difficult to quantify in most studies, and therefore, contribute to the random noise seen in the measured outcome (e.g. usually change from baseline HAMD score). However, addition of these

cyclical functions can reduce the unexplained variability in the data, making the effect of drug easier to evaluate.

$$HAMD(t) = DiseaseProgress(t)$$
$$+ SAD_{amp} \cos\left(\frac{2\pi}{12}(Month - Phase)\right). \quad (3.9)$$

In this equation, DiseaseProgress(t) is the function used to describe the general disease trajectory (e.g. a transit function or indirect response model), $SAD_{amp}$ and Phase define the amplitude of the seasonal change in HAMD and the time of the peak worsening of HAMD, respectively. "Month" is the month the observation was made. "Phase" is the interval of time to complete a cycle. For studies of sufficient duration, the application of a linked cosine function can be useful to characterize the underlying periodicity of the disease. A periodic function can also be valuable for other diseases that exhibit cyclical behavior such as psoriasis and osteoporosis.

### 3.3.1.2 Alzheimer's Disease

AD is the most commonly occurring disease within the group of disorders known as "dementias" with a rising global prevalence. AD is an irreversible, progressive neurodegenerative disorder, characterized by gradual cognitive deficits associated with abnormal behavior, and personality changes, which ultimately leads to dementia. The pattern of cell loss and mental function in normal aging is different from the pattern observed patients with AD (Yew et al. 1999). The histopathological hallmarks of AD are neurofibrillary tangles and amyloid plaques.

Currently, there is no cure for AD, nor can its progression be reversed. However, there are several agents approved for the symptomatic treatment of AD including cholinesterase inhibitors (e.g. donezepil, rivastigmine, galantamine) and memantine. Cholinesterase inhibitors are used in mild to moderate AD to prevent the breakdown of acetylcholine, which is believed to be important for memory and thinking. As AD progresses,

however, the brain produces less acetylcholine and cholinesterase inhibitors therefore eventually lose their effectiveness. Memantine is prescribed to treat moderate to severe AD and is an N-methyl D-aspartate (NMDA) antagonist that works by regulating glutamate, which when produced in excessive amounts may lead to brain cell death. Recently, attention has been given to prevention of formation of neurofibrillary tangles and amyloid plaques since they are found in the cerebral cortex of AD patients and are thought to be responsible for the neuronal loss seen in the brain. It is believed that strategies for preventing and/or altering amyloid fibril formation represent therapeutic values (Schenk et al. 1995; Kisilevsky 1996). A number of other treatments, including vitamin E (which has become less frequently used (Dysken et al. 2009), estrogen (Henderson 2009) and antiinflammatory drugs (Szekely et al. 2008) have shown some promising early results, but are not yet proven for routine use. There is increasing evidence that diet and cholesterol may play a role in the development of the plaques (Solomon and Kivipelto 2009). Controlled clinical trials of statins are assessing whether the rate of decline in AD can be modified or slowed by these medications.

Disease progression for AD is based on several measurements, including the mini mental state examination (MMSE), dementia rating scale (DRS), clinical dementia rating (CDR), and the Alzheimer's disease assessment scale – cognitive (ADAS-Cog). Magnetic resonance imaging (MRI) and positron emission tomography (PET) are also used to evaluate structural and functional alternations in the brain. These assessments have different scales and most provide a summary measure of a variety of cognitive, emotional, and physical performance attributes. A listing of some of the more commonly used assessment scales is presented in Table 3.2. The majority of scales start at low values and the scores increase as impairment increases.

Comparison of disease progression and drug activity across studies that have employed different metrics of disease progression is therefore difficult. Chan and Holford (2001) evaluated the natural progression of AD across several

**Table 3.2** Overview of commonly utilized scales for assessment of Alzheimer's disease status

| Measurement scale | Abbreviation | Component evaluated | Range |
|---|---|---|---|
| Alzheimer's disease assessment scale | ADAS | Total | 0–120 |
| | | Noncognitive | 0–50 |
| | ADAS-Cog | Cognitive | 0–70 |
| Blessed dementia scale | BDS | Total | 0–27 |
| | | ADL | 0–16 |
| | | Cognitive | 0–17 |
| Blessed information memory concentration | BIMC | – | 0–33 |
| Behavior rating scale for dementia | BRSD | Total | 0–164 |
| Clinical dementia rating (in six categories) | CDR | – | 0–3 |
| Clinician's interview-based impression of change | CIBIC | – | 1–7 |
| Sum of boxes (global CDR) | CDR-SB | – | 0–18 |
| Dementia rating scale[a] | DRS | – | 0–144 |
| Extended scale for dementia | ESD | – | 0–250 |
| Global deterioration scale | GDS | – | 0–7 |
| Mini mental state examination[a] | MMSE | – | 0–30 |
| Progressive deterioration scale | PDS | – | 0–100 |
| Severe impairment battery[a] | SIB | – | 0–100 |

[a]Lower scores are associated with greater impairment

common assessments. Despite obtaining the absolute values of disease status at different time points and expressing the changes as a percentage of the baseline value, this comparison showed a fairly wide range of progression rates. At 5 years, percent change from baseline ranged from approximately 100 to 400% across all studies and scores compiled. When evaluated separately, the rate of progression of AD is generally slow. Imbimbo et al. (1999) reported an annual worsening of 10.2 points on the ADAS-Cog scale. Birks (2006) compared the effects of donepezil, galantamine, and rivastigmine in people with mild, moderate, or severe AD. Based on the results of 13 randomized, double blind, placebo controlled trials over treatment for periods of 6 months and 1 year, these treatments produced improvements in cognitive function, on average −2.7 points (95% confidence interval −3.0 to −2.3), in the midrange of the 70 point ADAS-Cog scale. The small improvement may be partly due to study assessment differences, or it may be due to the limited duration of treatment.

In general, study durations for trials evaluating AD are 2 years or less; thus, the pattern of drug modification of natural disease progression is applicable only for a relatively short period of time. Therefore, while AD progression over the entire course of the disease is asymptotic because most scales of disease status have a limiting value, most disease progression models used for AD are linear. However, the use of a linear model for progression may overestimate the rate of disease progression if the progression is asymptotic.

In 1992, Holford and Peace (Holford and Peace 1992a, b) utilized a linear model of disease progression to describe the change in AD over time. The model also incorporated a function to describe a transient improvement for patients randomized to placebo, and a third function to describe the effect of drug. The overall function to assess the status at any time $t$ is given in the equation below.

$$S(t) = S_0 + \alpha t + \text{PD}(Ce_{\text{placebo}}) + \text{PD}(Ce_{\text{active}}).$$
(3.10)

In this equation, $S(t)$ is the assessment at time ($t$), $S_0$ is the baseline observation, $\alpha$ is the rate of progression, PD(Ce) is the effect of either drug or placebo, where Ce is a concentration in an effect compartment to allow for a lag between the initiation of treatment and onset of measurable
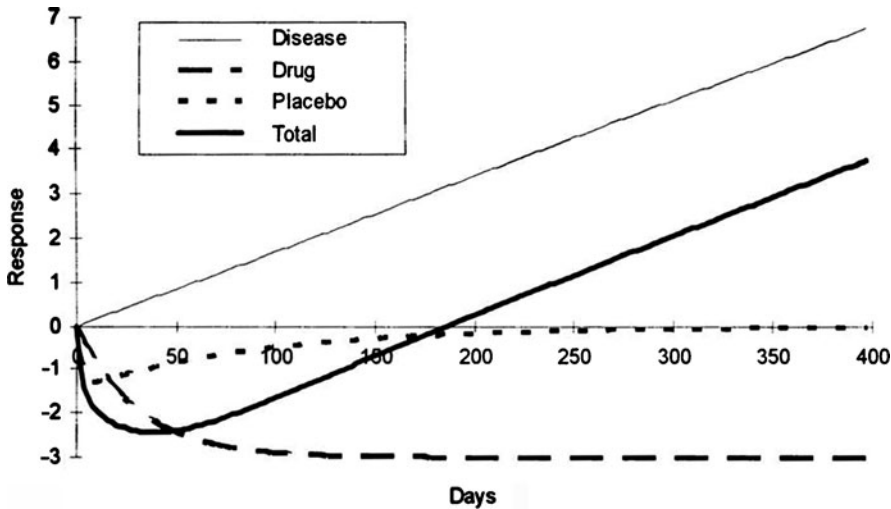
**Fig. 3.6** Progression of Alzheimer's disease – Taken from Holford and Peace (1992a, b). The observed score for Alzheimer's disease (*heavy solid line*) is a sum of several functions including the natural progression, a placebo effect, and a drug effect

improvement. This function is presented in Fig. 3.6 below.

In general, model-based results have shown consistent estimates of disease progression and have identified modest symptomatic benefit of treatment. Gobburu et al. (2001) utilized a similar model to describe the effects of rivastigmine on AD progression. This evaluation described computerized neuropsychological test battery (CNTB) scores, although the authors were not able to correlate drug exposure to improvement in CNTB. Ito et al. (2010) conducted a systematic review of published data from 1990 to 2008 of all available cholinesterase inhibitor studies as well as clinical studies that evaluated the rate of deterioration in AD patients. The authors developed a linear model describing the longitudinal response in the AD based on change from baseline ADAS-Cog in patients with mild to moderately severe AD. An $E_{max}$ type model was developed to describe the symptomatic benefit of active treatment. Brooks et al. (1993) proposed a triphasic linear model to describe the time course of AD. This model incorporates a lag time or a latent phase before the start of the period of constant rate of deterioration, followed by a resistance phase where there is no further worsening of disease status. While the triphasic model has more flexibility than the simple linear model, over the limited duration of a clinical trial there appears to be little difference in model performance.

### 3.3.2 Models for Hematopoiesis

Hematopoiesis is the process of forming and maintaining stable populations of blood cells in the body. When this process is disturbed either through disease or chemically mediation (e.g. through administration of chemotherapy), the first cell population to be affected is usually neutrophils (which have a life span in the blood of only 6–8 h) followed by platelets (with a 10-day life span). Anemia develops more slowly, over a much longer span of time (since the red blood cells have a 120-day lifespan).

All blood cells develop from pluripotent stem cells found in the bone marrow. These stem cells are able to proliferate as well as differentiate into the different types of blood cells, and are able to renew themselves. The pluripotent stem cell is the progenitor of two multipotential stem cell lines: the myeloid and the lymphoid lines. Myeloid stem cells are precursors of granulocytes,
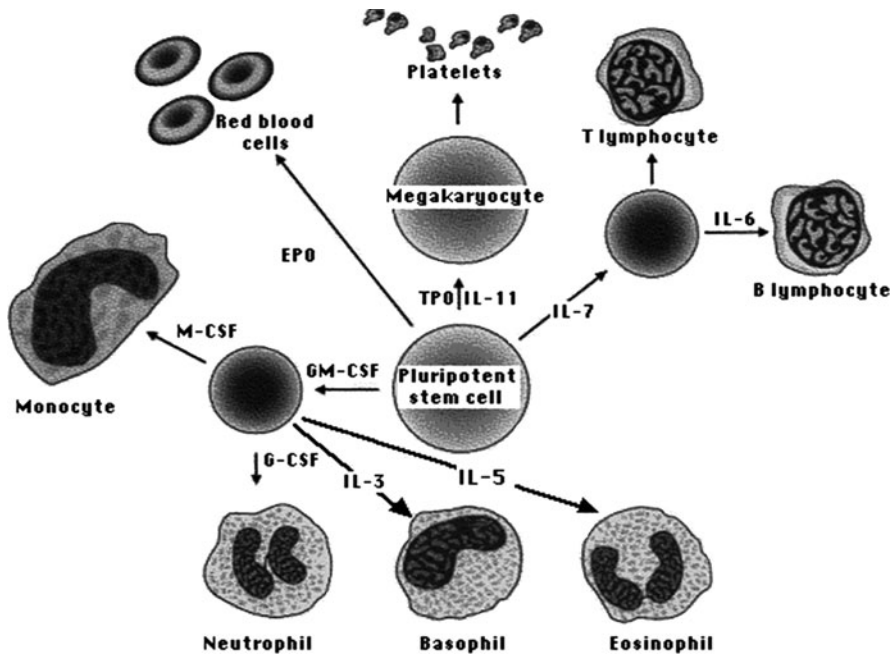
**Fig. 3.7** Hematopoietic maturation. Hematopoiesis involves a complex process that is controlled by precursor cell availability and cytokines. All cells arise from a pluriponent stem cell, then differentiate during the maturation process as shown above is determined by cell specific cytokines

monocyte, red blood cells, and platelets. Lymphoid stem cells are precursor of lymphocytes. The production of blood cells is largely controlled by feedback. When the demand for production of cells of a particular type of cells increases or the levels of the cells fall in blood, cytokines are released that stimulate stem cells to differentiate and mature into blood cells. The cytokines are specific for each cell type. A schematic pathway for the hematopoietic process is provided in Fig. 3.7. As can be seen, there are several cytokines that can stimulate the differentiation and maturation of various cell populations.

### 3.3.2.1 White Blood Cells and Neutropenia

Although it is somewhat less common than anemia or thrombocytopenia, neutropenia can develop if neutrophils are depleted faster than the bone marrow can produce new ones. This can occur with some types of acute bacterial infections, allergic disorders, and drug treatments, particularly chemotherapeutic regimens. In addition, certain autoimmune diseases can induce the

formation of antibodies that target neutrophils, resulting in neutropenia. In addition, an enlarged spleen may result in neutropenia because the enlarged spleen traps and destroys neutrophils more efficiently than a small spleen.

Neutropenia can also develop if the production of neutrophils in the bone marrow is reduced, as can occur in with cancer, viral infections such as influenza, bacterial infections such as tuberculosis, myelofibrosis, or deficiencies of vitamin $B_{12}$ or folate. Radiation therapy that involves areas of the bone involved in white cell production may also result in neutropenia. Many drugs, including phenytoin, chloramphenicol, sulfa drugs, and chemo therapeutic agents, as well as certain toxins (e.g. benzene and insecticides) can also impair the bone marrow's ability to produce neutrophils.

Because one of the primary causes of neutropenia is administration of chemotherapeutic agents, and neutropenia is one of the more common dose-limiting toxicities associated with the administration of chemotherapeutic agents (e.g. paclitaxel; Rowinsky et al. 1993), more attention has been paid to developing models to

describe the time course of neutropenia following chemotherapy than to describing neutropenia arising from other conditions. Empirical models such as the $E_{max}$ model have been used to relate summary measures of drug exposure to the nadir white cell count (Egorin et al. 1986; Hantel et al. 1990; Erlichman et al. 1991). Attempts to correlate the degree of neutropenia with steady-state paclitaxel concentrations have been tried but were generally unsuccessful (Rowinsky et al. 1999). The degree of neutropenia has also been associated with the length of time that drug concentrations exceed a critical threshold concentration (Eisenhower et al. 1994; Gianni et al. 1995). Consequently, the pharmacokinetic/pharmacodynamic relationship between paclitaxel exposure and neutropenia has often been described using a threshold model (Gianni et al. 1995; Henningsson et al. 2001, 2003). Karlsson et al. (1998) proposed a more elaborate model relating drug exposure, time above a threshold concentration, between the concentration–time profile of free paclitaxel and the decrease in white blood cell or neutrophil count.

Another frequently used approach is to link the grade of neutropenia with a summary measure of exposure using logistic regression (Mould et al. 2002). This approach is commonly taken when there are insufficient data (e.g. neutrophil counts over time) to describe the data using a continuous function or when there is not enough time to do a more fully developed semimechanistic model. Both logistic and empirical models are often used to describe the data obtained from a particular dose regimen; they are easy to develop and implement. However, logistic mod-

els have limited utility to extrapolate to other doses or dose regimens. In order to better characterize the relationship between drug exposure and neutropenia, more mechanistic models are preferable as these models are also capable of providing better predictions of untested doses and schedules.

One of the issues associated with developing a mechanistic model for neutropenia was the long lag between drug exposure and response. For paclitaxel, the onset of neutropenia occurs 8–10 days following treatment and recovery is not complete until day 15–21. Various indirect effect type models were tested to account for this lag between drug administration and effect (Minami et al. 1998). However, the model currently in vogue is a transit-type semiphysiological model developed by Friberg et al. (2000), which appears to work well across a variety of antineoplastic agents (Friberg et al. 2002). A schematic for this model is presented in Fig. 3.8.

Granulocyte colony-stimulating factor (G-CSF) is produced by monocytes, fibroblasts, and endothelial cells and is a physiologic regulator of neutrophil production and function and is used in the treatment of neutropenia. G-CSF is an endogenous cytokine that regulates the production of neutrophils by stimulating neutrophil progenitor proliferation (Zsebo et al. 1986; Welte et al. 1987) and differentiation (Duhrsen et al. 1988). G-CSF is cleared by glomerular filtration and also undergoes clearance through binding to receptors on the surface pluripotent stem cells as well as on neutrophils (Kotto-Kome et al. 2004). Binding to the pluripotent cells affects the differentiation of the stem cells with eventual

**Fig. 3.8** Schematic of white blood cell transit model. A schematic for white blood cell maturation is provided above. This model has a precursor compartment, three transit compartments, and a compartment for observed cell counts. The model has a feedback loop that will regulate cell counts to mimic the hemostasis
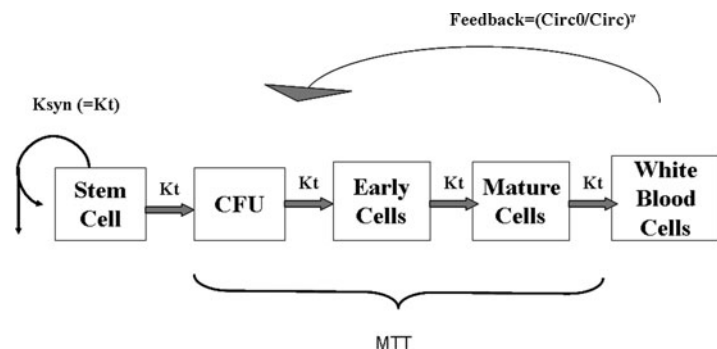
maturation to neutrophils. Binding to neutrophils plays a critical role in hemostasis, increasing clearance of G-CSF from both endogenous and exogenous sources when cell counts are high as a means of controlling neutrophil count by a feedback mechanism (Terashi et al. 1999), or reducing clearance when neutrophil counts are low. This feedback mechanism is reflected in the model for neutropenia proposed by Friberg et al. (2000). Because G-CSF works to increase circulating neutrophils, receptor-mediated clearance of G-CSF increases the course of treatment based on individual response (Kuwabara et al. 1996). Terashi et al. (1999) have also shown that G-CSF receptor density increases on neutrophils in the presence of G-CSF, further increasing its clearance. Consequently, there is a strong pharmacokinetic–pharmacodynamic interaction with this agent and therefore, a physiological limitation to the pharmacodynamic activity of G-CSF. There are other feedback mechanisms, including interactions between other cytokines. For example, inhibition of binding of G-CSF by human neutrophils has been observed in the presence of excess unlabeled human granulocyte-macrophage colony-stimulating factor (GM-CSF), suggesting competition or down modulation by GM-CSF of the G-CSF receptor. Finally, there is also a potential mechanism referred to as "lineage steal" (Papaldo et al. (2006) where administration of one cytokine (e.g. GCSF) can transiently reduce the pool of pluripotent stem cells available for maturation into other cell lines resulting in mild anemia or thrombocytopenia. This has been reported in patients (Papaldo et al. 2006) although as seen below, cancer itself as well as chemotherapy can result in anemia, making this process difficult to evaluate.

### 3.3.2.2 Red Blood Cells and Anemia

In the early 1950s, investigators reported that red blood cells exist for a fixed duration of time (Mollison 1952–1953) or lifespan. Most estimates for the lifespan of a red blood cell in healthy patients are approximately 120 days. The effect of diseases such as leukemia (Berlin et al. 1951) and renal impairment (Chaplin and Mollison 1953) were subsequently found to shorten red cell lifespan, resulting in anemia. For patients with renal impairment, properties of the uremic environment such as inflammation, increased oxidative stress and uremic toxins may result in premature changes in red cell membrane and cytoskeleton. Exposure of antigenic sites and breakdown of the phosphatidylserine asymmetry may therefore increase red blood cell phagocytosis (Kruse et al. 2008).

As with renal failure, cancer-related anemia can be caused by a number of factors. It can occur as a direct effect of the tumor, it may be due to products of the cancer cells, or it may develop as a result of the cancer treatment itself. A listing of some of the causes for anemia arising as a direct effect of the neoplasm is presented in Table 3.3. Other causes of anemia in malignancy include known substances or proteins produced by the cancer. Excessive amyloid deposition and antibody formation are primary compounds produced by neoplasm that can cause anemia. The deposits of amyloid in myelomas and amyloidosis can be extensive enough to replace the bone marrow. The development of antibodies in chronic lymphocytic leukemia, lymphoma, and sometimes solid tumor malignancies can lead to immune hemolytic anemias.

**Table 3.3** Tumor based causes of cancer-related anemia

| Clinical cause of anemia | Types of cancer |
| --- | --- |
| Exogenous blood loss (acute or chronic) | Gastrointestinal malignancies |
| | Head and neck cancer |
| | Genitourinary cancers |
| | Cervical and vaginal cancers |
| Intratumor bleeding | Sarcomas |
| | Bulky melanomas |
| | Hepatoma |
| | Ovarian cancer |
| | Adrenocortical tumors |
| Anemia due to erthrophagocytosis | Histicytic medullary reticulosis |
| | Histiocytic lymphomas |
| | Other histiocyctic neoplasms |
| Bone marrow replacement | Leukemias |
| | Lymphomas |
| | Myelomas |
| | Carcinomas (breast, prostate) |

Furthermore, development of microangiopathic hemolytic anemia, which is seen in some solid tumor malignancies, may result from procoagulants released from cancers. While the hemoglobin trajectory in patients with cancer is usually confounded by concomitant treatment with chemotherapy or radiotherapy, at least one report has been published illustrating the hemoglobin time course in patients with cancer not receiving chemotherapy or radiotherapy (Smith et al. 2003).

Regardless of the cause of the anemia, individual response to treatment depends on both red blood cell lifespan and red blood cell production rate. Consequently, PK/PD models for hematological processes involving red blood cell formation generally assume that red blood cells are produced by a zero- or first-order process, survive for a specific cell lifespan, and then are lost to circulation. Furthermore, models predicting erythropoietin-induced changes in red blood cells or hemoglobin are generally dependent on estimates of both red blood cell production rate and lifespan.

Several structural models have been proposed for describing red blood cell or hemoglobin production. An early approach using a modified indirect pharmacodynamic model assumed that cells were produced at a constant rate, survived for a specific duration, and were then lost to circulation. The rate of cell loss was set equal to the production rate but the loss was delayed by the cell lifespan (Krzyzanski et al. 1999). This model was successfully applied to describe the change in red blood cells after administration of erythropoietin in cynomolgus monkeys (Ramakrishnan et al. 2003); however the model required the use of delay differential equations (DDEs) in order to track the cell population lifespan, making it difficult to implement. An updated model was developed that included a precursor pool, and the DDEs were modified using a numerical method of steps to facilitate analysis (Perez-Ruixo et al. 2005). The model was further altered by inclusion of a transit type model used to describe neutropenia (Friberg et al. 2000, 2002) with a precursor pool (Agoram et al. 2006) which considerably simplified the numerical methodology required to solve the differential equations (DEs) and removed the need for DDEs entirely. A somewhat further simplified model has been proposed (Holford and Sheiner 1982; Mould 2007) that does not include a precursor pool and utilizes endogenous levels of EPO to establish the baseline Hb level.

A schematic of this later, simplified model is presented in Fig. 3.9. The equations for the model are presented afterwards. One of the notable differences in this model from that published by Friberg et al. is that the red blood cell count or
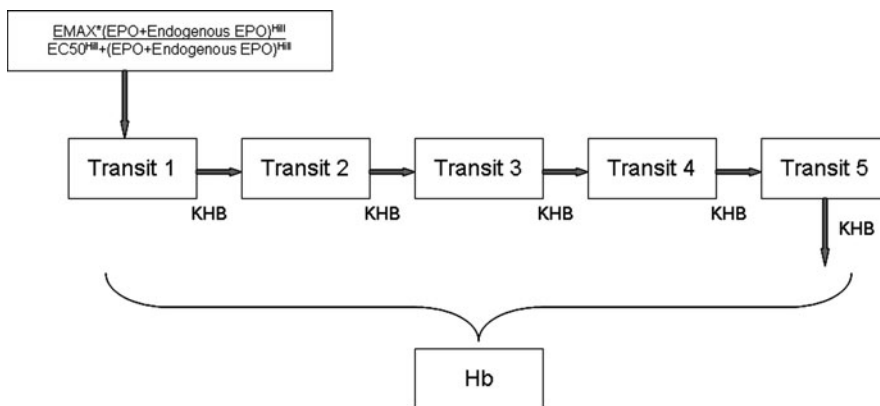


**Fig. 3.9** Schematic of red blood cell transit model. A schematic for red blood cell maturation is provided above. This model has a precursor compartment that is dependent on endogenous erythropoietin, five transit compartments, and a compartment for observed cell counts. In order to mimic lifespan, cell count is the sum of all compartments. Unlike white cells there is no feedback loop

hemoglobin level is taken as the sum of the total amounts in each of the transit compartments. This is done to allow the model to behave more like a lifespan model. In addition this model has neither the feedback that was included in the transit model for white cells, nor the loss from the first compartment. The lack of feedback is because red cell production is not regulated based on present cell counts, but rather by oxygen levels.

One of the shortcomings of the model is that it does not include the influence of iron levels. Clinical experience suggests that correcting iron deficiency can reduce the need for erythropoietin by enhancing its effectiveness. Low iron levels can also result the loss of response over time (Rizzo et al. 2002). Consequently, models of anemia should include cotherapy with iron supplements as well as transfusions administered to account for changes in the trajectory of disease.

$$\text{KHB} = \frac{1}{\text{MRT}}$$
$$\text{KHB}n = \text{KHB5}$$
$$\text{RHBO} = \frac{E_{\max}C_{\text{endogenous}}}{(\text{EC50} + C_{\text{endogenous}})}$$
$$\text{HB0} = \frac{\text{RHB0}}{\text{KHB}}$$
$$\text{Total} = C_{\text{exogenous}} + C_{\text{endogenous}}$$
$$\text{DRHB} = \frac{E_{\max}\text{Total}}{(\text{EC50} + \text{Total})}$$
$$\text{DADT}(1) = \text{DRHB} - \text{KHB}nA(1)$$
$$\text{DADT}(2) = \text{KHB}n(A(1) - A(2))$$
$$\text{DADT}(3) = \text{KHB}n(A(2) - A(3))$$
$$\text{DADT}(4) = \text{KHB}n(A(3) - A(4))$$
$$\text{DADT}(5) = \text{KHB}n(A(4) - A(5))$$
$$\text{Hb} = A(1) + A(2) + A(3) + A(4) + A(5)$$
$$(3.11)$$

### 3.3.3 Models Describing Growth

There are many therapeutic areas that utilize disease progression models of growth, including bacterial infection, viral infection, and cancer. Several examples of models for growth are presented in the following sections. More discussion on odeling tumor growth can be found in Chap. 1.

#### 3.3.3.1 Cancer and Tumor Growth

The way in which cancer can cause death varies depending on the type of cancer and the parts of the body affected. The metastatic patterns for tumors are variable, as are tumor growth rates. However, as a rule, the cause of death is due to the mass effect of the tumor, which occurs when cancer spreads to a part of the body that carries out an essential function. For example, if a tumor is growing in part of the digestive tract, it can prevent the digestion and absorption of food, or it can block the digestive tract so that food cannot pass through the intestines. When such blockages occur, then nutrients from the food can't be absorbed and poor nutrition and issues ensuring from body wasting arising from the mass effect of the tumor will contribute to death. In other cases, organ failure, necrosis, and infection can eventually lead to death.

The effect of anticancer drugs on solid tumors is usually categorized based on the criteria outlined in the Response Evaluation Criteria in Solid Tumors (RECIST) Group (Eisenhauer et al. 2009). This method classifies the response of the tumor to a particular therapeutic intervention into one of four categories: complete response (CR), partial response (PR), stable disease (SD) and progressive disease (PD). The advantage of the RECIST criteria is that it offers a uniform response criterion that standardizes the measurement and interpretation of tumor responses across clinical trials, allowing cross-comparison between various treatment modalities. Other metrics of tumor response to treatment involve evaluation of survival at some key endpoint (Mould et al. 2006), disease free survival, or time to disease progression.

However, the use of categorical response inherently reduces the amount of information being evaluated. Using other related markers such as cancer antigens (e.g. CEA or CA15-3) have not been helpful, as these markers are not closely related to tumor mass although they are recognized as prognostic factors at time of diagnosis. Consequently, the evaluation of tumor size as a

continuous scale assessment has been proposed as being potentially more useful for relating tumor response to individual levels of drug exposure. Because assessments of tumor growth usually require sophisticated imaging techniques for accurate measurements, and the fact that patients often have multiple metastatic sites of disease, the use of continuous tumor measurements has not yet gained widespread application as an end point for drug effect modeling in clinical trials. Development of a model to account for metastasis is particularly important in this setting. The ability to determine the initiation time of metastatic growth would be a valuable tool to determine the likelihood of a patient having metastatic recurrence. As should be expected, the predicted initiation time for metastases depends on the disease progression model. Therefore, if a model predicts an early initiation time for metastatic growth relative to the time of diagnosis, then treatment strategy would be different than if the metastasis were unlikely to have been initiated. In the former case, chemotherapy would be a primary treatment option and in the latter, surgery and radiation would likely be preferred.

Breast cancer is one of the most common solid tumors in women. Mortality rates for breast cancer across the entire population within the United States have remained largely unchanged since 1970 (Bailar and Gornik 1997). Despite the fact that most breast cancer patients are treated with cytotoxic chemotherapy at the reported optimal schedule, a significant percentage of patients relapse and die. The Oxford Overview (Early Breast Cancer Trialists' Collaborative Group) reported the recurrence-free and survival rates at 10 years for women receiving multiagent chemotherapy as 44 and 51%, respectively.

Developing a better understanding of the natural history of breast cancer through the use of disease progression models may suggest more effective treatments and has been investigated over the past 25 years. A variety of models have been proposed to describe the natural history of breast cancer. In the sixties, Laird used the Gompertz function to describe the growth of solid tumors (Laird 1964). More recent work on breast cancer tumor growth includes models developed by Speer et al. (1984), Koscielny et al. (1985), Norton and Simon (1977, 1986), and Spratt et al. (1993).

The Gompertz model (Gompertz 1825) has been the basis of many models of solid tumor growth. The Gompertz model is a modification of exponential growth, with the addition of a decreasing growth rate over time that causes the cancer to asymptotically approach a limiting size, referred to as its carrying capacity. This limited growth is attributed to several factors, including hypoxia and the lack of nutrients. The use of this model stems from data obtained in several in vivo studies in which the Gompertz function described the growth dynamics of the tumor (Norton et al. 1976). However, Speer, among others, found evidence that cancer cells can enter a dormant phase, and that the original Gompertz equation could not account for this observed dormant phase. Thus, the Gompertz function has been modified to account for cells to existing in multiple phases. In the equation below, the Gompertz function was modified to allow for a resistant (dormant) subpopulation of cells and a sensitive or growing population.

$$
\begin{aligned}
\frac{dR_s}{dt} &= K_{RS}R_r + \beta R_s(\beta_{max} - R_s) \\
&\quad - \left[ K_{SR} + \left( 1 + \frac{E_{max}C_p}{EC50 + C_p} \right) K_{SO} \right] R_s \\
\frac{dR_r}{dt} &= K_{SR}R_s - K_{RS}R_r
\end{aligned}
$$

$$(3.12)$$

In this equation, $R_r$ is the resistant population and $R_s$ is the sensitive population. $K_{RS}$ is the rate constant of transfer from resting to sensitive and $K_{SR}$ is the rate constant of transfer from sensitive to resting. $\beta_{max}$ is the maximum carrying capacity, and $\beta$ is the growth rate. $E_{max}$ and $EC_{50}$ represent the maximum activity of the drug and the concentration at half maximal effect, respectively. $C_p$ is the concentration of the drug. As has been seen with other models of disease progression, concentration can be replaced by an effect compartment concentration to allow for the delay between drug administration and

**Fig. 3.10** Gompertz growth patterns for varying treatment regimens. Cell counts following administration of different doses of cytotoxic drug. With this model, it can be seen that even with a very high dose, cell count appears to drop to 0 but will regrow. This model then can mimic relapse following chemotherapy
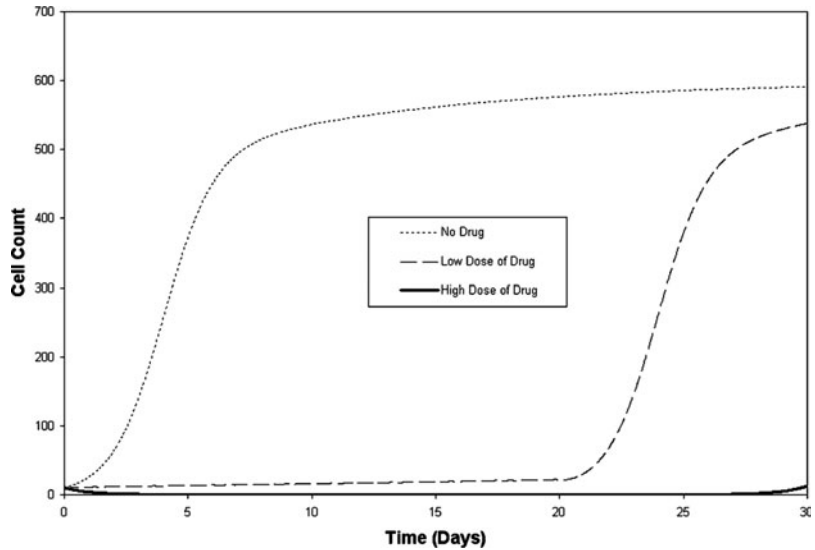
observed change in tumor growth patterns. This function provides the growth patterns seen in Fig. 3.10.
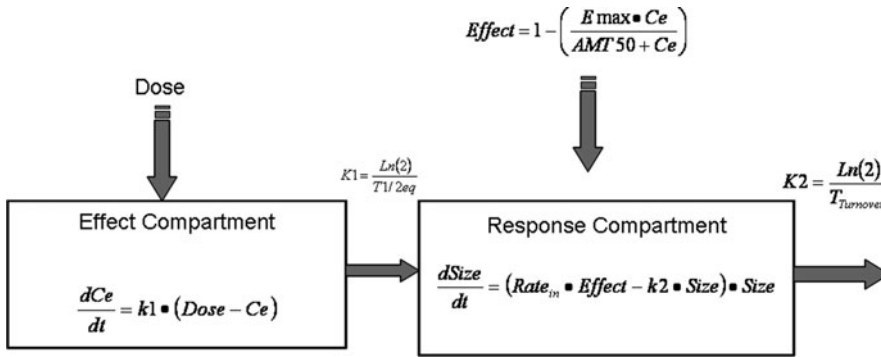
However, the Gompertz function presented does not account for metastatic disease which is a shortcoming.

Norton and Simon (1986) assumed that all tumor growth, regression, and regrowth followed Gompertzian kinetics. Their model describes the initial response to chemotherapy as cell death or depopulation. Based on the Gompertz model, as the tumor regresses, its growth fraction increases. If following treatment the asymptotic limit (where kill rate and repopulation are equal) exceeds one cell, a cure cannot occur. Consequently, the only way to cure the disease is to eradicate every metastatic cell. This evaluation supported the administration of adjuvant chemotherapy to patients with early stage breast cancer following tumor resection.

However, other issues must be considered in any disease progression model for cancer. Firstly, tumor cells often exhibit resistance through expression of multidrug resistance transporters (MDR). In addition, the resistance of cancer cells to chemotherapeutic agents may be a consequence of clonal selection, where the surviving subpopulation following treatment is resistant to that agent or class of agents. The Goldie–Coldman model (Goldie and Coldman (1979) attempted to incorporate the theory of the evolution of clonal drug resistance into a disease progression model. Their model incorporates a fixed nonzero probability that any new daughter cell will be a resistant mutant at each cell division of an unmutated tumor cell. At diagnosis (e.g. a tumor of approximately $10^9$ cells), this model estimates that drug-resistant cells are present. Also, with an increasing tumor cell population, the probability that a double mutant is created is also increased.

Although breast cancer models have been used for many years, models for other tumors have not been evaluated to the same extent. For example, several models for nonsmall cell lung cancer, which may be an easier disease to describe as the primary tumor is often the cause of death, have recently been reported. Tham et al. (2008) also employed a disease progression model for nonsmall cell lung cancer based on the Gompertz function. This model also used an effect or link compartment to allow for the delay between treatment and reduction in tumor size. A schematic of this model is presented in Fig. 3.11. The evaluation was driven only by effects of the antineoplastic agent on a primary

$$Effect = 1 - \left( \frac{E\max \bullet Ce}{AMT50 + Ce} \right)$$

$$K1 = \frac{Ln(2)}{T1/2eq}$$

$$K2 = \frac{Ln(2)}{T_{Turnover}}$$

**Effect Compartment**

$$\frac{dCe}{dt} = k1 \bullet (Dose - Ce)$$

**Response Compartment**

$$\frac{dSize}{dt} = (Rate_{in} \bullet Effect - k2 \bullet Size) \bullet Size$$

**Fig. 3.11** Schematic of Gompertz model – derived from Tham et al. (2008). A schematic for tumor growth dynamics is presented above. Here, a link or effect compartment is used to allow for a delay between the administration of

drug and a change in tumor size. The effect site concentration (Ce) is used to drive the $E_{max}$ model that decreases tumor cells

tumor target and thus did not include models for metastatic sites and tumor cell resistance. Therefore the model was able to capture the overall change in tumor size following chemotherapy. However, the authors were not able to correlate individual drug exposure with tumor regression, possibly due to the small size of the study evaluated. Wang et al. (2009) also developed a model for nonsmall cell lung cancer. This later work utilized pooled data from several studies and a mixed exponential decay and linear growth model for tumor size as shown below. In this equation, $TS_i$ is the individual tumor size at some time $t$, BASE is the individual primary tumor size measured at baseline, $SR_i$ is the shrinkage rate, and $PR_i$ is the growth rate under a specific treatment course.

$$TS_i(t) = BASE_i\, e^{-SR_i t} + PR_i t. \qquad (3.13)$$

What was particularly important in this work is that the authors were able to link the tumor size to overall survival. The combined model identified other prognostic factors for survival, including East Coast Oncology Group (ECOG) status, baseline tumor size, and tumor size at week 8 following treatment. This model may be useful to make comparisons of various chemotherapeutic regimens and may provide insight to patient response.

### 3.3.3.2 Viral Growth

Acquired immune deficiency syndrome (AIDS) is a severe immunological disorder that is caused by the human immunodeficiency retrovirus (HIV). AIDS arises as a defect in cell-mediated immune response that is manifested by increased susceptibility to opportunistic infections and to certain rare cancers, especially Kaposi's sarcoma. The Center for Disease Control (CDC) estimated that at the end of 2006, approximately 1,106,400 persons in the United States were living with HIV infection, with 21% undiagnosed (Garnett and Holford, Abstract Measurement 2006 Meeting) and that approximately 56,300 people were newly infected with HIV (Hall et al. 2008). CD4+ lymphocytes are the cells primarily infected by HIV. During treatment with antiviral agents, the number of CD4+ lymphocytes generally increases as the viral load decreases. It is the loss of CD4+ lymphocytes that results in the immunosuppression.
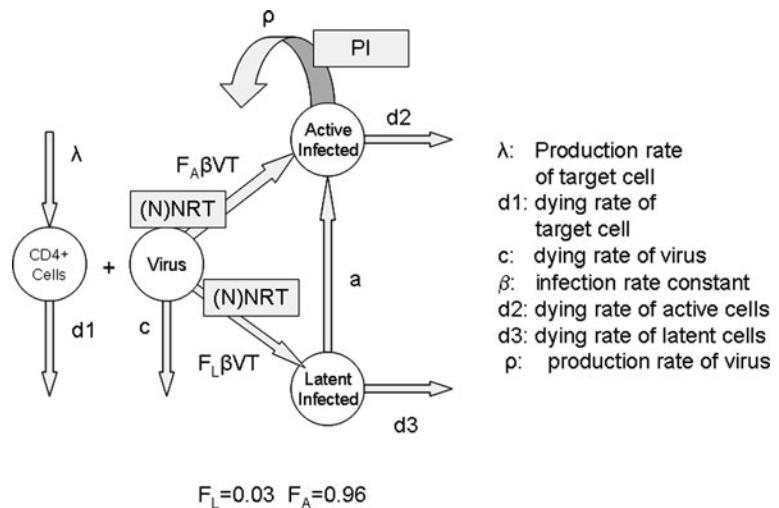
HIV viral detection was initially elusive. In the early 1990s HIV detection methods were not well established, with high assay variability (Sloand et al. 1991). Consequently, CD4+ cell count was generally used as a predictor of magnitude of response to treatment. Sale et al. (1993) conducted a post-hoc analysis of data obtained from 1,423 asymptomatic HIV-positive patients with CD4+ cell counts less than 500 mm³. Patients were dosed at 500 or 1,500 mg/day

zidovudine, or placebo. The main outcome measure was change in the CD4+ cell counts over time. The authors reported that early initiation of treatment with zidovudine resulted in a larger increment in the CD4+ cell count. In addition, the increment in CD4+ cell count is very long lived. The model suggested that zidovudine does not change the underlying course of HIV infection but simply delays the time course of CD4+ cell loss. However, drug exposure was not found to be a predictor of response to treatment in the dose range studied. Similarly, Stein and Drusano (1997), using a model somewhat more elaborate than Sale et al. investigated the relationships between changes in CD4+ counts over 24 weeks during treatment with indinavir at dosages of at least 2.4 g/day. Baseline CD4+ counts were linked to the time-weighted average CD4+ cell count through a nonlinear effect model. The loss of CD4+ cells after the initiation of indinavir therapy was estimated simultaneously by fitting a series of differential equations to the data using a linked lymph node-blood (two-compartment) system in which there was a constant rate of generation, first-order transfer rate constants between compartments, and first-order rate constants of CD4+ cell loss in the absence or presence of indinavir. The results of this evaluation suggested that the CD4+ cell count at the start of therapy is correlated to both the decrease in the destruction rate of CD4 cells and the degree of change in the CD4 lymphocytes on therapy. The work also indicated that a low initial CD4+ cell count is associated with high CD4+ cell turnover and a reduced ability of the immune system to increase absolute CD4+ cell levels after viral suppression, which is consistent with a decreased regenerative capacity with progression of disease.

However, viral infections have complex growth patterns (Bonhoeffer et al. 1997), and while the CD4+ cells are the target, models for viral load are an important component of the disease. Funk et al. (2001) developed a model that described the dynamics of CD4+ cells and viral load after initiation of antiretroviral therapy. The authors also distinguished between actively, latently, persistently, and defectively infected cells The model simultaneously described HIV-1 RNA, peripheral blood mononuclear cell (PBMC)-gag RNA, proviral DNA, and CD4+ cell counts. A schematic of this model is presented in Fig. 3.12. With this model, the authors were able to estimate the replicative capacity of the virus. The authors reported that HIV can maintain an ongoing infection only in actively infected cells. In latently and persistently infected cells the viral reproductive rate is considerably smaller, indicating that these compartments contribute little to the total basic



**Fig. 3.12** Schematic of viral growth model. A more complex model schematic for viral growth accounts for actively infected cells and latent cells because the response to treatment will be different. There is also the possibility that latent cells can convert to active cells

reproductive rate and cannot maintain an ongoing infection in the absence of actively infected cells.

Rosario et al. (2005) developed a model that built upon the earlier work published by Funk. The authors integrated models for pharmacokinetics, pharmacodynamics, and viral growth (disease progression) to predict the effect of a new antiviral agent maraviroc on viral load. After the model was developed, a range of oral doses for maraviroc with potential activity was simulated to help guide the early clinical trials of this agent.

The development of resistance in HIV strains to current antiviral therapy is an important component of therapeutic outcome (Kuritzkes 2007). Resistance is thought to be partly attributable to poor compliance (Kilby et al. 2000) and to suboptimal therapy. In both situations, viral clones have an opportunity for regrowth and have possibly undergone selection for resistance to treatment. Labbé and Verotta (2006) developed a model characterizing variability in the long-term response to HIV treatment. The model was used to quantify the effect of physiological variables, adherence to treatment or previous exposure to treatment, on the dynamics of HIV-1 RNA. The authors reported that patients with previous exposure to treatment show faster death rates for HIV-1, and that higher adherence to treatment was associated with lower reproductive ratio. The importance of compliance in viral dynamics was further confirmed in a model developed by Radisavljevic-Gajic (2009) who demonstrated viral regrowth attributed to poor compliance.

As was mentioned earlier, suboptimal treatment can also contribute to poor clinical outcome of HIV therapy. Ioannidis et al. (2000) modeled the regrowth of HIV in patients who were not receiving optimal antiviral therapy. The rates of viral load increase were shown to be similar to those reported in patients whose therapy has been interrupted. Variability among viral rebound in suboptimally dosed patients with HIV may depend on viral fitness, target cell availability and extent of immune reconstitution.

Developing models to account for resistant subpopulations is not straightforward. RNA viruses are often described as molecular quasispecies due to their genetic diversity, which is a direct consequence of high mutation rates. According to this theory, RNA virus populations cannot be understood in terms of individual viral clones, as they are clouds of interconnected mutants. Cuevas et al. (2005) developed a viral growth model to examine the fitness of individual clones, which seems to be determined mainly by the ability to complete infection cycles more quickly. According to the authors, viral clone fitness was systematically higher for initial clones than for their derived populations. In addition to environmental changes, such as initiation of cellular defense mechanisms following infection, the differences in fitness are attributable to high RNA virus mutation rates.

Models of viral growth and dynamics need to incorporate a wide variety of submodels, including compliance, development of resistant subpopulations, active and latent infections, and target cell growth. As a consequence of the variability in viral subpopulations, compliance, and individual response to therapy, Wu et al. (2005) reported that it may be necessary to individualize the HIV treatment regimen in order to optimize response.

### 3.3.4 Osteoporosis

Measurement of bone mineral density (BMD) is used to diagnose osteoporosis, and fracture risk generally increases when BMD decreases. Monitoring changes in BMD over time can be used to estimate an individual's rate of bone loss, and therefore can be used to confirm response to treatment. However, the precision of BMD for determining a change in fracture risk is compromised by two factors: (1) there are errors of accuracy inherent in the testing methods which increase the variance of the assessment. These errors, taken together with the normal variation of BMD in the population mean over seasonal changes, necessitate the collection of

observations over a prolonged period of time in order to accurately assess changes; (2) BMD is not the only physiological factor that contributes to bone strength and fracture risk. Other factors such as race and concomitant disease can affect bone strength and fracture risk. The lack of predictive precision of BMD for change in fracture risk means that the usefulness of BMD as a surrogate marker of fracture risk reduction in clinical trials is somewhat limited and can be difficult to estimate.

In 1994, Pors Nielsen et al. reported that continuous treatment with hormone replacement therapy resulted in a pronounced rise in lumbar spine bone density. They also reported the rate spontaneous decline in lumbar spine bone density in untreated patients averaged 1.86% per year. However, they also noted that there was a significant bone loss from the lumbar spine during the last year of active treatment, suggesting that following initiation of hormone replacement therapy, lumbar spine bone density rises to a certain level and subsequently declines. These data were evaluated using a disease progression model, with the decay of BMD over time in untreated patients being described using a linear disease progression model with a slope equal to the annual rate of bone mineral loss (Fig. 3.13, lower panel). The placebo adjusted change from baseline in BMD seen in patients receiving treatment was described using a disease modifying model (model 1) and a symptomatic model (model 2). The fit of these two disease progression models is presented in the upper panel of Fig. 3.13. The results of their evaluation suggested a symptomatic benefit rather than a disease modifying benefit of treatment.

As mentioned earlier, BMD measurements exhibit seasonal changes over time. Figure 3.14 shows a regular pattern in the BMD observations that can be described using a linked cosine model to capture the periodicity in the data. Utilizing a linear disease progression model with a linked cosine function to account for seasonal changes and a disease modifying effect of drug produces the disease progression curves shown in Fig. 3.15.

$$\text{Wave}(t) = \text{Amp} \cos\left(\frac{2\pi}{12}(\text{Month} - \text{Phase})\right)$$
$$\text{Slope} = \alpha(1 - \text{DrugEffect})$$
$$\text{BMD}(t) = S_0 + \text{Wave}(t) + \text{Slope Month} + \varepsilon_{\text{additive}}$$

(3.14)

In the above equations, Amp is the amplitude of the cosine function, Month is the month the observation was taken, Phase is the phase of the wave, $\alpha$ is the slope of untreated BMD decay, $S_0$ is the baseline BMD value, and DrugEffect is the scaled effect of drug either via concentration or other summary measure of exposure such as dose or AUC.

Changes in BMD can also be described using an indirect effect type function, where the change in BMD is described using a differential equation as shown below and the schematic is presented in Fig. 3.16.

$$\text{Wave}(t) = \text{Amp} \cos\left(\frac{2\pi}{12}(\text{Month} - \text{Phase})\right)$$
$$R_{\text{formation}} = R_{\text{formation0}} \exp(-kt)$$
$$\frac{\text{dBMT}}{\text{d}t} = \text{Wave}(t) + R_{\text{formation}} - R_{\text{loss}}$$
$$\text{BMD}(t) = S_0 + \text{DrugEffect} + \int_0^t \frac{\text{dBMT}}{\text{d}t} + \varepsilon_{\text{additive}}$$

(3.15)

The linked cosine model is the same as has been implemented previously. In this model, $R_{\text{formation}}$ is the rate of calcium deposition in the bone, which decreases over time. The rate of change of BMD (dBMT/dt) is dependent on the cosine and the balance of formation and loss rates. The overall bone density at any time $t$ is the baseline density plus a drug effect and the integral of the overall BMD. This model was applied by Holford et al. (2001) to describe the effect of pamidronate on bone density.

The Women's Health Initiative estrogen–progestin trial in 2003 was the first randomized clinical trial demonstrating that combination postmenopausal hormone therapy reduces the risk of fracture at the hip, vertebrae, and wrist (Cauley et al. 2003). Garnett and Holford
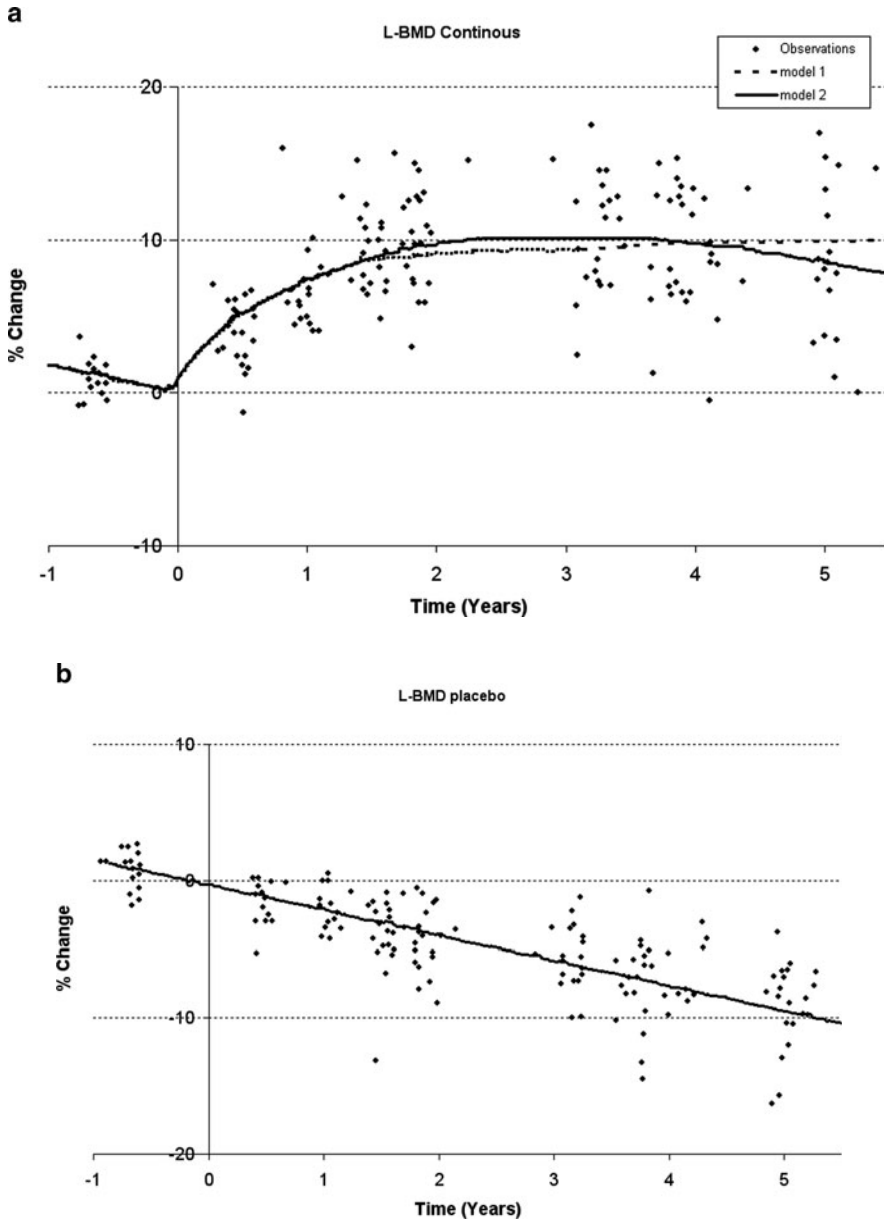
**Fig. 3.13** Percent change from baseline of lumbar spine bone mineral density over time – derived from Pors Nielsen et al. (1994). Placebo adjusted change from baseline in bone mineral density was described using a disease mod-ifying model (model 1) and a symptomatic model (model 2). The upper panel represents active treatment and the lower panel is the change in density for placebo

(Garnett and Holford, Abstract Measurement 2006 Meeting) attempted to develop a model correlating drug treatment, change in BMD, and fracture risk. However, they were not able to correlate BMD with fracture probability, finding that the important predictors of fracture risk were baseline BMD and treatment status, but not the change in BMD from untreated disease. In a separate assessment of data obtained in another study (No Authors listed. J Bone Miner Res.
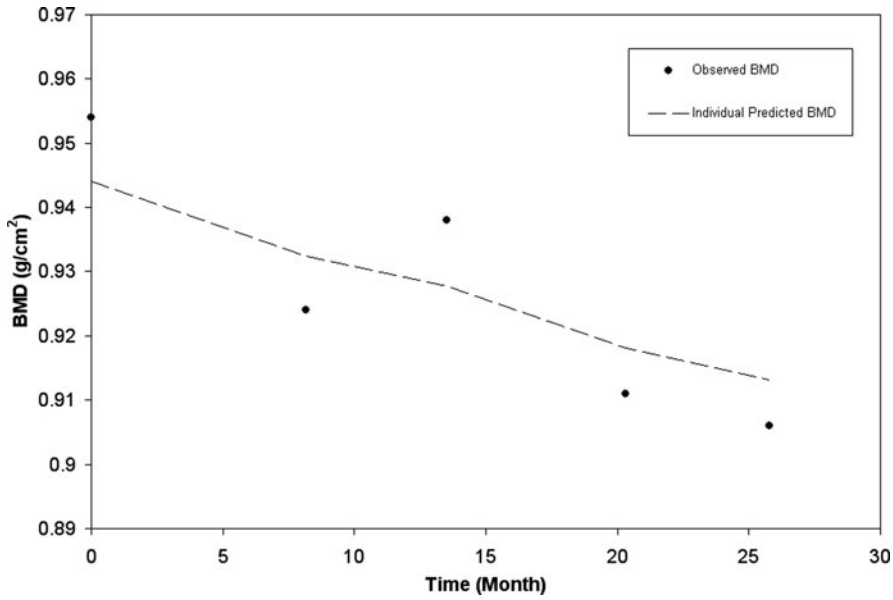
**Fig. 3.14** Decay of untreated lumbar spine bone mineral density over time showing periodicity. Bone mineral density changes with season, increasing during the summer months and decreasing in the winter. The observed bone density measurements oscillate in addition to decreasing over time in an untreated subject. Failing to account for this periodicity can increase the residual unexplained variability in a model
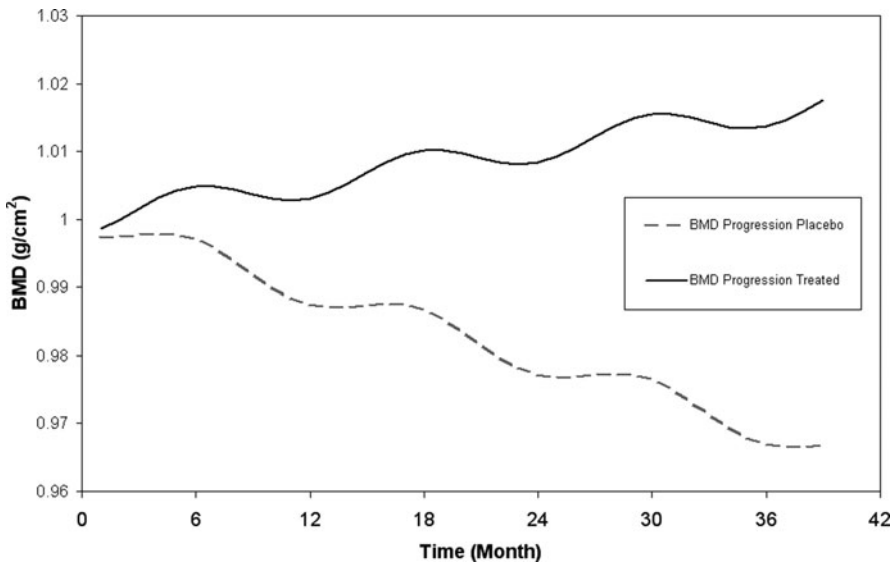


**Fig. 3.15** Simulated bone mineral density over time in treated and untreated states. Simulated time course of bone mineral density for treated and untreated patients over time can provide valuable insights into the magnitude of change expected following treatment with an investigational agent

2002) after adjusting for age, the risk of incident vertebral fracture was found to increase by a factor of 1.4 (95% CI, 1.2–1.8) per decrease of 0.1 g/cm$^2$ in BMD at the spine. Similarly, Johnell et al. (2005) found that for the prediction of any osteoporotic fracture (and any fracture), there

**Fig. 3.16** Schematic diagram of indirect effect model for osteoporosis. Bone density is a function of calcium deposition and loss and can be described using a standard indirect effect type model as shown here. Drug effect or disease can then affect either the deposition or removal in this system
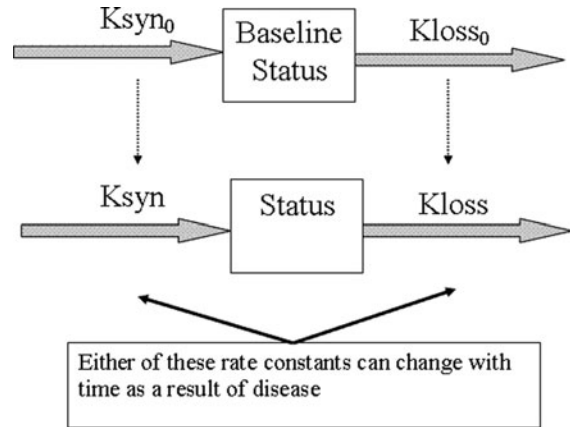


was a higher gradient of risk the lower the BMD. Other authors (Mackey et al. 2007; Henry et al. 2006) have also reported that vertebral BMD and hip BMD were both associated with risk of non-spine fracture. Models correlating exposure, changes in BMD and associated risk of fracture are still an area for exploration.

## 3.4 Study Designs for Evaluating Disease Progression and Drug Effects

The high failure rate of new drug development programs has been well documented (Mould et al. 2009) as less than 10% of the compounds that enter clinical trials are approved for use. Further, a high percentage of drugs that do not discontinue from drug development and are filed with the Food and Drug Administration (FDA) for marketing approval are not approved (Fig. 3.17). The reasons for failure are varied, but are often related to insufficient activity or undesirable adverse events.

In addition, with increasing pressure to reduce the cost of health care, improving clinical trial design and removing drug candidates that are unlikely to be successful at an early stage of development has become essential. These challenges in the "critical path" of drug development are discussed in a 2004 publication by the US FDA (Zsebo et al. 1986). Disease–drug-trial models are recommended as tools that can be used to streamline and improve drug develop-

ment and decision making in the FDA critical path document. Several groups have recommended model-based drug development (Zhang et al. 2006; Lalonde et al. 2007) with the goal of providing explicit, reproducible, and predictive models for optimizing drug development plans and facilitating critical decision making.

There are numerous examples of simulated study designs based on disease progression models. One early example was proposed by Holford and Peace (1992a, b) to improve the ability to assess drug effect for Tacrine in AD. The proposed design was an enrichment design, with patients receiving random doses of drug for fixed intervals of time. Lockwood et al. (2006) used the same linear AD disease progression model to investigate eight trial designs, including Latin square, incomplete block, and parallel group, as well as two composite designs that included both crossover and parallel group arms. The authors concluded that the use of simulation resulted in the decision to use a 4 × 4 Latin square rather than the originally proposed 12-week parallel group trial, resulting in savings of approximately US$4M in direct costs and a firm decision 8–12 months earlier than anticipated. Mould et al. (2007) reported that D-optimization, which minimizes the projected variance–covariance of a model, could be used as a tool to explore study designs once a disease progression model was established. The use of D-optimization provided candidate study designs and response assessment times more
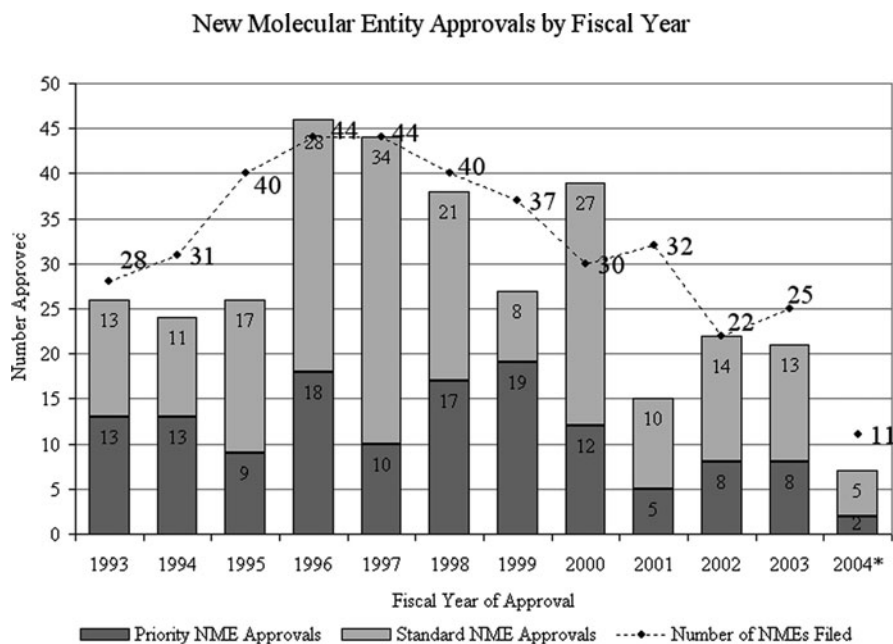
**Fig. 3.17** New molecular entity approval by the FDA by fiscal year – taken from Powell (2005). A frequency histogram of approvals for new molecules from 1993 to 2004. The number of approvals has fallen over the past several years

easily than formal clinical trial simulation, and the resulting study designs did not impact the power to detect drug effect using traditional approaches.

One of the more interesting aspects of disease progression modeling has been the concept of the ability to detect disease modifying effects for a candidate drug. One of the early study designs proposed to distinguish drug activity was a washout design. Chan et al. (2007) reported on a study (ELLDOPA) that was designed to detect a difference between placebo and levodopa treated arms in the total unified Parkinson's disease rating scale (UPDRS) taken at baseline and following 2 weeks levodopa washout after 40 weeks of treatment. The total UPDRS response was simulated with different assumptions on levodopa effect (e.g. symptomatic effect both with and without disease modifying activity) and washout speed of symptomatic effect for levodopa based on a model that had been developed from earlier longitudinal data (DATATOP). The results of this study did not support the concept that levodopa may hasten the disease progression, but rather, it appears to slow down the rate

of the disease progression. The clinical study failed to demonstrate any evidence of levodopa worsening early stage disease progression. Lastly, the data suggested that a 2-week washout period was insufficient to eliminate the symptomatic benefits of levodopa.

However, there have been concerns expressed about the appropriateness of using washout studies to evaluate drug effects (Hung and Schwarzschild (2007). Furthermore, as seen with the findings from the ELLDOPA trial, washout periods for drug effect can be protracted. Two simulated scenarios of a fast onset and washout and a slow onset and washout for drug effect are shown in Fig. 3.18, panel A and panel B, respectively. In panel A, when drug onset and washout are fast, the disease modifying and symptomatic effects can be clearly distinguished. However, as can be seen in panel B, when drug effect has a slow onset and slow washout, the disease modifying and symptomatic behaviors are less distinct. Therefore, the distinction between a disease modifying drug activity and symptomatic activity must be based on clinical use and observed activity.
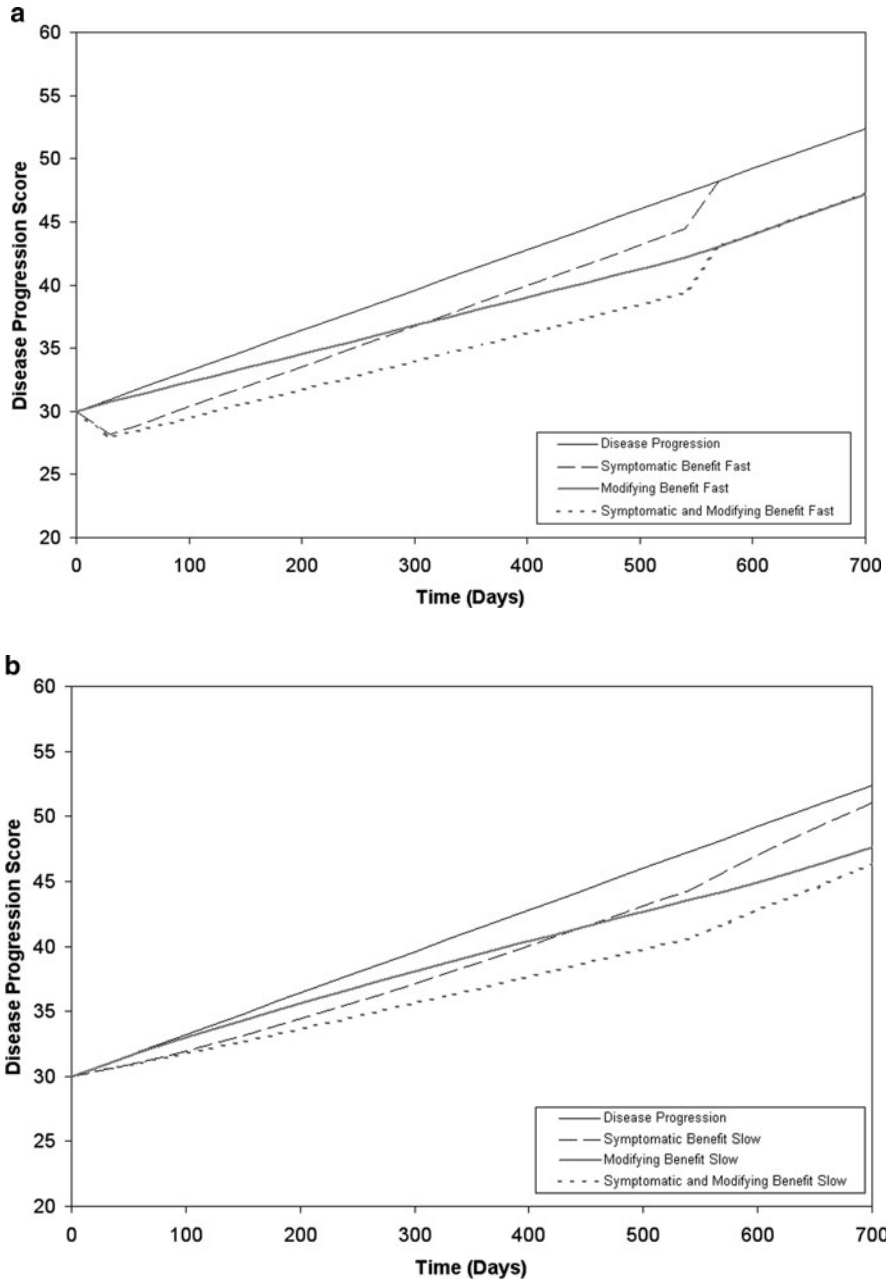
**Fig. 3.18** Effects of washout on determining drug activity. In these figures, the effect of washout can be seen. For panel A, patient status rapidly returns to follow the natural time course clearly suggesting the drug has only symptomatic effect because the drug effect wears off quickly. In panel B the status never returns to the natural time course, suggesting that the drug has an effect on disease progression. However, this is due to the slow washout of the drug which was simulated to exert only symptomatic benefit

A randomized delay or staggered start study design was proposed as one means of assessing drug effect. This design was tested to separate symptomatic from disease modifying effects of rasagiline (TEMPO) (Parkinson Study Group 2004). Comparison of the change in total UPDRS

Score from baseline to 12 months showed lower values in the group that received rasagiline immediately compared with the delayed start group, suggesting a disease modifying effect. However, evaluation of the time course of drug effect did not rule out a slow onset symptomatic effect. These findings, and other published opinions (Clarke 2004), cast doubt on the utility of a staggered start study design. Ploeger and Holford (2009) conducted a simulation based evaluation comparing washout and staggered start study designs. The authors reported that for the simulation model used, including a washout period in which the patients are followed up after cessation of treatment substantially increases the power to distinguish different treatment effect types (washout: 80%; delayed start: 60%).

Clearly, study design issues must be considered for every drug and disease being evaluated. Practical considerations as well as ethical issues need to be taken into account. However, modeling, simulation, and other tools such as D-optimization can be important in designing an informative trial that provides robust information on drug activity.

## 3.5  Summary

Both the power to detect drug effect and predictive power can be achieved by the application of disease progression modeling. Certainly their application provides a more rational basis for dealing with missing data than imputation methods such as LOCF. Combined with pharmacokinetic and pharmacodynamic models, models of disease progression can provide insights into understanding the time course and management of degenerative disease. While empirical models can help improve the power to detect drug effect, physiologically based models can provide a platform for exploration of alternative and combination therapies prior to clinical trial, and such efforts should be routinely included in the "learn and confirm" process of drug development.

Currently, there are numerous diseases for which these models have been developed and applied. Many chronic degenerative diseases such as AD, Parkinson's disease, and acute phases of schizophrenia have been characterized. However, there are still many therapeutic areas that have seen limited model based evaluations. One of the issues associated with development of such models is that the progression of many diseases is very slow, necessitating collection of data over long periods of time. Furthermore, it is unusual to have long-term observational data from untreated patients as most receive treatment for their disease. The effect of the standard treatment on the symptoms and disease progression need to be accounted for in any evaluation. Finally, owing to the variability in the individual patient progression and their response to treatment, data from large numbers of subjects is usually required to develop such models. The efforts of regulatory authorities such as the US FDA in developing and publishing models of disease progression based on data collected across a wide variety of studies should prove to be a useful resource.

The development of models for disease progression is not a new practice. However, the routine development and use of disease progression models in drug development is relatively new. The advantage of such models is that, once developed and qualified, they can be used to improve future study designs for new agents to allow better detection of drug effect. Many failures seen in late phase trials are attributed to the lack of differentiation from placebo (i.e. the trials fail to demonstrate the effectiveness of the new treatment over the comparator). While there are many literature reports of the use of pharmacokinetic/pharmacodynamic modeling and simulation to improve decision making and dose selection, incorporation of disease progression models should allow more efficient planning and more informative study design during the early phases of drug development. Methods such as D-optimization can be utilized once the appropriate models are established to reduce the number of observations required to assess treatment effectiveness.

The use of disease progression models in the drug development process is likely to continue to expand as more models are developed and the benefits of such assessments become more widely recognized. Furthermore, as the understanding of various aspects of diseases improves, these models will require adjustment and improvement to reflect increased understanding of the mechanistic basis of disease.

## References

Agoram B, Heatherington AC, Gastonguay MR. Development and evaluation of a population pharmacokinetic—pharmacodynamic model of darbepoetin Alfa in patients with nonmyeloid malignancies undergoing multicycle chemotherapy. AAPS J 8(3):E552–63 (2006)

Bailar JC III, Gornik HL. Cancer undefeated. N Engl J Med 336:1569–74 (1997)

Berlin NI, Lawrence JH, Lee HC. The life span of the red blood cell in chronic leukemia and polycythemia. Science 114(2963):385–7 (1951)

Birks J. Cholinesterase inhibitors for Alzheimer's disease. Cochrane Database Syst Rev (1):CD005593 (2006)

Bonhoeffer S, May RM, Shaw GM, Nowak MA. Virus dynamics and drug therapy. Proc Natl Acad Sci U S A 94(13):6971–6 (1997)

Brooks JOD, Kraemer HC, Tanke ED, Yesavage JA. The methodology of studying decline in Alzheimer's disease. J Am Geriatr Soc 41:623–28 (1993)

Cauley JA, Robbins R, Chen Z, Cummings SR, Jackson RD, LaCroix AZ, LeBoff M, Lewis CE, McGowan J, Neuner J, Pettinger M, Stefanick ML, Wactawski-Wende J, Watts NB, for the Women's Health Initiative Investigators. Effects of estrogen plus progestin on risk of fracture and bone mineral density. JAMA 290:1729–38 (2003)

CDC. HIV Prevalence Estimates – United States, 2006. MMWR 57(39):1073–6 (2008)

Chan PLS, Holford NHG. Drug treatment effects on disease progression. Ann Rev Pharmacol Toxicol 41:625–59 (2001)

Chan PL, Nutt JG, Holford NH. Levodopa slows progression of Parkinson's disease: external validation by clinical trial simulation. Pharm Res 24(4):791–802 (2007)

Chaplin H Jr, Mollison PL. Red cell life-span in nephritis and in hepatic cirrhosis. Clin Sci (Lond) 12(4):351–60 (1953)

Clarke CE. A 'cure' for Parkinson's disease: can neuroprotection be proven with current trial designs? Mov Disord 19(5):491–498 (2004)

Cosson V, Gomeni R. Modelling placebo response in depression using a mechanistic longitudinal model approach. PAGE 14 (2005) Abstr 818 [http://www.page-meeting.org/?abstract=818]

Cuevas JM, Moya A, Sanjua R. Following the very initial growth of biological RNA viral clones. J Gen Virol 86:435–43 (2005)

Dayneka NL, Garg V, Jusko WJ. Comparison of four basic models of indirect pharmacodynamic responses. J Pharmacokinet Biopharm 21(4):457–78 (1993)

Diggle P, Kenward MG. Informative drop-out in longitudinal data analysis. Appl Stat 43:49–93 (1994)

Duhrsen U, Villeval JL, Boyd J, et al. Effects of recombinant human granulocyte colony-stimulating factor on hematopoietic progenitor cells in cancer patients. Blood 72:2074–81 (1988)

Dworkin RH, Katz J, Gitlin MJ. Placebo response in clinical trials of depression and its implications for research on chronic neuropathic pain. Neurology 65 (12 Suppl 4):S7–19 (2005)

Dysken MW, Kirk LN, Kuskowski M. Changes in vitamin E prescribing for Alzheimer patients. Am J Geriatr Psychiatry 17(7):621–4 (2009)

Early Breast Cancer Trialists' Collaborative Group: Systemic treatment of early breast cancer by hormonal, cytotoxic, or immune therapy. 133 randomised trials involving 31,000 recurrences and 24,000 deaths among 75,000 women. Early Breast Cancer Trialists' Collaborative Group

Egorin MJ, Van Echo DA, Whitacre MY, Forrest A, Sigman LM, Engisch KL, Aisner J. Human pharmacokinetics, excretion, and metabolism of the anthracycline antibiotic menogaril (7-OMEN, NSC 269148) and their correlation with clinical toxicities. Cancer Res 46:1513–20 (1986)

Eisenhauer EA, Therasse P, Bogaerts J, Schwartz LH, Sargent D, Ford R, Dancey J, Arbuck S, Gwyther S, Mooney M, Rubinstein L, Shankar L, Dodd L, Kaplan R, Lacombe D, Verweij J. New response evaluation criteria in solid tumours: Revised RECIST guideline (version 1.1). Eur J Cancer 45:228–47 (2009)

Eisenhower EA, ten Bokkel Huinink WW, Swenerton KD, et al. European Canadian randomized trial of paclitaxel in relapsed ovarian cancer: high dose versus low dose and long versus short infusion. J Clin Oncol 12:654–66 (1994)

Emslie GJ, Ryan ND, Wagner KD. Major depressive disorder in children and adolescents: clinical trial design and antidepressant efficacy. J Clin Psychiatry. 66(Suppl 7):14–20 (2005)

Erlichman C, Moore M, Kerr IG, Wong B, Eisenhauer E, Zee B, Whitfield LR. Phase 1 pharmacokinetic and pharmacodynamic study of a new anthrapyrazole, CI-937 (DUP937). Cancer Res 51:6317–22 (1991)

Ernst E, Resch KL. Concept of true and perceived placebo effects. BMJ 311:551–553 (1995)

Food Drug Adm. 2004. Innovation or stagnation: challenges and opportunity on the critical path to new medical products. http://www.fda.gov/oc/initiatives/criticalpath/whitepaper.html

Friberg LE, Freijs A, Sandstrom M, Karlsson MO. Semi-physiological model for the time course of leukocytes after varying schedules of 5-fluorouracil in rats. J Pharmacol Exp Ther 295(2):734–40 (2000)

Friberg LE, Henningsson A, Maas H, Nguyen L, Karlsson MO. Model of chemotherapy-induced myelosuppression with parameter consistency across drugs. J Clin Oncol 20(24):4713–21 (2002)

Funk GA, Fischer M, Joos B, Opravil M, Günthard HF, Ledergerber B, Bonhoeffer S. Quantification of in vivo replicative capacity of HIV-1 in different compartments of infected cells. J Acquir Immune Defic Syndr 26(5):397–404 (2001)

Garnett C, Holford N. Bone mineral density progression to dropout and time-to-fracture: application to post menopausal women taking hormone replacement therapy. Abstract Measurement 2006 Meeting. http://www.lacdr.nl/index.php3?c=87

Gianni L, Kearns CM, Giani A, et al. Nonlinear pharmacokinetics and metabolism of paclitaxel and its pharmacokinetic/pharmacodynamic relationships in humans. J Clin Oncol 13:180–90 (1995)

Gobburu JVS, Lesko LJ. Quantitative disease, drug, and trial models. Annu Rev Pharmacol Toxicol 49: 291–301 (2009)

Gobburu JV, Tammara V, Lesko L, Jhee SS, Sramek JJ, Cutler NR, Yuan RJ. Pharmacokinetic–pharmacodynamic modeling of rivastigmine, a cholinesterase inhibitor, in patients with Alzheimer's disease. Clin Pharmacol 41(10):1082–90 (2001)

Goldie JH, Coldman AJ. A mathematic model for relating the drug sensitivity of tumors to their spontaneous mutation rate. Cancer Treat Rep 63:1727–33 (1979)

Gompertz B. On the nature of the function expressive of the law of human mortality, and on a new mode of determining the value of life contingencies. Philos Trans R Soc Lond 115:513–85 (1825)

Gruwez B, Dauphin A, Tod M. A mathematical model for paroxetine antidepressant effect time course and its interaction with pindolol. J Pharmacokinet Pharmacodyn 32(5–6):663–83 (2005)

Hall HI, Ruiguang S, Rhodes P, Prejean J, An Q, Lee LM, Karon J, Brookmeyer R, Kaplan EH, McKenna MT, Janssen RS; HIV Incidence Surveillance Group. Estimation of HIV incidence in the United States. JAMA 300:520–9 (2008)

Hantel A, Donehower RC, Rowinsky EK, Vance E, Clarke BV, McGuire WP, Ettinger DS, Noe DA, Grochow LB. Phase 1 study and pharmacodynamics of piroxantrone (NSC 349174), a new anthrapyrazole. Cancer Res 50:3284–8 (1990)

Hedlung JL, Vieweg BW. The Hamilton rating scale for depression. J Operat Psych 10(2):149–65 (1979)

Henderson VW. Estrogens, episodic memory, and Alzheimer's disease: a critical update. Semin Reprod Med 27(3):283–93 (2009)

Henningsson A, Karlsson MO, Vigano L, Gianni L, Verweij J, Sparreboom A. Mechanism-based pharmacokinetic model for paclitaxel. J Clin Oncol 19:4065–73 (2001)

Henningsson A, Sparreboom A, Sandstrom M, Freijs A, Larsson R, Bergh J, Nygren P, Karlsson MO. Population pharmacokinetic modeling of unbound and total plasma concentration of paclitaxel in cancer patients. Eur J Cancer 39:1105–14 (2003)

Henry MJ, Pasco JA, Sanders KM, Nicholson GC, Kotowicz MA. Fracture risk (FRISK) score: Geelong osteoporosis study. Radiology 241:190–6 (2006)

Holford NH, Peace KE. Methodologic aspects of a population pharmacodynamic model for cognitive effects in Alzheimer patients treated with tacrine. PNAS 89 (23):11466–70 (1992)

Holford NH, Peace KE. Results and validation of a population pharmacodynamic model for cognitive effects in Alzheimer patients treated with tacrine. Proc Natl Acad Sci U S A 89(23):11471–5 (1992)

Holford NH, Sheiner LB. Understanding the dose–effect relationship: clinical application of pharmacokinetic–pharmacodynamic models. Clin Pharmacokinet 6:429–53 (1981)

Holford NHG, Sheiner LB. Kinetics of pharmacologic response. Pharmacol Ther 16:143–66 (1982)

Holford NHG, Bååthe S, Karlsson MO. Auckland bones and summer sun. PAGE 10 (2001) Abstr 231 [http://www.page-meeting.org/?abstract=231]

Holford N, Li J, Benincosa L, Birath M. Population disease progress models for the time course of HAM-D score in depressed patients receiving placebo in antidepressant clinical trials. PAGE 11 (2002) Abstr 311 [http://www.page-meeting.org/?abstract=311]

Holford NHG, Mould DR, Peck CC. Disease progression models. In Principles of Clinical Pharmacology, 2nd Edition. Editor: A Atkinson. Academic Press, New York, NY (2006)

http://www.wired.com/medtech/drugs/magazine/17-09/ff_placebo_effect?currentPage=all

Hung AY, Schwarzschild MA. Clinical trials for neuroprotection in Parkinson's disease: overcoming angst and futility? Curr Opin Neurol 20(4): 477–483 (2007)

Imbimbo BP, Verdelli G, Martelli P, Marchesini D. Two year treatment of Alzheimer's disease with eptastigmine. The Eptastigmine Study Group. Dement Geriatr Cogn Disord 10(2):139–47 (1999)

Ioannidis JP, Havlir DV, Tebas P, Hirsch MS, Collier AC, Richman DD. Dynamics of HIV-1 viral load rebound among patients with previous suppression of viral replication. AIDS 14(11):1481–8 (2000)

Ito K, Ahadieh S, Corrigan B, French J, Fullerton T, Tensfeldt T; Alzheimer's Disease Working Group. Disease progression meta-analysis model in Alzheimer's disease. Alzheimers Dement 6(1):39–53 (2010)

Jacqmin P, Gieschke R, Jordan P, Steimer J-L, Goggin T, Pillai G, Snoeck E, Girard P. Modeling drug induced changes in biomarkers without using drug concentrations: Introducing the K-PD model. PAGE 10

(2001) Abstr 232 [http://www.page-meeting.org/?abstract=232]

Johnell O, Kanis JA, Oden A, Johansson H, De Laet C, Delmas P, Eisman JA, Fujiwara S, Kroger H, Mellstrom D, Meunier PJ, Melton LJ III, O'Neill T, Pols H, Reeve J, Silman A, Tenenhouse A. Predictive value of BMD for hip and other fractures. J Bone Miner Res 20 (7):1185–94 (2005)

Jonsson EN, Sheiner LB. More efficient clinical trials through use of scientific model-based statistical tests. Clin Pharmacol Ther 72(6):603–14 (2002)

Karlsson MO, Molnar V, Bergh J, Freijs A, Larsson R. A general model for time-dissociated pharmacokinetic–pharmacodynamic relationship exemplified by paclitaxel myelosuppression. Clin Pharmacol Ther 63: 11–25 (1998)

Khan A, Schwartz K. Study designs and outcomes in antidepressant clinical trials. Essent Psychopharmacol 6(4):221–6 (2005)

Khan A, Detke M, Khan SRF, Mallinckrodt C. Placebo response and antidepressant clinical trial outcome. J Nerv Ment Dis 191(4):211–8 (2003)

Kienle GS, Kiene H. The powerful placebo effect: fact or fiction? J Clin Epidemiol 50:1311–8 (1997)

Kilby JM, Goepfert PA, Miller AP, Gnann JW Jr, Sillers M, Saag MS, Bucy RP. Recurrence of the acute HIV syndrome after interruption of antiretroviral therapy in a patient with chronic HIV infection: A case report. Ann Intern Med 133(6):435–8 (2000)

Kisilevsky R. Anti-amyloid drugs: Potential in the treatment of diseases associated with aging. Drugs Aging 8:75–83 (1996)

Koscielny S, Tubiana M, Valleron AJ. A simulation model of the natural history of human breast cancer. Br J Cancer 52:515–24 (1985)

Kotto-Kome AC, Fox SE, Lu W, Yang BB, Christensen RD, Calhoun DA. Evidence that the granulocyte colony-stimulating factor (G-CSF) receptor plays a role in the pharmacokinetics of G-CSF and PegG-CSF using a G-CSF-R KO model. Pharmacol Res 50(1):55–8 (2004)

Kruse A, Uehlinger DE, Gotch F, Kotanko P, Levin NW. Red blood cell lifespan, erythropoiesis and hemoglobin control. Contrib Nephrol 161:247–54 (2008)

Krzyzanski W, Ramakrishnan R, Jusko WJ. Basic pharmacodynamic models for agents that alter production of natural cells. J Pharmacokinet Biopharm 27 (5):467–89 (1999)

Kuritzkes DR. HIV resistance: frequency, testing, mechanisms. International AIDS Society – USA 15 (5):150–4 (2007)

Kuwabara T, Kobayashi S, Sugiyama Y. Pharmacokinetics and pharmacodynamics of a recombinant human granulocyte colony-stimulating factor. Drug Metab Rev 28(4):625–58 (1996)

Labbé L, Verotta D. A non-linear mixed effect dynamic model incorporating prior exposure and adherence to treatment to describe long-term therapy outcome in HIV-patients. J Pharmacokinet Pharmacodyn 33 (4):519–42 (2006)

Laird AK. Dynamics of tumor growth. Br J Cancer 18:490–502 (1964)

Lalonde RL, Kowalski KG, Hutmacher MM, Ewy W, Nichols DJ, Milligan PA, Corrigan BW, Lockwood PA, Marshall SA, Benincosa LJ, Tensfeldt TG, Parivar K, Amantea M, Glue P, Koide H, Miller R. Model-based drug development. Clin Pharmacol Ther 82:21–32 (2007)

Lee YJ, Ellenber JH, Hirtz DG, Nelson KB. Analysis of clinical trials by treatment actually received: is it really an option? Stat Med 10:1595–605 (1991)

Little RJA, Rubin DB. Statistical analysis with missing data. Wiley, New York (1987)

Little RJ, Rubin DB. Causal effects in clinical and epidemiological studies via potential outcomes: concepts and analytical approaches. Annu Rev Public Health 21:121–45 (2000)

Little R, Yau L. Intent-to-treat analysis for longitudinal studies with drop-outs. Biometrics 52(4):1324–33 (1996)

Lockwood P, Ewy W, Hermann D, Holford N. Application of clinical trial simulation to compare proof-of-concept study designs for drugs with a slow onset of effect; an example in Alzheimer's disease. Pharm Res 23(9):2050–9 (2006)

Mackey DC, Eby JG, Harris F, Taaffe DR, Cauley JA, Tylavsky FA, Harris TB, Lang TF, Cummings SR; Health, Aging, and Body Composition Study Group. Prediction of clinical non-spine fractures in older black and white men and women with volumetric BMD of the spine and areal BMD of the hip: the Health, Aging, and Body Composition Study. J Bone Miner Res 22(12):1862–8 (2007)

Magnusson A. An overview of epidemiological studies on seasonal affective disorder. Acta Psychiatr Scand 101 (3):176–84 (2000)

Minami H, Sasaki Y, Saijo N, Ohtsu T, Fujii H, Igarashi T, Itoh K. Indirect-response model for the time course of leukopenia with anticancer drugs. Clin Pharmacol Ther 64:511–21 (1998)

Mollison PL. The life-span of red blood-cells. Lect Sci Basis Med 2:269–86 (1952–1953)

Mould DR. Development of models of disease progression. In *Pharmacometrics: The Science of Quantitative Pharmacology*. Editors: E Ette and P Williams. John Wiley and Sons, Hoboken, NJ, pp. 547–579 (2007)

Mould DR, Holford NHG, Schellens JHM, Beijnen JH, Hutson PR, Rosing H, ten Bokkel Huinink WW, Rowinsky EK, Schiller JH, Russo M, Dane G. Pooled pharmacokinetic and adverse event analysis of topotecan in patients with solid tumors. Clin Pharmacol Ther 71(5):334–48 (2002)

Mould DR, Fleming GF, Darcy KM, Spriggs D. Population analysis of a 24-hour paclitaxel infusion in advanced endometrial cancer: A Gynecologic Oncology Group Study. Br J Clin Pharmacol 62(1):56–70 (2006)

Mould DR, Denman NG, Duffull S. Using disease progression models as a tool to detect drug effect. Clin Pharmacol Ther 82(1):81–6 (2007)

Mould DR, Molnar SA, Thomas T. Modeling and simulation as tools to improve drug development. Congressional Modeling and Simulation Website. September 2009

No Authors listed. The relationship between bone density and incident vertebral fracture in men and women. J Bone Miner Res 17(12):2214–21 (2002)

Norton L, Simon R. Growth curve of an experimental solid tumor following radiotherapy. J Natl Cancer Inst 58:1735–41 (1977)

Norton L, Simon R. The Norton–Simon hypothesis revisited. Cancer Treat Rep 70:163–9 (1986)

Norton L, Simon R, Brereton HD, Bogden AE. Predicting the course of Gompertzian growth. Nature 264:542–5 (1976)

Papaldo P, Ferretti G, Di Cosimo S, Giannarelli D, Marolla P, Lopez M, Cortesi E, Antimi M, Terzoli E, Carlini P, Vici P, Botti C, Di Lauro L, Naso G, Nisticò C, Mottolese M, Di Filippo F, Ruggeri EM, Ceribelli A, Cognetti F. Does granulocyte colony-stimulating factor worsen anemia in early breast cancer patients treated with epirubicin and cyclophosphamide? J Clin Oncol 24:3048–55 (2006)

Parkinson Study Group. A controlled, randomized, delayed-start study of rasagiline in early Parkinson disease. Arch Neurol 61(4):561–6 (2004)

Perez-Ruixo JJ, Kimko HC, Chow AT, Piotrovsky V, Krzyzanski W, Jusko WJ. Population cell life span models for effects of drugs following indirect mechanisms of action. J Pharmacokinet Pharmacodyn 32 (5–6):767–93 (2005)

Pillai G, Gieschke R, Goggin T, Jacqumin P, Schimmer RC and Steimer J-L. A semimechanistic and mechanistic population PK-PD model for biomarker response to ibrandronate, a new bisphosphonate for the treatment of osteoporosis. Br J Clin Pharmacol 58 (6):618–31 (2004)

Ploeger BA, Holford NH. Washout and delayed start designs for identifying disease modifying effects in slowly progressive diseases using disease progression analysis. Pharm Stat 8(3):225–38 (2009)

Pors Nielsen S, Bärenholdt O, Hermansen F, Munk-Jensen N. Magnitude and pattern of skeletal response to long term continuous and cyclic sequential oestrogen/progestin treatment. Br J Obstet Gynaecol 101 (4):319–24 (1994)

Powell R. Drug–disease modeling and simulation applied to improve drug development & regulatory decisions (2005). http://www.dkma.dk/db/filarkiv/5664/biosimulationfdaviews.pdf

Radisavljevic-Gajic V. Optimal control of HIV-virus dynamics. Ann Biomed Eng 37(6):1251–61 (2009)

Ramakrishnan R, Cheung WK, Farrell F, Joffee L, Jusko WJ. Pharmacokinetic and pharmacodynamic modeling of recombinant human erythropoietin after intravenous and subcutaneous dose administration in cynomolgus monkeys. J Pharmacol Exp Ther 306 (1):324–31 (2003)

Rizzo JD, Lichtin AE, Woolf SH, Seidenfeld J, Bennett CL, Cella D, et al. Use of epoetin in patients with cancer: evidence-based clinical practice guidelines of the American Society of Clinical Oncology and the American Society of Hematology. J Clin Oncol 20 (19):4083–107 (2002)

Rosario MC, Jacqmin P, Dorr P, van der Ryst E, Hitchcock C. A pharmacokinetic–pharmacodynamic disease model to predict in vivo antiviral activity of maraviroc. Clin Pharmacol Ther 78(5):508–19 (2005)

Rowinsky EK, Eisenhauer EA, Chaudry V, Arbuck SA Donehower RC. Clinical toxicities encountered with paclitaxel (Taxol). Semin Oncol 20(Suppl 3):1–15 (1993)

Rowinsky EK, Jiroutek M, Bonomi P, Johnson D, Baker S. Paclitaxel steady-state plasma concentrations as a determinant of disease outcome and toxicity in lung cancer patients treated with paclitaxel and cisplatin. Clin Cancer Res 5:767–74 (1999)

Sale M, Sheiner LB, Volberding P, Blaschke TF. Zidovudine response relationships in early human immunodeficiency virus infection. Clin Pharmacol Ther 54 (5):556–66 (1993)

Schenk DB, Rydel RE, May P, et al. Therapeutic approaches related to amyloid-β peptide and Alzheimer's disease. J Med Chem 38:4141–54 (1995)

Shang E, Gibbs MA, Landen J, Denman NG, Krams M, Russell T, Mould DR. Model based analysis of placebo response in major depression. ACCP, Cambridge, MA, September (2006).

Shang Y, Gibbs MA, Landen JW, Krams M, Russell T, Denman NG, Mould DR. Evaluation of structural models to describe the effect of placebo upon the time course of major depressive disorder. J Pharmacokin Pharmacodyn 36:63–80 (2009)

Sheiner LB. Learning versus confirming in clinical drug development. Clin Pharmacol Ther 61:275–91 (1997)

Sheiner LB. Is intent-to-treat analysis always (ever) enough? Br J Clin Pharmacol 54:203–11 (2000)

Sheiner LB, DB Rubin. Intention-to-treat analysis and the goals of clinical trials. Clin Pharmacol Ther 57 (1):6–15 (1995)

Sloand E, Pitt E, Chiarello R, Nimo GJ. HIV Testing: State of the art. JAMA 266:2861 (1991)

Smith RE Jr, Tchekmedyian NS, Chan D, Meza LA, Northfelt DW, Patel R, et al. A dose- and schedule-finding study of darbepoetin alpha for the treatment of chronic anaemia of cancer. Br J Cancer 88(12):1851–8 (2003)

Solomon A, Kivipelto M. Cholesterol-modifying strategies for Alzheimer's disease. Expert Rev Neurother 9 (5):695–709 (2009)

Speer JF, Petrosky VE, Retsky MW, Wardell RH. A stochastic numerical model of breast cancer growth that simulates clinical data. Cancer Res 44:4124–30 (1984)

Spratt JA, von Fournier D, Spratt JS, Weber EE. Decelerating growth and human breast cancer. Cancer 71:2013–9 (1993)

Stein DS, Drusano GL. Modeling of the change in CD4 lymphocyte counts in patients before and after administration of the human immunodeficiency virus protease inhibitor indinavir. Antimicrob Agents Chemother 41(2):449–53 (1997)

Szekely CA, Breitner JC, Fitzpatrick AL, Rea TD, Psaty BM, Kuller LH, Zandi PP. NSAID use and dementia risk in the Cardiovascular Health Study: role of APOE and NSAID type. Neurology 70(1):17–24 (2008)

Terashi K, Oka M, Ohdo S, Furukubo T, Ikeda C, Fukuda M, Soda H, Higuchi S, Kohno S. Close association between clearance of recombinant human granulocyte colony-stimulating factor (G-CSF) and G-CSF receptor on neutrophils in cancer patients antimicrobial agents and chemotherapy. Antimicrob Agents Chemother 43:21–4 (1999)

Tham LS, Wang L, Soo RA, Lee SC, Lee HS, Yong WP, Goh BC, Holford NH. A pharmacodynamic model for the time course of tumor shrinkage by gemcitabine + carboplatin in non-small cell lung cancer patients. Clin Cancer Res 14(13):4213–8 (2008)

Wang Y, Sung C, Dartois C, Ramchandani R, Booth BP, Rock E, Gobburu J. Elucidation of relationship between tumor size and survival in non-small-cell lung cancer patients can aid early decision making in clinical drug development. Clin Pharmacol Ther 86 (2):167–74 (2009)

Welte K, Bonilla MA, Gillio AP, et al. Recombinant human G-CSF. Effects on hematopoiesis in normal and cyclophosphamide treated primates. J Exp Med 165:941–8 (1987)

Wu H, Huang Y, Acosta EP, Rosenkranz SL, Kuritzkes DR, Eron JJ, Perelson AS, Gerber JG. Modeling long-term HIV dynamics and antiretroviral response: effects of drug potency, pharmacokinetics, adherence, and drug resistance. J Acquir Immune Defic Syndr 39 (3):272–83 (2005)

Yew DT, Wong HW, Li WP, Lai HW, Yu WH. Nitric oxide synthase neurons in different areas of normal aged and Alzheimer's brains. Neuroscience 89:675–86 (1999)

Zhang L, Sinha V, Forgue ST, Callies S, Ni L, Allerheiligen SR. Model-based drug development: the road to quantitative pharmacology. J Pharmacokinet Pharmacodyn 33:369–93 (2006)

Zsebo KM, Cohen AM, Murdock DC, et al. Recombinant human granulocyte colony-stimulating factor: Molecular and biological characterization. Immunobiology 172:175–84 (1986)

# The Use of Dried Blood Spots for Concentration Assessment in Pharmacokinetic Evaluations

**4**

Tapan K. Majumdar and Danny R. Howard

**Abstract**

This chapter reviews the technology and application of Dried Blood Spot (DBS) sampling techniques. In part due to its relative simplicity, DBS has begun to receive increased use in the pharmaceutical industry, particularly where blood or plasma sample volumes are small, are difficult to collect, store, process, or transport. This chapter presents methods and techniques, highlights applications, and discusses benefits and drawbacks associated with its use in pharmacokinetics.

## 4.1 Introduction

Sensitive, specific, and robust assessment of drug and metabolite concentrations have become an essential part of characterization of nearly every new molecular entity intended for medical treatment. In both nonclincal and clinical safety studies, biological fluids such as blood, plasma, or serum are analyzed to determine the concentrations of target compounds and their metabolites. Relative exposure assessment through toxicokinetic (TK) and pharmacokinetic (PK) evaluation permits comparison across species and subsequent characterization of safety thresholds. Comparison of exposure or concentration to response permits the selection of optimal doses

and regimens where the medical benefit is maximized against the risk of adverse events. The evaluations for drug interactions, dose adjustments for special treatment populations, coadministration with food, formulation comparability, and bioequivalence rely heavily on PK observations determined from measured drug concentrations.

Traditionally, blood has been the primary biological sampling matrix, with the plasma or serum fraction serving as the most common biofluid for in vivo concentration assessment. Blood is sampled because, unlike other matrices (e.g., urine, saliva, cerebral spinal fluid) it is relatively convenient to obtain in a variety of species, usually allows for frequent measurement at prespecified time points, and is available in volumes needed for most modern analytical methods.

There are drawbacks however to traditional blood collection methods. In small animals, such as mice, serial sampling is often not possible and therefore PK assessments are highly variable composite profiles. It is frequently not possible,

D.R. Howard (✉)

Drug Metabolism and Pharmacokinetics, Translational Sciences, Novartis, One Health Plaza, East Hanover, NJ 07936, USA

e-mail: dan.howard@novartis.com

or desirable, to collected repeated venipuncture or the required blood volumes from some special patient populations, such as the elderly or very young. Special processing is necessary to ensure stability – refrigerated centrifugation, addition of antioxidants or stabilizing agents, and freezing at temperatures below −20°C are commonly required for each sample obtained. Not all clinical sites, particularly those of developing countries are equipped to handle these requirements. If the sample cannot be analyzed at the collection site, shipping procedures must be designed to ensure sample integrity and protection of shipping personnel from contamination or infection should damage to the sample tube occur.

A nontraditional sample collection technique based on DBS has been employed since early 1960s (Guthrie and Susi 1963; Fujimoto et al. 1989; Howe and Handelsman 1997; Peng et al. 2000; Filippi et al. 2009). DBS is a micro-volume sampling technique where ≤100 μL of whole blood is collected as a spot on a cellulose matrix known as the DBS card. Traditional sampling techniques typically require at almost 0.5 mL of blood. Two or more blood spots are collected per sample on each card. The cards are dried and shipped to a bioanalytical or clinical lab for the determination of analytes in the dry blood spot. A portion of the DBS on the card may be removed with a hole-punch of specified size (usually 3 mm or more in diameter), or may be sampled directly from the card using specialized equipment. If a punch is taken, the target analytes are extracted from this disc and the liquid extract is used directly for bioanalysis using liquid chromatography with variety of detectors, including mass spectrometry.

The DBS method does not generally require difficult or special sample preparation or handling techniques, and each sample requires only a fraction of the blood volume of traditional methods. With the availability of the very low level quantification and high throughput capabilities of tandem mass spectrometry (MS/MS), this technique has recently begun to receive attention from drug development laboratories (Liang et al. 2009; Spooner et al. 2009; Barfield et al. 2008;

Mauriala et al. 2005; Beaudette and Bateman 2004; De Haan et al. 2004) for use in pharmaceutical drug development programs. This novel sampling method is less invasive, requires minimal training, and reduces processing time at the collection site and may permit shipment and storage at ambient temperatures. Because it is a micro-volume sampling technique, it can be used in serial bleeding of small animals such as rat or mouse where sparse sampling technique (Nedelman et al. 1995) is typically used due to limitations in sample volume for TK sampling. Accuracy of the data in the micro-volume sampling technique is comparable to traditional methodologies.

The less invasive nature of DBS and use of micro-volume blood samples have made it a very useful sampling method for neonatal and juvenile subjects. Collection of blood samples for diagnosis of inborn error of metabolism has been routinely performed since 1960s (Guthrie and Susi 1963; Hill et al. 1967) through DBS. According to a report published by the Center for Disease Control and Prevention, as of 2001, public health laboratories screened more than 95% of all newborns in the United States for inborn metabolic disorders (Mei et al. 2001) using the DBS technique. Over last 47 years the DBS sampling technique has been used for both the qualitative and quantitative screening of wide varieties of diagnostic compounds and biomarkers (De Jesus et al. 2009; Chalcraft and Britz-McKibbin 2009; Al-Dirbashi et al. 2008; de Wilde et al. 2008; Searles et al. 2008; Oglesbee et al. 2008; Wang et al. 2005; Bowron et al. 2005; Febriani et al. 2004; Constantinou et al. 2004; O'Broin and Gunter 1999; Chace et al. 1993; Spence et al. 1993).

Pathogens from blood or plasma samples collected for the diagnosis of infectious diseases may contaminate surroundings by spill or from broken containers. The DBS samples, on the other hand, are safe from such inconveniences. Due to this advantage, DBS has been extensively used for collecting blood samples from epidemiological studies involving HIV, malaria, and other infectious diseases globally (Versteeg and Mens 2009; Lofgren et al. 2009; Tani et al. 2008;

Ngo-Giang-Huong et al. 2008; Creek et al. 2008; Burhenne et al. 2008; Steegen et al. 2007; Brambilla et al. 2003; Barbi et al. 2001). DBS also have been widely used for therapeutic drug monitoring (TDM) in hospitals and clinical laboratories (Edelbroek et al. 2009; Wilhelm et al. 2009a, b; van der Heijden et al. 2009; Cheung et al. 2008; Hoogtanders et al. 2007; AbuRuz et al. 2006).

A wide variety of both small and large molecular compounds have been detected and quantified using whole blood collected as DBS. These include: amino acids, vitamins, antibiotics, enzymes, nucleic acids, hormones, thyroglobulin, trace elements, specific antibodies, antigens, and genotyping (Damen et al. 2009; ter Heine et al. 2009a; ter Heine et al. 2009b; Eyles et al. 2009; Fingerhut 2009a; Lofgren et al. 2009; Liang et al. 2009; Otero-Santos et al. 2009; Tani et al. 2008; Janzen et al. 2008; Garcia et al. 2008; Al-Dirbashi et al. 2008; Alfazil and Anderson 2008; Higashi et al. 2008; Ngo-Giang-Huong et al. 2008; Creek et al. 2008; Barfield et al. 2008; Steegen et al. 2007; Koal et al. 2005; Deng et al. 2005; Brambilla et al. 2003; Green et al. 2002; Adam et al. 2000; Parker et al. 1995; Chace et al. 1993; Spence et al. 1993; Worthman and Stallings 1994; Lemonnier et al. 1991; McGarrity et al. 1984; Mizuta et al. 1982).

This chapter aims to review on the use of the DBS sampling technique, and to highlight the wide array of applications of this novel sampling technique including discussion for quantitative method validation applicable for pharmaceutical development.

## 4.2   Components and Methods

### 4.2.1   DBS Card Types

Neonatal screening facilities and epidemiological centers around the world accept DBS as a reliable sampling method comparable to traditional methods using capillary pipettes, test tubes, centrifuges, and freezers for collection and preservation of plasma and blood samples. The DBS sampling technique requires a suitable paper matrix, a needle, capillary pipettes, drying racks, a bag with desiccant for storage of paper matrices in dry condition and a punching tool for use in the bioanalytical lab. The details of the procedure have been documented by the National Committee on Clinical Laboratory Standard (NCCLS) and Newborn Screening Quality Assurance Program (NSQAP) at the Centers for Disease Control and Prevention (CDC) in several publications (Hannon et al. 2003; Mei et al. 2001).

The DBS cards are composed of a cellulose matrix (filter paper) of specific pore size and thickness. Dr. Robert Guthrie in his seminal 1963 publication described the use of a piece of thick, very absorbent filter paper made from high purity cotton (Schleicher and Schuell #903, later known as Whatman 903) to measure phenylalanine for the diagnosis of phenylketonuria in newborns (Guthrie and Susi 1963). Whatman 903 paper provides an accurate and reproducible absorption of blood specimens in line with National Committee on Clinical Laboratory Standards (NSQAP) that has been approved and registered by the FDA as a Class II IVD Medical Device. The NSQAP has developed an isotopic method to assess the paper's uniformity and absorption characteristics of the DBS matrices (Edelbroek et al. 2009).

The traditional filter paper manufacturer Whatman is now a subsidiary of General Electric Healthcare Division (http://www.whatman.com). They manufacture and supply several types of DBS cards both uncoated and coated with proprietary reagents. Four common types of DBS cards used for biological sampling are FTA DMPK-A (coated and known as FTA card), FTA DMPK-B (coated and know as FTA elute card), FTA DMPK-C (not coated and known as 31ETF), and 903 (uncoated and similar to DMPK-C card but less controlled in terms of quality specifications). Two additional types of uncoated cards (226 and 227) are manufactured by Ahlstrom (http://www.ahlstrom.com). The FTA DMPK-A and FTA DMPK-B cards were designed for nucleic acid analysis and according to the manufacturer, both cards are chemically treated with proprietary reagents that, upon contact,

**Fig. 4.1** A DBS card with different volumes on the imprinted circles
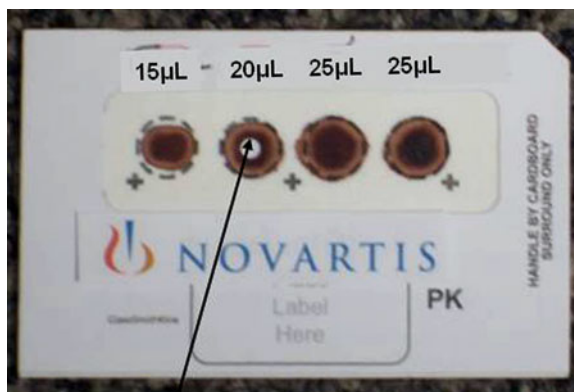


A 3 mm punch from the center of the spot

lyse cells, denature proteins, inactivate enzymes and pathogens, and prevent the growth of bacteria. Basically, these coated cards were prepared to lyse both cellular and nuclear membranes to expose nucleic acids with good stability for storage and analysis. Each of these cards has four circles (diameter 1 cm) imprinted for sampling area and encased in a paper frame shown in Fig. 4.1. The use of the coated cards has been reported in recent publications for the exposure assessment of drugs and metabolites in both clinical and toxicological studies (Filippi et al. 2009; Liang et al. 2009; Spooner et al. 2009; Barfield et al. 2008; Mauriala et al. 2005; Beaudette and Bateman 2004). Many compounds have been shown to be stable on the coated cards for at least 2 months at room temperature (Beaudette and Bateman 2004).

## 4.2.2 Specimen Collection on DBS Cards

For quantitative bioassay used in PK studies, a whole blood sample is collected from a toe or finger-prick. The puncture site is cleansed with 70% isopropanol and dried prior to puncture. Whole blood is then collected in capillary pipettes coated with EDTA as anticoagulant. Alternatively, blood can be collected by venipuncture or from indwelling catheters into EDTA tubes.

The total volume of blood needed depends on the sensitivity requirement of the bioassay and the detection method. For example, the current tandem mass spectrometric instruments have very high sensitivity and require very low sample volume for the analysis of most compounds. Typically, a 50 μL aliquot of blood per time point is sufficient to obtain three spots of 15 μL each in three of the imprinted circles on each DBS card (appropriately labeled) using a capillary pipette (Spooner et al. 2009; Liang et al. 2009; Barfield et al. 2008). The pipette tip is held just above the card and a drop is allowed to form and soak into the surface of the card. The pipette tip is not allowed touch the surface of the card as this may damage the paper leading to issues with sample homogeneity. Samples from small animals such as rat and mouse can be collected via the tail vain (Mauriala et al. 2005; Beaudette and Bateman 2004). Sampling for neonatal screening, therapeutic drug monitoring or other diagnostic purposes, whole blood is obtained via a toe- or finger-pricks (Edelbroek et al. 2009; Hannon et al. 2003; Mei et al. 2001).

## 4.2.3 Drying of DBS Cards

After sample collection, the DBS cards are dried for typically 2 h on a card rack at room temperature (Spooner et al. 2009; Barfield et al. 2008).

The drying time depends on the card type and the sample volume. In our laboratory, we studied precise drying time and found that FTA DMPK-A and FTA DMPK-B cards are completely dry after 20 min of storage on the bench at room temperature (23°C) for a blood spot volume of 20 μL. As mentioned above, these two cards are coated with ingredients that prevent bacterial growth. The uncoated cards may be subject to bacterial growth if the card is not completely dry, and this may impact determination of the analyte concentrations in the sample (Mei et al. 2001).

### 4.2.4 Stability of Target Analytes, Packaging, and Shipping

Many compounds were found to be more stable on DBS matrix compared to blood or plasma matrices (Edelbroek et al. 2009). Stability on the DBS card depends on the chemistry of the compounds. Because the blood spots must be dried on the surface of the cards, volatile or air sensitive compounds cannot be reliably collected on DBS cards. Light sensitive compounds need special handling whether they are on DBS cards or not. Typically, the dry cards are stored in zip-closure bags containing a desiccant package. Compounds in DBS matrix have been successfully stored under this condition for up to 2 months (Beaudette and Bateman 2004). However, for long-term storage, the bags are stored at −20°C (Fingerhut et al. 2009b; Mei et al. 2001). One of the conveniences of using DBS card is that the samples can be shipped at ambient temperatures without the possibility of exposure to blood pathogens. Ambient temperatures are difficult to maintain during shipping and the temperature may rise up to 60°C for a long period during shipping. Therefore, to ensure stability of the compounds, the effect of temperature on the stability of the compounds on the DBS cards should either be tested during method validation, or the temperature should be controlled during shipment. DBS cards containing unstable compounds and compounds without stability information should be shipped in dry ice to ensure stability.

## 4.3 Bioassay Using the DBS Card Matrix

### 4.3.1 Introduction

Depending on the type of application, the DBS matrix may be subjected to qualitative, semiquantitative, and quantitative analysis. One of the benefits of the application of the DBS technique is that the semiquantitative or qualitative analysis from the blood spots can be directly performed without extraction using a mass spectrometer equipped with a desorption electrospray ionization (DESI) or matrix assisted laser desorption ionization (MALDI) source. Samples collected on DBS matrix have been analyzed using a variety of biological and analytical techniques. The first published method for DBS samples used a microbial assay (Guthrie and Susi 1963). There are published assays based on immunological techniques (Boemer et al. 2009; Worthman and Stallings 1994; Lemonnier et al. 1991; Mizuta et al. 1982). Qualitative assay of DBS samples were also performed using nuclear magnetic resonance spectroscopy (Constantinou et al. 2004). Recent DBS assay methods are mostly based on liquid chromatography-tandem mass spectrometry (LC-MS/MS). The speed and sensitivity of MS/MS made the DBS sampling useful and cost effective for PK and TK studies in pharmaceutical research and development.

A validated method is needed for the quantitative analysis of drugs and metabolites collected in the DBS card matrix. If the method is needed for exposure assessment in support of preclinical or clinical studies, the validation should be completed according to regulatory guidelines (US Food and Drug Administration, Guidance for Industry: Bioanalytical Method Validation, May 2001).

The coated cards have proprietary chemicals in the matrix that may cause matrix effects and ion suppression in MS/MS detection. Therefore, matrix effects and ion suppression should be investigated when using a mass spectrometric detection method for the bio-assay. Assay validation for DBS matrix is more time consuming

than that in a liquid bio-matrix (plasma, serum, or whole blood) due to the steps needed to study some effects that are specific to DBS card matrix only. The effects such as chromatographic partitioning, blood volume, and hematocrit effects have been discussed for samples collected on DBS cards (Mei et al. 2001; Adam et al. 2000; Holub et al. 2006; Newman et al. 2009; Wilhelm et al. 2009a; Liang et al. 2009). While the hematocrit value in a whole blood sample impacts the concentration of analytes in blood, the chromatographic effect is negligible in the DMPK-A and DMPK-B cards. Since DBS is a dry matrix, freeze-thaw stability study is not applicable. However, as previously indicated, the stability of DBS matrix under shipping conditions (e.g., at 60°C) must be evaluated during the validation process.

## 4.3.2   Preparation of Standards and Quality Control Samples

Stock solutions for standard and quality control (QC) samples are prepared separately using the pre-weighed amount of each analyte and dissolving in a suitable solvent. The stock solutions are diluted in whole blood within the dynamic range of the assay method for the preparation of the standard and QC samples. It is also common practice to make working solutions in plasma matrix (from the stock solutions) at high concentrations and these solutions are then diluted in whole blood to prepare the standard and QC samples. In order to minimize dilution of the blood matrix, it is important that the volume of the spiking solution be maintained less than 5% of the total volume during the preparation of standard and QC matrices. Typically less than 50 μL of the standard or QC in whole blood is used on each spot using the procedure described in the "Specimen collection on DBS" section. Calibration standards are made fresh on the day of analysis. The QC samples are prepared, dried, and stored with the study samples to mimic the same storage conditions. The cards containing the calibration standards need to be dried completely before punching any disc from these cards.

## 4.3.3   Sample Extraction and Analysis

After drying the DBS cards spotted with whole blood, the blood proteins are precipitated on the paper matrix. Depending on the sensitivity requirement of the assay, one or more discs of specific diameter (e.g., 3 mm) is punched out of each DBS and transferred to a specified well in a 96-well plate. A Harris Uni-Core punching tool (http://www.tedpella.com/histo_html/unicore.htm) is commonly used for manual punching. The punching tools of punches of different sizes are shown in Fig. 4.2. This punching step of DBS cards can be automated using the BSD1000 GenePunch automated punch system (http://www.bsdrobotics.com). There is also the semi-automated BSD600-DUET punch system shown in Fig. 4.3 that can be used for punching DBS cards. The supplier in the USA for both these robots is ID Biological Systems (http://www.id-biological.com).

The BSD1000 robot has been designed to accommodate commonly used DBS cards. The cards are preloaded into a card magazine. The system automatically scans the sample area to determine possible areas for punching the card. It has a module for punching of disks into 96-well plates. This unit also has the BSD Low-Pressure Air System, with a humidifier, which reduces the effects of static electricity. The instrument has highly flexible software and barcode reading capability that provides positive identification of card magazines, samples, standards, controls, and plates throughout the whole process. The software generates a comma-delimited ASCII file after every run. This file can be exported into the LIMS or another downstream instrument for further use. The unit can scan the sample (or controls and standards) barcodes determined in the input file and punch the number of disks required into specified wells of the 96-well plate. The unit will only punch the sample if the barcode scanned is identical to the one in the input file.

**Fig. 4.2** Harris Uni-Core punching tools of different diameters for manual punch (with permission from Ted Pella, Inc.)



**Fig. 4.3** BSD600-DUET Semi-automated punch system (with permission from BSD Robotics)

The extraction process involves dissolving the target analytes from the paper discs in a solvent and subsequent analysis of the extract. For a regular off-line extraction, a specified volume of extraction solvent (e.g., methanol) is pipetted into each well. The internal standard used for LC/MS methods is already dissolved in the extraction solvent. An automated liquid handler (e.g., Tomtec Quadra 4) can be used to add the extraction liquid to the 96-well plate. The plate is then sealed and mixed on an automatic shaker. The plate can also be briefly kept in a sonication bath to facilitate the extraction process if needed. The plate is then centrifuged and a specific volume (e.g., 50 μL) of liquid is removed from each well using the automated liquid handler (e.g., Tomtec Quadra 96) and transferred to a clean 96-well plate. The extracts can be dried under dried nitrogen gas and the residue is reconstituted in a suitable solvent if needed. The plate is placed on an autosampler for analysis. The off-line extraction procedure described here is most common, though an online extraction procedure for punched DBS samples has been reported recently (Déglon et al. 2009). A preliminary assessment of direct quantitative analysis of drugs in DBS samples has been investigated and reported by Abu-Rabie and Spooner (2009) using a CAMAG thin-layer chromatography mass spectrometer interface (TLC-MS). The method was simple, saved time, and did not involve high-performance liquid chromatographic (HPLC) separation. The method sensitivity was higher than the regular method using the off-line extraction of punched spots. However, the authors acknowledged that the introduction of internal standard needs to be investigated for such direct on-line method.

Since the early 2000s, the most commonly used detection methods have been based on liquid chromatography-mass spectrometric (LC-MS or LC-MS/MS) detection (Spooner et al. 2009; Wilhelm et al. 2009a; Otero-Santos et al. 2009; Liang et al. 2009; van der Heijden et al. 2009; ter Heine et al. 2009a; ter Heine et al. 2009b; Barfield et al. 2008; Higashi et al. 2008; Koal et al. 2005; Lai et al. 2001). It is the high selectivity and sensitivity of recent MS/MS instruments

that has made DBS amenable to PK studies in pharmaceutical research and development. It is important to evaluate matrix effects and ion suppression during the validation of LC-MS based methods (US Food and Drug Administration, Guidance for Industry: Bioanalytical Method Validation, May 2001). Other reported analytical techniques include assays based on liquid chromatography-fluorescence (LC-FL) detection (Kand'ár and Žáková 2009; Jansson et al. 2003), liquid chromatography-photodiode array (LC-PDA) detection (Wilhelm et al. 2009b), liquid chromatography-ultra violet (LC-UV) detection (Ntale et al. 2009; Dean et al. 2006), LC-coulometric electrode array (LC-EC) detection (Melby et al. 2005), gas chromatography-mass spectrometric (GC-MS) detection (Deng et al. 2005), and immunological detection (Boemer et al. 2009; Worthman and Stallings 1994; Lemonnier et al. 1991; Rattenbury and Taylor 1988; Lampe et al. 1987; Li et al. 1986).

### 4.3.4 Special Considerations for DBS Sampling

*Selection of DBS card:* Different types of cards are available and the signal intensity of the same compound may vary greatly due to the card matrix. Internal data shown below in Table 4.1 illustrates the mean ($n = 3$) signal intensity for compound A on FTA DMPK-B and on FTA DMPK-A type cards varies by as much as 60%. Therefore, it is very important to experiment with different types of cards during the assay development and select the card matrix that maximizes the signal intensity of the analyte.

**Table 4.1** Selection of the card matrix

| Card type | Peak area of compound A | Mean ($n = 3$) |
|---|---|---|
| FTA DMPK-A (FTA) | 5,790 6,610 6,350 | 6,250 |
| FTA DMPK-B (FTA-Elute) | 9,270 10,600 10,235 | 10,035 |

*Sample homogeneity on the DBS:* Homogeneous distribution of analytes on the entire area of the blood spot is very important. The homogeneity may depend on the blood volume, interaction of the compound with the red blood cells (RBC) and type of DBS card used. This test is performed during method development and validation because the standards and the QC samples are prepared using blood of specific volume and hematocrit value (discussed later) but the spot volume of the actual samples may vary due to less control during sample collection and physiological condition of the subject. For example the samples collected by tail bleeding of animals or skin-pricking of human subjects may vary in volume and the hematocrit value. If the analyte distribution is heterogeneous on the DBS matrix, the analyte concentration of the punched disc sampled from the center of the spot will be higher than those of the peripheral region of the spot. In a paper published from Centers for Disease Control and Prevention (Mei et al. 2001) an accuracy difference of 13% was reported in 6 mm punched discs from the center of the DBS when the blood volume varied from 25 to 125 μL and the results was reproducible between two different sources of DBS cards.

The effect of blood volume on FTA-Elute (FTA DMPK-B) card was studied with dextromethorphan and its metabolite (Liang et al. 2009). An accuracy difference of <10% was observed for the quality control samples when the blood volume was changed from 25 to 50 μL. The effect of blood volume on the accuracy was less than 5.5% when a spotted blood volume of 10 or 20 μL was compared with 15 μL for acetaminophen (Spooner et al. 2009). An acceptable accuracy difference of ±15% is acceptable according to the FDA guidance for quality control samples. Our laboratory has observed a precision of 8.9% or less for the test compound, shown in Table 4.2.

*Dried blood spots (whole blood) vs. plasma data:* Plasma is typically preferred over whole blood for the assessment of systemic exposure due to conveniences in storage, processing for analysis and homogeneity. In both plasma and whole blood (as a fluid or as DBS matrix), the

**Table 4.2** Response of compound A in different punched discs in the same dried blood spot on FTA DMPK-B card

| Nominal conc. (ng/mL) | Peak area | Mean (n = 3) | CV (%) |
|---|---|---|---|
| 20 | 834 816 779 | 810 | 3.46 |
| 200 | 8,666 7,907 7,253 | 7,942 | 8.90 |

concentration of any compound is affected by the blood-to-plasma distribution, the hematocrit value, and systemic clearance. According to Rowland and Emmons (2010), for drugs showing less variability in fraction unbound in plasma ($f_u$) and blood cell-to-unbound plasma concentration ratio ($\rho$) the use of whole blood or DBS as an alternative to plasma is acceptable. However, for compounds with large variability in either $f_u$ or $\rho$, it may be important to include correction for these factors, since this variability can confound both PK and PK/pharmacodynamic interpretations. For compounds with a low value of blood-to-plasma ratio close to 0.55 the variability in $f_u$ is important when using whole blood or DBS for exposure assessment. For compounds with large blood-to-plasma ratio >2 the variability in $\rho$ is critical. All these ratios can be evaluated in vitro using blood obtained from the study species of interest prior to implementing the use of whole blood or DBS for exposure assessment (Rowland and Emmons 2010).

*The Hematocrit effect:* The hematocrit, also known as packed cell volume (PCV), is expressed as the percent volume occupied by red blood and other cells in the whole blood. It is normally 48% (range 42–52%) for adult men and 42% (range 36–48%) for adult women and 28–68% for neonates (Purves et al. 2004). The effect of hematocrit on DBS can be severe for erythrocyte bound compounds because uneven diffusion of the compounds on the card may result in spot heterogeneity especially when using uncoated card matrix. It is advisable to maintain the hematocrit parameter of the standard and quality control samples close to the mean value for the patient population used in the study. As mentioned above, the effects of the hematocrit and the blood-to-plasma distribution ratio are dependent on the compound. For example, the DBS analysis of cyclosporine A was not affected by the hematocrit (HT) value when studied in quality control samples in blood containing 20–70% HT values (Wilhelm et al. 2009a). Similarly, the DBS analysis of 25-hydroxy vitamin D2 and 25-hydroxy vitamin D3 concentrations were not affected when studied at HT values of 40–60% (Newman et al. 2009). In a study examining the influence of HT and localization of punch in DBS on levels of amino acids and acylcarnitines were studied, the hematocrit values of 20–60% severely affected the analyte concentrations (Holub et al. 2006). The sampling of thyroxine on an uncoated matrix showed HT effects when studied using ^{125}I-thyroxine in blood containing HT values of 30–70% (Mei et al. 2001).

## 4.4 Review of Applications

The DBS technique has been used for both qualitative and quantitative determination of a wide variety of compounds in diagnostic and pharmaceutical laboratories. Compounds analyzable in whole blood, serum, or plasma can be analyzed from DBS provided they are nonvolatile and nonreactive to air. Some of the compounds analyzed using DBS include nucleic acids (DNA and RNA), enzymes, enzyme inhibitors, amino acids, hormones, biomarkers, vitamins, antibiotics, antiepileptics, antivirals, antimalarials, antitussive, anticonvulsant, alkaloids, immunosuppressants, thyroglobulin, trace elements, sugars, carnitine, cholesterol, glutathione, and acetaminophen. Applications of this technique include TDM, neonatal screening, epidemiological studies (mostly associated with TDM and newborn screening), PK/TK studies and determinations of various diagnostic compounds.

*Therapeutic drug monitoring (TDM):* Therapeutic drug monitoring can be essential for effective drug treatment management, and is commonly employed in hospitals and clinics. The use of blood spot cards is a simple method of sampling

blood for quantitative determination of drugs and metabolites for TDM (Edelbroek et al. 2009; Wilhelm et al. 2009; van der Heijden et al. 2009; Cheung et al. 2008; Hoogtanders et al. 2007; AbuRuz et al. 2006; Abu Ruz et al. 2010). TDM of several immunosuppressive drugs has been reported using DBS technique. DBS assay of cyclosporin A has been developed for monitoring blood concentrations in patients using both immunological (Lampe et al. 1987) and LC-MS/MS techniques (Wilhelm et al. 2009). The immunoassay used 20 μL blood per spot and the samples on DBS matrix were shown to be stable for at least 4 weeks at room temperature. The method precision was 11.5% for quality control (QC) samples at 0.25 mg/L. The LC-MS/MS assay was validated for a dynamic range of 25–1,440 μg/L. The assay showed a negligible matrix effect and had a recovery of 97% for cyclosporine A in QC samples. The DBS were stable for a period of at least 17 days in the refrigerator at 4°C.

An LC-MS/MS assay for everolimus was reported for TDM in stable renal transplant patients (van der Heijden et al. 2009). The sample volume used on the blood spot was 30 μL and the standard curve range was 2–30 μg/L. The DBS samples were stable for 32 days at 4°C and for 3 days at 60°C. An assay for tacrolimus, based on LC-MS/MS detection, was reported in which a 30 μL aliquot of blood per spot was used (Hoogtanders et al. 2007). The assay range was 1–30 μg/L, stabilities at different temperatures were studied. The tacrolimus concentrations of 24 stable out patients were similar when compared by DBS vs. whole blood quantification.

Determination of metformin in DBS has been reported using only 10 μL blood (AbuRuz et al. 2006). The method was applied for the analysis of blood spots taken from diabetic patients to assess adherence to medications and to evaluate the relationship between metformin level and metabolic control of diabetes. The method used reversed phase HPLC separation with UV detection. The method recovery of metformin was more than 84%. The limits of detection and quantification were 90 and 150 ng/mL, respectively. The intra- and inter-day precision (measured by CV%) was less than 9%. The accuracy (measured by relative error, %) was less than 12%. Stability analysis showed that metformin was stable for at least 2 months when stored at −70°C. A similar HPLC-UV method has been recently reported for the therapeutic drug monitoring of Lamotrigine in DBS by Abu Ruz et al. (2010).

Quantification of antiretroviral drugs in DBS samples using LC-MS/MS was reported (Koal et al. 2005). The study used DBS from HIV/AIDS patients as the basis for TDM. This study included seven protease inhibitors amprenavir, nelfinavir, indinavir, lopinavir, saquinavir, ritonavir, atazanavir and two non-nucleoside reverse transcriptase inhibitors nevirapine, and efavirenz. Reserpine was used as the internal standard. The DBS samples were punched out and extracted using 50:50 methanol/0.2 M zinc sulfate (v/v) as extraction reagent. The limits of detection were 8–70 ng/mL, the lower limits of quantification (LLOQ) were 41–102 ng/mL, the linear concentration ranges were 41–10,000 ng/mL, the accuracies were 92–113%, and the QC recoveries were 62–94%. The ion suppressions of the compounds in the ionization source were investigated and were comparable to data obtained from human plasma. Significant correlations between real patient plasma and DBS were obtained for samples containing lopinavir, atazanavir, ritonavir, saquinavir, and efavirenz.

For the quantitative determination of the HIV-integrase inhibitor raltegravir in human plasma, DBS, and peripheral blood mononuclear cell (PBMC) lysate, an assay was developed and validated using LC-MS/MS (ter Heine et al. 2009a). The study also included the qualitative analysis of the main metabolite, raltegravir-glucuronide. Raltegravir was extracted from 50 μL of human plasma by protein precipitation using a mixture of methanol and acetonitrile. Extraction from DBS was performed with a mixture of methanol, acetonitrile, and 0.2 M zinc sulfate in water (1:1:2, v/v/v) and extraction from cell lysate was performed using 50% methanol in water. The method was validated over a range of 50–10,000 ng/mL in plasma and DBS and a range of 1–500 ng/mL in PBMC lysate. Dibenzepine was used as the internal standard. The

method showed good specificity, accuracy, precision, and robustness. Accuracies ranged from 104 to 105% in plasma, 93 to 105% in DBS, and 82 to 113% in PBMC lysate. The respective precisions over the concentration range were less than 6, 11, and 13% in plasma, DBS, and PBMC lysate, respectively. The method was used for therapeutic drug monitoring and pharmacological research in HIV-infected patients treated with raltegravir.

Quantification of etravirine (TMC125) in plasma, DBS, and PMBC lysate by LC-MS/MS has been published by ter Heine et al. (2009b). The method was validated over a range of 25–5,000 ng/mL in plasma, 50–10,000 ng/mL in DBS and 5–2,500 ng/mL in PBMC lysate, respectively. The respective accuracies ranged from 89 to 106% in plasma, 94 to 109% in DBS, and 91 to 105% in PBMC lysate. Precisions ranged from 1.9 to 14% in plasma, 4.7 to 20% in DBS, and from 3.1 to 11% in PBMC lysate. The assay was successfully used for therapeutic drug monitoring in HIV-infected patients treated with etravirine.

The antiepileptic drug topiramate for TDM has been assayed using LC-MS/MS (la Marca et al. 2008). The linear calibration curve range was 0.5–50 mg/L in DBS with a correlation coefficient of 0.999. The precision varied from 2.13–11.85% in the concentration range of 0.5–50 mg/L, and the accuracy varied from 93.9–111%. The data observed in this method was comparable with those obtained using a commercially available fluorescence-polarization immunoassay (FPIA) kit.

A rapid and simple enzyme-linked immunosorbent assay (ELISA) was developed for the detection of the antimalarial drug quinine in urine, serum, and DBS (Rowell and Rowell 1987). The assay had a limit of detection of 3 μg/L, using 5 μL of blood on DBS. No cross-reactivity was observed with commonly administered drugs. The assay was used to screen samples of DBS and urine from a volunteer after taking a dose of 300 mg of quinine. In another study the antimalarial drug methylene blue was assayed using LC-MS/MS methods from whole blood, DBS, and plasma (Burhenne

et al. 2008). The assay methods were developed according to FDA guidelines. Extraction was performed using aqueous acetonitrile. Sample extracts were chromatographed on a mixed mode column (cation exchange/reversed phase) using an aqueous ammonium acetate/acetonitrile gradient. The methods were linear within 75–10,000 ng/mL concentration range. The respective inter-batch accuracies of the whole blood, plasma, and paper spot methods varied between −4.5 to +6.6, −3.7 to +7.5, and −5.8 to +11.1%, respectively. The corresponding precisions varied from 3.8 to 11.8%. After a single 500 mg oral dose, the methylene blue concentrations were detectable for up to 72 h in plasma. The methods were applied in clinical studies on healthy individuals and malaria patients.

A method for simultaneous determination of antimalarial drugs chloroquine, proguanil, and their metabolites from a whole blood sample (80 μL) collected on DBS was developed (Lejeune et al. 2007). The method was based on HPLC-UV (254 nm). The assay was linear in the range of 150–2,500 ng/mL for chloroquine and metabolite and 300–2,500 ng/mL for proguanil and cycloguanil. Both inter- and intra-batch precisions were below 10.3%. The stability of the compounds and metabolites on DBS was evaluated at temperatures −20, 4, 20, and 50°C for 1, 5, and 20 days. Decrease in the chloroquine and proguanil levels were observed under the storage conditions. The assay showed good accuracy, precision, and was suitable for use in PK and epidemiological studies on antimalarial treatments.

A bioassay method was developed and validated for the quantitative determination of sulfadoxine (SD) and sulfamethoxazole (SM) in 0.1 mL of capillary blood sampled on DBS (Malm et al. 2008). Extraction was performed using a solid phase method. Analytes were detected with an UV lamp at 256 nm. The lower limit of quantitation was 5 μmol/L for both analytes. The precisions were 4.2 and 3.9% for SD and SM, respectively. Three brands of sampling papers were compared with respect to absorption properties, extraction recoveries, and precision. Punching out DBS instead of

cutting spots into strips prior to extraction was also evaluated. The importance of uniformity of the sampling paper, sample volume, and the benefits of DBS were discussed. Avoiding possible preanalysis errors resulted in more accurate and precise data in this study.

A sensitive and specific HPLC-MS/MS assay for the simultaneous determination of the antibiotics vincristine and actinomycin-D in human DBS has been published (Damen et al. 2009). The analytes were extracted from the punched-out disk (0.25 in. diameter) and sonicated for 15 min in a mixture of acetonitrile-methanol-water (1:1:1, v/v/v) containing vinorelbine as the internal standard. The standard curve range for vincristine was 1–100 ng/mL and that for actinomycin-D was 2–250 ng/mL. The assay was suitable for application in clinical studies involving vincristine and actinomycin-D.

The use of a simple pre-column derivatization method for the determination of aminoglycoside antibiotics (Ags) has been reported (Tawa et al. 1998). The stability of the o-phthalaldehyde (OPA) derivatives of the Ags obtained using β-mercaptopropionic acid (β-MP) was investigated using a HPLC-Fluorescence detection method. One of the fluorescent derivatives of sisomicin was stable for at least 6 h in 50% methanol. The method was applied to rabbit whole blood samples collected after subcutaneous injection of 1 mg/kg of the Ags, using DBS on filter paper punched disks. The detection limits of sisomicin and netilmicin in the DBS were 0.053 and 0.50 μg/mL, respectively. The method allowed monitoring Ags in blood at therapeutic levels.

A simple method based on LC-UV (334 nm) detection has been reported for the antituberculosis drug rifampicin in human plasma and DBS (Allanson et al. 2007). Extraction from plasma was performed using a solid phase cartridge and that from DBS was performed using acetonitrile as the solvent. The recovery of rifampicin from plasma and blood spots was 84.5 and 65.0%, respectively. The assay was linear over the concentration range of 0.5–20 μg/mL. The limit of quantification was 0.5 μg/mL in plasma and 1.5 μg/mL in blood spots. Both intra-day and inter-day precision data showed reproducibility (R.S.D. ≤8.0%, $n = 9$). Stability studies showed rifampicin was stable in plasma for up to 9 h after thawing, up to 9 h in extract. Five patient samples were analyzed using the methods described. A correlation was found between the concentrations of rifampicin in plasma and blood spots ($r^2 = 0.92$). This method was proposed as a means of therapeutic drug monitoring of rifampicin in patients with tuberculosis.

A commonly used enzyme immunoassay was modified for the measurement of theophylline in plasma and DBS (Rattenbury and Taylor 1988). The recovery of theophylline added to samples was 62–76%. The correlation of results from the spots with those from plasma was 0.965. In an earlier publication by Li et al. (1986), an assay for theophylline in which DBS was used successfully as an alternative matrix for quantification of theophylline using a modified FPIA. The method provided results comparable with those of the conventional serum assay. Results from 64 pairs of DBS and serum specimens analyzed by the respective FPIA methods yielded the correlation of 0.988. A major advantage of the FPIA was that it required only basic laboratory skills. When coupled with the use of DBS, this system was effective in remote theophylline monitoring, particularly suited for home care. The major conclusion from both of these two papers was that theophylline concentration was identical when measured in plasma, serum, and DBS.

*Neonatal Screening:* Newborn screening to identify infants with treatable congenital disorders is carried out worldwide. The use of novel analytical instrumentation, such as tandem mass spectrometry (MS/MS), has expanded the ability to screen for more than 50 metabolic diseases with a single DBS. The feature that makes metabolic disorders particularly amenable to screening is the presence of specific small-molecule metabolites. The relatively simple and less invasive nature of DBS sampling and the use of micro volume blood make it a very useful sampling method for neonatal and juvenile subjects. The early published articles on the use of DBS technique were in the area of newborn screening (Guthrie and Susi 1963; Hill et al. 1967). This

is an application area where the largest number of published articles using the DBS sampling technique has been observed.

Lysosomal storage disorders (LSDs) comprise more than 40 genetic diseases that result in the accumulation of products that would normally be degraded by lysosomal enzymes. A tandem mass spectrometry (MS/MS) based method is available for newborn screening for five LSDs (De Jesus et al. 2009). Many clinical screening laboratories are initiating pilot studies to evaluate the incorporation of this method into their screening process. The authors developed and evaluated DBS quality control (QC) materials for LSDs and used the MS/MS method to investigate their suitability for LSD QC monitoring. This method involves incubation of 3.2 mm punches from DBS controls for 20–24 h with assay cocktails containing substrate and internal standard and subsequently analysis using MS/MS. Samples were run in triplicate for 3 consecutive days. Results were reported as product-to-internal standard ratios and enzyme activity units (μmol/L/h). Enzyme activity interday precision (CV%) for the high, medium, and low series were 3.4–14.3% for galactocerebroside α-galactosidase, 6.8–24.6% for acid α-galactosidase A, 7.36–22.1% for acid sphingomyelinase, 6.2–26.2% for acid α-glucocerebrosidase, and 7.0–24.8% for lysosomal acid α-glucosidase. Stability assessment of DBS samples stored at −20 and 4°C showed minimal enzyme activity loss over a period of 187 days. DBS stored at 37 and 45°C had lower activity values over the 187 day evaluation time. Suitable QC materials for newborn screening of LSDs were developed for laboratories performing LSD screening using DBS.

Newborn screening of mucopolysaccharidosis-I is done by monitoring the activity of the enzyme α-L-iduronidase. A new α-L-iduronidase substrate has been synthesized for monitoring the enzyme activity for a method using LC-MS/MS (Blanchard et al. 2008). The assay used a DBS on a newborn screening card as the enzyme source. The enzyme reaction conditions and procedures for the assay, including the concentration of substrate, the reaction pH, and the incubation time were optimized. The α-L-iduronidase activity

measured for five patients with mucopolysaccharidosis-I was well below that found for ten randomly chosen newborns. Inter- and intra-assay precision values were less than 10%.

Chalcraft and Britz-McKibbin (2009) reported a capillary electrophoresis-electrospray ionization-mass spectrometry (CE-ESI-MS) assay for neonatal screening that allowed the direct analysis of amino acids, acylcarnitines, and their stereoisomers from DBS. Online sample preconcentration allowed the quantification of metabolites with poor sensitivity in complex biological samples without ion suppression or isomeric/isobaric interferences. Method validation parameters showed accurate quantitation of 20 different amino acid and acylcarnitine biomarkers associated with inborn error of metabolism in neonates.

Phenylketonuria (PKU) is one of the most common inborn errors of metabolism caused by mutations in the gene for phenylalanine hydroxylase and resulting in elevated levels of phenylalanine (Phe) and decreased level of tyrosine (Tyr) in the blood. The determination of Phe and Tyr is the most reliable approach for the diagnosis of PKU. An HPLC-fluorescence method for the simultaneous measurement of Phe and Tyr in samples of DBS and plasma has been developed and evaluated recently (Kand'ár and Žáková 2009). The intra-assay and inter-assay precisions were below 10%. The method recoveries of Phe and Tyr were 92.0 and 103%, respectively, and the limit of detection was 10.0 and 5.0 μmol/L, respectively.

Tyrosinemia type-I (TYR-1) is a disorder that causes early death if left untreated. Newborn screening for this condition is problematic due to the diagnostic marker, succinylacetone which requires a separate first-tier analysis based on the tyrosine concentration. Turgeon et al. (2008) developed a new assay that simultaneously quantifies acylcarnitines, amino acids, and succinylacetone in DBS by flow injection tandem mass spectrometry (FIA-MS/MS). The extraction of 3/16 in. DBS punches were performed with 0.3 mL methanol containing amino acid and acylcarnitine stable isotope-labeled internal standards. The extract was derivatized with butanol and

hydrochloric acid. In parallel, the extraction of succinylacetone was done from the residual filter paper with 0.1 mL of a 15 mmol/L hydrazine solution containing the internal standard $^{13}C_5$-succinylacetone. The derivatized aliquots were combined in acetonitrile for MS/MS analysis. Elevated levels of succinylacetone were observed in retrospectively analyzed newborn samples of 11 TYR-1 patients. The duration of storage of the samples was 1 week–52 months with original succinylacetone and tyrosine concentrations 13–81 and 65–293 µmol/L, respectively.

An improved diagnostic method for tyrosinemia type-1 based on quantifying succinylacetone in DBS by ultra-performance liquid chromatography (UPLC) MS/MS has been published (Al-Dirbashi et al. 2008). Succinylacetone extracted from a single 3/16 in. disk from DBS was derivatized with dansylhydrazine. The derivatized extract was analyzed by UPLC-MS/MS. The calibration curve was linear within the range 0.2–100 µmol/L. Intra-day ($n = 13$) and inter-day ($n = 10$) variations were less than 10%. The cutoff level of succinylacetone in DBS from healthy infants obtained by the method was 0.63 µmol/L ($n = 151$). In DBS from patients with established tyrosinemia type 1 ($n = 11$), concentration of succinylacetone was 6.4–30.8 µmol/L.

Second-tier LC-MS/MS assays of DBS has been reliably used for the screening congenital adrenal hyperplasia (CAH) where the primary methods were based on immunoassays. 21-Hydroxylase enzyme deficiency CAH is one of the target diseases in many newborn screening programs. Affected newborns may show slightly elevated levels of 17-OH-progesterone (17-OHP) in the routine immunoassay screening test. The diagnosis of 11β-hydroxylase deficiency was made by a second-tier LC-MS/MS from DBS (Peter et al. 2008). This method was very helpful in the work-up of elevated 17-OHP observed in immunoassays. It was reported that existing immunoassays of 17-OHP suffer from cross-reactivity mostly with steroid sulfates leading to false positive concentrations of 17-OHP (Fingerhut 2009a). The authors used a second-tier LC-MS/MS method on diethyl ether extract of DBS

and found two distinct subgroups of initially false positive cases.

It was thought that17α-hydroxypregnenolone (17-OHPreg) was one of the major causes of the false elevated 17-OHP levels. To test this hypothesis an LC-MS/MS method was developed that enabled the simultaneous determination of 17-OHPreg and 17-OHP in DBS (Higashi et al. 2008). The application of the method showed that the blood level of 17-OHPreg was elevated in the very-low birth weight ($<1,500$ g) infants compared to those in the normal birth weight ($>2,500$ g) infants ($P < 0.05$). However, the 17-OHPreg concentration was not high enough to cause the false positive results in the enzyme immunoassay-based screening and it was considered that the false positive results came from other endogenous components rather than 17-OHPreg.

Stored DBS cards are a valuable source for postmortem investigations to evaluate the cause of death in early childhood. Fatty acid oxidation disorders, carnitine cycle disorders, and acidurias during neonatal screening have been done by detecting acylcarnitine profiles from DBS. However, diagnostic uncertainties arising from the unknown stability of acylcarnitines and free carnitine during prolonged storage have been a problem in the screening process. Stability of acylcarnitines and free carnitine in DBS samples has been reported by Fingerhut et al. (2009b). The authors reported that at $-18°C$ acylcarnitines were stable for at least 330 days. If stored for more than 2 weeks at room temperature, acylcarnitines were hydrolyzed to free carnitine and the corresponding fatty acids. The rate of decay was logarithmic and dependent on the chain length of the acylcarnitines. Short-chain acylcarnitines hydrolyzed quicker than long-chain acylcarnitines.

Many treatable disorders such as Wilson disease are characterized by absent or diminished large proteins in plasma or within circulating blood cells, for which there are currently no cost-effective screening methods. An assay for quantifying ceruloplasmin (CP) in DBS for newborn screening of Wilson disease has been recently reported (de Wilde et al. 2008). In this

method, CP-specific peptides from DBS samples digested by trypsin were quantified using isotopically labeled peptide internal standards using LC-MS/MS. The calibration curve was linear from 200 to 950 mg/L. Intra-assay precision for CP concentrations of 250, 350, and 550 mg/L was 9.2, 10.7, and 10.2%, respectively. Inter-assay precision for 19 different batches was 8.9, 5.8, and 6.9%, respectively. A method comparison study on previously tested patient samples for CP gave comparable results with lower limit of quantification of 7 mg/L. This approach may be used for newborn screening of other treatable genetic conditions, such as primary immunodeficiencies, that have large proteins as biomarkers.

Congenital hypothyroidism is a disease associated with severe developmental and physical morbidities. An ELISA method has been developed to quantify thyroid stimulating hormone (TSH) levels on newborn DBS (Boemer et al. 2009). The method was accurate over a concentration range from 17.48 to 250 mIU/L. Based on 99.5 percentile of a 16,459 newborn population the cut-off was fixed at 20.1 mIU/L and validated against normal and pathological neonatal populations.

Thyroid dysfunction is more common in individuals with Down's syndrome (DS) than in the general population. DBS is an excellent and simple means of sampling infants and adolescents for measurement of TSH to screen for thyroid dysfunction. Murphy et al. (2008) reported the clinical assessment of 394 children for thyroid dysfunction including the screening of 305 children (aged 4 months–18.9 years) for hypothyroidism using capillary whole blood TSH sample on DBS. Thyroid dysfunction was detected in 4.6% of the children. The parents of the children reported minimal distress by finger-prick screening.

A well known assay (Gen-Probe Aptima assay) for human immunodeficiency virus type 1 (HIV-1) RNA has been adapted for the diagnosis of HIV infection in infants by using DBS (Kerr et al. 2009). The assay was very sensitive and specific. In another article, testing was performed on 617 DBS from HIV-exposed infants in five countries using an ultra-sensitive p24 antigen assay (Cachafeiro et al. 2009). The sensitivity was 94.4% (67/71) and the specificity was 100% (431/431) for infants with DBS specimens ≤20 months old. DBS older than 30 months demonstrated only 72.2% sensitivity (39/54) ($P < 0.001$) but displayed 100% specificity (61/61). Lofgren et al. (2009) reported a procedure for the assessment of a DBS-based HIV-1 RNA service for remote healthcare facilities in a low-income country Tanzania. A method comparison and operational evaluation of DBS RNA against conventional tests for early infant diagnosis of HIV and HIV RNA quantitation was performed under field conditions in Tanzania. DBS samples were prepared and plasma was frozen at −80°C for shipment. DBS samples were mailed and plasma samples were couriered to a central laboratory for testing using the Abbott m2000 system. Infant diagnosis DBS samples were also tested for HIV-1 DNA by ROCHE COBAS AmpliPrep/COBAS TaqMan System. Results of DBS RNA were compared with conventional tests. DBS provided HIV-1 RNA results comparable to conventional methods to remote healthcare facilities.

The country of Botswana has high antenatal human immunodeficiency virus (HIV) prevalence (33.4%). Infant HIV diagnosis is challenging in resource-limited settings, and HIV prevalence among HIV-exposed infants in Botswana is unknown. DBS polymerase chain reaction (PCR) provided a feasible method to identify the HIV-infected children population (Creek et al. 2008). Collection and testing of DBS was successfully integrated into routine infant care in the public health system. The staff in 15 clinics and a hospital were trained to obtain DBS on HIV-exposed infants age 6 weeks–17 months receiving routine care. Roche Amplicor 1.5 DNA PCR testing was performed on the samples on 1931 HIV-exposed infants age 6 weeks–17 months, of whom 136 (7.0%) were HIV infected.

Searles et al. (2008) published a study in which the feasibility of obtaining DBS from newborn screening archives for subjects in epidemiologic studies was evaluated. These specimens were used for genotyping, and for the evaluation of potential for bias in their use. The

authors attempted to locate DBS at Washington State archives for 230 participants in a previous case-control study of childhood cancer, who were born between 1978 and 1990. Specimens for 203 (88%) children were retrieved, including 199 (94%) born in months when a DBS catalog was available. Genotyping assays were completed for all the specimens. Among the controls the genotype distributions were similar to existing results.

In summary, monitoring of treatment with HIV viral load and resistance testing, as recommended in industrialized countries, is rarely available in resource-limited settings due to high costs and stringent requirements for storage and transport of plasma. DBS are easy to collect and store, and can be a convenient alternative to plasma. Recently, a number of studies have demonstrated the feasibility and reliability of using DBS to monitor viral load and genotypic resistance (Johannessen et al. 2009).

*Pharmacokinetic and TK applications:* Extensive use of DBS sampling techniques has been reported for newborn screening, therapeutic drug monitoring, and epidemiology. However, the PK and TK applications of DBS have been very limited. The use of DBS for TK studies involving small animals will result in ethical and financial benefit for the studies. The micro volume samples used in DBS will allow serial bleeding of small animals, like mice and rats. It is possible for these samples to be taken from the main study groups, limiting or possibly eliminating the need for additional satellite animals specifically to assess exposure, and therefore, reducing the number of animals used per study. Fewer animals will translate into reduced costs for test article, husbandry, and labor.

Beaudette and Bateman (2004) reported a method for obtaining PK data from rats using DBS for discovery stage exposure assessment of drug candidates to facilitate the decision making for lead optimization. The analysis method had high selectivity, high sensitivity, and the speed offered by the liquid chromatography-tandem mass spectrometry (LC-MS/MS). Another discovery stage study in rats reported on the pharmacokinetics of a cathepsin K inhibitor

using DBS as the sample matrix (Mauriala et al. 2005). Metabolites were initially detected from microsomal incubations and characterized using tandem mass spectrometry. Microsomal results were then used to design a multiple reaction monitoring (MRM) method with MS/MS for the detection of parent drug and metabolites. DBS extracts collected from the rat PK study were analyzed. The circulating metabolites were detected using MRM and their identities confirmed on the basis of fragment ion spectra collected simultaneously. The use of DBS provided a means for reanalysis of PK samples for metabolite identification without the need for complex sample storage and preparation in this study.

In a TK study in dogs, the animals were orally administered acetaminophen and whole blood samples were collected on DBS (15 µL per spot) at different time points to assess the drug exposure (Barfield et al. 2008). Methanol extracts of the DBS samples were analyzed using HPLC-MS/MS. In this study, the quantitative analysis of a drug extracted from DBS provided good quality TK data while minimizing the volume of blood withdrawn from the animals. DBS assays have been recently applied to several TK studies for acetaminophen and dexamethasone administered to beagle dogs and rats (Liang et al. 2009). The acetaminophen data were similar to those observed by Barfield et al. (2008).

There have been a limited number of reported applications of DBS in human PK assessments. In a clinical study involving hyperphenylalaninaemia, the oral loading test with tetrahydrobiopterin (BH4) was used to differentiate the variants of hyperphenylalaninaemia and to screen for BH4-responsive patients (Zurfluh et al. 2006). The outcome of the loading test was dependent on the genotype, dosage administered, and pharmacokinetics of BH4. A total of 71 patients with hyperphenylalaninaemia (mild to classic) were administered 20 mg/kg of BH4 according to different protocols ($1 \times 20$ mg and $2 \times 20$ mg). The blood BH4 concentrations were measured in DBS at different time points (0–48 h) post administration. Maximal BH4 concentrations ($C_{max}$) were measured 4 h ($T_{max}$) after BH4 administration in 63 out of 71 patients. After

24 h, the blood levels of BH4 dropped to 11% of $C_{max}$. The PK parameters for BH4 in blood were: $T_{max} = 4$ h, $AUC_{(0-32h)} = 370$ nmol $\times$ h/g Hb (hemoglobin), and $T_{1/2}$ values for absorption was 1.1 h, for distribution was 2.5 h, and for elimination was 46.0 h. Among the mild PKU patients, 97% responded to BH4 administration. Another recent study data has been reported on the pharmacokinetics of tetrahydrobiopterin (BH4) following oral loadings with three single dosages in patients with PKU (Gramer et al. 2009). In this study, the authors reported that BH4 pharmacokinetics were variable between patients in terms of absolute levels of BH4 metabolites after BH4 dosing.

In a clinical PK study, ten patients with chronic asthma were given oral doses of 424 mg choline theophyllinate at 09.0 h and 848 mg at 21.0 h for 4 days. At regular intervals during day 1 and day 4 of treatment theophylline concentrations were measured in plasma and DBS by fluorimmunoassay (Hibberd et al. 1986). The day and night time exposure data (PK parameters) of asymmetrical doses of slow release choline theophyllinate were compared at day 1 and at day 4 of treatment when steady state had been achieved. From all the patients and at all the time points throughout the study (179 measurements), theophylline measured from extracted DBS showed a close correlation with plasma concentrations, the regression line was $y = 0.785x + 0.056$, $r = 0.989$. Theophylline concentrations measured in blood spots were slightly lower than those measured in plasma, but exhibited the same PK profile as measured in plasma.

Therapeutic hypothermia reduces mortality and neurologic impairment in neonates with hypoxic-ischemic encephalopathy. Topiramate exerts a neuroprotective effect in asphyxiated neonatal animal models. The influence of hypothermia on the pharmacokinetics of topiramate was evaluated in a clinical study in which asphyxiated neonates were treated with prolonged whole-body hypothermia and topiramate (Filippi et al. 2009). Thirteen newborns were treated with mild or deep whole body hypothermia for 72 h. All the subjects were orally administered with 5 mg/kg of topiramate once a day for the first

3 days of life, and seven subjects had concomitant phenobarbital treatment. Topiramate concentrations were measured on serial DBS sampling of the newborn subjects. Topiramate concentrations reached a virtual steady state in nine newborns. PK parameters $C_{max}$, $C_{min}$, $T_{max}$, $T_{1/2}$, and AUC values were calculated after topiramate administration for these nine newborns. With respect to normothermic infants, the time of maximal concentration ($T_{max}$) was mildly delayed and apparent total body clearance was lower, suggesting slower absorption and elimination. The PK parameters did not differ significantly between infants on deep vs. mild hypothermia and in those on topiramate monotherapy vs. add-on phenobarbital. Most neonates on prolonged hypothermia treated with 5 mg/kg of topiramate once a day exhibited drug concentrations within the reference range for the entire treatment duration.

Recently, a paper has been published on the use of DBS as a sample collection technique for clinical pharmacokinetics (Spooner et al. 2009). In this article the authors used acetaminophen as a compound to demonstrate the utility of DBS sampling technique for in human PK studies for drug development. The bioanalytical method used HPLC-MS/MS for analyzing acetaminophen from human blood (15 µL) collected on DBS. Method validation parameters were discussed for the standard curve range of 25–5,000 ng/mL. Validation parameters such as precision, accuracy, linearity, sensitivity, selectivity and effect of the spotted blood volume, the influence of the blood spotting device, and the temperature of the spotted blood were discussed. The validated method was successfully applied to a clinical study involving single oral dose of 500 mg and 1 g acetaminophen.

*Various diagnostic applications:* A fast, simple, and reproducible method for the quantitative determination of steroid hormones has been reported by Janzen et al. (2008). In this method corticosterone, deoxycorticosterone, progesterone, 17α-hydroxy progesterone, 11-deoxycortisol, 21-deoxycortisol, cortisol, androstenedione, testosterone, and dihydrotestosterone were quantified in micro-volume of serum and in DBS samples

using LC-MS/MS. No derivatization was needed. The validation showed excellent precision, sensitivity, recovery, and linearity with correlation coefficients of greater than 0.992.

Low levels of 25-hydroxyvitamin D (25OHD), during early childhood development, was associated with a range of adverse health outcomes. An assay based on DBS samples was developed (Eyles et al. 2009) where 25-hydroxyvitamin D3 (25OHD3) and 25 hydroxyvitamin D2 (25OHD2) were extracted from 3.2 mm DBS punches, and derivatized with 4-phenyl-1,2,4-triazoline-3,5-dione (PTAD) prior to analysis using LC-MS/MS. Validation parameters such as precision, accuracy, and the impact of storage conditions were assessed. The limit of detection was <1 nmol/L, and 2 nmol/L for 25OHD3 and 25OHD2, respectively. The mean 25OHD3 concentrations in 118 archived DBS varied from 4.8 to 67.8 nmol/L. Another LC-MS/MS method for the determination of 25-OHD2 and 25-OHD3 in DBS has also been recently reported by Newman et al. (2009).

An improved method for the measurement of retinol in DBS on filter paper has been reported (Erhardt et al. 2002). Retinol was extracted by acetonitrile protein precipitation followed by n-hexane extraction and was analyzed by HPLC. The intra- and inter-assay variability was <6%, the detection limit was 0.1 μmol/L, and the method recovery was 97% in spiked samples. DBS retinol consistently decreased 18–23% during the 1st week of storage. After 1 week, retinol remained stable in the blood spots at 23°C for more than 3 months. O'Broin and Gunter (1999) developed and evaluated a method for the determination of folate from DBS samples. In this method, folate was eluted from DBS by sonication in 5 g ascorbic acid/L containing 0.1% (by volume) Triton X-100. The method recovery was >95%, the inter-and intra-assay precision was <8 and <9%, respectively.

Orfanos et al. (1980) reported a method for quantitative determination of glutathione from DBS samples. The sample preparation involved elution of the analyte from a small disk of dried blood spotted on filter paper. After enzymatic reduction of oxidized glutathione, total glutathione in the eluate was measured colorimetrically with 5,5′-dithiobis(2-nitrobenzoic acid) reagent. The stability of the total oxidized glutathione in the DBS was assessed. The results from the method were compared with a spectrophotometric method that used liquid blood and the results were in good agreement. The method may be useful in early detection of 5-oxoprolinuria and some forms of nonspherocytic hemolytic anemia.

Perchlorate is an environmental pollutant that is frequently detected in drinking water and foods. High exposure to perchlorate can inhibit the thyroid's uptake of iodine leading to developmental abnormalities in fetuses and newborns. Otero-Santos et al. (2009) developed a method for analyzing perchlorate in the DBS of newborns. The method used methanol extraction of ten discs of 3.2 mm from DBS spots. The extract was dried, reconstituted, and analyzed in by ion chromatography interfaced with electrospray ionization tandem mass spectrometry. The lower limit of quantitation for the method was 0.10 ng/mL and the precision varied from 5.8 to 16.2%. Using the method, perchlorate was detected in 100% of the DBS collected from 100 newborns.

## 4.5    Advantages and Disadvantages of Using DBS

*Advantages:* DBS offers many advantages including (1) the DBS technique uses less than 0.1 mL of whole blood with many recent applications using less than 20 μL. Such low-volume sampling enables serial bleeding of small animals, newborn subjects, and critically ill patients for exposure assessment, (2) for TK studies the use of DBS will result in using fewer animals, less test article (costly at the development phase) for dosing the animals, (3) the procedure is less invasive and samples can be collected from human subjects by simple finger pricking which may improve subject comfort in clinical studies, (4) the coated DBS card matrix lyses cells, inactivates pathogens, denatures blood proteins and enzymes, and stabilizes the target compounds. Hence, DBS are considered nonhazardous and

cards may be shipped in zippered bags containing desiccants, (5) the sample collection procedure is economical because there is no need for centrifugation, sub-aliquoting, and freezing (needed for plasma collection), (6) cost of shipping is much less than tradition plasma samples because it may not require special packaging with dry ice typically used for plasma samples, (7) the storage of the DBS cards is simpler than storing conventional plasma samples, (8) there is also significant time and cost saving during bioanalysis of DBS samples compared to the plasma or serum samples. The bioassay involves a simple one step solvent extraction using minimum amount of solvent, no need for expensive solid-phase extraction (SPE) cartridges, and there is no need to assess freeze-thaw stability during the method validation process, (9) Compounds that can be analyzed from plasma, serum or whole blood can be easily analyzed using the DBS technique, and (10) Another convenience is that semiquantitative or qualitative analysis of DBS samples can be directly performed without extraction using mass spectrometers equipped with DESI or MALDI. For these many reasons, DBS are ideal for phase II/III studies in developing countries and very convenient for population PK studies.

*Disadvantages:* The DBS sampling cannot be used for volatile and air sensitive compounds. Light sensitive compounds still require special handling. Ultra-low quantitation limit (pg/mL) may be limited for DBS due to the utilization of micro-volume amount of sample. Therefore, DBS sampling may not be suitable for monitoring drugs and metabolites where the blood concentrations are very low. This limitation is expected to be resolved using detector with higher sensitivity in the near future. There are only two manufacturers for DBS cards, currently.

DBS data is dependent on blood/plasma distribution of the target compounds and will provide low exposure data for compounds with high distribution in plasma. In this situation, the plasma method will provide higher exposure values than DBS or whole blood. As for any whole blood assessment, care should be taken when comparing results of different matrices. Automation is currently limited for DBS. A variety of robotics for accurate punching of DBS cards and for

high-throughput bioassay is not yet available. The coated card has proprietary matrix components known to cause both ion suppression and matrix effects in some LC-MS/MS assays. The method validation for DBS bioassay is more time consuming, and require additional experiments such as evaluation of spot homogeneity of analytes, hematocrit effect, effect of blood volume on analyte concentrations, and effect of storage at high temperature (e.g., 60°C) needed to mimic the shipping conditions.

## 4.6 Regulatory Considerations

Regulatory authorities accept systemic drug exposure data from biological fluids such as plasma, serum, and whole blood (US Food and Drug Administration. C. F. R. 60, 11264 1995; ICH Harmonized Tripartate Guideline 1994). The DBS sampling technique is similar to using whole blood and has been in use for more than 45 years for neonatal screening of in born errors of metabolism, therapeutic drug monitoring, and epidemiological screening, and for systemic exposure monitoring of varieties of biologically active compounds (Guthrie and Susi 1963; Edelbroek et al. 2009; Spooner et al. 2009). The existing DBS cards provide an accurate and reproducible absorption of blood specimens and much better quality than Whatman 903 paper which met the quality in line with National Committee on Clinical Laboratory Standards (NSQAP). The FDA approved the Whatman 903 paper as a class II medical device. DBS is a simple, convenient, and accurate matrix for exposure and concentration assessment in whole blood. Bioassay on DBS can be successfully validated using currently established guidelines provided by drug regulatory authorities.

## 4.7 Summary

The dried blood sampling technique has been in use since early 1960s. The procedure is less invasive and the DBS specimens are very easy to collect, dry, and transport. The DBS has been

widely used for neonatal screening, therapeutic drug monitoring, epidemiological studies, and monitoring of many biologically active compounds.

There are both advantages as disadvantages of using DBS as a sampling tool. This sampling techniques has been only recently been used in drug development laboratories. The current limitation of DBS in quantifying low systemic concentrations of analytes can be expected to be resolved with more sensitive detectors in the near future.

For diagnostic and semiquantitative applications in clinical laboratories, the DBS can be a very useful tool. DBS assays may be validated to comply with regulatory guidelines. With the observed growing interest from pharmaceutical companies and the potential benefits to be gained by both patients and researchers, we can expect DBS to quickly become an important new tool for the development of new medicines in pharmaceutical research and development programs.

## References

Abu-Rabie P, and Spooner N. Direct Quantitative Bioanalysis of Drugs in Dried Blood Spot Samples Using a Thin-Layer Chromatography Mass Spectrometer Interface. *Anal. Chem.* 2009; 81:10275–10284

Abu Ruz S, Al-Ghazawi M, and Al-Hiari Y. A Simple Dried Blood Spot Assay for Therapeutic Drug Monitoring of Lamotrigine. *Chromatographia.* 2010; 71:1093–1099

AbuRuz A, Millership J, and McElnay J. Dried Blood Spot Liquid Chromatography Assay for Therapeutic Drug Monitoring of Metformin. *J. Chromatogr. B Analyt. Technol. Biomed. Life Sci.* 2006; 832:202–207

Adam BW, Alexander JR, Smith SJ, Chace DH, Loeber JG, Elvers LH, and Hannon WH. Recoveries of Phenylalanine from Two Sets of Dried-Blood-Spot Reference Materials: Prediction from Hematocrit, Spot Volume, and Paper Matrix. *Clin. Chem.* 2000; 46:126–128

Al-Dirbashi OY, Rashed MS, Jacob M, Al-Ahaideb LY, Al-Amoudi M, Rahbeeni Z, Al-Sayed MM, Al-Hassnan Z, Al-Owain M, and Al-Zeidan H. Improved Method to Determine Succinylacetone in Dried Blood Spots for Diagnosis of Tyrosinemia Type 1 Using UPLC-MS/MS. *Biomed. Chromatogr.* 2008; 22:1181–1185

Alfazil AA, and Anderson RA. Stability of Benzodiazepines and Cocaine in Blood Spots Stored on Filter Paper. *J Anal Toxicol.* 2008; 32:511–515

Allanson AL, Cotton MM, Tettey JNA, and Boyter AC. Determination of Rifampicin in Human Plasma and Blood Spots by High Performance Liquid Chromatography With UV Detection: A Potential Method for Therapeutic Drug Monitoring. *J. Pharm. Biomed. Anal.* 2007; 44:963–969

Barbi M, Binda, S, Caroppo S, Primache V, Dido P, Guidotti P, Corbetta C, and Melotti D. CMV gB Genotypes and Outcome of Vertical Transmission: Study on Dried Blood Spots of Congenitally Infected Babies. *J. Clin. Virol.* 2001; 21:75–79

Barfield M, Spooner N, Lad R, Parry S, and Fowles S. Application of Dried Blood Spots Combined with HPLC-MS/MS for the Quantification of Acetaminophen in Toxicokinetic Studies. *J Chromatogr B Analyt Technol Biomed Life Sci.* 2008; 870:32–37

Beaudette P, and Bateman KP. Discovery Stage Pharmacokinetics Using Dried Blood Spots. *J. Chromatogr. B Analyt. Technol. Biomed. Life Sci.* 2004; 809:153–158

Blanchard S, Sadilek M, Scott CR, Turecek F, and Gelb MH. Tandem Mass Spectrometry for the Direct Assay of Lysosomal Enzymes in Dried Blood Spots: Application to Screening Newborns for Mucopolysaccharidosis I. *Clin. Chem.* 2008; 54:2067–2070

Boemer F, Bours V, Schoos R, Hubert P, and Rozet E. Analytical Validation Based on Total Error Measurement and Cut-off Interpretation of a Neonatal Screening TSH-Immunoassay. *J. Chromatogr. B Analyt. Technol. Biomed. Life Sci.* 2009; 877:2412–2417

Boy RG, Henseler J, Mattern R, and Skopp G. Determination of Morphine and 6-Acetylmorphine in Blood with Use of Dried Blood Spots. *Ther. Drug Monit.* 2008; 30:733–739

Bowron A, Barton A, Scott J, and Stansbie D. Blood Spot Homocysteine: A Feasibility and Stability Study. *Clin. Chem.* 2005; 51:257–258

Brambilla D, Jennings C, and Aldrovandi G. Multicenter Evaluation of Use of Dried Blood and Plasma Spot Specimens in Quantitative Assays for Human Immunodeficiency Virus RNA: Measurement, Precision, and RNA Stability. *J. Clin. Microbiol.* 2003; 41:1888–1893

Burhenne J, Riedel KD, Rengelshausen J, Meissner P, Müller O, Mikus G, Haefeli WE, and Walter-Sack I. Quantification of Cationic Anti-Malaria Agent Methylene Blue in Different Human Biological Matrices Using Cation Exchange Chromatography Coupled to Tandem Mass Spectrometry. *J. Chromatogr. B Analyt. Technol. Biomed. Life Sci.* 2008; 863:273–282

Cachafeiro A, Sherman GG, Sohn AH, Beck-Sague C, Fiscus, and Susan A. Diagnosis of Human Immunodeficiency Virus Type 1 Infection in Infants by Use of Dried Blood Spots and an Ultrasensitive p24 Antigen Assay. *J. Clin. Microbiol.* 2009; 47:459–462

Chace DH, Millington DS, Terada N, Kahler SG, Roe CR, and Hofman LF. Rapid Diagnosis of Phenylketonuria by Quantitative Analysis for Phenylalanine and Tyrosine in Neonatal Blood Spots by Tandem Mass Spectrometry. *Clin. Chem.* 1993; 39:66–71

Chalcraft KR, and Britz-McKibbin P. Newborn Screening of Inborn Errors of Metabolism by Capillary Electrophoresis-Electrospray Ionization-Mass Spectrometry: A Second-Tier Method with Improved Specificity and Sensitivity. *Anal. Chem.* 2009; 81:307–314

Cheung CY, van der Heijden J, Hoogtanders K, Christiaans M, Liu YL, Chan YH, Choi KS, van de Plas A, Shek CC, Chau KF, Li CS, van Hooff J, and Stolk L. Dried Blood Spot Measurement: Application in Tacrolimus Monitoring Using Limited Sampling Strategy and Abbreviated AUC Estimation. *Transpl. Int.* 2008; 21:140–145

Constantinou MA, Papkonstantinou E, Benaki D, Spraul M., Shulpis K, Koupparis MA, and Mikros E. Application of Nuclear Magnetic Resonance Spectroscopy Combined with Principal Component Analysis in Detecting Inborn Errors of Metabolism Using Blood Spots: A Metabonomic Approach. *Anal. Chim. Acta.* 2004; 511:303–312

Creek T, Tanuri A, Smith M, Seipone K, Smit M, Legwaila K, Motswere C, Maruping M, Nkoane T, Ntumy R, Bile E, Mine M, Lu L, Tebele G, Mazhani L, Davis MK, Roels TH, and Kilmarx PH. Early Diagnosis of Human Immunodeficiency Virus in Infants Using Polymerase Chain Reaction on Dried Blood Spots in Botswana's National Program for Prevention of Mother-to-Child Transmission. *Pediatr. Infect. Dis. J.* 2008; 27:22–26

Damen CW, Rosing H, Schellens JH, and Beijnen JH. Application of Dried Blood Spots Combined with High-Performance Liquid Chromatography Coupled with Electrospray Ionisation Tandem Mass Spectrometry for Simultaneous Quantification of Vincristine and Actinomycin-D. *Anal. Bioanal. Chem.* 2009; 394:1171–1182

Dean CJ, Bockmann MR, Hopwood JJ, Brooks DA, and Meikle PJ. Detection of Mucopolysaccharidosis Type II by Measurement of Iduronate-2-Sulfatase in Dried Blood Spots and Plasma Samples. *Clin. Chem.* 2006; 52:643–649

Déglon J, Thomas A, Cataldo A, Mangin P, and Staub C. On-Line Desorption of Dried Blood Spot: A Novel Approach for the Direct LC/MS Analysis of Micro-Whole Blood Samples. *J. Pharm. Biomed. Anal.* 2009; 49:1034–1039

De Haan GJ, Edelbroek P, and Segers J. Gestation-Induced Changes in Lamotrigine Pharmacokinetics: A Monotherapy Study. *Neurology.* 2004; 63:571–573

De Jesus VR, Zhang XK, Keutzer J, Bodamer OA., Muhl A, Orsini JJ, Caggana, M, Vogt RF, and Hannon WH. Development and Evaluation of Quality Control Dried Blood Spot Materials in Newborn Screening for Lysosomal Storage Disorders. *Clin. Chem.* 2009; 55:158–164

de Wilde A, Sadilkova K, Sadilek M, Vasta V, and Hahn SH. Tryptic Peptide Analysis of Ceruloplasmin in Dried Blood Spots Using Liquid Chromatography-Tandem Mass Spectrometry: Application to Newborn Screening. *Clin. Chem.* 2008; 54:1961–1968

Deng C, Ji J, Zhang L, and Zhang X. Diagnosis of Congenital Adrenal Hyperplasia by Rapid Determination of 17α-Hydroxyprogesterone in Dried Blood Spots by Gas Chromatography/Mass Spectrometry Following Microwave-Assisted Silylation. *Rapid Commun. Mass Spectrom.* 2005; 19:2974–2978

Edelbroek PM, van der Heijden J, and Stolk LML. Dried Blood Spot Methods in Therapeutic Drug Monitoring: Methods, Assays, and Pitfalls. *Ther Drug Monit.* 2009; 31:327–336

Erhardt JG, Craft NE, Heinrich F, and Biesalski HK. Rapid and Simple Measurement of Retinol in Human Dried Whole Blood Spots. *J. Nutr.* 2002; 132:318–321

Eyles D, Anderson C, Ko P, Jones A, Thomas A, Burne T, Mortensen PB, Nørgaard-Pedersen B, Hougaard DM, and McGrath J. A Sensitive LC/MS/MS Assay of 25OH Vitamin D3 and 25OH Vitamin D2 in Dried Blood Spots. *Clin. Chim. Acta.* 2009; 403:145–151

Febriani ADB, Sakamoto A, Ono H, Sakura N, Ueda K, Yoshii C, Kubota M, and Yanagawa J. Determination of Total Homocysteine in Dried Blood Spots Using High Performance Liquid Chromatography for Homocystinuria Newborn Screening. *Pediatr. Int.* 2004; 46:5–9

Filippi L, La Marca G, Fiorini P, Poggi C, Cavallaro G, Malvagia S, Pellegrini-Giampietro DE, and Guerrini R. Topiramate Concentrations in Neonates Treated with Prolonged Whole Body Hypothermia for Hypoxic Ischemic Encephalopathy. *Epilepsia.* 2009; 50:2355–2361

Fingerhut R. False Positive Rate in Newborn Screening for Congenital Adrenal Hyperplasia (CAH)-Ether Extraction Reveals Two Distinct Reasons for Elevated 17α-Hydroxyprogesterone (17-OHP) Values. *Steroids.* 2009; 74:662–665

Fingerhut R, Ensenauer R, Röschinger W, Arnecke R, Olgemöller B, and Roscher AA. Stability of Acylcarnitines and Free Carnitine in Dried Blood Samples: Implications for Retrospective Diagnosis of Inborn Errors of Metabolism and Neonatal Screening for Carnitine Transporter Deficiency. *Anal. Chem.* 2009; 81:3571–3575

Fujimoto T, Tawa R, and Hirose S. Determination of Sisomicin in Eluate from Dried Blood Spots on Filter Paper Disc for Monitoring of Blood Levels in Rats, by Reversed-Phase High-Performance Liquid Chromatography after Precolumn Fluoromertic Derivatization. *Chem. Pharm. Bull.* 1989; 37:174–176

Gramer G, Garbade SF, Blau N, and Lindner M. Pharmacokinetics of tetrahydrobiopterin following oral loadings with three single dosages in patients with phenylketonuria. *J. Inherit. Metab. Dis.* 2009; 32:52–57

Green MD, Mount DL, and Nettey H. High-Performance Liquid Chromatographic Assay for the Simultaneous

Determination of Sulfadoxine and Pyrimethamine from Whole Blood Dried Onto Filter Paper. *J. Chromatogr. B Analyt. Technol. Biomed. Life Sci.* 2002; 767:159–162

Guthrie R, and Susi A. A Simple Phenylalanine Method for Detecting Phenylketoneuria in Large Populations of Newborn Infants. *Pediatrics.* 1963; 32:338–343

Hannon W, Boyle J, Davin B, Marsden A, McCabe ERB, Schwartz M, Scholl G, Therrell BL, Wolfson M, and Yoder F. Blood Collection on Filter Paper for Neonatal Screening Programs, 4th Approved Standard, NCCLS Document LA4–A5. Vol 23. Wayne, PA: National Committee for Clinical Laboratory Standards; 2003:21

Hibberd SG, Alveyn C, Coombes EJ, and Holgate ST. Acute and Chronic Pharmacokinetics of Asymmetrical Doses of Slow Release Choline Theophyllinate in Asthma. *Br. J. Clin. Pharmacol.* 1986; 22:337–341

Higashi T, Nishio T, Uchida S, Shimada K, Fukushi M, and Maeda M. Simultaneous Determination of 17α-Hydroxypregnenolone and 17α-Hydroxyprogesterone in Dried Blood Spots from Low Birth Weight Infants Using LC-MS/MS. *J. Pharm. Biomed. Anal.* 2008; 48:177–182

Hill JB, Summer GK, and Hill HD. Modifications of the Automated Procedure for Blood Phenylalanine. *Clin. Chem.* 1967; 13:77–80

Holub M, Tuschl K, Ratschmann R, Strnadová KA, Mühl A, Heinze G, Sperl W, and Bodamer OA. Influence of Hematocrit and Localisation of Punch in Dried Blood Spots on Levels of Amino Acids and Acylcarnitines Measured by Tandem Mass Spectrometry. *Clin. Chim. Acta.* 2006; 373:27–31

Hoogtanders K, van der Heijden J, Christiaans M, Edelbroek P, van Hooff JP, and Stolk LML. Therapeutic Drug Monitoring of Tacrolimus with the Dried Blood Spot Method. *J. Pharm. Biomed. Anal.* 2007; 44:658–664

Howe CJ, and Handelsman DJ. Use of Filter Paper for Sample Collection and Transport in Steroid Pharmacology. *Clin. Chem.* 1997; 43:1408–1415

ICH Harmonised Tripartate Guideline, Code S3A, 1994

Jansson Å, Gustafsson LL, and Mirghani RA. High-Performance Liquid Chromatographic Method for the Determination of Quinine and 3-Hydroxyquinine in Blood Samples Dried on Filter Paper. *J. Chromatogr. B Analyt. Technol. Biomed. Life Sci.* 2003; 795:151–156

Janzen N, Sander S, Terhardt M, Peter M, and Sander J. Fast and Direct Quantification of Adrenal Steroids by Tandem Mass Spectrometry in Serum and Dried Blood Spots. *J. Chromatogr. B Analyt. Technol. Biomed. Life Sci.* 2008; 861:117–122

Johannessen A, Troeseid M, and Calmy A. Dried Blood Spots Can Expand Access to Virological Vonitoring of HIV Treatment in Resource-Limited Settings. *J. Antimicrobial Chemother.* 2009; 64:1126–1129

Kand'ár R, and Žáková P. Determination of Phenylalanine and Tyrosine in Plasma and Dried Blood Samples Using HPLC With Fluoresence Detection. *J. Chromatogr. B Analyt. Technol. Biomed. Life Sci.* 2009; 877:3926–3929

Kerr R, Ryan JS, Player G, Fiscus SA, and Nelson JA. Qualitative Human Immunodeficiency Virus RNA Analysis of Dried Blood Spots for Diagnosis of Infections in Infants. *J. Clin. Microbiol.* 2009; 47:220–222

Koal T, Burhenne H, Roemling R, Svoboda M, Resch K, and Kaever V. Quantification of Antiretroviral Drugs in Dried Blood Spot Samples by Means of Liquid Chromatography/Tandem Mass Spectrometry. *Rapid Commun. Mass Spectrom.* 2005; 19:2995–3001

la Marca G, Malvagia S, Filippi L, Fiorini P, Innocenti M, Luceri F, Pieraccini G, Moneti G, Francese S, Dani FR, and Guerrini R. Rapid Assay of Topiramate in Dried Blood Spots by a New Liquid Chromatography-Tandem Mass Spectrometric Method. *J. Pharm. Biomed. Anal.* 2008; 48:1392–1396

Lai CC, Tsai CH, Tsai FJ, Lee CC, and Lin WD. Rapid Monitoring Assay of Congenital Adrenal Hyperplasia with Microbore High-Performance Liquid Chromatography/ Electrospray Ionization Tandem Mass Spectrometry from Dried Blood Spots. *Rapid Commun. Mass Spectrom.* 2001; 15:2145–2151

Lampe D, Scholtz D, Prumke HJ, Blank W, and Huller H. Capillary Blood, Dried on Flter Paper, as Sample for Monitoring Cyclosporin A Concentrations. *Clin. Chem.* 1987; 33:1643–1644

Lejeune D, Souletie I, Houze S, Le Bricon T, Le Bras J, Gourmel B, and Houze P. Simultaneous Determination of Monodesethylchloroquine, Chloroquine, Cycloguanil and Proguanil on Dried Blood Spots by Reverse-Phase Liquid Chromatography. *J. Pharm. Biomed. Anal.* 2007; 43:1106–1115

Lemonnier F, Masson J, Laroche D, Travert J, and Travert G. Free Thyroxin Measured in Dried Blood Spots from Normal, Low-Birth-Weight, and Hypothyroid Neonates. *Clin. Chem.* 1991; 37:2114–2117

Li PK, Lee JT, Conboy KA, and Ellis EF. Fluorescence Polarization Immunoassay for Theophylline Modified for Use with Dried Spots on Filter Paper. *Clin. Chem.* 1986; 32:552–555

Liang X, Li Y, Barfield M, and Ji QC. Study of Dried Blood Spots Technique for the Determination of Dextromethorphan and its Metabolite Dextrorphan in Human Whole Blood by LC-MS/MS. *J. Chromatogr. B Analyt. Technol. Biomed. Life Sci.* 2009; 877:799–806

Lofgren SM, Morrissey AB, Chevallier CC, Malabeja AI, Edmonds S, Amos B, Sifuna DJ, von Seidlein L, Schimana W, Stevens WS, Bartlett JA, and Crump JA. Evaluation of a Dried Blood Spot HIV-1 RNA Program for Early Infant Diagnosis and Viral Load Monitoring at Rural and Remote Healthcare Facilities. *AIDS.* 2009; 23:2459–2466

Malm M, Lindkvist J, and Bergqvist J. Importance of Pre-Analytical Factors Contributing to Measurement Uncertainty, When Determining Sulfadoxine and

Sulfamethoxazole from Capillary Blood Dried on Sampling Paper. *J. Chromatogr. Sci.* 2008; 46: 837–843

Mauriala T, Chauret N, Oballa R, Nicoll-Griffith DA, and Bateman KP. A Strategy for Identification of Drug Metabolites from Dried Blood Spots Using Triple-Quadrupole/ Linear Ion Trap Hybrid Mass Spectrometry. *Rapid Commun. Mass Spectrom.* 2005; 19: 1984–1992

McGarrity GJ, Constantopoulos G, and Barranger JA. Effect of Mycoplasma Infection on Pyruvate Dehydrogenase Complex Activity of Normal and Pyruvate Dehydrogenase Complex-Deficient Fibroblasts. *Exp. Cell Res.* 1984; 151:557–562

Mei JV, Alexander JR, Adam BW, and Hannon WH. Use of Filter Paper for the Collection and Analysis of Human Whole Blood Specimens. *J. Nutr.* 2001; 131: 1631S–1336S

Melby MK, Wantanabe S, Whitten PL, and Worthman CM. Sensitive High-Performance Liquid Chromatographic Method Using Coulometric Electrode Array Detection for Measurement of Phyroestrogens in Dried Blood Spots. *J. Chromatogr. B Analyt. Technol. Biomed. Life Sci.* 2005; 826:81–90

Mizuta H, Miyal K, Ichihara K, Amino N, Harada T, Nose O, and Tanizaqa O. Radioimmunoassay of "Free Thyroxin" in Dried Blood Spots on Filter Paper-Preliminary Observations on the Effective Differentiation of Subjects with Congenital Hypothyroidism from Those with Subnormal Thyroxin-Binding Globulin and Normal Subjects. *Clin. Chem.* 1982; 28:505–508

Murphy J, Philip M, Macken S, Meehan J, Roche E, Mayne PD, O'Regan M, and Hoey HMCV. Thyroid Dysfunction in Down's Syndrome and Screening for Hypothyroidism in Children and Adolescents Using Capillary TSH Measurement. *J. Pediatr. Endocrinol. Metab.* 2008; 21:155–163

Nedelman JR, Gibiansky E, and Lau DTW. Applying Bailer's Method for AUC Confidence Intervals to Sparse Sampling. *Pharm. Res.* 1995; 12:124–128

Newman MS, Brandon TR, Groves MN, Gregory WL, Kapur S, and Zava DT. A Liquid Chromatography/ Tandem Mass Spectrometry Method for Determination of 25-Hydroxy Vitamin D2 and 25-Hydroxy Vitamin D3 in Dried Blood Spots: A Potential Adjunct to Diabetes and Cardiometabolic Risk Screening. *J. Diabetes Sci. Technol.* 2009; 3:156–162

Ngo-Giang-Huong N, Khamduang W, Leurent B, Collins I, Nantasen I, Leechanachai P, Sirirungsi W, Limtrakul A, Leusaree T, Comeau AM, and Lallemant M. Early HIV-1 Diagnosis Using In-House Real-Time PCR Amplification on Dried Blood Spots for Infants in Remote and Resource-Limited Settings. *J. Acquir. Immune Defic. Syndr.* 2008; 49:465–471

Ntale M, Ogwal-Okeng JW, Mahindi M, Gustafsson LL, and Beck O. A Field-Adapted Sampling and HPLC Quantification Method for Lumefantrine and its Desbutyl Metabolite in Whole Blood Spotted on Filter Paper. *J. Chromatogr. B Analyt. Technol. Biomed. Life Sci.* 2009; 876:261–265

O'Broin SD, and Gunter EW. Screening of Folate Status with Use of Dried Blood Spots on Filter Paper. *Am. J. Clin. Nutr.* 1999; 70:359–367

Oglesbee D, Sanders KA, Lacey JM, Magera MJ, Casetta B, Strauss KA, Tortorelli S, Rinaldo P, and Matern D. Second-Tier Test for Quantification of Alloisoleucine and Branched-Chain Amino Acids in Dried Blood Spots to Improve Newborn Screening for Maple Syrup Urine Disease (MSUD). *Clin. Chem.* 2008; 54: 542–549

Orfanos AP, Naylor EW, and Guthrie R. Ultramicromethod for Estimation of Total Glutathione in Dried Blood Spots on Filter Paper. *Anal. Biochem.* 1980; 104:70–74

Otero-Santos M, Delinsky AD, Valentin-Blasini L, Schiffer J, and Blount BC. Analysis of Perchlorate in Dried Blood Spots Using Ion Chromatography and Tandem Mass Spectrometry. *Anal. Chem.* 2009; 81:1931–1936

Parker SP, Taylor MB, Ades AE, Cubitt WD, and Peckham C. Use of Dried Blood Spots for the Detection and Confirmation of HTLV-I Specific Antibodies for Epidemiological Purposes. *J. Clin. Pathol.* 1995; 48:904–907

Peng SH, Segura J, Farre M, and De La Torre X. Oral Testosterone Administration Detected by Testosterone Glucuronidation Measured in Blood Spots Dried on Filter Paper. *Clin. Chem.* 2000; 46:515–522

Peter M, Janzen N, Sander S, Korsch E, Riepe FG, and Sander J. A Case of 11β-Hydroxylase Deficiency Detected in a Newborn Screening Program by Second-Tier LC-MS/MS. *Horm. Res.* 2008; 69:253–256

Purves WK, David S, Gordon H, and Craig HH. Life: The Science of Biology (7th edn.). Sunderland, MA: Sinauer Associates; 2004:954

Rattenbury JM, and Taylor T. Measurement of Theophylline in Dried Blood Spots by Spectrophotometric Enzyme Immunoassay. *Ann. Clin. Biochem.* 1988; 25:650–653

Rowland M, and Emmons GT. Use of Dried Blood Spots in Drug Development: Pharmacokinetic Considerations. *AAPS J.* 2010; 12:290–293

Rowell V, and Rowell FJ. Rapid Enzyme-Linked Immunosorbent Assay (ELISA) With a Visual End-Point for Detecting Quinine in Urine, Serum, and Dried Blood Spots. *Analyst.* 1987; 112:1437–1439

Searles NS, Mueller BA, and De Roos AJ. Newborn Screening Archives as a Specimen Source for Epidemiologic Studies: Feasibility and Potential for Bias. *Ann. Epidemiol.* 2008; 18:58–64

Spence WC, Morris JE, Pass K, and Murphy PD. Molecular Confirmation of α1-Antitrypsin Genotypes in Newborn Dried Blood Specimens. *Biochem. Med. Metab. Biol.* 1993; 50:233–40

Spooner N, Lad R, and Barfield M. Dried Blood Spots as a Sample Collection Technique for the Determination of Pharmacokinetics in Clinical Studies: Considerations

for the Validation of a Quantitative Bioanalytical Method. *Anal. Chem*. 2009; 81:1557–1563

Steegen K, Luchters S, Demecheleer E, Dauwe K, Mandaliya K, Jaoko W, Plum J, Temmerman M, and Verhofstede C. Feasibility of Detecting Human Immunodeficiency Virus Type 1 Drug Resistance in DNA Extracted from Whole Blood or Dried Blood Spots. *J. Clin. Microbiol*. 2007; 45:3342–3351

Tani H, Tada Y, Sasai K, and Baba E, Improvement of DNA Extraction Method for Dried Blood Spots and Comparison of Four PCR Methods for Detection of Babesia Gibsoni (Asian Genotype) Infection in Canine Blood Samples. *J. Vet. Med. Sci*. 2008; 70:461–467

Tawa R, Matsunaga H, and Fujimoto T. High-Performance Liquid Chromatographic Analysis of Aminoglycoside Antibiotics. *J. Chromatogr. A*. 1998; 812:141–150

ter Heine R, Hillebrand MJ, Rosing H, van Gorp EC, Mulder JW, Beijnen JH, and Huitema ADR. Quantification of the HIV-Integrase Inhibitor Raltegravir and Detection of its Main Metabolite in Human Plasma, Dried Blood Spots and Peripheral Blood Mononuclear Cell Lysate by Means of High-Performance Liquid Chromatography Tandem Mass Spectrometry. *J. Pharm. Biomed. Anal*. 2009a; 49:451–458

ter Heine R, Rosing H, van Gorp EC, Mulder JW, Beijnen JH, and Huitema AD. Quantification of Etravirine (TMC125) in Plasma, Dried Blood Spots and Peripheral Blood Mononuclear Cell Lysate by Liquid Chromatography Tandem Mass Spectrometry. *J. Pharm. Biomed. Anal*. 2009b; 49:393–400

Turgeon C, Magera MJ, Allard P, Tortorelli S, Gavrilov D, Oglesbee D, Raymond K, Rinaldo P, and Matern D. Combined Newborn Screening for Succinylacetone, Amino Acids, and Acylcarnitines in Dried Blood Spots. *Clin. Chem*. 2008; 54:657–664

U.S. Food and Drug Administration. C. F. R. 60, 11264, 1995

U.S. Food and Drug Administration. Guidance for Industry on Bioanalytical Method Validation. C. F. R. 66 (100), 28526, 2001

van der Heijden J, de Beer Y, Hoogtanders K, Christiaans M, de Jong GJ, Neef C, and Stolk L. Therapeutic Drug Monitoring of Everolimus Using the Dried Blood Spot Method in Combination with Liquid Chromatography-Mass Spectrometry. *J. Pharm. Biomed. Anal*. 2009; 50:664–670

Versteeg I, and Mens PF. Development of a Stable Positive Control to be Used for Quality Assurance of Rapid Diagnostic Tests for Malaria. *Diag. Microbiol. Infec. Dis*. 2009; 64:256–260

Wang D, Eadala B, Sadilek M, Chamoles NA, Turecek F, Scott CR, and Gelb MH. Tandem Mass Spectrometric Analysis of Dried Blood Spots for Screening of Mucopolysaccharidosis I in Newborns. *Clin. Chem*. 2005; 51:898–900

Wilhelm AJ, den Burger JCG, Vos RM, Chahbouni A, and Sinjewel A. Analysis of Cyclosporin A in Dried Blood Spots Using Liquid Chromatography Tandem Mass Spectrometry. *J. Chromatogr. B Analyt. Technol. Biomed. Life Sci*. 2009a; 877:1595–1598

Wilhelm AJ, den Burger JCG, Chahbouni A, Vos RM, and Sinjewel A. Analysis of Mycophenolic Acid in Dried Blood Spots Using Reversed Phase High Performance Liquid Chromatography. *J. Chromatogr. B Analyt. Technol. Biomed. Life Sci*. 2009b; 877:3916–3919

Worthman CM, and Stallings JF. Measurement of Gonadotropins in Dried Blood Spots. *Clin. Chem*. 1994; 40:448–453

Zurfluh MR, Fiori L, Fiege B, Ozen I, Demirkol M, Gartner KH, Thony B, Giovannini M, and Blau N. Pharmacokinetics of Orally Administered Tetrahydrobiopterin in Patients with Phenylalanine Hydroxylase Deficiency. *J. Inherit. Metab. Dis*. 2006; 29:725–731

# Microdosing: Pharmacokinetic and Metabolism Data Early in the Drug Development Process

# 5

Graham Lappin

**Abstract**

Microdosing is the use of low, sub-pharmacologic doses (typically in the microgram range using less than 100th lower than the anticipated therapeutic dose and usually with the drug radiolabeled with $^{14}$C) to study the pharmacokinetics of a drug in early clinical development. The concept of microdosing has been around for over a decade and is now finding application in drug development. Although questions of dose linearity remain, insights to the reasons of non-linearity, should it occur, are now beginning to be understood. Microdosing is also being used to obtain early knowledge of drug metabolism, enabling better selection of drug candidates for full development.

## 5.1 Introduction

A microdose study is performed at a very early stage of drug development to obtain preliminary pharmacokinetic or distribution data on a drug candidate in human volunteers. The concept of obtaining early pharmacokinetic data in humans prior to Phase 1 clinical trials was first suggested in the latter part of the 1990s, with the first data published in 2003, albeit as a summary in a review article (Lappin and Garner 2003). As its name implies, the dose administered in a microdose study is very small, the amount being defined by both the EMEA (2004) and FDA (2006) as 100th

of the predicted pharmacologic dose or 100 μg whichever is the smaller. These small doses are assumed to be inherently safer than pharmacologically active doses and therefore the regulatory authorities will approve human microdose studies based upon limited preclinical safety evaluation. This enables the drug candidate to be administered to human volunteers earlier and with less expenditure compared to a Phase 1 clinical study (Lewis 2009). Microdosing therefore circumvents many of the obstacles to the administration of drugs at proposed therapeutic dose levels to humans at an early stage of drug development. Microdosing studies, however, should have no pharmacologic effect on the subjects and are used solely to gain information on the metabolism and pharmacokinetics of a candidate drug in humans, albeit at very low concentrations.

To date, the microdose studies reported in the literature have been with small molecule drugs

G. Lappin
Xceleron, The BioCentre, Innovation Way, York YO10 5NY, UK
e-mail: graham.lappin@xceleron.com

rather than therapeutic proteins. The FDA (2006) regulatory guideline classifies a microdose of protein product as a maximum dose of 30 nM, but to the author's knowledge, no such microdose study has been conducted (unless by PET, see below). Although there is no intrinsic reason why microdose studies could not be performed with protein products, there are good reasons why microdosing studies with antibodies, other than those with soluble target antigens, may not be applicable. The pharmacokinetics of these substances are known to be nonlinear below concentrations where the target ligand is unsaturated, due to target mediated disposition (Wang et al. 2008). Unless otherwise stated therefore, this chapter is concerned with human microdosing studies with small molecules.

Prior to the publication of the first summary microdose data (Lappin and Garner 2003) numerous studies had been performed utilising sub-pharmacological doses of drug candidates in conjunction with the imaging technique, Positron Emission Tomography (PET), although these were not necessarily called microdose studies at the time. In retrospect, however, it can be argued all PET studies utilising drugs labelled with a positron-emitting isotope meet the definition of a microdose study (Wagner et al. 2008). PET is an imaging technique that utilises relatively short-lived positron-emitting radioisotopes and is therefore largely concerned with the study of drug distribution over comparatively short periods of time, rather than the determination of pharmacokinetics to a point where elimination is essentially complete. Moreover, because of the short radioactive half-lives of positron emitting isotopes, PET studies are virtually always carried out using the intravenous route of administration and therefore do not study absorption kinetics. PET is nevertheless a widely used and very powerful technology and the reader is referred to a number of reviews (Bergstrom et al. 2003; Bauer et al. 2008; Wagner et al. 2008). PET is not considered further in this chapter as the focus is on what might be termed "classical" pharmacokinetics.

The general design of a microdose study would typically consist of four to eight human volunteers, typically young, healthy, males but not necessarily so, as female volunteers have been used previously (Lappin et al. 2006a, b). The volunteers are administered a maximum of 100 µg of a candidate drug. There is no theoretical restriction to the route of administration although most commonly, microdoses have been given orally or intravenously (IV). Following administration, samples of blood (plasma) and sometimes excreta are collected and analysed to determine the concentration of parent drug (and sometimes metabolites) over time. Where plausible, biopsies might be taken to provide some information on the drug's distribution (Lappin et al. 2007). From these concentration–time data, the pharmacokinetics of the drug can then be characterised. Since microdosing is often used to select a drug for full development from a number of candidates, several microdose studies might be performed in parallel so comparative data are acquired (Madan et al. 2008). Microdose studies are not performed routinely and are best applied to situations where certain pharmacokinetic parameters are the key drivers to the selection of a drug candidate for further development and where the traditional methods of predicting the drug's pharmacokinetics in humans from in vitro data (e.g. in silico modelling, animal models or allometric scaling) are believed to be unreliable.

## 5.2 Analytical Methods

Because very low doses of drug are administered in a microdose study, the plasma concentrations are consequently very low and therefore highly sensitive analytical techniques are necessary to measure the drug concentration. A discussion of the analytical modalities may be found outside this chapter with a number of reviews being available (Lappin et al. 2009). Accelerator Mass Spectrometry (AMS) and LC-MS/MS have been commonly used to determine drug concentrations in biological samples, such as plasma, obtained from microdose studies.

AMS, although becoming more widely applied, is not a routinely available analytical

method. AMS is an isotope ratio technique, first developed for radiocarbon dating in the 1970s (Bennett et al. 1977, 1978) and applied to biomedical research in the 1990s (Garner 2000). AMS can be applied to a wide range of isotopes but $^{14}C$ is the most widely used in biomedical work since it can be incorporated into the core structure of organic molecules. Biological samples (e.g. blood, plasma, excreta) are oxidised to produce $^{14}CO_2$, then reduced to carbon, in a process known as graphitisation. The graphite thereby produced, typically 2 mg, is placed into the AMS ion source. Carbon ions are accelerated to very high energy to facilitate efficient isotopic separation and measurement (Lappin 2006).

Figure 5.1 shows a schematic of how biological samples, using plasma as the example, are typically analysed by AMS. An aliquot of the plasma can be analysed without any chromatographic separation to provide the total $^{14}C$ concentration (i.e. the sum of parent drug and metabolites). Samples can also be extracted and analysed by some chromatographic method such as HPLC or UPLC. Because of the necessity for graphitisation, there is currently no routine interface between HPLC and AMS. To generate chromatograms therefore, it is necessary to collect fractions of the chromatographic eluant and graphitise each fraction separately (Lappin and Garner 2004, 2005). If all the fractions collected across a chromatogram are analysed, a complete metabolite profile can be generated (an example of a chromatogram is shown in Figs. 5.6–5.8). Alternatively, selected fractions can be analysed by AMS, for example at the retention time corresponding to the parent drug, and its concentration then determined. [As an aside, for parent drug analysis, analytical losses have to be taken into account to determine the mass per volume concentration (Lappin et al. 2008)]. Determination of parent drug concentration enables concentration–time plots to be generated along with the calculation of pharmacokinetic parameters (an example is shown in Fig. 5.2).

Under the right circumstances, AMS can achieve analytical sensitivities in the femtogram to attogram range ($10^{-15}$ to $10^{-18}$ g) which is typically one thousand to one million times more sensitive than LC-MS/MS (Hellborg and Skog 2008). For a fuller description of AMS and how it is applied to biomedical research, the reader is referred to (Lappin 2006). As an isotope ratio technique, AMS requires the drug to be



**Fig. 5.1** A schematic showing options for sample analysis using AMS
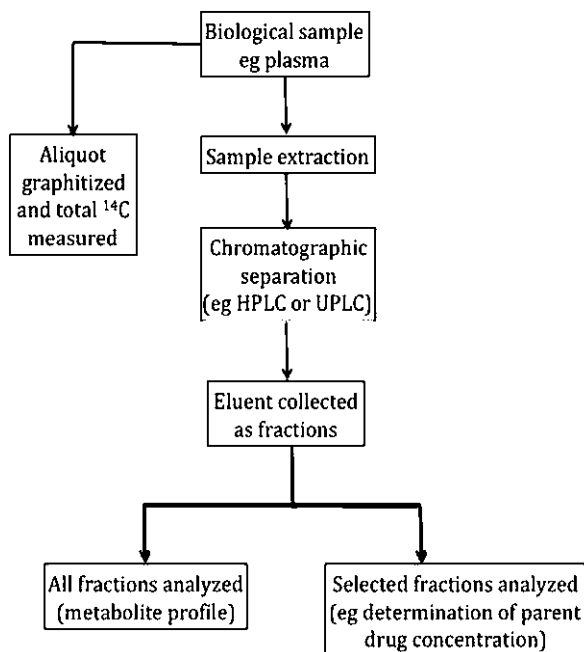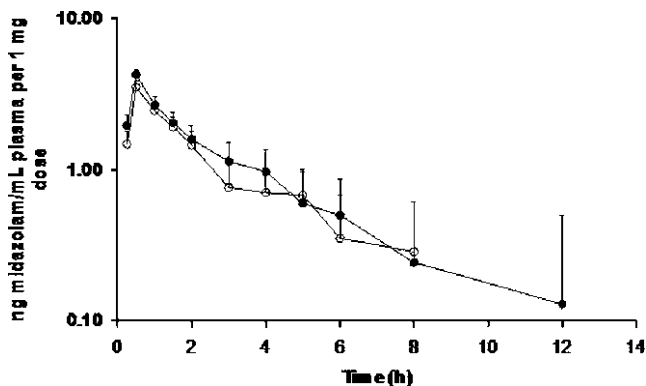
**Fig. 5.2** An example of a normalised dose plot. The plot has been taken from Lappin et al. (2006a, b) and shows a comparison of log-linear concentration–time plot for a 100 μg oral microdose (*open circles*) and 7.5 mg oral therapeutic dose (*filled circles*) of midazolam to healthy volunteers (error bars are standard error, $n = 6$). The plasma drug concentration on the *Y*-axis was presented normalised to a 1 mg dose. The shapes of the plots closely align showing the linearity of the pharmacokinetics over the 75-fold dose range

enriched with a rare isotope, almost always [14]C (Lappin and Garner 2004; Lappin and Stevens 2008). When AMS is chosen as the analytical method therefore, some customised radiosynthetic chemistry is necessary to produce the ^{14}C-labelled drug. This effort, unless combined with the requirement of ^{14}C-drug for other purposes such as regulatory animal or human metabolism studies, is potentially an extra cost burden compared to standard development plans. In addition, ^{14}C-drugs are radioactive and therefore the exposure to radioactivity administered to human volunteers must be considered. When designed around the use of AMS however, the levels of radioactivity administered to human volunteers are kept very low (typically less than 1 μCi) and hence, the study does not require specific approval by regulatory authorities for the administration of radioactivity (although the regulatory authorities should be informed or consulted regarding the study in advance).

## 5.3    Nomenclature

Microdosing is a relatively recent innovation. The terminology is also relatively new and some incertitude has entered the nomenclature. It is therefore worth clarifying some of the terminology, which is summarised in Table 5.1.

Microdosing studies are sometimes referred to as Phase 0 studies or, more precisely, human Phase 0.

Some observers have not favoured the term Phase 0, although it is becoming common parlance and there are many advantages in using this description (Kinders et al. 2007; Eliopoulos et al. 2008). Phase 0 describes studies in humans prior to Phase 1 and are performed at doses lower than those intended for therapeutic use. Microdose studies are classified as Phase 0, but the terms are not necessarily interchangeable; microdose studies are in effect a subset of Phase 0 studies. Phase 0 studies can also include studies in humans where the dose is greater than 100 μg and where some pharmacologic effects are manifest (Gutierrez and Collyar 2008). The regulatory authorities require more preclinical safety data than microdose studies to allow a "low pharmacologic dose" study to proceed, but still less than required for a full Phase 1 (FDA 2006). This chapter is focused on true microdosing studies, rather than Phase 0 per se.

There has been some confusion over the use of the term microdosing and occasionally it has been incorrectly applied. Much of this confusion has arisen from various applications of AMS, as this technique can be applied to microdose-related but nevertheless distinctly different areas of drug development (Brown et al. 2005). A number of

**Table 5.1** Clarification of some of the terminology surrounding microdosing

| Nomenclature | Explanation |
| --- | --- |
| Human Phase 0 | Studies on humans prior to Phase 1. The studies are conducted at either sub-pharmacologic doses or low doses that exhibit some pharmacologic action. These studies are performed under regulatory guidelines (e.g. the FDA's Exploratory IND) that allow the studies to be conducted based on reduced preclinical safety data compared to a Phase 1 study |
| Microdose | A category of human Phase 0 study where the dose is defined as 100th of the pharmacologic dose or 100 μg, whichever is the lower value (30 nM for protein products) |
| Low specific activity ADME studies | Sometimes confused with a microdose study, a low specific activity ADME study uses doses of drug relevant to therapeutic doses but with low levels of $^{14}C$. The definition of "low" is typically 1 uCi (37 kBq) per subject or less |
| IV Tracer study | A study where a low mass of $^{14}C$-drug is administered IV to human volunteers along with a therapeutic dose of non-labelled drug by the extravascular route. The tracer allows for IV pharmacokinetics to be obtained in humans at therapeutically relevant systemic drug concentrations but without the need to conduct IV preclinical safety toxicology or extensive IV formulation. This type of study is not classified as a microdose study as it is performed in a Phase 1 setting |

publications have appeared on the use of AMS in human absorption, distribution, metabolism and excretion (ADME) studies where the levels of $^{14}C$ in terms of the radioactivity dosed was comparatively low (Garner et al. 2002; Beumer et al. 2007). It is, however, incorrect to term these types of ADME studies as "microdosing" as the total mass of drug administered is in the therapeutic dose range. The confusion may have arisen from the fact that only very small amounts of $^{14}C$-drug are included in the total mass of the dose but it is the total mass of drug administered that defines a microdose study. Such "low radioactivity" ADME studies are in fact no different from any other human ADME study, it is just the specific radioactivity of the drug administered is lower than normally used.

Another type of study which has been commonly confused with microdosing is the so-called "intravenous tracer study". In these studies, a low dose (≤100 μg) of $^{14}C$-drug is administered intravenously (IV) to human volunteers close to the time when a non-labelled pharmacologic dose is given by the extravascular route, usually orally. Plasma samples are collected over time and each sample is analysed by a technique such as LC-MS/MS to measure the total drug concentration and also by HPLC followed by AMS to measure the $^{14}C$-drug concentration.

The IV dose, being so low does not contribute significantly to the overall systemic concentration, permits LC-MS/MS data to provide the pharmacokinetics of the extravascular dose and the AMS data to provide the pharmacokinetics of the IV dose. The overall plasma concentrations are dependent upon absorption of the pharmacologic oral dose and therefore by definition are at pharmacologically relevant concentrations. Thus, the IV pharmacokinetics are relevant to the pharmacologic dose, not the "microdose" administered IV. This technique was first developed in the 1970s using stable isotopic labels (Browne et al. 1993; Fairweather-Tait and Dainty 2002) as way of removing artefacts in absolute bioavailability determinations where there may be unequal clearance between the oral and IV administrations. The use of isotopic tracer for the IV dose (stable or radioisotope) is a better study design in this respect and the method has been used on and off for over 30 years. The method has been updated recently and used in conjunction with AMS, whereupon confusion in the terminology then arose. The technique has the advantage that the very low IV dose can often be justified without conducting preclinical safety studies for this route of administration, providing there are toxicology data from the oral route and sufficient exposure information. Of course,

appropriate preclinical safety evaluations have to be conducted for the oral dose given at a therapeutically relevant dose level. In addition, the low concentration of the IV dose only requires rudimentary effort for formulation. The IV administered $^{14}$C-drug acts as a tracer, tracking the passage of the IV dose, which is where these types of studies have gained their name "intravenous tracer study". It is however, incorrect and sometimes confusing to call these microdose studies. An example of a study using an IV tracer is Sarapa et al. 2005. The IV tracer approach is reviewed by (Lappin et al. 2006a, b).

## 5.4 Pharmacokinetic-Dose Linearity

There has been much debate about how well the pharmacokinetics of a microdose might predict the pharmacokinetics at a higher pharmacologic dose (Harenberg 1998; Lappin and Garner 2006; Bertino et al. 2007; Rowland 2007) and there are a number of publications that review the comparisons in some detail (Lappin and Garner 2008;

Ings 2009). It is not the purpose of this chapter to restate the conclusions of these reviews but the published data at the time of writing is summarised in Table 5.2. The published data constitutes a growing body of evidence to support the utility of microdosing although there is still some way to go in order to fully assess this technique. Nevertheless, a better understanding is growing for those properties of a drug that might lead to significant non-linearity in the pharmacokinetics seen between a microdose and a therapeutic dose. Of the 18 drugs reported in the literature so far, 15 demonstrated linear pharmacokinetics within a factor of 2 between a microdose and a therapeutic dose.

To compare the linearity of a microdose with a pharmacologic dose, the concentration–time data can be plotted on separate graphs, typically using the classical log-linear plot, however, the data are more meaningful when plotted normalised against dose. Time of sampling is plotted on the X-axis and the concentrations of the drug in plasma per 1 mg dose are plotted on the Y-axis. The dose against which the data are normalised could be any unit of mass but 1 mg seems to be

**Table 5.2** Summary of published data where the pharmacokinetics observed at a microdose has been compared to those from a therapeutic dose

| Drug | Linearity (and dose range)[a] | Species | References |
|---|---|---|---|
| A-1A adrenoceptor | Linear 5–500 μg | Human | (Lappin and Garner 2003) |
| 7-deaza-2′-C-methyl-adenosine | Linear 0.02–1 mg/kg | Dog | (Sandhu et al. 2004) |
| Fluconazole | Linear 0.001–5 mg | Rat | (Balani et al. 2006) |
| Tolbutamide | Linear 0.001–5 mg | Rat | |
| MLNX | AUC non-linear | Rat | |
| Warfarin | Non-linear distribution | Human | (Lappin et al. 2006a, b) |
| Midazolam | Linear 0.1–5 mg | Human | |
| Diazepam | Linear 0.1–10 mg | Human | |
| ZK-253 | Linear 0.1–50 mg | Human | |
| Fexofenadine | Linear 0.1–50 mg | Human | (Yamane et al. 2007) |
| Zidovudine | Linear 0.02–1 mg | Human | (Vuong et al. 2007) |
| Diphenhydramine | Linear 0.1–50 mg | Human | (Madan et al. 2008) |
| NBI-1 | Linear 0.1–50 mg | Human | |
| Antipyrine | Linear 0.17–1670 μg/kg | Rat | (Ni et al. 2008) |
| Carbamazepine | Linear 0.17–1670 μg/kg | Rat | |
| Metoprolol | Some non-linearity | Rat | |
| Atenolol | Linear 1.67–1670 μg/kg | Rat | |
| Digoxin | Linear 1.67–1670 μg/kg | Rat | |

[a]Pharmacokinetics described as linear if the parameter for a microdose, when normalised for the therapeutic dose is within a factor of 2

becoming the convention (Fig. 5.2). The shapes of the curves can be compared directly and if they overlay each other are considered to be dose linear.

The shape of the plasma concentration–time curve is an important consideration, although often forgotten in the literature, where data are frequently only reported as mean pharmacokinetic parameters. An example of a case where the microdose and pharmacologic dose were linear is presented in Fig. 5.2. Strictly speaking, units of, for example, pg/mL per 1 mg dose can be mathematically expressed as the reciprocal of the volume, but this expression does not immediately describe the situation and therefore the more descriptive (if mathematically less precise) units of mass/volume per mass of dose is immediately more meaningful.

## 5.5 Dose Routes

There is a great deal of benefit to the inclusion of an intravenous dose in a microdose study, even when the drug is only destined for oral administration. The intravenous dose provides the fundamental pharmacokinetic parameters of clearance (CL) and volume of distribution (V) without the confounding effect of bioavailability (F).

Microdose studies are typically cross-over designs. If both an oral dose and an intravenous dose are included in the study design, an estimate of the absolute oral bioavailability can be obtained. As an example, the author was involved in a study where the plasma concentrations following the oral microdose were very much lower than anticipated. It was concluded that the drug had unexpected limited absorption, but when the intravenous data were obtained, it became apparent the low plasma concentrations were explained by a very high volume of distribution of several thousand litres and the drug was virtually 100% bioavailable (unpublished data).

There are currently no published data for microdose studies other than by oral or IV routes of administration, although the author has conducted one microdose study for a dermally applied compound. Using the dermal route opens up another consideration as both the total dose administered and the surface concentration (i.e. $\mu g/cm^2$ of skin) have to be taken into account. The rate of absorption through the skin is dependent upon the surface area concentration, whilst the total amount absorbed over the study duration (i.e. systemic exposure) is dependent upon the total amount placed on the surface of the skin, the rate of absorption, and the time the drug remained on (or possibly in) the skin. On this basis, the total dose applied in the dermal microdose study was 100th the pharmacologic dose, thus qualifying it as a microdose, but the surface concentration was kept the same as that intended for clinical use by limiting the area of skin to which the drug was applied to 100th of that exposed during a therapeutic clinical study. In this way the systemic exposure was at "microdose concentrations" but the rate of absorption was the same as expected in clinical use.

## 5.6 Isotopic Tracers in Microdosing

LC-MS/MS has been successfully used for the determination of parent drug in plasma and other body fluids in microdosing studies (e.g. Bertino et al. 2007; Ni et al. 2008). On the other hand, at the outset of a study, it is difficult to predict the likely plasma drug concentration, which may be very low as shown in the example above where the drug had an unexpectedly high volume of distribution. For many microdose studies therefore, researchers choose the most sensitive analytical technique available, which is currently AMS. AMS is an isotope ratio technique and therefore has the potential disadvantage that the drug has to be isotopically labelled, typically with $^{14}C$.

Figure 5.1 shows a schematic of how biological samples are typically analysed by AMS. An aliquot of the plasma can be analysed to determine the total $^{14}C$ concentration (i.e. unchanged drug together with metabolites) or the sample can be extracted, analysed by HPLC and selected fractions (e.g. those corresponding to parent drug) analysed by AMS. Consequently, two sets of

concentration–time data are generated, one for total $^{14}$C expressed as mass equivalents per millilitre of plasma (e.g. pg equiv/mL) and another for unchanged parent drug, expressed as mass per volume of plasma (e.g. pg/mL). These data can then be plotted on the same axes. Examples of these plots are shown in Figs. 5.3–5.5. The respective Areas Under the Curve (AUCs) can be calculated from the concentration–time data and presented as a ratio quantifying the proportion of the parent drug to total metabolites in circulation (typically as a percentage of AUC$_{parent}$ to AUC$_{total}$).



**Fig. 5.3** Plasma log-linear concentration–time plot for an intravenous microdose (100 μg) of fexofenadine to healthy human volunteers. The concentration for total $^{14}$C (*filled circles*) is plotted with unchanged drug (*open circles*). The plots are virtually superimposable, with 85% of the plasma $^{14}$C representing parent drug (based on the AUCs). Error bars are standard deviation, $n = 6$
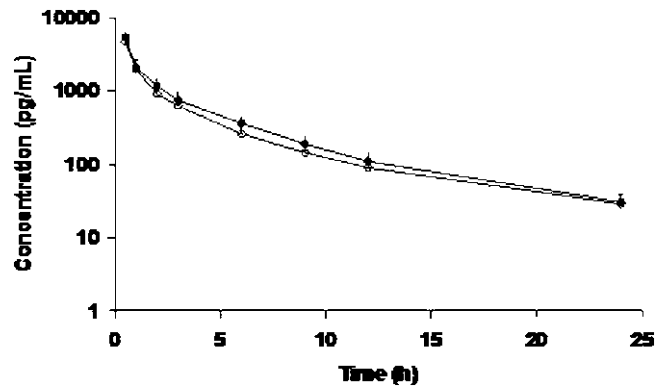


**Fig. 5.4** Log-linear plasma concentration–time plots from a microdose study with midazolam. Total $^{14}$C (*filled circles*) is plotted together with concentration of parent drug (*open circles*) in plasma following an intravenous administration to healthy volunteers. Error bars are standard error, $n = 6$
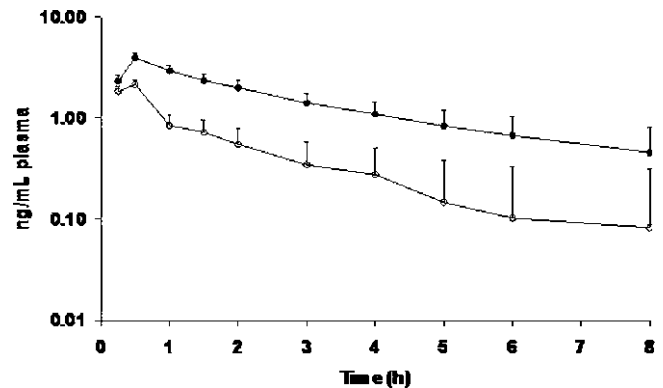


**Fig. 5.5** Log-linear plasma concentration–time plots from a microdose study with midazolam. Total $^{14}$C (*filled squares*) is plotted together with concentration of parent drug (*open squares*) in plasma following an oral administration to healthy volunteers. Error bars are standard error, $n = 6$
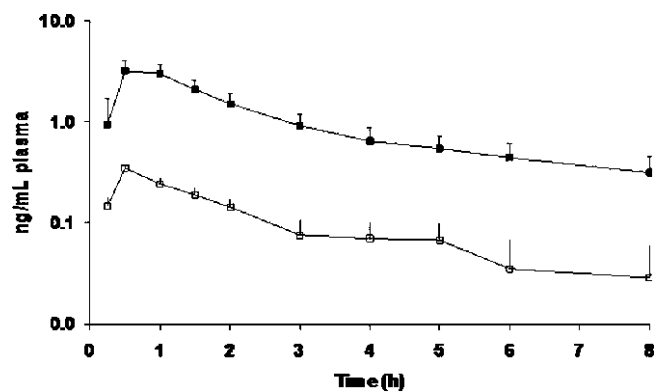
Care has to be taken in the interpretation of these data as it provides information only with regard to the point of measurement. For example, if plasma is analysed in this way then the data may not provide complete information on the metabolism of the drug outside the plasma compartment. Tolbutamide exemplifies this situation as it is well metabolised in the body but it is the parent drug that is the dominant species in circulation and therefore plasma contains virtually no metabolites (Matin and Rowland 1973). From plasma data alone, it might therefore be incorrectly surmised that tolbutamide is not significantly metabolised.

An example of how total $^{14}C$ and parent drug concentration data are compared is shown in Fig. 5.3. As part of a microdose study, fexofenadine was $^{14}C$ labelled and administered IV (100 µg) to six human volunteers (Lappin et al. 2010). The amount of radioactivity administered was 7.4 kBq, 200 nCi. Plasma was collected from the volunteers over time and analysed by AMS for total $^{14}C$ and for unchanged parent drug using HPLC followed by AMS analysis of the isolated fraction at the retention time of parent drug. Figure 5.3 shows that the concentration–time plot for total $^{14}C$ and for parent fexofenadine in plasma track each other very closely. The $AUC_{parent}$ to $AUC_{total}$ showed 85% of the plasma radioactivity was parent drug, and hence by difference, 15% of the plasma radioactivity was metabolites. This was consistent with the known limited metabolism of fexofenadine (Chen 2007).

Further insights into the metabolism of a candidate drug can be gained when the total $^{14}C$ and parent drug plots are compared for the oral and IV doses. The results from a microdose study with midazolam are presented in Figs. 5.4 and 5.5 (modified from Lappin et al. 2006a, b). Midazolam, a benzodiazepine derivative, is a short-acting sedative typically used during short-term surgical procedures. Following an intravenous dose of 100 µg $^{14}C$-midazolam (7.4 kBq, 200 nCi) to six human volunteers, at the first sampling time point (0.25 h), the plasma concentration of total $^{14}C$ was similar to parent drug (Fig. 5.4). The concentration of total $^{14}C$ and parent drug then rapidly diverged with time, as

midazolam was metabolised. Following an oral 100 µg dose of $^{14}C$-midazolam (7.4 kBq, 200 nCi) the concentration of total $^{14}C$ and parent midazolam were significantly different from the first plasma sampling (Fig. 5.5). The lower concentration of parent midazolam compared to total $^{14}C$ reflects the high first pass metabolism of this drug. The absolute bioavailability of midazolam, calculated from the respective AUCs for both the oral and IV microdose was approximately 22%, which compares well with reported values for higher therapeutic doses (Heizmann et al. 1983). The relatively low bioavailability of midazolam, however, was shown to be due to first pass metabolism rather than any limitation of absorption. By conducting a microdose cross-over study (IV and oral dosing) with $^{14}C$-midazolam therefore, it was possible to obtain a clearer description of how the drug was handled by the body, albeit at a low dose. Knowledge about the bioavailability of a drug and whether a low bioavailability is due to limitations of absorption or first pass effects can be pivotal to the drug's development. Poor absorption can be possibly tackled by reformulation whereas first pass effects are not formulation-dependent and may require other approaches such as the development of a prodrug. By employing a microdosing study, this information can be gained at the earliest possible stages in human volunteers, prior to conducting a full preclinical safety toxicology package supporting Phase 1.

## 5.7  Metabolite Profiling in Microdose Studies

Samples of plasma or other biological samples generated in a microdose study can be extracted and chromatographically analysed to generate a full metabolite profile (Fig. 5.1). The presence of the $^{14}C$-tracer ensures that all the metabolites are revealed, assuming the metabolites still retain the $^{14}C$ isotope in the structure, even if obscure catabolic pathways are involved. Moreover, $^{14}C$ is fully quantitative, allowing for the quantification of parent and metabolites, even if the chemical structures of the metabolites are uncertain.

Metabolite profiles from microdose studies are produced using very low doses (≤100 μg), so there is a question as to whether the metabolism will be the same at higher pharmacologic doses. There are, in fact, surprisingly little data in the literature showing full metabolic profiles from microdose studies and so two examples are presented here (unpublished data) as shown in Figs. 5.6–5.8.

[14C]-diazepam was intravenously administered as a microdose (100 μg) or a therapeutic dose (10 mg) to six healthy male volunteers. For both dose levels, 7.4 kBq (200 nCi) was administered. Plasma samples were taken periodically and those taken 24 h after dosing were pooled across subjects, making two pools, one for the 100 μg dose and one for the 10 mg dose. The plasma pools were extracted and analysed
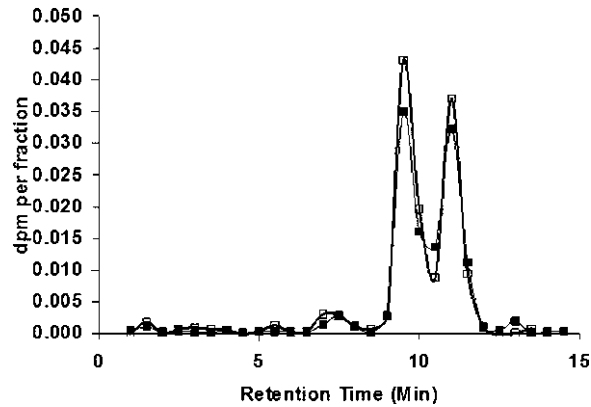


**Fig. 5.6** Chromatographic profiles of plasma from human volunteers administered [14C]-diazepam intravenously at doses of 100 μg (*open squares*) or 10 mg (*filled squares*). The profiles were produced by analysing HPLC fractions with AMS (results of individual fraction analysis shown by data points – see text). The peak at retention time of approximately 11 min is parent diazepam. The peak at a retention time of approximately 9 min is 4-hydroxy-diazepam. The two profiles were virtually identical. (Note the scale on the *Y*-axis. The metabolite profile of diazepam was generated by injecting just 0.2 dpm onto the HPLC column, demonstrating the extreme sensitivity of AMS)
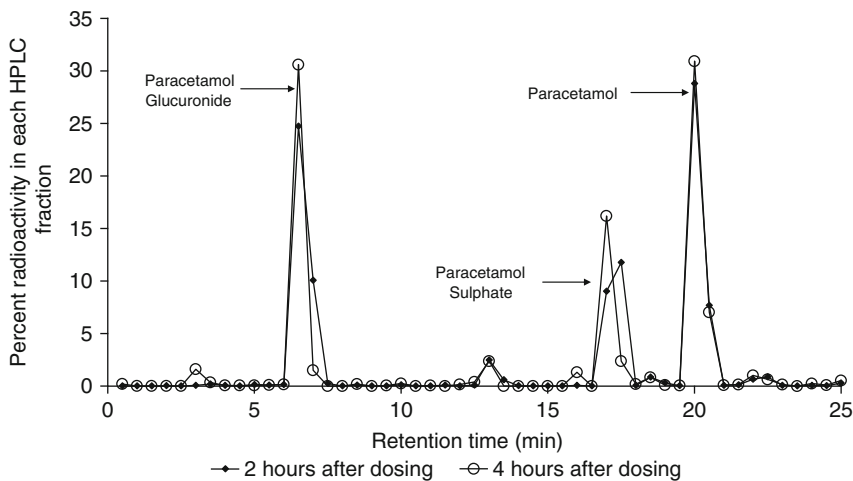


**Fig. 5.7** Chromatographic metabolite profile of plasma, 2 (*filled squares*) and 4 h (*open circles*) after the oral administration of 100 μg [14C]-paracetamol to human volunteers. (Results of individual fraction analysis shown by data points – see text)
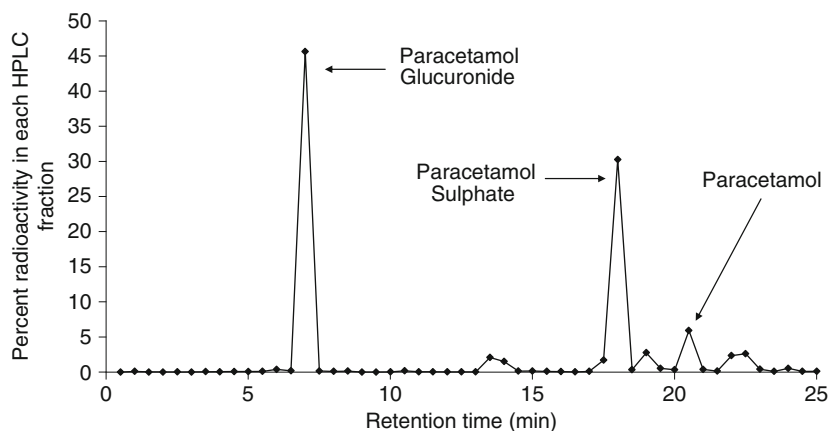
**Fig. 5.8** Chromatographic metabolite profile of urine 0–24 h after the oral administration of 100 μg (200 nCi) $^{14}$C-paracetamol to human volunteers. (Results of individual fraction analysis shown by data points – see text)

by HPLC, using conditions described in Lappin et al. (2006a, b). The eluant from the HPLC was collected as a series of fractions. Each fraction was then graphitised (see above) and analysed by AMS. The resulting chromatographic metabolite profile is shown in Fig. 5.6. The peak at a retention time of approximately 11 min is unchanged diazepam. The peak at retention time of approximately 9 min is 4-hydroxy-diazepam. The two profiles were virtually identical despite a 100-fold difference in dose.

In a separate research study undertaken as part of the European Microdosing AMS Partnership Programme (unpublished at the time of writing but with the latest results given at http://www.EUMAPP.com) the metabolic profiles in plasma and urine derived from human subjects administered a microdose of [$^{14}$C]-paracetamol (acetaminophen in the USA) was investigated by HPLC followed by AMS analysis. Data from the radiochromatograms generated from the microdose were compared with data for the therapeutic doses published in literature. Paracetamol is a widely used analgesic and antipyretic. It is absorbed rapidly from the gastrointestinal tract and is metabolised primarily in the liver by conjugation to form paracetamol–glucuronide and paracetamol–sulphate. These major polar conjugates are excreted by the kidneys in the urine. A minor fraction is metabolised via hepatic cytochrome P450 to a highly reactive alkylat-

ing metabolite (N-acetyl-p-benzoquinoneimine). This metabolite rapidly conjugates with glutathione and is eventually excreted in the urine as cysteine and mercapturic acid conjugates. In situations of overdose, the glutathione conjugation pathway is saturated resulting in toxic concentrations of the active N-acetyl-p-benzoquinone imine.

In the research study, six healthy male volunteers were orally administered 100 μg, 7.4 kBq (200 nCi) $^{14}$C-paracetamol. Plasma and urine samples were collected periodically following dosing. Plasma collected at 2 or 4 h after oral administration was pooled across subjects. Urine was pooled across subjects from 0 to 24 h. Plasma extracts and urine were analysed by HPLC using the method of (Vertzoni et al. 2003). The HPLC eluant was collected as a series of fractions across the chromatogram and analysed by AMS. The reconstructed radiochromatogram for plasma and urine are shown in Figs. 5.7 and 5.8, respectively. The principal metabolites observed in the profiles were unchanged paracetamol and its sulphate and glucuronide conjugates, which was consistent with what would be expected from the known metabolic pathway of paracetamol. The quantities of each of these compounds were compared to results previously published and the comparisons are shown in Figs. 5.9–5.11. For both 2 and 4 h after dosing, the proportions of paracetamol to the glucuronide and sulphate

conjugates present in plasma were very similar (Figs. 5.9 and 5.10, respectively). In all cases, the glucuronide was the most abundant species, followed by unchanged paracetamol and then the sulphate. In urine, the proportions of paracetamol to the glucuronide and sulphate conjugates were also consistent, with the glucuronide being most abundant, followed by the sulphate and then unchanged paracetamol. Interestingly, unchanged paracetamol is not always detected in urine

demonstrating differences in the data can occur from study to study (Pabba et al. 2002). Notwithstanding this, the microdose predicted the metabolism of paracetamol over a dose range of 15,000-fold very well. These data were consistence with those of Tozuka et al. (2010).

Although the use of an isotopic tracer can be very useful in revealing the pattern of metabolites and their quantities, it is nevertheless worth remembering that if unknown metabolites are
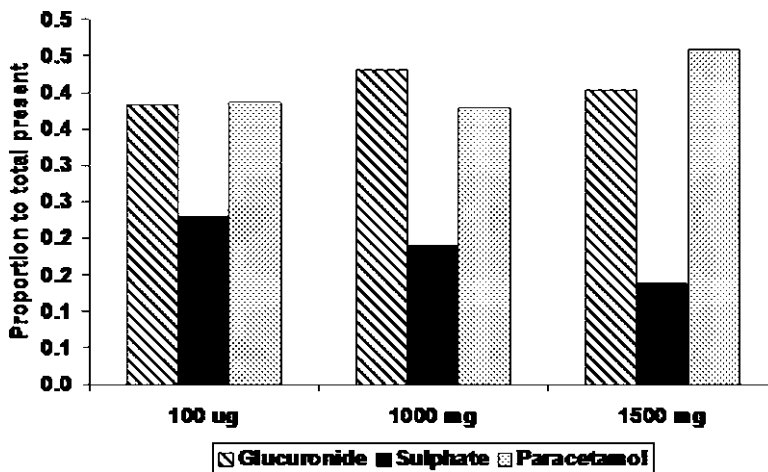


**Fig. 5.9** Comparison of relative amounts of unchanged paracetamol paracetamol–sulphate and paracetamol–glucuronide present in plasma across a 10,000-fold dose range 2 h after oral dosing. [100 μg data generated in the author's laboratory, 1,000 mg data after Jensen et al. (2004) and 1,500 mg dose data after Prescott (1980)]
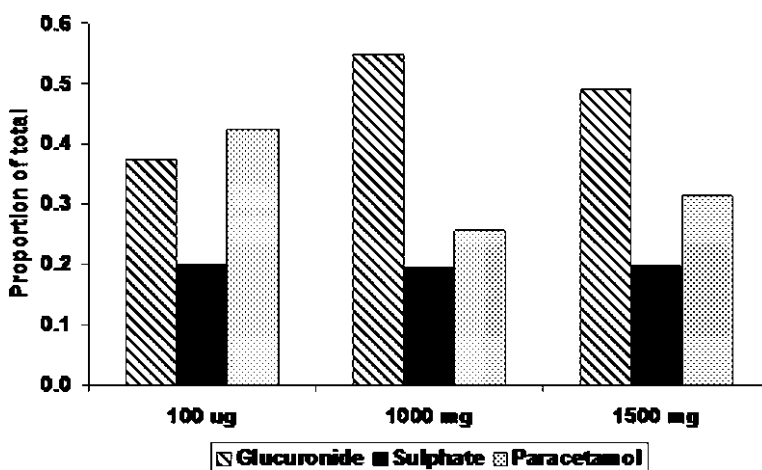


**Fig. 5.10** Comparison of relative amounts of unchanged paracetamol, paracetamol–sulphate and paracetamol–glucuronide present in plasma across a 10,000-fold dose range 4 h after oral dosing. [100 μg data generated in the author's laboratory, 1,000 mg data after Jensen et al. (2004) and 1,500 mg dose data after Prescott (1980)]
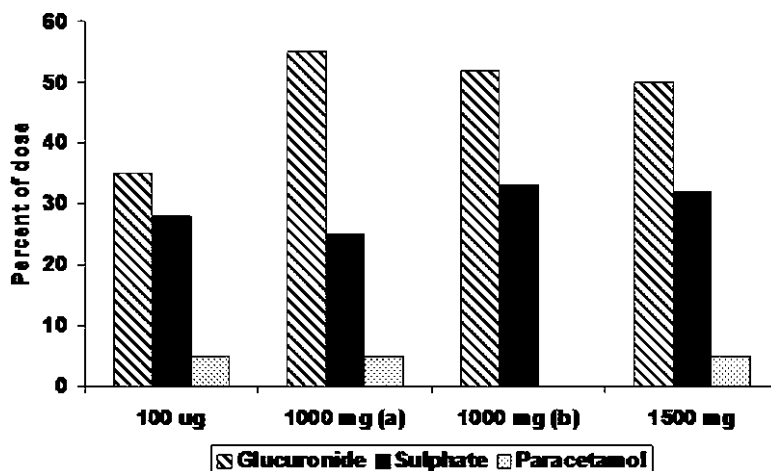
**Fig. 5.11** Comparison of relative amounts of unchanged paracetamol, paracetamol–sulphate and paracetamol–glucuronide present in 0–24 h urine across a 15,000-fold dose range. (1,500 mg dose data after (Prescott 1980), 1,000 mg (a) dose data after Jenson et al. Comparison of relative amounts of unchanged paracetamol, paraceta-mol–sulphate and paracetamol–glucuronide present in plasma across a 10,000-fold dose range 4 h after oral dosing. [100 μg data generated in the author's laboratory, 1,000 mg (a) data after Jensen et al. (2004), 1,000 mg (b) data after Pabba et al. (2002) and 1,500 mg dose data after Prescott (1980)]

revealed, structural elucidation can be very challenging given the potentially very low concentrations encountered following microdosing. The occurrence of unique human metabolites is however, rare and therefore putative identification can usually be made by chromatographic retention time comparison with, for example, laboratory animal studies. In addition, it should be remembered that microdose data are preliminary and if a unique human metabolite was observed, even if it's full chemical structure was unknown, this in itself is very valuable information in terms of the further development of the drug. Such information would enable drug developers to critically assess the future potential of the compound and perhaps realign future regulatory studies to address species-specific metabolism at an earlier stage than would otherwise be thought necessary.

## 5.8   Linear and Non-linear Pharmacokinetics

At overdose levels of paracetamol, metabolites from the glutathione-pathway appear in plasma and urine. It is probably unrealistic to expect a microdose study with paracetamol to predict these effects as the dose used is well below that which would cause any enzyme saturation. The chromatogram shown in Figs. 5.7 and 5.8, however, do possess some minor unidentified peaks and it is interesting to speculate that some glutathione-related metabolites might have been formed in the microdose study. The point is nevertheless illustrated that generally, non-linearities that appear in the kinetics due to the saturation of some system (such as certain enzymes) will occur at higher doses rather than lower doses. For example, it might be speculated that because of the high first pass observed with midazolam, at very low doses, the midazolam presented to CYP-3A4 in the GI-tract and liver would be at such a low concentration that all of the compound would be metabolised and no unchanged parent drug would be measured in the systemic circulation. This, however, was not observed. The equilibrium of formation of metabolites from midazolam was maintained throughout the dose range examined (100 μg to 7.5 mg). Presumably, if the midazolam dose were high enough to saturate CYP-3A4, then non-linearities in the pharmacokinetics would result.

Similar speculations were made with fexofenadine, a substrate for the efflux transporter Pg-P. Given the very low concentrations expected in the GI-tract following a microdose of fexofenadine, the Pg-P system would be expected to pump any absorbed fexofenadine out of the epithelial cells of the small intestine and hence prevent the drug from being absorbed into the hepatic portal vein. As with midazolam, however, when microdose (100 µg) and therapeutic dose (60 mg) data for fexofenadine were compared, the pharmacokinetics observed for the microdose predicted those at the therapeutic dose very well (Lappin et al. 2010; Yamane et al. 2007). The equilibrium between the amount of drug absorbed through the GI-tract and that which was pumped out by P-gP was therefore apparently maintained over the 100 µg to 60 mg dose range. Non-linearities in the amount of fexofenadine absorbed are however, known to occur at higher doses (240 mg) where saturation of the P-gP system is likely to occur (Robbins et al. 1998).

Of course, there are situations where non-linear pharmacokinetics are observed at lower doses, as illustrated by the aforementioned target mediated disposition observed with antibodies. Another example would be warfarin. Due to the presence of a low-capacity, high-affinity binding site, coupled with a low volume of distribution, the kinetics prior to the drug's elimination phase were non-linear at lower doses (Levy et al. 2003; Lappin et al. 2006a, b).

## 5.9 Summary

A microdose, defined as 100th of the predicted pharmacologic dose of drug or 100 µg whichever is the smaller, is administered to human volunteers prior to Phase 1 studies to obtain an early readout of pharmacokinetics. The low dose is assumed to be inherently safer than a pharmacologically active dose and therefore the regulatory authorities will approve human microdose studies based upon limited preclinical safety evaluation. A question as to how well microdose data will predict the pharmacokinetics at higher therapeutically relevant doses arises, but there is a growing body of published studies where such dose comparisons can be made, and to date there is around 80% of orally administered microdose studies and 100% intravenous microdose data predicted the pharmacokinetics at higher doses within a factor of 2. As well as providing data on the pharmacokinetics of the parent drug, microdosing can also be used to obtain an appreciation of its metabolism. Provided the candidate drug is $^{14}$C labelled, the isotopic tracer can be used to provide qualitative and quantitative metabolic data, albeit at low doses. Such early data can help drug developers assess the future potential of a drug candidate and schedule the regulatory studies to best address any issues of metabolism of pharmacokinetics.

## References

Balani, S. K., Nagaraja, N. V., Qian, M. G., Costa, A. O., Daniels, J. S., Yang, H., Shimoga, P. R., Wu, J. T., Gan, L. S., Lee, F. W. and Miwa, G. T., 2006. Evaluation of microdosing to assess pharmacokinetic linearity in rats using liquid chromatography-tandem mass spectrometry. Drug Metab Dispos 34 (3), 384–388.

Bauer, M., Wagner, C. C. and Langer, O., 2008. Microdosing studies in humans: the role of positron emission tomography. Drugs R D 9 (2), 73–81.

Bennett, C. L., Beukens, R. P., Clover, M. R., Gove, H. E., Liebert, R. B., Litherland, A. E., Purser, K. H. and

Sondheim, W. E., 1977. Radiocarbon dating using electrostatic accelerators: negative ions provide the key. Science 198 (4316), 508–510.

Bennett, C. L., Beukens, R. P., Clover, M. R., Elmore, D., Gove, H. E., Kilius, L., Litherland, A. E. and Purser, K. H., 1978. Radiocarbon dating with electrostatic accelerators: dating of milligram samples. Science 201 (4353), 345–347.

Bergstrom, M., Grahnen, A. and Langstrom, B., 2003. Positron emission tomography microdosing: a new concept with application in tracer and early clinical drug development. Eur J Clin Pharmacol 59 (5–6), 357–366.

Bertino, J. S., Jr., Greenberg, H. E. and Reed, M. D., 2007. American College of Clinical Pharmacology position statement on the use of microdosing in the drug development process. J Clin Pharmacol 47 (4), 418–422.

Beumer, J. H., Garner, R. C., Cohen, M. B., Galbraith, S., Duncan, G. F., Griffin, T., Beijnen, J. H. and Schellens, J. H., 2007. Human mass balance study of the novel anticancer agent ixabepilone using accelerator mass spectrometry. Invest New Drugs 25 (4), 327–334.

Brown, K., Dingley, K. and Turteltaub, K. W., 2005. Accelerator Mass Spectrometry for Biomedical Research. In A. L. Burlingame (Ed.) *Methods in Enzymology*. New York, Academic Press. 402.

Browne, T. R., Szabo, G. K., McEntegart, C., Evans, J. E., Evans, B. A., Miceli, J. J., Quon, C., Dougherty, C. L., Kres, J. and Davoudi, H., 1993. Bioavailability studies of drugs with nonlinear pharmacokinetics: II. Absolute bioavailability of intravenous phenytoin prodrug at therapeutic phenytoin serum concentrations determined by double-stable isotope technique. J Clin Pharmacol 33 (1), 89–94.

Chen, C., 2007. Some pharmacokinetic aspects of the lipophilic terfenadine and zwitterionic fexofenadine in humans. Drugs R D 8 (5), 301–314.

Eliopoulos, H., Giranda, V., Carr, R., Tiehen, R., Leahy, T. and Gordon, G., 2008. Phase 0 trials: an industry perspective. Clin Cancer Res 14 (12), 3683–3688.

EMEA, 2004. EMEA, Position Paper on Non-clinical Safety Studies to Support Clinical Trials with a Single Microdose. Position paper CPMP/SWP/2599, 23 June 2004.

Fairweather-Tait, S. J. and Dainty, J., 2002. Use of stable isotopes to assess the bioavailability of trace elements: a review. Food Addit Contam 19 (10), 939–947.

FDA, 2006. Food and Drug Administration US Department of Health and Human Services Guidance for Industry Investigators and Reviewers. Exploratory IND Studies. January 2006.

Garner, R. C., 2000. Accelerator mass spectrometry in pharmaceutical research and development – a new ultrasensitive analytical method for isotope measurement. Curr Drug Metab 1 (2), 205–213.

Garner, R. C., Goris, I., Laenen, A. A., Vanhoutte, E., Meuldermans, W., Gregory, S., Garner, J. V., Leong, D., Whattam, M., Calam, A. and Snel, C. A., 2002. Evaluation of accelerator mass spectrometry in a

human mass balance and pharmacokinetic study-experience with 14C-labeled (R)-6-[amino(4- chlorophenyl) (1-methyl-1H-imidazol-5-yl)methyl]-4-(3-chlorophenyl)-1- methyl-2(1H)-quinolinone (R115777), a farnesyl transferase inhibitor. Drug Metab Dispos 30 (7), 823–830.

Gutierrez, M. and Collyar, D., 2008. Patient perspectives on phase 0 clinical trials. Clin Cancer Res 14 (12), 3689–3691.

Harenberg, J., 1998. Review of pharmacodynamics, pharmacokinetics, and therapeutic properties of sulodexide. Med Res Rev 18 (1), 1–20.

Heizmann, P., Eckert, M. and Ziegler, W. H., 1983. Pharmacokinetics and bioavailability of midazolam in man. Br J Clin Pharmacol 16 Suppl 1, 43S–49S.

Hellborg, R. and Skog, G., 2008. Accelerator mass spectrometry. Mass Spectrom Rev 27 (5), 398–427.

Ings, R., 2009. Microdosing: a valuable tool for accelerating drug development and the role of bioanalytical methods in meeting the challenge of this new concept. Bioanalysis 1 (7), 1293–1305 DOI: 10.4155/BIO.09.107.

Jensen, L. S., Valentine, J., Milne, R. W. and Evans, A. M., 2004. The quantification of paracetamol, paracetamol glucuronide and paracetamol sulphate in plasma and urine using a single high-performance liquid chromatography assay. J Pharm Biomed Anal 34 (3), 585–593.

Kinders, R., Parchment, R. E., Ji, J., Kummar, S., Murgo, A. J., Gutierrez, M., Collins, J., Rubinstein, L., Pickeral, O., Steinberg, S. M., Yang, S., Hollingshead, M., Chen, A., Helman, L., Wiltrout, R., Simpson, M., Tomaszewski, J. E. and Doroshow, J. H., 2007. Phase 0 clinical trials in cancer drug development: from FDA guidance to clinical practice. Mol Interv 7 (6), 325–334.

Lappin, G. J., 2006. Biomedical Accelerator Mass Spectrometry. Radiotracers in Drug Development. Boca Raton, USA, Taylor & Francis.

Lappin, G. and Garner, R. C., 2003. Big physics, small doses: the use of AMS and PET in human microdosing of development drugs. Nat Rev Drug Discov 2 (3), 233–240.

Lappin, G. and Garner, R. C., 2004. Current perspectives of 14C-isotope measurement in biomedical accelerator mass spectrometry. Analytical Biochemistry 378 (2), 356–364.

Lappin, G. and Garner, R. C., 2005. The use of accelerator mass spectrometry to obtain early human ADME/PK data. Expert Opin Drug Metab Toxicol 1 (1), 23–32.

Lappin, G. and Garner, R. C., 2006. A review of human phase 0 and microdosing clinical trials following the US food and drug administration exploratory investigational new drug studies guidance. Int J Pharm Med 30 (3), 159–165.

Lappin, G. and Garner, C., 2008. The utility of microdosing over the past 5 years. Expert Opin Drug Metab Toxicol 4 (12), 1499–1506.

Lappin, G. and Stevens, L., 2008. Biomedical accelerator mass spectrometry: recent applications in metabolism and pharmacokinetics. Expert Opin Drug Metab Toxicol 4 (8), 1021–1033.

Lappin, G., Kuhnz, W., Jochemsen, R., Kneer, J., Chaudhary, A., Oosterhuis, B., Drijfhout, W. J., Rowland, M. and Garner, R. C., 2006. Use of microdosing to predict pharmacokinetics at the therapeutic dose: experience with 5 drugs. Clin Pharmacol Ther 80 (3), 203–215.

Lappin, G., Rowland, M. and Garner, R. C., 2006. The use of isotopes in the determination of absolute bioavailability of drugs in humans. Expert Opin Drug Metab Toxicol 2 (3), 419–427.

Lappin, G., Warrington, S., Honeybourne, D., Sanghera, D., Dowen, S., Lister, N., Islam, K. and Lociuro, S., 2007. Concentrations of AR-709 in plasma and key compartments of the lungs after microdosing. Poster presented at the Interscience Conference on Antimicrobial Agents and Chemotherapy. Chicago, USA.

Lappin, G., Simpson, M., Shishikura, Y. and Garner, C., 2008. High-performance liquid chromatography accelerator mass spectrometry: correcting for losses during analysis by internal standardization. Anal Biochem 378, 93–95.

Lappin, G., Wagner, C., Langer, O. and Merbel, V. D., 2009. New ultrasensitive detection technologies and techniques for use in microdosing studies. Bioanalysis 1 (2), 357–366.

Lappin, G., Shishikura, Y., Jochemsen, R., Weaver, R. J., Gesson, C., Houston, B., Oosterhuis, B., Bjerrume, O.J., Rowland, M. and Garner, C., 2010. Pharmacokinetics of fexofenadine: Evaluation of a microdose and assessment of absolute oral bioavailability. Eur J Pharm Sci 40: 125–131.

Levy, G., Mager, D. E., Cheung, W. K. and Jusko, W. J., 2003. Comparative pharmacokinetics of coumarin anticoagulants L: physiologic modeling of S-warfarin in rats and pharmacologic target-mediated warfarin disposition in man. J Pharm Sci 92 (5), 985–994.

Lewis, D. F., 2009. Early human studies of investigational agents: dose or microdose. Br J Clin Pharmacol 67 (3), 277–279.

Madan, A., O'Brien, Z., Wen, J., O'Brien, C., Farber, R. H., Beaton, G., Crowe, P., Oosterhuis, B., Garner, R. C., Lappin, G. and Bozigian, H. P., 2008. A pharmacokinetic evaluation of five H1 antagonists after an oral and intravenous microdose to human subjects. Br J Clin Pharmacol 67 (3), 288–298.

Matin, S. B. and Rowland, M., 1973. Determination of tolbutamide and chlorpropamide in biological fluids. J Pharm Pharmacol 25 (2), 186–188.

Ni, J., Ouyang, H., Aiello, M., Seto, C., Borbridge, L., Sakuma, T., Ellis, R., Welty, D. and Acheampong, A., 2008. Microdosing assessment to evaluate pharmacokinetics and drug metabolism in rats using liquid chromatography-tandem mass spectrometry. Pharm Res 25 (7), 1572–1582.

Pabba, S. K., Bolla, S., Kandhagatla, R., Chaluvadi, M. R. and Krishna, D. R., 2002. Paracetamol metabolism in Indian population. Arzneimittelforschung 52 (10), 769–772.

Prescott, L. F., 1980. Kinetics and metabolism of paracetamol and phenacetin. Br J Clin Pharmacol 10 Suppl 2, 291S–298S.

Robbins, D. K., Castles, M. A., Pack, D. J., Bhargava, V. O. and Weir, S. J., 1998. Dose proportionality and comparison of single and multiple dose pharmacokinetics of fexofenadine (MDL 16455) and its enantiomers in healthy male volunteers. Biopharm Drug Dispos 19 (7), 455–463.

Rowland, M., 2007. Commentary on ACCP position statement on the use of microdosing in the drug development process. J Clin Pharmacol 47 (12), 1595–1596; author reply 1597–1598.

Sandhu, P., Vogel, J. S., Rose, M. J., Ubick, E. A., Brunner, J. E., Wallace, M. A., Adelsberger, J. K., Baker, M. P., Henderson, P. T., Pearson, P. G. and Baillie, T. A., 2004. Evaluation of microdosing strategies for studies in preclinical drug development: demonstration of linear pharmacokinetics in dogs of a nucleoside analog over a 50-fold dose range. Drug Metab Dispos 32 (11), 1254–1259.

Sarapa, N., Hsyu, P. H., Lappin, G. and Garner, R. C., 2005. The application of accelerator mass spectrometry to absolute bioavailability studies in humans: simultaneous administration of an intravenous microdose of 14C-nelfinavir mesylate solution and oral nelfinavir to healthy volunteers. J Clin Pharmacol 45 (10), 1198–1205.

Tozuka, Z., Kusuhara, H., Nozawa, K., Y, H., lkushima, I, lkeda, T. and Sugiyama, Y., 2010. Microdose study of L4C-Acetaminophen with accelerator mass spectrometry to examine pharmacokinetics of parent drug and metabolites in healthy subjects. Clin Pharmacol Ther 88(6): 824–830.

Vertzoni, M. V., Archontaki, H. A. and Galanopoulou, P., 2003. Development and optimization of a reversed-phase high-performance liquid chromatographic method for the determination of acetaminophen and its major metabolites in rabbit plasma and urine after a toxic dose. J Pharm Biomed Anal 32 (3), 487–493.

Vuong, L. T., Ruckle, J. L., Blood, A. B., Reid, M. J., Wasnich, R. D., Synal, H. A. and Dueker, S. R., 2007. Use of accelerator mass spectrometry to measure the pharmacokinetics and peripheral blood mononuclear cell concentrations of zidovudine. J Pharm Sci 97 (7), 2833–2843 DOI 10.1002/jps.21160.

Wagner, C. C., Muller, M., Lappin, G. and Langer, O., 2008. Positron emission tomography for use in microdosing studies. Curr Opin Drug Discov Devel 11 (1), 104–110.

Wang, W., Wang, E. Q. and Balthasar, J. P., 2008. Monoclonal antibody pharmacokinetics and pharmacodynamics. Clin Pharmacol Ther 84 (5), 548–558.

Yamane, N., Tozuka, Z., Sugiyama, Y., Tanimoto, T., Yamazaki, A. and Kumagai, Y., 2007. Microdose clinical trial: quantitative determination of fexofenadine in human plasma using liquid chromatography/electrospray ionization tandem mass spectrometry. J Chromatogr B Analyt Technol Biomed Life Sci 858 (1–2), 118–128.

# Metabolite Testing in Drug Development

**6**

Angus N. R. Nedderman and Don K. Walker

## Abstract

A significant consideration during the development of drug candidates is the impact of metabolites on efficacy and safety. Following the publication of the Metabolites in Safety Testing (MIST) guidance by the FDA in 2008, the focus on defining appropriate strategies to underwrite metabolite safety has intensified. Many analytical technologies are available to determine the identity and abundance of metabolites and further approaches continue to emerge. Furthermore, the scientific debate in recent years has enabled a pragmatic case-by-case approach to understand the significance of the metabolic pathways of novel compounds. In this respect, a number of key considerations apply, notably the specific structure, pharmacological activity, abundance, pharmacokinetics and physicochemical properties of individual metabolites, together with the administered dose of the parent compound. By considering all these factors, appropriate strategies can be defined to derive fit-for-purpose data to ensure that the safety and efficacy profiles of candidate compounds are properly understood.

## 6.1 Introduction

Metabolite characterisation is recognised to be a key component of the drug discovery and development continuum due to its potential impact on the clearance, efficacy, and safety of drug candidates (Korfmacher et al. 2001; Watt et al. 2003). In the development phase, defined as the period following nomination of a drug candidate, monitoring of the unmetabolized drug, or "parent", during clinical and safety programmes is standard practise. However, for most drug candidates, metabolic clearance strategies are also necessary to ensure the impact of metabolic products on safety and efficacy is understood. Knowledge of the pharmacokinetics and pharmacodynamics of drug metabolites may prompt further investigation to understand the role that metabolites can have on drug response. The publication of the FDA Metabolites in Safety Testing (MIST) guidance in 2008 (FDA Guidance 2008) has brought metabolite safety issues into sharper focus, and much thought has been given to the

A.N.R. Nedderman (✉)

Department of Pharmacokinetics, Dynamics and Metabolism, IPC 664, Pfizer Global Research and Development, Ramsgate Road, Sandwich, Kent CT13 9NJ, UK
e-mail: angus.nedderman@pfizer.com

application of strategies to ensure the safety of metabolites will be assessed as drug development programmes proceed through clinical testing and ultimately to registration. A core principle of the FDA MIST guidance is the identification of disproportionate human metabolites, defined as those drug-related components present in human circulation at steady-state at higher exposures than observed within toxicology studies. This chapter will discuss approaches employed to generate these metabolism data, the interpretation of metabolism data in the context of safety assessments, and strategic considerations to ensure safety is adequately assessed throughout the drug discovery and development process.

## 6.2 Methodologies to Generate Metabolism Data

### 6.2.1 Metabolism Studies in Drug Discovery

Metabolite identification studies in drug discovery are typically conducted with mass spectrometry as the primary tool and use a variety of approaches and instrumentation to generate supporting structural information (Prakash et al. 2007). Additional technologies and strategies, such as NMR spectroscopy or chemical derivatisation, can be used to provide more specific structural data. However, practical considerations, including time, costs, and the high failure rate of clinical candidates' translation to useful medicines, can limit their routine application during the discovery phase. Indeed, the optimal approach to discovery metabolism studies is to ensure that fit-for-purpose data are generated efficiently and projects can apply this knowledge within an optimal time frame.

Recent technological developments have enabled metabolism studies to be conducted earlier in the discovery process in order to more routinely influence chemical design. Notably, in silico prediction tools (Cruciani et al. 2005; Testa et al. 2005), on-line approaches to characterising metabolites (Van Liempd et al. 2007) and high-resolution MS and HPLC methods (Castro-Perez

et al. 2005) have grown in popularity within the pharmaceutical industry and provide rapid metabolite characterisation data to increase confidence in efficacy and safety understanding.

### 6.2.2 Metabolite Scouting in Early Development

Regardless of the diligence with which discovery metabolism studies are undertaken, it is important to generate in vivo human metabolism data early in drug development in order to validate the findings in the discovery phase. Whilst it is feasible for definitive metabolism data to be generated using radiolabelled compound in the early stages of development, such studies are typically conducted in Phase II due to their cost and complexity. Therefore, metabolite "scouting" a term applied to the qualitative and semiquantitative analysis of metabolites using cold, or non-radiolabelled, compound is a common strategy during single and multiple-dose studies in healthy volunteers. Whilst the analytical approaches are similar to those employed during the discovery phase, further diligence may be required to provide semiquantitative information in order to underwrite human safety.

Metabolite quantitation without radiolabelled material or an authentic standard is not trivial, although many technologies exist that can be utilised (Wright et al. 2009). Notably, metabolite quantitation using NMR spectroscopy continues to grow in popularity with recent advances in sensitivity. Historically used for fluorinated compounds (Scarfe et al. 1999) where endogenous compounds provide no interfering signals, NMR has recently been applied to the quantitation of non-fluorine containing compounds (Dear et al. 2008; Espina et al. 2009). Although emerging quantitative techniques may be attractive, the key to metabolite quantitation during metabolite scouting is an assessment of relative, rather than absolute, abundance, such that mass spectrometric or UV detection are appropriate approaches in many cases. Therefore, a typical scouting strategy is to compare metabolic profiles, ideally at steady state, between clinical and nonclinical toxicology

studies. Information on the relative abundance and structure of metabolic products at this stage is important with regard to on- and off-target pharmacological activity and will be discussed within the strategic considerations section.

### 6.2.3   Definitive Metabolism Studies in Drug Development

Definitive metabolism data in humans and animal species are typically generated following administration of radiolabelled compound, thus enabling the detection and accurate quantitation of all drug-related material, assuming that the position of radiolabel is appropriate and metabolism does not yield any unlabelled components. A variety of approaches are available for radiochemical analysis, including a number of methods to quantify low-levels of radioactivity, which are typically required for the analysis of plasma samples (Nassar et al. 2003; Nedderman et al. 2004; Boernsen et al. 2000).

One technique that provides quantitative data of exquisite sensitivity, albeit without the capability to provide direct structural information, is accelerator mass spectrometry (AMS). This approach has had something of a renaissance following the publication of the MIST guidance (FDA guidance 2008). Historically used for carbon dating (Bennett et al. 1977) and biomedical investigations (Elmore et al. 1990), AMS has been applied to ADME studies for a number of years (Kaye et al. 1997), and provides robust metabolite quantitative data of exceptional sensitivity (Young et al. 2001; Garner et al. 2002). Technologies to provide structural information during the ADME programme are as described earlier, although the definitive nature of these studies means that more frequent use of resource-intensive technologies such as NMR are applied to generate specific structural data. Assessment of metabolite profiles across species is facile for definitive studies, and the identification of disproportionate human metabolites cannot be excluded at this typically late stage of the development programme. Such a finding may necessitate a return to additional safety, pharma-

cokinetic, or toxicology studies to support human safety characterisation.

### 6.2.4   Case Study

A good example of an emerging metabolite profile has been illustrated for the non-nucleoside reverse transcriptase inhibitor (NNRTI), lersivirine (UK-453061). In vitro studies conducted during the discovery phase identified N-dealkylated and hydroxylated metabolites; information which, together with pharmacokinetic data from toxicology species, provided the basis for the predicted human pharmacokinetic profile (Allan et al. 2008). In early development, plasma samples from first-in-human studies confirmed the presence of the hydroxylated components (with additional information on the relative abundance of the two positional isomers) but showed only trace levels of the N-dealkylated metabolite. In addition, an abundant glucuronide conjugate of parent was identified together with a carboxylic acid metabolite formed by oxidation of the alcohol function (Fig. 6.1) and some additional phase II conjugates. The information from these studies prompted further studies to confirm the presence of the carboxylic acid metabolite in toxicology species at sufficient exposure in order to demonstrate appropriate safety cover. A human radiolabelled ADME study with lersivirine was subsequently conducted during phase II, which confirmed the major routes of metabolism identified through the metabolite scouting and provided additional information around minor metabolic products as well as definitive quantitation of the individual routes both in the systemic circulation and the excreta.

### 6.3   Pharmacokinetic Considerations

### 6.3.1   Physicochemical Aspects

When considering the pharmacokinetic behaviour of drug metabolites, a useful first point of reference is the physicochemical properties. These can provide valuable information on the
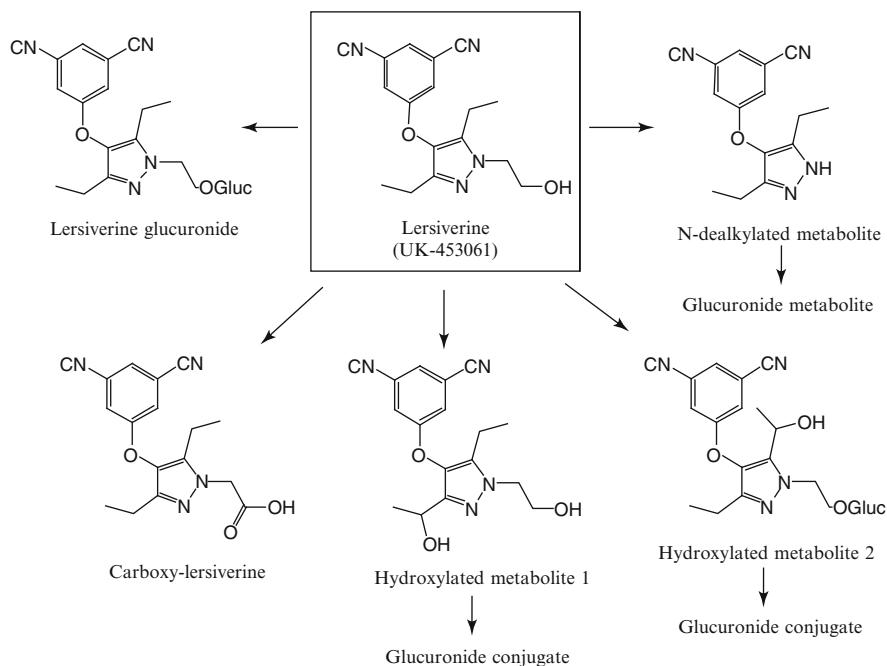
**Fig. 6.1** Major metabolic pathways for lersivirine (UK-453,061). Nonclinical in vitro studies demonstrated formation of the hydroxylated and N-dealkylated metabo- lites. Metabolite scouting in human plasma identified the glucuronide conjugate of parent and the carboxylic acid

rate and route of clearance, tissue distribution and plasma protein binding. In general, metabolism converts lipophilic drug molecules into more polar metabolites in order to facilitate their removal from the body. The increase in polarity may be substantial, such as in the case of glucuronide conjugates. The polarity change may be more subtle, for example in the case of oxidative metabolism resulting in hydroxylation or dealkylation of small aliphatic units. Increased polarity facilitates the removal of drug-derived metabolites via passive filtration in the kidneys and may increase susceptibility to biliary excretion via the bile. This is illustrated for the cholinesterase inhibitor SM-10888, where pharmacokinetic properties of individual metabolites were determined in rat and related to physicochemical properties (Yabuki et al. 1994). Hydroxylation of the parent molecule resulted in an approximate reduction of 0.6 units in the log $D_{7.4}$ value and renal clearance increased almost fourfold. Direct glucuronidation of the parent molecule resulted in a 3.6 unit reduction in log $D_{7.4}$ with a 100-fold increase in the renal

clearance. Whilst this compound illustrates the general rule that metabolism increases polarity and thus increases clearance; it also provides an example of a metabolic product (a ketone) which has increased lipophilicity resulting in lowered clearance. In order to enable effective renal clearance by passive processes, it is generally regarded that a log $D_{7.4}$ value below 0 is required (Smith et al. 1996). Hence the absolute lipophilicity of the parent molecule and the degree of polarity introduced by metabolism will determine if a metabolite is susceptible to renal clearance. For highly lipophilic molecules such as amiodarone (Log $D_{7.4} > 5.0$), relatively small changes in lipophilicity due to N-dealkylation do not greatly enhance the ability to clear metabolites from the body (Holt et al. 1983).

In addition to the impact that the change in physicochemistry imparts on the clearance of molecules, metabolic transformation can also influence other disposition characteristics. Tissue affinity and plasma protein binding are dependent on the physiochemical properties of a molecule. In general, decreasing lipophilicity

will reduce the affinity for tissue and plasma protein binding due to decreased hydrophobic interactions.

However, there may be cases where changes in the physicochemistry result in additional specific interactions leading to increased binding. It is well recognised that carboxylic acids exhibit particularly high plasma protein binding due to their ionic interaction with albumin (Smith et al. 1996). Hence metabolic transformations that yield a carboxylic acid metabolite can show increased plasma protein binding which may result in decreased availability for clearance and, potentially, pharmacological effect. An example is provided by the angiotensin II receptor antagonist losartan and its pharmacologically active metabolite EXP3174. In this case, the metabolite has higher plasma protein binding than the parent compound (Christ 1995) due to oxidation of the alcohol function to an acid. A more subtle impact on tissue disposition due to changing physicochemistry was encountered in the discovery of the calcium channel blocker amlodipine. In this case, the primary amine amlodipine was first observed as a metabolite of the dimethyl tertiary amine analogue, which possessed a long duration of action due, in large part, to formation of amlodipine as a metabolite (Humphrey 1996). Amlodipine possesses a large volume of distribution, larger than those of the secondary and tertiary amine analogues, and this has been attributed to a specific ion-pair interaction between the amine and acidic phos-

pholipid headgroups present in cell membranes. The large volume of distribution (21 L/kg) results in a long elimination half-life of around 35 h in man (Stopher et al. 1988).

## 6.3.2   Metabolite Kinetics

Schematically the formation and elimination of drug metabolites can be represented as shown in Fig. 6.2. In this scheme the amount of metabolite in the body (M) is governed by the balance between its formation (determined by the amount of parent molecule ($D$) and its rate constant for elimination ($k$) and fraction metabolised to the particular metabolite ($f_m$)) and its elimination (determined by the amount of metabolite (M) and the rate constant for metabolite elimination ($k_m$)). The concentration of the metabolite ($C_m$) can be described mathematically but requires information on its volume of distribution ($V_d$) according to the following equation (Clark and Smith 1986):

$$C_m = \frac{f_m \times D}{V_d} \frac{k}{k_m - k} \left( e^{-kt} - e^{-k_m t} \right) \qquad (6.1)$$

In the majority of cases the rate constant for metabolite elimination is larger than the rate constant for parent drug elimination, reflecting that metabolites are more readily eliminated from the body than the parent molecule. In
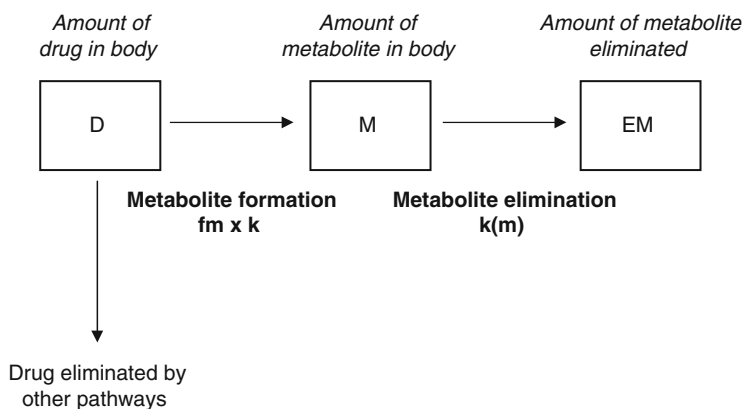


**Fig. 6.2**  Schematic representation of the formation and elimination of metabolites

addition, metabolites are generally more polar than parent compound resulting in a reduced volume of distribution. These two factors of higher clearance (Cl) and reduced volume of distribution (Vd) will generally mean that the half-life of a metabolite would be shorter than that of the parent molecule if it was administered directly.

In reality, the observed half-lives of metabolites are often the same as parent molecule as their elimination becomes formation rate-limited where the decline in the concentration of parent drug limits the rate of formation and hence elimination of the metabolite. Mathematically when "$k_m$" is significantly larger than "$k$" the term "exp $(-k_m t)$" in (6.1) becomes negligible and the change in metabolite concentration is a function of the rate constant for parent drug elimination (i.e. "$k$").

While formation rate-limited metabolite pharmacokinetics are the more common situation, there are numerous examples where metabolites exhibit elimination rate-limited pharmacokinetics ($k >> k_m$). Examples include parent drug molecules which are particularly susceptible to rapid metabolic clearance resulting in metabolites which no longer possess such a vulnerable site of metabolism; this is of course an intrinsic design principle of prodrugs, like esters, which are cleaved to yield more slowly eliminated pharmacologically active moieties. An example of an intrinsically designed prodrug is the ACE inhibitor enalapril which has a short elimination half-life but is rapidly hydrolysed to the carboxylic acid active moiety enalaprilat which has an elimination half-life of about 35 h (Ulm et al. 1982). Other examples of longer-lived metabolites include metoprolol and its hydroxylated metabolite and nitroglycerin and its dinitrate metabolites.

### 6.3.3 Population Variability and Drug Metabolites

Increasingly, population variability in drug response is recognised as an important consideration in the evaluation of new medicines. Pharmacogenetic determinants of drug response include genetic polymorphisms of drug metabolising enzymes and transporters which impact the pharmacokinetics of the compound and hence the resultant pharmacological effects (Eichelbaum et al. 2006). The influence of genetic polymorphism on pharmacokinetics may also need to be extended to drug metabolites, particularly when these possess pharmacological activity in their own right.

Probably the best known genetic polymorphism amongst drug metabolising enzymes is the CYP2D6 polymorphism with multiple forms of the enzyme present within the population and absence of active protein in approximately 7% of the Caucasian population. The antimuscarinic agent tolterodine is extensively metabolised by CYP2D6 and its pharmacokinetics show marked variation between CYP2D6 extensive metabolisers (EMs) and poor metabolisers (PMs). However, due to the pharmacodynamic contribution from the active metabolite of tolterodine, which is formed by CYP2D6, the genetic polymorphism appears to have little impact on the antimuscarinic effect probably due to the additive effect of parent compound and metabolite (Brynne et al. 1998). Thus pharmacogenetic considerations should include active metabolites in the overall assessment of population variability on drug effect.

## 6.4 Strategic Considerations

### 6.4.1 Timing of Metabolism Studies

The FDA MIST guidance refers to the need to generate metabolism data "as early as possible" in drug development in order to appropriately underwrite safety. As a result, some pharmaceutical companies have accelerated the definitive ADME programmes for novel compounds, often administering low levels of radioactivity in early clinical studies and using AMS analysis to generate metabolism data (Lappin and Stevens 2008). Whilst this is a valid approach, its cost and time effectiveness may be questioned given the high concordance between animal and human

metabolism (Smith 1991) and the technologies that are available to identify metabolites in the absence of radiolabel. For this reason, a more pragmatic approach may be to conduct diligent metabolite scouting on plasma samples from Phase I clinical studies and toxicology species and then complete definitive radiolabelled studies later in development. Typically this will be after evidence is obtained supporting the potential utility of the drug candidate as a medicine, and when the time, effort and expense of synthesising the appropriate radiolabel(s) and bioanalytical standards are justified. Early radiolabelled studies may well be appropriate, for instance, when specific metabolism issues need to be addressed early in drug development in order to inform safety concerns or to generate definitive data to provide appropriate context around an in vitro safety observation.

## 6.4.2  Metabolite Monitoring Strategies

In the absence of radiolabelled material, robust and reliable quantitative data for metabolite exposure are best obtained via formal metabolite monitoring during clinical and safety programmes, typically using validated LC-MS/MS assays. However, since this approach requires synthesis of an authentic standard, precise structural definition of the metabolite is required. It may also necessitate potentially laborious analytical method development and possibly require an isotopically-labelled internal standard. For these reasons, quantitative assays for metabolites can prove costly and should not be undertaken lightly.

Metabolite identification studies during drug discovery should yield valuable information well in advance of clinical and safety study design in order to inform the metabolite monitoring strategy. Typically, formal metabolite monitoring in clinical studies will only be necessary in Phase I following identification of an active metabolite of significant abundance relative to parent compound, as such a metabolite may affect the clinical safety and efficacy of the administered drug.

As a rule of thumb, unless a metabolite is expected to contribute more than 25% relative potency to parent (based on free exposure and pharmacological activity (Smith and Obach 2005)), then routine quantitation need not be employed. Thus, discovery metabolism studies should be designed to provide sufficient information to enable synthesis and subsequent pharmacology testing of the metabolite. Whilst the activity of a metabolite can in principle be determined by on-line activity profiling (Van Liempd et al. 2007), the common approach involves synthesis and testing driven by a combination of abundance (allowing for the caveats associated with quantitative data in the absence of authentic standards and/or radiolabelled material) and a knowledge of the pharmacophore of the parent compound and the metabolite structure. Even when an active metabolite is identified in drug discovery, it may still be appropriate to apply a degree of pragmatism to the monitoring strategy and conduct an informal semiquantitative analysis of the metabolite in question during the first-in-human study, the data from which can inform the need to continue to a formal monitoring strategy in subsequent studies. This approach allows for the possibility that an active metabolite may be a minor component relative to parent compound in patients, and therefore, its impact on safety and efficacy may be negligible. It should be remembered, however, that the extent of plasma protein binding of a metabolite may be lower than the parent compound and the relative potency can be greater than the parent. Under these circumstances, a metabolite may make a greater contribution to the pharmacological effect than judged simply on a comparison of total concentration or exposure.

Whilst data generated during drug discovery will guide the initial metabolite monitoring strategy, subsequent metabolite scouting studies in human plasma from Phase I clinical studies should be used to refine the monitoring approach. These data inform decisions to either terminate formal monitoring of a metabolite found subsequently to be a minor component, or can initiate monitoring of a component not previously detected in vitro, but which is found to represent

a significant component in terms of safety or, possibly efficacy.

Furthermore, definitive metabolism data generated using radiolabelled material can also affect the monitoring strategy. Even though these data will not typically be generated until Phase 2 of clinical development, the information is usually necessary to underwrite safety during Phase 3 development and to inform the clinical drug-interaction programme.

### 6.4.3 The Significance of Disproportionate Human Metabolites

It is well known that unique human metabolites are rare (Leclercq et al. 2009), reflecting the similarity of drug metabolising pathways between humans and laboratory animal species (Smith 1991). However, scenarios where metabolites may not be unique but have higher relative exposures in humans than in animal species are more common and in such circumstances, it is appropriate that additional safety considerations are made. Indeed, such thinking is integral to the FDA's MIST guidance document. Within this document, metabolite considerations are framed into a decision tree. The first consideration for a human metabolite is its relative abundance in the systemic circulation compared to parent compound. If this is less than 10% then the metabolite can be considered not to pose a safety concern. For those metabolites that exceed 10% relative to parent then a consideration of their safety risk is required. The choice of a level of 10% was made to provide consistency with other FDA and Environmental Protection Agency guidance. For these metabolites the next consideration is with regard to their systemic exposure in the toxicology species. If at least one animal species used in the toxicology programme demonstrates adequate exposure (approximately equal to or greater than human exposure) then it can be assumed that the metabolites' contribution to the overall safety profile has been assessed. Importantly the guidance recognises that although metabolites may occur

in higher proportions in humans compared to animals in toxicology studies, in many cases, the higher doses used in toxicology studies result in overall higher systemic exposures of drug and metabolites which means that the animals have been exposed to higher absolute amounts of metabolites and thus metabolite safety has been adequately assessed. The guidance uses the term "disproportionate drug metabolite" which is defined as a metabolite that exceeds 10% of parent systemic exposure and is present only in humans or present in humans at higher plasma concentrations than are encountered in the animals used in the nonclinical studies.

Whilst the MIST guidance lays out the fundamental principles of metabolite safety assessments, a number of additional areas are worthy of further specific consideration. First, the guidance states that it is appropriate to consider metabolites accounting for 10% or more of the parent AUC in human plasma. Although this is an appropriate consideration, designed to guard against unnecessary responses to underwrite the safety of metabolites of extremely low abundance, it is less readily applied to extensively metabolised compounds, where many metabolites may occur at high proportions of parent compound. In these circumstances, it is pragmatic to focus on the most abundant metabolites that represent more than 10% of the total drug-related material, as a threshold for considerations of metabolite safety testing. This limitation of the guidance has been recognised within the FDA and provides further rationale for the need for case-by-case assessments (Atrakchi 2009). In all cases, any metabolite structure that raises a specific safety concern (e.g. structural alert), irrespective of amount, should be given due consideration. Secondly, a case has been made that absolute, rather than relative, abundance is the key consideration, and therefore the administered dose should be taken into account (Smith and Obach 2006). Thus, metabolites of low dose compounds are less likely to give rise to safety issues while even low level (in% terms) metabolites may be a cause for concern if the dose level is very high, as the circulating concentration and/or total body burden may impart significant

chemical stress. A third consideration is around the specific structure of the metabolites in question. Metabolites of similar structure to the parent compound, such as those arising from hydroxylation or demethylation, are likely to have on- or off-target pharmacological activity similar to the parent molecule and thus are worthy of further consideration.

Metabolites of very different structure to the parent drug are highly unlikely to possess similar activity, though they may have off-target effects. Caution should be exercised, however, in dismissing the potential safety concerns of all metabolites that are structurally unrelated to the parent compound. In particular, any metabolites resulting from reactive metabolic pathways are indicative of a mechanism that may give rise to safety concerns. Such "smoking gun" metabolites, including methylcatechols or migrated acyl glucuronides, should be given serious consideration, and may only be identified in excreta, showing that although plasma metabolites are typically of key importance, those present in excreta cannot be ignored. An example of a "smoking gun" metabolite was observed for the 5-lipoxygenase inhibitor zileuton, where an N-acetylthiophene metabolite was detected in urine, indicative of the formation of a reactive sulphoxide component (Joshi et al. 2004) (Fig. 6.3). The therapeutic use of zileuton is limited due to hepatotoxicity, possibly as a result of this metabolic pathway.

One final consideration noted in the FDA guidance is that some structures may be considered benign, regardless of the relative abundance in humans and animal species. Notably, ether glucuronides are cited in the guidance as components that should not give rise to safety concerns, due to the likelihood that they will be pharmacologically inactive and the fact that they typically have low volumes of distribution and rapid clearance due to their polarity. However, whilst ether glucuronides are typically benign, there are examples where such conjugates do possess on-target pharmacological activity, such as morphine 6-glucuronide which is an opioid mu agonist of 50-fold greater potency than the parent compound (Gong et al. 1991). Furthermore,
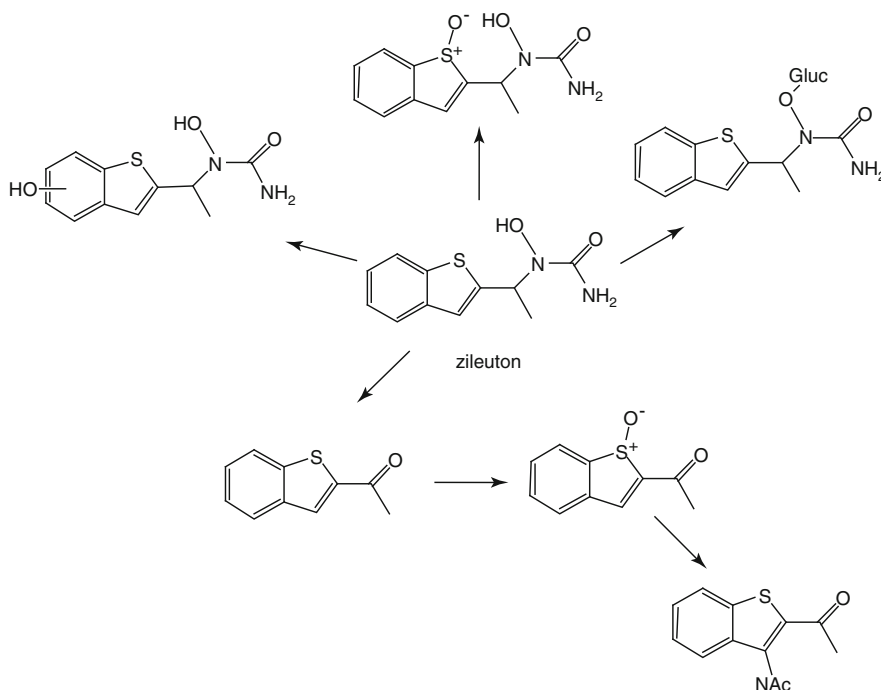


**Fig. 6.3** Metabolic pathways of zileuton, including formation of an N-acetylthiophene metabolite via a reactive sulphoxide intermediate

alternative classes of phase II conjugate do need to be given due consideration from a safety perspective, most notably acyl glucuronides, which have been shown to form covalent adducts to proteins, a mechanism that may be implicated in toxicity (Bailey and Dickenson 1996). Caveats and considerations such as those described in this section show that safety considerations for metabolites must be made on a case-by-case basis, applying sound reasoning to ensure that safety is appropriately underwritten.

## 6.5 Strategies to Underwrite the Safety of Disproportionate Human Metabolites

Whilst the occurrence of disproportionate metabolites is relatively rare, on the occasions when they are encountered, a strategy will be required to understand the safety profile of the particular chemical entity. It should be recognised that the MIST guidelines state that provided a metabolite is present in approximately equivalent absolute concentrations in at least one toxicology species at the NOAEL then its safety can be considered qualified, barring some unusual safety consideration. Even in situations where a metabolite is not adequately exposed in the toxicology programme there may be justification that specific toxicity testing is not required if there is a clear case that the particular structure can be shown to be devoid of hazard (e.g. ether glucuronides). In those cases where exposures to a human metabolite is not covered in safety studies then essentially two alternatives remain: the parent compound may be examined in a different non-clinical species to see if any of these provide adequate exposure to the metabolite or the metabolite may be directly administered to an animal species. The actual safety studies that need to be carried out with such a metabolite should be determined on a case-by-case basis taking into account regulatory guidance such as the International Conference on Harmonisation M3 Guidance for Non-Clinical Safety Studies (ICH Guidance M3, 2009), the disease indication and the risk assessment. In a situation where

the direct administration of a metabolite might be required there may need to be additional consideration concerning the route of administration should the metabolite not be orally absorbed. This in itself may add further complexity to the interpretation of data where route-specific effects could potentially contribute to the safety profile (Prueksaritanont et al. 2006). The specific testing of metabolites in general toxicology, genotoxicity studies, reproductive toxicology studies and carcinogenicity studies has been discussed within the scientific literature (Baillie et al. 2002). In addition, in vitro safety studies can be utilised to identify particular risks associated with metabolite structures.

An example where additional safety testing was conducted for a specific metabolite was reported recently for the acyl coenzyme A: cholesterol acyltransferase (ACAT) inhibitor pactimibe (Kotsuma et al. 2008). An oxidative metabolite of pactimibe, R-125528, formed by CYP3A4, is cleared by CYP2D6 (Fig. 6.4) and significant accumulation of R-125528 was observed after chronic administration of pactimibe to CYP2D6 poor metabolisers during the clinical programme. In order to fully characterise the safety following administration of pactimibe to humans, additional safety studies were conducted for R-125528 to show the exposure of R-125528 could be tolerated in animals significantly in excess of the exposure observed in clinical studies.

## 6.6 Summary

The publication of the FDA's MIST guidance in 2008 has precipitated renewed interest and significant activity in the field of metabolite characterisation to underwrite the safety of novel compounds. Although the derivation of metabolism data is a holistic process, conducted throughout drug discovery and development, particular focus is applied to the early development phase, where the opportunity to generate in vivo data in humans presents itself for the first time. For this reason, much effort is being expended on the development of approaches to generate information of metabolite structure,
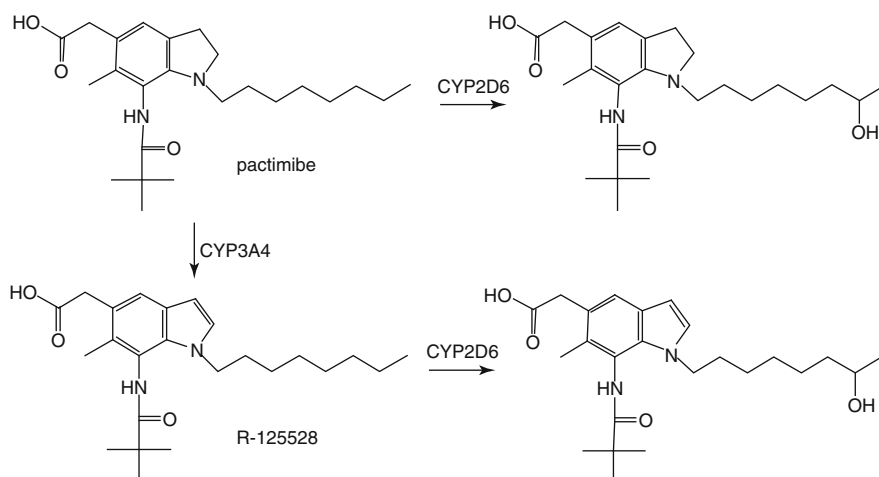
**Fig. 6.4** Metabolic scheme for the ACAT inhibitor pactimibe, showing formation and clearance routes for the metabolite R-125528

abundance and pharmacological activity during this phase of development. Technologies such as accelerator mass spectrometry have generated significant interest and undoubtedly have a place in the safety assessment process. Such approaches, however, are unlikely to achieve routine utility in early development until their cost effectiveness and speed are improved. Thus, the improvement of existing methodologies and the development of novel technologies to generate key metabolism data will remain an area of substantial focus.

Regardless of the available technologies, the key to metabolite safety assessments is to consider each case individually, rather than follow specific rules and such thinking is specifically laid out in the FDA guidance. Thus considerations around the relevance of structure, activity, pharmacokinetics, abundance and dose to the overall safety profile of a compound are critical to appropriately addressing safety concerns. Such thinking, based on the generation of fit-for-purpose data at the appropriate phase of drug discovery and development, will ensure that the correct decisions can be made around metabolite monitoring strategies, disproportionate metabolites and subsequent alterations to clinical and safety programmes, thereby ensuring that human safety is consistently and adequately addressed.

## References

Allan G, Davis J, Dickins M, Gardner I, Jenkins T, Jones H, Webster R, Westgate H. Pre-clinical pharmacokinetics of UK-453,061, a novel non-nucleoside reverse transcriptase inhibitor (NNRTI), and use of in silico physiologically based prediction tools to predict the oral pharmacokinetics of UK-453,061 in man. *Xenobiotica* 2008; **38**: 620–640.

Atrakchi AH. Interpretation and considerations on the safety evaluation of human drug metabolites. *Chem Res Toxicol* 2009; **22**: 1217–1220.

Bailey MJ, Dickenson RG. Chemical and immunochemical comparison of protein-adduct formation of four carboxylate drugs in rat liver and plasma. *Chem Res Toxicol* 1996; **9**: 659–666.

Baillie TA, Cayen MN, Fouda H, Gerson RJ, Green JD, Grossman SJ, Klunk LJ, LeBlanc B, Perkins DG, Shipley LA. Contempory issues in toxicology: drug metabolites in safety testing. *Toxicol Appl Pharmacol* 2002; **182**: 188–196.

Bennett CL, Beukens RP, Clover MR, Gove HE, Liebert RB, Litherland AE, Purser KH, Sondheim WE. Radiocarbon dating using electrostatic accelerators: negative ions provide the key. *Science* 1977; **198**: 508–510.

Boernsen KO, Floeckher JM, Bruin GJM. Use of a microplate scintillation counter as a radioactivity detector for miniaturised separation techniques in drug metabolism. *Anal Chem* 2000; **72**: 3956–3959.

Brynne N, Dalen P, Alvan G, Bertilsson L, Gabrielsson J. Influence of CYP2D6 polymorphism on the pharmacokinetics and pharmacodynamics of tolterodine. *Clin Pharmacol Ther* 1998; **63**: 529–539.

Castro-Perez JM, Plumb R, Granger JH, Beattie I, Joncour K, Wright A. Increasing throughput and information

content for in vitro drug metabolism experiments using ultra-performance liquid chromatography coupled to a quadrupole time-of-flight mass spectrometer. *Rapid Commun Mass Spectrom* 2005; **19**: 843–848.

Christ, D.D. Human plasma protein binding of the angiotensin II receptor antagonist losartan potassium (DuP 753/MK 954) and its pharmacologically active metabolite EXP3174. *J Clin Pharmacol* 1995; **35**: 515–520.

Clark B, Smith DA. *An introduction to pharmacokinetics, 2nd edition,* 1986. Blackwell Scientific Publications, Oxford, UK.

Cruciani G, Carosati E, De Boeck B, Ethirajulu K, Mackie C, Howe T, Vianello R. Metasite: understanding metabolism in human cytochromes from the perspective of the chemist. *J Med Chem* 2005; **48**: 6970–6979.

Dear GJ, Roberts AD, Beaumont C, North SE. Evaluation of preparative high performance liquid chromatography and cryoprobe-nuclear magnetic resonance spectroscopy for the early quantitative estimation of drug metabolites in human plasma. *J Chromatog B* 2008; **876**: 182–190.

Eichelbaum M, Ingelman-Sundberg M, Evans WE. Pharmacogenomics and individualised drug therapy. *Annu Rev Med* 2006; **57**: 119–137.

Elmore D, Bhattacharyya MH, Sacco-Gibson N, Peterson DP. Calcium-41 as a long-term biological tracer for bone resorption. *Nucl Inst Methods Phys Res* 1990; **B52**: 531–535.

Espina R, Yu L, Wang J, Tong Z, Vashishtha S, Talaat R, Scatina J, Mutlib A. Nuclear magnetic resonance spectroscopy as a quantitative tool to determine the concentrations of biologically produced metabolites: implications in metabolites in safety testing. *Chem Res Toxicol* 2009; **22**: 299–310.

FDA Guidance for Industry. Safety Testing of Drug Metabolites 2008, www.fda.gov/downloads/Drugs/GuidanceComplianceRegulatoryInformation/Guidances/ucm079266.pdf (accessed June 3, 2009)

Garner RC, Goris I, Laenen AAE, Vanhoutte E, Meuldermans W, Gregory S, Garner JV, Leong D, Whattam M, Calam A, Snel CAW. Evaluation of accelerator mass spectrometry in a human mass balance and pharmacokinetic study – experience with ^{14}C-labelled (*R*)-6-[Amino(4-chlorophenyl)(1-methyl-1*H*-imidazol-5-yl)methyl]-4-(3-chlorophenyl)-1-methyl-2 (1*H*)-quinolinone (R115777), a farnesyl transferase inhibitor. *Drug Metab Disp* 2002; **30**: 823–830.

Gong Q-L, Hedner T, Hedner J, Bjorkman R, Nordberg C. Antinociceptive and ventilatory effects of the morphine metabolites: Morphine-6-glucuronide and morphine-3-glucuronide. *Eur J Pharmacol* 1991; **193**: 47–56.

Holt DW, Tucker GT, Jackson PR, Storey GCA. Amiodarone pharmacokinetics. *Am Heart J* 1983; **106**: 840–847.

Humphrey MJ. Application of metabolism and pharmacokinetic studies to the drug discovery process. *Drug Metab Rev* 1996; **28**: 473–489.

ICH Guidance for Industry. M3 Nonclinical Safety Studies for the Conduct of Human Clinical Trials for Pharmaceuticals 2009, www.fda.gov/downloads/Drugs/GuidanceComplianceRegulatoryInformation/Guidances/ucm073250.pdf (accessed June 3, 2009)

Joshi EM, Heasley BH, Chordia MD, Macdonald TL. In vitro metabolism of 2-acetylbenzothiophene: relevance to zileuton hepatotoxicity. *Chem Res Toxicol* 2004; **17**: 137–143.

Kaye B, Garner RC, Mauthe RJ, Freeman SPHT, Turteltaub KW. A preliminary evaluation of accelerator mass spectrometry in the biomedical field. *J Pharm Biomed Anal* 1997; **16**: 541–543.

Korfmacher WA, Bryant MS, Cox KA, Ng K, Veals J, Clarke N, Hsieh Y, Ringden D, Tansdler P, Wainhaus S, White RE. Strategies for optimising the use of mass spectrometry for drug metabolism participation in new drug discovery. Adv Mass Spectrom 2001; **15**: 679–680.

Kotsuma M, Tokui T, Freudenthaler S, Nishimura K. Effect of CYPD6 polymorphism on pharmacokinetics of a novel ACAT inhibitor, pactimibe and its unique metabolite, R-125528. *Int J Clin Pharmacol Ther* 2008; **46**: 545–555.

Lappin G, Stevens L. Biomedical accelerator mass spectrometry: recent applications in metabolism and pharmacokinetics. *Exp Opin Drug Metabol Toxicol* 2008; **4**: 1021–1033.

Leclercq L, Cuyckens F, Mannens GSJ, de Vries R, Timmerman P, Evans DC. Which human metabolites have we MIST? Retrospective analysis, practical aspects, and perspectives for metabolite identification and quantification in pharmaceutical development. *Chem Res Toxicol* 2009; **22**: 280–293.

Nassar AE-F, Bjorge SM, Lee DY. On-line liquid chromatography-accurate radioisotope counting to coupled with a radioactivity detector and mass spectrometer for metabolite identification in drug discovery and development. *Anal Chem* 2003; **75**: 785–790.

Nedderman ANR, Savage ME, White KL, Walker DK. The use of 96-well Scintiplates to facilitate definitive metabolism studies for drug candidates. *J Pharm Biomed Anal* 2004; **34**: 607–617.

Prakash C, Shaffer CL, Nedderman A. Analytical strategies for identifying drug metabolites. *Mass Spectrom Rev* 2007; **26**: 340–369.

Prueksaritanont T, Lin JH, Baillie TA. Complicating factors in safety testing of drug metabolites: kinetic differences between generated and preformed metabolites. *Toxicol Appl Pharmacol* 2006; **217**: 143–152.

Scarfe GB, Wright B, Clayton E, Talyor S, Wilson ID, Lindon JC, Nicholson JK. Quantitative studies on the urinary metabolic fate of 2-chloro-4-trifluoromethylaniline in the rat using ^{19}F-NMR spectroscopy and directly coupled HPLC-NMR-MS. *Xenobiotica* 1999; **29**: 77–91.

Smith DA. Species differences in metabolism and pharmacokinetics: are we close to an understanding? *Drug Met Rev* 1991; **23**: 355–373.

Smith DA, Obach RS. Seeing through the mist: abundance versus percentage. Commentary on metabolites in safety testing. *Drug Metab Dispos* 2005; **33**: 1409–1417.

Smith DA, Obach RS. Metabolites and safety: what are the concerns and how should we address them? *Chem Res Toxicol* 2006; **19**: 1570–1579.

Smith DA, Jones BC, Walker DK. Design of drugs involving the concepts and theories of drug metabolism and pharmacokinetics. *Med Res Rev* 1996; **16**: 243–266.

Stopher, D.A., Beresford, A.P., Macrae, P.V., Humphrey, M.J. The metabolism and pharmacokinetics of amlodipine in humans and animals. *J Cardiovasc Pharmacol* 1988; **12**: S55–S59.

Testa B, Balmat A-L, Long A, Judson P. Predicting drug metabolism – an evaluation of the expert system METEOR. *Chem Biodiv* 2005; **2**: 872–885.

Ulm EH, Hichens M, Gomez HJ, Till AE, Hand E, Vassil TC, Biollaz J, Brunner HR, Schelling JL. Enalapril maleate and a lysine analogue (MK521): disposition in man. *Br J Clin Pharmacol* 1982; **14**: 357–362.

Van Liempd SM, Kool J, Meerman JH, Irth H, Vermeulen NP. Metabolic profiling of endocrine-disrupting compounds by on-line cytochrome P450 bioreaction coupled to on-line receptor affinity screening. *Chem Res Toxicol* 2007; **20**: 1825–1832.

Watt AP, Mortishire-Smith RJ, Gerhard U, Thomas T. Metabolite identification in drug discovery. Drug Discov Dev 2003; **6**: 57–65.

Wright P, Miao Z, Shilliday B. Metabolite quantitation: detector technology and MIST implications. *Bioanalysis* 2009; **1**: 831–845.

Yabuki M, Mine T, Iba K, Nakatsuka I, Yoshitake A. Pharmacokinetics of SM-10888 and its metabolites depending on their physicochemical properties. *Drug Metab Dispos* 1994; **22**: 294–297.

Young G, Ellis W, Ayrton J, Hussey E, Adamkiewicz B. Accelerator mass spectrometry (AMS): recent experience of its use in a clinical study and the potential future of the technique. *Xenobiotica* 2001; **31**: 619–632.

# The -Omics in Drug Development

**7**

Majid Y. Moridani, Robyn P. Araujo, Caroline H. Johnson, and John C. Lindon

## Abstract

New advancement in genomics, proteomics, and metabonomics created significant excitement about the use of these relatively new technologies in drug design, discovery, development, and molecular-targeted therapeutics by identifying new drug targets and better tools for safety and efficacy studies in preclinical and clinical stages of drug development as well as diagnostics. In this chapter, we will briefly discuss the application of genomics, proteomics, and metabonomics in drug discovery and development.

## 7.1 Pharmacogenomics in Drug Development

### 7.1.1 Introduction

Genomics, proteomics, and metabonomics are new tools and techniques that are increasingly used in the optimization process in drug development and discovery. Although each of these tools has its own advantages and limitations, the expectation is that the use of these technologies will increase the current success rate of drug

discovery and development. Here, each of these branches of study will be discussed separately.

The completion of the Human Genome Project generated a significant amount of information related to inherited materials, which in turn, created new hope for the development of novel medicines based on a patient's genetic makeup. This new information has made it possible to understand the underlying biology of disease processes in greater detail, which can potentially be used to recategorize diseases into new subtypes and stages, which may require different therapeutic approaches and medical interventions. Studies have demonstrated that variations in drug responses exist between different individuals, genders, age groups, and ethnic populations (Anderson 2008; Gomez and Ingelman-Sundberg 2009). These differences are attributed to variations in a single gene or multiple genes interacting with environmental factors. Understanding how these variations influence the pathophysiology of diseases and lead to variations in drug response

M.Y. Moridani (✉)

Department of Pharmaceutical Sciences, School of Pharmacy, Texas Tech University HSC, 1406 S Coulter Drive, Amarillo, TX 79106, USA
and
Department of Pediatrics, School of Medicine, Texas Tech University HSC, Amarillo Research Building, Amarillo, TX 79106, USA
e-mail: majid.moridani@ttuhsc.edu

and toxicity can ultimately improve drug discovery and development processes.

Pharmacogenetics and pharmacogenomics are closely related sciences that deal with inter-individual variations in genomic information (Kalow 2006). Pharmacogenetics looks at the influence of a single gene on a drug response. A number of classic genetic examples that influence phenotypes by single gene variations exist, including alcaptonuria, phenylketonuria, butyryl cholinesterase, *N*-acetyltransferase, and CYP2D6 enzyme. These single gene variations result in altered metabolism in endogenous substrates or drugs such as succinylcholine, isoniazid, and debrisoquine. For instance, individuals who are *N*-acetyltransferase slow metabolizers, taking regular doses of isoniazid have better efficacy responses to the drug than individuals who metabolize the drug normally. Adverse drug reactions, however, are seen more often in the slow metabolizer group. Pharmacogenomics, on the other hand, looks at the whole genome with an aim to develop reliable biomarkers that accurately predict drug responses, adverse drug reactions, dose requirements, susceptibility to disease, and disease stages. Pharmacogenomics is heavily dependent upon technology and statistical analyzes of complex data to investigate many genes and gene patterns by simultaneously looking at structure and expression of many different genes. These new technologies have the ability to look at low, medium, or large scale genotyping or expression analyzes using DNA and RNA materials derived from blood or tissue samples obtained from patients and healthy subjects for comparison studies. However, in order to be able to utilize these genetic markers in drug design, clinical practice, and drug development, they need to be clearly linked to clinical information and endpoints such as efficacy, pharmacokinetics, safety/adverse reactions, disease state, and disease predisposition. In the following we discuss a number of technical, regulatory, and scientific advances in the use of genomics in drug discovery and development.

## 7.1.2 Genomics in Drug Discovery

Drug discovery is a time consuming and expensive process with a high rate of failure (Kola and Landis 2004; McHale 2008). For instance, 20% of the candidate molecules fail during preclinical toxicology. An additional 10% fail due to pharmacokinetic limitations during preclinical assessment. Another 15% of drug development molecules fail due to safety and toxicity concerns during clinical studies. These high rates of failure in drug discovery and development require strategies to improve target identification, lead optimization, better clinical trial planning, identification of new disease targets, and the drug development process.

Genomic technology may enable the identification of toxicological failures as early as possible and may significantly reduce drug development costs associated with animal use, consumables, and infrastructure-related costs, as well as scientists' time. The technology can be used for cross disease applications for various unrelated diseases, organ system targets rather than candidate targets, molecular pathway targets rather than disease target, and prediction of likely variability in biology and populations.

Genomic and mRNA expression studies can be extremely powerful tools in the assessment of drug efficacy and toxicology which in turn can improve drug development process. Using the genomic approach, biological endpoints can be assessed instead of traditional pharmacological responses. mRNA profiling can assist in the validation and evaluation of drug targets, and organ targets sharing the same expression profile and pathways leading to efficacy and toxicity. By using multiple targets, mRNA-profiling makes it possible to identify toxicity in major organs such as liver, kidney, and vascular system, instead of utilizing traditional histopathology techniques which may not be as sensitive. By looking at specific mechanisms and structure-based toxicity all the organs that can serve as a target can be examined. One of the advantages of expression profiling is that it can also be used to study RNA regulation and as a surrogate for protein-expression studies.

Moreover, genomic biomarkers can be used to enrich early clinical studies with individuals most likely to respond to the drugs or least likely to develop adverse drug reactions. Failure to determine efficacy in a targeted subpopulation of patients who are positive or negative for certain biomarkers may prevent the need for larger clinical trials, which require significant investments in time and financial resources. In other words, genomic information has significant utility in identifying failing drug candidates as early as possible in drug discovery pipeline (Burczynski 2009; Ferrer-Dufol and Menao-Guillen 2009).

Another way to improve the drug development process is by developing new targets and using molecular pathways such as receptors and their underlying signal transduction. Genomic advances and the completion of the Human Genome Project have significantly increased the number of drug targets from 500 to 3,000. Pharmaceutical industries have currently developed drugs for 120 of the original 500 targets; hence, a large number of drug targets remain to be explored. Genetic markers can also be used to find new indications for drugs in development by investigating the effect of the most common genetic variations in the drug target (protein, receptor, channel, transporter, or enzyme) and correlating this with disease risk across a wide range of diseases. This will provide invaluable information regarding possible interindividual differences in drug response, efficacy, toxicity, adverse drug reactions, and pharmacokinetic endpoints.

Cell culture is a necessary part of the drug discovery process. Specific target drug and their polymorphic variants can be expressed in cell culture for screening purposes. In addition, animal models are extensively used in toxicological and efficacy studies as part of drug development. The genetics of the animals can be altered to create new disease model or for enhanced toxicological and efficacy studies. Similar to the Human Genome Project, various Animal Genome Projects are either underway or have been completed. For instance, the mouse is extensively used in drug research discovery and development. Hence, the Mouse Genome Project (http://www.ncbi.nlm.nih.gov/projects/genome/guide/mouse/;

Boguski 2002) can provide invaluable information regarding the relevance of diseases in mice to those in humans and preclinical results to those of clinical trial outcomes.

Briefly, genomic technology has the potential for identifying drug responders from nonresponders, populations at-risk for adverse reactions, and drug response outliers. Genomic technology can be used for new biomarker association studies, drug dose adjustments, selective recruitment of patients to enrich clinical trials with individuals carrying specific molecular characteristics, for differentiating new drugs from first-line therapy by targeting a subpopulation of patients who will benefit mostly from the therapy, and in the investigation of drug action/toxicity mechanisms and molecular pathways.

### 7.1.3 Examples of Technological Advances in Genomics Research

Technology is no longer a limiting factor in genomics research. The major barriers for widespread implementation of genomics in drug discovery, clinical trials, and clinical practice are related to DNA/RNA sample collection and storage guidelines, the amount of quality data needed for a test or group of biomarkers to be considered as required or recommended by the FDA, the number of samples needed for statistical validity and analyzes, and the regulatory challenges for clinical trials in a global research environment. Lack of education among scientists and clinicians is another barrier for efficient use of genomic information in drug development and clinical practice. Currently, these challenges are being addressed at ongoing interactions between numerous regulatory agencies, industries, academia, and interest groups. In the following, we discuss a number of examples from Affymetrix (http://www.affymetrix.com) and Illumina (http://www.illumina.com) to highlight technological advances made in this area.

Affymetrix and Illumina are leading manufacturers of microarray technology that enable the screening of thousands to millions of single

nucleotide polymorphisms (SNPs) and copy number variants (CNV) on a single chip. An example of the microarray technology is Affymetrix's GeneChip Microarray (Dalma-Weiszhausz et al. 2006; http://www.affymetrix.com), which can be used for both targeted genotyping and whole-genome association studies. The GeneChip Systems enable successful association studies with a targeted approach that offers flexible multiplexing from 3,000 to 20,000 SNPs per assay. The Affymetrix technology can also be used for Whole Genome Association (WGA) studies, covering 1.8 million genetic markers of SNPs and probes for the detection of CNV. The Affymetrix SNP Array includes large numbers of genetic variations on a single array providing maximum panel power and coverage of the genome on a single chip. Another example from Affymetrix is the DMET Plus Premier Pack (http://www.affymetrix.com), which contains a comprehensive group of pharmacogenetic markers for drug metabolism investigation. It includes approximately 2,000 drug metabolism markers related to 225 genes and provides coverage of common and rare SNPs, insertions, deletions, tri-alleles, and CNV.

Illumina also developed genotyping technologies that can assist with sequencing, whole-genome SNP genotyping, CNV analyzes, focused and custom SNP genotyping, linkage analyzes, biomarker validation, screening, molecular testing, and methylation profiling. For instance, Infinium HD BeadChips technology (http://www.illumina.com/pages.ilmn?ID=40) is capable of screening between 300,000 and 1,000,000 genetic markers for two to twelve samples per single chip. The Semi-Custom Human1M-Duo+ and HumanHap550-Quad+ products from Illumina allow for two to four samples per BeadChip to be screened for 60,000 SNPs per sample. Another example from Illumina includes Human-CytoSNP-12 which allows for screening 12 samples per bead for common cytogenetic abnormality studies. This BeadChip contains approximately 300,000 genetic markers associated with about 300 syndromes. In addition, technology is available from Illumina for genome-wide mRNA expression- and microRNA expression-profiling

and degraded RNA, such as those derived from formalin-fixed paraffin-embedded-tissue. Sequencing technology is also available from Illumina for genome sequencing, transcriptome analysis, gene regulation, epigenetic analysis, and multiplex sample sequencing for up to 12 samples per bead.

## 7.1.4 Examples of FDA Cleared Devices for Genetic Testing

Here, a number of FDA-cleared devices will be discussed to highlight both technological and regulatory advances made in this area. As first example, the Roche Amplichip CYP450 Test, which was introduced in 2005, was the first FDA-cleared pharmacogenetic test for the analysis of the CYP2D6 and CYP2C19 genes (http://www.amplichip.us; Hillman and Nikoloff 2009; de Leon et al. 2009). These genes are involved in the metabolism of many drugs in use on the market. The AmpliChip CYP450 Test determines a patient's genotype and can predict if a phenotype is a poor, intermediate, extensive, or ultrarapid metabolizer. The AmpliChip CYP450 can be used when planning the inclusion and exclusion criteria for clinical trials and in medical practice for use in dose adjustment. However, one should also note that other clinical information and the patient medical history should be also taken into account before making a decision for dose adjustments based on genetic tests.

Another example of an FDA-cleared device, the MammaPrint (Agendia, http://usa.agendia.com/en/mammaprint.html; van't Veer et al. 2002), is a gene expression profiling test to assess the risk of cancer recurrence in patients with breast cancer. MammaPrint, approved for marketing in 2007, is the first in vitro diagnostic multivariate index assay (IVDMIA) to receive FDA approval. The test is based on the expression of 70 genes in the tumor for determining the risk of breast cancer recurrence (Fig. 7.1, reproduced with permission from Agendia). If breast cancer is detected early, the tumor can be removed by surgical intervention, and most patients can fully recover. However, 30% of patients with breast cancer in stage I or II develop metastases within 5–10 years
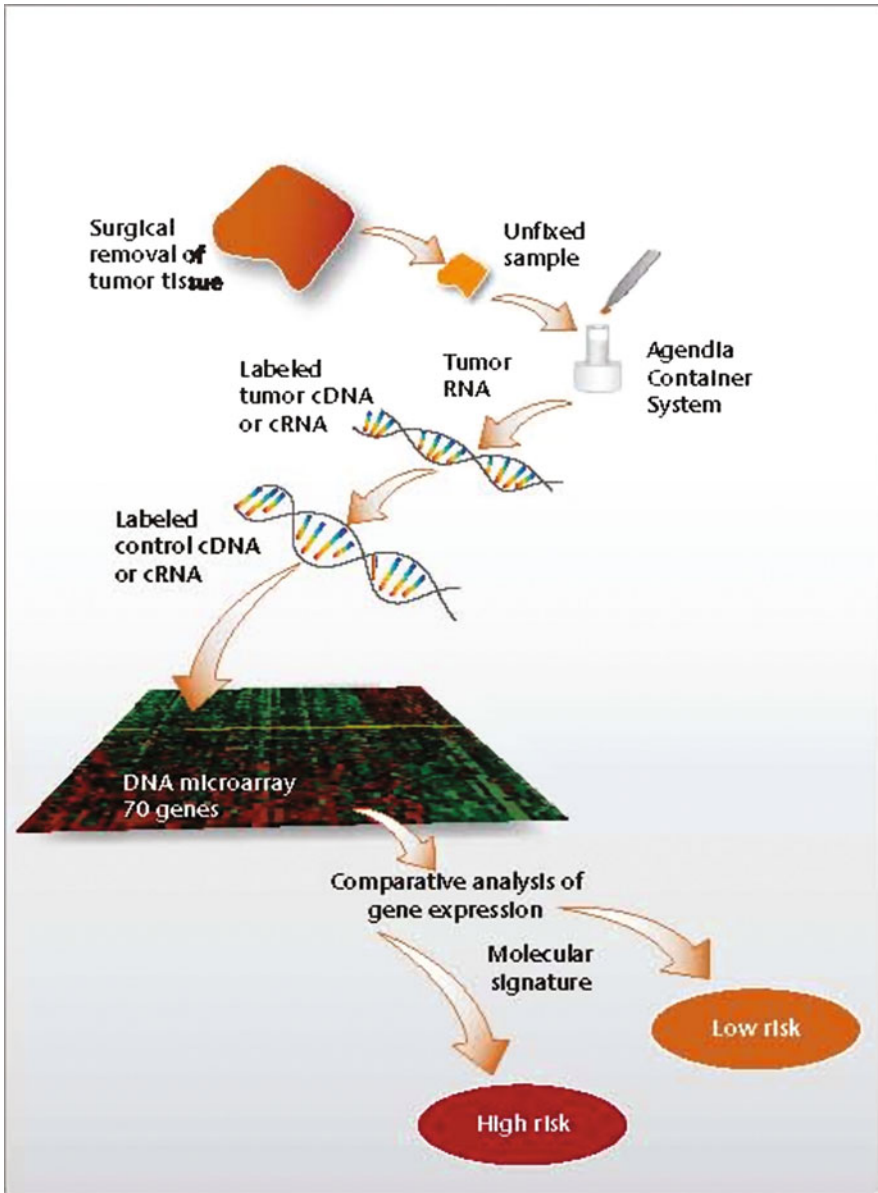
**Fig. 7.1** *MammaPrint: Classification of breast cancer tumor sample into high risk and low risk of recurrence of the disease* (http://usa.agendia.com/en/mammaprint.html). MammaPrint is an in vitro diagnostic multivariate index assay (IVDMIA) based on the expression of 70 genes in the tumor for determining the risk of breast cancer recurrence. The test helps to stratify tumors into high and low risk of relapse. Patients with high risk of relapse need systemic therapy. Reproduced with permission from Agendia

after surgery. The test helps to stratify tumors into high and low risk of relapse. Patients with high risk of relapse need systemic therapy. Before the MammaPrint test became available, it was not possible to accurately stratify patients, hence approximately 70% of the patients who would

not benefit from systemic therapy received it unnecessarily. In this group, adverse drug reactions could often have been eliminated if the tumors had been stratified to the low risk of relapse category. To maximize its clinical utility, one should also bear in mind that the MammaPrint

results are indicated for use by physicians as prognostic markers which should be used in combination with other clinical laboratory tests and data.

The list of FDA-approved genotyping kits also includes the Trugene HIV-1 test (Bayer) which is a sequence-based assay targeted at the protease and reverse transcriptase regions of the HIV-1 genome. These regions of the virus genome code for drug resistance against antiretroviral protease and reverse transcriptase inhibitors. When resistance develops, the patient's viral load can increase, worsening clinical prognosis, and eventually accelerating the development of drug-resistant viruses. Drug-resistant patients may be subjected to severe side effects of antiviral drugs despite having no hope of benefiting from drug therapy. The Trugene HIV-1 test permits early identification of drug-resistant viruses, and hence of identifying patients who will not benefit from antiviral therapy (http://www.research.bayer.com).

Another example from this series is the Invader UGT1A1 Molecular Assay (Genzyme), which is an in vitro diagnostic test that detects two polymorphisms in the UGT1A1 gene: the normal UGT1A1*1 allele and the mutation UGT1A1*28 allele in genomic DNA. The UGT1A1 enzyme is responsible for the metabolism of irinotecan, a drug used to treat metastatic colorectal cancer. The active metabolite of irinotecan is metabolized and deactivated by the UGT1A1 enzyme. UGT1A1 activity is diminished in individuals with genetic UGT1A1*28 polymorphism. Colorectal patients with reduced UGT1A1 activity are at significantly increased risk of developing severe neutropenia when treated with irinotecan (http://www.genzymegenetics.com). This test will help identify patients with a greater risk of developing irinotecan toxicity. In addition to approving the device, it is interesting to note that the FDA has recommended UGT1A1 testing before prescribing irinotecan, but stopped short of requiring the test for its prescription (http://www.fda.gov).

The PathVysion HER-2 DNA Probe Kit (Abbott), another example of an FDA approved devices, is designed to detect amplification of the HER-2/neu gene *via* fluorescence in situ hybridization (FISH) in formalin-fixed paraffin-embedded human breast cancer tissue specimens (http://www.pathvysion.com). The test results are intended for use in combination with other clinical and pathologic information used as prognostic factors in stage II, node-positive breast cancer patients. The test is also used to predict disease-free and overall survival in patients treated with adjuvant chemotherapy. The PathVysion HER-2 DNA test is one of the two tests required by the FDA as an aid in the assessment of patients who are candidates to receive Trastuzumab therapy (http://www.fda.gov).

### 7.1.5 Examples of FDA "Required" or "Recommended" Genetic Biomarkers

Here, we discuss a number of genetic biomarkers that are required or recommended by FDA for their testing in drug therapy. The FDA has generated a "Table of Valid Genomic Biomarkers in the Context of Approved Drug Labels" on which tests are indicated as "required," "recommended," or "for information only" (http://www.fda.gov; Moridani 2009). In addition, the FDA has issued a document entitled "Guidance for Industry Pharmacogenomic Data Submissions" to encourage research and voluntary data submissions from pharmaceutical industry (http://www.fda.gov/cder/guidance/6400fnl.pdf). The following examples highlight the regulatory advancements in the use of genomics information in guiding drug selection or dose adjustment.

The "required" tests are indicated for identifying potential responders (http://www.fda.gov; Moridani 2009). The tests are required because drugs are shown to have an enhanced efficacy in the subpopulation of patients who tested positive for the biomarker. The FDA's required tests provide information about patients infected with CCR5-tropic HIV-1, EGFR-positive colorectal cancer, Her2/neu-positive breast cancer, and Philadelphia chromosome-positive acute lymphoblastic leukemia (Ph+ ALL) with resistance or intolerance to prior therapy. The above four "required" tests are approved for the

following drugs: Maraviroc (CCR5-tropic HIV-1), Cetuximab (colorectal cancer), Trastuzumab (breast cancer), and Dasatinib (Ph+ ALL), respectively. Required tests are currently used for drug selection and identification of responders; all in the area of cancers and infectious disease.

The FDA has also indicated a number of tests as "Recommended" Tests, which assist with dose selection/adjustment to prevent a drug's severe toxicities/side effects and/or to enhance a drug's efficacy, but it stopped short of requiring them prior to drug prescription. The recommended biomarker tests include: protein C deficiency, CYP2C9 and VKORC1 variants (for Warfarin), G6PD deficiency (Rasburicase and Dapsone), HLA-B*1502 (Carbamazepine), LDL receptor deficiency or mutation testing (Atorvastatin), HLA-B*5701 (Abacavir), TPMT (Azathioprine, Thioguanine, and Mercaptopurine), UGT1A1 (Irinotecan), and urea cycle disorder deficiency (for Valproic acid, Sodium Phenylacetate, Sodium Benzoate, and Sodium Phenylbutyrate). LDL receptor deficiency or mutation testing is the only test in this category that is recommended to enhance efficacy through dose adjustment for Atorvastatin, whereas the rest of the listed recommended tests serve to reduce the incidence and severity of drug toxicity.

It is interesting to note that recommended tests are commonly performed for dose selection/adjustment. Currently, they have no use in identifying responders from nonresponders. The tests are recommended because of the known association between the biomarkers, drug doses, and toxicity/efficacy, as observed in clinical studies. The tests are not on the FDA required test list because: (a) no prospective clinical studies have been undertaken to show that the utilization of such tests actually changes any clinical endpoint, (b) clinicians have other tests at their disposal to guide them in dose selection/adjustment (e.g. INR for warfarin therapy), and (c) physicians can use the presentation of toxicities or lack of clinical response to guide them for subsequent dose adjustments.

FDA also enlisted a third category of genetic biomarkers known as "for information only." Although the tests classified by FDA as "for information only" are valid genomic markers they require additional clinical evidence before elevating them to the FDA's recommended test or required test categories (http://www.fda.gov). There are many biomarkers and drugs are listed under this category. Examples of biomarkers in this category include: C-KIT expression, deletion of chromosome 5q, EGFR expression, G6PD deficiency, Ph+ chromosome responders, PML/RAR alpha fusion gene (retinoic acid receptor responders and nonresponders), and variants of drug metabolizing enzymes CYP2C19, CYP2C9, CYP2D6, DPD, UGT1A1, and NAT (http://www.fda.gov). These biomarkers may find utilization in identifying responders from nonresponders or in dose selection/adjustment to enhance drug efficacy and safety. As new clinical information becomes available, some of these biomarkers may be recategorized as required tests or recommended tests.

### 7.1.6  Concluding Remarks

The Human Genome Project created significant excitement about using genomics and expression-profiling information in drug design, discovery, and development by identifying new drug targets and better tools for safety and efficacy studies in preclinical and clinical stages of drug development. Genomic information can also be useful in clinical practice and in planning clinical trials by aiding in the identification of responders and nonresponders, the prediction of adverse drug reactions, dose optimization, risk assessment in disease predisposition, and prognosis. However, it should be noted that genomic information must be used in connection with patients' medical history and not as a replacement for medical judgment. As with other tests, it too has limitations. Some of these limitations can be overcome by using proteomics and metabonomics, which will be discussed in the following subsections.

## 7.2 Proteomics in Drug Development

In recent years, the growing interest in elucidating the "organization and dynamics of the metabolic, signaling and regulatory networks through which the life of the cell is transacted" (Anderson et al. 2000) has spawned powerful proteomic technologies that now make it possible "to generate quantitative protein expression data on a scale and sensitivity comparable to that achieved at the genetic level" (Anderson et al. 2000). With the era of molecular medicine now upon us, these proteomics technologies and approaches are becoming increasingly important to the fields of drug discovery and drug development as we attempt to acquire a new level of knowledge about how a potential drug target is wired into the control circuitry of a complex cellular signaling network.

As we discuss in this section, the exquisite sensitivity and specificity of many of these new technologies, such as reverse-phase protein microarrays and laser capture microdissection (LCM), provide rich and detailed proteomic profiles comprising hundreds of phospho-protein end points, enabling tiny clinical specimens to undergo a thorough molecular analysis. Coupled with a new generation of tools to create, screen, test and evaluate targeted chemical compounds to modulate the activities of the cell's protein workforce, these technological advances are now creating unique opportunities to study and treat a wide range of human diseases with an efficacy hitherto unimagined.

Progress in proteomics technology is now being made at all levels of the disease detection and treatment spectrum, from the development of nanoparticles to detect incipient asymptomatic disease *via* the capture of disease-relevant protein peptides, to the wide-angle proteomic profiling of tiny clinical specimens to yield extensive molecular information on the activation states of potential drug targets.

In this section, we present an overview of a number of key proteomics technologies and conceptual advances germane to the fields of drug discovery and development. We begin with a consideration of some key recent technical developments, which together have resulted in a paradigm shift in our study of human disease at the level of cellular proteins. In the ensuing discussion, we outline some of the critical challenges in drug development and pharmacoproteomics today, and identify some novel ideas in the development of molecular-targeted regimens that offer promise in addressing some of those challenges.

### 7.2.1 Recent Advances in Serum Proteomics and the Promise of Early Disease Detection

The study of the human plasma proteome is now assuming an ever greater importance in the detection and treatment of disease, and is thought to hold the key to a revolution in disease diagnosis and therapeutic monitoring (Anderson and Anderson 2002). Indeed, since plasma continually perfuses the body's tissues, it is thought to contain most, if not all, human proteins (at least in fragment form) (Araujo et al. 2008) and represents the largest and deepest version of the human proteome present in any clinical sample (Anderson and Anderson 2002), thereby supplying the richest and most detailed source of information about the physiological state of the body. For this reason, plasma (or its close cognate, serum) has a pivotal role to play in early disease detection, since abnormal physiological states are expected to leave some specific fingerprint in the composition of circulating proteins (Anderson 2005) in the blood, so that the onset of disease may be detected by the altered presence or abundance of the constituent molecular species in serum (Tirumalai et al. 2003). The early detection of diseases such as cancer, which may be asymptomatic until an advanced and often incurable stage, holds the promise of improved clinical outcomes, with an associated reduction in disease related mortality and morbidity (Diamandis and van der Merwe 2005).

One of the great complexities of the serum proteome, however, is its extraordinarily wide dynamic concentration range, with more than

ten orders of magnitude of concentration separating the high-abundance resident proteins such as albumin from the rarest proteins now detected clinically (Tirumalai et al. 2003). It is critical to appreciate that the pathophysiological state of the body's tissues is predominantly reflected in the low molecular weight (LMW) and low-abundance (LA) region of the serum proteome which contains the low-level tissue leakage and active secretion of a mixture of small intact proteins and proteolytic fragments of large proteins. Consequently, these LMW/LA protein markers, or "biomarkers," have become the focus of the experimental and clinical quests for diagnostic or prognostic information.

Owing to these technical and analytical challenges, early attempts to characterize this LMW/LA region of the serum proteome involved a separation process (using affinity methods, for example (Tirumalai et al. 2003)) whereby the high abundance, high molecular mass proteins such as albumin, thyroglobulin, and immunoglobulins were removed from the serum sample in order to isolate the LMW/LA region of interest for subsequent analysis and study. This approach was based on the assumption that the small protein fragments exist in a free, uncomplexed state. However, it is now becoming apparent that large and relatively abundant proteins such as albumin can act as carrier proteins within the blood, binding a range of physiologically important molecules such as hormones, cytokines, and lipoproteins (Tirumalai et al. 2003) along with a spectrum of enzymatically generated and proteolytically clipped protein fragments (Petricoin and Liotta 2004). Therefore, discarding the high molecular mass portion of a serum sample almost certainly means dispensing with much of the protein complement germane to the study of disease.

Now at the dawn of a new era in molecular diagnostics, with the urgent need to discover novel biomarkers that are useful for disease diagnosis, mathematical modeling and analysis (see (Araujo et al. 2008) and references therein) have spawned an intense interest in the concept of creating nanoscale harvesting particles which could act as even more efficient harvesters of disease-related biomarkers than natural harvesters such as albumin. Indeed, the design and development of such "nanoharvesters" are currently well underway. Luchini et al. (2008), for example, have introduced an affinity bait molecule into N-isopropylacrylamide to produce a "smart" nanoscale hydrogel particle that performs three independent functions in one step, in solution: (a) molecular size sieving, (b) affinity capture of all solution-phase target molecules, and (c) complete protection of the sequestered proteins and peptides from enzymatic degradation. This new technology represents a unique and rapid method for blood-derived biomarker isolation and analysis.

These technological developments presage a future in which patients could potentially be screened for various early-stage (and as yet asymptomatic) diseases such as cancer with an out-patient infusion of biocompatible nanoparticles (Geho et al. 2007). The infused particles with their intrinsic "barcode" (Geho et al. 2007) could later be sorted from a blood sample, with their molecular content subsequently extracted and identified using mass spectrometry-based tools. Should this screening procedure reveal a biomarker signature associated with a high probability of a particular early-stage cancer, for example, subsequent clinical procedures could then be used to identify any atypical mass or lesion in the organ of interest if it exists, and to procure a biopsy sample for further analysis. Thus, this nanotechnology-based early-detection field is beginning to open up possibilities for the early detection of curable disease, rather than simply better detection of advanced disease (Araujo et al. 2008). See references (Geho et al. 2007; Liotta and Petricoin 2008) for further details on these exciting possibilities.

As elaborated in the sections to follow, we can envision a future in which such a biopsy sample could be subjected to further processing and analysis *via* the various sensitive and powerful proteomics technologies available today, in order to gain insight into the function of activated signaling pathways in the procured cells, thereby developing a rational basis for devising an individualized molecular-targeted therapeutic regimen.

## 7.2.2 New Developments in the Proteomic Profiling of Patient Tissue Samples

In the context of cancer drug development in particular, it is widely recognized that each patient's tumor is unique with its own set of pathogenic molecular derangements (Araujo et al. 2007a). While individualized therapeutic strategies have been used in medicine for quite some time (Wulfkuhle et al. 2006), an ever increasing armamentarium of molecular-targeted anticancer drugs is becoming available for clinical use is generating a pressing need to develop new techniques for accurately identifying those patients who will derive the greatest benefit from a given drug. It is important to note, in this connection, that while tumors of the same type often display genetic variation from patient to patient, they often share similarities at the level of protein signaling pathways.

Recent technical innovations such as LCM and reverse phase protein microarrays (RPAs), in particular, now make it possible to segregate pure populations of tumor cells from stromal tissue obtained from small patient biopsies, and to survey the expression levels and activation states of hundreds of signaling proteins within these cell populations (Araujo et al. 2007a). This is a vitally important advance in pursuing the goal of individualizing cancer therapies in view of the fact that signaling proteins are, themselves, the targets of many of the new anticancer drugs currently available or under development.

The advantages of the RPA profiling technology are many. RPAs do not require direct labeling of the sample analyte, which often destroys the epitope that is being detected, and do not utilize a two-site antibody sandwich, which often limits the repertoire of analytes that can be effectively measured. Therefore, there is no experimental variability introduced due to analyte labeling yield, sandwich antibody affinity mismatch, or epitope masking (Liotta et al. 2003). In addition, the RPA array format is capable of extremely sensitive detection, with detection levels approaching attogram amounts of a given analyte (Paweletz et al. 2001). Third-generation amplification chemistries now available can be used for highly sensitive detection (King et al. 1997). For example, coupling the detection antibody with highly sensitive tyramide-based avidin/biotin signal amplification systems combined with quantum dots can yield detection sensitivities down to fewer than 1,000 molecules/spot. Using commercially available automated equipment, RPAs exhibit excellent within-run and between-run analytical precision (3–10% coefficient of variance) (Paweletz et al. 2001).

## 7.2.3 Challenges Ahead for Individualized Molecular Medicine

A small handful of outstanding successes points to the potential for a major revolution in the treatment of human disease in the area of molecular-targeted therapeutics. The extraordinary success of the small-molecule ABL kinase inhibitor imatinib mesylate (Gleevec/Novartis) in the treatment of chronic myelogenous leukemia (CML), for example, has made this targeted therapy the "poster child" for the concept that strict dependency on certain key oncogenic mutations could apply to a wide range of spontaneously occurring human cancers (Evan 2006). More recently, somatic mutations within the kinase domain of the epidermal growth factor receptor (EGFR) have emerged as important predictors of responsiveness to the EGFR tyrosine kinase inhibitor gefitinib (Iressa/AstraZeneca) for patients with nonsmall-cell lung cancer (NSCLC) (Lynch et al. 2004). Even the problem of tumor recurrence in these responsive NSCLC and CML tumor types reveals that the majority of relapses involve resistance mutations in the target kinase, rather than an altogether novel oncogenic expedient, which suggests that room for evolutionary maneuver in surviving tumor cells is highly constrained, even in the face of genomic instability (Araujo et al. 2007a).

With protein kinases now representing a major focus of today's drug discovery efforts,

a key question now looms for the field of cancer drug development: How can the abundance of proteomic data – now made available *via* the technological advances described in Sect. 7.2.2 – be used to reveal an effective therapeutic strategy for a given patient's tumor, with its own unique molecular profile? It is tempting to believe that these rich and information-dense representations of protein signaling are able, by themselves, to provide vital clues on the nature of the signaling mechanisms underpinning the disease at hand – pointing to hyperactive/underactive pathways, ectopic expression of proteins, presence or absence of an important feedback mechanism, or some other key feature.

However, in view of the modest progress in drug development and clinical implementation over recent years, it is becoming increasingly apparent that this level of knowledge may not be enough to understand the function of a proposed therapeutic target within the context of the cellular network. Indeed, the static patterns revealed in proteomic profiles, no matter how rich and detailed, are not a proxy for the cellular mechanisms regulated by the profiled molecules (Araujo et al. 2007a). A number of insightful articles have entered the literature in recent years, highlighting the many advanced computational approaches becoming available to parse high-dimensional "omic" data in order to discern key features of the underlying signaling networks and processes (Janes and Lauffenburger 2006), as well as more mechanistic and predictive "simple–complexity"-based modeling approaches that focus on overarching control mechanisms orchestrating cellular signal transduction (Araujo and Liotta 2006; Araujo et al. 2007a, b). These later approaches, in particular, have been foundational in introducing the drug discovery and development communities to the crucial concept that a protein's suitability as a therapeutic target is determined largely by the nature of its contribution to the signaling network's control circuitry, rather than by its aberrant activity per se (Araujo et al. 2007b).

Beyond the problem of identifying effective techniques to selectively modulate aberrantly activated signaling pathways with target-based drugs, toxicity remains an additional challenge (Geho et al. 2005). The narrow "therapeutic index" of much of the existing pharmacopeia means that only a very restricted dosing range produces therapeutic benefit with tolerable toxicity, with doses outside of this range producing either unacceptable toxicity or insufficient therapeutic benefit (Araujo et al. 2004). Recent theoretical studies of intracellular signaling have focused on a new concept in the treatment of disease – "network-targeted" combination therapy – which holds the promise of circumventing many of these shortcomings. In this new approach, the emphasis is on distributing drug delivery among a multiplicity of targets, rather than concentrating the therapeutic intervention at a single signaling molecule (Araujo et al. 2004; Araujo et al. 2005; Araujo et al. 2007a) (Fig. 7.2).

Combination therapies afford at least five key benefits in comparison with monotherapies:

1. For a given drug dose at each molecular target, the attenuation of downstream signals is significantly enhanced when a multiplicity of targets is chosen rather than a single target, particularly when the nodes are serially linked (Araujo et al. 2005) (see Fig. 7.2).

2. The desired response may be produced with lower doses of the necessary agent when multiple nodes are targeted, rather than a single node in isolation (Araujo et al. 2004; Araujo et al. 2005). Not only could this property reduce the harmful side effects of drugs in current use, but it may impart clinical applicability to a huge compendium of agents which, of themselves, are too toxic at their therapeutically effective doses. This new concept may therefore spawn an enormous new repertoire of molecular-targeted drugs for clinical evaluation.

3. The location of target nodes in relation to the local architecture of the signaling network has important implications for the effectiveness of the therapy (Araujo et al. 2004; Araujo et al. 2007a, b). Nodes embedded in negative feedback loops may represent very poor targets in some cases (Sauro and Kholodenko 2004), for
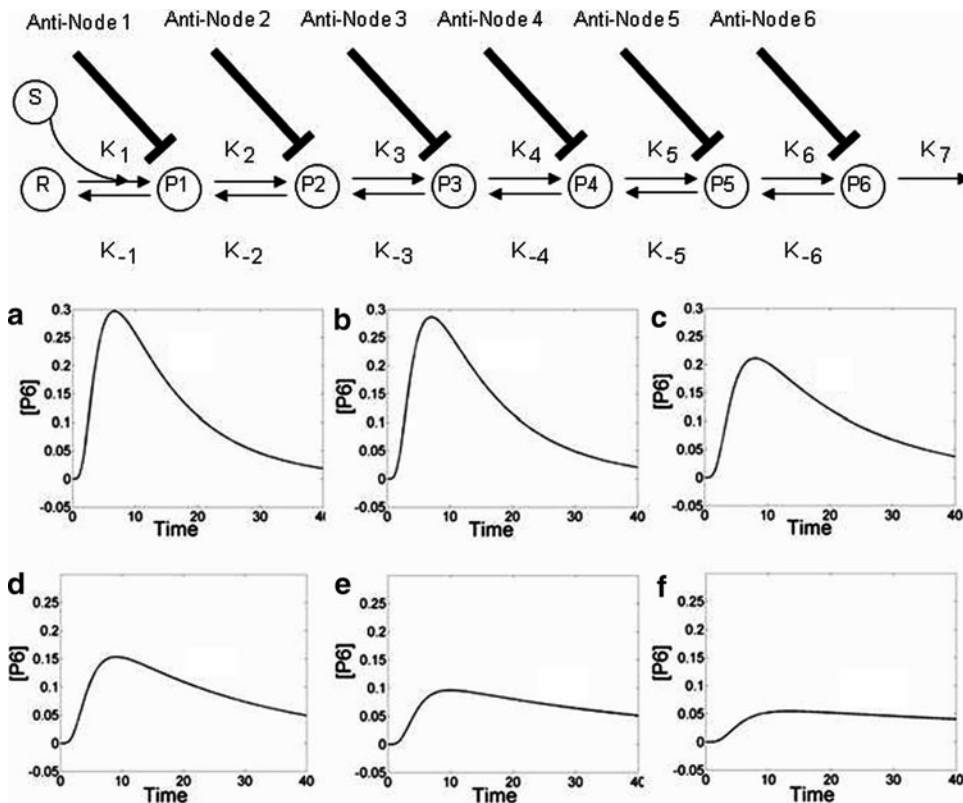
**Fig. 7.2** *(adapted from Araujo et al.* 2004*): A model of the effects of network-targeted combination therapy, applied to a simple stereotypical signaling cascade.* Graphs depict the temporal evolution of a biochemical signal as it progresses through a six-node network comprising proteins P1 through P6, in response to the binding of a stimulus, S, to a cell-surface receptor, R. (**a**): the unperturbed network (no targeted inhibitors); (**b**) node 1 inhibited with a dose of IC50; (**c**) nodes 1 and 2 each inhibited simultaneously with doses of IC50; (**d**) nodes 1 through 3 each inhibited with doses of IC50; (**e**) nodes 1 through 4 each inhibited with doses of IC50; (**f**) nodes 1 through 6 each inhibited with doses of IC50. As shown, as more nodes are added to the treatment regimen, the output signal progressively diminishes. Note that the biochemical signal under consideration (represented on the vertical axis, [P6]) is the activation level of the most downstream protein, P6 (see Araujo et al. 2004 for modeling equations, parameters, and further details on the mathematical model)

example, since the automatic control characteristics of this signaling motif have the tendency to constrain the system response to follow a defined set point and resist the effects of any disturbances. Moreover, recent theoretical studies (Araujo et al. 2004) provide circumstantial evidence that receptors, being at the most upstream location in a signaling cascade, may represent quite poor targets. This is an important consideration in view of the number of drugs developed to target receptors (Iressa, Herceptin, etc.). On the other hand, receptors may represent a less complex therapeutic target in comparison with downstream nodes embedded in more complicated network architectures involving interpathway cross talk and feedback loops (Araujo et al. 2004).

4. One of the consequences of the markedly nonlinear relationships between kinetic parameters and concentrations of signaling proteins is the nonadditive attenuation of signals for a multiplicity of target nodes, in comparison with targeting the same nodes individually (Araujo et al. 2005). Signal attenuation may therefore be synergistic, producing an

extra inhibition that is not due to an extra dose of drug. We may therefore view this bonus inhibition as entirely nontoxic (Geho et al. 2005).

5. As demonstrated recently by mathematical modeling (Araujo et al. 2007a), one of the most promising aspects of network-targeted combination therapies is their potential to combat the problem of tumor resistance. A combination of inhibitors that target a sensitive signaling pathway at multiple nodes reduces the necessity for each individual drug to exert a significant influence on its own target. In this way, a more robust and potent regimen results, which reduces the opportunities for resistant clones to emerge from within the tumor mass (Araujo et al. 2007a).

## 7.2.4 Concluding Remarks

As we have briefly outlined in this subchapter, the promise of pharmacoproteomics for the integrated coupling of diagnosis with therapeutic intervention represents a new paradigm, and suggests new directions for the development and application of molecular-targeted therapeutics in the future. This expanding field is surging with potential, with innovations in molecular network analysis, risk stratification, early disease detection, development of individualized targeted therapies and posttherapy monitoring.

## 7.3 Metabonomics in Drug Development

Systems biology is usually viewed as a way of integrating data over many aspects and levels of molecular biology, the main levels of which are genomics, transcriptomics, proteomics, and metabonomics (also called metabolomics), i.e., multivariate analyzes at the genome, gene transcription, protein and metabolite levels, respectively. Metabonomics, in the context of systems biology, focuses on understanding the biochemical effects of a systematic change on a biological system brought about by an intervention, whether it is the result of a biological stimulus, genetic manipulation, or drug intervention (Nicholson and Lindon 2008). Such systematic metabolic profiling and their temporal changes caused by lifestyle, environment, genetic or xenobiotic effects are usually achieved through the analysis of biofluids and tissues by nuclear magnetic resonance (NMR) spectroscopy and mass spectrometry (MS), and the spectral data interpreted using chemometric techniques (Lindon et al. 2006).

Metabonomics is particularly important in systems biology because it provides a "top-down" approach that gives an integrated view of the biochemistry as opposed to "bottom-up" studies where the effects of an individual gene, or groups of genes, are investigated (Nicholson and Lindon 2008). Relating genomic and transcriptomic data to actual observed biological endpoints can be challenging because the linked effects between specific genes, the possibility of adaptive effects in the organism, and complex highly nonlinear interactions between gene expression and environmental factors can affect risk. In addition, at present, proteomics methods can be somewhat labor-intensive and not high-throughput, although major advances as detailed in this chapter are being made. However, it is advantageous to integrate all these technologies despite their different levels of biological control and their very different temporal effects. It is also necessary to recognize that pharmacological or toxicological effects at the metabonomic level can induce adaptation effects at the proteomic or transcriptomic levels. The environment and lifestyle of the organism also has a large effect at all stages of molecular biology, and this variation has to be considered and integrated into any analysis. A major input comes from the symbiotic gut microflora that have their own ecosystem of diverse metabolic processes that interact with the host and for which, in many cases, the genomes are not known.

Here we describe the main analytical technologies that are involved in the analysis of metabonomic samples and the role that metabonomics

can play in the preclinical and clinical regimes in drug development. We also summarize the important emerging fields of pharmacometabonomics and metabolic phenotyping since these will be of importance for personalized healthcare and the understanding of health risk factors.

## 7.3.1 Analytical Techniques

The analysis of biological samples for metabonomic studies have been predominantly carried out using proton ($^1$H) NMR spectroscopy, but increasingly, MS coupled to a separation system such as gas chromatography (GC), high-performance liquid-chromatography (HPLC), or ultra-performance liquid-chromatography (UPLC), is being used, albeit often in a more targeted approach. It is also possible to hyphenate these techniques for accurate metabolite identification; the most general of these is HPLC-NMR-MS, in which the eluting HPLC peak is split, with parallel analysis by directly coupled NMR and MS techniques.

NMR spectroscopy is a nondestructive technique that is highly effective for metabolic profiling and for metabolite identification (Claridge 2008). It is not as sensitive as MS but recent developments in cryoprobe technology have increased the sensitivity by up to a factor of 5 by cooling the detector coil and preamplifier to ~20 K, through a reduction of thermal noise in the electronics of the spectrometer. Two-dimensional (2-D) NMR spectroscopy can also enhance information recovery and aid in metabolite discovery by increasing signal dispersion and revealing the connectivities between signals. 2-D J-resolved (JRES) experiments have proved very useful by which peaks from macromolecules are attenuated, and the projection of the 2-D spectrum on to the chemical-shift axis yields a fingerprint of peaks from only the most highly mobile small molecules, with the added benefit that all of the spin-coupling peak multiplicities are removed to give single peaks for each proton. Data acquisition is also possible on intact tissue samples using high resolution magic-angle-spinning (MAS) NMR spectroscopy. The

tissue is spun rapidly at an angle of 54.7° relative to the applied magnetic field, which reduces many effects of line broadening. Thus an integrated physiological interpretation of both biofluid and tissue data can be made. In order to analyze all the different types of biological samples, specific NMR pulse sequences are used. Observed peak intensities can be edited on the basis of their molecular diffusion coefficients (to attenuate small molecule peaks) or on NMR relaxation times (to attenuate large molecule peaks).

Examples of some of these different types of NMR spectroscopic analysis for human blood plasma are shown in Fig. 7.3. This gives the standard one-dimensional $^1$H NMR spectrum with the water peak suppressed (Fig. 7.3a), a $^1$H NMR spectrum acquired using the CPMG pulse sequence which causes attenuation of peaks from macromolecules (Fig. 7.3b), and a spectrum edited on the basis of molecular diffusion coefficients (Fig. 7.3c), which removes peaks from fast diffusing small molecule metabolites, thus being complementary to the CPMG result. Figure 7.3d shows a skyline projection of a 2-D JRES spectrum.

MS is generally coupled to HPLC for metabonomic studies on biofluids, and both positive and negative ion mode MS are usually acquired. Tandem MS/MS experiments can also be performed in which fragments ions can be further analyzed to provide more structural information. UPLC which operates at around 12,000 psi with a smaller 1.7 μm reversed-phase packing material gives better chromatographic peak resolution than HPLC, with a ~ tenfold increase in speed and three- to fivefold increase in sensitivity. This reduces the problem of ion suppression in the MS from coeluting peaks.

MS and NMR spectroscopy are complementary analytical tools for metabonomic analysis and combining both techniques provides the optimal means to obtain full molecular characterization. In order to analyze the complex data sets that are produced *via* these methods, a number of chemometric tools have been developed and applied. Unsupervised methods such as principal components analysis (PCA) simply look for
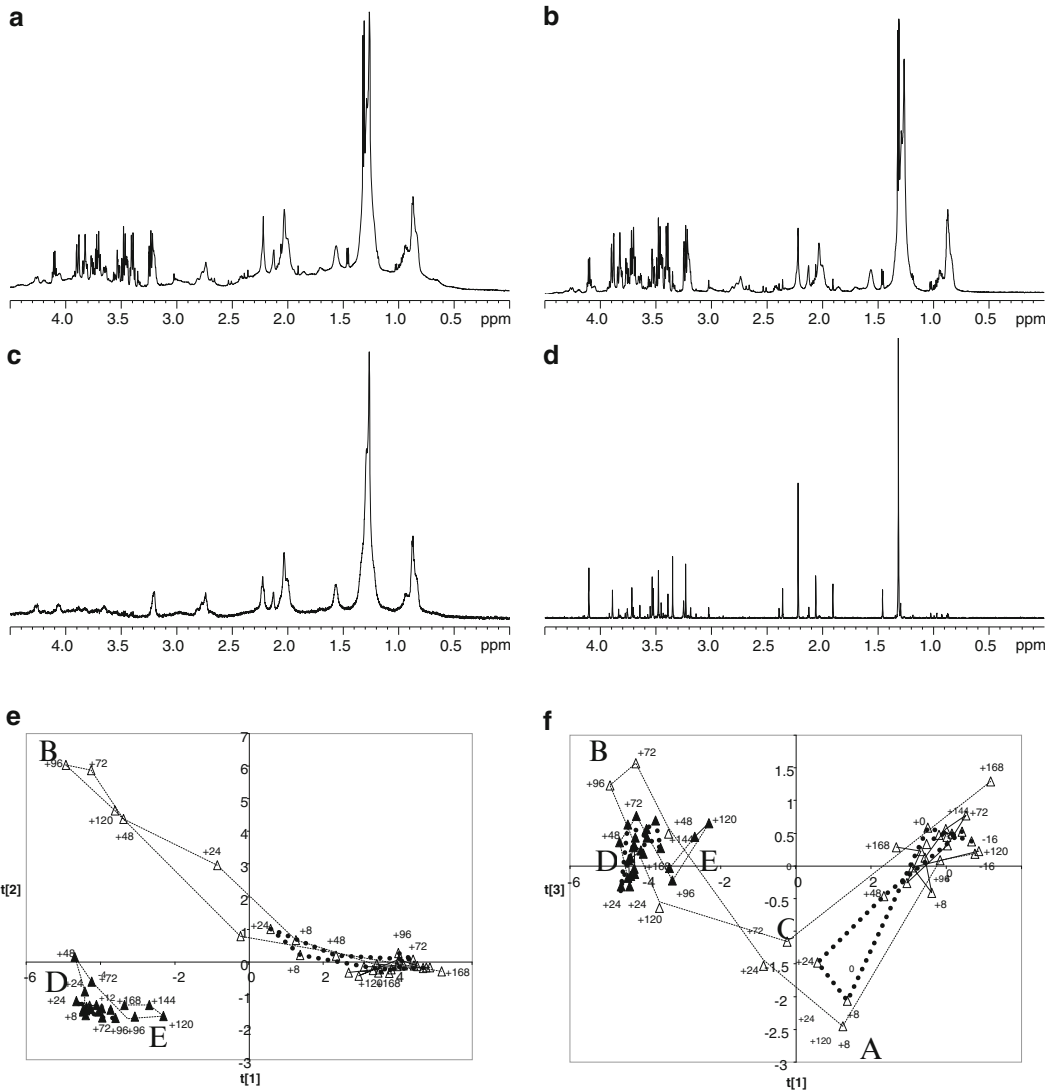
**Fig. 7.3** (**a**) Standard one-dimensional ¹H NMR spectrum of human blood plasma with the water peak suppressed, (**b**) a spin-echo ¹H NMR spectrum of the same sample acquired using the Carr-Purcell-Meiboom-Gill (CPMG) pulse sequence which causes attenuation of peaks from macromolecules, (**c**) a ¹H spectrum of the same sample edited on the basis of molecular diffusion coefficients which removes peaks from fast diffusing small molecule metabolites, (**d**) the skyline projection of a two-dimensional spectrum acquired using the J-resolved pulse sequence. In its two-dimensional form, this spectrum shows NMR chemical shifts and spin-coupling patterns in orthogonal directions. When the two-dimensional spectrum is projected on to the chemical shift axis, it results in a single line for each multi-

plet, from only the most mobile metabolites, (**e**) mean trajectories of PC1 vs. PC2 scores for NMR spectra from urines from hydrazine-treated rats and mice and (**f**) mean trajectories of PC1 vs. PC3 scores for urines from hydrazine-treated rats and mice illustrating the different magnitudes and direction of metabolic effect in the rat and mouse. Key: filled triangle, mice; open triangle, rats; full line, control group; broken line, high dose (mice 250 mg/kg, rats 90 mg/kg); thick dotted line, low dose groups (mice 100 mg/kg, rats 30 mg/kg). Key points of inflection in the trajectories are labeled **a–e** for the high dose rat and mouse. Parts (**e**) and (**f**) reproduced with permission from Bollard et al. (2005)

clusters or patterns of similarity in the data to give an understanding of the relationships between samples and sample class. PCA expresses the variation in a data set using a smaller number of factors or principal components. Using "supervised" methods such as partial least squares (PLS), multiparametric data sets can be modeled so that a class or other response variable of separate samples (a "validation set") can be predicted based on a series of mathematical models derived from the original data or "training set" (Lindon et al. 2001). PLS relates a data matrix of spectral intensity values to a matrix containing measurements of a response for those samples. PLS can show how the time axis can influence a data set, which is useful when analyzing the progression of a disease. It can also be combined with discriminant analysis (DA) to establish the optimal position to place a discriminant surface which separates classes.

New statistical spectroscopic methods for improving structural identification of metabolites have been established. Statistical total correlation spectroscopy (STOCSY) takes advantage of the colinearity of the intensity variables for the multiple peaks of a metabolite whose concentration varies across a set of NMR spectra, so that correlations from NMR peaks belonging to the same molecule can be identified (Cloarec et al. 2005). The method calculates statistical correlation matrices for individual spectral data points corresponding to data points of interest, and plots the correlation coefficients as a pseudo-NMR spectrum, allowing all peaks from the same molecule to be identified. An extension of STOCSY, statistical heterospectroscopy (SHY) allows for the coanalysis of data sets obtained by both NMR spectroscopy and MS. Chemical-shift data from NMR and $m/z$ data from MS can be cross-correlated. This has been demonstrated using 600 MHz ^{1}H NMR and UPLC-TOF-MS data acquired from the analysis of rat urine in control and hydrazine (a model liver toxin) treated animals (Wilson et al. 2005; Crockford et al. 2006). This approach has the potential to correlate data from any two spectroscopic or indeed other multivariate analytical measurements such as transcriptomics.

## 7.3.2 Preclinical Drug Development

The selection of candidate drugs for clinical development remains one of the greatest challenges facing the pharmaceutical industry. One key factor that has to be achieved is the absence of drug adverse effects. Metabonomics has a recognized role in toxicity assessment and can be used for definition of the metabolic characteristics of normal animals and the classification of the target organ or region of toxicity, the biochemical mechanism of that toxin, the identification of combination biomarkers of toxic effect and evaluation of the time-course of the effect, e.g. the onset, evolution, and regression of toxicity. There have been many studies using ^{1}H NMR spectroscopy of biofluids to characterize drug toxicity going back to the 1980s, and the role of metabonomics and magnetic resonance in toxicological evaluation of drugs has been comprehensively reviewed (Lindon et al. 2004).

The usefulness of metabonomics for the evaluation of xenobiotic toxicity effects was comprehensively explored by the COMET group (Consortium on Metabonomics in Toxicology), formed between five pharmaceutical companies and Imperial College, London (Lindon et al. 2003) to develop methodologies for the acquisition and evaluation of metabonomic data generated using ^{1}H NMR spectroscopy of urine and blood serum from rats and mice for preclinical toxicological screening of candidate drugs. Predictive models of toxicity were constructed using NMR-based metabonomic data (around 35,000 NMR spectra), taking into account the whole time course of toxicity. Databases of spectral and conventional results were generated for a wide range of model toxins and treatments (147 in total) and these served as the basis for successful computer-based expert systems for toxicity prediction (Lindon et al. 2005).

Some toxins were studied in both the mouse and the rat in order to evaluate species differences and examples of this are shown in Fig. 7.3e and f. PCAs based on urine ^{1}H NMR spectra from both mice and rats administered the liver toxin hydrazine are shown. Despite the much higher relative

dose used in the mice the mean metabolic trajectories for the mice are much less extensive than those for the rat (Bollard et al. 2005).

A follow-up project, COMET-2, is on-going with the aim of improved understanding of biochemical mechanisms of toxicity relevant to pharmaceutical development. Here, NMR spectroscopy, LC-MS, and *in vitro* and *in vivo* labeling studies are being carried out with the aim of determining the mechanisms of action of model toxic xenobiotics. One system that has been studied by COMET-2 is galactosamine hepatotoxicity since this shows high variation between animals and the mechanism of its effect is unknown (Coen et al. 2007).

Most studies have limited themselves to metabonomics but a few have attempted to integrate data from different -omics into a systems biology view. These include investigations of the liver toxicity of acetaminophen and Methapyrilene using both transcriptomics and metabonomics (Coen et al. 2004; Coen et al. 2007; Craig et al. 2006). So far, this is not usually done at the level of coanalyzing data from different -omics, but more usually at the level of defining altered metabolic pathways from the two studies, and then identifying commonality and unifying observations.

### 7.3.3 Clinical Studies

There are many studies using NMR-based metabonomics for probing the altered metabolic status in a wide variety of human diseases and most have been summarized and reviewed recently (Lindon et al. 2007). Many used only low numbers of subjects and while statistically valid connections have been made between NMR spectral profiles and disease, the discovery of real biomarkers of disease remains elusive and the biological relevance of metabolic differences is often not fully explained.

One area of application of NMR-based metabonomics that has already been used effectively in the clinic is the diagnosis of inborn errors of metabolism. Diabetes, Alzheimer's disease, osteoarthritis, and male infertility have also all been studied through NMR spectroscopic analysis of

plasma, cerebrospinal fluid, synovial fluid and seminal fluid, respectively. The analysis of urine has also been particularly insightful for the investigation of drug overdose, renal transplantation, and other various renal diseases. Some metabonomics studies have been carried out on tissue samples to examine prostate cancer, renal cell carcinoma, breast cancer, Duchenne muscular dystrophy, cardiac arrhythmia, and cardiac hypertrophy. Cancer metabonomic studies have however now progressed to serum analysis and subsequent diagnosis of epithelial ovarian cancer (Odunsi et al. 2005). Tissues themselves can be studied using HR-MAS NMR spectroscopy and published examples include prostate cancer, renal cell carcinoma, breast cancer and various brain tumors. One study that has attempted to fully coanalyze and integrate plasma data from metabonomics and proteomics has been the study of human prostate tumor xenografts in mice (Rantalainen et al. 2006).

Cardiovascular disease has been investigated for many years using $^1$H NMR spectroscopy of plasma or serum and there are many published examples concentrating on lipoprotein composition (Ala-Korpela 2008). The diagnosis of coronary artery disease based upon the metabolic profile in blood plasma has been attempted (Kirschenlohr et al. 2006) and conflicting results obtained. However, this type of study is fraught with the problem that most subjects are already on some form of drug therapy such as statin administration and this can confuse diagnostic findings unless taken into account as reported (Brindle et al. 2002).

### 7.3.4 Pharmacometabonomics and Personalized Healthcare

As personalized healthcare becomes more achievable, drug treatments will have to be tailored to an individual to achieve maximal efficacy and avoid adverse reactions. The subject of pharmacogenomics was established to base such decisions on a person's genome, investigating the genetic make-up of different individuals (their genetic polymorphisms) and their varying

abilities to handle pharmaceuticals both for their beneficial effects and for identifying adverse effects. However, this cannot provide information on lifestyle or symbiotic gut microfloral effects and an alternative approach to probe intersubject variability in response to drug treatment is to use metabolic profiling as demonstrated by the prediction of the metabolism and toxicity of a dosed substance, based solely on the analysis and modeling of a predose metabolic profile (Clayton et al. 2006). This approach, which has been termed "pharmacometabonomics," is sensitive to both the genetic and modifying environmental influences, including gut microfloral effects that determine the basal metabolic fingerprint of an individual, since these will also influence the outcome of a drug intervention. In this first exemplification, acetaminophen was administered to rats and a link was observed between the predose urinary metabolite profile and the variable extent of both the liver damage sustained after dosing and the pattern of xenobiotic metabolism. This concept has now been demonstrated in humans for the first time, and a key biomarker of acetaminophen metabolism was shown to be a human/gut microbial co-metabolite (Clayton et al. 2009). The potential of this approach for personalized healthcare is clear and ultimately adverse drug reactions could be avoided and drugs and dose levels targeted more effectively according to the metabolic characteristics of the individual. The possibility of stratifying patients as suitable or not for drug clinical trials also becomes evident.

## 7.3.5 Population-Wide Studies for Disease Risk Assessment

The incorporation of metabolic profiling components into large-scale human population studies such as biobanks or epidemiological cohorts is increasing, including retrospective analysis of samples. These large studies present practical and logistical challenges, but they are feasible, and metabonomics is well suited to characterizing the metabolic phenotypes of populations, being particularly relevant for high risk populations with a prevalence of pathological or pre-pathological conditions. These studies can allow insight into the prevalence of disease, and coanalysis of the metabolic profile with a range of factors such as diet, medication, and other lifestyle factors to elucidate risk levels is possible (Holmes et al. 2008). Using large-scale metabolic phenotyping from 17 populations in China, Japan, USA, and UK, geographic metabolic differences were shown to be greater than gender differences, and it was seen that even those populations that are genetically similar can be very dissimilar metabolically and also have different disease propensities. For example the Japanese and Chinese are genetically similar, but have different metabolic phenotypes, and their disease types are also different. Through pairwise comparisons across countries, a large variation in the metabolic phenotype was observed between Japanese subjects that live in Japan, and Japanese resident in the USA. In this study, novel urinary biomarkers related to blood pressure were also identified that indicated a link between diet and gut microbial activity. This study therefore showed how environmental factors such as lifestyle and diet can have a large affect on the incidence of disease, irrespective of genetics. This also has implications regarding the targeting of therapies to appropriate populations.

## 7.3.6 Concluding Remarks

In summary, it is apparent that metabonomics will have significant future influence on the drug development and discovery process. Metabonomic analysis has a high level of biological reproducibility, high throughput, and low cost per sample and analyte. In addition biofluid analysis is minimally invasive, and biomarkers are closely identifiable with real biological endpoints. A further advantage of metabonomics is that interspecies comparison of metabolic biomarkers is potentially easier than for transcriptomics or proteomics. Against this, some problems have been highlighted with the multiple analytical technologies (sensitivity and dynamic range) and the complexity of the data sets. Continuing developments

of these techniques will overcome these issues. Currently standards for data and operations are being set up, but there is still the need for regulatory agencies to be trained in the data interpretation and for more well trained practitioners.

The ultimate goal of systems biology must be the integration of data acquired from living organisms at the genomic, protein, and metabolite levels. Transcriptomics, proteomics and, metabonomics will all play an important role in this. Through understanding the total biology of an organism *via* the combination of these -omics technologies and taking into account the environmental, genetic, and temporal effects on them, an improved understanding of the causes and progression of human diseases will be achieved. With the twenty-first century goal of personalized healthcare, the improved design and development of new and better targeted pharmaceuticals should also be attainable.

## 7.4 Considerations for the Application of the -Omics in Drug Development

In this section, we discuss how the technologies presented can be incorporated into nonclinical and clinical investigations. From a practical point of view, we also discuss what we should consider when planning clinical trial protocols, informed consent, and handling and storing of samples and data. The techniques used to analyze the data are also briefly outlined.

### 7.4.1 Informed Consent

Like any other study, clinical trial should be explained in a study protocol for which an approval should be sought from the Institutional Review Board (IRB). It is important to realize that informed consent is a process of obtaining permission for voluntary participation in a clinical trial rather than simply explaining the study protocol to volunteers for legal reasons. The key component for informed consent is the infor-

mation that should be presented in a manner that the potential volunteers can easily understand. For practical reasons, the number of elements should be clearly indicated in the protocol and verbally explained to the potential subjects. For instance, whether the participation in the study is optional or mandatory, or whether the samples collected will be used for definitive or tentative analysis of certain biomarkers. The difference between optional or mandatory participation and tentative or definitive analysis should be clearly explained to the potential participants. For instance, optional participation does not exclude the volunteer to enroll in a clinical trial, which may or may not benefit the subject. On the other hand, if the subject declines providing a sample for subsequent mandatory analysis, he or she is automatically disqualified from enrolling in that clinical trial. In definitive analysis, all the samples will be analyzed for specified biomarkers, whereas in tentative analysis samples are stored and analyzed when needed. Regardless of the study type, participants are permitted to withdraw from the clinical trial at any given time. For example, if a subject enrolls as a volunteer in a mandatory definitive clinical trial to provide a sample for genomic analysis, the subject is permitted to withdraw from the study. However, all the samples collected prior to the time of withdraw can be still used in subsequent analysis without the subject's consent.

The code of Federal Regulations 21 CFR 50 discusses the protection of human subjects in research (21 CFR Part 50 and Protection of Human Subjects FDA http://www1.va.gov/oro/apps/compendium/Files/21CFR50.htm. Accessed December 21, 2009). The specific requirements for consent form 21 CFR section 50.25 contain eight basic elements with six additional elements when appropriate and are given as follows (http://www.accessdata.fda.gov/scripts/cdrh/cfdocs/cfcfr/CFRSearch.cfm?FR=50.25):

(A) Basic elements of informed consent: when seeking informed consent, the following information shall be provided to each subject:
  1. A statement that the study involves research, an explanation of the purposes of the research and the expected duration

of the subject's participation, a description of the procedures to be followed, and identification of any procedures which are experimental.

2. A description of any reasonably foreseeable risks or discomforts to the subject.

3. A description of any benefits to the subject or to others which may reasonably be expected from the research.

4. A disclosure of appropriate alternative procedures or courses of treatment, if any, that might be advantageous to the subject.

5. A statement describing the extent, if any, to which confidentiality of records identifying the subject will be maintained and that notes the possibility that the Food and Drug Administration may inspect the records.

6. For research involving more than minimal risk, an explanation as to whether any compensation and medical treatments are available if injury occurs and, if so, what they consist of, or where further information may be obtained.

7. An explanation of whom to contact for answers to pertinent questions about the research and research subjects' rights, and whom to contact in the event of a research-related injury to the subject.

8. A statement that participation is voluntary, that refusal to participate will involve no penalty or loss of benefits to which the subject is otherwise entitled, and that the subject may discontinue participation at any time without penalty or loss of benefits to which the subject is otherwise entitled.

(B) Additional elements of informed consent: when appropriate, one or more of the following elements of information shall also be provided to each subject:

1. A statement that the particular treatment or procedure may involve risks to the subject (or to the embryo or fetus, if the subject is or may become pregnant) which are currently unforeseeable.

2. Anticipated circumstances under which the subject's participation may be terminated by the investigator without regard to the subject's consent.

3. Any additional costs to the subject that may result from participation in the research.

4. The consequences of a subject's decision to withdraw from the research and procedures for orderly termination of participation by the subject.

5. A statement that significant new findings developed during the course of the research which may relate to the subject's willingness to continue participation will be provided to the subject.

6. The approximate number of subjects involved in the study.

(C) The informed consent requirements in these regulations are not intended to preempt any applicable Federal, State, or local laws which require additional information to be disclosed for informed consent to be legally effective.

(D) Nothing in these regulations is intended to limit the authority of a physician to provide emergency medical care to the extent the physician is permitted to do so under applicable Federal, State, or local law (http:// www.accessdata.fda.gov/scripts/cdrh/cfdocs/ cfcfr/CFRSearch.cfm?FR=50.25).

Additional considerations should be given if a pharmacogenomic test is planned. This is because there are always special concerns about privacy of the participants when genetic tests are used. It is generally acceptable to have two separate consent forms, one for general procedure and another for genetic testing component. From an operational perspective, this makes it even easier to present complex materials to participants in separate forms. This strategy is especially useful for optional clinical trials where refusal of participation in genomic research/biomarker discovery component will not prevent the eligibility and enrolment of the main clinical trial.

## 7.4.2  Considerations for Handling and Storing Samples and Data

The protocol should discuss standard methods and procedures used in sample collection, sample storage, sample identification, sample integrity, and sample collection for future use, as well as data storage and data handling. The duration of sample storage is important and it should therefore be indicated in the protocol. This is especially important in sample collection for future use. Generally, sample collection for future uses is permitted by the IRB for a specific drug class, disease and therapeutic area, and specified duration of the study. Another important consideration is the protection of patient privacy which can be achieved by de-identification process of samples, in which a link between de-identified samples and original information is maintained, or by anonymization, in which the link is permanently removed. From a practical point of view, the process of de-identification and anonymization can influence the degree of enrolment as some individuals prefer the latter method because researchers are not able to link the results back to the patients' identity. Although anonymization permits pharmaceutical decision making based on the results obtained from the biomarker–phenotype correlation study, it has consequence for regulatory decision making. This is because regulatory agencies may wish to examine the integrity of the data. One should also note that the research is now conducted in a global environment and therefore global regulations should be taken into account before clinical trial planning as regulations vary among countries. The area of consideration should include standard methods and procedures used in sample collection, sample storage, sample identification, sample integrity, sample collection for future use, data storage, data handling, and the shipment of the samples to other parts of the world for genomic, proteomic, and metabonomic analyzes.

Specific considerations should be given to the type of samples collected for subsequent biomarker analysis in drug discovery process. For instance, blood samples are excellent sources for DNA and RNA, which can be extracted from leukocyte and whole blood. The latter source and method of collection suffer from the presence of a significant amount of mRNA from erythrocytes source. Generally, the blood samples can be collected in an EDTA vacutainer blood sample collection tube, stored at 4°C, and shipped overnight for DNA and RNA collection. This method is more practical for a multicenter clinical trial. For the best recovery and stability, high yield can be achieved if DNA and mRNA are extracted immediately and stored at −70°C. Serum and plasma samples are widely used in protein and metabonomic research projects. The storage of serum and plasma samples at −20°C is generally satisfactory. Citrate, EDTA, and heparin vacutainer blood collection tubes can be used for plasma collection; however, each can cause interference with the measurement of biomarkers depending on the technologies used. The use of serum samples for the discovery of small peptides should be avoided as many of the small peptides can bind to larger molecules as carriers, which may be lost during coagulation process.

Tissue biopsied samples can be used as paraffin embedded and fresh or frozen samples. Major concerns related to this type of samples include the stability and recovery rate of mRNA and microRNA for genomic expression research and the quality of proteins needed in proteomic research. For instance, paraffin-embedded samples diminish the quality and yield of RNA extraction. Sample contamination with other cell types present in a biopsied specimen is a major concern, which requires specific consideration. Precision sample removal using laser capture microdissection (LCM) can significantly improve the quality of sample collection by removing specific cell populations needed for biomarker studies from the surrounding tissue. Urine samples are used in metabonomic and drug toxicological studies. Generally, urine samples are unstable and need to be stored at −20°C. Stability and integrity of analyte should be taken into account when urine samples are used.

### 7.4.3 Application of the -Omics in Drug Discovery

As an example of application in drug discovery, biomarkers can be used for better planning of clinical trials as shown in Fig. 7.4. Integration of biomarkers in clinical trial planning can assist in helping explaining outliers or variability in pharmacokinetics data, subject enrolment for inclusion/exclusion in clinical trials, and the identification
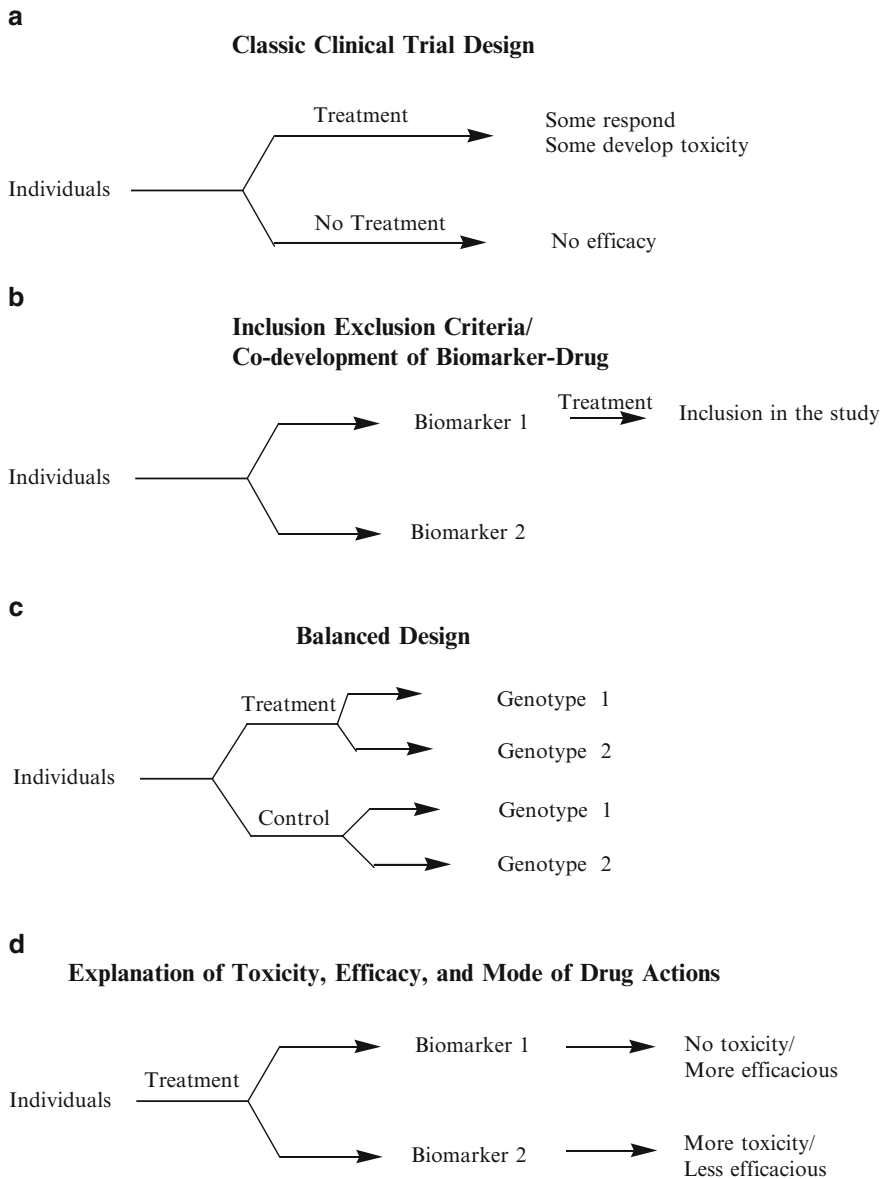


**Fig. 7.4** *The application of biomarkers in clinical trial designs.* (**a**) Classic clinical trial design, no biomarkers are used in selection of patients to receive a specific therapy. (**b**) Biomarkers can be used as inclusion/exclusion criteria to receive a therapeutic intervention. (**c**) Balanced design is a clinical trial design in which the biomarkers are included in the treatment and control arms of the study. Balanced design can potentially explain how the biology of biomarkers influences therapeutic outcomes. (**d**) Biomarkers can also be used in search of explanation for toxicity and efficacy in a subpopulation of patients who received the therapy

of responders from nonresponders, and those who may be at increased risk of developing toxicity. Biomarkers can be also used to make an informed strategic decision whether the clinical trial should continue or be stopped. In the following, we discuss two examples to illustrate how biomarkers can be incorporated into clinical investigations and drug discovery process.

*Imatinib Mesylate – Gleevec*® *(BCR-ABL kinase inhibitor)*. Imatinib is used in the treatment of a number of cancers such as CML, gastrointestinal stromal tumors (GISTs), and acute lymphoblastic leukemia (ALL). Imatinib was developed using principles of rational drug design by Novartis in late 1990s and received FDA approval in 2001. Investigators first screened chemical libraries against defective BCR-ABL protein, the tyrosine kinase product of Philadelphia chromosome mutation, to identify a compound that can inhibit BCR-ABL protein, which remains in active form. The active site of ABL-BCR tyrosine kinase has a binding site for ATP on which imatinib can bind and therefore inhibit its activity (Druker and Lydon 2000). The results from clinical trials (Druker et al. 2001b) not only provided evidence for the BCR-ABL role in CML, but also demonstrated the potential for the development of drugs based on specific biomarker present in diseases. In another clinical trial by the same group (Druker et al. 2001a), BCR-ABL protein was used as

inclusion criteria for recruiting CML and ALL patients (Fig. 7.5). BCR-ABL enzyme is present in all cases of CML but only in 20% of cases of ALL. The conclusion of the trial was that the BCR-ABL tyrosine kinase inhibitor imatinib had substantial activity in CML and Ph-positive ALL.

*Trastuzumab – Herceptin*® *and Tamoxifen (Breast Cancer Therapy)*. In addition to chemotherapy, trastuzumab (Herceptin®) and tamoxifen are widely used in the treatment of breast cancer patients by targeting Her2-axis and the hormone-axis pathways (Toi et al. 2005). Figure 7.6 illustrates a simplified decision tree for choosing appropriate drug treatment based on molecular markers of Her-2, estrogen receptor, progesterone receptor, and CYP2D6 metabolizing enzyme (http://www.nccn.org/professionals/physician_gls/PDF/breast.pdf). In breast cancer therapy, trastuzumab, a monoclonal antibody that binds Her2, is used in the treatment of women with Her2-overexpressing breast cancer. Although Her2 overexpression is useful in making decision who will receive trastuzumab, only about one-third of patients with Her-2 overexpression respond to trastuzumab treatment (Toi et al. 2005). Therefore, there is a need to find additional predictive response markers in order to identify patients who likely to benefit from trastuzumab treatment (Beano et al. 2008).

The other drug tamoxifen is used in the treatment of ER+ (estrogen receptor positive) breast



**Inclusion/Exclusion**

ALL patients
- 20% of patients BCR-ABL positive → Receive Imatinib
- 80% of patients BCR-ABL negative → Not receive Imatinib
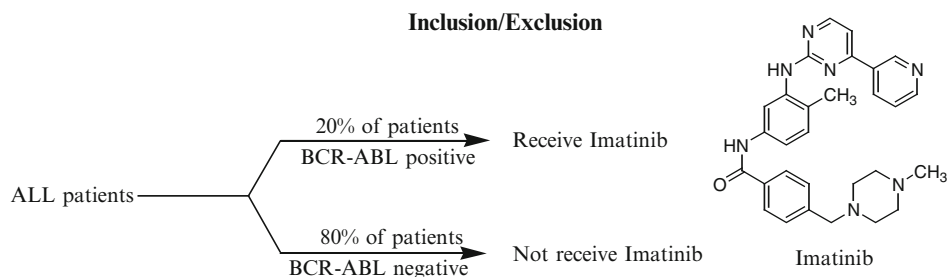
Imatinib

**Fig. 7.5** *Clinical trial planning for imatinib therapy in acute lymphoblastic leukemia*. The inclusion of BCR-ABL positive acute lymphoblastic leukemia (ALL) patients in clinical trial enriches the clinical trial with a population of patients who are more likely to respond to imatinib. For instance, a clinical trial of imatinib in ten BCR-ABL positive ALL patients will lead to substantial therapeutic response in all ten patients (100% response

rate). In contrast, if BCR-ABL marker is not used as an inclusion criterion for patient enrolment, a minimum of 50 ALL patients are needed to observe substantial therapeutic response to imatinib in ten patients (20% response rate). Hence, the inclusion of biomarkers as a criterion in patient recruitment can significantly reduce the cost of clinical trial and improve the attrition rate in drug discovery

**Decision Tree in Breast Cancer Therapy**
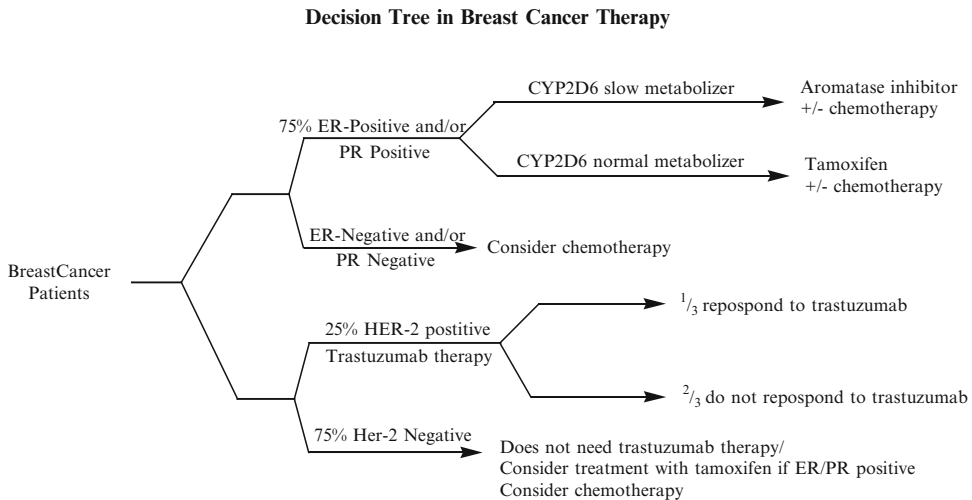


**Fig. 7.6** *Decision tree for making therapeutic choices depends on molecular markers in breast cancer patients.* 75% of breast cancer patients have tumors which over-express estrogen receptor (ER) and are good candidates to receive hormonal therapy with tamoxifen. 25% of patients have tumors that overexpress Her-2 and are good candidates to receive trastuzumab. The tumors that overexpress both biomarkers are good candidate to receive both tamoxifen and trastuzumab
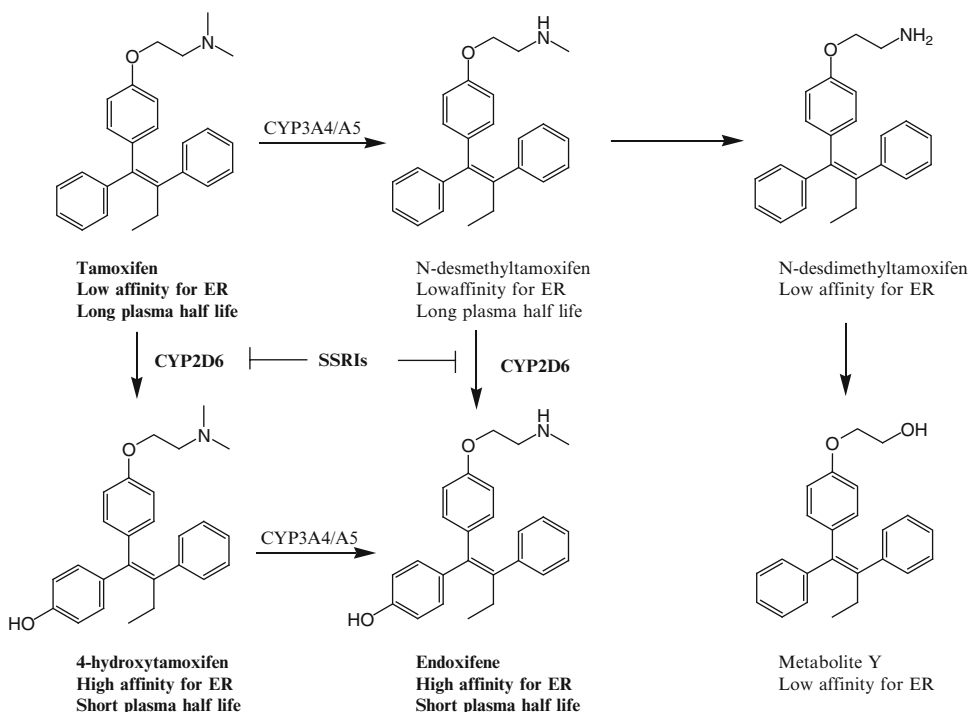


**Fig. 7.7** *The role of CYP2D6 genetic polymorphism and drug–drug interaction in metabolic bioactivation of pro-drug tamoxifen to active drug endoxifen.* SSRIs, selective serotonin reuptake inhibitors; ER, estrogen receptor. The normal activity of CYP2D6 liver enzyme is needed for bioconversion of tamoxifen to endoxifen. CYP2D6 genetic polymorphism can diminish or abolish the bioconversion of tamoxifen to active drug endoxifen. SSRIs antidepressant drug–CYP2D6 interaction prevents bioactivation of tamoxifen to endoxifen leading to the development of tamoxifen resistance in breast cancer patients

cancer in women (Blanchard et al. 2005). However, a fraction of patients who receive tamoxifen does not respond to the therapy or develop tamoxifen resistance. Recently, it was reported that CYP2D6 genetic polymorphism was responsible for underlying molecular mechanism in tamoxifen resistance. This is because tamoxifen is a prodrug and needs to be activated by CYP2D6 and CYP3A4 liver enzymes to its active form endoxifen which has a higher affinity for estrogen receptor (Fig. 7.7) (Desta et al. 2004; Wang et al. 2004). CYP2D6 slow metabolizers may benefit more from aromatase inhibitors. Patients who are menopausal may benefit from ovarian ablation. For additional information on association between CYP2D6 polymorphisms and outcomes among women with breast cancer treated with tamoxifen, please refer Schroth et al. (2009).

Another mechanism for development of tamoxifen resistance includes drug–drug interaction involving the CY2D6 enzyme. Many breast cancer patients suffer from depression and hence need to receive selective serotonin reuptake inhibitor (SSRI) antidepressant prescription drugs which can cause drug–drug interaction by inhibiting CYP2D6 enzyme and limiting the bioconversion of prodrug tamoxifen to its active drug endoxifen (Jin et al. 2005; Beckmann et al. 2009).

As outlined above, the use of breast cancer biomarkers is an excellent example to illustrate the utility of the –omic information in nonclinical and clinical setting to address important questions related to underlying mechanisms by which patients are not responding to specific therapy or developing drug resistance. Such biomarkers can be used in the identification of patients who may benefit from trastuzumab, tamoxifen, aromatase inhibitor, or a combination.

### 7.4.4 Considerations for Statistical Analysis in Microarrays

Microarrays offer great promises for drug design, drug discovery, target identification, hypothesis generation, comparative genomics, diagnostics, prognostics, personalized medicine, and in the understanding of molecular mechanism,

biochemical pathways, and gene networks (Fan and Ren 2006). In the discovery stage, a vast amount of data is generated when microarray experiments are conducted which makes the interpretation of microarray results very difficult. To obtain meaningful information from microarray data, researchers need to utilize powerful statistical analysis methods. In principle, microarray data analysis requires a different statistical analysis from traditional statistical methods, because it attempts simultaneous inferences on thousands of genes where only a small fraction of genes are statistically different. Furthermore, consideration should be given to a number of statistical problems which arise during microarray data analysis as a result of multiple testing. For each statistical test performed, there is some probability to make erroneous inferences. Several incorrect inferences can inadvertently happen in an analysis that includes multiple statistical tests. Hence, researchers can easily arrive at inaccurate conclusions. Pounds (2006) discusses how to estimate and control multiple testing error rates. Briefly, to minimize the chance of arriving at incorrect conclusions, important attention should be given to sample size, statistical power, statistical methods, and the type of software used when planning microarray experiments. The statistical techniques that are widely used in microarray data analysis include fold-change, clustering, classification, genetic network analysis, and simulation (Hanai et al. 2006). Subsequently, the candidate biomarker should be validated in separate experiments to minimize the chance of making incorrect inferences. The softwares that are mainly used in microarray data analysis include R software (http://www.r-project.org/) and Bioconductor (http://www.bioconductor.org). The latter is the most comprehensive software that is used in gene expression data analysis.

## 7.5 Summary

Genomics, proteomics, and metabonomics are finding widespread application in drug discovery, diagnostics, and clinical medicine. Technology is

becoming a less important barrier in the application of the -omics technology in drug development. The major barriers in widespread uptake of the -omics in the drug development process include the lack of regulatory and research guidelines in a global research environment, lack of physician and scientist training, interpretation of results, and the complex nature of the data generated in the preclinical and clinical stages of drug development.

## References

21 CFR Part 50, Protection of Human Subjects (FDA) http://www1.va.gov/oro/apps/compendium/Files/21CF-R50.htm. Accessed December 21, 2009

Ala-Korpela M. Critical evaluation of 1H NMR metabonomics of serum as a methodology for disease risk assessment and diagnostics. Clin Chem Lab Med 2008;46:27–42.

Anderson L. Candidate-based proteomics in the search for biomarkers of cardiovascular disease. J Physiol 2005;563:23–60.

Anderson GD. Gender differences in pharmacological response. Int Rev Neurobiol 2008;83:1–10.

Anderson NL, Anderson NG. The human plasma proteome: history, character, and diagnostic prospects. Mol Cell Proteomics 2002;1:845–867.

Anderson NL, Matheson AD, and Steiner S. Proteomics: applications in basic and applied biology. Curr Opin Cell Biol 2000;11:408–412.

Araujo RP, Liotta LA. A control theoretic paradigm for cell signaling networks: a simple complexity for a sensitive robustness. Curr Opin Chem Biol 2006;10:81–87.

Araujo RP, Doran C, Liotta LA, and Petricoin EF. Network-targeted combination therapy: a new concept in cancer treatment. Drug Discov Today Ther Strateg 2004;1:425–433.

Araujo RP, Petricoin EF, and Liotta LA. A mathematical model of combination therapy using the EGFR signaling network. Biosystems 2005;80:57–69.

Araujo RP, Liotta LA, and Petricoin EF. Proteins, drug targets and the mechanisms they control: the simple truth about complex networks. Nat Rev Drug Discov 2007;6:871–880.

Araujo RP, Petricoin EF, and Liotta LA. Mathematical modeling of the cancer cell's control circuitry: paving the way to individualized therapeutic strategies. Curr Signal Transduction Ther 2007;2:145–155.

Araujo RP, Petricoin EF, and Liotta LA. Critical dependence of blood-borne biomarker concentrations on the half-lives of their carrier proteins. J Theor Biol 2008;253:616–622.

Beano A, Signorino E, Evangelista A, Brusa D, Mistrangelo M, Polimeni MA, Spadi R, Donadio M, Ciuffreda L, Matera L. Correlation between NK function and response to trastuzumab in metastatic breast cancer patients. J Transl Med 2008;6:25.

Beckmann MW, Koelbl H, Weinshilboum RM, Ingle JN, Eichelbaum M, Schwab M, Brauch H. Association between CYP2D6 polymorphisms and outcomes among women with early stage breast cancer treated with tamoxifen. JAMA 2009;302(13):1429–1436.

Blanchard R, Nguyen A, Ullmer L, Hayden J, Lemler S, Weinshilboum RM, Rae JM, Hayes DF, Flockhart DA. CYP2D6 genotype, antidepressant use, and tamoxifen metabolism during adjuvant breast cancer treatment. J Natl Cancer Inst 2005;97(1):30–39.

Bollard ME, Keun HC, Beckonert O, Ebbels TMD, Antti H, Nicholls AW, Shockcor JP, Cantor GH, Stevens G, Lindon JC, Holmes E, and Nicholson JK. Comparative metabonomics of differential hydrazine toxicity in the rat and mouse. Toxicol Appl Pharmacol 2005;204: 135–151.

Brindle JT, Antti H, Holmes E, Tranter G, Nicholson JK, Bethell HW, Clarke S, Schofield PM, McKilligin E, Mosedale DE, and Grainger DJ. Rapid and noninvasive diagnosis of the presence and severity of coronary heart disease using 1H-NMR-based metabonomics. Nat Med 2002;8:1439–1444.

Burczynski ME. Pharmacogenomic approaches in clinical studies to identify biomarkers of safety and efficacy. Toxicol Lett 2009;186(1):18–21.

CFR – Code of Federal Regulations Title 21 http://www.accessdata.fda.gov/scripts/cdrh/cfdocs/cfcfr/CFRSearch.cfm?FR=50.25. Accessed December 21, 2009

Claridge TDW (2008) High-resolution NMR techniques in organic chemistry. Elsevier Science, Oxford.

Clayton TA, Lindon JC, Cloarec O, Antti H, Charuel C, Hanton G, Provost JP, Le Net JL, Baker D, Walley RJ, Everett JR, and Nicholson JK. Pharmaco-metabonomic phenotyping and personalized drug treatment. Nature 2006;440:1073–1077.

Clayton TA, Baker D, Lindon JC, Everett JR, and Nicholson JK. Pharmacometabonomic identification of a significant host-microbiome metabolic interaction affecting human drug metabolism. PNAS USA 2009; 106:14728–14733.

Cloarec O, Dumas ME, Craig A, Barton RH, Trygg J, Hudson J, Blancher C, Gauguier D, Lindon JC, Holmes E, and Nicholson J. Statistical total correlation spectroscopy: an exploratory approach for latent biomarker identification from metabolic 1H NMR data sets. Anal Chem 2005;77:1282–1289.

Coen M, Ruepp SU, Lindon JC, Nicholson JK, Pognan F, Lenz EM, and Wilson ID. Integrated application of transcriptomics and metabonomics yields new insight into the toxicity due to paracetamol in the mouse. J Pharm Biomed Anal 2004;35:93–105.

Coen M, Hong YS, Clayton TA, Rohde CM, Pearce JT, Reily MD, Robertson DG, Holmes E, Lindon JC, and

Nicholson JK. The mechanism of galactosamine toxicity revisited; A metabonomic study. J Proteome Res 2007;6:2711–2719.

Craig A, Sidaway J, Holmes E, Orton T, Jackson D, Rowlinson R, Nickson J, Tonge R, Wilson I, and Nicholson J. Systems toxicology: integrated genomic, proteomic and metabonomic analysis of methapyrilene induced hepatotoxicity in the rat. J Proteome Res 2006;5:1586–1601.

Crockford DJ, Holmes E, Lindon JC, Plumb RS, Zirah S, Bruce SJ, Rainville P, Stumpf CL, and Nicholson JK. Statistical heterospectroscopy, an approach to the integrated analysis of NMR and UPLC-MS data sets: application in metabonomic toxicology studies. Anal Chem 2006;78:363–371.

Dalma-Weiszhausz DD, Warrington J, Tanimoto EY, and Miyada CG. The affymetrix GeneChip platform: an overview. Meth Enzymol 2006;410:3–28.

de Leon J, Susce MT, Johnson M, Hardin M, Maw L, Shao A, Allen AC, Chiafari FA, Hillman G, Nikoloff DM. DNA microarray technology in the clinical environment: the AmpliChip CYP450 test for CYP2D6 and CYP2C19 genotyping. CNS Spectr. 2009;14 (1):19–34.

Desta Z, Ward BA, Soukhova NV, Flockhart DA. Comprehensive evaluation of tamoxifen sequential biotransformation by the human cytochrome P450 system in vitro: prominent roles for CYP3A and CYP2D6. J Pharmacol Exp Ther 2004;310(3):1062–1075.

Diamandis EP, van der Merwe DE. Plasma protein profiling by mass spectrometry for cancer diagnosis: opportunities and limitations. Clin Cancer Res 2005;11:963–965.

DMET™ Plus Premier Pack.

Druker BJ, Lydon NB. Lessons learned from the development of an Abl tyrosine kinase inhibitor for chronic myelogenous leukemia. J Clin Invest 2000;105:3–7. PMID 10619854

Druker BJ, Sawyers CL, Kantarjian H, Resta DJ, Reese SF, Ford JM, Capdeville R, and Talpaz M. Activity of a specific inhibitor of the BCR-ABL tyrosine kinase in the blast crisis of chronic myeloid leukemia and acute lymphoblastic leukemia with the Philadelphia chromosome. N Engl J Med 2001;344(14):1038–1042.

Druker BJ, Talpaz M, Resta DJ, Peng B, Buchdunger E, Ford JM, Lydon NB, Kantarjian H, Capdeville R, Ohno-Jones S, and Sawyers CL. Efficacy and safety of a specific inhibitor of the BCR-ABL tyrosine kinase in chronic myeloid leukemia. N Engl J Med 2001;344 (14):1031–1037.

Evan GI. Can't kick that oncogene habit. Cancer Cell 2006;10:345–347.

Fan J, Ren Y. Statistical analysis of DNA microarray data in cancer research. Clin Cancer Res 2006;12 (15):4469–4473.

Ferrer-Dufol A, Menao-Guillen S. Toxicogenomics and clinical toxicology: an example of the connection between basic and applied sciences. Toxicol Lett 2009;186(1):2–8.

Geho DH, Petricoin EF, Liotta LA, and Araujo RP. Modeling of protein signaling networks in clinical proteomics. Cold Spring Harb Symp Quant Biol 2005;70:517–524.

Geho DH, Luchini A, Garaci E, Belluco C, Petricoin E, and Liotta LA. Nanotechnology in clinical proteomics. Nanomedicine (Lond) 2007;2:1–5.

GeneChip Microarray System. http://www.affymetrix. com/support/technical/other/genechip_system_brochure. pdf. Accessed June 1, 2009.

Gomez A, Ingelman-Sundberg M. Pharmacoepigenetics: its role in interindividual differences in drug response. Clin Pharmacol Ther 2009;85(4):426–430.

Hanai T, Hamada H, Okamoto M. Application of bioinformatics for DNA microarray data to bioscience, bioengineering and medical fields. J Biosci Bioeng 2006;101(5):377–384.

Hillman G, Nikoloff DM. DNA microarray technology in the clinical environment: the AmpliChip CYP450 test for CYP2D6 and CYP2C19 genotyping. CNS Spectr 2009;14(1):19–34.

Holmes E, Loo RL, Stamler J, Bictash M, Yap IK, Chan Q, Ebbels T, De Iorio M, Brown IJ, Veselkov KA, Daviglus ML, Kesteloot H, Ueshima H, Zhao L, Nicholson JK and Elliott P. Human metabolic phenotype diversity and its association with diet and blood pressure. Nature 2008;453:396–400. http://www.affymetrix.com/support/technical/byproduct.affx?product=dmet_2 Accessed June 1, 2009.

Infinium HD BeadChips technology http://www.illumina. com/pages.ilmn?ID=40 Accessed June 1, 2009.

Invader UGT1A1 molecular assay. http://www.genzymegenetics.com/testmenu/tests/cancer/gene_p_testmenu_can_test_ugt1a1.asp Accessed June 1, 2009.

Janes KA, Lauffenburger DA. A biological approach to computational models of proteomic networks. Curr Opin Chem Biol 2006;10:73–80.

Jin Y, Desta Z, Stearns V, Ward B, Ho H, Lee KH, Skaar T, Storniolo AM, Li L, Araba A, Blanchard R, Nguyen A, Ullmer L, Hayden J, Lemler S, Weinshilboum RM, Rae JM, Hayes DF, Flockhart DA. CYP2D6 genotype, antidepressant use, and tamoxifen metabolism during adjuvant breast cancer treatment. J Natl Cancer Inst 2005;97(1):30–39.

Jones D. Pathways to cancer therapy. Nat Rev Drug Discov 2008;7:875–876.

Kalow W. Pharmacogenetics and pharmacogenomics: origin, status, and the hope for personalized medicine. Pharmacogenomics J 2006;6(3):162–165.

King G, Payne S, Walker F, and Murray GI: A highly sensitive detection method for immunohistochemistry using biotinylated tyramine. J Pathol 1997;183: 237–241.

Kirschenlohr HL, Griffin JL, Clarke SC, Rhydwen R, Grace AA, Schofield PM, Brindle KM, and Metcalfe JC. Proton NMR analysis of plasma is a weak predictor of coronary artery disease. Nat Med 2006;12: 705–710.

Kola I, Landis J. Can the pharmaceutical industry reduce attrition rates? Nat Rev Drug Discov 2004;3:711–715.

Lindon JC, Holmes E, and Nicholson JK. Pattern recognition methods and applications in biomedical magnetic resonance. Prog Nucl Magn Reson Spectrosc 2001;39:1–40.

Lindon JC, Nicholson JK, Holmes E, Antti H, Bollard ME, Keun H, Beckonert O, Ebbels TM, Reilly MD, Robertson D, Stevens GJ, Luke P, Breau AP, Cantor GH, Bible RH, Niederhauser U, Senn H, Schlotterbeck G, Sidelmann UG, Laursen SM, Tymiak A, Car BD, Lehman-McKeeman L, Colet JM, Loukaci A, and Thomas C. Contemporary issues in toxicology – The role of metabonomics in toxicology and its evaluation by the COMET project. Toxicol Appl Pharmacol 2003;187:137–146.

Lindon JC, Holmes E, and Nicholson JK. Toxicological applications of magnetic resonance. Prog Nucl Magn Reson Spectrosc 2004;45:109–143.

Lindon JC, Keun HC, Ebbels TMD, Pearce JMT, Holmes E, and Nicholson JK. The Consortium for Metabonomic Toxicology (COMET): aims, activities and achievements. Pharmacogenomics 2005;6:691–699.

Lindon JC, Holmes E, and Nicholson JK. Metabonomics techniques and applications to pharmaceutical research & development. Pharm Res 2006;23:1075–1088.

Lindon JC, Nicholson JK, and Holmes E (2007) The handbook of metabonomics and metabolomics. Elsevier, The Netherlands.

Liotta L, Petricoin E. Nanomedicine – the power of proteins: a conversation with Lance Liotta and Emanual Petricoin. Interview by Barbara J Culliton. Health Aff (Millwood) 2008;27:w310–w314.

Liotta LA, Espina V, Mehta AI, Calvert V, Rosenblatt K, Geho D, Munson PJ, Young L, Wulfkuhle J, and Petricoin EF. Protein microarrays: Meeting analytical challenges for clinical applications. Cancer Cell 2003;3:317–325.

Luchini A, Geho DH, Bishop B, Tran D, Xia C, Dufour RL, Jones CD, Espina V, Patanarut A, Zhou W, et al. Smart hydrogel particles: biomarker harvesting: one-step affinity purification, size exclusion, and protection against degradation. Nano Lett 2008;8:350–361.

Lynch TJ, Bell DW, Sordella R, Gurubhagavatula S, Okimoto RA, Brannigan BW, Harris PL, Haserlat SM, Supko JG, Haluska FG, et al. Activating mutations in the epidermal growth factor receptor underlying responsiveness of non-small-cell lung cancer to gefitinib. N Engl J Med 2004;350:2129–2139.

MammaPrint. http://usa.agendia.com/en/mammaprint.html Accessed June 1, 2009.

Mark S. Boguski. Comparative genomics: The mouse that roared. Nature 2002;420:515–516.

McHale D (2008) Applications of pharmacogenomics in drug discovery, 73–87 in: Cohen N (ed) Pharmacogenomics and personalized medicine. Humana Press, Clifton, UK

Moridani, Pharmacogenomics Testing: "Required", "Recommended", or "For Information Only". PGx Highlights 2009;1(1):6–7. http://www.aapspharmaceutica.com/inside/focus_groups/PGX/imagespdfs/PGxHighlightsJun2009.pdf Accessed June 1, 2009.

Mouse Genome Resources. http://www.ncbi.nlm.nih.gov/projects/genome/guide/mouse/ Accessed May 29, 2009.

NCCN Clinical Practice Guidelines in Oncology: Breast Cancer. http://www.nccn.org/professionals/physician_gls/PDF/breast.pdf Accessed December 19, 2009

Nicholson JK, Lindon JC. Systems biology: Metabonomics. Nature 2008;455:1054–1056.

Odunsi K, Wollman RM, Ambrosone CB, Hutson A, McCann SE, Tammela J, Geisler JP, Miller G, Sellers T, Cliby W, Qian F, Keitz B, Intengan M, Lele S, and Alderfer JL. Detection of epithelial ovarian cancer using 1H-NMR-based metabonomics. Int J Cancer 2005;113:782–788.

PathVysion HER-2 DNA Probe Kit. http://www.pathvysion.com/WhyPathVysionisrightforyourpatients_934.aspx Accessed June 1, 2009.

Paweletz CP, Charboneau L, Bichsel VE, Simone NL, Chen T, Gillespie JW, Emmert-Buck MR, Roth MJ, Petricoin IE, and Liotta LA. Reverse phase protein microarrays which capture disease progression show activation of pro-survival pathways at the cancer invasion front. Oncogene 2001;20:1981–1989.

Petricoin EF, Liotta LA. SELDI-TOF-based serum proteomic pattern diagnostics for early detection of cancer. Curr Opin Biotechnol 2004;15:24–30.

Pounds SB. Estimation and control of multiple testing error rates for microarray studies. Brief Bioinform 2006;7(1):25–36.

Rantalainen M, Cloarec O, Beckonert O, Wilson ID, Jackson D, Tonge R, Rowlinson R, Rayner S, Nickson J, Wilkinson RW, Mills JD, Trygg J, Nicholson JK, and Holmes E. Statistically integrated metabonomic-proteomic studies on a human prostate cancer xenograft model in mice. J Proteome Res 2006;5:2642–2655.

Roche Amplichip CYP450 Test. http://www.amplichip.us/?gclid=CM6Nr9Oo6poCFR0Sagodqi7PBw Accessed June 1, 2009.

Sauro HM, Kholodenko BN. Quantitative analysis of signaling networks. Prog Biophys Mol Biol 2004;86:5–43.

Schroth W, Goetz MP, Hamann U, Fasching PA, Schmidt M, Winter S, Fritz P, Simon W, Suman VJ, Ames MM, Safgren SL, Kuffel MJ, Ulmer HU, Boländer J, Strick R, Beckmann MW, Koelbl H, Weinshilboum RM, Ingle JN, Eichelbaum M, Schwab M, and Brauch H. Association between CYP2D6 polymorphisms and outcomes among women with early stage breast cancer treated with tamoxifen. JAMA 2009;302 (13):1429–1436

Tirumalai RS, Chan KC, Prieto DA, Issaq HJ, Conrads TP, and Veenstra TD. Characterization of the low molecular weight human serum proteome. Mol Cell Proteomics 2003;2(10):1096–1103.

Toi M, Horiguchi K, Bando H, Saji S, and Chow LW. Trastuzumab: updates and future issues. Cancer Chemother Pharmacol. 2005;56(Suppl 1):94–99.

Trugene HIV-1 test. http://www.research.bayer.com/edi-
    tion_16/16_HIV_Test_en.pdfx Accessed June 1,
    2009.
U.S. FDA, Guidance for Industry Pharmacogenomic Data
    Submissions.    http://www.fda.gov/cder/guidance/
    6400fnl.pdf Accessed May 29, 2009.
U.S. FDA. Table of Valid Genomic Biomarkers in the
    Context of Approved Drug Labels. http://www.fda.
    gov/Drugs/ScienceResearch/ResearchAreas/Pharmaco-
    genetics/ucm083378.htm Accessed December 15, 2009.
van't Veer LJ, Dai H, van de Vijver MJ, He YD, Hart AA,
    Mao M, Peterse HL, van der Kooy K, Marton MJ,
    Witteveen AT, Schreiber GJ, Kerkhoven RM, Roberts
    C, Linsley PS, Bernards R, and Friend SH. Gene
    expression profiling predicts clinical outcome of
    breast cancer. Nature 2002;415(6871):530–536.

Wang DY, Fulthorpe R, Liss SN, and Edwards EA. Iden-
    tification of estrogen-responsive genes by comple-
    mentary deoxyribonucleic acid microarray and
    characterization of a novel early estrogen-induced
    gene: EEIG1. Mol Endocrinol 2004;18(2):402–411.
Wilson ID, Nicholson JK, Castro-Perez J, Granger JH,
    Johnson KA, Smith BW and Plumb RS. High resolu-
    tion "ultra performance" liquid chromatography cou-
    pled to oa-TOF mass spectrometry as a tool for
    differential metabolic pathway profiling in functional
    genomic studies. J Proteome Res 2005;4:591–598.
Wulfkuhle JD, Edmiston KH, Liotta LA, and Petricoin
    EF. Technology insight: pharmacoproteomics for can-
    cer – promises of patient-tailored medicine using pro-
    tein microarrays. Nat Clin Pract Oncol 2006;3:
    256–268.

# Optimal Design of Pharmacokinetic–Pharmacodynamic Studies

**8**

Lee-Kien Foo and Stephen B. Duffull

**Abstract**

This chapter provides an overview of the theory and application of optimal design with the focus on PKPD studies. Different optimality criteria for parameter estimation and model discrimination, together with various methods to estimate sampling window are discussed. Some practicality issues, design tips, ways to assess the design performance, and available software are addressed with an example to demonstrate the applicability of optimal design to PKPD studies.

## 8.1    Introduction

Setting up and running efficient and experimentally successful studies is an essential part of the drug development process. Inefficiencies and experimental failure associated with poorly or costly (nonparsimonious) designs are wasteful of limited physical and human resources. An efficient study is one that optimizes the balance between what is to be learnt and the resource constraints available to the researcher. Within this definition, the absence of study constraints and unlimited resources should yield maximally informative studies. However, the absence of limiting conditions is not realistic and hence formal methods to optimize the efficiency of the

design of experiments have received significant attention in the statistical literature.

Perhaps the first formal application of optimal design technique was performed by Smith (1918), in her work for optimizing polynomials. Although there were significant advances in optimizing the design of studies in the following years it took until 1981 when the first application of the theory of optimal design for nonlinear models reached the pharmacokinetic literature (D'Argenio 1981). In this work, D'Argenio introduced the concepts and showed the design of pharmacokinetic studies was not only amenable to these techniques, but the gain in terms of parsimony could be considerable.

Around the same time, more complex methods for analysis of pharmacokinetic data were introduced (Sheiner and Beal 1983), which allowed data from many individuals to be analyzed simultaneously. The NONMEM program introduced by Sheiner and Beal was a pioneering breakthrough for the application of nonlinear mixed effects modeling. The benefits of nonlinear

S.B. Duffull (✉)
School of Pharmacy, University of Otago, P.O. Box 56, Dunedin, New Zealand
e-mail: stephen.duffull@otago.ac.nz

mixed effects modeling allowed researchers to relax many logistical constraints which meant population pharmacokinetic studies could be performed in the target patient population, thereby maximizing the clinical utility of the pharmacokinetic information collected. Despite the benefits evident from the population approach, however, the design of these studies was considerably more complex and prone to failure. It was almost 20 years later before the first work appeared that provided a method for optimizing the design of nonlinear mixed effects models (Mentré et al. 1997). This work included a population pharmacokinetic example. Since this time the pharmaceutical literature has exploded with new methods and applications for optimal study design.

The aim of this chapter is to provide a brief overview of the theory and application of optimal design for population pharmacokinetic and pharmacokinetic–pharmacodynamic studies.

## 8.2 Theory of Optimal Design

In general, clinical trials provide two types of information: (1) the hypothesis test, i.e., *is the drug effective?* and (2) *what are the characteristics of the drug that confer effectiveness?* These questions have been posed under the framework of "learning and confirming" where the hypothesis testing in studies of type 1 constitute a confirming trial and studies of type 2 constitute a learning trial (Sheiner 1997).

The distinction between study types lies not in the quality of the study but in the type of information provided. Study type 1 provides confirmation about the utility of a drug and Study type 2 supports the science underpinning the claimed therapeutic utility. The confirming trial relies on a study design robust enough to provide a maximal probability the study will successfully test the hypothesis. In contrast, the learning trial relies on an experimental design exquisitely sensitive to the study conditions. A highly sensitive study maximizes the signal from any given change in the underlying system. It is the latter study type that predominates in pharmacokinetics, i.e., one

where we wish to characterize pharmacokinetic properties of the drug in question.

The sensitivity of a study can be formally described as the rate of change in the response of interest to a change in the parameter of interest. We assess this as the derivative, which we can compute easily using numerical methods, where

$$\frac{df}{d\theta} = f'(\theta) = \lim_{h \to 0} \frac{f(\theta + h) - f(\theta - h)}{2h}.$$

$\theta$ is a parameter of interest, $f$ is our response variable, and $h$ a change in the value of $\theta$, which is usually taken to be as small as practical. Since most pharmacokinetic models have more than one parameter, we would rewrite the notation as a partial derivative,

$$\frac{\partial f}{\partial \theta_1} = f'(\theta_1) = \lim_{h \to 0} \frac{f(\mathbf{\theta}, \theta_1 + h) - f(\mathbf{\theta}, \theta_1 - h)}{2h};$$
$$\mathbf{\theta} = (\theta_2 \ldots \theta_p)^{\mathrm{T}},$$
(8.1)

where, T is the transpose of the vector. Maximizing the derivative of the model with respect to the parameter values of interest will maximize our investigation's information content and, therefore, what we will learn.

### 8.2.1 Linear Regression

We introduce the derivation of optimal design within the framework of linear models. Linear regression models the linear relationship between the observed response $y$ and one or more covariates where:

$$\mathbf{y} = \mathbf{X}\mathbf{\theta} + \mathbf{\epsilon}; \ \ \epsilon \overset{\mathrm{iid}}{\sim} N(0, \sigma^2). \qquad (8.2)$$

$\mathbf{\theta}$ is a vector of coefficients, $\mathbf{X}$ is a matrix of covariates and $\mathbf{\epsilon}$ a vector of random errors which we assume to be independently and identically distributed with mean 0 and variance $\sigma^2$. The expectation and variance of $y$ are given by $E[\mathbf{y}] = \mathbf{X}\mathbf{\theta}$ and $V[\mathbf{y}|\mathbf{X}\mathbf{\theta}] = \sigma^2$.

Various methods have been developed for parameter estimation in linear regression. The simplest and most commonly used is ordinary least square (OLS). OLS methods minimize the sum of the squared residuals (SS), which is given by $SS = (\mathbf{y} - \mathbf{X}\boldsymbol{\theta})^T(\mathbf{y} - \mathbf{X}\boldsymbol{\theta})$. We can find the values of $\boldsymbol{\theta}$ that minimize the sum of squares by solving for $\boldsymbol{\theta}$ when the derivative of the sum of squares given $\boldsymbol{\theta}$ equals zero. This gives rise to $\boldsymbol{\theta} = (\mathbf{X}^T\mathbf{X})^{-1}\mathbf{X}^T\mathbf{y}$. For simplicity we assume the variance $\sigma^2$ is homoscedastic. The variance–covariance matrix of estimation is therefore $\mathbf{V} = (\mathbf{X}^T\mathbf{X})^{-1}$. The smaller the variance–covariance matrix, the more precise the estimates of $\boldsymbol{\theta}$. It can be seen that if the derivatives of the model are computed with respect to the parameter vector $\boldsymbol{\theta}$ (as per (8.1)), the sensitivity matrix is given by $\mathbf{X}$ and the product of the sensitivity matrices (which is termed the Fisher information matrix, $\mathbf{M}_F$) will yield $\mathbf{X}^T\mathbf{X}$.

The associated standard error (SE) for the vector of coefficients $\boldsymbol{\theta}$ is given by the square root of the diagonal entries of the variance–covariance matrix. Since SE is a function of the covariate $\mathbf{X}$ only, thus optimizing $\mathbf{X}$ will minimize the SE. According to the Cramér–Rao inequality (Cramér 1946; Rao 1945), the Fisher information matrix is the lower bound of the variance–covariance matrix $\mathbf{V} \geqslant \mathbf{M}_F^{-1}$ (note here that this inequality implies that the difference of the inverse of the Fisher information matrix from the variance–covariance matrix will be positive definite). Therefore the standard error can be approximated with the inverse of the Fisher information matrix.

Using the simple linear regression model $y = \theta_1 + \theta_2 x$ the expected value of $\mathbf{Y}$ is equal to $E[y] = \mathbf{X}\boldsymbol{\theta}$

$$E\begin{bmatrix} y_1 \\ y_2 \\ \vdots \\ y_n \end{bmatrix} = \begin{bmatrix} 1 & x_1 \\ 1 & x_2 \\ \vdots & \vdots \\ 1 & x_n \end{bmatrix} \begin{bmatrix} \theta_1 \\ \theta_2 \end{bmatrix}.$$

Locating values of $x_i$; $i = 1, \ldots, n$ that minimize the variance–covariance matrix of estimation, thus minimizing the SE, is equivalent to maximizing the Fisher information matrix since the Fisher information matrix is the inverse of variance–covariance matrix. If two designs are considered – one where Design 1 has six values of $x_i$ evenly spaced over the range and one (Design 2) where the values of $x_i$ are optimized so that they minimize the variance–covariance matrix $\mathbf{V}$, then for Design 2 all the values of $x_i$ are located at only two points on the line, with three points at the lowest and three points at the highest value of the range (Fig. 8.1). Note that it is not necessary to know the values of $\theta_1$ or $\theta_2$ to optimize the design for linear regression. In this particular example optimizing the location of the values of $x_i$ significantly improves the efficiency of the design.

## 8.2.2 Nonlinear Regression

Now consider models nonlinear in the parameter values. The same process is followed but the sensitivity matrix is now also a function of the unknown parameter values. As an example, consider an instantaneous input single compartment model of the form:

$$y_j = f_j + \varepsilon_j; \ \varepsilon_j \overset{\text{iid}}{\sim} N(0, \sigma^2). \tag{8.3}$$

where, $f_j = \dfrac{D}{Vd} \exp\left(-\dfrac{CL}{Vd} t_j\right)$.

CL and Vd are clearance and volume of distribution. The predicted concentration $f$ changes over time $t$ for a drug given dose $D$.

The first partial derivative of this model with respect to CL is

$$\frac{\partial f}{\partial CL} = \frac{-Dt}{Vd^2} \exp\left(-\frac{CL}{Vd} t\right)$$

omitting the index $j$ for simplicity. If $D = Vd = 1$ and $CL = \ln(2)$, then the concentration $f$ and the absolute value of the sensitivity of the concentration to the changes in CL for different values of $t$ is shown in Fig. 8.2. The sensitivity matrix can be extended to include all partial derivatives for all parameters $(\theta_i; \ i = 1, \ldots, p)$ at time
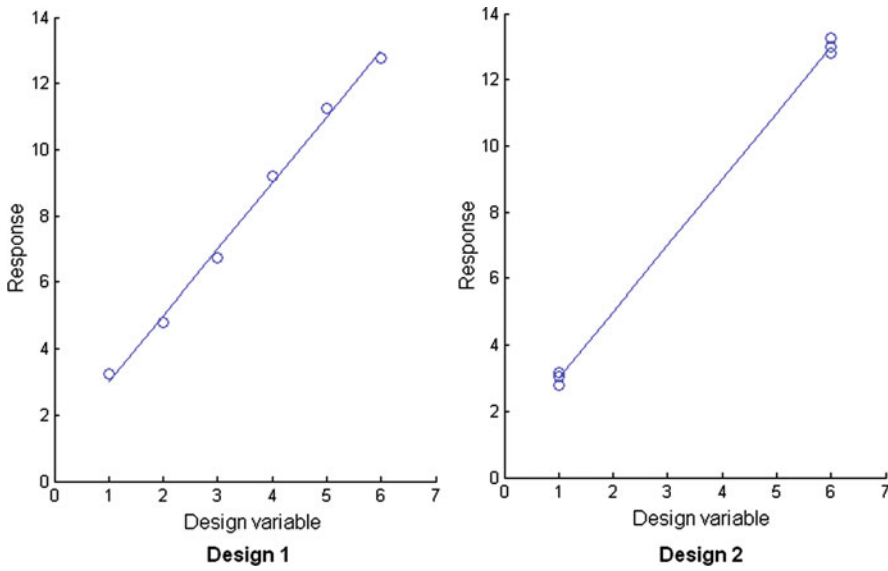
**Fig. 8.1** Design $1 - x_i$ evenly spaced over the range. Design $2 - x_i$ located at only two points at the lowest and highest value of the range
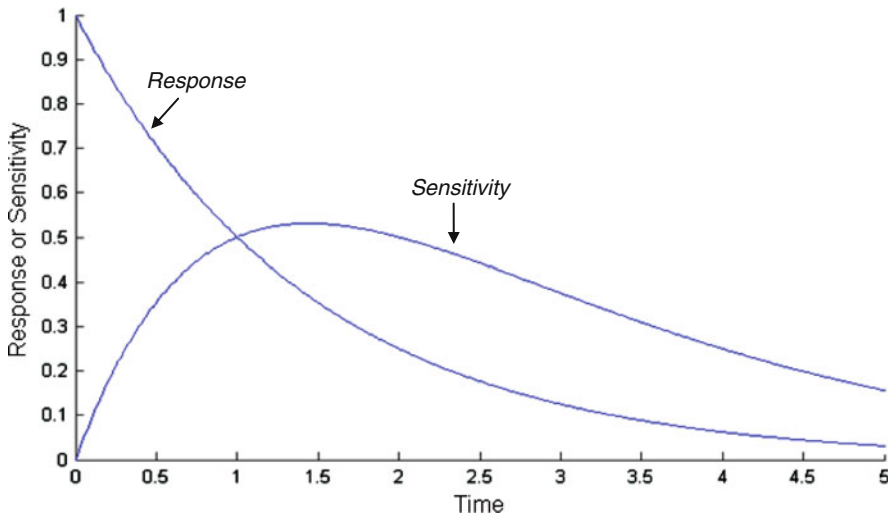


**Fig. 8.2** The function value and the sensitivity of the concentration to changes in CL for different $t$ values

points of interest $(t_j; \; j = 1, \ldots, n)$, which is then termed the Jacobian matrix:

$$\mathbf{J} = \begin{bmatrix} \dfrac{\partial f(t_1)}{\partial \theta_1} & \cdots & \dfrac{\partial f(t_1)}{\partial \theta_p} \\ \vdots & \ddots & \vdots \\ \dfrac{\partial f(t_n)}{\partial \theta_1} & \cdots & \dfrac{\partial f(t_n)}{\partial \theta_p} \end{bmatrix}.$$

For the instantaneous input single compartment model $p = 2$ and

$$\mathbf{J} = \begin{bmatrix} \dfrac{\partial f(t_1)}{\partial \mathrm{Vd}} & \dfrac{\partial f(t_1)}{\partial \mathrm{CL}} \\ \vdots & \vdots \\ \dfrac{\partial f(t_n)}{\partial \mathrm{Vd}} & \dfrac{\partial f(t_n)}{\partial \mathrm{CL}} \end{bmatrix},$$

$$
= \begin{bmatrix}
\frac{D}{\mathrm{Vd}^2}\left(\frac{\mathrm{CL}}{\mathrm{Vd}}t_1 - 1\right) & \\
\times \exp\left(-\frac{\mathrm{CL}}{\mathrm{Vd}}t_1\right) & \frac{-Dt_1}{\mathrm{Vd}^2}\exp\left(-\frac{\mathrm{CL}}{\mathrm{Vd}}t_1\right) \\
\vdots & \vdots \\
\frac{D}{\mathrm{Vd}^2}\left(\frac{\mathrm{CL}}{\mathrm{Vd}}t_n - 1\right) & \\
\times \exp\left(-\frac{\mathrm{CL}}{\mathrm{Vd}}t_n\right) & \frac{-Dt_n}{\mathrm{Vd}^2}\exp\left(-\frac{\mathrm{CL}}{\mathrm{Vd}}t_n\right)
\end{bmatrix}.
$$

In the case of linear regression, the Fisher information matrix for the linear regression model was introduced as $\mathbf{M}_F = \mathbf{X}^T\mathbf{X}$. Here the sensitivity matrices for the linear case are replaced with the Jacobian matrices and the Fisher information matrix is written as $\mathbf{M}_F = \mathbf{J}^T\mathbf{J}$. Note that $\mathbf{J} = \mathbf{X}$ for linear models.

### 8.2.3 Accounting for Random Noise

In our derivation of the information matrix for linear and nonlinear models, random error has been ignored. In doing so, the model is forced to have an implicit additive variance structure. All designs, however, must consider how reliable response measurements can be determined at different sampling times since there is always random noise in an experiment. If there were no experimental noise then, on the basis of the signal to noise ratio, every design would be the optimal design. If the random noise in an experiment, referred as the residual unexplained variability (RUV), exceeds the variability in the response, then the design will be poor since any information contained in the response will be overwhelmed in the random noise of the experiment. Hence, the response should be weighted by the random noise, or RUV.

The Fisher information matrix weighted by the random noise is, therefore, $\mathbf{M}_F = \mathbf{J}^T\mathbf{\Sigma}^{-1}\mathbf{J}$ for the nonlinear regression model and $\mathbf{M}_F = \mathbf{X}^T\mathbf{\Sigma}^{-1}\mathbf{X}$ for linear model where in both cases $\mathbf{\Sigma} = \sigma^2 \cdot \mathbf{I}_n$ and $\sigma^2$ is defined in either (8.2) or (8.3) and $\mathbf{I}_n$ is the identity matrix of dimension $n$, where $n$ is the number of observations.

In pharmacokinetic studies, there are three common forms of error models. Since the Jacobian matrix is weighted by the residual error,

**Table 8.1** Common error models and variance structures

| Error model | Notation | Variance |
|---|---|---|
| Additive | $y_j = f_j + \varepsilon_j$ | $\sigma^2 = \sigma_{\mathrm{add}}^2$ |
| Proportional | $y_j = f_j \cdot (1 + \varepsilon_j)$ | $\sigma_j^2 = \sigma_{\mathrm{prop}}^2 \cdot f_j^2$ |
| Combined | $y_j = f_j \cdot (1 + \varepsilon_{1,j})$ $+ \varepsilon_{2,j}$ | $\sigma_j^2 = \sigma_{\mathrm{prop}}^2 \cdot f_j^2$ $+ \sigma_{\mathrm{add}}^2$ |

different error models will affect the informativeness of the design. The three error models are shown in Table 8.1 and the sensitivity of the response ($f$) to CL over the range of times for each of the error models is shown in Fig. 8.3.

The importance of error model specification is most obvious in the proportional error model. It is seen in Fig. 8.3 that the design becomes exponentially more informative as the concentrations decline (exponentially). This error model implies that as the concentration approaches zero, the error approaches zero and hence the design would be optimal. Clearly this is an unreasonable assertion and it highlights the inappropriateness of this particular error structure.

### 8.2.4 Nonlinear Mixed Effects Regression

Finally, the notation for a nonlinear mixed effects regression model is introduced. This model consists of a two-stage hierarchy:

Stage 1 – model for the data

$$
y_{ij} = f(x_{ij}, \theta_i) + \varepsilon_{ij}; \ \varepsilon_{ij} \overset{\mathrm{iid}}{\sim} N(0, \sigma^2).
$$

Stage 2 – model for heterogeneity

$$
\theta_i = g(z_i, \theta) + \eta_i; \ \eta_i \overset{\mathrm{iid}}{\sim} N(0, \omega).
$$

The parameters of interest include both the fixed effects and the variance of the random effects, $\Phi = (\theta_1, \ldots, \theta_p, \omega_1, \ldots, \omega_q, \sigma^2) = (\boldsymbol{\theta}, \Omega, \Sigma)$. In contrast to fixed effects models, for nonlinear mixed effects regression, neither the expectation $E[\mathbf{y}]$ nor the variance $\mathbf{V}$ are available in closed form. It is usual to therefore linearize the model around the random effects using a first order Taylor series approximation to give:
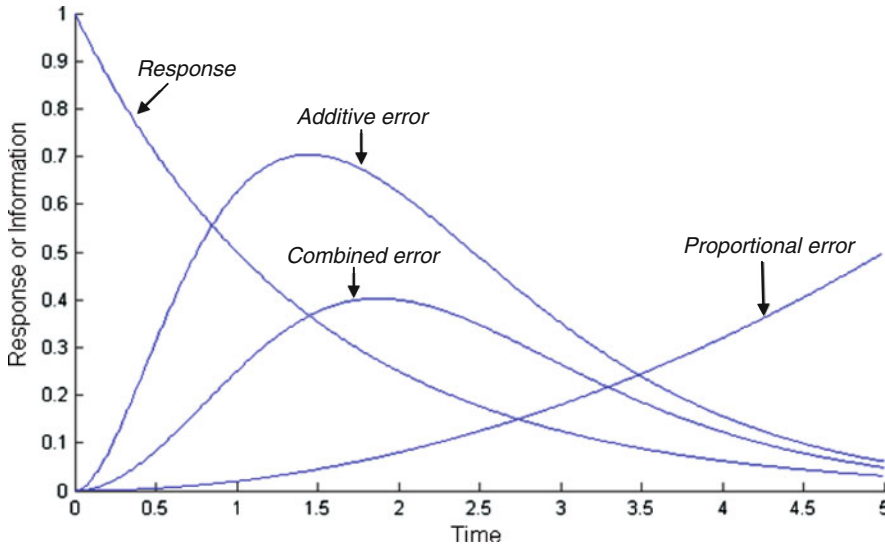
**Fig. 8.3** The graph shows how different error models affect the informativeness of the design

$$E[\mathbf{y}] \approx f(x_j, \boldsymbol{\theta}) \text{ and } \mathbf{V} \approx \mathbf{J}^{\mathrm{T}}\boldsymbol{\Omega}\mathbf{J} + \boldsymbol{\Sigma}.$$

The Fisher information matrix for a nonlinear mixed effects regression model is then given by

$$\mathbf{M}_{\mathrm{F}}(\boldsymbol{\Phi}, \Xi) = \begin{bmatrix} \mathbf{A}(E, \mathbf{V}) & \mathbf{C}(E, \mathbf{V}) \\ \mathbf{C}'(E, \mathbf{V}) & \mathbf{B}(E, \mathbf{V}) \end{bmatrix}$$

$$\mathbf{A}(E, \mathbf{V}) = 2\mathbf{J}\mathbf{V}^{-1}\mathbf{J} + \mathrm{tr}\left(\frac{\partial \mathbf{V}}{\partial \theta_n} V^{-1} \frac{\partial \mathbf{V}}{\partial \theta_m} \mathbf{V}^{-1}\right);$$

$$m \& n = 1, \ldots, p$$

$$\mathbf{B}(E, \mathbf{V}) = \mathrm{tr}\left(\frac{\partial \mathbf{V}}{\partial \lambda_n} \mathbf{V}^{-1} \frac{\partial \mathbf{V}}{\partial \lambda_m} \mathbf{V}^{-1}\right);$$

$$m \& n = 1, \ldots, q$$

$$\mathbf{C}(E, \mathbf{V}) = \mathrm{tr}\left(\frac{\partial \mathbf{V}}{\partial \lambda_n} \mathbf{V}^{-1} \frac{\partial \mathbf{V}}{\partial \theta_m}\right);$$

$$m = 1, \ldots, p; \ n = 1, \ldots, q$$

$$\boldsymbol{\Phi} = (\theta_1, \ldots, \theta_p, \omega_1, \ldots, \omega_q, \sigma^2) \text{ and}$$
$$\boldsymbol{\lambda} = (\omega_1, \ldots, \omega_q, \sigma^2)$$

where $\mathrm{tr}(\cdot)$ is the trace function.

### 8.2.5 Defining a Population Design

A population design is the sum of the information from each patient in the study. In the above notation $\Xi$ was used to represent a population design. Here, $\Xi$ is defined by

$$\Xi = \begin{bmatrix} \xi_1 & \cdots & \xi_N \\ w_1 & \cdots & w_N \end{bmatrix} \text{ and } \xi = \begin{bmatrix} x_1 & \cdots & x_n \\ v_1 & \cdots & v_n \end{bmatrix}.$$

The variables $N$, $w$, $x$, and $v$ are used to denote the number of elementary designs, the weighting for each elementary design, the support points within an elementary design and the weighting for each of the support points, respectively. If there were the same number of elementary designs as there were patients in the study then $\xi$ would represent an individual design for a single patient much as would be considered for the nonlinear regression example above. It is inefficient to consider a separate design for each patient since logistical issues would forbid a study protocol that listed out a different design for every patient in a particular study! It is therefore usual to consider $\xi$ to be an elementary design for which a proportion of patients $w$ are assigned. A cohort of patients who are assigned

to a single elementary design is termed as a group of patients with the patients within any given group being considered exchangeable. The simplest population design would therefore have a single elementary design, i.e., $N = 1$, providing a single group of patients. This type of design is similar to the designs used prior to the advent of nonlinear mixed effects modeling software. If there is more than 1 elementary design it is straightforward to deduce that each elementary design may have fewer support points than there are fixed effects parameters to estimate since there will be borrowing strength between groups of patients. In the following equation we show the information matrix for a population design as the sum of the information matrices from the $N$ groups of patients as

$$\mathbf{M}_{\text{F}}(\boldsymbol{\Phi}, \boldsymbol{\Xi}) = \sum_{k=1}^{N} n_k \mathbf{M}_{\text{F}_k}(\boldsymbol{\Phi}, \xi_k).$$

For further discussion on sparse designs see Duffull et al. (2005).

For the purposes of this chapter $x$ will be considered to be a sampling time, but this is not a requirement of population optimal designs and realistically any controllable independent variable could be included as a potential design variable, including dose, infusion duration and so forth. It is important to note that optimizing over multiple conditionally independent variables simultaneously on continuous space is not a simple problem.

## 8.2.6  Optimality Criteria

An optimal design is one in which the $M_{\text{F}}$ matrix is maximized in some manner. The process of optimizing the Fisher information matrix is usually simplified by computing a criterion that summarizes the size (or volume) of the matrix. The choice of the criterion will depend on what the researcher wishes to learn. The most commonly used summary measures are the alphabetic optimality criteria (Atkinson and Donev 1992). Generally A, C, D, E, G, L, Q, and V criteria (some of

which will be discussed shortly) have been used to optimize a design for parameter estimation where the design is conditioned in a prior point estimate of the parameter value. The multiple letter optimality in particular, ED and EID (Walter and Pronzato 1987), API (D'Argenio 1990), HClnD (Foo and Duffull 2010) have been used where the design is conditioned in a prior distribution of the likely values of the parameters. Criteria for model discrimination include Ds and T optimality.

The D-optimality criterion, which refers to the determinant of a matrix, is the most commonly used summary measure of the "bigness" of a matrix in PKPD. The criterion is given by

$$\Psi_{\text{D}} = \det \begin{bmatrix} \mathbf{M}_{\text{F}_{1,1}} & \mathbf{M}_{\text{F}_{1,2}} \\ \mathbf{M}_{\text{F}_{2,1}} & \mathbf{M}_{\text{F}_{2,2}} \end{bmatrix}$$
$$= \mathbf{M}_{\text{F}_{1,1}} \times \mathbf{M}_{\text{F}_{2,2}} - \mathbf{M}_{\text{F}_{1,2}} \times \mathbf{M}_{\text{F}_{2,1}}.$$

The determinant is defined as the volume of the joint confidence ellipsoid when taken on the variance–covariance matrix. Minimizing the determinant of the variance–covariance matrix is equal to maximizing the determinant of the $M_{\text{F}}$ matrix since $\left| M_{\text{F}}^{-1} \right| = \left| M_{\text{F}} \right|^{-1}$ and $\log \left| M_{\text{F}}^{-1} \right| = -\log \left| M_{\text{F}} \right|$ which is a useful finding since inverting a scalar (e.g. a determinant) is considerably easier than inverting a large matrix, where $|\cdot|$ denotes the determinant.

The value of $\Psi_{\text{D}}$ has no intrinsic meaning but values can be compared empirically and the largest one relates to the better design. A $\Psi_{\text{D}}$ may be transformed into an efficiency rating when comparing to another $\Psi_{\text{D}}$ by taking the ratio to the $p$th root (where $p = $ total number of parameters).

$$\text{Eff} = \left( \frac{\Psi_{\text{D}}(1)}{\Psi_{\text{D}}(2)} \right)^{\frac{1}{p}}.$$

The efficiency (Eff) which is expressed as a fraction provides some indication of the approximate number of patients required for Design 1 to be equivalently informative to Design 2. For example if Eff $= 0.5$, then for a single group design the number of patients in Design 1 needs to be doubled to achieve the same efficiency as Design 2.

## 8.3 Application of Optimal Designs

In this section particular issues pertinent to the application of optimal design to population pharmacokinetic–pharmacodynamic studies will be considered. In the following subsection, designs robust to misspecification of the prior parameter values and misspecification of the likely model will be discussed. Later subsections deal with designs for discrimination between competing models, a framework for considering designs for multiple response (MR) models, and finally an introduction to sampling windows.

### 8.3.1 Robust Designs

Two main sources of uncertainty should be taken into account prior to conducting the experiment: (1) uncertainty in the model space and (2) uncertainty in the parameter space. In both cases it is natural to consider optimizing the prior information that is available. For the special case of linear models, only uncertainty in the likely model space is necessary (since the Fisher information matrix for linear regression does not depends on the parameter values), whereas for nonlinear models it is also important to establish designs that are robust to the prior initial estimate of the parameter values.

#### 8.3.1.1 Designs Robust to the Parameter Space

There are a variety of criteria available for summarizing the Fisher information matrix over a distribution of possible prior parameter values. Three criteria will be briefly introduced: ED, API, and HClnD. Each of these criteria involves evaluating the determinant of the Fisher information matrix over the prior distribution of the parameter values.

As noted in the section on nonlinear mixed effects regression, the parameters of interest for a nonlinear mixed effects model include both the fixed effects and random effects, $\Phi = (\boldsymbol{\theta}, \boldsymbol{\Omega}, \boldsymbol{\Sigma})$. It is common to use Monte Carlo simulations to generate the underlying parameter space for the purpose of robust designs. However, this may be computationally impractical for models of high dimension. It is important that the distributional form for each parameter should ensure that only legal values are generated, for instance this could mean a multivariate log-normal distribution for fixed effects parameters, an inverse Wishart distribution for the variance–covariance matrix of the between subject effects and an inverse gamma distribution for the distribution of the residual variance. Fortunately, the computational burden can be eased since the value of the variance of the between-subject random effects parameters often has limited influence on the support points for the design and, hence, the dimensionality can be reduced by considering uncertainty (i.e. a prior) on the fixed effects parameters only.

The ED-optimality criterion (Walter and Pronzato 1987; and for applications see Hooker et al. 2003) optimizes the design by maximizing the expectation of the determinant of the Fisher information matrix over the prior of the parameters so that

$$\Psi_{ED} = \begin{array}{c} \arg \max \\ \Xi \end{array} (E[|\mathbf{M}_F(\boldsymbol{\theta}, \Xi)|])$$

$$= \begin{array}{c} \arg \max \\ \Xi \end{array} \int_{-\infty}^{\infty} \cdots \int_{-\infty}^{\infty} |\mathbf{M}_F(\boldsymbol{\theta}, \Xi)|$$

$$\times g(\boldsymbol{\theta}) \, d\theta_1 \dots \theta_p \text{ and}$$

$E[\cdot]$ is the expectation value and $g(\boldsymbol{\theta})$ is the joint prior distribution of the parameters.

The API-optimality criterion (D'Argenio 1990) optimizes the design by maximizing the expectation of the logarithmic of the determinant of the Fisher information matrix over the prior of the parameters

$$\Psi_{API} = \begin{array}{c} \arg \max \\ \Xi \end{array} (E[\log(|\mathbf{M}_F(\boldsymbol{\theta}, \Xi)|)])$$

$$= \begin{array}{c} \arg \max \\ \Xi \end{array} \int_{-\infty}^{\infty} \dots \int_{-\infty}^{\infty} \log(|\mathbf{M}_F(\boldsymbol{\theta}, \Xi)|) \times g$$

$$\times (\boldsymbol{\theta}) \, d\theta_1 \dots \theta_p.$$

The API method is similar in spirit to ED optimality. It is usual in both methods to use

Monte Carlo simulations to solve for the multiple integrals and these would usually be set up over a definite integral space. Recent work suggests that the API design has more consistent properties compared to ED design and generally performs slightly better in terms of providing designs with lower standard errors (Foo et al. submitted). However, this work has only incorporated models of low dimensionality where the integrals could generally be solved in closed form.

A relatively new criterion is hypercube D-optimality (HClnD), which uses the same technique as product D-optimality (Zhu and Wong 2000) and has been shown to be consistent and as accurate as ED and API but generally 100-fold faster (Foo and Duffull 2010; Foo et al. submitted). HClnD-optimality criterion optimizes the design over extrema regions of the parameter domain

$$\Psi_{\mathrm{HC}In\mathrm{D}} = \mathop{\arg\max}_{\Xi} \left( \sum_i^m \log\left( \left| \mathbf{M}_{\mathrm{F}}(\boldsymbol{\theta}^{\{i\}}, \Xi) \right| \right)^{\frac{1}{p}} \right),$$

where there are $m$ combinations of parameter values with each set representing a vertex on a "hypercube." Generally, the parameter set would be taken at the 95% confidence intervals so that a two parameter model, the hypercube, would be formed from $m = 4$ sets of parameters.

| Parameter set $i$ | Parameter values |
|---|---|
| 1 | $\theta_{1,L}, \theta_{2,L}$ |
| 2 | $\theta_{1,H}, \theta_{2,L}$ |
| 3 | $\theta_{1,L}, \theta_{2,H}$ |
| 4 | $\theta_{1,H}, \theta_{2,H}$ |

$L$ and $H$ represent low and high values for the parameter, respectively.

Other similar applications of this criterion have been published (Waterhouse et al. 2005; McGree et al. 2007; Hennig et al. 2007; Roos et al. 2008).

### 8.3.1.2 Designs Robust to the Model Space

Developing designs robust to the model space may arise under many settings. In the first setting there may be uncertainty on the form of the final model, perhaps a nonlinearity in the disposition phase is suspected, and a design is required to perform well over a range plausible alternative candidate models (see for example Waterhouse et al. 2005; Roos et al. 2008). The second scenario may arise where there is more than one drug being administered at the same time, perhaps a drug–drug interaction study, and hence the design should perform well over both drugs. From a design perspective these scenarios are equivalent.

Let us consider the example where there are two possible models M1 and M2, M1 ≠ M2, where

$$M1 = \theta_1^{\{1\}} \exp(-\theta_2^{\{1\}} \cdot t),$$

$$M2 = \theta_3^{\{2\}} \frac{\theta_1^{\{2\}}}{\theta_1^{\{2\}} - \theta_2^{\{2\}}} (\exp(-\theta_2^{\{2\}} \cdot t)$$
$$- \exp(-\theta_1^{\{2\}} \cdot t)).$$

We use the index $\{i\}$ to denote the model. Here the product D-optimal design can be used to derive design that is robust to the uncertainty in the model space (Zhu and Wong 2000). Product D-optimality is similar to HClnD in that it combines the information across models by summing the log of the determinants

$$\Psi_{\mathrm{PD}} = \mathop{\arg\max}_{\Xi_{\mathrm{PD}}} \left( \sum_i^m \log\left( \left| \mathbf{M}_{\mathrm{F}}(\boldsymbol{\theta}^{\{i\}}, \Xi_{\mathrm{PD}}) \right| \right)^{\alpha_i/p_i} \right),$$

which provides a similar solution to Bayesian model averaging (Hoeting et al. 1999). Product D-optimality differs from HClnD in that the value of $\alpha$, the weighting for each model, can be specified and the dimension of the model $p_i$ is not necessarily the same for all models. The efficiency of the product design for estimation of the parameters under any given model, e.g., M1, can then be compared to the D-optimal design for this model in order to assess the loss of efficiency associated with optimizing over a number of competing models as

$$\mathrm{Eff}_{\mathrm{M1}} = \left( \frac{|\mathbf{M}_{\mathrm{F}}(\boldsymbol{\Phi}_1, \hat{\Xi}_{1_{\mathrm{PD}}})|}{|\mathbf{M}_{\mathrm{F}}(\boldsymbol{\Phi}_1, \hat{\Xi}_{1_{\mathrm{D}}})|} \right)^{\frac{1}{p_1}}.$$

In this notation, $\hat{\Xi}_{1_{PD}}$ is the design optimized under the product D-optimal criterion for M1 and $\hat{\Xi}_{1_D}$ is the design optimized under the D-optimal criterion for M1 only.

### 8.3.2 Model Discrimination

Criteria for model discrimination differ from criteria for parameter estimation. Indeed designs that are optimal for discrimination are generally suboptimal for parameter estimation and vice-versa (Atkinson 2008; Waterhouse et al. 2009). Hence optimizing a design solely for discrimination does not guarantee that the design will perform well for parameter estimation. Indeed the work of McGree et al. (2008) addresses potential compound criteria that could be used to incorporate design criteria that are naturally opposed (such as D and T optimality).

The two most commonly used criteria for model discrimination are T and $D_S$-optimality. T-optimal designs are so-called because they maximize the design for model discrimination using an F-test, where T denotes *testing* (Atkinson and Fedorov 1975a; Atkinson and Fedorov 1975b). The T-optimality criterion follows a standard mini-max framework where for two models M1 and M2, M1 $\neq$ M2, predictions of the concentration are made from M1 and M2 is fitted to this data thereby providing parameter estimates for M2 by minimizing the sum of squared differences. At the next stage, times are selected that maximize the sum of squared differences between M1 and M2 under the current parameter estimates for M2. Given these new time points model predictions are made from M1 and M2 is fitted to these predictions. The process is then repeated. This is shown as

$$\text{Step 1}: \hat{\boldsymbol{\theta}}^{\{2\}}(\hat{\xi}) = \arg\min_{\boldsymbol{\theta}^{\{2\}}} \sum (M1 - M2(\hat{\xi}, \boldsymbol{\theta}^{\{2\}}))^2,$$

$$\text{Step 2}: \hat{\xi} = \arg\max_{\xi} \sum (M1 - M2(\xi, \hat{\boldsymbol{\theta}}^{\{2\}}))^2.$$

For the first iteration of step 1 an initial estimate of the design ($\xi_0$) is substituted for the

T-optimized design $\hat{\xi}$. Note, T-optimality does not require that the two models are nested.

$D_S$-optimality is essentially D-optimality where a subset of the parameters is considered to be nuisance parameters. This procedure can be used for model discrimination if M1 and M2 are nested and share a common structure, i.e., M1 $\subset$ M2. Accurate estimation of the noncommon parameters present in M2 will enable M2 to be distinguished from M1. However as with T-optimality, designs that are $D_S$-optimal may be degenerate for parameter estimation for both M1 and M2.

The criterion is provided by partitioning the information matrix into submatrices that contain the parameters of interest and nuisance parameters separately. Here we are only interested in the information matrix for the parameters of M2 that are not shared by M1, shown here as $\mathbf{M}_{F_{2,2(M2)}}$

$$\mathbf{M}_{F_{(M1M2)}} = \det \begin{bmatrix} \mathbf{M}_{F_{1,1(M1M2)}} & \mathbf{M}_{F_{1,2(M1M2)}} \\ \mathbf{M}_{F_{2,1(M1M2)}} & \mathbf{M}_{F_{2,2(M2)}} \end{bmatrix},$$

$$\Psi_{D_S} = \left| \mathbf{M}_{F_{2,2(M2)}} \right| = \frac{\left| \mathbf{M}_{F_{(M1M2)}} \right|}{\left| \mathbf{M}_{F_{1,1(M1M2)}} \right|}.$$

### 8.3.3 Multiple Response Models (MR)

There are at least three types of MR model frameworks that may occur in PKPD. All of these models are linked by common fixed effects. We use $A$ to denote the amount of drug input into the system. (1) Nested unidirectional where

$$A \rightarrow B \rightarrow C,$$

for example PKPD and parent and metabolite models. Here $B$ and $C$ could be the concentration of parent and metabolite in the plasma. The responses in these models are linked by common fixed effects. (2) Nested bidirectional,

$$A \rightarrow B \leftrightarrow C.$$

For example, a pharmacokinetic model where observations are taken from two compartments in

equilibrium (e.g. plasma ($B$) and cerebrospinal fluid ($C$)). And finally, (3) Nonnested,

$$A \rightarrow B \ \& \ A \rightarrow C,$$

which might arise in the situation in which there are two clearance mechanisms that run in parallel and the end products of both are measured. Under the unidirectional nested model framework $A \rightarrow B \rightarrow C$ multiple responses ($B$) and ($C$) from administration of $A$ can be estimated from a single design. The conditional nature allows observations in $C$ to inform about the relationships from $A \rightarrow B$ and $B \rightarrow C$ whereas observations in $B$ only inform on $A \rightarrow B$. For PKPD we would have,

$$\text{Dose} \overset{\text{PK}-\text{model}}{\rightarrow} \text{Concentration} \overset{\text{PD}-\text{model}}{\rightarrow} \text{Effect}.$$

The information matrix for multiple response models is provided by summing the information about each parameter over each response (as per Draper and Hunter 1966 for a fixed effects model).

$$M_{\mathrm{F}} = \sum_{i=1}^{m} \sum_{j=1}^{m} \sigma_{ij} \mathbf{J}_i^{\mathrm{T}} \mathbf{J}_j,$$

where, $\mathbf{J}$ is the usual sensitivity matrix. Using more specific notation for a PKPD model then the PK data would provide the following information.

$$\mathbf{M}_{\mathrm{F_{PK|PK}}} = \begin{bmatrix} \mathbf{M}_{\mathrm{F_{1,1(PK|PK)}}} & 0 \\ 0 & 0 \end{bmatrix}.$$

The symbol "|" is used to denote that the information matrix is conditioned on specific data, for example $M_{\mathrm{F_{PK|PK}}}$ denotes the information matrix for the pharmacokinetics parameters conditioned on observing pharmacokinetic data. The PD responses provide information about the PK and PD models

$$\mathbf{M}_{\mathrm{F_{PKPD|PD}}} = \begin{bmatrix} \mathbf{M}_{\mathrm{F_{1,1(PK|PD)}}} & \mathbf{M}_{\mathrm{F_{1,2(PKPD|PD)}}} \\ \mathbf{M}_{\mathrm{F_{2,1(PKPD|PD)}}} & \mathbf{M}_{\mathrm{F_{2,2(PD|PD)}}} \end{bmatrix}.$$

The information matrix for the PKPD multiple response is thus given

$$M_{\mathrm{F_{PKPD|PKPD}}} = M_{\mathrm{F_{PK|PK}}} + M_{\mathrm{F_{PKPD|PD}}}.$$

The story has been generalized from fixed effects models and the computation of designs for PKPD is based on the same principles as used in NONMEM using the first-order method. Details and applications are provided by: McGree et al. (2009), Hooker and Vicini (2005), Waterhouse et al. (2005) and Gueorguieva et al. (2006).

### 8.3.4 Sampling Windows

Sampling windows represent a time window of opportunity where nearly optimal samples can be taken (Fig. 8.4). It is impossible for any executed clinical study to conform exactly to an optimal design where in this case the design will be suboptimal and termed "unplanned suboptimality," and represents a design in which the researcher did not plan for execution error. Sampling windows provide a mechanism for "planned suboptimality" where the researcher optimizes regions in which some level of execution error will have minimal effect on the performance of the design. Currently, three techniques have been proposed to estimate sampling windows: (1) analytical solution, (2) numerical estimation of windows and (3) POSTHOC simulation of windows. Newer methods based on adaptive designs have also been proposed (Duffull et al.).

#### 8.3.4.1 Analytical Solution
An analytical solution has been proposed based on the equivalence theorem for a fixed effects model. The equivalence theorem, which has also been proposed to apply to mixed effects models (Bogacka et al. 2005), states that (amongst other statements) the standardized variance of the prediction $d(t, \xi*, \boldsymbol{\theta})$ at $t$, defined as

$$d(t, \xi, \boldsymbol{\theta}) = \mathbf{J}(t_i, \boldsymbol{\theta}) \mathbf{M}_{\mathrm{F}}^{-1}(\xi, \boldsymbol{\theta}) \mathbf{J}^{\mathrm{T}}(t_i, \boldsymbol{\theta})$$
$$\text{for } t_i = t_1, \ldots, t_n,$$

will always be $\leq p$ and that $d(t, \xi*, \theta) = p$ at the optimum values of $t$ where $p$ is the number of
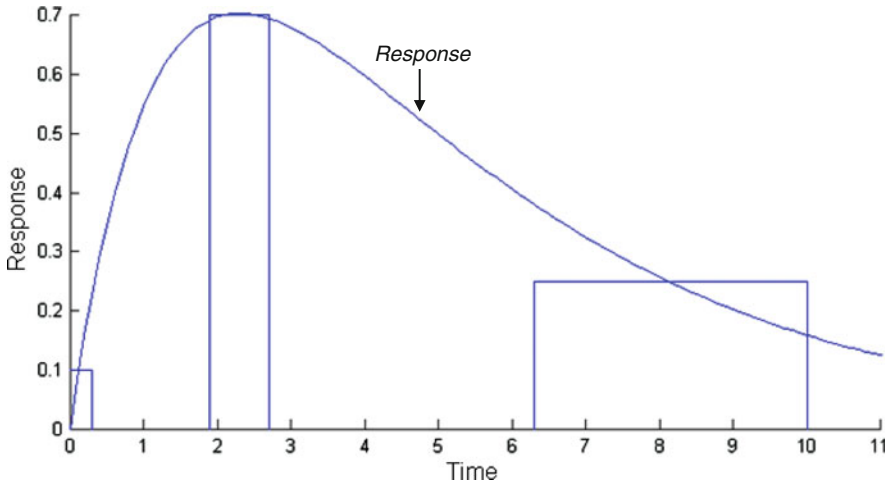
**Fig. 8.4** Graph shows three sampling windows for a nonlinear response model
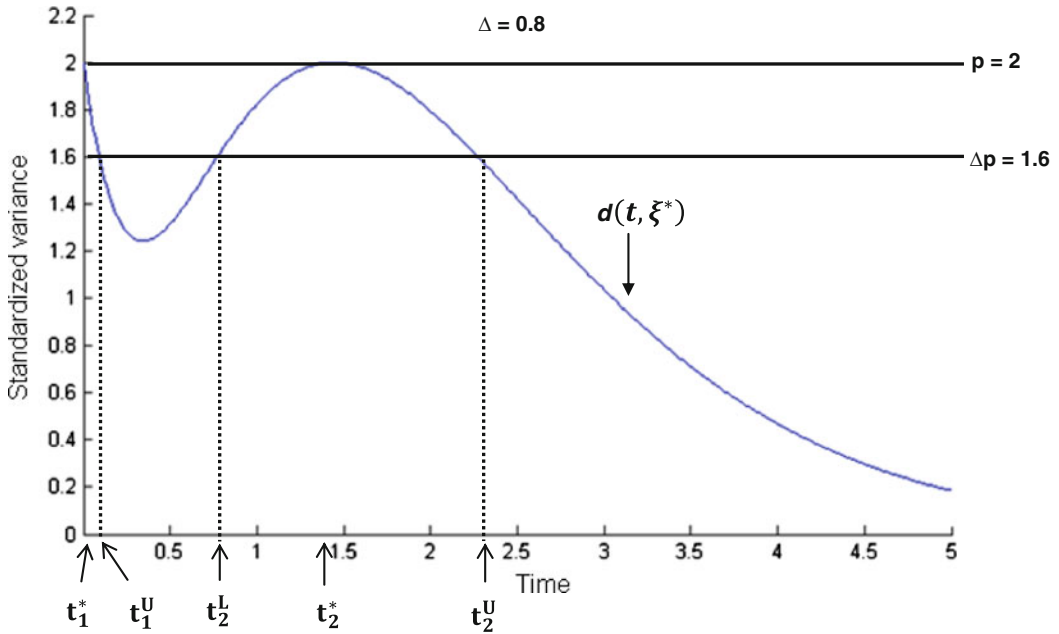


**Fig. 8.5** An example of the surface of the standardized variance and sampling windows

parameters (Atkinson and Donev 1992) and $\mathbf{J}(t_i, \theta)$ is the *i*th row in the Jacobian matrix. An example of the surface of the standardized variance is given in Fig. 8.5. This method does not currently link the loss $\Delta$ to a specific loss of efficiency but this could be performed easily. This method has analytical appeal as an exact

solution, but cannot be expressed explicitly for nonlinear mixed effects models.

### 8.3.4.2 Numerical Estimation of Windows

Two basic approaches have been proposed for this problem. The first method optimizes the length of a fixed set of sampling windows

assuming the windows are symmetric ($\pm \delta W$) around the optimal sampling times (Graham and Aarons 2008). An estimate of $\delta$ could then be included in the design. The assumption of symmetry and a uniform size of $\delta$ makes the method more difficult to use in a practical sense. Later research relaxed the assumption of symmetry. The second main method was based on constructing a finite set of potential sampling windows and then searching over the sampling window space to see which sampling windows appear to perform best (Ogungbenro and Aarons 2008) which is quite an appealing process as long as the user specifies at least one *good* set of sampling windows.

### 8.3.4.3 POSTHOC Simulation of Windows
An early description of this method (Duffull et al. 2001) is similar in spirit to a simplified profile likelihood method for determining a 95% confidence interval on a parameter (for estimation). The method is termed POSTHOC since the optimal design is estimated first and then the sampling windows computed subsequently. The method involves fixing all but one sampling time and then varying this sampling time until the efficiency of the design falls to some predefined value (say 80% of the efficiency of the optimal design). The method provides marginal estimates of the sampling windows. The main issue with this method is that the windows may not be sufficiently conservative since they do not account for correlation between samples. Despite this, the method has been used with success (Green and Duffull 2003). A Monte Carlo version has also been used where the joint windows are estimated by simulation (see for example Roos et al. 2008). This method avoids the less conservative pitfalls of the marginal estimates.

## 8.4 Practicalities

In this section we outline a framework for the application of the theory of optimal design for solving population pharmacokinetic or pharmacokinetic–pharmacodynamic problems. This includes a brief discussion of the design space,

some design tips and methods of assessment of the final design.

### 8.4.1 Design Space

In this section, basic components of the design, model, and parameter space are reviewed. In many cases the designer will not be the person who originally conceived the study and indeed there are some benefits of separating these processes. An initial interview process is essential to ensure that the study will meet the needs of the principle investigator while ensuring that it has a high probability of success. Typically, the designer must be familiar with the basic layout of the research study including the maximum number of patients that can be enrolled, the dosing schedule, the study layout (double blind, open label, cross-over), dates and times of clinic visits and the maximum number of samples per patient, as well as the likelihood of dropouts based on the investigator's prior experience. In addition, the designer should be aware of potential constraints on the design space and importantly the flexibility of these constraints. All constraints should be considered relative since experimental failure due to excessively tight constraints is an ultimate failure of a trial and the designer's role often requires a formal assessment of the constraints. In particular, a nonexhaustive list of typical constraints might include: samples are constrained to be the same for all groups (i.e. one sampling schedule), dose levels are fixed, samples from within a period of time (e.g. 8 h postdose) are constrained to be the same, some samples may be fixed (e.g. trough samples [it is a common misconception that trough samples are useful for estimating AUC]), samples may arise from complex procedures and cannot be readily repeated within a specified period of time, samples may be required within a defined period of time postdose, samples from multiple response models may be constrained to be at the same time (e.g. plasma drug concentration and plasma biomarker measurement) or may be required to be at different times (e.g. plasma drug concentration and blood pressure measurement).

All of these constraints form the basis for setting out the design space. Some, or many, of these constraints may have been decided arbitrarily by the principle investigator without critical thought.

In addition to design constraints the designer must also be critical of the model and parameter space. Considering a diverse model space helps your design to be robust to assumptions about the model. It should be noted that development teams often strive to find the best *single* model for their data. There is no reason to assume that this model will also be the best model for any new study design, e.g., a best model from a Phase 1 study is not necessarily going to be best for a Phase 2 study (see Roos et al. 2008 for an example of this). Questions the designer may ponder are: *what models could conceivably have described the prior data?* and *is there evidence of nonlinearity?* This latter question may require designs optimal for both parameter estimation and model discrimination. If there are uncertainties in the model space then there will almost certainly be uncertainty in the parameter space. Considering a diverse parameter space helps your design to be robust to assumptions about the parameter values. Some questions that the designer may ponder: *could patients in the new study have a lower or higher value of clearance than expected? Is a drug interaction possible? Would a greater than anticipated clearance affect the assay performance?*

## 8.4.2   Design Tips

Every design will have some individuality, which means that a standard recipe to solve the design problem is likely to provide suboptimal designs or perhaps even designs that fail. Despite this there are some practical considerations for designing studies. The first and, arguably, most important step is to ensure that the model(s) being used as the basis for the study design describe the potential data. When designing an experiment there is no data to let you assess whether your coded model is correct (and an error of units can have disastrous effects). It is therefore essential that the designer ensures that the model they are using as the basis of their design matches (or is able to match) the predictions of a model from a previous analysis.

Constructing a design provides an ideal opportunity for the designer to informally check the identifiability of the parameters of the proposed model. This process is not intended to replace formal identifiability theory, and is rather like a pleasant side effect of the design process. Simply, the Fisher information matrix for a model that is not identifiable will be rank deficient (i.e. have a column and a row of zeros) and therefore yield a determinant of zero. There are two types of identifiability: structural (*a priori*) identifiability and deterministic (*a posterior*) identifiability. Both can be assessed in the framework of design. Structural identifiability is used to refer to a model that has 1 or more parameters that cannot be locally identified irrespective of the intensity of the study design, for example attempting to estimate the fraction of drug absorbed for an oral dose when only oral dosing is being considered. Deterministic identifiability is more subtle and describes a model that is structurally identifiable but given the study constraints gives exceedingly poor parameter estimates and a determinant close to zero. Structural identifiability can be tested by assessing the information matrix using an impossibly intensive design with the thought that if this design doesn't work then something is wrong. Deterministic identifiability can be tested by assessing the information matrix for the most intensive (but allowable) design within the study constraints, for example a study where blood samples are not allowable within the first few hours will provide exceedingly poor estimates of a the model parameters of a rapid input phase.

Finally, here are some tips on developing designs. You will notice that the need for an optimization run, i.e., a formal numerical optimization process, is indeed rather uncommon.

1. Determine the maximum allowable design and evaluate its performance for the models under consideration. No optimization is needed to assess this.

2. Reduce the maximal design and assess the loss of design performance. No optimization needed to assess this.

3. Explore benefits of early versus late sampling and samples taken on the first dose or a dose at steady state. No optimization needed to assess this.

4. Establish a set of designs that appear to work well and optimize these to locate a currently optimal design.

5. Determine the sensitivity of the design to any assumptions that may have been made, i.e., the loss of efficiency given a change in a variable of interest.

### 8.4.3   Assessment of the Performance of the Design

A design that is optimal is not necessarily guaranteed to perform well in practice. It is possible to choose an optimal design from a set of candidate designs where all the candidates are poor. The performance question is therefore, *how well does the design fair when it is used in conjunction with the analysis software that will be used in the actual study*? This question can be answered with the use of simulation-estimation techniques. A common technique is to simulate a large number of data sets under the design and model(s), then fit the candidate models to these data and assess the parameter estimates. For an unbiased model, the standard deviation of the distribution of the set of parameter estimates is an empirical estimate of the asymptotic standard error. These values should agree with those predicted from the Fisher information matrix.

### 8.5   Software

There are numerous software programs available for optimizing the design of population pharmacokinetic and pharmacokinetic–pharmacodynamic studies (Mentré et al. 2007). Important differences are inherent in the platform they use

(some rely on the presence of R or MATLAB) or on their range of built-in features. These include robust design features, the ability to handle a variety of design constraints and types of models. Selected software details are presented below.

The earliest design software was based on population Fisher-information matrix (PFIM), which was developed in S (PFIM_S) and MATLAB (PFIM_M) simultaneously in 1999 (Retout et al. 2001). PFIM, which has a graphical user interface (GUI) called the PFIM interface, has been further developed and now runs under R as a set of scripts from the command line in R. POPT (Population OPTimal design) was developed from the MATLAB version of PFIM. POPT requires MATLAB to run and uses the MATLAB script functionality to describe models. WinPOPT (Windows Population OPTimal design) is a Windows GUI version of POPT and runs as a standalone program. It contains most of the same features as POPT. PopDes (population design) is a graphic user interface for a set of script/function applications written in MATLAB and requires MATLAB to run. PopED (population optimal experimental design – note this software also uses the ED-optimality criterion) is a GUI for a set of script/function applications written for MATLAB and requires either MATLAB or O-Matrix to run. PkStaMp (pharmacokinetic sampling times allocation – Matlab platform) is a graphic user interface of a set of scripts/functions written in MATLAB and runs as a standalone program. All software except PkStaMp are freely available for download.

Note, at the time of writing this chapter all software can be identified easily using the Google search engine, except POPT which can be located using the term "WinPOPT."

### 8.6   Examples

The application of optimal design is illustrated through an example of designing a population study for a drug following a one compartment first order input PK model of the form:

$$C_{ij} = \frac{D_i \text{ka}_i}{\text{Vd}_i(\text{ka}_i - \text{k}_i)}$$
$$\times \left[ \exp(-\text{k}_i \cdot t_{ij}) - \exp(-\text{ka}_i \cdot t_{ij}) \right] + \varepsilon_{ij};$$
$$\text{k}_i = \frac{\text{CL}_i}{\text{Vd}_i} \text{ and } \varepsilon_{ij} \overset{iid}{\sim} N(0, \Sigma).$$

CL and Vd are clearance and volume of distribution, ka is the rate constant of absorption (per time). The $j$th plasma concentration $C$ for individual $i$ changes over time $t$ for a drug given dose $D_i$. The fixed effects parameters of this model are CL, Vd, and ka which have arbitrary values 4, 20, and 1, respectively. The variance of the random effects parameters of CL, Vd, and ka are assumed to be the same, independent and lognormal with value equals to 0.1. Combined error model with variance of the proportional error $\sigma_{\text{prop}}^2$ equals to 0.1 and variance of the additive error $\sigma_{\text{prop}}^2$ equals to 0.05 is also assumed (see Table 8.2 for parameter values).

The software WinPOPT is used to optimize the population study of 100 patients. Four blood samples will be collected from each patient. A single elementary design consisting of four time points to collect the blood samples is decided. The dose given to each patient is 100 mg with dose interval 24 h (the upper bound of sampling times). Three sampling schedules, an empirical design, an optimal design using the D-optimality criterion (as per Sect. 8.3), and a robust design using HClnD (as per Sect. 8.4.1) will be considered.

### 8.6.1 Evaluation of an Empirical Design

The first design is an empirical sampling schedule with sampling times fixed at 1, 4, 8, and 12 h postdose. The empirical design is evaluated with WinPOPT where the determinant of Fisher information matrix is given as $6.42 \times 10^{15}$. The normalized determinant which is the value of the determinant raise to the power of one over the number of parameters in the model, for this design is 181. The utility of a design can be determined by using the asymptotic estimates of the estimation standard error of all eight parameters provided in the WinPOPT output. The smaller

**Table 8.2** Parameter values for one-compartment first-order input PK model

| Parameter | CL | Vd | ka | $\sigma_{\text{CL}}^2$ | $\sigma_{\text{V}}^2$ | $\sigma_{\text{ka}}^2$ | $\sigma_{\text{prop}}^2$ | $\sigma_{\text{add}}^2$ |
|-----------|----|----|----|------|------|------|------|------|
| Value | 4 | 20 | 1 | 0.1 | 0.1 | 0.1 | 0.1 | 0.05 |

**Table 8.3** Percentage standard error of parameter estimates in empirical design and D-optimal design

| Parameter | CL | Vd | ka | $\sigma_{\text{CL}}^2$ | $\sigma_{\text{V}}^2$ | $\sigma_{\text{ka}}^2$ | $\sigma_{\text{prop}}^2$ |
|-----------|----|----|----|------|------|------|------|
| Empirical design SE (%) | 4 | 6 | 10 | 19 | 30 | 96 | 7 |
| D-optimal design SE (%) | 4 | 5 | 7 | 21 | 26 | 54 | 7 |

the estimation standard error means the design will result in an estimate that is more reliable. In practice, the estimation standard error is considered as acceptable if the value is less than some predefined limit; for example, it is often desirable for the standard error of the fixed effects parameters to be <20% and <50% for variance of the random-effects parameters. The percentage standard error of the three fixed effects parameters CL, Vd, and ka are 4, 6, and 10%, respectively for the empirical design. The percentage standard error of the variance of the three random effects parameters are 19, 30, and 96%, respectively. The percentage standard error of the variance of the proportional error is 7%. Here we have fixed the additive error component since its value is of minimal importance and we know that omitting the value will yield inappropriate optimal designs (as per discussion in Sect. 8.2.3). We also know that the best estimate of the additive variance will arise from a predose blood sample which, in this circumstance, will not be considered further. The percentage standard errors are presented in Table 8.3.

### 8.6.2 D-Optimal Design

The design is then optimized with the inbuilt *exchange algorithm* in WinPOPT, where the optimal sampling times are found to be 0.301, 3.84, 3.84, and 12.8 h postdose. The D-optimal design consists of three unique time points with

repetition of one of the time points. The repetition of a time point does not mean that we can omit one sample (e.g. omitting 3.84 h) by taking only three samples instead of four as the standard error of estimates will be higher if we do so. Rather the repeated time point provides two important interpretations: (1) given there are three fixed effects parameters and therefore there should be only three unique time points then a repetition of a time point indicates that an optimal design has been found since no new unique time points should become evident no matter how many more samples are taken and (2) that the time point at about 4 h is important and while we would not recommend taking two blood samples at exactly the same time we would recommend taking two samples within the same sampling window centered on this time. The determinant of the Fisher information matrix for the optimal design is $4.66 \times 10^{16}$ and the normalized determinant is 241. The increase in the determinant value indicates that the optimal sampling schedule is a better design. The efficiency of the empirical design as compared to the optimal design can be calculated by taking the ratio of the normalized determinants (as per the calculation for efficiency in Sect. 8.3). The efficiency value of 0.75 indicates that the number of patients in the empirical design needs to be about 33% more to achieve same efficiency as the optimal design.

The percentage standard error of CL, Vd, and ka in the optimal design are shown in Table 8.3. On average, the standard error values are lower for the optimal design than those from the empirical design for both the fixed and variance of the random effects parameters. Note that the variance of the random effects parameter of CL which is marginally higher which is compensated for by a highly significant decrease in the standard error of the variance of the random effects parameter of ka.

### 8.6.3 Robust Design

Although the optimal design is efficient, it will be suboptimal and perhaps even fail if the nominal parameter values are very different from the true (but unknown) values associated with the forth

**Table 8.4** Combinations of the values of the three fixed-effects parameters for eight component models used in the HClnD-optimal design

| Parameter set | CL | Vd | ka |
|---|---|---|---|
| 1 | 2 | 10 | 0.5 |
| 2 | 2 | 10 | 2 |
| 3 | 2 | 40 | 0.5 |
| 4 | 2 | 40 | 2 |
| 5 | 8 | 10 | 0.5 |
| 6 | 8 | 10 | 2 |
| 7 | 8 | 40 | 0.5 |
| 8 | 8 | 40 | 2 |

coming study. A robust design method can be used to account for the uncertainty in the parameter space. Here we use HClnD as per Sect. 8.3.1. In this setting, the parameter assumes values at the extrema of an interval around the fixed effects values. We only consider the uncertainty on the fixed effects parameter values for CL, Vd, and ka. The robust design is conducted for this population study by constructing vectors of all combinations of parameter sets with CL taking a value of either 2 or 8; Vd a value of either 10 or 40, and ka as 0.5 or 2. Eight component models were developed where each model has a different vector of parameter values with different combinations of the parameter values are shown in Table 8.4. The HClnD-optimal design is achieved via the multiple model single response method in WinPOPT. The final sampling times for the HClnD design are 0.301, 1.86, 5.29, and 15.9 h postdose. The normalized determinant values for the eight models range from 81 to 415. The percentage standard error of each parameter is given in Table 8.5. For CL the standard errors range from 4 to 9%, Vd from 4 to 28%, and ka from 7 to 24%. When compared to the optimal design (above) the relative efficiencies of the eight component models ranged from 0.34 to 1.72.

There are four unique sampling times with no repetitions in the robust design, while the model only has three fixed-effects parameters. This relaxation of the general rule that a unique sampling time is required for each fixed effects parameter occurs when parameters adopt significantly different values. The divergent parameter values result in a split of the regions where

192 L.-K. Foo and S.B. Duffull

**Table 8.5** Percentage standard error of parameter estimates for eight component models used in HClnD-optimal design

| Parameter set | SE (%) | | | | | | |
|---|---|---|---|---|---|---|---|
| | CL | Vd | ka | $\sigma_{CL}^2$ | $\sigma_V^2$ | $\sigma_{ka}^2$ | $\sigma_{prop}^2$ |
| 1 | 4 | 7 | 9 | 19 | 32 | 55 | 6 |
| 2 | 4 | 4 | 7 | 19 | 22 | 60 | 7 |
| 3 | 9 | 8 | 12 | 65 | 30 | 75 | 8 |
| 4 | 6 | 5 | 8 | 51 | 23 | 72 | 7 |
| 5 | 4 | 28 | 24 | 22 | 159 | 124 | 8 |
| 6 | 4 | 6 | 9 | 22 | 33 | 78 | 12 |
| 7 | 5 | 10 | 14 | 36 | 54 | 103 | 10 |
| 8 | 5 | 5 | 9 | 32 | 30 | 80 | 9 |

sampling times are most informative. From the standard error value in Table 8.5, we also see that some parameter sets fairly well (e.g. parameter set 1) and some fairly poor (e.g. parameter set 5); in particular, this is the case for the standard error of the variances of the random effects of $V$ and ka. The component model with parameter set 5 provides the most stress on the design as the half-life of elimination is short and only limited drug remains towards the end of the sampling interval. In addition, the similarity of the rate constant for absorption and rate constant for elimination makes differentiation of these processes more challenging. One hopes that this particular scenario is an unlikely occurrence. Nevertheless, the design could be enriched to accommodate this particular set if it was felt likely to be plausible.

## 8.7 Summary

The design of PK and PKPD studies is often overlooked in the imperative to conduct studies that aim to show the safety and efficacy of new medicinal compounds. In some circumstances the design may be chosen from one that has been conducted previously in the hope that it will perform well in the new circumstances of the current study. The result may be a design that fails to identify key PK or PKPD features of the medicinal compound or a design that places an excessive load on diminishing resources. The use of optimal design methods are becoming widely accepted in industry and these methods offer a formal process to evaluate and identify designs that are both parsimonious as well as carry a high probability of success.

## References

Atkinson AC. DT-Optimum Designs for Model Discrimination and Parameter Estimation. *J Stat Plan Inference* 2008; 138:56–64

Atkinson AC, and Donev AN. Optimum Experimental Designs. Oxford Statistical Science Series 8, Vol. 8. Oxford: Clarendon Press 1992

Atkinson AC, and Fedorov VV. The Design of Experiments for Discriminating Between Two Rival Models. *Biometrika* 1975a; 62(1):57–70

Atkinson AC, and Fedorov VV. Optimal Design: Experiments for Discriminating Between Several Models. *Biometrika* 1975b; 62(2):289–303

Bogacka B et al. ICODOE. Memphis 2005

Cramér H. Mathematical Methods of Statistics. Princeton, NJ: Princeton University Press 1946

D'Argenio DZ. Incorporating Prior Parameter Uncertainty in the Design of Sampling Schedules for Pharmacokinetic Parameter Estimation Experiments. *Math Biosci* 1990; 99(1):105–118

D'Argenio DZ. Optimal Sampling Times for Pharmacokinetic Experiments. *J Pharmacokinet Biopharm* 1981; 9:739–756

Draper NR, and Hunter WG. Design of Experiments for Parameter Estimation in Multiresponse Situations. *Biometrika* 1966; 53:525–533

Duffull SB, Graham G, Mengersen K, and Eccleston J. Evaluation of the Pre-posterior Distribution of Optimized Sampling Times for the Design of Pharmacokinetic Studies. *J Biopharm Stat* [in press]

Duffull SB, Mentré F, and Aarons L. Optimal Design of a Population Pharmacodynamic Experiment for Ivabradine. *Pharm Res* 2001; 18:83–89

Duffull S, Waterhouse T, and Eccleston J. Some Considerations on the Design of Population Pharmacokinetic Studies. *J Pharmacokinet Pharmacodyn* 2005; 32 (3–4):441–457

Foo L-K, McGree J, Eccleston J, and Duffull S. Comparison of Robust Criteria for D-Optimal Design. *Manuscript submitted for review*.

Foo L-K, and Duffull S. Methods of Robust Design of Nonlinear Models with an Application to Pharmacokinetics. *J Biopharm Stat* 2010; 20(4):886–902

Graham G, and Aarons L. Optimum Blood Sampling Time Windows for Parameter Estimation in Population Pharmacokinetic Experiments. *Stat Med* 2006; 25:4004–4019

Green B, and Duffull SB. Prospective Evaluation of a D-Optimal Designed Population Pharmacokinetic

Study. *J Pharmacokinet Pharmacodyn* 2003; 30 (2):145–161

Gueorguieva I, Aarons L, Ogungbenro K, Jorga KM, Rodgers T, and Rowland M. Optimal Design for Multivariate Response Pharmacokinetic Models. *J Pharmacokinet Pharmacodyn* 2006; 33:97–124

Hennig S, Waterhouse TH, Bell SC, France M, Wainwright CE, Hugh M, Charles BG, and Duffull SB. A D-Optimal Designed Population Pharmacokinetic Study of Oral Itraconazole in Adult Cystic Fibrosis Patients. *Br J Clin Pharmacol* 2007; 63(4):438–450

Hoeting JA, Madigan D, Raftery AE, and Volinsky CT. Bayesian Model Averaging: A Tutorial. *Stat Sci* 1999; 14(4):382–417

Hooker A, and Vicini P. Simultaneous Population Optimal Design for Pharmacokinetic–Pharmacodynamic Experiments. *AAPS J* 2005; 7:E759–E785

Hooker AC, Foracchia M, Dodds MG, and Vicini P. An Evaluation of Population D-Optimal Designs Via Pharmacokinetic Simulations. *Ann Biomed Eng* 2003; 31:98–111

McGree JM, Duffull SB, Eccleston JA, and Ward LC. Optimal Design for Studying Bioimpedance. *Physiol Meas* 2007; 28:1465–1483

McGree JM, Eccleston JA, and Duffull SB. Compound Optimal Design Criteria for Nonlinear Models. *J Biopharm Stat* 2008; 18(4):646–661

McGree JM, Duffull SB, and Eccleston JA. Simultaneous Versus Sequential Optimal Design for Pharmacokinetic–Pharmacodynamic Models with FO and FOCE Consideration. *J Pharmacokinet Pharmacodyn* 2009; 36:101–123

Mentré F, Maller A, and Baccar D. Optimal Design in Random-Effects Regression Models. *Biometrika* 1997; 84(2):429–442

Mentré F, Duffull S, Gueorguieva I, Hooker A, Leonov S, Ogungbenro K, and Retout S. Software for Optimal Design in Population Pharmacokinetics and Pharmacodynamics: a Comparison. PAGE 16 2007 Abstr 1179 [http://www.page-meeting.org/?abstract=1179]

Ogungbenro K, and Aarons L. Optimization of Sampling Windows Design for Population Pharmacokinetic Experiments. *J Pharmacokinet Pharmacodyn* 2008; 35:465–482

Rao CR. Information and the Accuracy Attainable in the Estimation of Statistical Parameters. *Bull Calcutta Math Soc* 1945; 37:81–89

Retout S, Duffull S, and Mentré F. Development and Implementation of the Population Fisher Information Matrix for the Evaluation of Population Pharmacokinetic Designs. *Comput Methods Programs Biomed* 2001; 65:141–151

Roos JF, Kirkpatrick CM, Tett SE, McLachlan AJ, and Duffull SB. Development of a Sufficient Design for Estimation of Fluconazole Pharmacokinetics in People with HIV Infection. *Br J Clin Pharmacol* 2008; 66:455–466

Sheiner LB. Learning Versus Confirming in Clinical Drug Development. *Clin Pharmacol Ther* 1997; 61 (3):275–291

Sheiner LB, and Beal SL. Evaluation of Methods for Estimating Population Pharmacokinetic Parameters. III. Monoexponential Model: Routine Clinical Pharmacokinetic Data. *J Pharmacokinet Biopharm* 1983; 11(3):303–319

Smith K. On the Standard Deviations of Adjusted and Interpolated Values of an Observed Polynomial Function and Its Constants and the Guidance They Give Towards a Proper Choice of the Distribution of Observations. *Biometrika* 1918; 12:1–85

Walter E, and Pronzato L. Optimal Experiment Design for Nonlinear Models Subject to Large Prior Uncertainties. *Am J Physiol* 1987; 253:530–534

Waterhouse TH, Redmann S, Duffull SB, and Eccleston JA. Optimal Design for Model Discrimination and Parameter Estimation for Itraconazole Population Pharmacokinetics in Cystic Fibrosis Patients. *J Pharmacokinet Pharmacodyn* 2005; 32(3–4):521–546

Waterhouse TH, Eccleston JA, and Duffull SB. Optimal Design Criteria for Discrimination and Estimation in Nonlinear Models. *J Biopharm Stat* 2009; 19:386–402

Zhu W, and Wong WK. Optimal Treatment Allocation in Comparative Biomedical Studies. *Stat Med* 2000; 19 (5):639–648

# Pharmacokinetic Studies in Pregnant Women

**9**

Jamie L. Renbarger and David M. Haas

**Abstract**

The only way to determine appropriate medication dosing during pregnancy is to evaluate the pharmacokinetics and pharmacodynamics of individual medications in pregnant women. This type of clinical investigation can present a variety of challenges and concerns. This chapter summarizes what is known about physiologic changes in pregnancy and the impact these changes can have on drug disposition, and provides a model approach for completing pharmacokinetic studies in women during pregnancy.

## 9.1 Introduction

Conventional drug development is generally conducted in the adult population and does not include women of reproductive age or pregnant women. The appropriate therapeutic use of drugs in pregnant women in order to ensure efficacy for the woman, as well as safety for the fetus, is a major concern for patients and health care professionals. Medication use during pregnancy is often necessary and sometimes critical to the health of both the mother and the child. Pharmacoepidemiological surveys indicate that about one half of all obstetric office visits involve a medication (Lee et al. 2006); 83% of women use at least one medication at some point during pregnancy (Headley et al. 2004) and nearly one third of all pregnant women use two or more drugs during pregnancy (Rubin et al. 1993). Although it has been increasingly recognized that a single standard dose is not appropriate for everyone, information-guided drug treatment for obstetric patients is still largely extrapolated from drug development trials conducted in men and nonpregnant women. Drug development research for pregnant women has also been largely excluded due to many concerns and potential risks including teratogenic, psychological, social, technical, ethical, and legal. As a result primarily of the tragic situation with thalidomide in the 1960s (McBride 1961), the focus of the majority of obstetric pharmacology studies in the past has been on drug safety – and specifically on avoiding harm to the fetus. However, given the myriad of physical, hormonal, and physiological changes occurring throughout pregnancy, it would be expected that drug disposition may also change during pregnancy.

J.L. Renbarger (✉)
Indiana University School of Medicine, Indianapolis, IN, USA
e-mail: jarenbar@iupui.edu

In recent years, the gap in knowledge in obstetric pharmacology has been recognized and there has been an increased focus on systematically evaluating the pharmacokinetics and pharmacodynamics of medications in pregnant women. This work has revealed continual changes in drug disposition throughout pregnancy (Tracy et al. 2005). In the case of many drug metabolizing enzymes and renal excretion of many drugs, activity can increase dramatically throughout pregnancy (Tracy et al. 2005), which has the potential to significantly decrease exposure of pregnant women to medications and could result in lack of efficacy with potentially serious consequences to both the mother and the child. However, this is not the case for all drugs or for all drug metabolizing enzymes. As such, application of dosing regimens developed for nonpregnant populations in pregnant women is not appropriate. Furthermore, extrapolating dosing of specific medications based on what is known about other medications, drug metabolizing enzyme activity, and renal function is also not appropriate at this time given the limited data available. With concerns about potential for teratogenicity, the vast majority of practitioners are reluctant to dose escalate medications for pregnant women above standard, published doses; however, in the case of some drugs, this may be required. The only way to determine appropriate medication dosing during pregnancy is to evaluate the pharmacokinetics and pharmacodynamics of individual medications in pregnant women. This type of clinical investigation can present a variety of challenges and concerns.

This chapter summarizes what is known about physiologic changes that occur during pregnancy, the impact these changes can have on drug disposition, and provides a model approach for completing pharmacokinetic studies in women during pregnancy. With the increased participation of obstetric patients in clinical trials, progress has been made in drug research and development, which provides valuable therapeutic information for pregnant women. However, information guiding drug usage for the majority of drugs used in during pregnancy is still scarce and incomplete. Furthermore, the

current therapeutic practice for the majority of medications used during pregnancy does not take into account the profound physiologic changes that take place during pregnancy. The use of drugs in pregnant women is largely based on an empiric understanding of dosage, safety and efficacy from nonpregnant women rather than scientific evidence. The lack of appropriate drug testing and research in pregnant women is a significant public health concern. Consequently, there is an urgent need to study drug metabolism, disposition, toxicity and efficacy in women during pregnancy in order to understand the significant differences in drug actions and responses during these critical times and to develop effective and safe therapeutic regimens and drugs.

## 9.2   Physiologic Changes During Pregnancy

A pregnant woman's body undergoes profound changes in anatomy, physiology, and metabolism to support the entire pregnancy, which ultimately support growth and development of the fetus. Such alterations are required to increase cardiac output and to maintain uteroplacental perfusion and fetal demands. However, these changes can have dramatic effects on drug disposition, pharmacokinetics, and pharmacodynamics. Failure to take these changes into consideration when using medications during pregnancy can result in a variety of consequences (compared to the nonpregnant state) including: (1) no significant changes; (2) decreased maternal exposure resulting in decreased drug efficacy; or (3) increased maternal exposure resulting in increased toxicity. The following is a summary of some of the important physical and physiological changes that occur during pregnancy.

*General changes*. There is an increase in both total body weight and body fat during pregnancy. The increase in weight is due in large part to increased body water in both intravascular (plasma volume) and extravascular spaces. In addition, along with the increase in plasma volume, there is a decrease in albumin concentration

during the second trimester with albumin reaching 70–80% of normal values by the end of pregnancy (Dean et al. 1980).

*Cardiac changes.* The cardiovascular system of the pregnant woman must meet the demands of both the mother and the fetus. Maternal cardiac output begins to increase by about 6 weeks of gestational age. Cardiac output ultimately increases by about 40% compared to the nonpregnant state due to an increase in heart rate and stroke volume combined with a 20–30% decrease in systemic capillary resistance (Clark et al. 1989). The maternal heart rate peaks in the third trimester with a 15% increase over the average heart rate in a nonpregnant woman. Maternal blood volume increases progressively during pregnancy by about 2 L or 30 to 50% more than the volume during the nonpregnant state (Naylor and Olson 2003). Furthermore, oncotic pressure also decreases during pregnancy – primarily as a reflection of the decline in albumin concentration (Chesnutt 2004).

*Respiratory changes.* Changes that occur in the respiratory system are a function of a combination of hormonal, biochemical, and mechanical changes. Ventilation and oxygen consumption are the major parameters that change during pregnancy. Minute ventilation increases by about 50% during pregnancy – primarily due to the increased metabolic rate, changes in the mechanics of breathing, and increases in progesterone concentration (Elkus and Popovich 1992; Crapo 1996). The change begins before the end of the first trimester and remains relatively constant throughout pregnancy (Chesnutt 2004). Oxygen consumption increases by 15–20% in singleton pregnancies in order to meet the increased demand placed on the mother by the growing fetus (Torgersen and Curran 2006).

*Renal changes.* Changes occurring in the renal system during pregnancy are a result of functional and structural adaptations (Torgersen and Curran 2006). By 16 weeks of gestational age, the glomerular filtration rate increases by 50% and remains elevated throughout pregnancy (Davison and Dunlop 1980). In addition, creatinine clearance increases during pregnancy resulting in lower serum creatinine, blood urea nitrogen, and uric acid concentrations (Davison 1987).

*Gastrointestinal changes.* Gastroesophageal reflux is a common problem during pregnancy. This can begin in the first trimester due to progesterone's causing smooth muscle relaxation resulting in lower esophageal sphincter relaxation. As pregnancy progresses, displacement of the stomach by the uterus can cause exacerbation of these symptoms (Chesnutt 2004). Gastric emptying and intestinal motility are also reduced during pregnancy secondary to smooth muscle relaxation by progesterone (Krauer and Krauer 1977; Dvorchik 1982; Anger and Piquette-Miller 2008) while gastric pH seems to increase throughout pregnancy (Krauer and Krauer 1977; Dvorchik 1982).

Nakai et al. reported a significant increase in the amount of hepatic blood flow after 28 weeks of gestational age (Nakai et al. 2002), resulting in increased delivery of drugs and toxins to the liver for metabolism. In addition, drug metabolism via hepatic metabolizing enzymes is altered during pregnancy. This is discussed in detail below.

## 9.3 Pharmacokinetic Considerations

The physiologic changes that occur during pregnancy can result in changes in pharmacokinetics. The majority of the research performed to date is observational in nature and involves small numbers of women. The information below is meant as a summary to guide development of pharmacokinetic studies to evaluate new agents for use in pregnant women.

### 9.3.1 Absorption

Given the changes that occur within the gastrointestinal tract during pregnancy, one could hypothesize that drug absorption would change in pregnant compared to nonpregnant women. At this point, there are limited data to document that any of these changes significantly affect drug absorption. Paracetamol (acetaminophen) is one

drug with evidence of a difference in absorption between pregnant and nonpregnant women. Simpson et al. (1988) studied single dose pharmacokinetics of paracetamol in 28 pregnant women compared to 14 nonpregnant controls and found a delay in paracetamol absorption in the women who were 12–14 weeks pregnant compared to the control group. Paracetamol is absorbed in the upper small bowel and as such the rate of absorption depends on the rate of gastric emptying. As such, the delay in gastric emptying during pregnancy is likely the cause for the difference in absorption between pregnant and nonpregnant women (Simpson et al. 1988). In contrast, small studies of other agents have revealed no difference in absorption between women during pregnancy and in the postpartum period. One example is sotalol, a β-receptor antagonist. O'Hare et al. (1983) studied the pharmacokinetics of intravenous and oral doses of sotalol in six women during the third trimester of pregnancy and again 6-weeks postpartum. They found the bioavailability to be 85–90% both during pregnancy and postpartum. Similar studies were performed in pregnant women with asymptomatic urinary tract infections receiving β-lactam antibiotics (ampicillin (Philipson 1977), cephradine (Philipson et al. 1987), or cefazolin (Philipson et al. 1987)), in whom bioavailability was evaluated during the second or third trimester of pregnancy and again at least 6-weeks postpartum. These studies found no difference in the bioavailability of these antibiotics during pregnancy compared to postpartum.

One problem with these trials is the small number of subjects studied – as such they are all significantly under-powered to evaluate the hypotheses that they are testing. Sample size is often a challenge in studying medications during pregnancy; however, a critical question is whether studies such as those described above add to the science or not – and in fact, whether they are helpful to practitioners prescribing medications to women during pregnancy and to the women themselves or not. In some cases, the studies may foster a false sense of security if they find no difference between pregnant and nonpregnant women. However, adequately powered studies may reveal the opposite results. A critical question for investigators to consider prior to publishing studies such as these is what impact the results may have.

### 9.3.2 Distribution

The increase in total body water associated with pregnancy creates a larger potential volume of distribution of hydrophilic drugs and the increase in body fat during pregnancy creates a larger potential volume of distribution for lipophilic drugs (Anger and Piquette-Miller 2008). These changes along with changes in protein binding during pregnancy could increase the apparent volume of distribution of many drugs thereby resulting in a decrease in initial concentration ($C_0$) after a loading dose and peak plasma concentration ($C_{max}$) after repeated dosing (Anderson 2005).

Another important factor to consider is the decrease in albumin plasma concentration, which begins in the second trimester and continues throughout the remainder of pregnancy to 70–80% of prepregnancy concentrations (Dean et al. 1980). In many cases, this change is partially off-set by an increase in drug metabolism that occurs with many enzymes during pregnancy (see Sect. 9.3.3). However, the decrease in protein binding can be clinically significant for a small number of drugs that are both highly protein bound and predominantly eliminated hepatically (Benet and Hoener 2002). One group for which this is important is low extraction ratio drugs in which therapeutic drug monitoring measures total plasma concentration. Given the gradual increase in the free fraction of these drugs throughout pregnancy, total plasma concentration will underestimate the amount of free drug available relative to the nonpregnant state. Examples of this type of drug include the anticonvulsants phenytoin and valproic acid (Yerby et al. 1990; Tomson et al. 1994a, b). The mean plasma concentration of phenytoin drops 56% over the course of pregnancy to its lowest level at the time of delivery and rising again in the postpartum period (Yerby

et al. 1990). However, the decrease in free phenytoin is only 31%. Phenytoin dose adjustments during pregnancy based on total plasma concentrations would result in a disproportionate increase in free phenytoin thereby potentially putting the fetus at risk for the teratogenic effects of the drug (Yerby et al. 1990).

The second group of drugs in which a drop in plasma protein binding can be clinically significant is the high extraction ratio drugs with narrow therapeutic indices administered intravenously. In the case of these drugs, the decrease in plasma protein binding associated with pregnancy could result in an increase in the free fraction of drug sufficient to fall outside of the therapeutic index resulting in increased side effects for the mother and potentially risks to the fetus (Yerby et al. 1990; Anderson 2005). Unfortunately, there are no published data in pregnancy evaluating pharmacologic changes of any such drugs.

### 9.3.3 Metabolism

The primary route of drug metabolism is via hepatic enzymes, including both phase I (oxidation) and phase II (conjugation) drug metabolizing enzymes. The activity of many of these enzymes is known to be altered during pregnancy; some are increased and some are decreased. Furthermore, overall hepatic clearance of drugs is dependent not only on drug metabolism, but also protein binding and blood flow to the liver – both of which are also altered during pregnancy (Morgan and Smallwood 1990). Consequently, the overall effect of pregnancy on drug metabolism is a very complex issue requiring systematic evaluation of individual drugs. The groups of enzymes most commonly involved in drug metabolism include the cytochrome P450 (CYP) enzymes, uridine diphosphate glucuronosyltransferases (UGT) and the N-acetyl transferases (NAT).

The *CYPs* are a multigene superfamily of hemoproteins that catalyze oxidation reactions of a multitude of both endogenous and exogenous compounds. Cytochrome P450 enzymes are present primarily in the liver but are also found in the gastrointestinal tract, kidneys, and lungs. In addition, to drug metabolism, this group of enzymes is important in hormone synthesis and metabolism, cholesterol synthesis, and vitamin D metabolism. Based on data from studies of drug metabolism during pregnancy, pregnancy appears to have different effects on the various CYP enzymes resulting in an increase in activity of CYP2A6, -2C9, -2D6, and -3A4 and a decrease in activity of CYP1A2 and -2C19.

*CYP1A2* is a member of the CYP superfamily involved in the metabolism of such things as caffeine, acetaminophen, theophylline, clozapine, and olanzapine. In the case of caffeine, multiple studies have evaluated the effect of pregnancy on its metabolism (Aldridge et al. 1981; Knutti et al. 1981; Bologa et al. 1991). These studies have all found that the half-life of caffeine is significantly longer during pregnancy compared to the half-life in postpartum women and nonpregnant control subjects, supporting the idea that CYP1A2 activity is decreased during pregnancy. These studies indicate that activity of this enzyme begins to decline during the first trimester and returns to baseline by 1 month postpartum. Based on these trials of caffeine metabolism, caffeine half-life increases from approximately 3.4 h in control subjects to 8.3 h in pregnant subjects (Aldridge et al. 1981; Knutti et al. 1981; Bologa et al. 1991). However, the confounding effect of volume of distribution cannot be ignored. Expression of CYP1A2 is also known to be induced by some polycyclic aromatic hydrocarbons, some of which are found in cigarette smoke. In addition, pharmacogenetic variability in CYP1A2 is an important determinant of the inducibility. In nonpregnant subjects, CYP1A2*1F is associated with higher inducibility of enzyme expression by smoking (Sachse et al. 2003). Nordmark et al. (2002) studied pregnant women to evaluate the effect of this allele on CYP1A2 expression during pregnancy. They studied women in their first trimester of pregnancy (740 nonsmokers, 164 smokers) including genotyping for the CYP1A2*1F allele and phenotyping of the CYP1A2 activity using caffeine as a probe drug. In contrast to the effects of

smoking seen in nonpregnant subjects, the investigators found no increased induction of CYP1A2 enzyme expression among pregnant carriers of the CYP1A2*1F compared to pregnant women who were not carriers of the variant allele (Nordmark et al. 2002).

CYP2A6 is the primary enzyme responsible for metabolism of nicotine as well as its primary metabolite, cotinine (Messina et al. 1997). Studies of nicotine and cotinine metabolism during pregnancy have revealed a significant increase in clearance of nicotine and cotinine as well as a decrease in nicotine half-life (Dempsey et al. 2002; Klein et al. 2004). This information is clinically relevant to the adequate prescribing of nicotine replacement during pregnancy. Given concerns about toxicity of the fetus secondary to exposure to medications and chemicals in utero, it is extremely uncommon for physicians to prescribe higher doses of medications during pregnancy than are recommended for nonpregnant women. However, in prescribing nicotine replacement, pregnant women are likely to need larger doses than nonpregnant people due to the increase in CYP2A6 activity during pregnancy. Furthermore, nicotine replacement therapy may be safer than smoking during pregnancy (Coleman 2007).

*CYP2C9* is an important enzyme in the metabolism of more than 100 drugs, including some drugs with narrow therapeutic indices (e.g., warfarin, phenytoin). Multiple single nucleotide genetic polymorphisms have been identified in the coding and regulatory regions of the *CYP2C9* gene (Garcia-Martin et al. 2006). Given the availability of therapeutic drug monitoring for phenytoin, a great deal of information is available about changes in phenytoin disposition during pregnancy (Chen et al. 1982; Bardy et al. 1987; Yerby et al. 1990; Tomson et al. 1994a, b). Phenytoin is metabolized by both CYP2C9 and CYP2C19; however, CYP2C9 catalyzes the major metabolic pathway (Bajpai et al. 1996). As described above, phenytoin clearance progressively increases beginning in the first trimester and continuing throughout pregnancy; thus indicating an increase in CYP2C9 activity during pregnancy. Furthermore, total plasma concentrations decrease more than do free plasma concentrations (due to the concomitant decrease in plasma albumin concentrations), which only significantly increased in the third trimester. Phenytoin dose adjustment is only necessary when the unbound concentration increases; therefore, this is only required for most women during the third trimester (Tomson et al. 1994a, b). While there are other CYP2C9 substrates commonly used during pregnancy, there are no available pharmacokinetic data on any of these medications. However, based on what is known about phenytoin, one would expect that CYP2C9 induction during pregnancy would require dosage increases for all substrates of this enzyme (Anderson 2005).

*CYP2C19* is a member of the CYP superfamily responsible for metabolism of such important drugs as proton pump inhibitors and some anticonvulsants. There are limited pharmacokinetic data related to CYP2C19 during pregnancy from which to make conclusions about changes in this enzyme that occur during pregnancy. One example is the antimalarial drug proguanil which is metabolized by CYP2C19 (Helsby et al. 1990). Two studies evaluating proguanil pharmacokinetics during pregnancy have both found a significant decrease in proguanil clearance during pregnancy (Ward et al. 1991; McGready et al. 2003); thus indicating a decrease in CYP2C19 activity during pregnancy. Furthermore, McGready et al. (2003) found that the inhibitory effect of pregnancy on CYP2C19 was only observed in the subjects who were extensive metabolizers; suggesting a possible genotype specific effect on CYP2C19 during pregnancy. The pharmacokinetics of nelfinavir, metabolized by both CYP3A4 and CYP2C19, has also been studied in pregnant women (see CYP3A4 section below). However, pharmacokinetic data on other commonly used CYP2C19 substrates are not available in pregnant women. Based on what is known about proguanil and CYP2C19 activity during pregnancy, one would expect that dosage requirements for drugs like the proton pump inhibitors would decrease during pregnancy.

*CYP2D6* is responsible for metabolism of many commonly used drugs and is one of the

most extensively studied CYP enzymes. Dextromethorphan is used as a probe drug of CYP2D6 activity and has been used to evaluate activity of this enzyme during pregnancy (Wadelius et al. 1997; Tracy et al. 2005). These studies have found an increase in the metabolism of dextromethorphan; thus potentially indicating an increase in CYP2D6 activity during the second and third trimesters of pregnancy in extensive metabolizers. In contrast, CYP2D6 activity seemed to decrease in the poor metabolizers (Wadelius et al. 1997). This type of divergent response does not seem possible and requires further investigation. Pharmacokinetic data are also available for the CYP2D6 substrates metoprolol (Hogstedt et al. 1983, 1985) and fluoxetine (Heikkinen et al. 2003; Ververs et al. 2009) during pregnancy and support this increase in CYP2D6 activity in extensive metabolizers during pregnancy (summarized in Table 9.1). Interestingly, the only time CYP2D6 induction is known to occur is during pregnancy. Based on this information, one would expect that for CYP2D6 extensive metabolizers, drug metabolized by this enzyme may require dose increases during the second and third trimesters of pregnancy.

*CYP3A4* is the most abundant of the CYP enzymes and is known to be responsible for metabolism of more than half of all drugs metabolized. Pharmacokinetic data are available for multiple substrates of this enzyme during pregnancy (see Table 9.1); however, the information is limited to the second and third trimesters. Midazolam is often used as a probe drug to evaluate CYP3A4 activity; and pharmacokinetics of midazolam has been investigated in pregnant women (Wilson et al. 1987; Andrew et al. 2008; Hebert et al. 2008). This study evaluated pregnant women awaiting elective cesarean section delivery, women in active labor, and nonpregnant women undergoing gynecologic procedures as control patients. The study found an increase in midazolam clearance in the women awaiting cesarean sections compared to the control subjects, but no difference in the women in active labor compared to the controls. Urinary secretion of cortisol and its metabolites has also been used as a nonspecific probe of CYP3A4

(Anderson 2005) activity and has been evaluated in pregnant women. Findings in pregnant women also support an increase in CYP3A4 activity during pregnancy (Ohkita and Goto 1990). Studies with CYP3A4 substrates, including nifedipine, carbamazepine, and multiple protease inhibitors, have also been performed during pregnancy (see Table 9.1). These findings support the conclusion that CYP3A4 activity is increased during the second and third trimesters (Anderson 2005).

Uridine diphosphate glucuronosyltransferases are an important group of phase II drug metabolizing enzymes. Activity of UGT1A4 during pregnancy is probably the best characterized of the UGT enzymes. The antiepileptic drug lamotrigine is metabolized by UGT1A4 and multiple studies have evaluated its pharmacokinetics during pregnancy – both alone (de Haan et al. 2004; Pennell et al. 2004) and in combination with other antiepileptic medications (Ohman et al. 2000; Tran et al. 2002). The results of these studies reveal a significant increase in lamotrigine clearance during pregnancy with a greater increase seen in the women on lamotrigine monotherapy (see Table 9.1); indicating an increase in UGT1A4 activity during pregnancy. The lesser increase in clearance in women on other antiepileptic medications is likely due to the fact that the enzyme induction associated with pregnancy is superimposed on the effect of enzyme inducing medications and is, therefore, not as great (Anderson 2005). Consequently, the relative dose increase required to maintain lamotrigine plasma concentrations during pregnancy in women on concomitant therapy with enzyme inducing antiepileptics should not be as great as the dose increase in lamotrigine required for women on monotherapy (Anderson 2005). Data related to medications metabolized by other UGT enzymes is limited (summarized in Table 9.1).

### 9.3.4 Excretion

The kidney is the main site for excretion of drugs. Renal excretion is dependent on a combination of glomerular filtration and tubular section in the

**Table 9.1** Effect of pregnancy on drug metabolism

| Drug | Pregnancy trimesters studied | Findings (relative to nonpregnant state) | Alteration in pregnancy | Reference |
|------|------|------|------|------|
| Caffeine | 1st, 2nd, 3rd, and postpartum | Caffeine $t_{1/2\beta}$ longer; clearance decreased; metabolic ratio of caffeine metabolites decreased | ↓CYP1A2 activity ↓NAT activity | (Aldridge et al. 1981; Knutti et al. 1981; Bologa et al. 1991; Tsutsumi et al. 2001; Tracy et al. 2005) |
| Carbamazepine | 1st, 2nd, 3rd, and postpartum | ↓ in total concentration; no change in unbound concentration | ↑CYP3A4 activity | (Yerby et al. 1990; Tomson et al. 1994a, b) |
| Dextromethorphan | 2nd, 3rd, and postpartum | ↑ in both O-demethylation and N-demethylation of dextromethorphan | ↑CYP2D6 activity ↑CYP3A4 activity | (Wadelius et al. 1997; Tracy et al. 2005) |
| Fluoxetine | 3rd and postpartum | ↑ ratio of norfluoxetine: fluoxetine | ↑CYP2D6 activity | (Heikkinen et al. 2003) |
| Lamotrigine | 1st, 2nd, 3rd, and postpartum | ↑CL | ↑NAT activity | (Ohman et al. 2000; Tran et al. 2002; de Haan et al. 2004; Pennell et al. 2004) |
| Metoprolol | 3rd and postpartum | ↑CL | ↑CYP2D6 activity | (Hogstedt et al. 1983; Hogstedt et al. 1985) |
| Midazolam | 3rd | ↑CL in C section patients; No difference in women in active labor (vs. nonpregnant women) | ↑ or ↔ CYP3A4 activity | (Wilson et al. 1987) |
| Nelfinavir | 2nd, 3rd, and postpartum | Nelfinavir oral clearance ↑ in pregnancy M8 concentrations ↓ in pregnancy | ↑CYP3A4 activity ↓CYP2C19 activity | (van Heeswijk et al. 2004; Bryson et al. 2008) |
| Nicotine | 2nd and 3rd | Nicotine and cotinine CL↑ 60 and 140%, respectively; $t_{1/2\beta}$ ↓ 50%; and conversion to cotinine ↑ 54% | ↑CYP2A6 activity | (Dempsey et al. 2002; Klein et al. 2004) |
| Nifedipine | 3rd | ↑CL | ↑CYP3A4 activity | (Prevost et al. 1992) |
| Paroxetine | 2nd and 3rd | Paroxetine concentrations progressively ↓ in ultrarapid and extensive metabolizers and ↑ in intermediate and poor metabolizers | ↑CYP2D6 activity in UM and EM ↓ or no change in CYP2D6 activity in IM and PM | (Ververs et al. 2009) |
| Proguanil | | ↓ proguanil CL during pregnancy (possibly only in CYP2C19 extensive metabolizers) | ↓CYP2C19 activity | (Ward et al. 1991; McGready et al. 2003) |
| Zidovudine | 3rd and delivery | ↑CL vs. no change | ↑ or ↔ NAT activity | (Watts et al. 1991; O'Sullivan et al. 1993) |

proximal tubule and tubular reabsorption in the distal tubule. Tubular secretion and reabsorption of drugs and endogenous compounds is dependent on a number of membrane transporters expressed in the kidneys. Changes in these saturable transporters during pregnancy and the associated changes in drug excretion during pregnancy are poorly characterized. Changes in glomerular filtration rate (GFR) during pregnancy have been evaluated. In one study, healthy women were evaluated during pregnancy and postpartum revealing a 50% increase in GFR

during the first trimester of pregnancy and a progressive increase in GFR throughout the remainder of pregnancy compared to postpartum (Davison and Dunlop 1980). This correlates with a change in renal hemodynamics at least through the second trimester, when renal blood flow has increased by as much as 80% (Dunlop 1981) followed by a decrease during the third trimester. This decrease in renal blood flow correlates with a decrease in GFR during the final 3 weeks of the third trimester of pregnancy documented by the same group of investigators (Davison et al. 1980).

Several drugs cleared by the kidneys unchanged (without being metabolized first) have been studied during pregnancy. This includes a number of antibiotics (Philipson 1977; Assael et al. 1979; Philipson and Stiernstedt 1982; Philipson et al. 1987; Heikkila and Erkkola 1991; Heikkila et al. 1992; Chamberlain et al. 1993; Nathorst-Boos et al. 1995; Andrew et al. 2007), beta blockers (Thorley et al. 1981; O'Hare et al. 1983; Hurst et al. 1998; Hebert et al. 2005, 2008), digoxin (Luxford and Kellaway 1983), lithium (Schou et al. 1973), low-molecular weight heparins (Blomback et al. 1998; Casele et al. 1999; Ensom and Stephenson 2004), and clonidine (Buchanan et al. 2009). These results reveal significant variability between drugs from no change in clearance during pregnancy to a greater than 100% increase in drug clearance during pregnancy. Many of the drugs studied have low protein binding as such the variability in renal clearance is likely to be related to differences in tubular secretion and reabsorption.

## 9.4    FDA Guidance

While there are known changes in physiology and drug metabolizing enzymes that occur during pregnancy that affect drug disposition, in many cases it is difficult to predict the results that these changes will have on individual drugs without systematically investigating each drug throughout pregnancy. As such, carrying out carefully planned pharmacokinetic–pharmacodynamic–pharmacogenetic studies during preg-

nancy is critical in order to optimize both the efficacy of the medication for the woman and the safety of the medication for both the woman and the fetus. The Food and Drug Administration (FDA) provides *Guidance for Industry*, which provides a basic framework for designing and conducting PK/PD studies in pregnant women. It provides recommendations to sponsors on how to assess the influence of pregnancy on pharmacokinetics as well as pharmacodynamics. Furthermore, it provides recommendations to clinical researchers and pharmacologists about issues to consider when designing PK studies in pregnant women. While it provides recommendations on when PK studies are appropriate during pregnancy, it does not address ways to assess efficacy or safety. FDA recommends using the guidance in conjunction with other guidances as well as pharmacology and clinical literature on design, conduct, and interpretation of PK studies. In addition, because of the specialized nature of doing research in pregnant women, FDA also recommends investigators planning obstetric pharmacology studies to obtain advice from experts in the fields of obstetrics, pediatrics, pharmacology, clinical pharmacology, pharmacometrics, statistics, and other applicable disciplines.

There is some debate as to who should be included in studies of medications during pregnancy. Some argue that given the large number of women who need medications during pregnancy, it is unethical to exclude them from trials of drugs. In contrast, many support only including women in trials for medications that they need therapeutically.

Studies in pregnant women must conform to all applicable regulations, including human subject protection. In addition, FDA recommends that all studies in pregnant women have Institutional Review Board Review and that informed consent be obtained from all participants. The Code of Federal Regulations (CFR Title 45 Subpart B 46.204) delineates the conditions under which pregnant women may be involved in PK studies. These include:

- *Preclinical studies, including studies on pregnant animals, and clinical studies, including studies on nonpregnant women, have been*

*conducted and provide data for assessing potential risk to pregnant women and fetuses; and*

- *The risk to the fetus is no greater than minimal and the purpose of the research is the development of important biomedical knowledge which cannot be obtained by any other means.*

The FDA Guidance recommends that PK studies be conducted in pregnant women in any of the following situations:

- *The drug is known to be prescribed in or used by pregnant women, especially in the second and third trimesters;*
- *For a new drug or indication, if there is anticipated or actual use of the drug in pregnancy;*
- *Use is expected to be rare, but the consequences of uninformed dosages are great;*
- *Pregnancy is likely to alter significantly the PK of a drug (e.g., renally excreted drug) and any of the above apply; and*
- *PK studies in pregnant women are NOT recommended if the drug is not used in pregnant women or the drug has known or highly suspect fetal risk.*

## 9.5　Study Design

In general, it is important to include both pharmacokinetics and pharmacodynamics when doing an obstetric pharmacology study. Furthermore, it is imperative to study medications during the second and third trimesters of pregnancy. Study during the first trimester is also important for medications used clinically during the early part of pregnancy. Utilizing an appropriate control group is also an important consideration. In some cases data are available from historical controls; however, in many cases a control group is necessary for one or more components of the study.

### 9.5.1　Participants

As stated above, in any obstetric pharmacology study, it is important to study subjects throughout pregnancy. This can be accomplished by enrolling women early during their pregnancies with continued follow-up throughout the pregnancy and into the postpartum period or by enrolling women on the medication being studied who are in different trimesters of pregnancy. In many cases, the drug under evaluation drives this decision. For example, in the case of an antidepressant that a woman may take throughout her pregnancy as well as postpartum, it would be most scientifically advantageous to enroll women early in pregnancy and to follow them into the postpartum period. This allows following the woman longitudinally such that changes in the medication's pharmacokinetics and pharmacodynamics across pregnancy can be monitored in subjects. Furthermore, if the subjects continue to be followed into the postpartum period or are enrolled prior to becoming pregnant, then the woman can be used as her own control. In contrast, when studying something that a woman may only be taking for a short period of time (e.g., an antibiotic), different women at various time-points in their pregnancy taking the drug would need to be enrolled. Enrolling a certain number of women in each trimester of pregnancy is a reasonable approach to take; however, pregnancy is a continuum and for drugs with a narrow therapeutic index, it might be important to enroll women over smaller time increments than a trimester. Furthermore, for any obstetric pharmacology clinical trial, enrolling subjects to narrower windows of time is likely superior; however, if this is not possible or practical, it is at least important to ensure that women enrolled in each trimester are dispersed evenly over the trimester at the time they are studied.

Development of appropriate inclusion and exclusion criteria is critical to ensuring an effective clinical trial. In most cases, obstetric pharmacology studies do not utilize healthy volunteers given the potential risk of unnecessary drug exposure to the fetus. As such, these trials typically have as an inclusion criterion that the woman is currently taking or planning to begin taking (as part of routine clinical care) the medication of interest. Furthermore, in studies of drug

disposition or efficacy, it is important to limit the population enrolled to women with singleton pregnancies (rather than multiparous pregnancies) given the likely confounding effects of variability in this factor. Age of the subject is also an important consideration. Pregnant adolescents should be considered as a separate population. If they are not excluded from a study, adolescents need to be adequately represented to allow analysis of this age group separately or be part of a large enough study population to allow for development of a pharmacologic model of the data. At the other end of the age spectrum, women over 40 years of age are often excluded from obstetric pharmacology studies given the potential for changes in drug disposition with age. In addition, women with serious illnesses (e.g., HIV, diabetes) not related to the study drug of interest need to be carefully considered for the potential to confound study data prior to determining eligibility criteria.

Drug interactions are an important consideration in developing exclusion criteria as well. Given the limited knowledge regarding changes in drug disposition during pregnancy, it is important to minimize the confounding effects of drug interactions in obstetric pharmacology studies, As such, it is often best to exclude patients known to be taking any moderate to strong enzyme inducers or inhibitors that may interact with the study drug of interest. Alternatively, if a particular drug combination commonly used in clinical practice includes a drug metabolizing inducer or inhibitor, it may be important to study such a combination.

### 9.5.2  Pharmacokinetics

The two alternatives for the pharmacokinetic portion of obstetric pharmacology studies are a standard full pharmacokinetic approach versus a population pharmacokinetic approach. The advantages of a full PK study are similar to that in a nonpregnant population and include: fewer subjects required and a comprehensive PK profile is generated from each subject. The advantages of a population PK study in an obstetric pharmacology study include: number of PK sampling times for each subject is limited, which can be of particular importance to a busy pregnant woman and given more subjects are enrolled, it facilitates enrollment across the range of gestational ages. Choice of sampling time-points is often similar for a drug to the time-point selected for a nonpregnant population; however, it is important to take into consideration what is already known about drug disposition during pregnancy so as not to miss critical time-points that may not be standard in a nonpregnant population. Optimal sampling (see Chap. 8) may also be an option.

### 9.5.3  Pharmacodynamics

As part of any obstetric pharmacology study, it is also important to systematically evaluate a medication's pharmacodynamics. Given the significant physiologic changes that occur during pregnancy, one cannot conclude that a drug's effects will be the same in pregnant and nonpregnant women at similar exposures. In addition, some conditions treated during pregnancy (e.g., hyperemesis gravidarum) are unique to pregnancy and evaluating a drug's pharmacodynamics is imperative to understanding appropriate treatment of the pregnancy-associated condition.

### 9.5.4  Control Group

Selecting an appropriate control group is a critical component to obstetric pharmacology studies. Furthermore, in some cases, the control groups differ for the pharmacokinetic and pharmacodynamic portions of a single study. Some examples of control groups include:

- Using a woman as her own control by studying her throughout pregnancy and in the postpartum period (control period)
- Using healthy pregnant women not on the medication as PD control group
- Using women with the same illness (e.g., depression) not on medication (due to personal

choice, physician recommendation, or another reason) as the PD control group
- Using nonpregnant women of childbearing age as the control group

Furthermore, for medications in which pharmacogenetic variability may be clinically relevant, it could also be important to enroll control subjects of various genotypes.

### 9.5.5 Pharmacogenetics

While investigating how pharmacogenetic variability affects a drug's pharmacokinetics and pharmcodynamics has permeated many areas of medicine; minimal work has been done in the area of obstetric pharmacogenetics. In terms of drug metabolizing enzymes, as discussed above, we are continuing to refine our knowledge about how enzyme expression and activity changes during pregnancy. The superimposed effect of pharmacogenetic variability on this has yet to be systematically investigated; however, it is possible that by taking pharmacogenetics into account, we may be able to explain some of the observed interindividual variability observed between pregnant women (similar to nonpregnant subjects). CYP2D6 is one example in which taking genotype into account has been important in an obstetric pharmacology study. Ververs et al. (2009) evaluated the effect of CYP2D6 genotype on paroxetine pharmacokinetics and efficacy during pregnancy. Recall that CYP2D6 activity generally increases during pregnancy (Hogstedt et al. 1983, 1985; Heikkinen et al. 2003; Tracy et al. 2005). In this study of paroxetine, they followed women throughout the second and third trimesters of pregnancy. They found for women who were extensive (EMs) and ultrarapid metabolizers (UMs) of CYP2D6, plasma paroxetine concentrations steadily decreased over the course of pregnancy. In contrast, in the CYP2D6 intermediate (IMs) and poor metabolizers (PMs), plasma paroxetine concentrations increased throughout pregnancy (Ververs et al. 2009). The group also assessed the women's depressive symptoms throughout

the course of pregnancy and found that depressive symptoms increased in the EM/UM group and did not change in the IM/PM group. This is one of the only examples of an obstetric pharmacology trial with a pharmacogenetic component that exists in the literature. However, it is an excellent example of why incorporation of pharmacogenetics into these studies can be extremely clinically relevant.

## 9.6 Summary

As demonstrated, several factors conspire to alter the behavior of drugs given to pregnant women. Pharmacokinetic–pharmacodynamic–pharmacogenetic studies are pivotal to assist with the rational prescribing of drugs to pregnant women. Understanding the physiologic and resulting pharmacokinetic changes can be used to develop the rationale for these studies in pregnancy. Utilizing the FDA guidance, an appropriate control group, and a scientifically sound study design should guide those in drug development. Developing drugs that may be used by pregnant women and testing them to ensure proper dosage and use are vitally important from the standpoint of therapeutic justice. This will allow health care practitioners to step out of the age of empiric therapeutics into an enlightened age of rational, informed prescribing of therapy in pregnancy.

## 9.7 The Future of the Field

The field of obstetric pharmacology has grown significantly over the past decade. The National Institutes of Health's (NIH) recognition of the need for additional research in this area prompted the establishment of the Obstetric-Fetal Pharmacology Research Unit Network with support from the Office of Research on Women's Health to provide the expert infrastructure needed to test therapeutic drugs during pregnancy. The Network of four U.S. academic medical centers allows researchers to conduct a whole new generation of safe, technically sophisticated, and complex studies that will help clinicians protect

the health of women, while improving birth outcomes and reducing infant mortality. It is possible that this group will expand in the coming years to further the scientific advancement in this arena. The NIH is currently utilizing specific program announcements in an attempt to stimulate additional research in this field. If measures such as this are not effective, mandates may be instituted requiring the study of medications in pregnant populations prior to FDA approval.

## References

Aldridge, A., J. Bailey, et al. (1981). "The disposition of caffeine during and after pregnancy." *Semin Perinatol* **5**(4): 310–4.

Anderson, G. D. (2005). "Pregnancy-induced changes in pharmacokinetics: a mechanistic-based approach." *Clin Pharmacokinet* **44**(10): 989–1008.

Andrew, M. A., T. R. Easterling, et al. (2007). "Amoxicillin pharmacokinetics in pregnant women: modeling and simulations of dosage strategies." *Clin Pharmacol Ther* **81**(4): 547–56.

Andrew, M. A., M. F. Hebert, et al. (2008). "Physiologically based pharmacokinetic model of midazolam disposition during pregnancy." *Conf Proc IEEE Eng Med Biol Soc* **2008**: 5454–7.

Anger, G. J. and M. Piquette-Miller (2008). "Pharmacokinetic studies in pregnant women." *Clin Pharmacol Ther* **83**(1): 184–7.

Assael, B. M., M. L. Como, et al. (1979). "Ampicillin kinetics in pregnancy." *Br J Clin Pharmacol* **8**(3): 286–8.

Bajpai, M., L. K. Roskos, et al. (1996). "Roles of cytochrome P4502C9 and cytochrome P4502C19 in the stereoselective metabolism of phenytoin to its major metabolite." *Drug Metab Dispos* **24**(12): 1401–3.

Bardy, A. H., V. K. Hiilesmaa, et al. (1987). "Serum phenytoin during pregnancy, labor and puerperium." *Acta Neurol Scand* **75**(6): 374–5.

Benet, L. Z. and B. A. Hoener (2002). "Changes in plasma protein binding have little clinical relevance." *Clin Pharmacol Ther* **71**(3): 115–21.

Blomback, M., K. Bremme, et al. (1998). "A pharmacokinetic study of dalteparin (fragmin) during late pregnancy." *Blood Coagul Fibrinolysis* **9**(4): 343–50.

Bologa, M., B. Tang, et al. (1991). "Pregnancy-induced changes in drug metabolism in epileptic women." *J Pharmacol Exp Ther* **257**(2): 735–40.

Bryson, Y. J., M. Mirochnick, et al. (2008). "Pharmacokinetics and safety of nelfinavir when used in combination with zidovudine and lamivudine in HIV-infected pregnant women: Pediatric AIDS Clinical Trials Group (PACTG) Protocol 353." *HIV Clin Trials* **9**(2): 115–25.

Buchanan, M. L., T. R. Easterling, et al. (2009). "Clonidine pharmacokinetics in pregnancy." *Drug Metab Dispos* **37**(4): 702–5.

Casele, H. L., S. A. Laifer, et al. (1999). "Changes in the pharmacokinetics of the low-molecular-weight heparin enoxaparin sodium during pregnancy." *Am J Obstet Gynecol* **181**(5 Pt 1): 1113–7.

Chamberlain, A., S. White, et al. (1993). "Pharmacokinetics of ampicillin and sulbactam in pregnancy." *Am J Obstet Gynecol* **168**(2): 667–73.

Chen, S. S., E. Perucca, et al. (1982). "Serum protein binding and free concentration of phenytoin and phenobarbitone in pregnancy." *Br J Clin Pharmacol* **13**(4): 547–52.

Chesnutt, A. N. (2004). "Physiology of normal pregnancy." *Crit Care Clin* **20**(4): 609–15.

Clark, S. L., D. B. Cotton, et al. (1989). "Central hemodynamic assessment of normal term pregnancy." *Am J Obstet Gynecol* **161**(6 Pt 1): 1439–42.

Coleman, T. (2007). "Recommendations for the use of pharmacological smoking cessation strategies in pregnant women." *CNS Drugs* **21**(12): 983–93.

Crapo, R. O. (1996). "Normal cardiopulmonary physiology during pregnancy." *Clin Obstet Gynecol* **39**(1): 3–16.

Davison, J. M. (1987). "Kidney function in pregnant women." *Am J Kidney Dis* **9**(4): 248–52.

Davison, J. M. and W. Dunlop (1980). "Renal hemodynamics and tubular function normal human pregnancy." *Kidney Int* **18**(2): 152–61.

Davison, J. M., W. Dunlop, et al. (1980). "24-hour creatinine clearance during the third trimester of normal pregnancy." *Br J Obstet Gynaecol* **87**(2): 106–9.

de Haan, G. J., P. Edelbroek, et al. (2004). "Gestation-induced changes in lamotrigine pharmacokinetics: a monotherapy study." *Neurology* **63**(3): 571–3.

Dean, M., B. Stock, et al. (1980). "Serum protein binding of drugs during and after pregnancy in humans." *Clin Pharmacol Ther* **28**(2): 253–61.

Dempsey, D., P. Jacob, III, et al. (2002). "Accelerated metabolism of nicotine and cotinine in pregnant smokers." *J Pharmacol Exp Ther* **301**(2): 594–8.

Dunlop, W. (1981). "Serial changes in renal haemodynamics during normal human pregnancy." *Br J Obstet Gynaecol* **88**(1): 1–9.

Dvorchik, B. H. (1982). "Drug disposition during pregnancy." *Int J Biol Res Pregnancy* **3**(3): 129–37.

Elkus, R. and J. Popovich, Jr. (1992). "Respiratory physiology in pregnancy." *Clin Chest Med* **13**(4): 555–65.

Ensom, M. H. and M. D. Stephenson (2004). "Pharmacokinetics of low molecular weight heparin and unfractionated heparin in pregnancy." *J Soc Gynecol Investig* **11**(6): 377–83.

Garcia-Martin, E., C. Martinez, et al. (2006). "Interethnic and intraethnic variability of CYP2C8 and CYP2C9 polymorphisms in healthy individuals." *Mol Diagn Ther* **10**(1): 29–40.

Headley, J., K. Northstone, et al. (2004). "Medication use during pregnancy: data from the Avon Longitudinal

Study of Parents and Children." *Eur J Clin Pharmacol* **60**(5): 355–61.

Hebert, M. F., D. B. Carr, et al. (2005). "Pharmacokinetics and pharmacodynamics of atenolol during pregnancy and postpartum." *J Clin Pharmacol* **45**(1): 25–33.

Hebert, M. F., T. R. Easterling, et al. (2008). "Effects of pregnancy on CYP3A and P-glycoprotein activities as measured by disposition of midazolam and digoxin: a University of Washington specialized center of research study." *Clin Pharmacol Ther* **84**(2): 248–53.

Heikkila, A. and R. Erkkola (1991). "Pharmacokinetics of piperacillin during pregnancy." *J Antimicrob Chemother* **28**(3): 419–23.

Heikkila, A., K. Pyykko, et al. (1992). "The pharmacokinetics of mecillinam and pivmecillinam in pregnant and non-pregnant women." *Br J Clin Pharmacol* **33**(6): 629–33.

Heikkinen, T., U. Ekblad, et al. (2003). "Pharmacokinetics of fluoxetine and norfluoxetine in pregnancy and lactation." *Clin Pharmacol Ther* **73**(4): 330–7.

Helsby, N. A., S. A. Ward, et al. (1990). "The pharmacokinetics and activation of proguanil in man: consequences of variability in drug metabolism." *Br J Clin Pharmacol* **30**(4): 593–8.

Hogstedt, S., B. Lindberg, et al. (1983). "Increased oral clearance of metoprolol in pregnancy." *Eur J Clin Pharmacol* **24**(2): 217–20.

Hogstedt, S., B. Lindberg, et al. (1985). "Pregnancy-induced increase in metoprolol metabolism." *Clin Pharmacol Ther* **37**(6): 688–92.

Hurst, A. K., A. Shotan, et al. (1998). "Pharmacokinetic and pharmacodynamic evaluation of atenolol during and after pregnancy." *Pharmacotherapy* **18**(4): 840–6.

Klein, J., P. Blanchette, et al. (2004). "Assessing nicotine metabolism in pregnancy – a novel approach using hair analysis." *Forensic Sci Int* **145**(2–3): 191–4.

Knutti, R., H. Rothweiler, et al. (1981). "Effect of pregnancy on the pharmacokinetics of caffeine." *Eur J Clin Pharmacol* **21**(2): 121–6.

Krauer, B. and F. Krauer (1977). "Drug kinetics in pregnancy." *Clin Pharmacokinet* **2**(3): 167–81.

Lee, E., M. K. Maneno, et al. (2006). "National patterns of medication use during pregnancy." *Pharmacoepidemiol Drug Saf* **15**(8): 537–45.

Luxford, A. M. and G. S. Kellaway (1983). "Pharmacokinetics of digoxin in pregnancy." *Eur J Clin Pharmacol* **25**(1): 117–21.

McBride, W. (1961). "Thalidomide and congenital abnormalities." *Lancet* **278**(7216): 1358.

McGready, R., K. Stepniewska, et al. (2003). "Pregnancy and use of oral contraceptives reduces the biotransformation of proguanil to cycloguanil." *Eur J Clin Pharmacol* **59**(7): 553–7.

Messina, E. S., R. F. Tyndale, et al. (1997). "A major role for CYP2A6 in nicotine C-oxidation by human liver microsomes." *J Pharmacol Exp Ther* **282**(3): 1608–14.

Morgan, D. J. and R. A. Smallwood (1990). "Clinical significance of pharmacokinetic models of hepatic elimination." *Clin Pharmacokinet* **18**(1): 61–76.

Nakai, A., I. Sekiya, et al. (2002). "Assessment of the hepatic arterial and portal venous blood flows during pregnancy with Doppler ultrasonography." *Arch Gynecol Obstet* **266**(1): 25–9.

Nathorst-Boos, J., A. Philipson, et al. (1995). "Renal elimination of ceftazidime during pregnancy." *Am J Obstet Gynecol* **172**(1 Pt 1): 163–6.

Naylor, D. F., Jr. and M. M. Olson (2003). "Critical care obstetrics and gynecology." *Crit Care Clin* **19**(1): 127–49.

Nordmark, A., S. Lundgren, et al. (2002). "The effect of the CYP1A2 *1F mutation on CYP1A2 inducibility in pregnant women." *Br J Clin Pharmacol* **54**(5): 504–10.

O'Hare, M. F., W. Leahey, et al. (1983). "Pharmacokinetics of sotalol during pregnancy." *Eur J Clin Pharmacol* **24**(4): 521–4.

Ohkita, C. and M. Goto (1990). "Increased 6-hydroxycortisol excretion in pregnant women: implication of drug-metabolizing enzyme induction." *DICP* **24**(9): 814–6.

Ohman, I., S. Vitols, et al. (2000). "Lamotrigine in pregnancy: pharmacokinetics during delivery, in the neonate, and during lactation." *Epilepsia* **41**(6): 709–13.

O'Sullivan, M. J., P. J. Boyer, et al. (1993). "The pharmacokinetics and safety of zidovudine in the third trimester of pregnancy for women infected with human immunodeficiency virus and their infants: phase I acquired immunodeficiency syndrome clinical trials group study (protocol 082). Zidovudine Collaborative Working Group." *Am J Obstet Gynecol* **168**(5): 1510–6.

Pennell, P. B., D. J. Newport, et al. (2004). "The impact of pregnancy and childbirth on the metabolism of lamotrigine." *Neurology* **62**(2): 292–5.

Philipson, A. (1977). "Pharmacokinetics of ampicillin during pregnancy." *J Infect Dis* **136**(3): 370–6.

Philipson, A. and G. Stiernstedt (1982). "Pharmacokinetics of cefuroxime in pregnancy." *Am J Obstet Gynecol* **142**(7): 823–8.

Philipson, A., G. Stiernstedt, et al. (1987). "Comparison of the pharmacokinetics of cephradine and cefazolin in pregnant and non-pregnant women." *Clin Pharmacokinet* **12**(2): 136–44.

Prevost, R. R., S. A. Akl, et al. (1992). "Oral nifedipine pharmacokinetics in pregnancy-induced hypertension." *Pharmacotherapy* **12**(3): 174–7.

Rubin, J. D., C. Ferencz, et al. (1993). "Use of prescription and non-prescription drugs in pregnancy. The Baltimore-Washington Infant Study Group." *J Clin Epidemiol* **46**(6): 581–9.

Sachse, C., U. Bhambra, et al. (2003). "Polymorphisms in the cytochrome P450 CYP1A2 gene (CYP1A2) in colorectal cancer patients and controls: allele frequencies, linkage disequilibrium and influence on caffeine metabolism." *Br J Clin Pharmacol* **55**(1): 68–76.

Schou, M., A. Amdisen, et al. (1973). "Lithium and pregnancy. II. Hazards to women given lithium during pregnancy and delivery." *Br Med J* **2**(5859): 137–8.

Simpson, K. H., A. F. Stakes, et al. (1988). "Pregnancy delays paracetamol absorption and gastric emptying in patients undergoing surgery." *Br J Anaesth* **60**(1): 24–7.

Thorley, K. J., J. McAinsh, et al. (1981). "Atenolol in the treatment of pregnancy-induced hypertension." *Br J Clin Pharmacol* **12**(5): 725–30.

Tomson, T., U. Lindbom, et al. (1994a). "Disposition of carbamazepine and phenytoin in pregnancy." *Epilepsia* **35**(1): 131–5.

Tomson, T., U. Lindbom, et al. (1994b). "Epilepsy and pregnancy: a prospective study of seizure control in relation to free and total plasma concentrations of carbamazepine and phenytoin." *Epilepsia* **35**(1): 122–30.

Torgersen, K. L. and C. A. Curran (2006). "A systematic approach to the physiologic adaptations of pregnancy." *Crit Care Nurs Q* **29**(1): 2–19.

Tracy, T. S., R. Venkataramanan, et al. (2005). "Temporal changes in drug metabolism (CYP1A2, CYP2D6 and CYP3A activity) during pregnancy." *Am J Obstet Gynecol* **192**(2): 633–9.

Tran, T. A., I. E. Leppik, et al. (2002). "Lamotrigine clearance during pregnancy." *Neurology* **59**(2): 251–5.

Tsutsumi, K., T. Kotegawa, et al. (2001). "The effect of pregnancy on cytochrome P4501A2, xanthine oxidase, and N-acetyltransferase activities in humans." *Clin Pharmacol Ther* **70**(2): 121–5.

van Heeswijk, R. P., Y. Khaliq, et al. (2004). "The pharmacokinetics of nelfinavir and M8 during pregnancy and post partum." *Clin Pharmacol Ther* **76**(6): 588–97.

Ververs, F. F., H. A. Voorbij, et al. (2009). "Effect of cytochrome P450 2D6 genotype on maternal paroxetine plasma concentrations during pregnancy." *Clin Pharmacokinet* **48**(10): 677–83.

Wadelius, M., E. Darj, et al. (1997). "Induction of CYP2D6 in pregnancy." *Clin Pharmacol Ther* **62**(4): 400–7.

Ward, S. A., N. A. Helsby, et al. (1991). "The activation of the biguanide antimalarial proguanil co-segregates with the mephenytoin oxidation polymorphism – a panel study." *Br J Clin Pharmacol* **31**(6): 689–92.

Watts, D. H., Z. A. Brown, et al. (1991). "Pharmacokinetic disposition of zidovudine during pregnancy." *J Infect Dis* **163**(2): 226–32.

Wilson, C. M., J. W. Dundee, et al. (1987). "A comparison of the early pharmacokinetics of midazolam in pregnant and nonpregnant women." *Anaesthesia* **42**(10): 1057–62.

Yerby, M. S., P. N. Friel, et al. (1990). "Pharmacokinetics of anticonvulsants in pregnancy: alterations in plasma protein binding." *Epilepsy Res* **5**(3): 223–8.

# Design, Conduct and Analysis of Thorough QT Studies

# 10

Tanya Russell, Daniel S. Stein, and David J. Kazierad

## Abstract

Torsades de Pointes (TdP) is a type of polymorphic ventricular tachycardia that can result in fainting and death. While there are genetic causes for TdP, such as ion channel mutations, drug-induced TdP can occur, an event that first gained prominence with the interaction between terfenadine and ketoconazole. While TdP itself cannot be studied in clinical trials due to its low rate of incidence, a biomarker for TdP is prolongation of the QT interval on an ECG. Today, almost every drug is expected to be evaluated for its potential to prolong QT interval. This chapter discusses measurement of QT intervals in clinical trials, the design and analysis of "thorough" QT studies, including the intersection–union test and concentration-QT modeling, as well as practical matters related to the International Conference on Harmonisation's E14 guidance.

## 10.1 Introduction and Background

In 1841 Matteucci demonstrated each heart beat was associated with electrical activity (Matteucci 1842). Over the ensuring years several investigators attempted to further describe the nature of the heart's electrical activity. The first human electrocardiogram was recorded by Augustus Waller in 1887 using a Lippmann capillary electrometer and indicated only two waves named $V_1$ and $V_2$ (Waller 1887). Willem Einthoven, after attending a demonstration by Waller in 1889, began a series of experiments to develop a more accurate and clinically suitable method of recording the heart's electrical activity (Zetterström 2009). The electrical activity occurring in four deflections was first demonstrated by Einthoven and were originally named ABCD (Hurst 1998). In 1895, Einthoven published an illustration where the ECG waves were named PQRST, probably to differentiate his corrected curve which had been superimposed on the uncorrected tracing. The mathematician Rene Descartes used P and Q to demonstrate points on a curve. Einthoven would have been instructed in this work during his education and it is the likely origin of the PQRST naming; in addition, by using these letters, he eliminated confusion between curves and allowed for later additions

T. Russell (✉)
Oncology Clinical Pharmacology, Pfizer, 10646 Science Center Drive (CB10/2503), San Diego, CA 92121, USA
e-mail: Tanya.russell@pfizer.com

(Hurst 1998). With the construction of the string galvanometer in 1901, Einthoven achieved his goal of making an instrument that could accurately record a full ECG recording from cutaneous input based on the Einthoven's triangle of bipolar currents using the right and left shoulder and the left leg as references (leads I, II, and III in the modern ECG). By 1906, Einthoven had published a report on normal and abnormal ECGs and by 1912 a comprehensive report on multiple cardiac pathologies (Einthoven 1912). An example of an ECG machine from 1912, which unlike today used salt solution buckets, can be found in Estes (2008). The ECG machine was in worldwide use within 20 years and Einthoven would win the Nobel Prize for his achievement in 1924 (Zetterström 2009). The additional unipolar limb leads (aVR, aVL, aVF, which are abbreviations for *a*ugmented *v*ector *r*ight, *l*eft, or *f*oot) and the precordial or ventricular leads ($V_1$–$V_6$) would come much later with the invention of more sophisticated electronics.

It is now known the electrical basis of the ECG is governed by different ion channels in the heart controlling sodium, calcium, and potassium influx and efflux – for which a full review is beyond the scope of this chapter (Ackerman and Clapman 1997; Tseng 2001; Wehrens et al. 2002). Mutations in the genes governing these channels can lead to serious diseases such as the long QT syndrome which can result in life threatening arrhythmias and death. The main channel responsible for the potassium-driven repolarization reflected by the QT interval is the human ether-a-go-go-related (hERG) or $I_{Kr}$ (Inward rapid potassium current). The hERG ion channel has multiple sites for binding by drugs and is the target of the class III antiarrthymic agents (Gralinski 2000; Tseng 2001). Binding of a drug to hERG can be competitive or noncompetitive with rapid or slow disassociation; therefore total drug concentration is used to assess risk. In vitro screening of drugs for potential risk of effects on cardiac conduction involves screening against the hERG channel and the isolated Purkinje fiber conduction system. In vivo drug dosing with full ECG telemetry monitoring to better assess the potential risk is typically performed

in dogs. All drugs shown clinically to cause potentially life threatening cardiac arrhythmias (such as torsades de pointes (TdP), a specific type of ventricular tachycardia) have been positive in hERG screening (Malik and Camm 2001). However, many drugs with a risk indicated from in vitro testing will not necessarily have an increased risk demonstrated in either animals or human evaluation. For additional information on the non-clinical assessment of ventricular repolarization, the reader may refer to the ICH S7B guidelines (International Conference on Harmonisation 2005b).

### 10.1.1 What Is "QTc" and Why Do We Measure It?

The QT interval duration is a reflection of the time from the beginning of ventricular depolarization marked by the QRS complex (ventricular contraction) to the repolarization of the cardiac conduction system marked by the end of the T wave (Fig. 10.1). The length of the entire cardiac cycle has to be shorter at higher heart rates in order for a higher heart rate to occur. The first two parts of the electrical activity, the P wave (representing atrial depolarization) and the QRS complex are relatively fixed, therefore the QT interval must shorten as the heart rate increases. To correct for changes in heart rate, the QT interval is normalized to a heart rate of 60 bpm; this corrected QT interval is known as the QTc interval.

The two most common formulae used to correct for the heart rate on the QT interval are Bazett's (1918) where the $QTcB = QT/(RR)^{1/2}$ and Fridericia's (1920) where the $QTcF = QT/(RR)^{1/3}$. At a heart rate of 60 bpm (RR = 1 s) both formulae agree and there is no correction. Other correction formulae will be discussed in a later section. An important reason for measuring the QTc interval is that prolongation of the interval is associated with an increased risk of potentially life threatening cardiac arrhythmias. This is seen on the ECG as TdP, a specific type of polymorphic ventricular tachycardia, known for its twisting form of wave pattern (see Fig. 10.2)
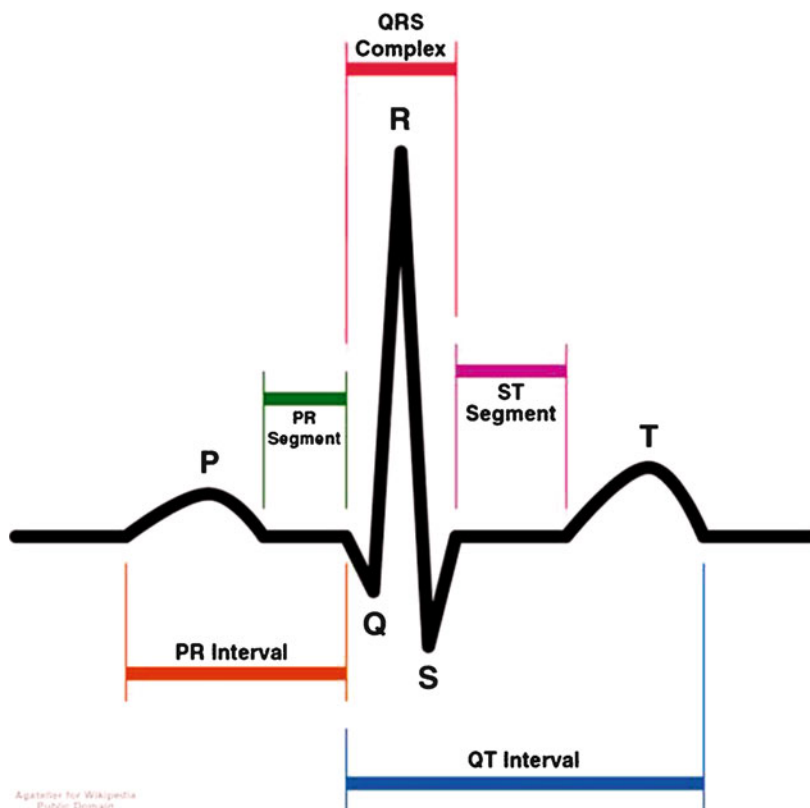
**Fig. 10.1** Example 12-lead ECG recording of lead II demonstrating the various interval measurements
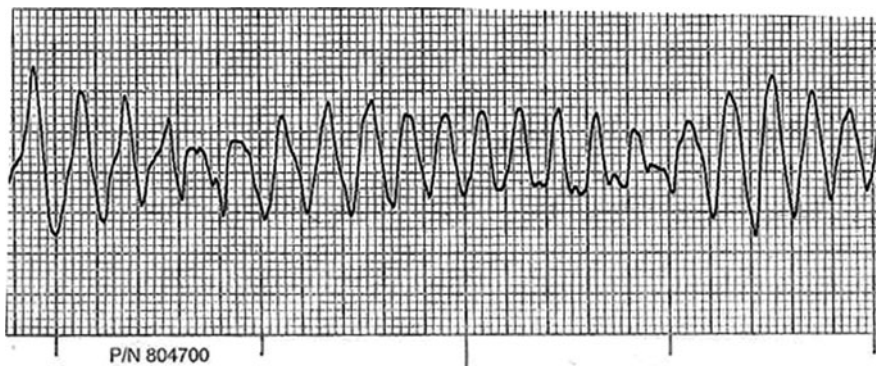


**Fig. 10.2** Example of a telemetry tracing of torsades de pointes

due to change of electrical axis of the QRS complex around the central isoelectric line.

Torsades de pointes can progress to ventricular fibrillation and death. Concern with TdP and drug induced arrhythmia began in the 1970s, but a significant increase in attention to the issue came in the 1990s when the non-sedating antihistamine terfenadine was associated with an increased incidence of arrhythmia and sudden death. Well known examples of dose related arrhythmia are the drugs sotalol (Bayer Healthcare Pharmaceuticals 2007) and dofetilide (Pfizer Inc. 2006).
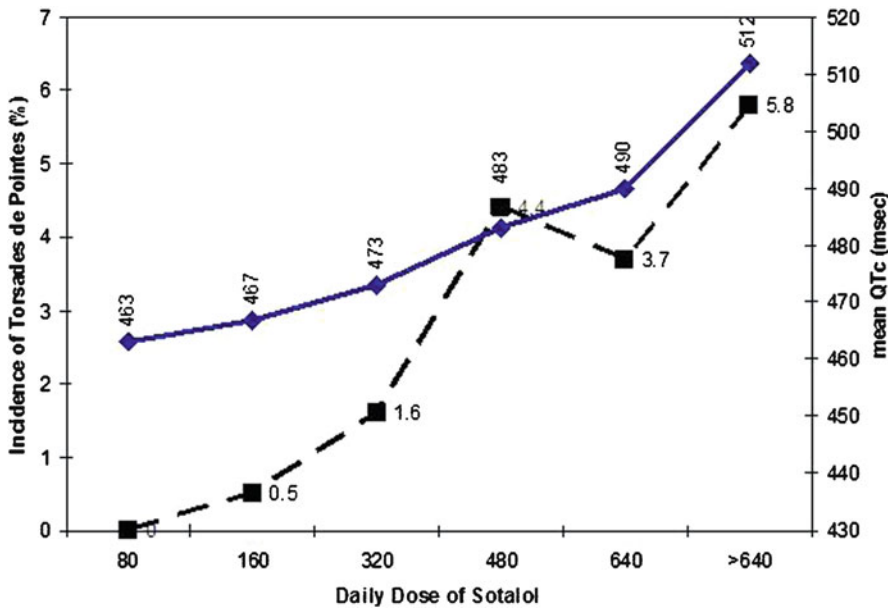
**Fig. 10.3** The relationship of sotalol dose to the increase in QTc intervals and occurrence of torsades ($N = 2,622$) – data from (Bayer Healthcare Pharmaceuticals 2007)

Sotalol, a non-selective beta blocker, given in large clinical trials had a well described relationship of increasing dose with an increase in mean QTc interval duration, and an increased incidence of sustained TdP (see Fig. 10.3).

Dofetilide, a class III antiarrhythmic drug causes QTc interval prolongation as part of its mechanism of action. In the data from large clinical trials, there was an association between increasing dose and TdP, and subsequently, an increased incidence of ventricular fibrillation, as well as the occurrence of TdP (see Fig. 10.4). These examples illustrate that as the QTc interval increases, the incidence of potentially life threatening ventricular arrhythmias increases and the occurrence of TdP is not the only ventricular arrhythmia that increases in risk. Both agents have significant labeling restrictions on their clinical use.

Terfenadine causes an average QTc interval increase in humans of 6 ms, but has been shown to increase to 23 ms with a tripling of dose or increase in parent drug exposure resulting from, for example, inhibition of its CYP3A4 metabolism (Gralinski 2000). These findings led to its withdrawal from the market which was followed

by a series of high-profile drug withdrawals of additional agents (e.g. cisapride, gemifloxacin) by health authorities because of QT interval prolongation-related safety issues. These events led health agencies to develop guidances regarding drug-induced QT interval prolongation.

## 10.2 Global Regulatory Guidance: ICH E14

### 10.2.1 ICH E14

The initial formal guidance concerning the potential for QT interval prolongation by non-cardiovascular drugs came in a 1997 "Points to Consider" from the Committee of Proprietary Medicinal Products (CPMP) of the European Medicines Evaluation Agency (Committee for Proprietary Medicinal Products 1997).

In 2001, the Therapeutic Products Directorate (TPD) of Health Canada published draft guidance on the assessment of QT interval prolongation potential on non-antiarrhythmic drugs. Like the CPMP document, the TPD draft proposed specific preclinical and clinical testing of new
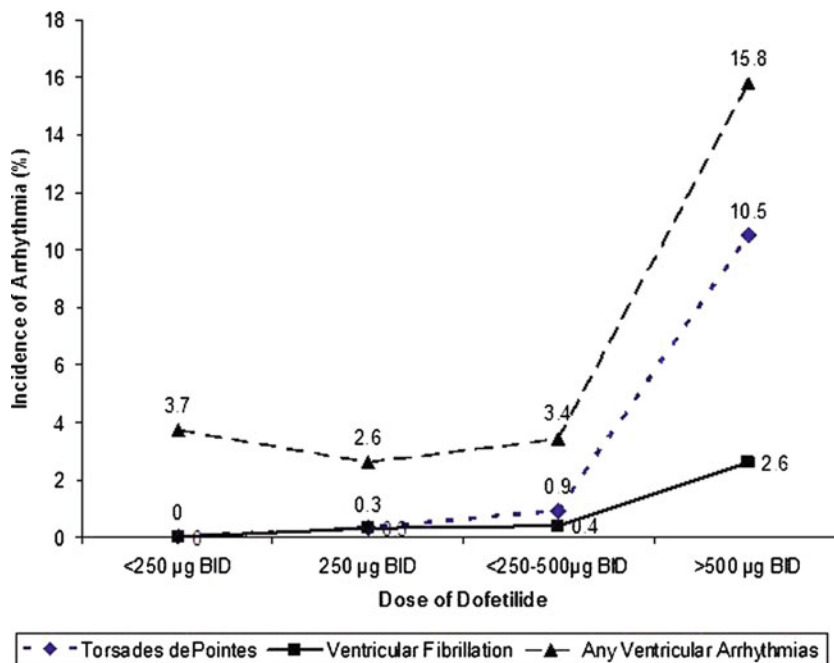
**Fig. 10.4**  The relationship of dofetilide dose to the incidence of any ventricular arrhythmia, torsades de pointes, and ventricular fibrillation ($N = 1,346$) – data from (Pfizer Inc. 2006)

compounds to identify potential QT interval prolongation. Working in conjunction with TPD, the United States Food and Drug Administration (FDA) revised the draft guidance and in November 2002 issued a preliminary clinical concept paper entitled "The Clinical Evaluation of QT/QTc Interval Prolongation and Proarrhythmic Potential for Non-Antiarrhythmic Drugs." The document was the focus of a February 2003 public meeting sponsored by FDA, TPD, Drug Information Association, and the North American Society of Pacing and Electrophysiology. Following the public meeting, the concept paper was revised and subsequently accepted by the International Conference of Harmonisation (ICH) for harmonization as guidance for industry that was finalized in May 2005 entitled, E14 Clinical evaluation of QT/QTc interval prolongation and proarrhythmic potential for non-antiarrhythmic drugs (International Conference on Harmonisation 2005a). A separate preclinical QT interval guidance preceded ICH E14 into the ICH process. The preclinical topic has been designated S7B [Guidance on the Nonclinical Evaluation of the Potential for Delayed Ventricular Repolarization (QT Interval Prolongation) by Human Pharmaceuticals] (International Conference on Harmonisation 2005b). The ICH includes among its members the United States Food and Drug Administration, the European Medicines Evaluation Agency and the Japan Ministry of Health, Labour and Welfare.

The ICH E14 guidance and its implications for drug development and approval will be outlined in further details in later sections. Briefly the guidance describes the assessment of potential for QTc interval prolongation in clinical trials and the need for a "Thorough QT/QTc study" (TQT study) with suggested methods of analysis and design. The overarching purpose of the recommendations is to characterize the proarrythmic risk of the drug. The results of the TQT study have significant implications for regulatory approval and for labeling in the context of the drug's overall risk-benefit in its intended population.

### 10.2.2 QT Interdisciplinary Review Team

In an effort to provide additional specific guidance to sponsors, the Center for Drug Evaluation and Research (CDER) at the FDA established the Interdisciplinary Review Team (IRT) in June 2006. The QT IRT includes clinical, statistical, pharmacology, and clinical pharmacology reviewers, and project and database management. The IRT is responsible for reviewing TQT study protocols and reports submitted by sponsors. Although the IRT provides a degree of standardization and consistency across various divisions within the FDA, the IRT's recommendations are nonbinding, and final decisions still reside with the individual therapeutic groups.

## 10.3 When to Conduct a Thorough QT Study

The ICH E14 guidance does not mandate the timing or conduct of a TQT study. It is the decision of each Sponsor and each project team to determine whether a TQT study is needed and the best time to conduct the TQT study in the development timeline. In general, this is a question to be discussed with regulatory agencies during the ongoing development program; such as part of an End-of-Phase 2 meeting. Because the purpose of the TQT study is to determine whether or not the drug has proarrhythmic risk; the results of the TQT study can influence the need and extent of ECG monitoring for Phase 2 and 3 trials and the risk-benefit assessment for the drug's approval by agencies, and its approved labeling. When the TQT study is positive, and demonstrates prolongation of the QT interval, the ICH E14 guidance recommends additional evaluation be performed in subsequent clinical trials. The purpose of the continued evaluation is to fully describe the effect of the drug on QT/QTc interval in the target patient population. For this characterization, it is important to collect ECGs around the time of the anticipated maximum drug effects based on the pharmacokinetics in the

population. If the TQT study is negative and there is no QT interval signal, then the routine safety monitoring of ECGs, as clinically indicated, is recommended for later studies.

At face value, the guidance suggests the TQT study should be conducted early in drug development, prior to Phase 2 or Phase 3 so additional ECG monitoring can be added to the Phase 2/3 protocols, if needed. However, in practice, it is not straightforward. As with any expenditure in drug development, there is a trade-off between obtaining information earlier in development, high attrition rates, and the cost of development. Because these studies are expensive, require relatively large subject numbers, multiple ECG's, and special ECG handling, the study conduct is a significant investment compared to other healthy subject trials. Investments spent early in the development timeline may be wasted if the drug does not progress. As a result of these trade-offs, a more pragmatic approach is often taken. The potential risk of the drug to prolong QTc interval and result in a positive TQT study should be assessed in early development by considering the preclinical data package (see ICH S7b guidance) (International Conference on Harmonisation 2005b) relative to QT/QTc prolongation. What is the potential for the drug to cause QT/QTc interval prolongation relative to the predicted concentrations needed for efficacy given the results from HERG channel, dog telemetry, general toxicology findings, etc.? In the first studies in humans, the ECGs can be recorded serially at time points to match a subset of the pharmacokinetic samples. The relationship between concentration and QTc interval can be explored across a wide range of doses and concentrations using a pooled analysis across the single and multiple dose tolerance studies. Categorical analysis of outliers as mentioned below is also helpful to understand the relative risk. If the early clinical data and preclinical data show a potential for QTc interval prolongation, then it may be wise to monitor ECGs in the patient trials. If the early clinical data and preclinical data indicate little to no risk of QTc interval prolongation, then a decision could be made to implement only routine ECG monitoring for safety in the patient trials. In

the later case, the Sponsor is accepting the risk inherent in assuming the TQT study will be negative and further monitoring in Phase 2/3 would not be required. In either case, the TQT study would then be conducted later in development either in parallel with Phase 2b or Phase 3 after proof of concept has been established.

In addition to general development timeline considerations, the availability of sufficient data to make an informed choice of the dose will also drive the timing of the TQT study. As is explained more fully in the section on dose, choosing the correct therapeutic and (when possible) supratherapeutic dose for the study is critical. If the TQT study is conducted too early in development, there is risk the doses used in the TQT study will not reflect the final therapeutic dose, which can impact the interpretation of the results and regulatory acceptance of the study.

A TQT study will be required for most drugs at the time of filing based on the current regulatory environment, although there are exceptions since some drugs cannot be studied in healthy subjects due to safety or tolerability concerns. This is often the case with cancer therapies due to cytotoxicity issues, but may also affect other therapeutic areas, such as schizophrenia where the drug may be tolerated at the therapeutic dose in patients, but not in healthy subjects. One alternative is to conduct the TQT study in the patient population, but this may present problems resulting from the potential for increased variability in the QTc interval in patients, increased potential for a false positive study with the parallel design (Hutmacher et al. 2008) and the potential use of other concomitant medications in the target population. Further, the use of placebo or even active controls in some patient populations may not be ethical. Alternative approaches have been suggested for oncology drugs. At a high level, the recommendation involves characterization of the ECG parameters across a wide range of doses (or concentrations) usually from the dose escalation study in patients. A separate ECG sub study under tightly controlled conditions in the target patient population preferably with concentration-QT interval modeling included could then be added to the

regulatory submission package to characterize the risk. Curigliano et al. (2008), Serapa and Britto (2008), and Rock et al. (2009) have all published in more detail on this topic. These alternate approaches should be discussed with the relevant regulatory authorities to gain acceptance of this package in lieu of the full package that includes a TQT study.

## 10.4   Measuring QT/QTc Intervals

### 10.4.1   Machine, Semi-Automated, and Manual Over-Read Methods

The techniques currently used for assessing ECG intervals can be classified into three broad categories: fully manual, fully automated, and semi-automated, or manual adjudication. When using a manual over-read technique, a human reader examines ECG waveforms and places reference marks at the beginning and the end of the intervals of interest, without the assistance of a computer algorithm. When manual measurements are made from ECG waveforms in a single lead, multiple (three or more) cardiac cycles are generally averaged to produce the final determination of interval duration. An advantage of this technique is that a trained reader reviews and interprets the ECG tracings and is able to identify potential artifacts such as T wave morphology changes or the presence of U waves, which may occur after the end of the T wave. These findings may often be seen in patient populations, especially those with existing cardiac disease. A disadvantage to this technique compared to automated approaches is the inherent inter- and intra-reader variability, especially when multiple measurements are performed over an extended period of time (e.g. several months). Core ECG laboratories, which act like a central laboratory for reading ECGs, performing manual over-read techniques should observe standard operating procedures based on prospectively defined criteria for determining the onset and offset of ECG intervals of interest, and all readers should be trained in the consistent application of these criteria (International Conference on

Harmonisation 2008). Although the ICH E14 document recommends the reader be skilled, it does not identify the specific training that is needed. Using a trained technician to read ECG recordings with a cardiologist review would be consistent with the ICH E14 guidance. In an effort to improve consistency in over-read values, the guidance recommends limiting the number of readers reviewing the ECG tracings. The guidance asks for assessment of intra- and inter-reader variability and suggests "a few skilled readers" (not necessarily a single reader) to analyze a whole TQT study, since increasing the number of readers may increase variability (International Conference on Harmonisation 2005a). It is recommended by some, however, that one reader should examine all the ECG tracings for the same subject throughout the trial.

For the fully automated (machine-read) approach, ECG interpretation relies entirely upon a computer algorithm for the measurement of ECG intervals. The algorithm used to derive QTc intervals from machine-read ECGs is not consistent among the different manufacturers and machines. It's useful to know which correction factor was used if the investigator is reading the initial machine recording output for real time safety monitoring at the clinical site. Most digital electrocardiographs are equipped with algorithms that perform measurements on global waveforms from all 12-leads. Although automated measurements have the advantage of being consistent and reproducible, they may be problematic and produce misleading results in the presence of a noisy baseline or when dealing with abnormal ECG rhythms, often resulting from low amplitude P or T waves, or overlapping U waves (International Conference on Harmonisation 2008). These issues are usually not a concern with ECG tracings collected from healthy subjects. The technology used for the construction and measurement of waveforms vary between different computerized algorithms and between different software versions within individual equipment manufacturers (see Sect. 10.5.2.1). Therefore, when using an automated approach, it is recommended the same brand of electrocardiograph be used for all subjects

in the trial. In comparison with manual methods, automated approaches offer advantages in terms of absolute repeatability of measurements, lack of reader errors related to fatigue and lapses of attention, and lower cost considerations.

The third approach to over-reading ECG recordings is the semi-automated or manual adjudication method. This technique uses a computer algorithm for the initial placement of reference marks on the waveforms to note where on the tracing the computer is making its measurements. A human reader then reviews the reference marks' placement, and performs adjustments when the computerized measurements are considered to be inaccurate. In an effort to ensure consistency between readers, it is important the laboratory performing the review of the automated measurements has prospectively defined criteria for determining when changes to computer-generated marks are corrected. This approach can have the advantage of greater consistency and reproducibility than fully manual readings, while providing an opportunity to correct any errors made by the algorithmic methods. In a review of 9,500 ECGs measured in healthy subjects using the semi-automated approach, only 10 (0.11%) of the recordings were corrected by the investigator (Darpo et al. 2006).

The ICH E14 guidance currently recommends either fully manual or semi-automated approaches for determining QT intervals in TQT studies. If a definitive TQT study has a positive finding for QT interval prolongation, the fully manual or semi-automated methods are currently recommended to describe the effect of the drug on the QT/QTc interval in an adequate number of patients from the target population (International Conference on Harmonisation 2005a). When the TQT study is negative, automated methods are adequate to assess routine ECG safety in later phase clinical trials (International Conference on Harmonisation 2005a, 2008). Currently, there are several companies working on developing and validating fully automated techniques. As these devices become available, the recommendations in the guidance for measuring ECG intervals could be modified.

Although manual ECG techniques have historically been preferred in studies of drug-related QT/QTc interval effects, manual techniques are susceptible to reader bias and variability. A recent analysis of ECG data using manual and machine-based techniques from three studies in healthy subjects demonstrated automated techniques were capable of detecting small changes in the QTc interval following a positive control that were similar to those with manual readings and arrived at the same conclusion (Darpo et al. 2006). Based on these findings, there is evidence that automated techniques are similar to manual over-reads for measuring QT intervals in healthy subjects (Darpo et al. 2006). In another comparison of manual and automated measurements of QT interval in healthy subjects, five TQT studies were evaluated (Fosser et al. 2009). Results from this analysis demonstrated that the fully automated, fully manual, and semi-automated methods all detected moxifloxacin-induced, baseline adjusted, placebo-subtracted mean changes in QTcF intervals. In general, manual and semi-automated techniques were associated with greater variability than a fully automated method, but all were comparable for the purpose of demonstrating assay sensitivity in healthy subjects (Fosser et al. 2009).

One instance when manual over-reading of ECG tracings may have a clear advantage over automated methods is when the study is being conducted in patients, especially those with cardiac disease (McLaughlin et al. 1996). Electrocardiograms from patients often exhibit altered T wave morphology relative to ECGs from healthy individuals. In a study comparing automated QT interval measurement techniques in cardiac patients and healthy subjects, the machine-read measurements were two times as variable as the manual reference performed by an experienced reader (McLaughlin et al. 1996).

### 10.4.2  Correction Methods

As noted earlier the two most common correction methods for the effect of heart rate on the QT interval are the Bazett's (1918), where the QTcB $= QT/(RR)^{1/2}$, and Fridericia's (Fridericia 1920), where the QTcF $= QT/(RR)^{1/3}$ (also called fixed correction methods). Both formulae have issues with overcorrection as the heart rate increases above 60 bpm and under correction below 60 bpm. While the Bazett method is commonly programmed into the automated ECG machine readouts, the Fridericia's correction is considered to be more accurate in most cases. As a result, the QTcF interval is often the default correction method used for summarization and analysis of the QTc interval data.

Other correction methods are available based on linear regression techniques, nonlinear or linear regression modeling on pooled data, and within subject data. For example, a common linear correction formula is the Framingham which is $QTc = QT + 0.154(1 - RR)$. Linear correction methods are applied to the placebo or baseline data to obtain the slope of the QT-RR interval relationship.

An Individual Correction method (or subject specific, QTcI) fits a regression model to the QT-RR baseline data from each subject. The two main issues with this method are (1) the need for several baseline measurements to get a good estimate and (2) the need for a wide range of heart rates. Guidance from Health Canada suggests greater than 100 QT-RR pairs should be included per subject and the RR should range from approximately 600–1,000 ms (Health Products and Food Branch 2009). The use of a 12-lead Holter where the continuous recording is sampled at multiple time points to collect the ECG parameters has been used to produce the requirement for several measurements. The heart rate issue is more difficult in healthy subjects. Methods such as exercise induced changes in heart rate have been suggested. The regulatory acceptance of these approaches in relevant regions should be explored before implementing these techniques or using QTcI interval as the primary endpoint.

A population based correction method (also called study specific or pooled correction) fits a mixed effects regression model to the pooled QT-RR data from all subjects within a study. While an individual method assumes a different

QT-RR relationship for each subject, the fixed and population based methods assume the QT-RR relationship is the same for all subjects. A population based correction is often explored as part of the population based concentration-QT interval analysis and has been accepted by the regulatory authorities as an alternative approach when QTcF intervals and QTcB intervals demonstrate significant correlation between QTc interval and RR interval. An example plot of QTc versus RR for three different corrections methods

demonstrating the varying degree of correlation is shown in Fig. 10.5.

While these other correction methods have been used to analyze ECG data, there is no consensus on whether they have a significant advantage over the common Fridericia's method (QTcF). In direct comparison of fixed, individual, and population methods on the same dataset the differences were negligible, indicating an effect on the individual but not the subject averaged mean QTc interval (Wang et al. 2008). One



$$QTcB = 477 - 0.0794 * RR$$

$$QTcF = 407 - 0.0098 * RR$$

$$QTcP = 398 + 0.0004 * RR$$
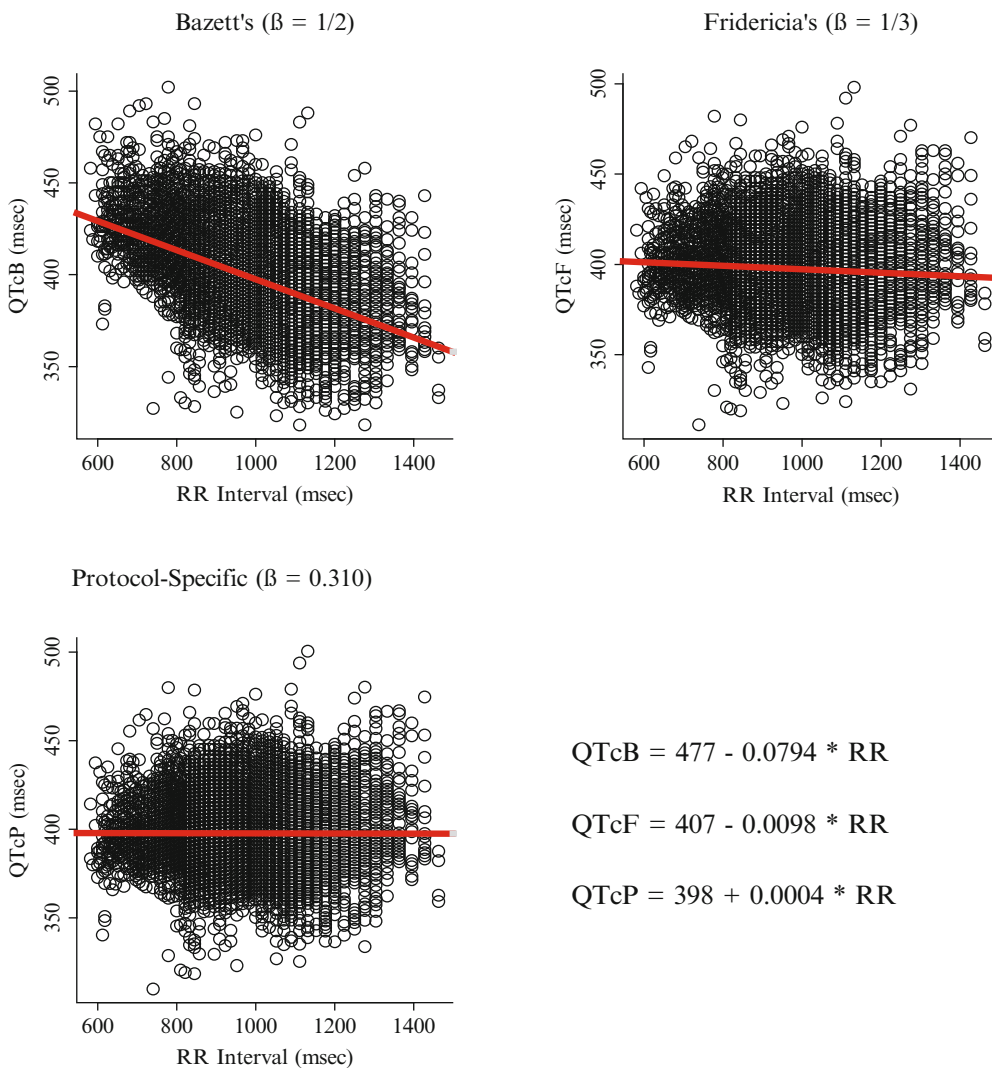
**Fig. 10.5** Plot of QTc by RR intervals for Bazett's, Fridericia's and a protocol-specific correction factors (Riley et al. 2006)

of the major limitations of the use of any of these alternate correction methods is that the broader clinical database will largely include only QTcB interval and/or QTcF interval collected from machine-read ECGs. This may make it difficult to summarize across studies and to fully assess risk at the time of submission.

### 10.4.3 Alternative QT Interval Assessment Approaches Under Consideration

The standard formulae for QT interval correction are heart-rate dependent. Therefore, if the drug causes a change in heart rate, the hysteresis effect in QT interval change with heart rate may lead to an overestimate of the QTc interval change. The adaptation to the acute change takes approximately 2 min to complete (Franz et al. 1988; Lau et al. 1988).

The RR binning method has been proposed as a means of controlling for heart rate. All the QT values are distributed according to their preceding RR interval into "bins" or groups. As an example, the estimate of the QT interval at 1,000 ms or QT interval at 60 bpm is determined from an average of the QT values in the 995–1,004 ms bin. A 12-lead Holter monitoring system which allows for continuous ECG assessment may be used for data collection. The differences in the estimated placebo corrected QTc interval change from baseline using this technique may or may not be different than using a simpler QTcF interval method (Extramiana et al. 2005; Malik et al. 2009). Because the averaged values are collected over a range of time points post dose, this approach results in under-estimation of the maximum QT/QTc prolongation (Health Products and Food Branch 2009).

A second approach is the estimate of the beat-to-beat confluence of ECG data or "clouds" (Fossa et al. 2005, 2007; Fossa 2008; Malik 2008). The premise is that methods to correct QT intervals are confounded by changes in autonomic state (normal physiological changes) and may not accurately reflect or quantify arrhythmogenic risk. To apply this technique, the beat-to-beat conflu-ence of ECG data is sequentially plotted. The nonparametric bootstrap resampling method is used to compute the mean of the uncorrected beat-to-beat QT interval value and the upper and lower 95% confidence intervals. A high quality digital 12-lead Holter system is used for data collection. Some validation of the method is completed (Fossa et al. 2007), and this technique is being explored as an alternative to traditional correction techniques.

These alternate approaches are still under investigation. Although there are examples where these methods have been accepted by regulatory authorities, discussion with the regulatory agencies is warranted prior to their submission.

## 10.5 Study Design Considerations

### 10.5.1 Subjects

#### 10.5.1.1 Patients or Healthy Subjects

One of the first considerations when designing a TQT study is the study population to be included in the trial. There are no regulatory requirements to conduct the TQT study in the patient population for which the study compound is being developed, and therefore, these studies are typically conducted in a healthy subject population. There is, however, one noted exception: when there are safety concerns limiting tolerability of the compound in healthy subjects. Examples include neuroleptics and cytotoxic agents. In these cases, it is prudent to conduct QT interval studies in the patient population in which the compound is being developed. Additional discussion of these situations can be found in the Sect. 10.3.

Regarding other demographic factors, there are no regulatory requirements to include or exclude subjects from the study-population based on age, gender or race. It is recognized, however, females have slower cardiac repolarization than males, which, on average, results in longer baseline QTc intervals (Stramba-Badiale et al. 1997). In addition, it has been reported females are at a greater risk of developing TdP associated with the use of certain cardiovascular

agents (Makkar et al. 1993). There are also data to support the existence of sex-related differences in the sensitivity of drug induced QT interval prolongation (Benton et al. 2000; Rodriguez et al. 2001). In one study, a single low dose infusion of ibutilide produced greater QT interval prolongation in females than males, independent of the concentrations of ibutilide (Rodriguez et al. 2001). In addition, this same study concluded females demonstrated greater QT interval variability in response to ibutilide depending on which phase of the menstrual cycle they were in when they received the drug. Women during menses and the ovulatory phase of the menstrual cycle had the greatest QTc interval response, relative to the luteal phase, thereby supporting a role for sex hormones in drug-related QT interval prolongation. Given this information, it is common to include sex as a covariate in the model for concentration-QTc interval analysis (see Sect. 10.6.2). Currently, there are no regulatory requirements to have gender balance in TQT studies provided the targeted indication is not gender-based; and there is no regulatory guidance for controlling the phase of menstrual cycle during a TQT study.

Another factor to consider in the TQT trial is the ethnicity of the study population. Ethnic variation in drug metabolizing enzymes, e.g. (CYP) 2C9, 2C19, and 2D6, are well known and may result in altered drug exposure (Shah 2005). While there does not appear to be inter-ethnic differences in QTc interval duration in the absence of drug (Mansi and Nash 2005), ethnic variability in the response to a challenge with a drug known to prolong QT intervals cannot be ruled out (Shah 2005). It is recognized ethnic differences exist in cardiac sodium and potassium channel variants in healthy individuals, potentially linking a genetic component to an individual's susceptibility to clinically significant drug induced QT interval prolongation (Ackerman et al. 2003; Shah 2005). Caucasians may be more susceptible to QT interval prolongation by hERG blockers than Asians (Shah 2005). The ICH E14 guidance recommends genotyping of patients should be considered for those who experience marked prolongation of the QT/QTc interval while on drug therapy (International Conference on Harmonisation 2005a).

There are other diseases and conditions reported to result in longer QT intervals, but the impact these factors have on QT interval assessment is unknown. Control of these conditions is less important, and is unlikely to be an issue in a crossover designed trial where subjects with these demographic factors serve as their own controls.

### 10.5.1.2 Inclusion/Exclusion Criteria to Consider

As stated above, the general recommendation is to conduct a TQT study in a healthy population of males and females, unless there are safety and tolerability concerns with administering the compound to a healthy population. Consequently, standard inclusion/exclusion criteria for healthy volunteer studies would apply. Particular attention should be given to excluding individuals who have history of risk factors for TdP, including cardiac disease, hypokalemia, or a family history of Long QT Syndrome. In addition, subjects who have repeated baseline QT/QTc intervals greater than 450 ms should be excluded from the TQT study. It is also important to limit all known and potential sources of QT/QTc variability, so the use of concomitant medications, especially those known to alter the QT/QTc interval should be excluded from the trial. If conducting the trial in patients, these additional criteria should also be considered and avoided including the exclusion of concomitant medications likely to prolong QT intervals.

## 10.5.2 Study Design

### 10.5.2.1 Equipment Considerations

The ECG database for TQT studies is generally derived from collecting 12-lead surface ECGs. The primary challenge in measuring the QT interval from 12-lead ECGs often involves the consistency of being able to accurately and reproducibly detect the end of the T wave. This, unfortunately, is not always such a simple

process. Changing T wave amplitudes and morphologies, often seen in cardiac patients can make this process a more challenging task. To confound matters even more, there is no standardized algorithm for QT interval measurement used in today's automated devices. Some ECG machines may identify selected leads and use a specific number of complexes for measuring QT intervals, while others may determine a global value across all 12-leads, often using the earliest onset of the Q wave and the latest offset of the T wave to calculate an integrated QT interval. In addition to using different leads, automated devices may also use various techniques to determine the offset of the T wave. These methods often rely on the amplitude and slope of the T wave. For example, the end of the T wave may be identified as the intercept of iso-electric level of the ECG tracing with a tangent line drawn to the point of the maximum T wave slope (McLaughlin et al. 1996). In a study that evaluated different model electrocardiographs manufactured by different companies, it noted that one company's brand consistently generated QT intervals 16–19 ms shorter than manually measured values, whereas another company's device consistently recorded values approximately 7 ms longer than the manual technique (Darpo et al. 2006). As a result of these differences in automated devices, it is important to standardize the brand and model of ECG machine used for the collection QT interval data when conducting a TQT study. The same machines used for baseline ECGs should also be used throughout the treatment phase of the study. Other important factors to consider when selecting ECG machines include the use of modern devices with the capability for digital signal processing, and which have been calibrated and serviced shortly before the study. In addition to consistency of automated devices, proper training of the operators is critically important to limit variability of ECG tracings and should include instruction of skin preparation for applying electrodes, correct and consistent lead placement and subject positioning. Although not widely used currently, an alternative to the 12-lead surface ECG is the digital 12-lead Holter monitor, such

as the Mortara 12-lead telemetry system (http://www.mortara.com), which allows for continuous collection of ECG recordings in contrast to older style machines which capture ECGs at distinct time intervals.

### 10.5.2.2  Parallel or Crossover

To fully assess a compound's potential to prolong the QT interval, the ICH E14 guidance recommends a minimum of four treatment arms which include placebo, positive control, and usually two doses of the study drug, one being the clinically relevant dose, the other being a supratherapeutic dose (see below). If the pharmacokinetic profile of the drug candidate is suitable, the preferred trial design for the TQT study is a cross-over design. This design allows for reduced within-subject variability and is more efficient by requiring fewer subjects. Additionally, a subject's response on study drug and active control can be compared to his or her own response on placebo. The possibility of carryover effect between treatment periods is absent or negligible since crossover studies are single dose with adequate washout between periods. The crossover design is also preferred if an individual correction approach (QTcI) is used to obtain the best heart rate correction for QT interval values.

Despite the advantages of using a crossover design, the use of a parallel design may be the more appropriate choice of design in some situations. Generally a parallel design is logistically more feasible when the properties of the study drug will result in either a long dosing period for multiple dose studies or a long washout period. In either case, the length of the study for a cross over design may be prohibitive. One example is a drug with a long elimination half-life that results in a long dosing period to attain steady-state or a long washout period between treatments to fully clear the drug and effects. Another example for using a parallel design is when a carryover effect is expected, such as with irreversible receptor binding or long-lived active metabolites. The choice of patients instead of healthy volunteers may also drive a parallel design because it may be less feasible or ethical to dose patients for the length of a cross over study.

### 10.5.2.3 Single or Multiple Dose

In general, the duration of dosing, or the dosing regimen should be sufficient to characterize the effect of the drug and its active metabolites at relevant concentrations and should be guided by available pharmacokinetic data for the compound. TQT studies can be conducted as single dose trials if the candidate is not significantly metabolized and does not show significant accumulation following repeat dosing, so the exposure observed after a single dose is equivalent to that seen at steady state (e.g. short half life drugs). Dosing conducted to steady state is recommended if there is significant accumulation of the parent compound or its metabolite(s). Some regulators and academic experts believe multiple dose studies are necessary to rule out delayed drug effects on cardiac tissues, which may not be apparent following a single dose administration. However, a single dose study is generally adequate as recommended in the ICH E14 guidance which states for drugs with short elimination half-lives and no metabolites, a single dose study may be sufficient (International Conference on Harmonisation 2005a).

For drug candidates that require steady state assessments, the active treatment arm(s) and placebo arm should all be dosed for the same duration, however, the positive control selected for the study only needs to be given long enough to have its expected effect on the QT/QTc interval, which in general may accomplished with a single dose.

### 10.5.2.4 Dose Selection

The doses selected to conduct the TQT study should take several considerations into account. According to the ICH E14 guidelines, doses should include the expected clinically therapeutic dose and a supratherapeutic dose (International Conference on Harmonisation 2005a). The highest dose selected must take safety and tolerability into account and the dose should attempt to cover the worst case scenario for the compound in regards to exposure. Selection of the supratherapeutic dose may be selected as the highest attainable dose for the compound, i.e., the maximum tolerated dose (MTD), or may

represent the dose necessary to achieve concentrations expected under conditions of maximal metabolic inhibition. For example, if the compound is a metabolic substrate of the cytochrome P450 (CYP) enzyme system, and drug interaction studies have demonstrated inhibition with the most potent inhibitor in the metabolic class, doses selected for the TQT study should be selected to mimic concentrations achieved in the drug interaction study. If issues with tolerability of the supratherapeutic doses are due to local irritation, then the use of a metabolic inhibitor to achieve higher concentrations may be considered in lieu of a supratherapeutic dose. However, the risk of the metabolic inhibitor's potential to prolong QT intervals should also be considered.

More recently a stepwise approach, similar to that taken for hepatic or renal studies, has been proposed. In this case, the study is conducted using only the supratherapeutic dose, the placebo and the active control. If the supratherapeutic dose has no effect on the QTc intervals (less than the threshold of regulatory concern), then the conclusion of a negative TQT study is held and it is assumed the therapeutic dose would likewise have no effect. If the supratherapeutic dose prolongs QT/QTc intervals, then the study would need to be repeated with the therapeutic dose (and possibly another interim dose) to characterize the risk at the therapeutic dose. Because of the additional time and cost to conduct a second study, this approach only seems wise if the risk of QTc interval prolongation with the supratherapeutic dose is extremely low. This approach should be discussed up front with the regulatory authorities to gain some agreement before proceeding.

### 10.5.2.5 Experimental Conditions

As with any well-designed clinical trial, it is important to control factors that may influence measurement variability as much as possible. For the TQT study, intrinsic variability in QT interval measurements may be influenced by such factors as the subject's heart rate, food ingestion and circadian rhythms. As a result, it is critical to try to control these variables through the design

of the study. Limiting a subject's activity levels during the trial, especially around the time of ECG measurement is very important for controlling fluctuations in heart rates. All scheduled ECGs should be performed after the subject has rested quietly for at least 10 min in a supine position. The absence of any environmental distractions in the clinic (TV, radio, conversation) during both the pre-ECG rest and the ECG recording period must be emphasized. As heart rates vary naturally throughout the day and night, the most common method for normalizing the effect of heart rate changes on the QT interval is through the use of established correction formulae (see above, Sect. 10.4.2). Other methods for controlling error include the use of replicate measurements at each ECG measurement time point, use of time-matched baselines to account for possible diurnal variation, and conducting the trials under conditions of a quiet environment, using consistent lead placement and using the same ECG machines for each subject.

Special attention should be given to ensure identical ECG lead placement in every treatment period, particularly for multiple ECGs on multiple study days. This may be achieved by clearly marking the individual sites for the placement of each lead on the subject with indelible ink. In some cases, it may be appropriate to repeat abnormal ECGs to rule out improper lead placement as contributing to an observed ECG abnormality. Supine body position with fully lowered headrest should also be consistently maintained for each ECG performed. In particular, changes in heart rate should be avoided. Whenever the nominal time points for different procedures coincide, the ECGs should always be collected prior to vital sign assessments and any concomitant blood draws or other procedures. If possible, ECGs should be collected at least 2–3 h after a meal in order to avoid the effect of food intake on the ECG (see below, Sect. 10.5.2.9). The time of meals should be standardized between study days.

### 10.5.2.6  Blinding and Randomization

The ICH E14 guidance states: "The 'thorough QT/QTc study' should be adequate and well-controlled, with mechanisms to deal with potential bias, including use of randomization, appropriate blinding, and concurrent placebo control group."

The placebo control for the potential effect of the investigational drug is important to remove the background variability affecting heart rate and the QT interval. The study drug and placebo are administered in a double-blinded and randomized fashion as a result.

When the ICH E14 guidance was first introduced, there was much discussion at conferences about the need to double-blind the active control treatment. The most recent communications from the agencies suggest blinding of the active control is not required for the trial. The Question and Answer document released to supplement the ICH E14 states, "The use of a double-blinded positive control does not appear to be essential, provided that the reading of ECGs is performed in a blinded manner . . . and the study is carefully designed to ensure that specified study procedures are followed uniformly. This means the same protocol for administering the test drug and placebo, taking blood samples and collecting the ECG data should also be used when administering the positive control. This does not mean that other aspects of the study, such as the duration of treatment with the positive control and the other treatment groups, would be identical. If blinding of the positive control is performed, common methods include the use of double-dummy techniques and over-encapsulation." (International Conference on Harmonisation 2008). This was further emphasized in a presentation by Garnett at a Drug Information Association meeting in 2008 (Garnett 2008). The point made in the presentation was that an analysis of moxifloxacin response across multiple studies did not indicate a difference based on blinding and that, in at least one instance, overencapsulation of the moxifloxacin for blinding caused poor absorption and a failed study. In the later case, concentration-QT interval analysis was used to demonstrate the active control effect (Garnett et al. 2008).

In addition to blinding the drug and placebo treatments, it is recommended that the reading of the ECGs for interval measurements have an element of blinding to remove reader bias. This

is discussed in the E14 Question and Answer document where it states, "core ECG laboratories blind subject, time (day) and treatment in order to reduce potential bias. The T wave analysis, which calls for all 12 leads, can be performed after the QT interval analyses and requires comparison to the baseline ECG; it can, however, be blinded as to treatment" (International Conference on Harmonisation 2008). Since digital ECGs are most commonly used, the ECG can be blinded during the data handling at the core laboratory after the ECG is transmitted, but before the reader measures the intervals. Usually subject, date and time identifiers, along with any machine read interpretations or intervals, are removed from the digital recording and replaced with a unique identifier prior to reading. The results can be merged with the identifier data after the reading using the common unique identifier. When using paper ECGs, the identifying information to be blinded can be recorded in the case report form and an opaque label with a unique identifier that is also recorded in the case report form is placed over the information printed on the ECG, effectively blinding the identifying information. Intervals (QT, RR, QRS, etc.) can be read independently, but the ECGs will need to be grouped by subject with the baseline identified for waveform evaluation and interpretation of the clinical findings of any arrhythmias. The core laboratories working in this area are quite experienced with these blinding issues.

### 10.5.2.7 Positive Control
As recommended by the ICH E14 Guidance document, TQT studies are required to include a positive control arm to validate study sensitivity. The positive control should show a significant increase in QTc intervals; i.e., the lower bounds of the one-sided 95% confidence interval (CI) must be above 0 ms. This finding demonstrates the trial is capable of detecting an increase in QTc intervals, a finding that is essential when concluding a negative result for the test drug is meaningful. The study should be able to detect a QTc interval effect of about 5 ms (the threshold of regulatory concern) if it is present. Therefore,

the magnitude of effect of the positive control is important. In selecting a positive control, sponsors of trials should use a positive control demonstrating an effect of greater than 5 ms (i.e., lower bound of a one-sided 95% CI > 5 ms). This approach has been proven to be useful in many regulatory cases. If, however, the positive control has too large an effect, the study's ability to detect a 5 ms QTc interval prolongation might be questioned. In this situation, the effect of the positive control could be examined at times other than the peak effect to determine whether an effect close to the threshold of regulatory concern can be detected. Importantly, the effect of the positive control (magnitude of peak and time course) should be reasonably similar to its usual effect. Results suggesting an underestimation of the QTc interval effect might question the assay sensitivity, thus jeopardizing the interpretability of the TQT study results (International Conference on Harmonisation 2005a).

Using these criteria, a single 400 mg dose of moxifloxacin has generally become the standard positive control, as it produces QTc interval prolongation in the range of 5–15 ms. The guidance also allows for other positive controls, preferably from the same drug mechanism class as the new chemical entity. The reproducibility of the positive control to produce a consistent prolongation in QTc interval in the range of interest (i.e., approximately 5–15 ms) must be well characterized and documented before using it in the TQT study. Otherwise, the risk of a failed study due to lack of assay sensitivity would be unacceptable. Moxifloxacin has been well accepted because the QTc interval prolongation is reproducible, well characterized and falls in the range of clinical concern. Blinding of the active control is discussed under Sect. 10.5.2.6.

### 10.5.2.8 ECG Collection Strategy
In general, when assessing QT/QTc interval changes, it is recommended to collect replicate ECGs (e.g. most commonly triplicate ECGs – defined as three single ECGs recorded approximately 1–2 min apart) around the nominal ECG time point for all scheduled baseline and on-treatment ECGs in TQT trials. Single ECGs

may be recorded at screening and at any post-study follow-up visits. One example of when replicate ECGs are not recommended is for studies in which the goal is to relate QT interval changes to drug exposure while plasma concentrations of the drug are changing rapidly (e.g. studies with IV bolus or short-term IV infusion of a compound).

The ECG schedule for clinical studies with intensive QT interval assessment must be designed with several caveats in mind. Analyses of various populations have demonstrated the QTc interval varies with the time of day, sleep/wake cycle, food, and other variables. Even after appropriately controlling for heart rate, statistically significant diurnal effects on QT/QTc intervals have been observed in some studies and must be taken into account. The time points at which ECGs are recorded in a TQT trial must capture the peak effect of the parent compound and any major metabolites. The goal of obtaining ECG analysis times is to characterize any QT interval changes with as few sampling times as possible. This can often be achieved with six to eight post-dose time-points. Due to the nature of the analysis, in which the greatest change from baseline values is the value of concern, the more time-points assessed, the higher likelihood of detecting false positive results. Using the fewest number of time-points will also allow for greater cost savings for the trial, especially when ECGs are captured in triplicate. The nominal sampling times for ECG collection should be based on the PK profile of the parent compound and any major metabolites, and should be appropriately scheduled around the $T_{max}$ of the compound being evaluated. It is recommended whenever an ECG is recorded, a PK sample should be collected immediately after collection of the ECG. The schedule of ECG time points after dosing should include the expected $C_{max}$ and $C_{min}$ for the plasma concentration of the molecule and, as appropriate, the time of maximum expected biologic response. For the positive control treatment, ECG sampling should include a minimum of about two to three time points near $T_{max}$ for the compound. For moxifloxacin, these time points should include at least 1, 2, and 4 h post-dose.

Additional ECG sampling times may be collected and often are recorded on the same schedule as the test drug. The parent and all relevant metabolites should be considered for both plasma and effect-related time points. Relevant metabolites are those either abundant or biologically active (see current guidance on metabolites in safety testing for more information). Biological activity of a metabolite in this context constitutes the activity on the primary pharmacological target and, in rare cases where the data are available, the hERG activity of human metabolites. Several additional time points must also be included in the post-dose ECG schedule to rule out delayed effects due to unknown metabolites or delayed physiological effects and also to provide some information as to whether or not the subjects have returned to approximate baseline values after dosing.

As stated above, sources of variability should be identified and controlled whenever possible. This variability may be separated into biologic variability and variability due to measurement error. Methods to control biologic variability, such as environmental factors, activity, food, and diurnal effects are described in more detail in the Sect. 10.5.2.5. Reducing measurement error may best be accomplished by collecting replicate measurements for QT/QTc interval assessment. A rationale for recording replicate ECGs is that the uncorrected QT interval is assumed to be a continuous parameter that is measured with error. The clinical assumption is that under controlled experimental conditions and a stable heart rate, the uncorrected QT interval does not vary much over several minutes and thus the biological variability is stable. Using the mean from replicate measurements is one way to reduce potential measurement error and obtain a more precise and reliable estimate of the subject's true response at a nominal time. To examine the effect of replicate measurements on QT interval assessment, a study was conducted in 32 healthy subjects to specifically address this question (unpublished data). Variability between single ECG measurements was compared to variability of triplicate measurements collected 2 min apart. In this study, all QT/QTc intervals

**Table 10.1** Intrasubject standard deviations for time-matched changes in QTcF interval (ms)

|              | Singlet ECGs | Triplicate ECGs | Reduction | % Reduction |
|--------------|--------------|-----------------|-----------|-------------|
| Automated    | 12.2         | 10.0            | 2.2       | 18          |
| Manual 1     | 14.7         | 9.2             | 5.5       | 37          |
| Manual 2     | 14.4         | 10.1            | 4.3       | 30          |

**Table 10.2** Intrasubject standard deviations for QTcF intervals measured from single ECGs and triplicate ECGs and the corresponding sample size

|                 | SD | $\delta = 0$ ms | $\delta = 5$ ms |
|-----------------|----|-----------------|-----------------|
| Single ECGs     | 14 | 44              | 79              |
| Triplicate ECGs | 9  | 20              | 30              |

were measured using both an automated method (values taken directly from the ECG machine) and a manual assessment conducted by two independent vendors specializing in manual over-read methods. Results from the study indicated that, whether manual or automated readings were used, triplicate ECGs reduced intra-subject variability. The Table 10.1 presents the intra-subject standard deviations for time-matched changes in QTcF intervals for automated measurements and two different manual methods.

Whether manual or automated readings were used, a reduction in intra-subject standard deviation was observed with triplicate ECGs compared to singlets, reaching about 10 ms. Table 10.2 shows the effect of triplicate ECGs on intra-subject standard deviations (SD) for QTcF intervals and corresponding sample sizes for a crossover study to compare study drug and placebo at one time post dose with the following assumptions: $\alpha = 0.05$ (one-sided test), 90% power, non-inferiority limit of 10 ms and under the null hypothesis a true mean difference $\delta$ between study drug and placebo of 0 or 5 ms.

Adjusting for baseline measurements is important for several reasons, including detection of carryover effects, accounting for potential diurnal changes, and reducing the influence of inter-subject differences. The two types of baseline assessments used in the TQT study are "time-matched" and "pre-dose." The decision on the type of baseline to collect is influenced by the study design and whether it is a parallel or

cross-over study. For parallel studies, one entire day is dedicated to obtaining baseline ECGs, occurring preferably 1 day prior to the first dosing day. This baseline is "time-matched" because ECGs are measured in triplicate at the same time points on the day prior to the first treatment day as on the treatment day. The baseline day is typically a treatment free day (no drug administered), but alternatively a placebo may be administered. Thus, common variables affecting QT intervals over the course of the day will be accounted for within each individual subject.

For crossover studies, a "pre-dose" baseline immediately prior to dosing (or within 30–60 min before dosing, depending on the number of assessments in the study protocol) in each period can be used as the period-specific baseline. Often a triplicate measurement recorded at three time points in the hour before the first treatment dose is used for the pre-dose baseline. The baseline is then the average of all the pre-dose measurements. The pre-dose baseline adjusts for between subject differences, but not for diurnal effects. The adjustment for diurnal effects is implicit in the assessment of time-matched drug to placebo differences and, hence, a baseline correction for diurnal effects is not needed.

### 10.5.2.9 Food Effect Considerations

The effect of food consumption on the QT interval has been evaluated in a limited number of studies with somewhat conflicting results. In one study, a 500 kcal formula meal was administered to 11 healthy males and females (Nagy et al. 1997). QTc interval changes were compared to a separate group of eight healthy males and females who received an equivalent volume of water. In the subjects receiving the liquid meal, QTc interval increased approximately 23 ms above baseline within 15 min of ingesting the

meal and stayed elevated for the study duration of 60 min, whereas the QTc interval decreased significantly following ingestion of water. The investigators also observed an increase in heart rate following meal consumption. In another study, the influence of food on electrocardiograms was evaluated in 12 healthy male subjects (Widerlov et al. 1999). A standardized meal was given 1.5 and 5.5 h after baseline assessments during separate sessions and compared to fasting in a three-way crossover design. Increases in heart rate, as well as alterations in T wave morphology were observed after the meals, but there was no change observed in the QTc interval. The effect of grapefruit juice on QTc interval prolongation has also been studied. In ten healthy male and female subjects who consumed a liter of grapefruit juice demonstrated a mean peak effect of 12.5 ms at 5 h and QTc interval prolongation persisting up to 8 h after ingestion of the grapefruit juice (Zitron et al. 2005).

Although the data are not conclusive, it may be prudent when conducting TQT studies to avoid measuring QTc intervals within 2–3 h after a meal, and prohibit grapefruit juice during the duration of the study.

## 10.6  Data Analysis

### 10.6.1  Statistical Analysis

#### 10.6.1.1  Sample Size Considerations

Sample size depends on the study design, planned analysis approach, and estimated variance of the primary endpoint. It is not uncommon to see sample sizes of 40–60 subjects for a crossover design study using the primary endpoint and analysis described in the ICH E14 guidance and in the analysis section below. Agin et al. (2008) cited simulations showing, that for the intersection–union test with a one-sided 5% significance level, a true mean drug effect of less than 5 ms and comparisons to placebo at 8–10 times post-dose, approximately 60 subjects would provide about 90% power if the noninferiority limit were set at 10 ms. The number of

subjects may be reduced as the ability to consistently measure the QT and RR intervals is improved and the variability in the QTc interval primary endpoint is reduced, as was discussed above under Sects. 10.5.2.1 and 10.5.2.8.

#### 10.6.1.2  Analyses of Central Tendency

The primary analysis described in the ICH E14 guidance seems straightforward at first glance, but stirred much debate of a statistical nature during the drafting of the original guidance and after the final guidance was released. Simulations assessing the false positive risk and suggestions for further refinement of the statistical approaches continue to appear in the literature.

The guidance recommends the primary analysis as, "...the largest time-matched mean difference between the drug and placebo (baseline-adjusted) over the collection period." Additionally it recommends analysis of changes around the $C_{max}$ for each individual could be included. This later point is generally accomplished by sampling ECGs around the anticipated pharmacokinetic $T_{max}$ of the drug. The objective of this analysis is to determine if the drug has an effect on cardiac repolarization using QT/QTc intervals as the surrogate endpoint. The "threshold for regulatory concern, ... is around 5 ms as evidenced by an upper bound of the 95% confidence interval around the mean effect on QTc interval of 10 ms." (International Conference on Harmonisation 2005a). The Question and Answers document for the E14 guidance addresses more specifically how this is to be calculated. The largest time-matched mean difference is to be calculated by comparing the mean QTc interval for the drug across the study population to the mean QTc interval for placebo across the study population at each time point. The largest time-matched mean difference is then the largest of these differences at any time point (International Conference on Harmonisation 2008).

The QT/QTc interval on-drug and on-placebo is to be baseline corrected for analysis. Often the double correction, once for baseline and once between drug and placebo is referred to as a "double delta" correction. The baseline used for correction is dependent on the study design

employed. As was mentioned above in the Sect. 10.5.2.8, a time-matched baseline is used for parallel group studies because it allows for the detection of diurnal pattern differences between subjects. A pre-dose baseline, composed of an average of ECGs collected just prior to the first dose of each cross-over treatment period, is used for cross-over studies.

The Pharmaceutical Research and Manufacturers Association (PhRMA) formed a group of statistical experts, the QT Statistics Expert Team (PhRMA QT SET) in December 2002 in response to the issuance of the joint United States Food and Drug Association (FDA)/Canada Therapeutic Products Directorate Concept Paper on the clinical evaluation of QT/QTc prolongation which was the predecissor to the ICH E14 guidance. This group contributed statistical comments during the drafting of the final ICH E14 guidance and has issued recommendations on the statistical methods to address the primary analysis in the guidance (Patterson et al. 2005; Agin et al. 2008). The recommendations of this group have been adopted as the statistical method of choice because of the difficulties in constructing a confidence interval for the largest difference in a series of population means.

The PhRMA QT SET and the E14 Statistics Group recommended the intersection–union test (IUT) (Berger 1982) to exclude a clinically relevant effect on the QT/QTc interval. "The parameter being tested at each time point $i$, $i = 1, \ldots, t$ is $\mu(D)i - \mu(P)i =$ population mean for change from baseline in QTcF intervals on-drug at time $i$ minus population mean for change from baseline in QTcF on-placebo at time $i$."

The null hypothesis of a positive QT/QTc effect and the alternative hypothesis of a negative QT/QTc effect can be expressed as the following statistical hypotheses:

$$Ho : \mu(D)i - \mu(P)i >= 10 \text{ ms for at least one } i$$

$$Ha : \mu(D)i - \mu(P)i < 10 \text{ ms for all } i.$$

The one-sided 95% upper confidence bound for $\mu(D)i - \mu(P)i$ is computed at each time point $i$. If the upper bounds of the $t$ confidence intervals for the difference between drug and placebo at every time point are below 10 ms then the confidence bound for the largest mean difference is also below the limit and the definition of a negative study by ICH E14 is satisfied (Agin et al. 2008).

Using the same basic statistical approach, this study will be deemed adequately sensitive to detect QT/QTc interval prolongation if the lower bound of the two-sided 90% confidence interval for mean differences between the active control and placebo at the most relevant post dose time point (generally at historical $T_{max}$) is greater than zero.

From a practical standpoint, the analysis of covariance is generally performed on the raw QTc intervals at each time point using a mixed effect repeated measures model with sequence, period, treatment and treatment-by-time interaction as fixed effects, subject within sequence as a random effect, baseline QTc interval as a covariate. Estimates of the adjusted mean differences (Test Drug − Placebo) and the two-sided 90% confidence intervals for each treatment and time are obtained from the model using linear contrasts.

While the IUT approach is the currently accepted method used to address the requirements of ICH E14, it is not without its issues. Eaton et al. (2006) explored some of the difficulties of constructing a one-sided confidence interval for a maximal mean change in QTc interval and proposed an approach consistent with that given above. They performed simulations to assess the performance of the method. The method appears to work well when the collection of mean changes from placebo (at each serial time point) has a distinct maximum coordinate. It, however, does not work well when all the values are close to or equal to the maximum (e.g. all mean differences from placebo are similar and close to the maximum) or when all values are close to zero. Hutmacher et al. (2008) found limitations resulting in larger false positive rates with the IUT, particularly when the parallel design is used and variability of the endpoint is large. As more studies are conducted using these techniques, it is likely further limitations will

be published and suggestions for alternative approaches may be forthcoming.

### 10.6.1.3 Categorical Analysis

In addition to the analysis of central tendency, the ICH E14 guidance recommends specific categorical analyses that should be summarized. Clinically important QT/QTc interval changes should be summarized based on the number and percentage of patients meeting or exceeding a predefined value and could be defined in terms of absolute QT/QTc interval intervals or change from baseline. It is recommended these analyses be separated by patients with normal versus elevated baseline QT/QTc intervals if the study includes patients with elevated baseline. This separation is more likely to be relevant when summarizing the QT/QTc interval data across studies rather than for the TQT study itself where the population is more homogeneous and typically healthy subjects.

There is no consensus regarding an absolute upper limit, however, for clinical trials, a prolongation of QTc intervals >500 ms or an absolute increase from baseline in QTcF intervals of >60 ms on treatment is generally considered to be a threshold for clinical concern. The ICH E14 guidance recommends summarizing the absolute changes and change from baseline as follows (International Conference on Harmonisation 2005a).

Absolute QTc Interval Prolongation:
- QTc interval >450 ms
- QTc interval >480 ms
- QTc interval >500 ms

Change from Baseline in QTc Interval:
- QTc interval increase from baseline >30 ms
- QTc interval increase from baseline >60 ms

### 10.6.2 Concentration-QTc Analysis

In the ICH E14 guidance, the analysis of the exposure-response relationship of drug concentrations to changes in QT/QTc interval was originally proposed as a secondary analysis, however, the guidance mentions there is active investiga-

tion ongoing regarding the role and method for exposure-response in the TQT study analysis. As this investigation continues to be published and presented, the important role of analyzing the concentration-QTc interval relationship has become apparent.

A recent article on the role of concentration-QT interval relationships written by reviewers at the United States Food and Drug Administration (Garnett et al. 2008) suggest both the formal statistical analyses and the concentration-QT interval analyses contribute to the ultimate determination of whether or not a drug prolongs the QT/QTc interval. Whereas the IUT method has fewer assumptions, the concentration-QT interval analysis is based on the pharmacology of drug-induced QT interval prolongation.

One critical piece to the acceptance of concentration-QT interval analysis is establishing some criteria around the method to be used. In this chapter, a population based approach to a rigorous concentration-QT interval analysis that has been accepted by regulatory authorities during product reviews is proposed, but it is acknowledged this is not the only acceptable approach. Agreement on a commonly accepted analysis plan is yet to occur. In response to the ongoing discussion, the Cardiac Safety Research Consortium (CSRC) has initiated a team led by Luana Pesco Koplowitz with broad representation from the pharmaceutical industry and regulatory agencies who are working on a white paper, "PK/PD analysis for QT evaluation." In addition to the CSRC team, the Optimizing QT Initiative Taskforce was established in December 2008 as a subteam to the PhRMA Clinical Pharmacology Technical Group. The objective of this taskforce is to optimize the performance characteristics of thorough QT trials by applying PK/PD methodologies. The taskforce plans to develop and rigorously evaluate exposure-response approaches to quantify the concentration-QT relationship and demonstrate that the statistical robustness of the approch is at least equivalent to the current statistical methods (i.e. IUT). The outcome of both these groups will significantly impact how concentration-QT data is analyzed and should be considered when developing the analysis plans

in the future. At the time of this writing, these white papers have not yet been released. It is important for the TQT study that a complete concentration-QT interval analysis plan be written in advance of data availability to avoid any perception of data mining or bias in order to interpret a "positive" study.

A three-step process is proposed for the concentration-QT interval analysis:

1. Evaluate the effect of the drug on heart rate;
2. Evaluate the methods for correcting the QT interval for heart rate and determine the best correction factor(s) to use for the primary endpoint; and
3. Evaluate the relationship between drug and relevant metabolite(s) and the QTc interval and any significant covariates affecting this relationship.

The first step in a concentration-QT interval analysis is to evaluate the effect of the drug on the heart rate. It is important to understand the effect on heart rate because the heart rate (or RR interval) is used to correct the QT interval. Fit a linear mixed effect model to the RR interval data.

$$
\begin{aligned}
RR_{ij} = \text{INT} + \eta_i^{(1)} + (\text{SLOPE} + \eta_i^{(2)}) \\
\times \text{CONC}_{ij} + \varepsilon_{ij}
\end{aligned} \tag{10.1}
$$

where, $RR_{ij}$ is the RR interval at the $j$th measurement for the $i$th individual, INT is the mean baseline RR interval estimated by the model when concentration is equal to 0 (baseline), $\text{CONC}_{ij}$ is the drug concentration observed matched with the RR interval at the $j$th measurement of concentration for the $i$th individual, and SLOPE is the population mean slope; $\eta_i^{(1)}$ and $\eta_i^{(2)}$ represent subject-specific random effects, which are assumed to be normally distributed with mean 0 and variance-covariance matrix $\Omega$; and $\varepsilon_{ij}$ represents the residual random variable with mean 0 and variance $\sigma^2$. Model diagnostics should be performed to assess the model adequacy. The 95% confidence interval estimate for the slope should be computed and if the interval contains zero then lack of effect may be concluded.

If there is no effect of the drug on heart rate, then subsequent analyses of the corrected QT interval are appropriate. If there is an effect of the drug on heart rate, then the heart rate effect will be confounded with the QT interval correction and may be problematic for quantifying the true effect of the drug on QT interval. One option might be to simultaneously fit the QT and RR intervals with concentration (sometimes called the "one-step" analysis), but this has not been widely employed. Correction factors other than QTcF and QTcB (e.g. individually corrected QT) may also be examined to obtain the best correction factor. Regardless, the effect of drug on QTc intervals must be carefully evaluated when the drug has an effect on heart rate.

The next step in the analysis is to examine different correction factors and determine the suitability of each. The purpose of the RR (or heart rate) correction is to obtain QTc interval values independent of the underlying heart rate. Because of the regulatory acceptance of the Fridericia's (QTcF) correction, the QTcF correction is often used in analysis as the primary endpoint unless there is significant issue with the correction. Bazett's (QTcB) correction is also routinely examined, more for historical reasons than because it gives the best correction. Often a population based correction factor is estimated for comparison as mentioned in the Sect. 10.4.2. The population correction factor can be estimated for the drug-free singlet ECG data using the following model:

$$
\begin{aligned}
\log(QT_{ij}) = \log(\text{INT}) + \eta_i^{(1)} \\
+ \beta_{\text{pop}} \log(RR_{ij}/1{,}000) + \varepsilon_{ij}
\end{aligned} \tag{10.2}
$$

where, $\log(QT_{ij})$ is the natural-log transformed QT interval at the $j$th measurement in the $i$th individual, INT is the mean QT interval evaluated at an RR interval of 1,000 ms, $\beta_{\text{pop}}$ represents the population estimate of the population correction factor. Other variables are as previously defined.

The appropriateness of these correction factors are assessed by determining the slope of the relationship between the corrected QT (QTc) interval and the RR interval using drug-free data (i.e. this can be only baseline data or both baseline and placebo). The appropriate correction

factor(s) should eliminate the correlation between QTc and RR. A linear mixed effects model should be fit to QTc versus RR intervals and the slope estimates can be used as the basis for the evaluation to compare among possible correction factors. An example of QTc and RR interval correlation for different correction factors is shown in Fig. 10.5.

The slope and intercept are parameters that define the linear relationship between QTc and RR intervals. Following the application of a correction factor to the QT data, if there is a correlation between QTc and RR intervals, the value of the slope parameter will be different from zero, indicating the correction factor is suboptimal and a relationship still exists between QTc and RR (heart rate) intervals. A confidence interval (CI) could be constructed using the standard error (SE) of the estimated parameter at a given confidence level to better evaluate the estimate of the slope parameter. A significant slope may be defined as the 95% CI (mean $\pm$ 1.96 $\times$ SE) excluding the null value. If both QTcF and QTcB exhibit significant correlation between QTc and RR, then other correction factors (as described above in the Sect. 10.4.2) may be examined to find the one with the least correlation. It is important to coordinate this analysis with the primary statistical analysis and use the same choice for the primary correction factor for both analyses.

The third step in the analysis is the examination of the concentration-QTc interval relationship. Garnett et al. (2008) reported most drugs that prolong the QT interval exhibit a dose- or concentration-QT interval relationship. Though a variety of pharmacodynamic models appear in the literature (Piotrovsky 2005), a simple linear mixed effects model can often be used to describe the exposure-response relationship. As part of any modeling exercise, the adequacy of modeling assumptions should be evaluated. This may be performed through the use of informative graphical exploration of the results with examination of the possibility of any delayed effect. Justification for the choice of the pharmacodynamic model (linear versus nonlinear) should be provided in advance of applying the model.

The following linear mixed model can be used:

$$QTc_{ij} = INT + SEX_i + \eta_i^{(1)}$$
$$+ (SLOPE + \eta_i^{(2)}) \times CONC_{ij} + \varepsilon_{ij}$$
$$(10.3)$$

where, $QTc_{ij}$ is the dependent variable at the $j$th measurement for the $i$th individual, INT is the baseline QTc interval value estimated by the model when concentration is equal to 0, $SEX_i$ is the difference in INT for females, $CONC_{ij}$ is the drug concentration observed at the same time as QTc for the $j$th measurement of concentration for the $i$th individual, and SLOPE is the population mean slope of the relationship between QTc and CONC; $\eta_i^{(1)}$ and $\eta_i^{(2)}$ represent subject-specific random effects, which are assumed to be normally distributed with mean 0 and variance-covariance matrix $\Omega$; and $\varepsilon_{ij}$ represents the residual random variable with mean 0 and variance $\sigma^2$. When triplicate QTc interval measurements are measured at each time point, the mean of the three QTc interval measurements is used for the analysis, although in theory, all replicate ECGS could be used in the analysis with the model expanded to include an additional variance component to account for replication. As was discussed above in the Sect. 10.5.1.1, gender is likely to have an effect on the relationship between concentration and QTc interval and is typically included in the initial model based on this assumption.

There is ongoing debate regarding which dependent variable should be used for the analysis. Garnett et al. (2008) advocate the use of the double delta QTc interval (baseline adjusted and difference between time-matched drug-placebo). This offers the advantage of being consistent with the primary statistical analysis. Alternatively, raw QTc or baseline adjusted QTc intervals may be used for the dependent variable with the inclusion of parameters in the model for baseline and/or post-dose placebo as appropriate (Russell et al. 2008). Figures 10.6, 10.7 and Table 10.3 show an example of the analysis of the effect of torcetrapib and its primary metabolite, BTFMBA, on QTcF intervals using these
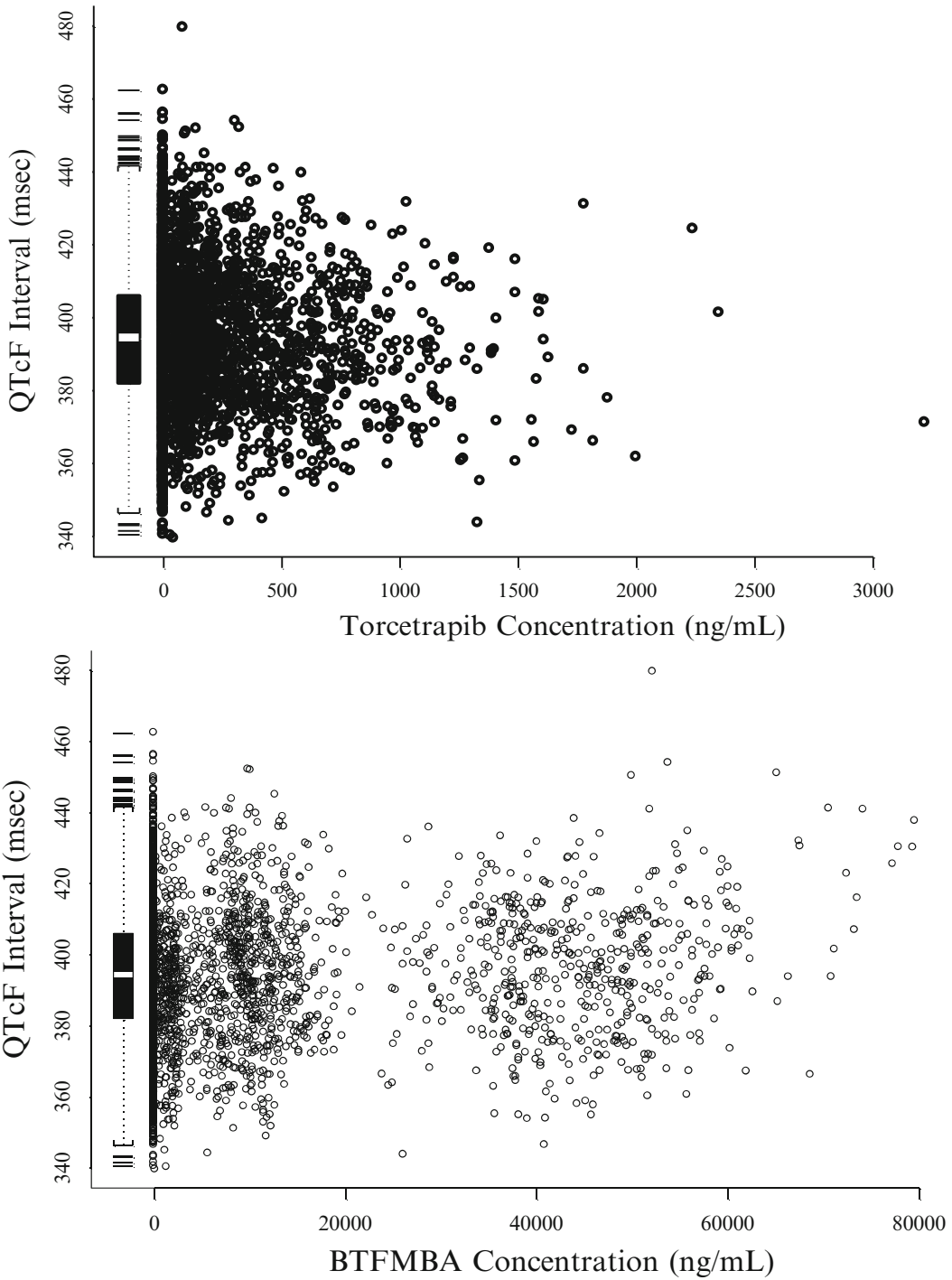
**Fig. 10.6** Observed Fridericia's-corrected QT interval versus torcetrapib and BTFMBA plasma concentrations (Riley et al. 2007)

**Fig. 10.7** Mean Torcetrapib and BTFMBA concentrations (*top*) and expected change from mean intercept versus time postdose (*bottom*) following administration of torcetrapib/atorvastatin 240/80 mg on day 21 (Riley et al. 2007)
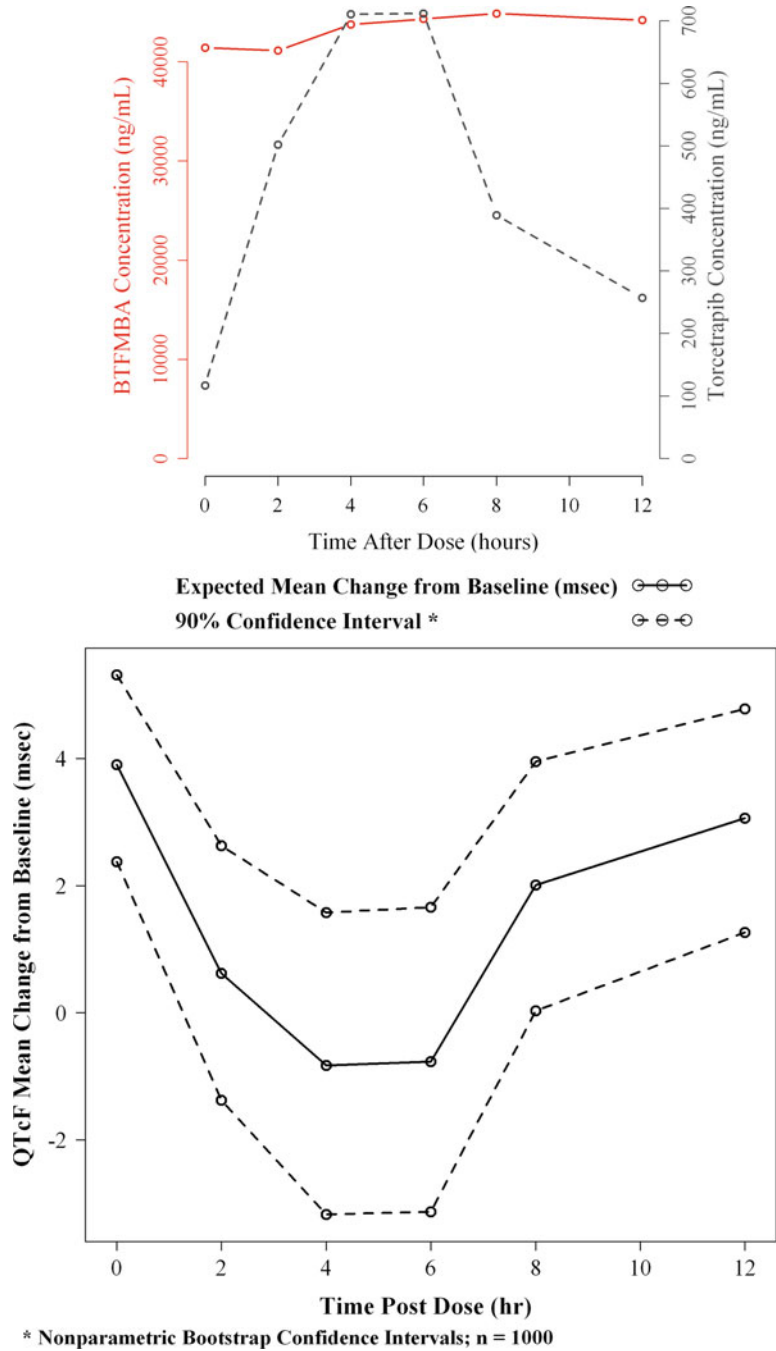
techniques. Figure 10.6 shows the observed concentration-QTcF data for both parent and metabolite, BTFMBA. Figure 10.7 shows the mean concentrations of the torcetrapib and BTFMBA and the expected mean change in QTcF from the intercept over time. In this case, the analysis showed a lack of effect of drug on QTc interval. Raw QTc interval was used as the dependent variable and baseline, placebo and sex were included in the model.

**Table 10.3** Modeling results of Fridericia's-corrected QTc interval versus torcetrapib and BTFMBA plasma concentration analysis (Riley et al. 2007)

| Parameter | Model | Para-meter estimate (%RSE[a]) | IIV[b] (%RSE[a]) | 95% CI[c] |
|---|---|---|---|---|
| Intercept (ms) | $INT = \theta_1 + \theta_2 \times PBO + \theta_3 \times SEX$ | | 13.8 (7.23)[d] | |
| Baseline | $\theta_1$ | 402 (0.289) | | (399, 404) |
| Placebo | $\theta_2$ | −1.11 (45.0) | | (−2.08, −0.358) |
| Sex effect for males | $\theta_3$ | −11.2 (12.9) | | (−13.9, −8.66) |
| Slope | $SLOPE = \theta_4 \times torcetrapib + \theta_5 \times BTFMBA$ | | | |
| Torcetrapib (ms/(ng/mL)) | $\theta_4$ | −0.00842 (11.1) | 0.00493 (49.8)[d] | (−0.00996, −0.00665) |
| BTFMBA (ms/ (μg/mL)) | $\theta_5$ | 0.118 (16.9) | 0.147 (34.0)[d] | (0.0793, 0.154) |
| Residual error (ms) | $\sigma$ | 9.92 (2.89)[d] | | |

[a]Percent relative standard error (%RSE) calculated as standard error/|parameter estimate| × 100
[b]IIV = interindividual variability expressed as standard deviations so that the reported values have the same units as the structural model parameters with which they are associated
[c]95% confidence interval (CI) derived from nonparametric bootstrap estimates ($n = 1,000$)
[d]%RSE of variance estimate
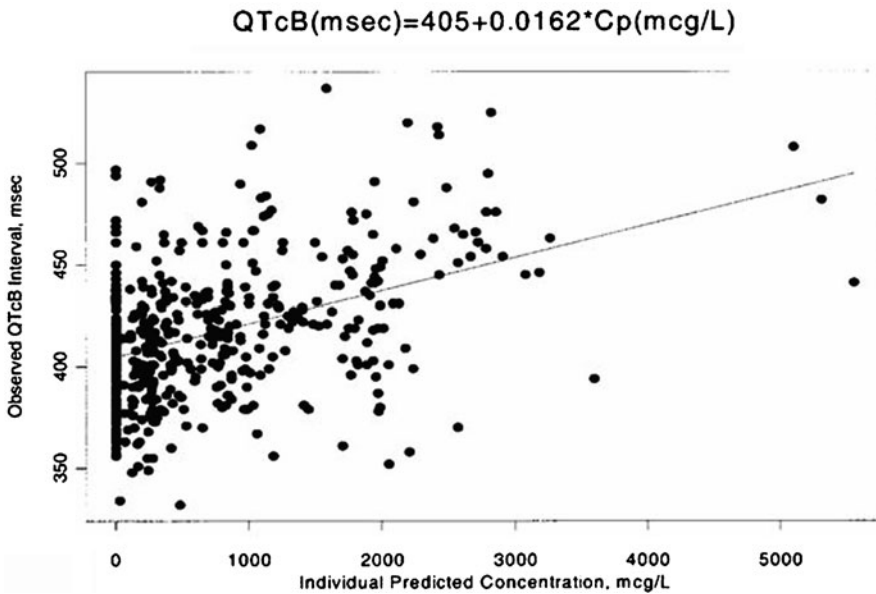


**Fig. 10.8** Sotalol effect on QTc intervals in pediatric subjects – observed QTc interval versus the individual (empirical Bayes) predicted sotalol concentration for all patients in the PK–PD study. Reprinted with kind permission from Springer Science + Business Media: (Shi et al. 2001)

As an alternative example, Fig. 10.8 shows an example of sotalol concentration versus QTcB intervals in pediatrics, where a significant effect on QTc intervals was demonstrated. Once the final model parameters are estimated, the predicted population average double delta QTc
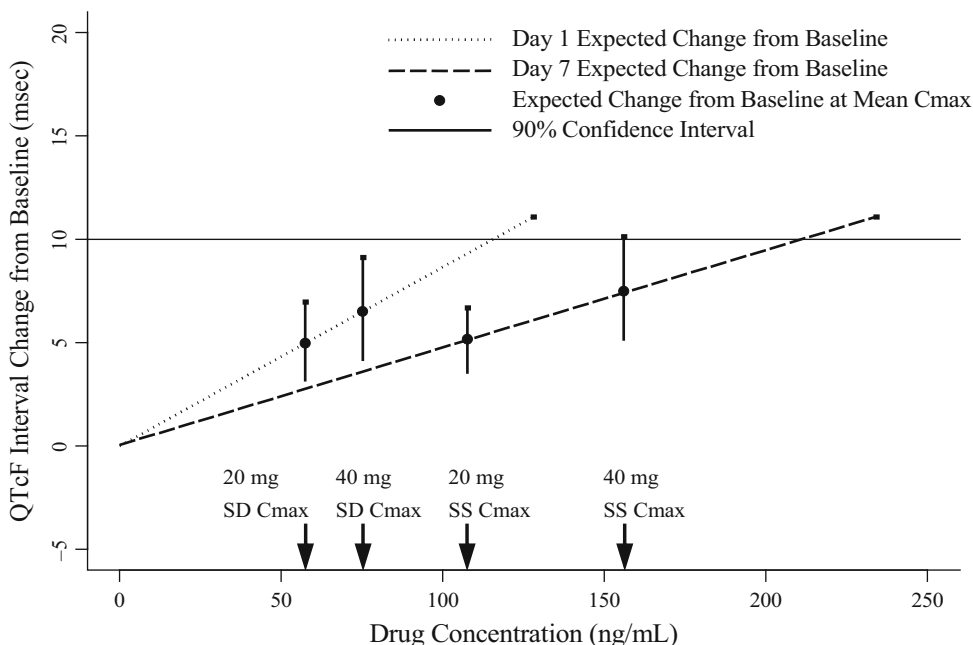
**Fig. 10.9** QTcF interval change from baseline versus plasma concentration following single and multiple oral doses. *Arrows* indicate the mean peak plasma concentration ($C_{max}$) after the single dose (SD) and at steady state after 7 days (SS). *Closed circles* and *vertical lines* are the model-predicted mean and 90% confidence interval QTcF. (Russell et al. 2008) The final, definitive version of this paper has been published in The Journal of Clinical Pharmacology 2008 by SAGE Publications, Inc., All rights reserved[©]

intervals and its corresponding upper 95% one-sided confidence interval boundaries may be evaluated at the average maximal plasma concentrations observed at the therapeutic and supratherapeutic doses (Garnett et al. 2008). This calculation can be used to assess the clinical relevance of the findings given the slope and the expected therapeutic concentration range. An example of one such analysis is presented in Fig. 10.9 looking at the predicted change in QTc intervals using the observed mean $C_{max}$ at the low end and high end of the expected therapeutic dose range.

## 10.7   Interpretation

The TQT study is designed to answer the basic question, "Does the drug cause an increase in QTc intervals that meets the threshold for regulatory concern?" The first part to interpreting the results of the TQT study is to assess whether or not the method was sufficiently sensitive to be able to detect a QTc interval increase of clinical concern. The positive control must show a significant increase in QTc intervals (i.e. the lower bound of the one-sided 95% confidence interval must be above 0 ms) and also be able to detect a mean maximal effect of about 5 ms. The effect of the positive control should be similar in the magnitude of maximum effect and time course to its usual effect as demonstrated in the literature and/or prior studies. If the positive control shows an effect greater than 5 ms, then the effect of the positive control could be examined at times other than the peak effect to determine whether or not an effect close to the 5 ms threshold of regulatory concern can be detected (International Conference on Harmonisation 2008). If these criteria are not met, then the assay sensitivity of the study will be called into question and it will be difficult to interpret the test drug results.

Assuming the study was sufficiently sensitive, if the upper bound of the 95% one-sided confidence interval for the largest time-matched mean difference of the drug on the QTc interval excludes 10 ms, then a negative TQT study can be declared based on the ICH E14 guidance. A concentration-QTc interval analysis that demonstrates a lack of positive slope is further confirmation of these results. A negative study gives reasonable assurance the mean effect of the drug on QTc intervals is not greater than approximately 5 ms. Consequently, the proarrhythmic risk of the drug should be low.

If the largest time-matched mean difference exceeds these thresholds, then the study will be positive. Once a study is determined to be positive, the analysis then focuses on characterizing the relative risk of the drug's effect on the QTc intervals. The drug may have a positive effect at the supratherapeutic dose, but not at the therapeutic dose. In this case, the compound's labeling may need to describe under what conditions the supratherapeutic concentrations and increased risk are likely to occur.

One of the most informative ways to help characterize the drug effect is to carefully review the concentration-QTc interval relationship. The concentration-QTc interval analysis will help to describe the concentrations and conditions under which the increase in QTc interval exceeds the threshold of concern. This, combined with an understanding of the sources of variability that will increase the drug concentrations, can provide greater understanding the relative risk-benefit of the drug. In the example shown in Fig. 10.9, the 20 mg dose at both single dose and steady state and the 40 mg single dose do not exhibit clinical relevant QTc interval increase. It is only with the administration of a 40 mg dose given to steady state that the drug effect on QTc interval begins to cross the limits of the threshold for clinical concern. In this particular example, the concentration-QTc interval analysis combined with an understanding of the drug receptor occupancy helped drive the dose selection for late-stage studies. In this example, the concentration-QTc interval analysis also teased out a different slope for the first day of

treatment compared to steady-state which helped to explain results observed in the statistical analysis (Russell et al. 2008). The concentration-QTc interval analysis may also help explain the results when the IUT analysis results are incongruent, e. g. highest dose has the smallest effect, time course of effect inconsistent between treatments, etc. (Hutmacher et al. 2008; Russell et al. 2008). In an example described by Hutmacher et al. (2008), the concentration-QTc interval results combined with simulations of the placebo data from the trial demonstrating a high likelihood of a false positive result led to a conclusion by the regulatory authority that the positive result of the IUT analysis was likely a spurious result. Subsequently, the product labeling for this drug referred to the concentration-QTc interval analysis and concluded the drug did not exhibit QTc interval prolongation.

Determining whether or not the test drug has a clinically relevant effect on QTc interval requires review of the full data package for the drug. All data, preclinical and clinical, on the QT/QTc interval and cardiac adverse events need to be reviewed and summarized at the time of marketing submission to determine the relative risk of the compound to prolong QT/QTc interval. The results of the TQT study will be one critical component to the risk assessment and will drive the need to characterize the risk more fully in the patient population.

## 10.8    Summary

The assessment of the proarrythmic risk of drugs has made significant progress since the early 1990s. The ICH E14 guidance and subsequent question and answer document give clear guidance for a Thorough QT study design that can be used to demonstrate that a drug does not cause a QTc interval increase of clinical concern. The design and conduct of the TQT study is becoming fairly standard. The use of a reduced design, similar to the approach used in the hepatic and renal impairment studies, has been proposed, but is not yet widely in use. The reduced design

approach only seems to be warranted if the risk of QTc prolongation is very low.

There are a few sections of the guidance, primarily regarding the analysis and interpretation of the results, for which investigation continues. The use of the IUT analysis as the primary statistical analysis for central tendency continues to come under some scrutiny. The primary concern seems to be around exploring the situations in which the IUT is prone to false positive results and proposing alternative analysis methods when these conditions exist.

The output of the working group formed by the Cardiac Safety Research Consortium and the Optimizing QT Initiative Taskforce should help to create a standard method for PK-QTc analysis. Once a standard analysis method is accepted, the PK-QTc interval analysis may take a larger role in the interpretation of the proarrhythmic risk.

# References

Ackerman, MJ and DE Clapman (1997). "Ion channels – Basic science and clinical disease." *N Engl J Med* **336**: 1575–1586.

Ackerman, MJ, DJ Tester, GS Jones, ML Will, CR Burrow and ME Curran (2003). "Ethnic differences in cardiac potassium channel variants: Implications for genetic susceptibility to sudden death and genetic testing for congenital long QT syndrome." *Mayo Clin Proc* **78**(12): 1479–1487.

Agin, MA, WS Aronstein, G Ferber, MC Geraldes, C Locke and P Sager (2008). "QT/QTc prolongation in placebo-treated subjects: A PhRMA collaborative data analysis." *J Biopharm Stat* **18**: 408–426.

Bayer Healthcare Pharmaceuticals (2007). Betapace (sotalol hydrochloride) package insert.

Bazett, HC (1918). "Analysis of the time relations of electrocardiograms." *Heart* **7**: 353–370.

Benton, RE, M Sale, DA Flockhart and RL Woosley (2000). "Greater quinidine-induced QTc interval prolongation in women." *Clin Pharmacol Ther* **67**(4): 413–418.

Berger, RL (1982). "Multiparameter hypothesis testing and acceptance sampling." *Technometrics* **24**(4): 295–300.

Committee for Proprietary Medicinal Products (1997). Points to Consider: The assessment of the potential for QT interval prolongation by non-cardiovascular medicinal products. **CPMP/986/96**.

Curigliano, G, G Spitaleri, HJ Fingert, F de Braud, C Sessa, E Loh, C Cipolla, T de Pas, A Goldhirsch and R Shah (2008). "Drug-induced QTc interval prolongation: A proposal towards an efficient and safe anticancer drug development." *Eur J Cancer* **44**: 494–500.

Darpo, B, M Agin, DJ Kazierad, G Layton, G Muirhead, P Gray and DK Jorkasky (2006). "Man versus machine: Is there an optimal method for QT measurements in thorough QT studies?" *J Clin Pharmacol* **46**: 598–612.

Eaton, ML, RJ Muirhead, JY Mancuso and S Kolluri (2006). "A confidence interval for the maximal mean QT interval change caused by drug effect." *Drug Inf J* **40**: 267–271.

Einthoven, W (1912). "The different forms of the human electrocardiogram and their significance." *Lancet* **1**: 853–861.

Estes, NAM (2008). "Review of electrical diseases of the heart." *N Engl J Med* **359**: 103.

Extramiana, F, P Maison-Blanche, MJ Cabanis, C Oretemann-Renon, P Beaufils and A Leenhardt (2005). "Clinical assessment of drug induced QT prolongation in association with heart rate changes." *Clin Pharmacol Ther* **77**: 247–258.

Fossa, AA (2008). "Review: The impact of varying autonomic states on the dynamic beat-to-beat QT-RR and QT-TQ interval relationships." *Br J Pharmacol* **154**: 1508–1515.

Fossa, A, T Wisialowski, A Magnano, E Wolfgang, R Winslow, W Gorczyca, K Crimin and D Raunig (2005). "Dynamic beat-to-beat modeling of the QT-RR interval relationship: Analysis of QT prolongation during alterations of autonomic state versus human ether a-go-go-related gene inhibition." *J Pharmacol Exp Ther* **312**(1): 1–11.

Fossa, A, T Wisialowski, K Crimin, E Wolfgang, J-P Couderc, M Hinterseer, S Kaab, W Zareba, F Badilini and N Sarapa (2007). "Analyses of dynamic beat-to-beat QT-TQ interval (ECG restitution) changes in humans under normal sinus rhythm and prior to an event of torsades de pointes during QT prolongation caused by sotalol." *Ann Noninvasive Electrocardiol* **12**(4): 338–348.

Fosser, C, G Duczynski, M Agin, P Wicker and B Darpo (2009). "Comparison of manual and automated measurements of the QT interval in healthy volunteers: An analysis of five thorough QT studies." *Clin Pharmacol Ther* **86**(5): 503–506.

Franz, MR, CD Swerdlow, LB Liem and J Schaefer (1988). "Cycle length dependence of human action potential duration in vivo. Effects of single extrastimuli, sudden sustained rate acceleration and deceleration, and different steady state frequencies." *J Clin Invest* **82**: 972–979.

Fridericia, LS (1920). "Die systolendauer im elektrokardiogram bei normalen menschen und bei herzkranken." *Acta Medica Scand* **53**: 469–486.

Garnett, C (2008). "Moxifloxacin needs to be given in a double-blind manner, i.e. The thorough QT study – counterpoint." *Drug Information Association*. Bethesda, MD.

Garnett, CE, N Beaslely, VA Bhattaram, PR Jadhav, R Madabushi, N Stockbridge, CW Tornoe, Y Wang, H Zhu and JV Gobburu (2008). "Concentration-QT relationships play a key role in the evaluation of proarrhythmic risk during regulatory review." *J Clin Pharmacol* **48**: 13–18.

Gralinski, MR (2000). "The assessment of potential for QT interval prolongation with new pharmaceuticals." *J Pharmacol Toxicol Methods* **43**: 91–99.

Health Products and Food Branch (2009). Guide for the analysis and review of QT/QTc interval data (Draft). Health Products and Food Branch, Minister of Public Works and Government Services Canada.

Hurst, JW (1998). "Naming of the waves in the ECG, with a brief account of their genesis." *Circulation* **98**: 1937–1942.

Hutmacher, MM, S Chapel, MA Agin, JC Fleishaker and RL LaLonde (2008). "Performance characteristics for some typical QT study designs under the ICH E14 Guidance." *J Clin Pharmacol* **48**: 215–224.

International Conference on Harmonisation (2005). ICH E14: The clinical evaluation of QT/QTc interval prolongation and proarrthythmic potential of non-132-antiarrhythmic drugs. *CHMP/ICH/2/04*, Federal Register October 20, 2005. **70**: 61134–61135.

International Conference on Harmonisation (2005). ICH S7B: The nonclinical evaluation of the potential for delayed ventricular repolarization (QT interval prolongation) by human pharmaceuticals. *CHMP/ICH/ 423/02*, Federal Register October 20, 2005. **70**: 61133–61134.

International Conference on Harmonisation (2008). ICH E14: The clinical evaluation of QT/QTc interval prolongation and proarrhythmic potential of non-132-antiarrhythmic drugs. Questions and Answers. *EMEA/ CHMP/ICH/310133/2008*, Federal Register November 18, 2008.

Lau, CP, AR Freeman, SJ Fleming, M Malik, AJ Camm and DE Ward (1988). "Hysteresis of the ventricular paced QT interval in response to abrupt changes in pacing rate." *Cardiovasc Res* **22**: 67–72.

Makkar, RR, B Fromm, RT Steinman, MD Meissner and MH Lehmann (1993). "Female gender as a risk factor for torsades de pointes associated with cardiovascular drugs." *JAMA* **270**: 2590–2597.

Malik, M (2008). "Beat-to-beat QT variability and cardiac autonomic regulation." *Am J Physiol Heart Circ Physiol* **295**: 923–925.

Malik, M and AJ Camm (2001). "Evaluation of drug-induced QT interval prolongation." *Drug Saf* **24**: 323–351.

Malik M, K Hnatkova, A Schmidt and P Smetana (2009). "Correction for QT/RR hysteresis in the assessment of drug-induced QTc changes – Cardiac safety of gadobutrol." *Ann Noninvasive Electrocardiol* **14**: 242–250.

Mansi, IH and IS Nash (2005). "Ethnic differences in electrocardiographic intervals and axes." *J Electrocardiol* **16**: 278–284.

Matteucci (1842). "Sur un phenomene physiologique produit par les muscles en contraction." *Ann Chim Phys* **6**: 339–341.

McLaughlin, NB, RWF Campbell and A Murray (1996). "Accuracy of four automatic QT measurement techniques in cardiac patients and healthy subjects." *Heart* **76**: 422–426.

Nagy, D, R DeMeersman, D Gallagher, A Pietrobelli, A Zion, D Daly and S Heymsfield (1997). "QTc interval (cardiac repolarization): Lengthening after meals." *Obes Res.* **5**: 531–537.

Patterson, S, MA Agin, R Anziano, T Burgess, C Chuang-Stein, A Dmitrienko, G Ferber, MC Geraldes, K Ghosh, R Menton, J Natarajan, W Offen, J Saoud, B Smith, R Suresh and N Zariffa (2005). "Investigating drug-induced QT and QTc prolongation in the clinic: A review of statistical design and analysis considerations: Report from the pharmaceutical research and manufacturers of America QT Statistics Expert Team." *Drug Inf J* **39**: 243–266.

Pfizer Inc. (2006). Tikosyn (dolfetilide) package insert.

Piotrovsky, V (2005). "Pharmakokinetic-pharmacodynamic modeling in the data analysis and interpretation of drug-induced QT/QTc prolongation." *AAPS J* **7**(3 Article 63): E609–E624.

Riley, S, D Sequeira, J French, J Mancuso, L Benincosa, R O'Sullivan, T Fullerton and T Russell (2006). "Population PK/PD evaluation of the QTcF interval-drug concentration relationship in healthy volunteers: A case study." *Am Soc Clin Pharmacol Ther* **79**: P29.

Riley, SP, R Labadie, S Terra, T Thuren, C Shear, T Russell, LJ Benincosa and MA Gibbs (2007). "Mixed effects exposure-response analysis and statistical assessment of heart rate corrected QTc for torcetrapib." *Am Soc Clin Pharmacol Ther* **81**: S73.

Rock, EP, HJ Finkle, BP Booth, CE Garnett, S Grant, RL Justice, RJ Kovacs, PR Kowey, I Rodriguez, WR Sanhai, C Strnadova, SL Targum, YI Tsong, K Uhl and N Stockbridge (2009). "Assessing proarrhythmic potential of drugs when optimal studies are infeasible." *Am Heart J* **157**(5): 827–836 e1.

Rodriguez, I, MJ Kilborn, L Xiao-Ke, JC Pezzullo and RL Woosley (2001). "Drug-induced QT prolongation in women during the menstrual cycle." *JAMA* **285**: 1322–1326.

Russell, T, SP Riley, JA Cook and RL Lalonde (2008). "A perspective on the use of concentration-QT modeling in drug development." *J Clin Pharmacol* **48**: 9–12.

Serapa, N and MR Britto (2008). "Challenges of characterizing proarrhythmic risk due to QTc prolongation induced by nonadjuvant anticancer agents." *Expert Opin Drug Saf* **7**(3): 305–318.

Shah, RR (2005). "Drugs, QTc interval prolongation and final ICH E14 guideline: An important milestone with challenges ahead." *Drug Saf* **28**: 1009–1028.

Shi, J, TM Ludden, AP Mclikian, MR Castonguay and PH Hinderling (2001). "Population pharmacokinetics and pharmacodynamics of sotalol in pediatric patients with supraventricular or ventricular tachyarrhythmia." *J Pharmacokinet Pharmacodyn* **28**(6): 555–575.

Stramba-Badiale, M, EH Locati, A Marinelli, J Courville and PJ Schwartz (1997). "Gender and the relationship between ventricular repolarization and cardiac cycle length during 24-h Holter recordings." *Eur Heart J* **18:** 1000–1006.

Tseng, GN (2001). "$I_{KR}$: The hERG channel." *J Mol Cell Cardiol* **33**: 835–849.

Waller, AD (1887). "A demonstration on man of electromotive changes accompanying the heart's beat." *J Physiol* **8**(5): 229–234.

Wang, Y, G Pan and A Balch (2008). "Bias and variance evaluation of QT interval correction methods." *J Biopharm Stat* **18**: 427–450.

Wehrens, XHT, MA Vos, PA Doevendans and HJJ Wellens (2002). "Novel insights in the congenital long QT syndrome." *Ann Intern Med* **137**: 981–992.

Widerlov, E, K-G Jostell, L Claesson, B Odlind, M Keisu and U Freyschuss (1999). "Influence of food intake on electrocardiograms of healthy male volunteers." *Eur J Clin Pharmacol* **55**: 619–624.

Zetterström, R (2009). "Nobel Prize to Willem Einthoven in 1924 for the discovery of the mechanisms underlying the electrocardiogram (ECG)." *Acta Paediatr* **98**: 1380–1382.

Zitron, E, E Scholz, R Owen, S Luck, C Kiesecker, D Thomas, S Kathofer, F Niroomand, J Kiehn, V Kreye, H Katus, W Schoels and C Karle (2005). "QTc prolongation by grapefruit juice and its potential pharmacological basis." *Circulation* **111**: 835–838.

# Contribution of Quantitative Whole-Body Autoradioluminography to the Early Selection and Development of Drug Candidates

# 11

Alain Schweitzer

### Abstract

Whole body autoradioluminography (WBA) utilizes radiolabeled compounds to assess the in situ tissue distribution of new chemical entities in laboratory animals and can be used to project dosimetry calculations in humans. The estimate of the tissue concentrations of radioactivity, along with the tissue distribution of radioactivity, allows for physiological-based pharmacokinetic–pharmacodynamic modeling and estimation of tissue half-life. This chapter provides a review of QWBA methods, methods, data interpretation, and applications to early drug development.

## 11.1 Introduction

The distribution of a radiolabeled drug and/or its metabolites in the tissues, matrices, and organs of a test animal is usually assessed during the course of the pharmacokinetic studies performed prior to the first clinical trials. Up to the early 1980s, the tissue distribution of radioactivity has been determined in most laboratories by dissection of the test animals at room temperature and subsequent processing of the organ and tissue samples by liquid scintillation counting. This method had the disadvantage of allowing postmortem diffusion of radioactive materials to occur in the tissues. Moreover no information was provided on the specific localization of the

radioactive materials in the tissues and organs. Whole-body film-autoradiography, a spatial radioactivity method which allows for the specific localization of radioactivity in the organs and tissues, was used only to fulfill the requirements of some regulatory authorities for registration of the new drug, i.e. in a very late development phase. One of the reasons of this limited use may have been the difficulty to obtain accurate quantitative information on a routine basis. This situation has started to change in the late 1980s as new spatial radioactivity imaging methods as well as new computer-based equipment specifically designed for the qualitative and quantitative interpretation of whole-body autoradiographs became available. The latter are based either on the generation and record of photo stimulated light (storage phosphor or autoradioluminography, the most widely used technology nowadays) or on direct counting of surface radioactivity visualized electronically.

A. Schweitzer

Drug Metabolism and Pharmacokinetics, Translational Sciences, Novartis, Basel CH 4002, Switzerland
e-mail: schweal4@hotmail.fr

Qualitative and quantitative whole-body film-autoradiography, autoradioluminography and direct nuclear counting have applications in numerous sciences; however, the objective of this chapter is to provide the reader with basic information on quantitative whole-body autoradioluminography (QWBA), and to discuss its typical applications, in the light of its strengths and weaknesses, in drug candidate selection, safety assessment, development, and life-cycle management.

## 11.2 Principle and Description of the Method

QWBA (also named phosphor-imaging or storage phosphor technology), film-autoradiography and direct nuclear counting are spatial radioactivity imaging methods that record the spatial distribution and the relationships of radioactive particles (i.e. beta particles emitted by $^{14}$C or $^{3}$H-labeled compounds) within an animal (definition derived from that proposed by Hahn 1983) after exogenous administration of a radiotracer. In QWBA, the most widely used method amongst the three ones mentioned above (Schweitzer 1995), whole-body animal sections are closely apposed to phosphor imaging plates, which represent the detection media. For description below, QWBA is divided into dosing, whole-body sectioning, imaging, and quantification of the image files.

Of course, practical details of the method may vary from one laboratory to another (survey by Solon et al. 2002). Thus, for the readers who wish a more detailed understanding of QWBA, specific courses are offered by many groups, including the Society of Whole-Body Autoradiography (SWBA) (http://www.autoradiography.net/) in the USA and the European Society of Autoradiography (ESA) in Europe (http://www.aopm80.dsl.pipex.com/esa/index.html).

### 11.2.1 Dosing and Administration Solution

The test compound is usually labeled with [$^{14}$C] or [$^{3}$H] in order to avoid a modification of its chemical structure; the rationale for the use of $^{3}$H is that much higher specific activities can be attained than with $^{14}$C, which is of key importance when very low nominal doses are selected (as for example for PET ligand identification studies, where the dose may be as low as 0.1 µg/kg body weight) and that the synthesis of tritium-labeled compounds is faster and less expensive than that of $^{14}$C-labeled ones. Of course, other radioisotopes may also be used, as for example $^{35}$S (Ullberg 1954) or $^{59}$Fe (Ullberg et al. 1961). The important parameter to consider is that the radiolabeled isotope does not modify the physical–chemical properties of the test compound, in particular its molecular structure, and has a half-life long enough to allow QWBA processing. In most laboratories, the typical radioactive dose is approximately 5 MBq/kg body weight with [$^{14}$C]- and 50 MBq/kg with [$^{3}$H]-labeled compounds.

Mainly for oral and topical administrations, it is advised to choose dosing formulations which remain frozen at the working temperatures, generally −20°C, in order to avoid contamination of the tissues surrounding the GIT or the application site during sectioning.

### 11.2.2 Whole-Body Sectioning

Whole-body animal sections are generally obtained according to the method of Ullberg (1977). At a predetermined time after dosing, the test animal is sacrificed and immediately deep-frozen by quenching for approximately 30 min (for a 200 g rat) into an *n*-hexane/dry ice mixture kept at −70°C. This "snap-freezing" avoids further distribution and diffusion of total radiolabeled components in the body. All subsequent procedures are performed at temperatures below −20°C to minimize diffusion of labeled material in the tissues.

The frozen carcass is rapidly shaved and embedded in a mold on a microtome stage by adding an ice-cold aqueous solution of 1–3% low or ultra-low viscosity sodium carboxymethylcellulose. Complete freezing of the embedding

block in an n-hexane/dry ice mixture at $-70°C$ lasts approximately 45 min and is followed by temperature stabilization overnight in a $-20°C$ freezer. The sectioning plan, i.e. coronal, sagittal, or frontal, must be predefined. For sagittal sectioning, the most widely used plan (Fig. 11.1), it is convenient to lay the animal on its right side so that the left side is uppermost in the block and is the first part to be sectioned. This arrangement facilitates earlier imaging of the spleen, stomach, and heart, since they lie toward the left side of the body and will be thus sampled while sectioning down to the midline. The coronal plan may be preferred to the sagittal one when comparative assessments in specific organs like kidney, lung, or brain are intended. For example, it may be preferred for evaluating the potential of a test compound as a fibrosis imaging biomarker when performing autoradiography studies in rat models of unilateral lung and kidney fibrosis.

Whole-body sections 10–50 μm thick are obtained by means of a cryomicrotome (e.g. CM3600, from Leica Biosystems GmbH, D-Nussloch, from Leica Microsystems GmbH, D-Nussloch). Although rats and mice are the most widely used species for QWBA studies in the pharmaceutical industry, larger laboratory animals such as rabbits, dogs, and monkeys may also be considered. The most common limitation is that the animal's carcass must fit into the largest available freezing frame block for sectioning ($40 \times 15 \times 15$ cm), or must be subdivided accordingly (Rico et al. 1978).

Once the first region of interest has been reached (trimming), several sections are obtained at varying depths, based on sectioning of the requisite organs, tissues and body fluids, by adhesion to a special adhesive tape. For calibration and further quantification, a block of $^{14}C$ or $^{3}H$ radiolabeled standards prepared in blood and assayed by liquid scintillation counting (Botta et al. 1985), is sectioned in the same manner and on the same day as the animals are sectioned.

Prior to returning the sections to room temperature, they are dehydrated in the cryomicrotome or with the help of an external freeze-dryer. When dehydration is carried out in the cryomicrotome cabinet, its duration depends on the selected temperature of dehydration, the number of sections being dehydrated, their position in the cabinet, and their thickness. Since residual water acts as a radiation absorber, this step should be long enough to allow for complete dehydration, especially when quantitation is foreseen. Usually, 48 h of dehydration in the cryomicrotome are regarded as a minimum. Using an external freeze-dryer, this step may last only a few minutes, but has to be repeated if a high number of sections have to be dried.

### 11.2.3 Imaging

Whole-body autoradiograms are obtained by means of the quantitative autoradioluminography (QWBA) method, which became commercially available in the late 1980s and early 1990s (Miyahara 1989; Hamaoka 1990; Shigematsu 1992; Shionoya 1992), although the physical phenomenon on which QWBA is based had been already discovered in 1975 (Luckey 1975). The radioactivity containing samples to be analyzed are exposed on an imaging plate which is scanned by a laser beam in a phosphor reader. The imaging plate is a flexible image sensor where very small crystals of photostimulable
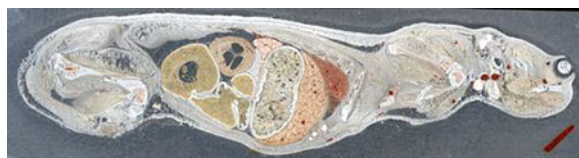


**Fig. 11.1**  (Sectioning plan and Artifacts) 40 μm thick sagittal section through the side of a male HanWIST rat, depicting hydronephrosis in the kidney; this abnormality was not observed in the other animals used in the study. The results of this rat were therefore not considered

phosphor of barium fluorobromide containing a trace amount of bivalent europium are uniformly coated 150–300 μm thick onto a polyester support film. Lattice defects are inherently present in the crystal. The grain size of the crystal is approximately 5 μm. Europium acts as a luminescence center. The luminescence mechanism of the BaFBr:Eu$^{2+}$ photostimulable phosphor can be summarized as follows: part of the Eu$^{2+}$ ions become Eu$^{3+}$ ions through primary excitation by ionizing radiation with electrons being released into the conduction band. These electrons are trapped into the Br-ion empty lattices of the crystal defects, and color centers of the metastable state are formed. When the photostimulated excitation light (PSL) to be absorbed by the color center is irradiated, the trapped electrons are liberated again into the conduction band. The bluish purple PSL released upon laser excitation is collected through the light collector guide to the photomultiplier tube and converted there to analog electric signals in chronological order and subsequently to digital signals. The protected imaging plates (not for weak beta-emitters as $^3$H) can be reused almost indefinitely, assuming they are handled with care.

For imaging, tissue and standard sections are placed on an overhead plastic foil or a cardboard. The tissue and standard sections are placed under controlled light conditions (strongly suggested although not mandatory) in direct and close contact with the imaging plates for typically 1–7 day(s) at room temperature in a lead-shielded box. Exposure in the latter will help to minimize the increase of the background signal. This is especially important for long exposures over 15 days. At the end of the exposure, the plates are first kept for 3–5 min in the dark, as the phosphostimulated light gets partly lost during the first seconds following the separation of the section from the imaging plate; they are then transferred into a phosphorimager, i.e. BAS 5000 (GE Healthcare, UK, formerly from Fuji Photo Film Co. Ltd., J-Tokyo), or Cyclone (Perkin Elmer, formerly from Packard, Meriden, CN, USA) (Schweitzer and Englert 1995) and scanned to produce an autoradiogram. Typical scanning steps are between 10 and 100 μm, and are either predefined by the equipment manufacturer or freely selected by the investigator.

## 11.2.4 Quantification

The specificity of quantification is that it uses image files and not the actual samples; the latter may thus be re-exposed and/or used for other or additional tasks. The major difficulty of quantification is due to the fact that the radioactivity concentrations (mol per weight unit of tissue) are derived from photostimulated light densities per unit of *area*.

The levels of radioactivity present in the tissues are determined by comparative densitometry and digital analysis of the whole-body autoradiogram. For quantification, calibration standards are prepared from fresh whole rat blood and a stock solution containing the same isotope as the one used for labeling the test compound. To assess the actual radioactivity concentrations in the calibration standard samples, samples of spiked blood are counted for total radioactivity in a liquid scintillation counter according to the standard liquid scintillation counting method (Botta et al. 1985). These values are used to generate a calibration curve during digital analysis. The background value is determined on each plate separately in a random manner in 10–20 areas surrounding the tissue and standard sections. In many QWBA laboratories, the limit of detection (LOD) is defined as the sum of the mean background and three standard deviations on the mean, and the quantification limit (LOQ) as three times the LOD, and the size of the areas used to determine the background value is normalized to that of the blood standards used to establish the calibration curve.

The concentrations of radioactivity in the tissues are calculated from the curve generated from the calibration samples present on the image plate. The resulting photostimulated light data files, usually automatically corrected by subtracting the background, are processed with the help of an image analyzer (e.g. MCID, Imaging Research, St. Catherines, Ontario, Canada). Taking into account the numerous parameters

influencing the efficiency in QWBA, which mainly include the extent of the tissue self-absorption, and the section, and image acquisition characteristics, it is essential to select an adequate calibrator and to work under fully normalized conditions in order to accurately estimate the radioactivity concentrations in the tissues. Blood samples of known radioactivity concentrations, processed under the same conditions as the samples to be analyzed, as suggested by Schweitzer et al. (1987) are excellent calibrators for all major tissues, except bone mineral and adipose tissue; for these tissues, correction factors are applied. In addition, the concentration of radioactivity in blood collected from each animal just prior to sacrifice may be used as a "reference" value, for further validation.

As suggested by Ito and Brill (1991), quality checks should be routinely performed. As a consequence of determinations performed in the author's laboratory using several hundreds 40 μm thick sections obtained in a Leica CM3600 cryomicrotome from $^3$H- and $^{14}$C-labeled liver and blood samples, the concentrations of radioactivity in blood and liver are determined on each section to assess the section-to-section thickness

**Table 11.1** Section thickness reproducibility and homogeneity

| SSTR $^{14}$C blood | SSTR $^{14}$C liver | SSTR $^3$H liver | TH $^{14}$C blood |
|---|---|---|---|
| 1.2–6.8% (3.3%) | 1.2–5.1% (3.3%) | 1.9–5.6% (2.9%) | 1.2–5.1% (2.8%) |

The section-to-section thickness reproducibility (SSTR) and thickness homogeneity (TH) are expressed as percents. The results were obtained with blood and liver sections from routinely performed $^{14}$C and $^3$H-QWBA studies. Ranges and mean values (in brackets) are given

reproducibility and thickness homogeneity, Based on the means and standard deviations on the means of the measured concentrations, the variability of the section-to-section thickness reproducibility and thickness homogeneity has been shown to be below 3.5% (Table 11.1), which corresponds to a thickness variation of 1.3 μm for a typical 40 μm thick section, and is thus fourfold less than the variation needed to impact on the results (Schweitzer, presentation at the 2007 SWBA meeting, Charleston, SC, USA).

## 11.3 Data Interpretation

### 11.3.1 Artifacts

For interpretation of the QWBA data, one has first to ensure that the results are not artifacts, most of which can be quite easily detected by skilled and experienced investigators. Artifacts may originate from the test animal health status (e.g. hydronephrosis, Fig. 11.1) and/or study design (e.g. anesthesia by means of carbon dioxide opens the blood–brain-barrier, and thus facilitates the entry of the test compound into the brain, see below).

Most artifacts however happen during the conduct of the study, analyses, or processing of samples. During the study they may result from incorrect or incomplete dose administration, drug precipitation at the blood pH value (Fig. 11.2), leakage of blood collected via cardiac puncture, or due to poor cannulation. Analyses and processing-related artifacts may be associated with undesired diffusion of the radiolabel, damaged knives, incorrect knife angle, debris, sledge speed, incomplete dehydration, due to inadequate



**Fig. 11.2** (Artifacts)
Whole-body autoradiograms of a median sagittal section of a male HanWIST rat at 5 min after IV dosing of a $^{14}$C-labeled drug. The *white areas* correspond to the high radioactivity concentrations. The *white dots* indicate that total radiolabeled components precipitated in blood shortly after dosing

drying duration, section stacking, thickness, temperature, and/or microtome overload, to the flake off of some tissues, and lack of image resolution due to poor intimate contact between the sample and the imaging plate. Contamination of the imaging plate due to improper cleaning and/or erasing will impair data imaging. Lastly, dark haze or flare in high radioactivity concentration areas has been observed, however, this was mainly with the first generation phosphorimagers.

Some artifacts, like those produced by impurities or degradation products due to a lower than optimal radiochemical purity of the test compound, are more difficult to detect. On a theoretical point of view, any radioactive side product amounting to over 0.6% of a typical radioactive dose may generate an autoradiogram, since 0.03 Bq/mg of tissue are routinely detectable under typical sectioning, exposure, and scanning conditions in $^{14}$C-QWBA, taking into account a radioactive dose of 5 MBq/kg body weight. Thus, concluding that a few tenths of percent of the radioactive compound are retained in the body or any single tissue may be incorrect and artifactual.

### 11.3.2 Qualitative Results Interpretation

From a qualitative point of view, autoradiograms should be interpreted in the light of the strengths and limitations of the method, and of the primary goal of the study. Comparing the autoradiographs to the original sections may facilitate the overall interpretation of the results, at least from an anatomical point of view. In addition, the tissue distribution at a given time point is the result of many different processes which occurred in the time between dosing and sacrifice. Thus, autoradiograms at any given time point post dose should be interpreted in the context of the results obtained at earlier time points.

The overall objective of a QWBA study is to provide information about uptake, distribution, retention, and/or accumulation of total radiolabeled components into tissues and organs.

The results obtained usually support several of the following areas: contribution to the selection of drug candidates, evaluation of potential toxicological issues, support of regulatory submissions, prediction of the radioexposure for the human to radioactive drug (e.g. human ADME studies), specific safety assessments including embryo-fetal transfer, transfer into the milk, and life-cycle management studies.

Compared to dissection of the animal followed by liquid scintillation counting of the tissue samples (another method allowing to assess the tissue distribution), QWBA offers many important advantages, thanks to the absence of diffusion of radioactivity in the sample and to optical resolution. Unlike other methods, the distribution of radioactivity is assessed even in the tissues and organs "contaminated" by a biological fluid. QWBA allows for a very precise localization of radioactivity in the organs and tissues independent of their size, location, and biological characteristics. Hence, the method allows assessment of the uptake, distribution, accumulation, and/or retention of total radiolabeled components in different brain areas, the ocular membranes, newly formed bone, embryos and fetuses, blood vessel wall, lymph nodes, collagen/elastine, etc.

QWBA also offers nearly optimal archiving possibilities. The results are documented as an image and a numeric data file, in contrast to the results obtained by liquid scintillation counting, which are in the form of numeric data files only. A potential drawback is that as databasing and computer imaging technology progresses, older file formats may no longer be "readable" by current software. Backward-compatibility of archived data and systems must be considered carefully when employing systems used to support drug development timelines known to span multiple generations of computer systems upgrades.

As with any other method, QWBA has also several limitations to be considered. First, QWBA provides data on the concentrations of total radiolabeled components, not of a single chemical entity, and does not allow for interpretation of data at the microscopic level, mainly

due to the relatively slow freezing rate which can allow ice crystals to develop and grow. In other words, strong statements on the relationship between the distribution, uptake or retention in a given tissue and the pharmacological activity of the test compound, including on receptor localization, should be avoided, as they are not realistic. Also, volatile metabolites are lost during dehydration. Other limitations, however of less importance, are related to the fact that QWBA is time-consuming. This can make it difficult to impossible to evaluate short-lived isotopes, like those used for radiopharmaceuticals. Other limitations can include the small sample sizes employed for each study, method or equipment limitations (e.g. minimal and maximal section thickness), high cost of the equipment and costs of the imaging plates, especially those for detecting weak β-emitters like tritium.

### 11.3.3  Quantitative Interpretation

QWBA offers a wide dynamic range over five orders of magnitude, and the response of the phosphorimagers is almost linear over the entire dynamic range. Thus quantification in QWBA is rather easy and is quite accurate even when using a limited number of internal standards. In addition, the limit of detection in QWBA is independent of the size of the sample, which is not the case for dissection methods. Hence, it is better for small samples compared to liquid scintillation counting (Schweitzer 1995). However, it is important to keep in mind that quantification in very small regions of interest (e.g. the ocular membranes of the rat) is less accurate than in large samples, due to the limited number of pixels analyzed. Specific software (e.g. MCID, http://www.mcid.co.uk/) provides the mean value and standard deviation of the individual measured pixel values, giving thus a scientific rationale to the investigator to keep or reject the results.

The peak concentrations of radioactivity, times of peak concentrations, and times of last concentrations above the limit of quantification in the time course of the study are usually recorded as observed. The concentrations are best expressed in molar units, as the exact nature and composition of the total radiolabeled components in the sample analyzed may be unknown. The tissue exposure, expressed as the area under the curve between time 0 and the time of last quantifiable concentration (AUClast) is calculated using the trapezoidal rule for those tissues and matrices where at least three data points above LOQ are available. The half-life of elimination is taken as $\ln(2)/\lambda z$, where $\lambda z$ (terminal elimination rate constant) is the slope of the log linear line from at least three of the last measurable data points in the terminal phase. Estimated half-lives values exceeding the time frame examined in the study should not be reported. The ratios of tissue/organ to blood peak concentrations of total radiolabeled components and of AUClast values are reported where possible. However, each time point assessed is "terminal," i.e. concentration data in the tissue are obtained at the time point of sacrifice only. Pharmacokinetic evaluations are performed using results from different animals; in addition, sufficient data points should be planned in the study design to allow for a realistic pharmacokinetic analysis. Assuming steady-state has been achieved, the accumulation factors of total radiolabeled components in the tissues after repeated dosing are calculated as exposure ratios from single dose and steady-state (e.g. AUC0-24 h after the last dose versus the AUC0-24 h after the single dose) in those tissues where at least three concentrations were greater than LOQ.

In order to estimate the overall residual radioactivity in the body, the mean radioactivity concentrations over at least six sections per animal (one per sectioning level) are determined and converted into percent of the administered dose by taking into account the animal weight, specific activity of the administrated formulation, volume administered, and dose.

## 11.4  Typical Applications of QWBA

QWBA has been used for decades in most major pharmaceutical companies to support regulatory submissions, estimate radioexposures for human

ADME studies, assess specific safety, and to profile compounds once available on the market (Shigematsu et al. 1995). These applications of QWBA are primarily those related to the precise information obtained with this technology, thanks to the fact that autoradiograms are obtained with a good resolution. Information on uptake, distribution, retention and/or accumulation of radioactive material can be obtained in all tissues, independent of their size. QWBA has been used to define exposures in tissues such as spleen white and red pulp, uveal tract, blood vessel wall, cartilage, specific cerebral and cerebellar regions, and various skin layers. Uptake, distribution, retention, and/or accumulation of drug related material within a single organ has been shown in the differentiation between the cortex, medulla, corticomedullar junction, and pelvis in the kidney and in the mottled distribution pattern of radioactivity within the liver or testis.

In the recent years, an increasing number of laboratories have decided to perform QWBA or to outsource QWBA studies on a routine basis in the very early phases of exploratory development. Application of QWBA in this area helps to contribute to the early selection of potential drug candidates, based on their distribution, uptake, and retention in specific tissues. Potchoiba and Nocerini (2004) described how they use $^3$H-QWBA to identify lead compounds early on during the drug discovery phase. This is in line with the statement by Solon et al. (2002), who concluded that QWBA is quickly becoming part of the battery of studies conducted during the lead optimization process to select optimal drug candidates.

## 11.4.1 Contribution to Early Selection of Drug Candidates

### 11.4.1.1 Central Nervous System

In the nervous system disease area, the assessment of the uptake, distribution, retention and/or accumulation of a drug candidate in the different anatomical regions of the brain is of particular importance. No other method achieves the level of detail needed for correct interpretation of the results. In general, taking into account that blood in brain represents 2–4% of the brain volume, and considering experimental uncertainties, brain/blood radioactivity AUClast ratios equal to or higher than 0.08 indicate that the compound and/or its metabolites passed significantly the blood–brain barrier. It is important to keep in mind that acidosis, as a consequence of anesthesia with carbondioxide (Mayhan et al. 1988), and hyperosmolar mannitol (Hiesiger et al. 1986) open the blood barrier, whose permeability may be also age-dependant (Bake and Sohrabji 2004) and increased by histamine (Gulati et al. 1985).

Foster et al. (2007) demonstrated that following single and multiple oral doses, the oral immunomodulatory drug FTY720 and its phosphorylated metabolite were specifically localized to the CNS white matter, preferentially along myelin sheaths, in similar concentrations, suggesting that FTY720 effectiveness is probably due to also to the neuroprotective influence of the phosphorylated compound in the central nervous system (Fig. 11.3).

In another example, the author investigated the distribution of different chemical classes of orally active AMPA receptor antagonists proposed for the treatment of epileptic patients. As the
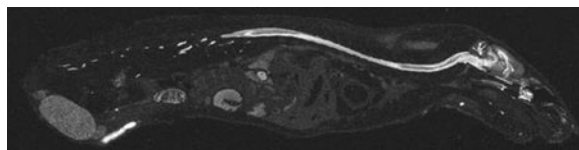


**Fig. 11.3** (Applications)
Whole-body autoradiogram of a median sagittal section of a male HanWIST rat at 72 h after po dosing of the $^{14}$C-labeled oral immunomodulatory drug FTY720. The *white areas* correspond to the high radioactivity concentrations.

The results show that FTY720 and its phosphorylated metabolite were specifically localized to the CNS white matter, preferentially along myelin sheaths

compounds of the di-phosphonate class have shown in the past a high and long lasting affinity and retention to/into bone mineral, the new drug candidates of a different structural class were evaluated on their particular affinity to the bone mineral. The particularity of this study is that the assessment needed only one animal per drug candidate (at 24 h following i.v. dosing) (Schweitzer, unpublished data, Fig. 11.4).

Another new interesting possible application of QWBA in the CNS area is the selection of potential ligands for positron emission tomography (PET). It has however to be mentioned that this selection is usually performed under very different experimental conditions (thaw-mounted sections from brain, short-living positron emitter isotope, for instance ^{11}C) (Wyss et al. 2007) than the ones described in this review, although radioactivity is detected by phosphorimaging. If using $\beta^-$ emitters, a challenge is the low nominal dose, often in the ng/kg body weight range, and the subsequent very low radioactive dose administered. In a recent study performed by the author with [3H]ABP688, a specific mGlu5 receptor antagonist whose uptake into the brain after IV dosing has been shown to be modified by pre-blocking (Wyss et al. 2007), the IV. dose ending up with <20% receptor occupancy was 0.5 µg/kg; the actual radioactive dose, 4.97 MBq/kg body weight, which is 10- to 20-fold lower than tritium a typical dose, necessitated 13 days of exposure.

### 11.4.1.2 Oncology

In oncology, the rapid and specific uptake into the tumor and long-lasting adequate concentrations of active compound in the tumor, combined with the low exposure of the other tissues represent the "basic" early selection criteria for compounds intended to be used in oncology indications. However, each company has its own criteria, which of course differ depending on the pharmacological class of the drug candidates.

For example, the author demonstrated with the help of QWBA that in female HsdNpa:Athymic Nude-nu mice, synthetic Hsp90 ATPase inhibitors foreseen for the treatment of solid tumors and hematological malignancies were rapidly and specifically taken up into the viable tumor (human breast cancer BT-474 tumor established from a solid, invasive ductal carcinoma of the breast), achieving levels in the tumor similar to that of blood at 5 min after a 30 mg/kg IV. dose; in addition, no radioactivity was detected in any tissue except the viable tumor (unchanged compound as demonstrated by MALDI-MSI, see below), and GIT content already at 24 h post dose (Schweitzer, unpublished data, Fig. 11.5).
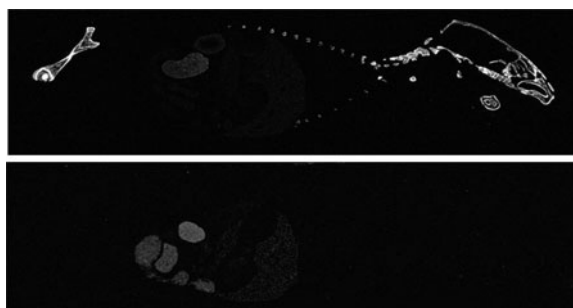


**Fig. 11.4** (Applications)
Whole-body autoradiograms of median sagittal sections of male HanWIST rats at 1 year after SC. administration (*top*) and 24 h after IV dosing of ^{14}C-labeled orally active AMPA receptor antagonists proposed for treatment of epileptic patients. The *white areas* correspond to the high radioactivity concentrations. The compound previously tested (di-phosphonate) (*top*) showed a high and long lasting affinity and retention to/into bone mineral. The drug candidate (different structural class than the previous compound) shows no retention in the bone mineral already at 24 h after IV dosing (*bottom*)
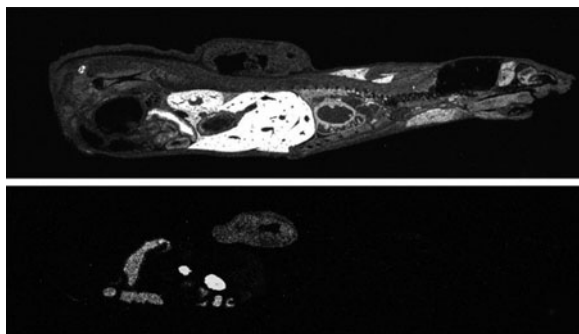
**Fig. 11.5** (Applications)
Whole-body autoradiograms of median sagittal sections of tumor bearing female HsdNpa:Athymic Nude-nu mice female at 5 min and 24 h after IV dosing of a $^{14}$C-labeled synthetic Hsp90 ATPase inhibitor foreseen for the treatment of solid tumors and hematological malignancies. The tumor was a human breast cancer BT-474 tumor established from a solid, invasive ductal carcinoma of the breast. The *white areas* correspond to the high radioactivity concentrations. The whole-body autoradiogram at the *top* shows that total radiolabeled components were rapidly and specifically taken up into the viable tumor, achieving levels similar to that of blood already at 5 min post dose; the whole-body autoradiogram at the *bottom* shows that no radioactivity was detected in any tissue except the viable tumor and GIT content already at 24 h post dose

Others have shown the utility of QWBA in oncology. Akel et al. (1986) showed that the uptake into the tumor of rats bearing chemically induced rhabdomyosarcoma of Ro 07-0582, a hypoxic cell radiosensitizer, was delayed, the tumor activity being highest as late as at 12 h after treatment. Fand et al. (1990) investigated the regional distribution of the $^{90}$Y-labeled anti-carcinoembryonic antigen monoclonal antibody NP-2 and its fragments within GW-39 colon carcinoma xenografts, and revealed specific anti-tumor uptake as well as significant accumulation of 90Y in the bones. These results demonstrate that QWBA is an effective tool for assessing the degree of penetration of immunoglobulins in tumors in which vascular patterns, local glucose metabolism, protein synthesis, and rapid cell proliferation indices may be characterized.

### 11.4.1.3 Infectious Diseases

In the infectious diseases area, blocking the CCR5 receptor is a promising therapeutic approach for the treatment of HIV infections; in fact, retroviruses are surrounded by an envelope consisting of a host cell-derived lipid bilayer and a virus-encoded envelope glycoprotein. For the virus to enter a target cell, the viral membrane must fuse with the plasma membrane of the cell, a process mediated by the envelope glycoproteins and transmembrane chemokine co-receptors, such as CCR5. As CCR2 can act as a co-receptor for HIV, CCR2 blockade, in addition to CCR5 inhibition, may provide additional benefit. Ideally, drug candidates should be highly potent antagonist for CCR2 and CCR5.

To test this, the author first showed that a new drug candidate was retained in the body and concentrated in the proximal intestinal wall; a second QWBA study was then done in CCR2/CCR5 homozygote knock-out and wild-type mice after po and IV dosing in order to differentiate between unspecific tissue binding and CCR2 and/or CCR5 receptor mediated tissue binding and distribution. The distribution patterns in the knock-out and wild-type mice were similar, indicating that the CCR2/CCR5 receptor is involved neither in the specific uptake nor retention of total radiolabeled components in the proximal small intestinal wall, leading to a "NO GO" decision for the test compound (Schweitzer, unpublished data, Fig. 11.6).

### 11.4.1.4 Imaging Biomarkers

QWBA is also a very promising tool for evaluating the potential of a test compound as an imaging biomarker. Nearly 45% of all deaths in the
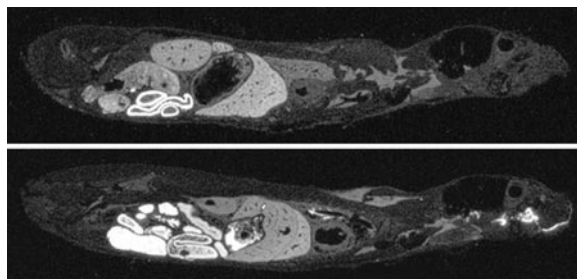
**Fig. 11.6** (Applications)
Whole-body autoradiograms of lateral sagittal sections of female CCR2/CCR5 homozygote knock-out (KO) and wild-type (WT) mice at 24 h after po dosing of a $^{14}$C-labeled drug. The *white areas* correspond to the high radioactivity concentrations. The similar distribution patterns in the KO and WT mice indicate that the CCR2/CCR5 receptor is involved neither in the specific uptake nor retention of total radiolabeled components in the proximal small intestinal wall
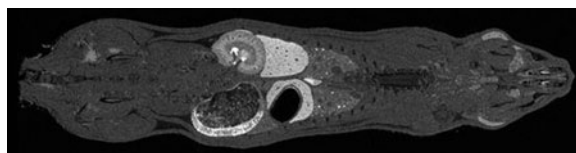


**Fig. 11.7** (Sectioning plan and Applications)
Whole-body autoradiogram of a coronal section of a male Sprague Dawley rat with unilateral kidney fibrosis at 4 h ($C_{max}$) after po dosing of a $^{14}$C-labeled drug candidate as a fibrosis imaging biomarker. The *white areas* correspond to the high radioactivity concentrations. The whole-body autoradiogram shows the differential uptake and distribution of total radiolabeled compounds in the intact and diseased kidneys

developed world are attributed to chronic fibro-proliferative diseases; however, early response imaging biomarkers for anti-fibrotic therapy are missing and represent a large unmet medical need. In this example, QWBA was performed in the rat models of unilateral kidney fibrosis. The UUO (unilateral ureteric obstruction) model is an experimental hydronephrosis model and is a widely used model for progressive renal fibrosis that is independent of hypertension or systemic immune disease. The obstructed kidney after UUO mimics in an accelerated manner the development of tubulointerstitial fibrosis, i.e. cellular infiltration, tubular proliferation and apoptosis, epithelial-mesenchymal transition, myofibroblast accumulation, increased extracellular matrix deposition, and tubular atrophy (Bascands and Schanstra 2005; Docherty et al. 2006). A selected autoradiogram of a coronal rat section showing the specific uptake and distribution in the intact and diseased kidney is depicted in Fig. 11.7 (Schweitzer, unpublished data).

## 11.4.2 Support of Toxicology and Pharmacokinetic Studies

One of the most typical applications of QWBA is the support of regular toxicology and toxicokinetic studies, by investigating the tissue distribution as a function of time in the same animal species under the same conditions as those of the toxicology studies (Busch 1977; Ahmed et al. 1993). The target tissues and target organs are detected and an overall estimation of the organ and tissue exposure is gained. In our laboratory, a routine QWBA tissue distribution evaluates 50–60 tissues at five to six different time points up to 168 h postdose. The data are used to better understand the overall pharmacokinetics and to predict the human exposure to radiation that might occur during the administration of radiolabeled drug in specialized clinical studies. The maximal radioactive dose for a typical human subject is estimated using the concentrations of total radiolabeled components in the

tissues and supplied weight factors to correct for the sensitivities to damage of the different tissues.

In relation to the latter, the assessment of the uptake, distribution, retention, and/or accumulation of total radiolabeled components into the melanin-containing organs is of particular importance, mainly since the toxicity studies in rodents are performed in albino animals and thus do not deliver exposure data in these area. QWBA is probably the best technique currently available to enable the evaluation of the affinity of a test compound to melanin, which is important for dosimetry calculations. In fact, due to the small sample size of the pigmented uveal tract of laboratory animals, tissue dissection followed by liquid scintillation counting may not allow to detect drug-derived radioactivity in this tissue. In contrast, as the limit of detection in phoshorimaging is almost independent of the sample size, evaluating the biodistribution of xenobiotics by QWBA not only provides pharmacokinetic data required for predicting the potential tissue deposition of an absorbed dose of radioactivity in man, but also allows for visual and quantitative evaluation of radioactivity in small anatomical structures that otherwise could not be detected or measured by conventional tissue combustion technology (Potchoiba et al. 1995).

The eye choroid is used to assess the potential uptake of the drug and/or its metabolites into melanin-containing structures. The presence and/or persistence of radioactive material in this tissue may be related to its specific uptake into the melanin-containing structures as well as to its uptake into other cells. Thus retention of radioactivity at late time points in the eye choroid of pigmented rats and not in albino rats indicates that there is a specific uptake of radioactive material in the melanin-containing structures (Fig. 11.8). A higher radioactivity concentration in the eye choroid of the pigmented rat at an early time point post dose than in the one at a late time point dose, usually after IV. dosing, indicates that this uptake is at least partly reversible (Zane et al. 1990). However, no clear relationship has been established between high affinity and chemical structure, except for polycyclic amines (chlorpromazine, chloroquine) and charged compounds. Thus, fluoroquinolones have been reported to have a high affinity for melanin. Tanaka et al. (2004) assessed the ocular tissue distribution and accumulation of radioactivity after repeated oral administration of $^{14}$C-levofloxacin and $^{14}$C-chloroquine in pigmented rats for 84 days. The melanin-containing ocular tissues, such as iris ciliary body and stratum pigment choroids sclera, showed a much higher concentration of radioactivity than other non-pigmented ocular
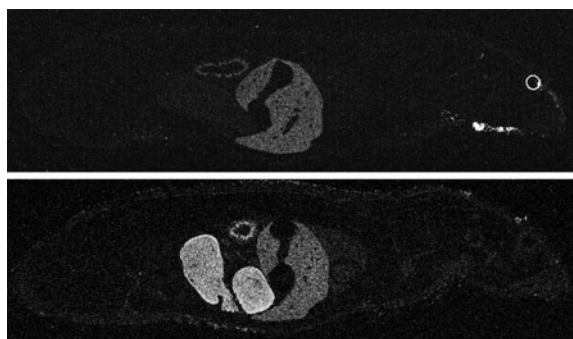


**Fig. 11.8** (Applications)
Whole-body autoradiograms of lateral sagittal sections of a male HanWIST rat (*top*) and a male Long Evans pigmented rat (*bottom*) at 168 h after po administration of a $^{14}$C-labeled drug candidate. The *white areas* correspond to the high radioactivity concentrations. Both autoradiograms show that residual radioactivity was observed in the liver, kidney, cortico medullar junction, and, to some extent in the lung and blood. The main difference between the albino and pigmented rats is that in the latter (*bottom*), total radiolabeled components are retained in the eye choroid, suggesting a specific uptake of the drug and/or its metabolites into the melanin-containing structures

tissues, and gradually increased with increasing dose number. The concentration and the extent of accumulation of radioactivity not only in melanin-containing ocular tissues but also in other non-pigmented ocular tissues, such as retina, after chronic oral administration of ^{14}C-levofloxacin once daily for 84 days were much lower than those after multiple dosing with ^{14}C-chloroquine under the same conditions, and concluded that based on these results levofloxacin would have a lower risk for ocular toxicity than chloroquine after chronic dosing. This statement might be questioned as the ocular toxicity of chloroquine has been shown to also be due to its retention in the visual area in the cerebral cortex (Liss et al. 1976).

### 11.4.3 Support of Regulatory Studies

QWBA is also of importance in those studies which have to be performed to fulfill the requirements of the regulatory authorities or agencies. Amongst others, QWBA allows to assess the placental transfer, distribution of radioactive material in the embryos and fetuses, and fetal exposure to the drug and/or its metabolites, supporting thus the teratology studies. Numerous examples of transfer into the embryo-fetal compartment have been published for pharmaceuticals (Ullberg et al. 1967; Ullberg 1971; Waddell 1972; Hemauer et al. 2008) (Fig. 11.9).

The extent of the transfer of radioactive material from maternal blood into the placenta is estimated from the placenta/blood AUClast ratio on day 13 and day 18 of gestation. A ratio >1 indicates that the radioactive material

present in blood is transferred into the placenta. Similarly, the extent of the transfer of compound-related material from placenta into the fetuses is estimated from the fetus/placenta AUClast ratio. The highest ratio indicates the highest extent of the placental transfer into the fetuses. As much of the radioactive material in the fetus will have bypassed the foetal liver, total radiolabeled components in the fetus are those present in the maternal blood and in the placenta, two compartments rather easy to analyze. However, the extent of the embryo-fetal transfer depends on many parameters: test species and stage of gestation, possibility of different pharmacokinetic profiles in the dam versus the fetus. Accumulation in the fetus does not necessarily mean damage to the fetus, just as the observation of fetal damage does not mean compound accumulation in the fetus. Other considerations must be taken, including possible contributions due to compound effects on seminal fluid, spermatozoids, and male sexual organs.

Recent examples of the use of QWBA in fetal transfer is the recent study by Bruin et al. (2008) which showed following oral administration of ^{14}C-labeled deferasirox (Exjade, ICL670) to female pregnant rats, the placental barrier was passed to a low extent and that approximately 3% of the dose was transferred into the breast milk. Other examples have been published for vitamins and chemicals; for instance, Ullberg et al. (1967) demonstrated that water-soluble vitamins (B12, B1, C) accumulate in the fetus by an active placental transport mechanism. Ullberg et al. (1961) showed also that ^{59}Fe achieved higher
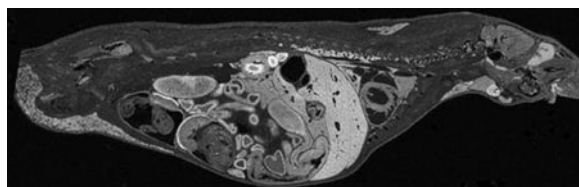


**Fig. 11.9** (Applications)
Whole-body autoradiograms of a median sagittal section of a female pregnant HanWIST rat at 8 h after po dosing of a ^{14}C-labeled drug. The *white areas* correspond to the high radioactivity concentrations. The radioactivity concentrations in the amnion, placenta, and fetus are higher than in the maternal blood, and total radiolabeled components passed the fetal blood–brain barrier

concentrations in fetal blood than in maternal blood already 20 min after oral dosing, and that 75% of the total radiolabeled components found in the fetus were concentrated in the fetal liver. Ahmed et al. (1993) demonstrated that [phenyl-U-$^{14}$C]tri-o-cresyl phosphate passed very well the placental barrier in pregnant mice.

QWBA also represents a good means to assess the transfer of drug related components into the milk in lactating dams, and the exposure of sucking pups. For estimating the fraction of the administered dose eliminated into the milk on day 1 post dose, a daily milk production in lactating rats of 15 mL (Sampson and Jansen 1984) and a constant production of milk over a 24-h period are assumed. For the assessment of the exposure of the pups, it is generally assumed that the litter size is ten and the weight of the pups on day 11 is 20 g (Pass and Freeth 1993), the pups absorb the sucked milk to an extent of 100%, all pups suck the same amount of milk, and that the produced milk is sucked by the pups quantitatively. Bruin et al. (2008) showed that, following oral dosing of $^{14}$C-labeled deferasirox (Exjade, ICL670) to female lactating dams, the sucking puppies were exposed to ICL670 and/or its metabolites; the highest $^{14}$C concentrations were detected in the kidney cortex, liver, lung, skin, and GIT content; the presence of radioactive milk was also evidenced in the pup stomach content (Fig. 11.10).
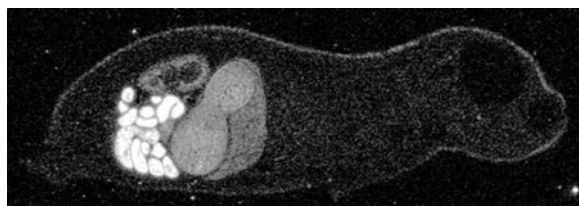
## 11.4.4 Life-Cycle Management

Although diclofenac (Voltaren®), an inhibitor of COX-2 and PGE-2 enzymes and a weak acid NSAID with pronounced analgesic, anti-inflammatory and antipyretic properties, prescribed for the treatment of a large variety of inflammation-related diseases, has been on the market since decades, its specific distribution into inflamed tissues has been only recently assessed after single oral administration of [$^{14}$C]diclofenac sodium to rats (Schweitzer et al. 2009). Diclofenac preferentially distributed into the carrageenan-induced inflamed tissues as early as 1 h after oral administration, which may contribute to the rapid therapeutic activity of the compound, and achieved exposures 26- and 53-fold higher in the inflamed neck and inflamed paw, respectively, of treated animals than in control rats. For all other tissues the distribution and exposure were similar for control and treated animals. Total radiolabeled components were rapidly eliminated from saline-injected sites (low blood flow, no inflammation, i.e. no accumulation of plasma proteins). These results consolidate the assumption that the blood circulation with its high albumin content might favor the drug uptake in well vascularized tissues as well as an increased expression of the COX-2, which is found in inflamed tissues, also evidenced by the rapid clearance of drug related material from non inflamed nape neck and



**Fig. 11.10** (Applications)
Whole-body autoradiogram of a sagittal section of a sucking pup at 8 h after po dosing ($C_{max}$) of $^{14}$C-deferasirox (ICL670) to a lactating dam. The *white areas* correspond to the high radioactivity concentrations. QWBA demonstrated that the sucking puppies were exposed to ICL670 and/or its metabolites; the highest $^{14}$C concentrations were detected in the kidney cortex, liver, lung, skin, and GIT content. In the autoradiogram below, the presence of radioactive milk was also evidenced in the pup stomach content

control footpad, in which blood vessels density is low.

The bisphosphonate, zoledronic acid, was shown to be initially rapidly eliminated from plasma and the non calcified tissues but only slowly from bone, whereas the terminal half-lives of elimination from the tissues were similar, suggesting redistribution of drug from the bone rather than prolonged retention in the latter (Weiss et al. 2008).

## 11.5 Outlook

Mass spectrometric imaging (MSI), also termed imaging mass spectrometry, has gained new momentum in the last couple of years with the development of matrix assisted laser desorption/ionization (MALDI) MSI (Caprioli et al. 1997). As QWBA detects total radiolabeled components and not a chemical entity, whole-body matrix-assisted laser desorption ionization combined to mass spectrometric imaging (WB-MALDI-MSI) using whole-body sections obtained as described above (with the exception of the dehydration step, see below) has become an alternative method in a growing number of laboratories in charge of pharmacokinetic studies (Rohner et al. 2005; Stoeckli et al. 2007a, b). The potential value of this technology for imaging applications in biomedical research was recognized early on by laboratories in academia and industry, with first efforts focusing on mapping of potential drug targets, disease biomarkers, and the lower mass range of most current drugs. The interest of MALDI MSI, although the method is only applicable to molecules that are ionizable by the MALDI process, results from the ability to simultaneously localize multiple label-free analytes in tissues, based on their molecular weights and fragmentation pattern, thereby providing valuable additional ADME information.

To perform a MALDI MSI analysis, the sample has to be attached to a metal plate and coated with matrix. Suitable sample preparation methods were developed which allow direct detection of compound from animal tissue sections by MALDI mass spectrometry (Stoeckli et al. 2007a). In fact, the sections are kept frozen until just before processing, fast freeze-dried, attached to metal plates, spray-coated with MALDI matrix and sputter coated with a thin film of gold. The sections prepared in this manner are introduced into the mass spectrometer, where the laser is used to raster over the tissue section, while acquiring a mass spectrum and/or fragmentation spectra from each laser spot. MALDI MSI is specific and rapid. This technology fits ideally into the field of existing technologies and will very likely expand in the future.

The major drawbacks of MALDI MSI are its lower sensitivity as compared to QWBA, and the difficulty to obtain accurate quantitative results, due to the substance specific ionization yield, tissue specific ion suppression, and dependency of detected signal on the amount/property of the deposited matrix. For example, as the signal suppression is very specific, depending on the tissue and substance, each substance needs to be calibrated in a separate experiment by spiking each tissue and measuring the resulting MALDI signal. In addition, not all compounds can be ionized equally well, limiting thus the application possibility of MALDI MSI.

The first example in which an IV administered unlabeled peptide has been used for MS imaging has been published by Stoeckli et al. (2007b). Mass spectrometric imaging was applied to assess compound distributions on whole-body sections of mice after IV dosing of a β-peptide and an α-peptide control. The animals were sacrificed at different time points after dosing, providing simultaneous spatial and kinetic information. No detection of the α-peptide control was observed at 1 h post-dose, while retention of the β-peptide was observed for longer than 24 h post-dose. Although tissue-dependent signal suppression was not accounted for, and there were no internal standards added for quantification, this study allowed for a rapid (relevant data obtained within 1 day) and cost efficient evaluation of the compound behavior in the animals, confirming that β-peptides are stable and distribute specifically in the tissues in vivo.

## Conclusion

In conclusion, QWBA has numerous applications in the pharmaceutical industry, and represents one of the key studies performed during the time course of the development of a drug, from early selection up to marketing support. Whole-body MALDI-MSI, an alternative powerful method providing information on the spatial distribution of label-free masses in sections similar to those used for QWBA, has been shown to nicely complement the latter. However, even if further technological improvements are to be anticipated, rendering MALDI-MSI more attractive, it is unlikely that this new method will completely replace QWBA in the near future in the applications described above.

## References

Ahmed, A.E., Jacob, S., Soliman, S., Ahmed, N., Osman, K., Loh, J.P., and Romero, N. Whole-body autoradiographic disposition, elimination and placental transport of [14C]tri-o-cresyl phosphate in mice. *J. Appl. Toxicol.* 1993; 13(4):259–267.

Akel, G., Benard, P., Canal, P., and Soula, G. Distribution and tumor penetration properties of a radiosensitizer 2-[14C]misonidazole (Ro 07-0582) in mice and rats as studied by whole-body autoradiography. *Cancer Chemother. Pharmacol.* 1986; 17:121–126.

Bake, S., and Sohrabji, F. 17beta-estradiol differentially regulates blood-brain barrier permeability in young and aging female rats. *Endocrinology* 2004; 145(12):5471–5475.

Bascands, J.L., and Schanstra, J.P. Obstructive nephropathy: Insights from genetically engineered animals. *Kidney Int.* 2005; 68:925–937.

Botta, L., Gerber, H.U., and Schmid, K. Measurement of radioactivity in biological experiments. In: Garrett, E.R. and Hirtz, J.L. (Eds), *Drug, Fate and Metabolism – Methods and Techniques*, Marcel Dekker, Inc., New York and Basel, 1985; vol. 5: pp. 99–134.

Bruin, G., Faller, T., Wiegand, H., Schweitzer, A., Nick, H., Schneider, J., Boernsen, K.-O., and Waldmeier, F. Pharmacokinetics, distribution, metabolism, and excretion of deferasinox and its iron complex in rats. *Drug Metab. Dispos.* 2008; 36:2523–2538.

Busch, U. Whole-body autoradiography (WBAR): Use for pilot studies of pharmacokinetics in rats. *Br. J. Clin. Toxicol.* 1977; 41(Suppl. 1):28–29.

Caprioli, R.M., Farmer, T.B., and Gile, J. Molecular imaging of biological samples: Localization of peptides and proteins using MALDI-TOF MS. *Anal. Chem.* 1997; 69:4751–4760.

Docherty, N.G., O'Sullivan, O.E., Healy, D.A., Fitzpatrick, J.M., and Watson, R.W.G. Evidence that inhibition of tubular cell apoptosis protects against renal damage and development of fibrosis following ureteric obstruction. *Am. J. Physiol. Renal Physiol.* 2006; 290:F4–F13.

Fand, I., Sharkey, R.M., and Goldenberg, D.M. Use of whole-body autoradiography in cancer targeting with radiolabeled antibodies. *Cancer Res.* 1990; 50:885s–891s.

Foster, C., Howard, L., Schweitzer, A., Persohn, E., Hiestand, P., Balatoni, B., Reuschel, R., Beerli, C., Schwartz, M., and Billich, A. Brain penetration of the oral iimmunomodulatory drug FTY720 and its phosphorylation in the central nervous system during experimental autoimmune encephalomyelitis: Consequences for mode of action in multiple sclerosis. *J. Pharmacol. Exp. Ther.* 2007; 323:469–476.

Gulati, A., Dhawan, K.N., Shukla, R., Srimal, R.C., and Dhawan, B.N. Evidence for the involvement of histamine in the regulation of blood-brain barrier permeability. *Pharmacol. Res. Commun.* 1985; 17(4):395–404.

Hahn, E.J. Autoradiography: A review of basic principles. *Am. Lab.* 1983; 15(7):64–71.

Hamaoka, T. Autoradiography of new era replacing traditional X-ray film. *Cell Technol.* 1990; 9:456–462.

Hemauer, S.J., Yan, R., Patrikeeva, S.L., Mattison, D.R., Hankins, G.D., Ahmed, M.S., and Nanovskaya, T.N. Transplacental transfer and metabolism of 17-alpha-hydroxyprogesterone caproate. *Am J Obstet Gynecol.* 2008; 199(2):169.

Hiesiger E.M., Voorhies R.M., Basler G.A., Lipschutz L.E., Posner J.B., and Shapiro W.R. Opening the blood-brain and blood-tumor barriers in experimental rat brain tumors: The effect of intracarotid hyperosmolar mannitol on capillary permeability and blood flow. *Ann. Neurol.* 1986; 19(1):50–59.

Ito, T., and Brill, A.B. Variation in thickness of the large cryosections cut for whole-body autoradiography. *Appl. Radiat. Isot.* 1991; 42(2):187–192.

Liss, R.H. In: Mehlman, M.A., Shapiro, R.E., and Blumenthal, H. (Eds), *Advances in Modern Toxicology: New Concepts in Safety Evaluation* Hemisphere, Washington, DC, 1976; vol. 1: pp. 273–305.

Luckey, G. US patent # 3, 859, 527, 1975.

Mayhan W.G., Faraci F.M., and Heistad D.D. Effects of vasodilatation and acidosis on the blood-brain barrier. *Microvasc. Res.* 1988; 35(2):179–192.

Miyahara, J. The imaging plate: A new radiation image sensor. *Chem. Today* 1989; 223:29–36.

Pass, D., and Freeth, G. The rat. *ANZCCART News* 1993; 6:4, Insert.

Pierson, J., Norris, J.L., Aerni, H.R., Svenningsson, P., Caprioli, R.M., and Andren, P.E. Molecular profiling of experimental parkinson's disease: Direct analysis of peptides and proteins on brain tissue sections by

MALDI mass spectrometry. *J. Proteome Res.* 2004; 3:289–295.

Potchoiba, M.J., and Nocerini, M.R. Utility of whole-body autoradiography in drug discovery for the quantification of tritium-labeled drug candidates. *Drug Metab. Dispos.* 2004; 32(10):1190–1198.

Potchoiba, M.G., Tensfeldt, T.G., Nocerini, M.R., and Silber, B.M. A novel quantitative method for determining the biodistribution of radiolabeled xenobiotics using whole-body cryosectioning. *J. Pharmacol. Exp. Ther.* 1995; 272(2):953–962.

Rico, A., Benard, P., Braun, J.P., and Burgat-Sacaze, V. Application of macroscopic autoradiography to large animals in veterinary pharmacokinetics: The distribution of sodium selenite labelled with $^{75}$Se in the pig. *Ann. Rech. Vét.* 1978; 9(1):25–32.

Rohner, T.C., Staab, D., and Stoeckli, M. MALDI mass spectrometric imaging of biological tissue sections. *Mech. Ageing Dev.* 2005; 126:177–185.

Sampson, D.A., and Jansen, G.R. Measurement of milk yield in the lactating rat from pup weight and weight gain. *J. Pediatr. Gastroenterol. Nutr.* 1984; 3(4):613–617.

Schweitzer, A. Spatial imaging of radioactivity in animal tissues and organs. In: Welling, P. (Ed.), *Pharmacokinetics: Regulatory-Industrial-Academic Perspectives*, 2nd edition, Marcel Dekker Inc., New York; 1995.

Schweitzer, A., Fahr, A., and Niederberger, W. A simple method for quantitation of $^{14}$C-whole-body autoradiograms. *Appl. Radiat. Isot.* 1987; 38(5):329–333.

Schweitzer, A., and Englert, D. Contribution of electronic autoradiography to the assessment of the site specific delivery of radiolabelled agents. *Q. J. Nucl. Med.* 1995; 42–44.

Schweitzer, A., Hasler-Nguyen, N., and Zijlstra, J. Preferential uptake of the non steroid anti-inflammatory drug diclofenac into inflamed tissues after a single oral dose in rats. *BMC Pharmacol.* 2009; 9:5.

Shigematsu, A. "Bao-Bei," or the powerful technology, in science of whole-body metabolism. Autoradioluminography. *Radioluminography* 1992; 1(3):115.

Shigematsu, A., Motoji, N., Hatori, A., and Satoh, T. Progressive application of autoradiography in pharmaceutical and metabolic studies for development of new drugs. *Regul. Toxicol. Pharmacol.* 1995; 22:122–142.

Shionoya, S. Mechanistic approach toward photostimulated luminography. *Radioluminography* 1992; 1(1):115.

Solon, E., and Kraus, L. Quantitative whole-body autoradiography in the pharmaceutical. Survey results on study design, methods and regulatory compliance. *J. Pharmacol. Toxicol. Meth.* 2002; 43:73–81.

Solon, E., Balani, S.K., and Lee, F.W. Whole-body autoradiography in drug discovery. *Curr. Drug Metab.* 2002; 3:451–462.

Stoeckli, M., Staab, D., and Schweitzer, A. Compound and metabolite distribution measured by MALDI mass spectrometric imaging in whole-body tissue sections. *Int. J. Mass Spect.* 2007; 260(2–3):195–202.

Stoeckli, M., Staab, D., Schweitzer, A., Gardiner, J., and Seebach, D. Imaging of a β-peptide distribution in whole-body mice sections by MALDI mass spectrometry. *J. Am. Soc. Mass Spectrom.* 2007; 18:1921–1924.

Tanaka, M., Takashina, H., and Tsutsumi, S. Comparative assessment of ocular tissue distribution of drug-related radioactivity after chronic oral administration of $^{14}$C-levofloxacin and $^{14}$C-chloroquine in pigmented rats. *J. Pharm. Pharmacol.* 2004; 56(8):977–983.

Todd, P.J., Schaff, T.G., Chaurand, P., and Caprioli, R.M. Organic ion imaging of biological tissue with MALDI and SIMS. *J. Mass Spectrom.* 2001; 36:355–369.

Ullberg, S. Studies on the distribution and fate of $^{35}$S-labeled benzylpenicillin in the body. *Acta Radiol. Suppl. (Stockh)* 1954; 118:1–110.

Ullberg, S. Autoradiography in fetal pharmacology. In: Boreus, L. (Ed), *Fetal Pharmacology Symposium*, Raven Press, New York, 1971; pp. 55–73.

Ullberg, S. The technique of whole-body autoradiography. Cryosectionning of large specimens. *Science Tools (The LKB Instr. J.)* Special Issue, 1977; 2–29.

Ullberg, S., Sorbo, B., and Clemedson, C.J. Distribution of radioactive iron in pregnant mice studies by whole-body autoradiography. *Acta Radiol.* 1961; 55:145–155.

Ullberg, S., Kristoffersson, H., Flodh, H., and Hanngren, A. Placental passage and fetal accumulation of labelled vitamin B12 in the mouse. *Arch. Int. Pharmacodyn. Ther.* 1967; 167:431–449.

Waddell, W.J. Localization and metabolism of drugs in the fetus. *Fed. Proc.* 1972; 31:52.

Weiss, H., Pfaar, U., Schweitzer, A., Wiegand, H., Skerjanec, A., and Schran, H. Biodistribution and plasma protein binding of zoledronic acid. *Drug Metab. Dispos.* 2008; 36:2043–2049.

Wyss, M.T., Ametamey S.M., Treyer V., Bettio A., Blagoev M., Kessler L.J., Burger C., Weber B., Schmidt M., Gasparini F., and Buck A. Quantitative evaluation of $^{11}$C-ABP688 as PET ligand for the measurement of the metabotropic glutamate receptor subtype 5 using autoradiographic studies and a beta-scintillator. *Neuroimage* 2007; 35(3):1086–1092.

Zane, P.A., Brindle, S.D., Gause, D.O., O'Buck, A.J., Raghavan, P.R., and Tripp, S.L. Physicochemical factors associated with binding and retention of compounds in ocular melanin of rats: Correlations using data from whole-body autoradiography and molecular modeling for multiple linear regression analysis. *Pharm. Res.* 1990; 7(9):935–941.

# Pharmacokinetics, Modeling, and Simulation in the Development of Sunitinib Malate: A Case Study

# 12

Brett E. Houk and Carlo L. Bello

### Abstract

Pharmacokinetics, modeling, and simulation are integral components of the drug development process, with potential impact on the regulatory approval process and approval language, as well as the clinical use of the drug. The US Food and Drug Administration and other regulatory agencies recommend inclusion of such analyses as part of the regulatory submission process. The pharmacokinetics, modeling, and simulation studies performed for the anti-cancer agent sunitinib malate are presented here as a case study. Population based pharmacokinetic and pharmacokinetic−pharmacodynamic studies supported the sunitinib dosing schedule in the regulatory submission process and have provided insights into optimal use of the drug. Sunitinib also illustrates some of the practical difficulties of evaluating exposure−response relationships in clinical trials in oncology.

## 12.1 Introduction

Pharmacokinetics, modeling, and simulation are integral components of the drug development process, with potential impact on the regulatory approval process and approval language, as well as the clinical use of the drug. Indeed, the US Food and Drug Administration (FDA) and other regulatory agencies recommend inclusion of such analyses as part of the regulatory submission process (FDA 1999 and 2003; International Conference on Harmonisation 1994).

We present the pharmacokinetics, modeling, and simulation studies performed for the anticancer agent sunitinib malate (SUTENT®, Pfizer Inc.) as a case study. Population based pharmacokinetic and pharmacokinetic−pharmacodynamic studies supported the sunitinib dosing schedule in the regulatory submission process and have provided insights into optimal use of the drug. Sunitinib also illustrates some of the practical difficulties of evaluating exposure−response relationships in clinical trials in oncology.

### 12.1.1 Introduction to Sunitinib

Sunitinib is an oral multitargeted tyrosine kinase inhibitor: a pyrrole-substituted 2-indolinone derivative with a molecular weight of 532.6 Da

B.E. Houk (✉)
Oncology Clinical Pharmacology, La Jolla, CA, USA
e-mail: Brett.houk@pfizer.com

(Sun et al. 2003). With receptor tyrosine kinase targets comprising the vascular endothelial growth factor receptors, the platelet-derived growth factor receptors, stem-cell factor receptor (KIT), FMS-like tyrosine kinase 3 (FLT3), colony-stimulating factor 1 receptor, and glial cell line-derived neurotrophic factor receptor (RET), sunitinib has demonstrated both antiangiogenic and direct antitumor activities in preclinical models (Pfizer Inc. 2010).

Sunitinib is approved multinationally for the treatment of advanced renal cell carcinoma (RCC) and gastrointestinal stromal tumor (GIST) after disease progression or intolerance to imatinib mesylate (Pfizer Inc. 2010). Sunitinib has also shown antitumor activity in other types of solid tumors, such as neuroendocrine tumors (Kulke et al. 2008) and non-small cell lung cancer (Socinski et al. 2008; Novello et al. 2009).

The sunitinib dosing schedule was determined in three phase I studies: two involving patients with advanced solid tumors and one involving patients with imatinib-resistant/intolerant GIST (Rosen et al. 2003; Faivre et al. 2006; Demetri et al. 2009). The doses tested in these studies ranged from 25 to 150 mg/day, with dose-limiting toxicities (including fatigue in all three studies) reported at doses $\geq 75$ mg/day. The maximum tolerated dose (MTD) was therefore determined to be 50 mg/day. The schedules that were tested included 2 weeks on treatment followed by 1 week off (Schedule 2/1), 2 weeks on followed by 2 weeks off (Schedule 2/2), and 4 weeks on followed by 2 weeks off (Schedule 4/2). The 50-mg dose on Schedule 4/2 was selected for phase II/III testing and approved for the treatment of patients with RCC and GIST (Pfizer Inc. 2010).

## 12.1.2 Sunitinib Pharmacokinetics

The pharmacokinetics of sunitinib in healthy subjects and cancer patients are well described (Pfizer Inc. 2010; Rosen et al. 2003; Faivre et al. 2006; Bello et al. 2007). Sunitinib is well absorbed following oral administration, with maximum plasma concentrations ($C_{max}$) observed within approximately 6−12 h ($t_{max}$). Sunitinib is metabolized primarily by cytochrome P450 (CYP) 3A4, leading to formation of the N-desethyl metabolite SU12662, which has similar inhibitory activity as the parent compound. SU12662 is the primary circulating metabolite derived from sunitinib, comprising 23−37% of the total exposure, and is also metabolized by CYP3A4, yielding a minor inactive metabolite. The combination of sunitinib and SU12662 therefore represents the total active drug in the plasma.

In in vitro studies, binding of sunitinib and SU12662 to human plasma protein was found to be 95% and 90%, respectively, with no concentration-dependence between 100 and 4,000 ng/mL. The apparent volume of distribution (Vd/F) for sunitinib was found to be 2,230 L. With doses of 25−100 mg, the area under the plasma concentration−time curve (AUC) and $C_{max}$ increased proportionately with dose. Sunitinib is eliminated primarily via the feces, with less than 16% excreted in urine. Total oral clearance (CL/F) was found to be 34−62 L/h, with interpatient variability of 40%.

Both sunitinib and SU12662 have been found to exhibit prolonged half-lives ($t_{1/2}$) of 40−60 h and 80−110 h, respectively. With repeated daily administration, the two compounds initially accumulated three- to fourfold and seven- to tenfold. Steady-state concentrations were achieved in 10−14 days, and no significant changes in the pharmacokinetics of either compound were observed with subsequent administration using the dosing schedules tested. At steady state, plasma concentrations of total drug (sunitinib plus SU12662) were found to be 62.9−101 ng/mL, corresponding well to the concentrations shown to provide inhibition of target receptor tyrosine kinases in preclinical studies ($\geq$ 50−100 ng/mL; Mendel et al. 2003). In these studies, sunitinib pharmacokinetics were found to be similar, whether healthy volunteers or patients with solid tumors were tested.

Three pharmacokinetic studies have directly assessed specific aspects of sunitinib administration. All three utilized an open-label, two-way crossover design. The effect of food on the oral bioavailability of sunitinib was tested in such a study involving 16 healthy subjects (Bello

et al. 2006a). Subjects received a 50-mg dose of sunitinib after a 10-h fast in one period and a high-fat, high-calorie meal in another period. Although in the fed state, sunitinib exposure increased slightly and formation/absorption of SU12662 was delayed, 90% confidence intervals (CIs) for $C_{\max}$ and AUC were within the $80-125\%$ bioequivalence range, indicating the absence of a food effect. These results showed that sunitinib can be administered without regard to food.

Two of the two-way crossover studies evaluated the impact of coadministration of inhibitors or inducers of CYP3A4 with sunitinib in healthy male subjects (Washington et al. 2003; Bello et al. 2006b). The first of these, involving 27 men, compared administration of one 10-mg dose of sunitinib alone on day 1 in one period with coadministration of the potent CYP3A4 inhibitor ketoconazole (400 mg) for 7 days with sunitinib on day 3 in the other period. Administration of sunitinib plus ketoconazole resulted in a 49% and a 51% higher mean total-drug $C_{\max}$ and AUC from time zero to infinity ($\mathrm{AUC}_{0-\infty}$), respectively, than that of sunitinib alone. Likewise, the other study involved 28 men who received a single 50-mg dose of sunitinib in one period and daily 600-mg doses of the potent CYP3A4 inducer rifampin for 17 days, with sunitinib coadministered on day 8, in the other period. Rifampin reduced sunitinib mean AUC from time zero to the last detectable concentration ($\mathrm{AUC}_{0-\mathrm{last}}$) and $\mathrm{AUC}_{0-\infty}$ (both 79%), $C_{\max}$ (56%), and $t_{1/2}$ (68%) and increased SU12662 $\mathrm{AUC}_{0-\mathrm{last}}$ (29%), $\mathrm{AUC}_{0-\infty}$ (26%), and $C_{\max}$ (137%); SU12662 $t_{1/2}$ was reduced (22%). Based on these results, the sunitinib prescribing information (Pfizer Inc. 2010) recommends that if sunitinib must be coadministered with a strong CYP3A4 inhibitor or inducer, dose-reduction to a minimum of 37.5 mg/day or dose-increase to a maximum of 87.5 mg/day, respectively, should be considered.

Finally, two studies have specifically evaluated sunitinib pharmacokinetics in special patient populations: those with impaired hepatic or renal function (Bello et al. 2010; Khosravan et al. 2010). Both studies employed an open-label, parallel-group study design. The first of these enrolled subjects with normal hepatic function or with mild (Child-Pugh-A) or moderate (Child-Pugh-B) hepatic impairment (eight subjects each). The study found that after administration of a single 50-mg dose of sunitinib, systemic exposure to sunitinib, SU12662, or total drug was not significantly different in patients with mild or moderate hepatic impairment than in subjects with normal hepatic function. These results suggested that there is no need to adjust the 50-mg starting dose in cancer patients with mild to moderate liver impairment. Renal impairment would not be expected to have a significant effect on the pharmacokinetics of sunitinib, given that urinary elimination is a minor route of sunitinib excretion. However, impaired renal function is common among patients with solid tumors, occurring in more than 50% of patients evaluated (Launay-Vacher et al. 2007), making this an important parameter to test. The second study evaluated subjects with normal renal function, severe renal impairment (but not requiring hemodialysis), or end-stage renal disease (ESRD) requiring hemodialysis (eight subjects each) given a single 50-mg dose of sunitinib. As expected, sunitinib and SU12662 pharmacokinetics in patients with severe renal impairment were similar to those of subjects with normal renal function. However, exposure to both compounds appeared to be lower in patients with ESRD requiring hemodialysis ($C_{\max}$, $30-38\%$ lower; $\mathrm{AUC}_{0-\infty}$, $31-47\%$ lower), but neither compound appeared to be eliminated from the body during hemodialysis. On this basis, it was concluded that the 50-mg dose of sunitinib may also be used to initiate treatment in these patients, but that tolerability should be monitored closely in case dose-modification becomes necessary.

### 12.1.3 Summary

- A suite of studies were conducted to characterize the basic pharmacokinetics of sunitinib and optimize treatment administration.
- The results of most of these studies formed a part of the sunitinib regulatory submission package for GIST and RCC and are summarized in the product prescribing information.

## 12.2 Population Pharmacokinetics of Sunitinib and SU12662 in Healthy Volunteers and Cancer Patients

While individual studies had previously found sunitinib pharmacokinetics to be similar between healthy volunteers and patients with solid tumors (Pfizer Inc. 2010), a variety of factors such as age, gender, race, body weight, and clinical performance status might be expected to affect sunitinib pharmacokinetics in individuals when analyzed across multiple studies. We therefore used a population approach to assess the pharmacokinetics of sunitinib and SU12662 and to assess covariates that might explain variability in exposure. Since studies with other tyrosine kinase inhibitors had shown correlations between high drug exposure and increased toxicity (Larson et al. 2008; Guo et al. 2008), a particular focus of our analysis was the identification of factors that increase exposure to sunitinib and/or SU12662 (Houk et al. 2009).

### 12.2.1 Patients

Data from 14 studies in which sunitinib was administered as a single agent (summarized in Table 12.1) involving a total of 590 patients were used in this analysis. Four of the studies involved healthy volunteers given a single dose of sunitinib of 10 or 50 mg, and one involved patients with acute myeloid leukemia (AML) given a single dose of 50−350 mg. The other nine were multiple-dose studies involving patients with metastatic RCC (mRCC), GIST, or various solid tumors who received 25−175-mg doses of sunitinib daily or every other day. Although patients had received a range of doses of sunitinib, the majority received the approved 50-mg/day starting dose, allowing us to evaluate the suitability of this dose in particular patient populations. The demographic and physiologic characteristics of the subjects are summarized in Table 12.2.

## 12.2.2 Model Development

In order to estimate population pharmacokinetic parameters (means and interindividual variability) for sunitinib and SU12662 and to identify potential covariates to explain any interindividual variability in the parameters (Beal and Sheiner 2006), nonlinear mixed-effects modeling was employed to analyze plasma concentration−time data for sunitinib and SU12662, which were modeled separately. An exponential error term was used to model interindividual variability in the main pharmacokinetic parameters (i.e., CL/F, Vd/F, and the absorption rate constant [$K_a$]). The estimate of interindividual variability was provided as percentage coefficient of variation (%CV), and residual variability was modeled as a proportional error structure; interindividual variability was also expressed as the variance (calculated as $[\%CV/100]^2$).

Base models for sunitinib and SU12662 were chosen using first-order conditional estimation with interaction. A two-compartment model (parameterized in terms of compartmental clearances and volumes) was found to describe the pharmacokinetic data for both sunitinib and SU12662. When plotted versus time after dose, observed concentrations were consistent with the two-compartment model, and population-predicted values agreed well with observed values, as did individual predicted concentrations. The base models selected were analyzed for covariate influence on the interindividual error terms.

Full models (including all potentially influential covariates that were identified) were then built using first-order conditional estimation with interaction. The continuous covariates evaluated were age, weight, and creatinine clearance (CrCL; a measure of renal function), whereas the categorical covariates evaluated were gender, race, tumor type, and Eastern Cooperative Oncology Group performance status (ECOG PS, a measure of patients' well-being on a scale of 0 [fully active, able to carry on all predisease performance without restriction] to 5 [dead]). All of these variables were assessed for potential effect on the CL/F of sunitinib and SU12662; only gender and weight were

**Table 12.1** Summary of studies included in the population-pharmacokinetic and pharmacokinetic–pharmacodynamic meta-analyses (Houk et al. 2009, 2010)

| Study number[*] | Study design and population | N[†] | Dosing schedule[‡] (weeks on/weeks off treatment) | Pharmacokinetic sampling | Pharmacodynamic evaluation[§] | Reference | Meta-analysis |
|---|---|---|---|---|---|---|---|
| **Single-dose studies** | | | | | | | |
| 001[a] | Randomized, double-blind, placebo-controlled single-dose study in healthy volunteers | 6 | 50 mg | Full: day 1 at 0, 0.5, 1, 1.5, 2, 2.5, 3, 3.5, 4, 4.5, 5, 5.5, 6, 6.5, 7, 7.5, 8–12, 16, 24, 30, 36, and 48 h postdosing | NA | Pfizer Inc., data on file | PK |
| 004 | Randomized, open-label two-way crossover study evaluating food effect in healthy volunteers | 16 | 50 mg | Full: day 1 at 0, 0.5, 1, 1.5, 2, 2.5, 3, 3.5, 4, 4.5, 5, 5.5, 6, 6.5, 7, 7.5, 8–12, 16, 24, 30, 36, 48, 72, and 216 h postdosing | NA | Bello et al. (2006a) | PK |
| 009[b] | Randomized, open-label two-way crossover study with/without concomitant ketoconazole in healthy volunteers | 27 | 10 mg (Ketoconazole: 400 mg po qd × 7 days) | Full: day 1 at 0–10, 12, 16, 24, 30, 36, 48, 72, 120, 168, 216, 312, 408, and 504 h postdosing | NA | Washington et al. (2003); Pfizer Inc., data on file | PK |
| 1001 | Open-label two-way crossover study with/without rifampin in healthy volunteers | 28 | 50 mg (Rifampin: 400 mg po qd × 7 days) | Full: day 1 at 0, 2, 4, 7, 8, 9, 12, 16, 24, 36, 48, 72, 144, 240, 288, 336, and 408 h postdosing | NA | Bello et al. (2006b) | PK |
| 006[c] | Open-label dose-escalation study in patients with acute myeloid leukemia | 29 | 50–350 mg | Full: day 1 at 0, 4, 6, 8, 10, 12, 24, and 48 h postdosing | NA | O'Farrell et al. (2003) | PK |
| **Multiple-dose studies** | | | | | | | |
| 002[a] | Dose-escalation study in patients with advanced solid tumors | 28 | 25–150 mg qd or qod 6-week cycles (4/2) | Full: cycle 1, days 1 and 27/28 at 0, 1, 2, 3, 3.5, 4, 4.5, 5, 5.5, 6, 6.5, 7, 8, 10, 12, 14, 16, and 24 h postdosing<br>Trough: days 2 and 29 and twice weekly during cycle 1 | Efficacy: baseline, day 28 of cycle 1, and day 28 of every third cycle thereafter; continuous safety assessment | Faivre et al. 2006; Pfizer Inc., data on file | PK; PK–PD |

(*continued*)

**Table 12.1** (continued)

| Study number[*] | N[†] | Dosing schedule[‡] (weeks on/weeks off treatment) | Pharmacokinetic sampling | Pharmacodynamic evaluation[§] | Reference | Meta-analysis |
|---|---|---|---|---|---|---|
| 005[a] | 41 | 25–75 mg qd or qod 6-week cycles (4/2) or 4-week cycles (2/2) | Full: first and last day of dosing in cycle 1 and last day of dosing in cycles 2–3 at 0, 1–8, 10, 12, 20, 24, and 48 h postdosing and cycle 1, day 14 of Schedule 4/2 at 0, 4, 6, 8, 10, 12, and 24 h postdosing Trough: once or twice weekly during cycles 1–3 | Efficacy: baseline and day 28 (Schedule 2/2) or day 40 (Schedule 4/2) of every even-numbered cycle; continuous safety assessment | Rosen et al. (2003); Pfizer Inc., data on file | PK; PK–PD |
| 016 | 12 | 50 mg qd 3-week cycles (2/1) | Full: cycle 1, days 1 and 14 and cycles 2–3, day 14 at 0, 1–8, 10, 12, 20, and 24 h postdosing Trough: cycle 1, day 7; cycles 2–3, days 1 and 7; days 1 and 14 thereafter | NA | Britten et al. 2008 | PK |
| 018 | 26 | 50–175 mg loading dose on day 1; 50 mg qd 3-week cycles (2/1) | Full: cycles 1–2, days 1 and 14 and cycle 3, day 14 (for maintenance dose >50 mg) at 0, 4, 6, 8, 10, 12, and 24 h; and cycle 1, day 14 at 72 and 120 h postdosing Trough: cycle 1, twice weekly on treatment; cycle 2, once weekly on treatment; days 1 and 14 thereafter | NA | Pfizer Inc., data on file | PK |
| 013 | 97 | 25–75 mg qd 6-week cycles (4/2), 4-week cycles (2/2), or 3-week cycles (2/1) | Full: first and last day of dosing in cycle 1 and last day of dosing in cycle 2 at 0, 1, 4, 6, 8, 10, 12, 24, and 48 h postdosing (n = 18) Trough: cycles 1–3, days 1 and 14 (all schedules) and day 28 (Schedule 4/2); cycles 4–6, day 1 | Efficacy: baseline and at the end of every even-numbered cycle; continuous safety assessment | Demetri et al. (2009); Pfizer Inc., data on file | PK; PK–PD |

| Study | Description | N | Dose | Sampling | Efficacy assessment | Reference | Analysis |
|---|---|---|---|---|---|---|---|
| 1004 | Double-blind, placebo-controlled, phase III study of single-agent sunitinib in patients with imatinib-resistant/intolerant GIST | 361 | 50 mg qd[d] 6-week cycles (4/2) | Trough: cycle 1, days 1, 14, and 28; days 1 and 28 thereafter | Efficacy: baseline and day 28 of every cycle; continuous safety assessment | Demetri et al. (2006, 2008) | PK; PK−PD |
| 1045 | Open-label, dose-escalation study in Japanese patients with imatinib-resistant/intolerant GIST (phase I part) | 12 | 25−75 mg qd 6-week cycles (4/2) | Full: cycle 1, days 1 and 28 at 0, 1, 2, 4, 6, 8, and 10 h and day 28 at 24 and 48 h postdosing; Trough: cycle 1, days 1, 2, 7, 14, 21, and 28 | NA | Shirao et al. (2010) | PK |
| 014 | Phase II study of single-agent sunitinib as second-line therapy in patients with mRCC | 63 | 50 mg qd[e] 6-week cycles (4/2) | Trough: cycles 1−4, days 1, 14, and 28; day 1 thereafter | Efficacy: baseline and day 28 of cycle 1 and every even-numbered cycle thereafter; continuous safety assessment | Motzer et al. (2006a) | PK; PK−PD |
| 1006 | Uncontrolled, study of single-agent sunitinib in patients with mRCC refractory to one prior cytokine therapy | 106 | 50 mg qd[d] 6-week cycles (4/2) | Trough: cycles 1, days 1, 14, and 28; cycles 2−4, days 1 and 28; day 1 thereafter | Efficacy: baseline and day 28 of cycles 1−4 and even-numbered cycles thereafter; continuous safety assessment | Motzer et al. 2006b | PK, PK−PD |

*Sunitinib administered as L-malate salt capsule unless otherwise stated: [a]free base powder in bottle; [b]L-malate salt in bottle; [c]free base and L-malate salt capsule

†Total number of patients in study

‡Dose reductions (if needed) in studies included in PK−PD meta-analysis as indicated: [d]dose range 25−50 mg qd; [e]dose range 25−75 mg qd

§Antitumor efficacy based on objective tumor assessments made using Response Evaluation Criteria in Solid Tumors (Therasse et al. 2000)

*NA* not applicable, *PK* population pharmacokinetic meta-analysis, *PK−PD* population pharmacokinetic−pharmacodynamic meta-analysis, *po* orally, *qd* once daily, *qod* once every other day

**Table 12.2** Summary of patient physiologic and demographic characteristics in the population pharmacokinetic metaanalysis

(a) Baseline demographics

| Demographic | No. of PK-evaluable subjects ($N = 590$) |
|---|---|
| Healthy volunteers | 73 |
| Cancer patients | 517 |
|    Solid tumors | 95 |
|    GIST | 241 |
|    mRCC | 152 |
|    Acute myeloid leukemia | 29 |
| Race | |
|    Caucasian | 505 |
|    Asian | 58 |
|    African American | 14 |
|    Other | 13 |
| Gender | |
|    Male | 398 |
|    Female | 192 |
| ECOG PS | |
|    0 | 297 |
|    1 | 259 |
|    2 | 33 |
|    3 | 1 |

(b) Summary values at screening (or first available measurement) of continuous covariates

| Variable | Age (years) | Weight (kg) | CrCL (mL/min)[a] |
|---|---|---|---|
| Minimum | 18 | 34.0 | 32.2 |
| 1st quartile | 44 | 64.0 | 74.1 |
| Mean | 53 | 77.6 | 98.2 |
| Median | 55 | 76.9 | 93.5 |
| 3rd quartile | 64 | 88.0 | 118 |
| Maximum | 87 | 168 | 347 |
| Total ($N$) | 590 | 590 | 587 |
| Standard deviation | 15 | 18.8 | 36.7 |

(c) Number of subjects within a range at screening (or first available measurement)

| Demographic (range at screening) | Subgroup | Healthy volunteers | Patients | All |
|---|---|---|---|---|
| Age, years (18–87) | <40 | 63 | 36 | 99 |
| | 40–60 | 10 | 275 | 285 |
| | 60–75 | 0 | 180 | 180 |
| | >75 | 0 | 26 | 26 |
| Weight, kg (34–168) | ≥135 | 0 | 6 | 6 |
| | 76 to <135 | 36 | 271 | 307 |
| | 41–75 | 37 | 237 | 274 |
| | ≤40 | 0 | 3 | 3 |
| CrCL, mL/min (32–347)[a] | >80 | 72 | 318 | 390 |
| | 50–80 | 1 | 168 | 169 |
| | 30–49 | 0 | 28 | 28 |
| | <30 | 0 | 3 | 3 |

[a]Excludes three subjects with low CrCL values (<1 mL/min; these are thought to be an artifact of the Cockroft-Gault estimation used)

Adapted with permission from the American Association for Cancer Research: Houk et al. (2009)

tested for potential effect on Vd/F. Screening to identify significant covariates was carried out using stepwise backward elimination.

The resulting final model for the sunitinib molecule included the effects of gender, Asian race, and tumor type (except AML) on CL/F and of body weight on Vd/F in the central compartment (Vd/F$_{central}$); and that for SU12662 included the effects of body weight, gender, Asian race, elevated ECOG PS, and tumor type (except AML) on CL/F and of body weight and gender on Vd/F$_{central}$. Final primary parameter estimates for both compounds are summarized in Table 12.3. The sunitinib absorption rate constant (K$_a$) was estimated to be 0.20/h (Table 12.3), corresponding to an absorption $t_{1/2}$ of 3.5 h. The SU12662 absorption and formation rate constant was 0.29/h, corresponding to a formation or appearance $t_{1/2}$ of 2.4 h. These estimates were then used to determine CL/F and Vd/F for sunitinib and SU12662 (Houk et al. 2009).

The goodness of fit of the final model was tested by plotting population-predicted versus observed concentrations, individual-predicted versus observed concentrations, weighted residuals versus population-predicted concentrations, and weighted residuals versus time (Fig. 12.1). Across the range of observations, individual predicted values agreed well with observed values. Weighted residuals were distributed evenly across the range of predicted concentrations and time. In a predictive check to assess model performance, the parameters from the final model and interindividual error estimates were used to simulate concentrations back into the observed data set. Simulated concentrations were found to agree well with observed concentrations, and no systematic bias was observed.

## 12.2.3 Effects of Covariates on Exposure

Of seven covariates tested, five (solid tumor, elevated ECOG PS, Asian race, gender, and body weight) described a portion of the variability in

CL/F for sunitinib and SU12662 (SU12662 only in the case of body weight). No relationship with age or renal function (CrCL) was found for either sunitinib or SU12662 CL/F. Both covariates tested (gender and body weight) explained some of the variability in sunitinib and SU12662 Vd/F.

Neither sunitinib nor SU12662 disposition was influenced by having AML. However, having a solid tumor did affect the disposition of both compounds: the estimations suggested that the CL/F for both sunitinib and the metabolite was lower in patients with solid tumors than in healthy adult volunteers. In GIST, sunitinib CL/F was 29% lower and SU12662 CL/F 22% lower; patients with mRCC exhibited a 26% lower sunitinib and SU12662 CL/F; and patients with mixed solid tumors exhibited a 27% lower sunitinib CL/F and 29% lower SU12662 CL/F. The effect of having solid tumors on CL/F was the most influential of all the covariates tested.

Elevated ECOG PS ($\geq 2$; representing patients with more debilitating disease) was found to have a small effect on SU12662 CL/F but not sunitinib CL/F. In patients with an elevated ECOG PS, CL/F for SU12662 was 7% lower. However, the effect was imprecisely estimated (96% CV) so that these results should be interpreted with caution.

The influence of Asian race on CL/F was examined relative to all other races (>85% Caucasian): CL/F was found to be 13% lower for sunitinib and 12% lower for SU12662. Compared with men, the CL/F of sunitinib and SU12662 for women was 9% and 26% lower, respectively, and Vd/F for SU12662 was 24% lower.

Body weight did not appear to correlate with sunitinib CL/F, although it correlated positively with Vd/F for sunitinib and with both Vd/F and CL/F for SU12662. For sunitinib, the Vd/F of a 40-kg individual was 26% lower than that of a 77-kg individual (the median body weight for the studies included in this analysis); for a heavier individual (100 kg), Vd/F was 13% higher. For SU12662, Vd/F was 28% lower and CL/F 18% lower for a 40-kg individual

**Table 12.3** Values of final primary parameter estimates for the final models for sunitinib and SU12662

| Parameter | Sunitinib | | | | SU12662 | | | |
|---|---|---|---|---|---|---|---|---|
| | Estimate (SE/estimate) | Inter-individual variability (%CV) | Inter-individual variability (variance)[a] | 95% CI | Estimate (SE/estimate) | Inter-individual Variability (%CV) | Inter-individual variability (variance)[a] | 95% CI |
| CL/F, L/h | 51.8 (4%) | 38% | 0.14 | 47.9 to 55.7 | 29.6 (3%) | 47% | 0.22 | 27.2 to 32.0 |
| Vd/F$_{central}$, L | 2,030 (4%) | 43% | 0.18 | 1,877 to 2,183 | 3,080 (4%) | 59% | 0.35 | 2,815 to 3,345 |
| K$_a$, L/h | 0.195 (7%) | 80% | 0.64 | 0.170 to 0.220 | 0.290 (7%) | 86% | 0.74 | 0.252 to 0.328 |
| Q/F, L/h | 7.22 (20%) | NA | NA | 4.44 to 10.00 | 23.3 (30%) | NA | NA | 9.64 to 37.0 |
| Vd/F$_{peripheral}$, L | 583 (9%) | NA | NA | 485 to 681 | 289 (27%) | NA | NA | 138 to 440 |
| Weight on CL/F | NA | NA | NA | NA | 0.296 (64%) | NA | NA | −0.074 to 0.666 |
| Weight on Vd/F | 0.459 (16%) | NA | NA | 0.318 to 0.600 | 0.510 (49%) | NA | NA | 0.024 to 0.996 |
| Gender on CL/F | −0.0876 (34%) | NA | NA | −0.145 to −0.030 | −0.274 (15%) | NA | NA | −0.354 to −0.294 |
| Gender on Vd/F | NA | NA | NA | NA | −0.241 (23%) | NA | NA | −0.339 to −0.133 |
| Asian race on CL/F | −0.130 (30%) | NA | NA | −0.206 to −0.054 | −0.123 (31%) | NA | NA | −0.198 to −0.048 |
| ECOG PS on CL/F | NA | NA | NA | NA | −0.0652 (96%) | NA | NA | −0.188 to 0.058 |
| GIST on CL/F | −0.285 (14%) | NA | NA | −0.361 to −0.209 | −0.224 (15%) | NA | NA | −0.289 to −0.159 |
| Solid tumor on CL/F | −0.269 (15%) | NA | NA | −0.349 to −0.189 | −0.287 (14%) | NA | NA | −0.366 to −0.208 |
| mRCC on CL/F | −0.258 (13%) | NA | NA | −0.323 to −0.193 | −0.257 (12%) | NA | NA | −0.316 to −0.198 |
| Proportional error | 0.146 (10%) | NA | NA | 0.118 to 0.174 | 0.0914 (7%) | NA | NA | 0.0782 to 0.105 |

[a]Calculated as $(\%CV/100)^2$

*CV* coefficient of variation, *NA* not available (covariates not found to have a significant effect when the full model was subjected to stepwise backward elimination were omitted from the final model), *SE* standard error of estimate

Note that F for the metabolite is the product of oral bioavailability and fraction metabolized, whereas F for the parent is only oral bioavailability

Reproduced and adapted with permission from the American Association for Cancer Research: Houk et al. (2009)
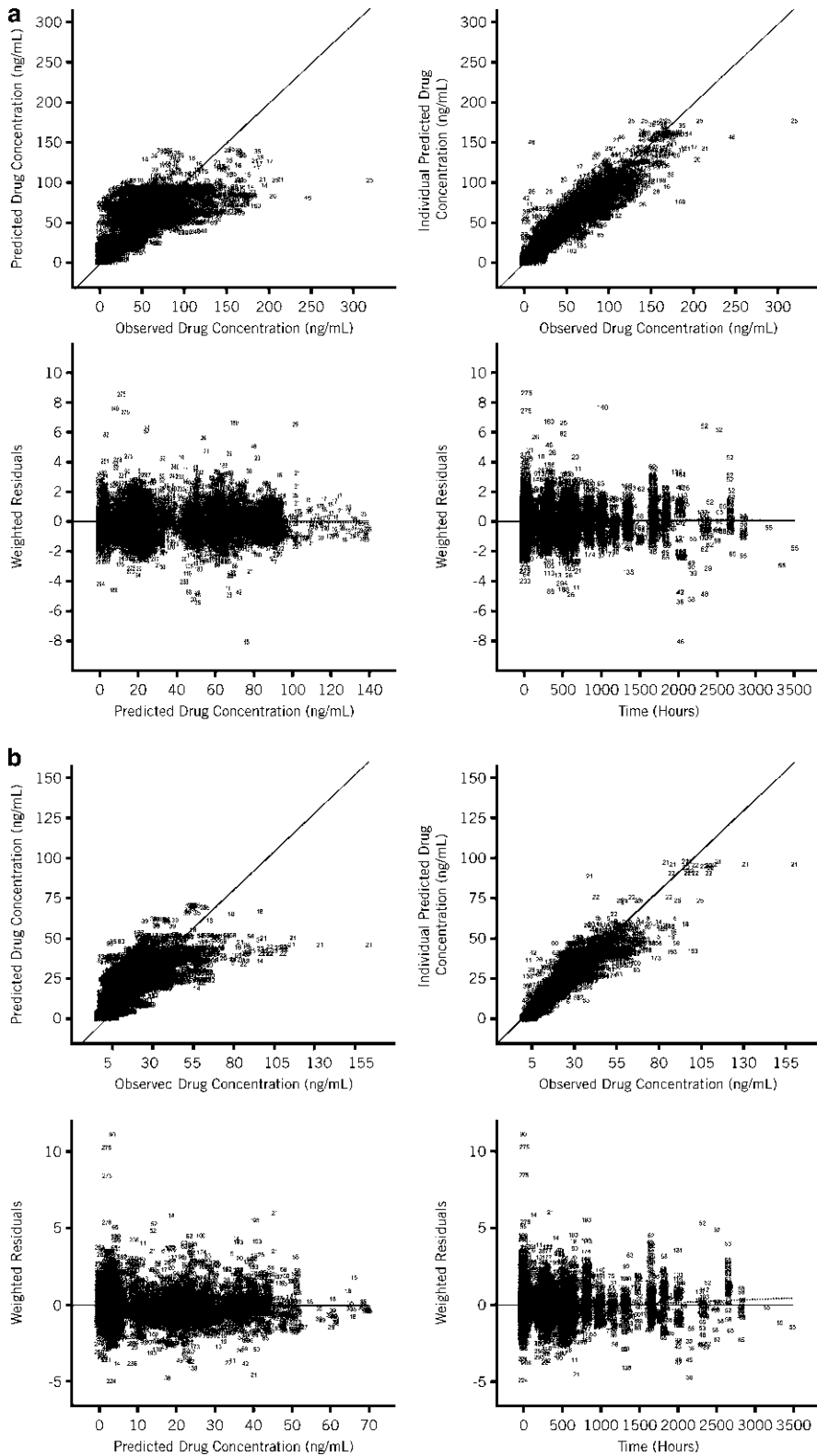
**Fig. 12.1** (continued)

than a 77-kg individual. Conversely, for a 100-kg individual compared to a 77-kg individual, Vd/F for SU12662 was 14% higher and CL/F was 8% higher.

## 12.2.4 Simulations

Monte Carlo simulations with the final models were performed to predict sunitinib, SU12662, and total-drug (sunitinib plus SU12662) exposures in the patient subpopulations identified using the demographic covariates shown to decrease CL/F and/or Vd/F. Potential differences in exposure were expressed relative to a 77-kg Caucasian male patient with mRCC and an ECOG PS of ≤1 (patients with GIST or other solid tumors were expected to behave similarly, since the effect of disease on CL/F was similar across solid tumor types). For each covariate combination, 10,000 subjects were simulated at steady state with 50 mg/day oral dosing. For each simulated subject, steady-state $C_{avg}$ (dose/[simulated clearance $\times$ 24 h]), AUC ($C_{avg} \times$ 24 h), and $C_{max}$ of both sunitinib and SU12662 were calculated. Additional considerations employed in the simulations can be found in the original publication (Houk et al. 2009).

The results of these simulations are summarized in Fig. 12.2. In Asians patients relative to patients of other ethnicities, sunitinib and total-drug AUC and $C_{max}$ were predicted to be 15% higher. In female relative to male patients, sunitinib AUC was predicted to be 10% higher and total-drug AUC, 17% higher, while $C_{max}$ was predicted to be almost as high (9% higher for sunitinib and 17% for total drug). The effects of other covariates in the simulations were smaller. A baseline ECOG PS ≥2 was predicted to increase total-drug AUC by 2% (due solely to lower SU12662 CL/F). In patients with

extremely low body weight (40 kg), total-drug AUC was predicted to be 6% higher (when compared with the median body weight of 77 kg), while high body weight (100 kg) was predicted to reduce total-drug AUC by 2%. In extreme cases, combinations of covariates were predicted to increase exposure levels more than any single covariate alone. In female Asian patients, for example, total-drug AUC was predicted to be 34% higher than in male non-Asian patients, and in a 40-kg female patient, total-drug AUC was predicted to be 25% higher.

In male Caucasian patients, the interindividual variability of total-drug AUC and $C_{max}$ was estimated to be 30% (variance, 0.09), while the predicted changes in total-drug AUC and/or $C_{max}$ among patients as a result of the individual covariates described above ranged from 2 to 17%. These findings indicated that the individual covariates evaluated minimally affected sunitinib and SU12662 pharmacokinetics, supporting the use of the recommended 50-mg/day sunitinib starting dose and minimizing the necessity for dose adjustment in these subpopulations.

## 12.2.5 Summary

- Separate models were developed for sunitinib and SU12662 (two-compartment models with first-order absorption and elimination).
- Pharmacokinetic parameters were estimated to be CL/F, 51.8 L/h and Vd/F$_{central}$, 2,030 L for sunitinib and CL/F, 29.6 L/h and Vd/F$_{central}$, 3,080 L for SU12662.
- Tumor type (except AML), Asian race, gender, body weight, and elevated ECOG PS described a portion of the variability in sunitinib and SU12662 CL/F, while gender and body weight explained some of the variability in sunitinib and SU12662 Vd/F$_{central}$.

**Fig. 12.1** (continued) Diagnostic goodness-of-fit plots for (**a**) sunitinib and (**b**) SU12662 final models, showing population and individual predicted versus observed concentrations, weighted residuals versus population predicted concentrations, and weighted residuals versus time. *Solid lines* represent the unity (population and individual predicted plots) or null value (weighted residual plots); *dotted lines* are Loess smooth trendlines. Reproduced and adapted with permission from the American Association for Cancer Research: Houk et al. (2009)
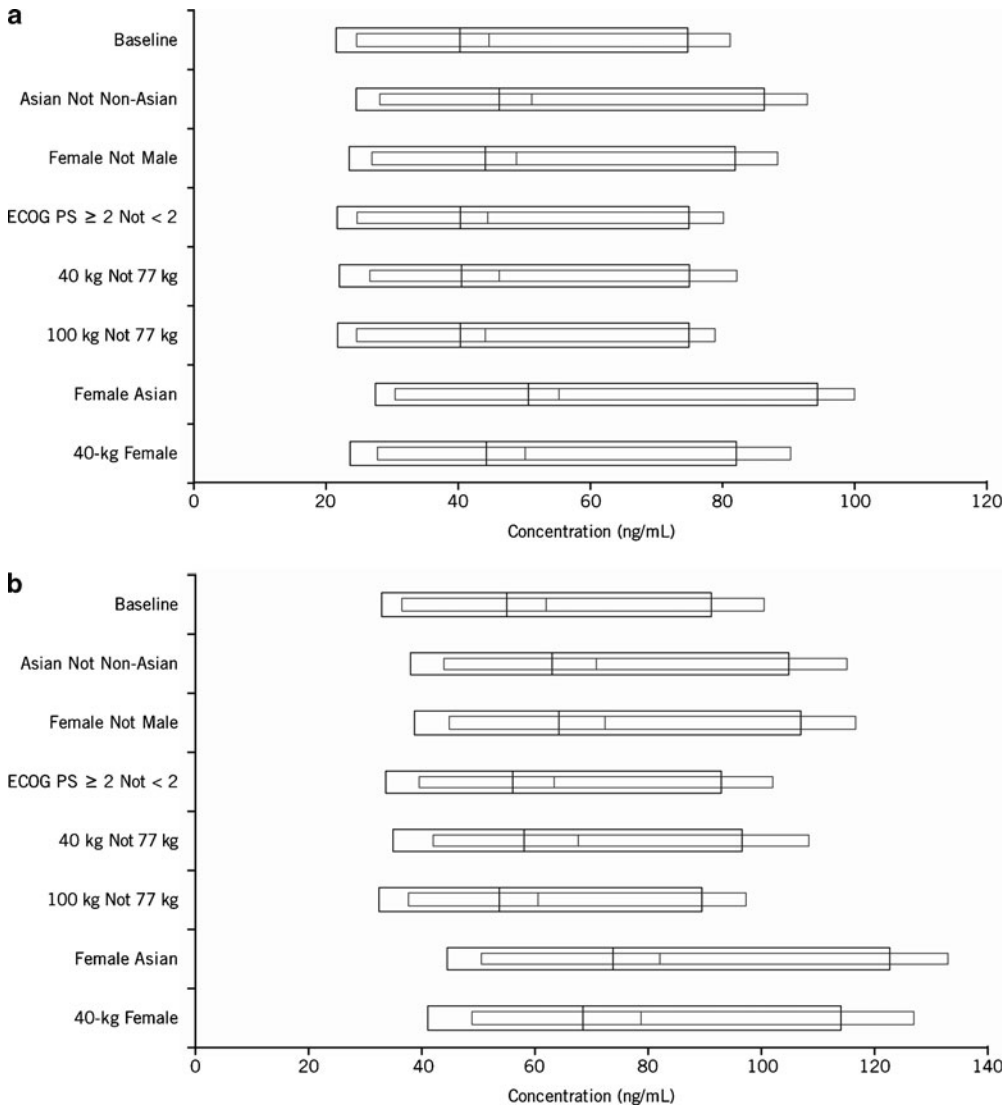
**Fig. 12.2** Simulation predictions of (**a**) sunitinib and (**b**) total drug exposures in covariate subpopulations compared with baseline (a 77-kg Caucasian male with mRCC and ECOG PS ≤ 1; patients with GIST or mixed solid tumors were expected to behave similarly). *Wide bars* represent $C_{avg}$ ($C_{avg} \times 24$ h = AUC) and *thinner bars* represent $C_{max}$. *Each bar* represents the fifth to 95th percentiles and the vertical line within the bar, the 50th percentile for the subpopulation. Reproduced and adapted with permission from the American Association for Cancer Research: Houk et al. (2009)

- The predicted differences in total drug (sunitinib plus SU12662) AUC and $C_{max}$ among patients as a result of the individual covariates ranged up to 17%.
- The magnitude of the predicted differences in exposure due to the covariates analyzed minimizes the necessity for dose adjustment in any of these subpopulations.

## 12.3 Pharmacokinetic–Pharmacodynamic Metaanalysis: Relationship Between Exposure to Sunitinib and Efficacy and Tolerability Endpoints

Building upon the population pharmacokinetic analyses and models described in the previous

section, we sought to characterize exposure—response relationships for efficacy and safety and to identify factors affecting sunitinib response in patients with solid tumors, GIST, and mRCC with the goal of optimizing sunitinib use (Houk et al. 2010).

## 12.3.1 Patients and Methods

Data for this analysis came from six of the studies summarized in Table 12.1. The analysis involved a total of 639 patients, 443 of whom had evaluable pharmacokinetic data; all had solid tumors (mRCC, GIST, and mixed solid tumors; Table 12.4). While the majority of patients received the approved dose of 50 mg (85%), sunitinib doses ranged from 25 to 150 mg, and final doses ranged from 25 to 100 mg. Sunitinib was administered once daily or every other day on any one of three treatment schedules: Schedules 4/2 (the approved schedule), 2/2, or 2/1.

Since only trough levels were available for the majority of patients, descriptive pharmacokinetic models for sunitinib and SU12662 were used (as described in the previous section) to obtain

best estimates of a variety of exposure measures for each patient in the six studies. These included trough plasma concentrations over time ($C_{\text{trough}}$, taking into account the patient's dosing history), the cumulative AUC over 28 days ($AUC_{\text{Cum28}}$; representing the 28 days of dosing on Schedule 4/2), and mean daily AUC at steady state ($AUC_{\text{ss}}$). Each parameter was calculated for sunitinib, SU12662, and total drug (sunitinib plus SU12662).

In exploratory analyses, measured efficacy and tolerability endpoints were assessed for distribution and plotted against measures of exposure. Potential relationships identified were evaluated using a linear regression model, and Pearson's correlation coefficients were computed and tested for statistical significance. Exposure measures that exhibited the highest correlations were chosen for further analysis. The potential effects of covariates on exposure–response were investigated by segmenting the patient population by covariate values and testing individual endpoint–exposure-measure relationships within each subgroup using linear regression. The covariates that were evaluated were gender, age, body mass index quartiles, race, baseline

**Table 12.4** Patient demographics and data summary by tumor type in the population pharmacokinetic−pharmacodynamic meta-analysis

| Characteristic | Solid tumors | GIST | mRCC | Pooled data |
|---|---|---|---|---|
| Number of evaluable patients | 69 | 401 | 169 | 639 |
| Number of patients with PK data | 69 | 225 | 149 | 443 |
| Number of patient-days of PD observations | 2,486 | 7,619 | 3,748 | 13,853 |
| Mean number of observations per patient | 36.0 | 19.0 | 22.2 | 21.7 |
| Duration of study data, mean $\pm$ SD (days) | 189 $\pm$ 174 | 146 $\pm$ 131 | 181 $\pm$ 117 | 160 $\pm$ 134 |
| Duration of study data, range (days) | 14–675 | 1–718 | 1–485 | 1–718 |
| Gender ($n$) | | | | |
| Male | 37 | 257 | 110 | 404 |
| Female | 32 | 144 | 59 | 235 |
| Race ($n$) | | | | |
| Caucasian | 35 | 384 | 154 | 573 |
| African American | 3 | 20 | 3 | 26 |
| Asian | 2 | 17 | 6 | 25 |
| Other | 1 | 8 | 6 | 15 |
| Mean age $\pm$ SD (year) | 55 $\pm$ 12 | 56 $\pm$ 12 | 57 $\pm$ 10 | 56 $\pm$ 12 |
| Mean weight $\pm$ SD (kg) | 72 $\pm$ 18 | 75 $\pm$ 18 | 85 $\pm$ 19 | 77 $\pm$ 19 |

*PD* pharmacodynamic, *PK* pharmacokinetic, *SD* standard deviation

Adapted from Houk et al. (2010) with kind permission of Springer Science and Business Media

diastolic blood pressure (DBP), dosing schedule (Schedules 4/2, 2/2, and 2/1), and tumor type (solid tumors, mRCC, and GIST). Models expressing the endpoint value and/or change of this value from baseline as a function of exposure measure were then developed in either S-PLUS or NONMEM using fixed- and mixed-effects modeling.

It should be noted that there are many constraints to identifying an exposure–response relationship in clinical trials in oncology. These include a frequent lack of placebo data and the narrow dose ranges generally administered (cancer treatment is usually initiated at the MTD). The latter constraint was a specific potential limitation in this model given the amount of data included from phase I studies in which patients received the lower and upper range of sunitinib dosing, the analysis of which may have been more relevant to exposure−toxicity than exposure−efficacy modeling. Although every effort was made to evaluate and minimize the impact, individual estimates of pharmacokinetic parameters may have been adversely impacted by the limited sampling in some patients and influenced by dose reductions or dose delays due to adverse events (AEs). Furthermore, because of individualized dose titration when a patient is on study, no two patients receive exactly the same dosing regimen throughout the entire study. Consequently, it is not possible to perform a dose−response analysis on parallel dose groups. The studies included in this analysis suffered from many of these limitations. Placebo data were only available from a small number of patients from one GIST study ($n = 59$, median of 62 days on placebo), making these the only data available for identification of baseline hazard rates for disease progression or AE occurrence. Additionally, as described above, the range of sunitinib doses administered was small and the vast majority of patients started treatment at 50 mg/day with individualized dose titration. Despite these challenges, employing fixed- and mixed-effects modeling approaches allowed relationships to be identified between exposure to sunitinib and efficacy and safety endpoints.

## 12.3.2 Effect of Exposure on Efficacy

We assessed the effect of exposure to sunitinib on a number of measures of efficacy. Two of these, which are key measures of efficacy in oncology trials, were time to tumor progression (TTP) and overall survival (OS). TTP is defined as the time from start of treatment to first documentation of objective tumor progression or death due to cancer and OS, as the time from start of treatment to death. Exposure ($AUC_{ss}$) was evaluated against both of these parameters using Kaplan–Meier analysis, in which patients were stratified by median $AUC_{ss}$ (less than the median $AUC_{ss}$ vs. greater than or equal to the median $AUC_{ss}$). Patients with the highest exposure to sunitinib exhibited longer TTP and OS across the different tumor types evaluated (Fig. 12.3) and similar results were obtained using total drug concentrations (sunitinib plus SU12662). Additionally, a time-to-event analysis carried out using a Weibull probability distribution model showed that $AUC_{ss}$ was significantly associated with longer TTP and OS in GIST and mRCC.

Another key oncology efficacy measure that we analyzed was objective response: a measure of tumor shrinkage based on computed tomography or magnetic resonance imaging. The standard criteria used (Response Evaluation Criteria in Solid Tumors; Therasse et al. 2000) define this as a complete response (CR), partial response (PR), stable disease (SD), or progressive disease (PD). Logistic regression was utilized to evaluate the relationship between objective responses (CRs and PRs) and exposure to sunitinib. Exposure correlated significantly with the probability of a PR or CR occurring in mRCC patients ($P = 0.00001$; Fig. 12.4). A similar trend that did not reach statistical significance was found for patients with GIST ($P = 0.06$) or solid tumors ($P = 0.28$; Fig. 12.4). This may have been due to the higher frequency of objective responses observed in patients with RCC (40−43%; Motzer et al. 2006a, b), compared with patients with GIST (7−8%; Demetri et al. 2006, 2009) or mixed solid tumors (10−27%; Faivre et al. 2006; Rosen et al. 2003). There
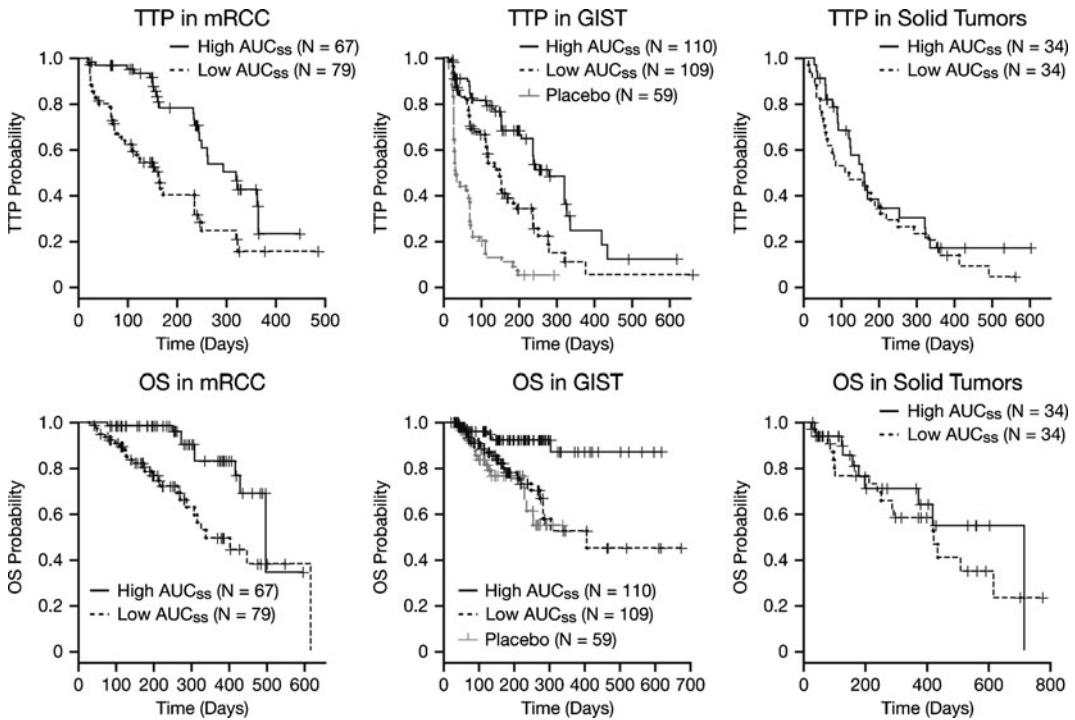
**Fig. 12.3** Relationship between average daily exposure (mean daily $AUC_{ss}$) to sunitinib and TTP/OS across tumor types. "High $AUC_{ss}$" denotes $AUC_{ss} \geq$ median (0.8, 0.6, and 0.7 μg·h/mL in patients with mRCC, GIST and solid tumors, respectively) and "low $AUC_{ss}$" denotes $AUC_{ss} <$ median. Reproduced and adapted from Houk et al. (2010) with kind permission of Springer Science and Business Media

was a significant correlation between the probability of SD and sunitinib exposure, both for patients with mRCC ($P = 0.002$) and patients with GIST ($P = 3 \times 10^{-9}$), but not patients with solid tumors ($P = 1.7$; Fig. 12.5). Taken together, these data suggested a trend toward a higher probability of tumor shrinkage (PR or CR) or halting of tumor growth (SD) in patients with higher exposure to sunitinib.

Tumor size changes over time were also analyzed using a tumor growth dynamics model, in which tumor growth kinetics were described as a function of sunitinib concentrations with a drug effect amplifying the tumor death rate (Houk et al. 2010). Model-based predictions of tumor sizes compared well with the observed study data for patients with either GIST or mRCC (Figs. 12.6 and 12.7), although an increase in the residuals and a larger under-prediction of tumor size after approximately 400 days were

observed in the diagnostic plots. The increased tumor size changes expected at doses of 25−50 mg/day on Schedule 4/2 for GIST and mRCC were simulated using the final model (Fig. 12.8). The simulations suggested that at a sunitinib dose of 50 mg/day, 38% more patients with mRCC and 23% more with GIST would be expected to achieve a 30% reduction in tumor size (the equivalent of a PR) than they would at a dose of 25 mg/day.

Taken together, these analyses demonstrated the importance of maintaining patients on a 50-mg dose of sunitinib and avoiding dosing interruptions or reductions during treatment. They also suggest that further analysis of alternative dosing schedules (e.g., Schedules 2/2 or 2/1 or a continuous daily dosing schedule) may be warranted to determine if these would benefit patients for whom it may not be possible to maintain a full dose.
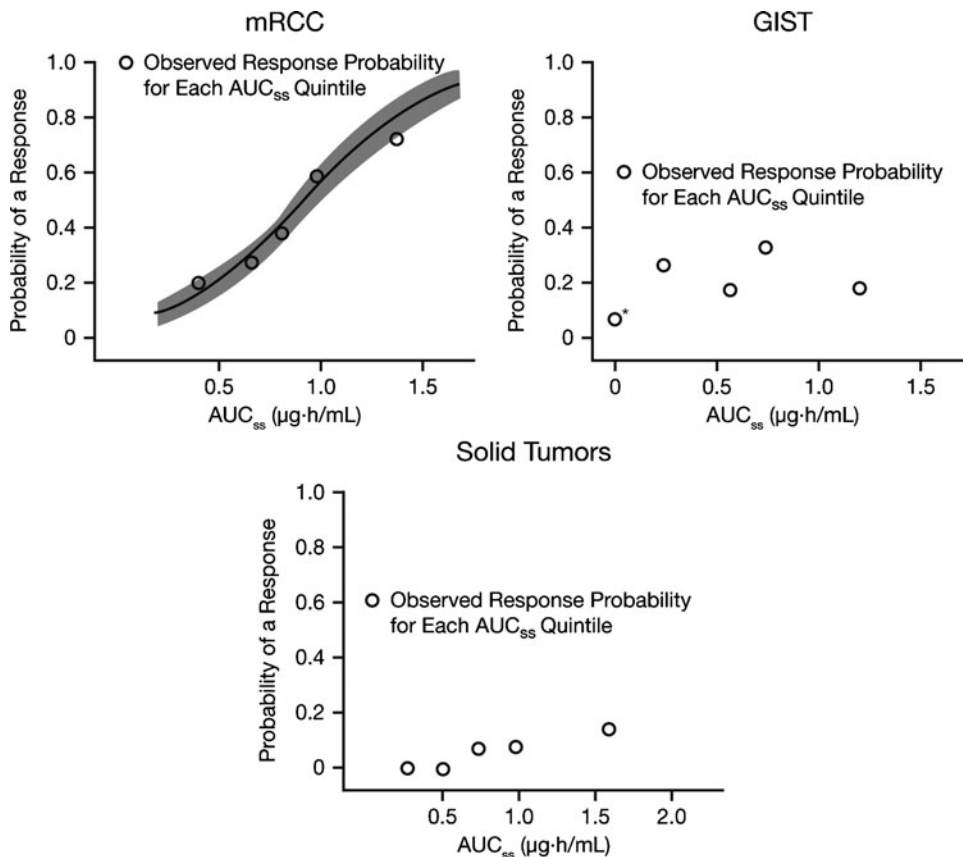
**Fig. 12.4** Probability of a PR or CR versus average daily exposure (mean daily $AUC_{ss}$) to sunitinib. *Line* represents model prediction and *shaded area* represents 95% CI. Modeling results are only displayed for the relationship displaying statistical significance. The *asterisk* in the $AUC_{ss}$ value of zero reflects the quintile of patients with GIST who received placebo rather than sunitinib. Adapted from Houk et al. (2010) with kind permission of Springer Science and Business Media

### 12.3.3 Effect of Exposure on Treatment-Related AEs

In patients with solid tumors enrolled in these studies, the most common sunitinib-related AEs of grade 3 severity (based on National Cancer Institute Common Terminology Criteria for Adverse Events version 3.0) were fatigue, hypertension, and neutropenia, and the most frequent treatment-related AE of grade 4 maximum severity was asymptomatic increased lipase (Pfizer Inc. 2007). Linear regression and Pearson's correlation coefficients were used for initial screening of these safety parameters against sunitinib exposure. Detailed exposure–response analysis was then carried out using the exposure measures demonstrating the highest correlations. Since there was less than a 5% correlation of lipase changes with any exposure measure, these were not evaluated further as a function of exposure.

*Fatigue*. Exposure (total-drug $AUC_{ss}$) was found to correlate with the incidence, but not severity, of fatigue. This relationship exhibited a distribution consistent with the existence of two patient sub-populations: one subpopulation that experienced fatigue (grade $\geq 1$) with a normally distributed range of fatigue scores and another subpopulation that did not display fatigue at any time during the study. Analysis of between-subject variability in an unconditional severity
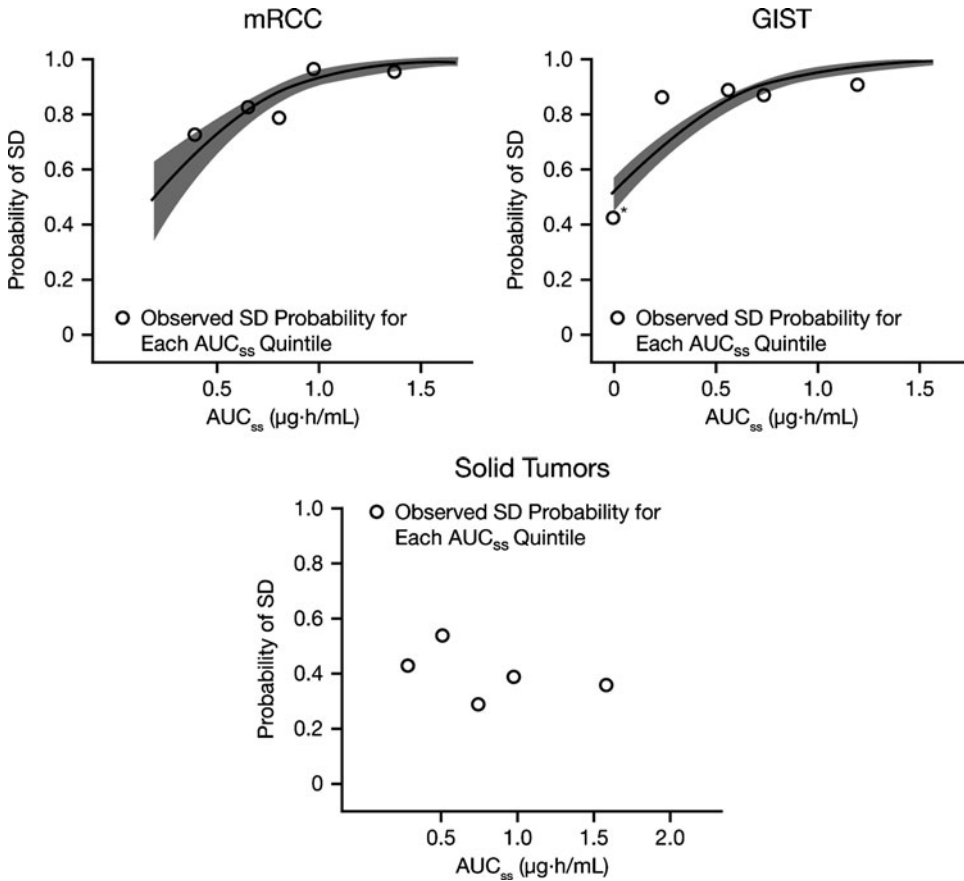
**Fig. 12.5** Probability of SD versus average daily exposure (mean daily $AUC_{ss}$) to sunitinib. *Lines* represent model prediction and *shaded areas* represent 95% CIs. Modeling results are only displayed for relationships displaying statistical significance. The *aster-isk* in the $AUC_{ss}$ value of zero reflects the quintile of patients with GIST who received placebo rather than sunitinib. Adapted from Houk et al. (2010) with kind permission of Springer Science and Business Media

model versus fatigue incidence supported this bimodal distribution. Based on a simulation with 1,000 patients, the $t_{1/2}$ for the appearance of fatigue was found to be 8 days, with the maximum level of fatigue (if experienced) therefore reached after one cycle of sunitinib treatment (Fig. 12.9). The model demonstrated a relationship between sunitinib exposure and the probability of experiencing grade $\geq 1$ fatigue in all three tumor types. At daily doses of 25 mg and 50 mg, the probabilities for GIST were predicted to be 46% and 65%; for mRCC, 57% and 74%; and for solid tumors, 85% and 92%, respectively.

*Neutropenia*. When correlation coefficients were calculated for the relationship between estimated exposure measures and observed absolute neutrophil count (ANC), the greatest correlation was found between $AUC_{Cum28}$ for total drug ($AUC_{Cum28Tot}$) and ANC. A negative relationship was found between ANC over the course of treatment, dose (Table 12.5), and $AUC_{cum28Tot}$ (Fig. 12.10). The slope of the exposure–response relationship was also significantly greater ($P < 0.05$) in patients with the highest baseline ANC (for a 10% increase in baseline ANC, patients had an approximately 3.5% greater ANC reduction). Furthermore, compared with patients with mixed solid tumors, patients with GIST or mRCC experienced 36% or 16% greater ANC reductions, respectively. Changes in ANC
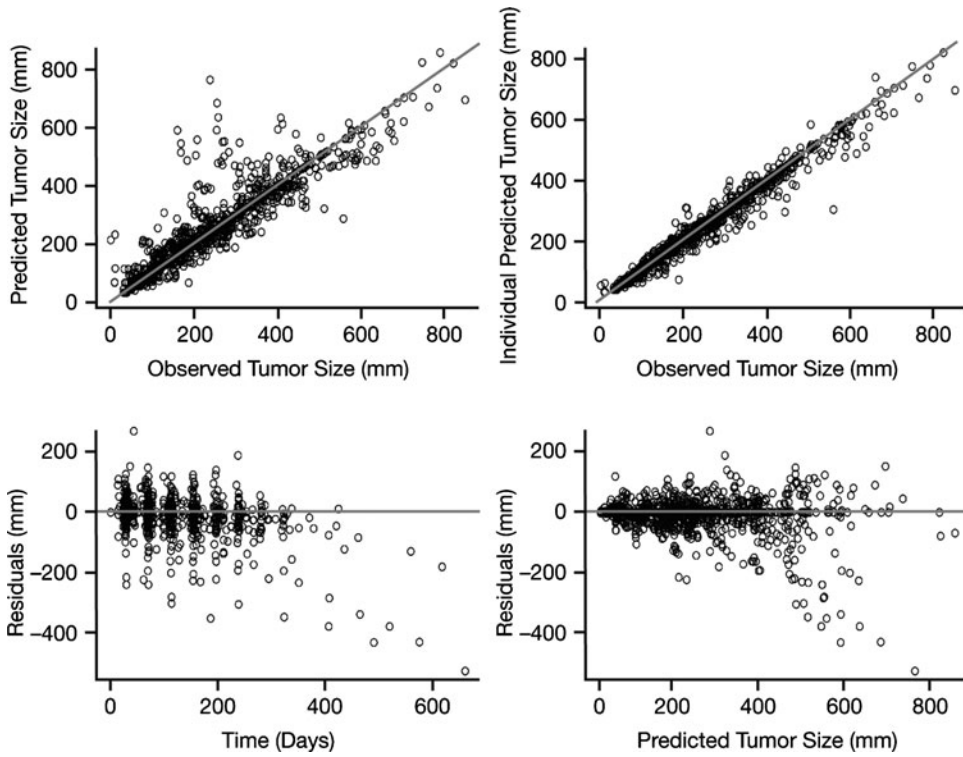
**Fig. 12.6** Diagnostic plots for the GIST tumor growth kinetics model. *Lines* represent the unity (population and individual predicted plots) or null value (weighted resid- ual plots). Reproduced and adapted from Houk et al. (2010) with kind permission of Springer Science and Business Media
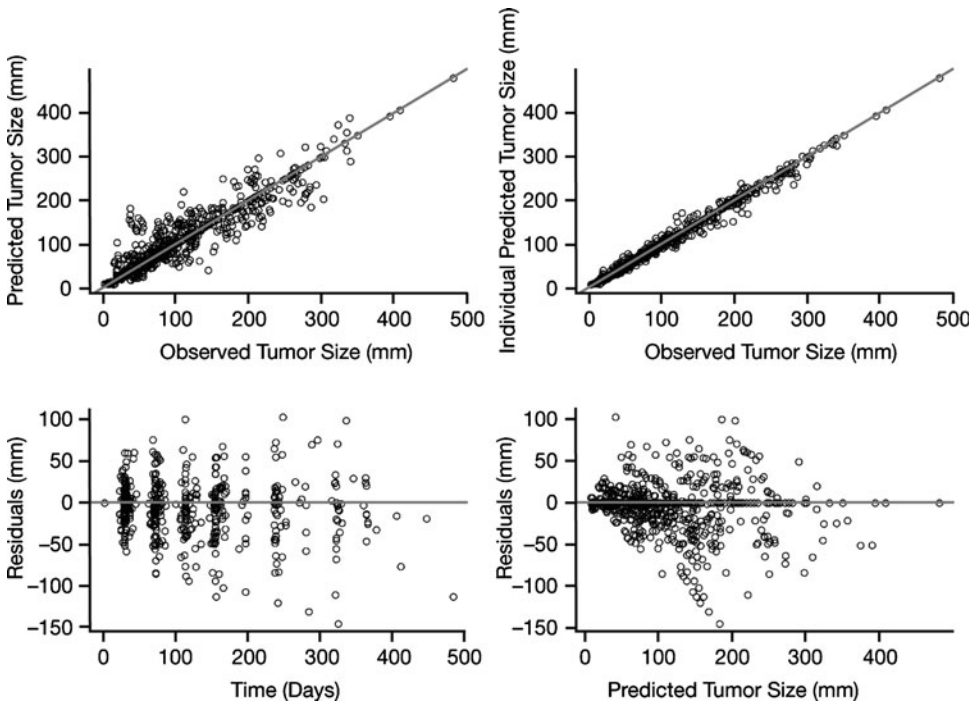


**Fig. 12.7** Diagnostic plots for the mRCC tumor growth kinetics model. *Lines* represent the unity (population and individual predicted plots) or null value (weighted residual plots). Reproduced and adapted from Houk et al. (2010) with kind permission of Springer Science and Business Media
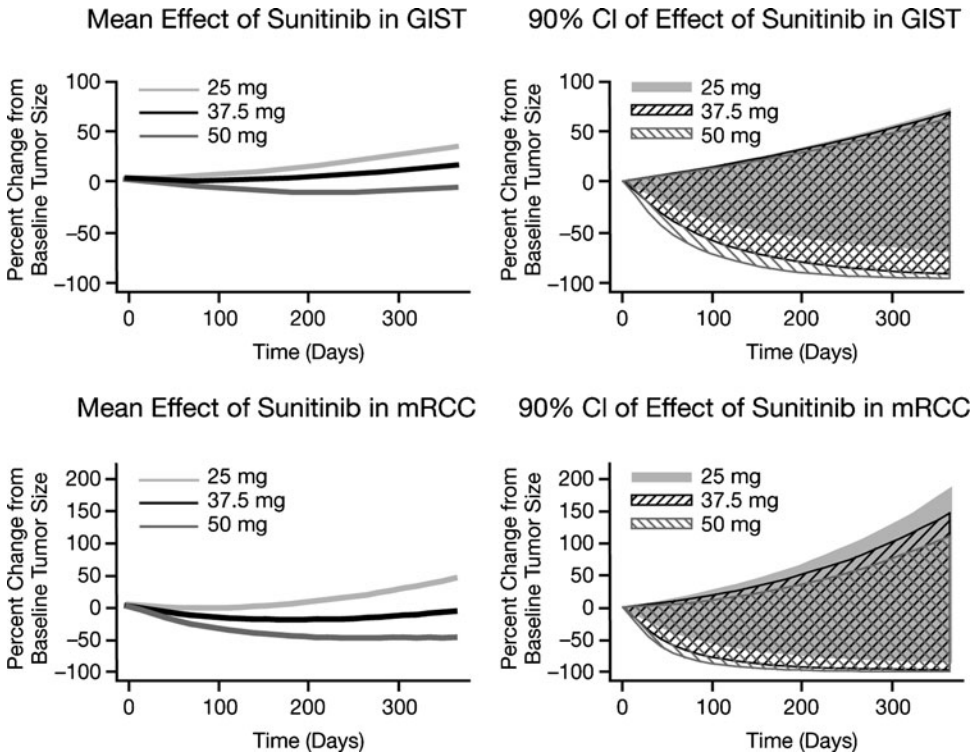
**Fig. 12.8** Simulated tumor size changes in patients with GIST or mRCC at doses between 25 and 50 mg daily on Schedule 4/2. Adapted from Houk et al. (2010) with kind permission of Springer Science and Business Media

**Fig. 12.9** Probability of experiencing fatigue over time based on a simulation with 1,000 patients. Adapted from Houk et al. (2010) with kind permission of Springer Science and Business Media
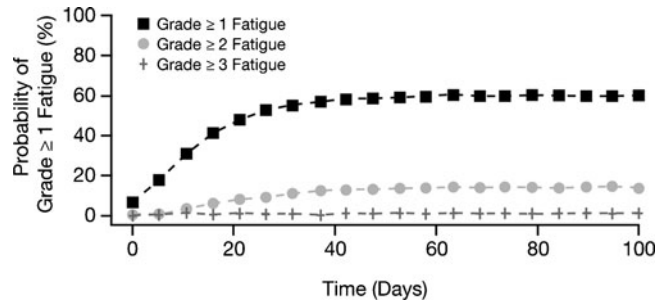


**Table 12.5** Estimates of typical ANC and percent reduction from baseline by sunitinib dose for each tumor type

| Dose of sunitinib (mg) | ANC, counts/nL (% reduction from baseline ANC value of 5 counts/nL) | | |
| --- | --- | --- | --- |
| | Solid tumors | GIST | mRCC |
| 25 | 4.3 (−13) | 4.1 (−18) | 4.2 (−15) |
| 50 | 3.7 (−26) | 3.2 (−36) | 3.5 (−30) |
| 75 | 3.0 (−39) | 2.3 (−54) | 2.7 (−45) |

Adapted from Houk et al. (2010) with kind permission of Springer Science and Business Media
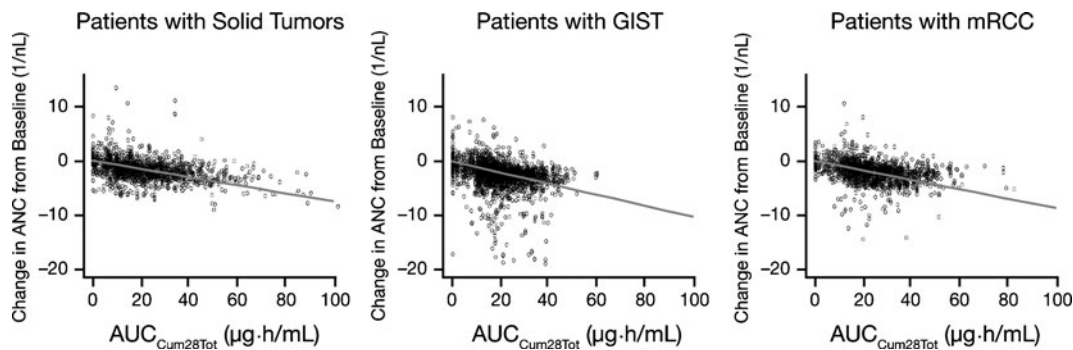
**Fig. 12.10** Observed and population-predicted (*solid line*) changes in ANC by sunitinib exposure ($AUC_{cum28Tot}$) in different tumor types. Reproduced and adapted from Houk et al. (2010) with kind permission of Springer Science and Business Media
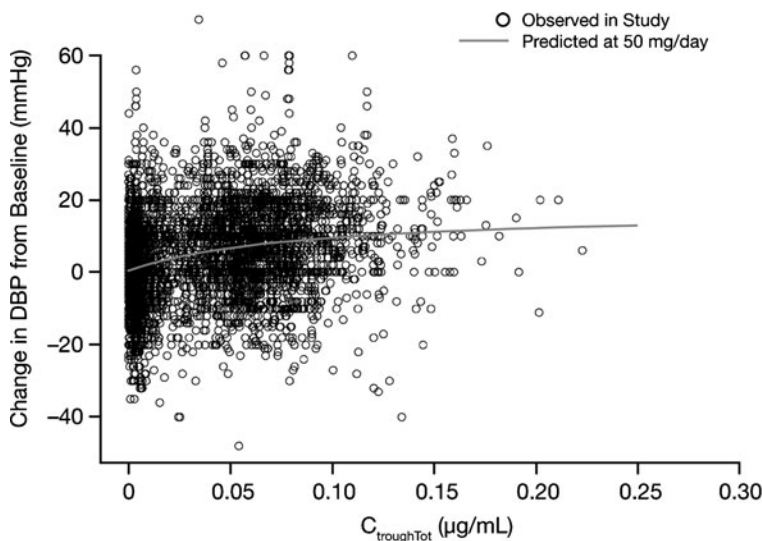


**Fig. 12.11** Observed and model-predicted changes in DBP by sunitinib exposure ($C_{troughTot}$) across all tumor types. Reproduced and adapted from Houk et al. (2010) with kind permission of Springer Science and Business Media

level occurred predominantly after one cycle of sunitinib treatment rather than in later cycles. Using this model, a solid tumor patient with a baseline ANC of 5 counts/nL was predicted to exhibit a decrease of 0.9 counts/nL at a dose of sunitinib 25 mg/day and 1.3 counts/nL at a dose of 50 mg/day.

*Elevated DBP.* DBP changes were found to correlate positively with total-drug $C_{trough}$ ($C_{troughTot}$), a relationship that was best described by a nonlinear ($E_{max}$) model (Fig. 12.11), rather than linear or power models. Baseline DBP across the population was estimated to be 74 mmHg, with an estimated interindividual variability (standard deviation) of approximately 10%. The maximum drug-mediated change in DBP was estimated to be 17 mmHg, with an interindividual variability of approximately 36% of this value. For the population on sunitinib 50 mg/day, the median $C_{trough}$ value was 0.068 μg/mL, below the estimated $C_{trough}$ value that achieves 50% of the maximum DBP increase (0.084 μg/mL), suggesting that a typical patient on sunitinib 50 mg/day would be expected to

experience a maximum elevation in DBP of 8 mmHg. An estimated 5-mmHg change in DBP was predicted for a 25-mg/day sunitinib dose.

## 12.3.4 Summary and Analysis

These analyses identified tentative relationships between sunitinib exposure and fatigue, neutropenia, and elevated DBP. As mentioned above, the paucity of placebo data and narrow range of doses limited these analyses, making it difficult to attribute these AEs to sunitinib alone rather than the disease process itself. Clinical experience has shown that at a dose of 50 mg/day on Schedule 4/2, all three of these AEs are generally mild to moderate in severity and manageable (Demetri et al. 2006, 2009; Motzer et al. 2006a, b).

The population pharmacokinetic analysis described in the previous section showed that certain patients in a given population treated with the same dose/schedule may experience increased exposure to sunitinib. In particular, these analyses identified female gender and low body weight as covariates that significantly increase exposure to sunitinib. Taken together with the pharmacokinetic−pharmacodynamic data, the results suggest that such patients may be at greater risk of fatigue, DBP elevation, or neutropenia. However, with these AEs generally being mild to moderate in severity and clinically manageable, the potentially higher risk should be balanced against the trend toward greater efficacy observed in patients with higher exposure to sunitinib.

### Conclusions

We have described how pharmacokinetics, modeling, and simulation have been employed within the clinical development program for sunitinib. The following conclusions can be drawn from these analyses:

- Increased exposure to sunitinib was associated with longer TTP, longer OS, a higher probability of an objective response, and greater tumor size decreases.

- Increased exposure was also associated with an increased risk of experiencing AEs; however, these were generally mild to moderate in severity.
- A 50-mg starting dose of sunitinib can provide clinical benefit with acceptably low risk of AEs.

While these analyses were not utilized in the design of sunitinib clinical trials, they figured prominently in the regulatory submission process. Indeed, the results of most of these analyses are reflected in the sunitinib prescribing information (Pfizer Inc. 2010), which notes, for example, that "population pharmacokinetic analyses of demographic data indicate that there are no clinically relevant effects of age, body weight, creatinine clearance, race, gender, or ECOG score on the pharmacokinetics of SUTENT or the primary active metabolite." Moreover, they have provided valuable guidance on the optimal use of sunitinib, highlighting the importance of maintaining sunitinib dosing to achieve maximum benefit from the drug.

## References

Beal SL, and Sheiner LB. NONMEM User's Guides. 2006

Bello CL, Bu H-Z, Patyna S, Kang P, Peng G, Pool W, Smeraglia J, Sherman L, Garrett M, and Klamerus K. A Phase I Mass-balance Study to Evaluate the Metabolism and Excretion of [$^{14}$C]-sunitinib in Healthy Male Subjects (abstract 9072). Poster presented at the Annual Meeting of the American Association for Cancer Research, Los Angeles, USA, 2007

Bello CL, Garrett M, Sherman L, Smeraglia J, Ryan B, and Toh M. Pharmacokinetics of Sunitinib Malate in Subjects with Hepatic Impairment. *Cancer Chemother Pharmacol* 2010; 66:699–707

Bello CL, Sherman L, Zhou J, Verkh L, Smeraglia J, Mount J, and Klamerus KJ. Effect of Food on the Pharmacokinetics of Sunitinib Malate (SU11248), a

Multi-targeted Receptor Tyrosine Kinase Inhibitor: Results from a Phase I Study in Healthy Subjects. *Anti-Cancer Drugs* 2006a; 17:353–358

Bello CL, Houk B, Sherman L, Sarapa N, Smeraglia J, Huang X, and Klamerus KJ. Pharmacokinetics of Sunitinib Malate (SU11248) Administered with/without Rifampin in Caucasian and Japanese Populations. Poster presented at the 17th International Congress on Anti-Cancer Treatment, Paris, France, 2006b

Britten CD, Kabbinavar F, Hecht JR, Bello CL, Li J, Baum C, and Slamon D. A Phase I and Pharmacokinetic Study of Sunitinib Administered Daily for 2 Weeks, Followed by a 1-week Off Period. *Cancer Chemother Pharmacol* 2008; 61:515–524

Demetri GD, Heinrich MC, Fletcher JA, Fletcher CDM, Van den Abbeele AD, Corless CL, Antonescu CR, George S, Morgan JA, Chen MH, Bello CL, Huang X, Cohen DP, Baum CM, and Maki RG. Molecular Target Modulation, Imaging, and Clinical Evaluation of Gastrointestinal Stromal Tumor Patients Treated with Sunitinib Malate After Imatinib Failure. *Clin Cancer Res* 2009; 15:5902–5909

Demetri GD, Huang X, Garrett CR, Schöffski P, Blackstein ME, Shah MH, Verweij J, Tassell V, Baum CM, and Casali PG. (2008). Novel Statistical Analysis of Long-term Survival to Account for Crossover in a Phase III Trial of Sunitinib (SU) vs. Placebo (PL) in Advanced GIST after Imatinib (IM) Failure. *J Clin Oncol 2008*; 26(15S):559s

Demetri GD, van Oosterom AT, Garrett CR, Blackstein ME, Shah MH, Verweij J, McArthur G, Judson IR, Heinrich MC, Morgan JA, Desai J, Fletcher CD, George S, Bello CL, Huang X, Baum CM, and Casali PG. Efficacy and Safety of Sunitinib in Patients with Advanced Gastrointestinal Stromal Tumour After Failure of Imatinib: a Randomised Controlled Trial. *Lancet* 2006; 368:1329–1338

Faivre S, Delbaldo C, Vera K, Robert C, Lozahic S, Lassau N, Bello C, Deprimo S, Brega N, Massimini G, Armand JP, Scigalla P, and Raymond E. Safety, Pharmacokinetic, and Antitumor Activity of SU11248, a Novel Oral Multitarget Tyrosine Kinase Inhibitor, in Patients with Cancer. *J Clin Oncol* 2006; 24:25–35

Food and Drug Administration. Guidance for Industry: Exposure–Response Relationships – Study Design, Data Analysis and Regulatory Applications, 2003. http://www.fda.gov/downloads/Drugs/GuidanceComplianceRegulatoryInformation/Guidances/ucm072109.pdf

Food and Drug Administration. Guidance for Industry: Population Pharmacokinetics, 1999. http://www.fda.gov/downloads/Drugs/GuidanceComplianceRegulatoryInformation/Guidances/ucm072137.pdf

Guo F, Letrent SP, Munster PN, Britten CD, Gelmon K, Tolcher AW, and Sharma A. Pharmacokinetics of a HER2 Tyrosine Kinase Inhibitor CP-724,714 in Patients with Advanced Malignant HER2 Positive Solid Tumors: Correlations with Clinical Characteristics and Safety. *Cancer Chemother Pharmacol* 2008; 62:97–109

Houk BE, Bello CL, Kang D, and Amantea M. A Population Pharmacokinetic Meta-analysis of Sunitinib Malate (SU11248) and its Primary Metabolite (SU12662) in Healthy Volunteers and Oncology Patients. *Clin Cancer Res* 2009; 15:2497–2506

Houk BE, Bello CL, Poland B, Rosen LS, Demetri GD, and Motzer RJ. Relationship between Exposure to Sunitinib and Efficacy and Tolerability Endpoints in Patients with Cancer: Results of a Pharmacokinetic/Pharmacodynamic Meta-analysis. *Cancer Chemother Pharmacol* 2010; 66:357–371

International Conference on Harmonisation. E4 Guidance for Industry: Dose–Response Information to Support Drug Registration, 1994. http://www.fda.gov/downloads/Drugs/GuidanceComplianceRegulatoryInformation/Guidances/ucm073115.pdf

Khosravan R, Toh M, Garrett M, La Fargue J, Ni G, Marbury TC, Swan SK, Lunde NM, and Bello CL. Pharmacokinetics and Safety of Sunitinib Malate in Subjects with Impaired Renal Function. *J Clin Pharmacol* 2010; 50:472–481

Kulke MH, Lenz HJ, Meropol NJ, Posey J, Ryan DP, Picus J, Bergsland E, Stuart K, Tye L, Huang X, Li JZ, Baum CM, and Fuchs CS. Activity of Sunitinib in Patients with Advanced Neuroendocrine Tumors. *J Clin Oncol* 2008; 26:3403–3410

Larson RA, Druker BJ, Guilhot F, O'Brien SG, Riviere GJ, Krahnke T, Gathmann I, Wang Y, and the IRIS (International Randomized Interferon vs STI571) Study Group. Imatinib Pharmacokinetics and its Correlation with Response and Safety in Chronic-phase Chronic Myeloid Leukemia: a Subanalysis of the IRIS Study. *Blood* 2008; 111:4022–4028

Launay-Vacher V, Oudard S, Janus N, Gligorov J, Pourrat X, Rixe O, Morere JF, Beuzeboc P, Deray G, and the Renal Insufficiency and Cancer Medications (IRMA) Study Group. Prevalence of Renal Insufficiency in Cancer Patients and Implications for Anticancer Drug Management: the Renal Insufficiency and Anticancer Medications (IRMA) Study. *Cancer* 2007; 110:1376–1384

Mendel DB, Laird AD, Xin X, Louie SG, Christensen JG, Li G, Schreck RE, Abrams TJ, Ngai TJ, Lee LB, Murray LJ, Carver J, Chan E, Moss KG, Haznedar JO, Sukbuntherng J, Blake RA, Sun L, Tang C, Miller T, Shirazian S, McMahon G, and Cherrington JM. In Vivo Antitumor Activity of SU11248, a Novel Tyrosine Kinase Inhibitor Targeting Vascular Endothelial Growth Factor and Platelet-derived Growth Factor Receptors: Determination of a Pharmacokinetic/Pharmacodynamic Relationship. *Clin Cancer Res* 2003; 9:327–337

Motzer RJ, Michaelson MD, Redman BG, Hudes GR, Wilding G, Figlin RA, Ginsberg MS, Kim ST, Baum CM, DePrimo SE, Li JZ, Bello CL, Theuer CP, George DJ, and Rini BI. Activity of

SU11248, a Multitargeted Inhibitor of Vascular Endo-thelial Growth Factor Receptor and Platelet-derived Growth Factor Receptor in Patients with Metastatic Renal Cell Carcinoma. *J Clin Oncol* 2006a; 24:16–24

Motzer RJ, Rini BI, Bukowski RM, Curti BD, George DJ, Hudes GR, Redman BG, Margolin KA, Merchan JR, Wilding G, Ginsberg MS, Bacik J, Kim ST, Baum CM, and Michaelson MD. Sunitinib in Patients with Meta-static Renal Cell Carcinoma. *JAMA* 2006b; 295: 2516–2524

Novello S, Scagliotti GV, Rosell R, Socinski MA, Brah-mer JR, Atkins JN, Pallares C, Burgess R, Tye L, Selaru P, Wang E, Chao R, and Govindan R. Phase II Study of Continuous Daily Sunitinib Dosing in Patients with Previously Treated Advanced Non-small Cell Lung Cancer. *Br J Cancer* 2009; 101: 1543–1548

O'Farrell AM, Foran JM, Fiedler W, Serve H, Paquette RL, Cooper MA, Yuen HA, Louie SG, Kim H, Nicholas S, Heinrich MC, Berdel WE, Bello C, Jacobs M, Scigalla P, Manning WC, Kelsey S, and Cherrington JM. An Innovative Phase I Clinical Study Demonstrates Inhibition of FLT3 Phosphorylation by SU11248 in Acute Myeloid Leukemia Patients. *Clin Cancer Res* 2003; 9:5465–5476

Pfizer Inc. SUTENT® Investigator Brochure, June 2007

Pfizer Inc. SUTENT® (Sunitinib) Prescribing Informa-tion, 2010. http://www.pfizer.com/files/products/uspi_sutent.pdf

Rosen L, Mulay M, Long J, Wittner J, Brown J, Martino A-M, et al. Phase I Trial of SU11248, a Novel Tyro-sine Kinase Inhibitor in Advanced Solid Tumors (abstract 765). Oral presentation at the 39th Annual Meeting of the American Society for Clinical Oncol-ogy (ASCO), Chicago, Illinois, USA. *Proc Amer Soc Oncol* 2003; 22:191

Shirao K, Nishida T, Doi T, Komatsu Y, Muro K, Li Y, Ueda E, and Ohtsu A. Phase I/II Study of Sunitinib Malate in Japanese Patients with Gastrointestinal Stro-mal Tumor After Failure of Prior Treatment with Imatinib Mesylate. *Invest New Drugs* 2010; 28: 866–875.

Socinski MA, Novello S, Brahmer JR, Rosell R, Sanchez JM, Belani CP, Govindan R, Atkins JN, Gillenwater HH, Pallares C, Tye L, Selaru P, Chao RC, and Scagliotti GV. Multicenter, Phase II Trial of Sunitinib in Previously Treated, Advanced Non-small-cell Lung Cancer. *J Clin Oncol* 2008; 26: 650–656

Sun L, Liang C, Shirazian S, Zhou Y, Miller T, Cui J, Fukuda JY, Chu JY, Nematalla A, Wang X, Chen H, Sistla A, Luu TC, Tang F, Wei J, and Tang C. Discovery of 5-[5-fluoro-2-oxo-1,2- dihydroindol-(3Z)-ylidenemethyl]-2,4- dimethyl-1H-pyrrole-3-car-boxylic acid (2-diethylaminoethyl)amide, a Novel Tyrosine Kinase Inhibitor Targeting Vascular Endo-thelial and Platelet-derived Growth Factor Receptor Tyrosine Kinase. *J Med Chem* 2003; 46:1116−1119

Therasse P, Arbuck SG, Eisenhauer EA, Wanders J, Kaplan RS, Rubinstein L, Verweij J, Van Glabbeke M, van Oosterom AT, Christian MC, and Gwyther SG. New Guidelines to Evaluate the Response to Treat-ment in Solid Tumors. European Organization for Research and Treatment of Cancer, National Can-cer Institute of the United States, National Cancer Institute of Canada. *J Natl Cancer Inst* 2000; 92: 205–216

Washington C, Eli M, Bello C, Schaaf L, Polasek E, Tan LH, et al. The Effect of Ketoconazole (KETO), a Potent CYP3A4 Inhibitor, on SU011248 Pharmaco-kinetics (PK) in Caucasian and Asian Healthy Sub-jects (abstract 553). *Proc Am Soc Oncol* 2003; 22:138

# The Clinical Significance of Drug Transporters in Drug Disposition and Drug Interactions

# 13

Thomas N. Thompson

**Abstract**

The field of drug transporters has exploded over the past 30 years. It is now known that transporters are located in virtually every organ and tissue in the body and are involved in every aspect of drug absorption, distribution, excretion, and even influence drug metabolism by regulating access to drug metabolizing enzymes. Because of their ubiquity and function, drug transporters profoundly influence drug pharmacokinetics and pharmacodynamics. Moreover, factors which influence drug transporter function, such as genetic polymorphisms or transporter based drug interactions, can have a major impact on drug efficacy and safety. This chapter summarizes the role of transporters in drug disposition, gives examples of their clinical relevance, and describes the emerging role of drug transporters in drug discovery and development.

## 13.1 Introduction

From the beginning of the modern era of pharmacotherapy, it has been the goal of scientists to rationally design, synthesize, and deliver agents to the systemic circulation of patients whereby they can reach their intended target, exert their effect, and have clinical benefit. Although this is regarded as a beneficent intervention, the human body (as do other mammalian bodies) recognizes our "beneficial drugs" as unwanted xenobiotics and has evolved an elaborate system of proteins that control systemic exposure by influencing the absorption, distribution, metabolism, and excretion (aka ADME) of said molecules.

After several decades of intense study, a fairly sophisticated understanding of the physicochemical properties necessary to gain systemic exposure exists, as well as the elaborate gauntlet of enzymes important in the metabolism and excretion of drugs. However, only relatively recently have scientists begun to recognize and understand another class of proteins, the so-called "drug transporters", that figure prominently in drug disposition. Drug transporters are important for gaining and restricting access to the systemic circulation, as well as influencing distribution to target organs, and excretion into bile and urine. Although transporters do not themselves catalyze changes to molecular structure, they work

T.N. Thompson
R&D Services Pharma consulting, 663 N. 132nd St, #126,
Omaha, NE 68154, USA
e-mail: tnt@rdservkc.com

in close coordination with drug metabolizing enzymes that do.

In addition to their role in drug and xenobiotic disposition, transporters are also pivotal in the uptake and distribution of key nutrients and critical endobiotics. It has been estimated that as much as 2% of the total genes in the human genome relate to transporters, which translates to approximately 700 transporter genes (Choudhuri and Klaassen 2006). Transporters are typically grouped into two broad categories known as "solute carrier transporters (SLC)" and ATP-binding cassette (ABC) transporters (Giacomini and Sugiyama 2006). The SLCs are largely responsible for uptake across many cell membrane barriers, whereas the ABC transporters are largely responsible for efflux back across cellular membranes. The SLCs are largely responsible for uptake across many cell membrane barriers, including intestinal epithelial cells, hepatocytes, and kidney proximal tubule cells. In contrast, the ABC transporters are largely responsible for efflux back across cellular membranes and are located in intestinal epithelial cells, hepatic canalicular membrane, the blood–brain barrier (BBB) and placenta.

Although the number of presumed transporters is large, a substantial number of those have yet to be identified and characterized, and only a comparatively small number of drug transporters are currently known to have clinical significance in the disposition of drugs. A recent review article by Giacomini et al. (2010) summarized the results of over 2 years of meetings of the International Transporter Consortium (ITC), a group of scientists from across all sectors of drug discovery, including academia, industry, and the United States Food and Drug Administration. This article lists 19 transporters as having the greatest known significance to human drug disposition. Indeed, even of these 19, the ITC focused their attention on a smaller subset of only seven transporters for which there is the greatest body of evidence for their role in human drug absorption, disposition, and drug interactions (Table 13.1).

Two of the seven transporters in the ITC review are in the ABC family of efflux transporters, namely P-glycoprotein (P-gp, aka multi-drug resistance protein 1 [MDR1]; Schinkel and Jonker 2003; Choudhuri and Klaassen 2006; Zhou 2008) and breast cancer resistance protein (BCRP, Schinkel and Jonker 2003; Mao and Unadkat 2005; Choudhuri and Klaassen 2006), both of which are located mainly in the intestinal epithelia, canalicular membrane of hepatocytes, and the BBB, although they are also known to be present in many other tissues, including tumor cells. The other five transporters are in the SLC family. Organic cation transporter 2 (OCT2, Koepsell et al. 2007) and the organic anion transporters 1 and 3 (OAT1, and OAT3, Nigam et al. 2007) are located in the kidney proximal tubule. Organic anion transporter proteins 1B1 and 1B3 (OATP1B1 and OATP1B3, Hagenbuch and Gui 2008) are located on the serosal membrane of hepatocytes. Although these seven transporters have received the most attention to date, the ITC acknowledged that future research will reveal major roles for other transporters in clinical drug therapy. Of note, in addition to the reviews cited above, the reader is referred to several other excellent recent reviews on OCTs (Wright 2005; Ciarimboli 2008) and OATs (VanWert et al. 2010).

## 13.2　Role of Transporters in Drug Disposition

In order to exert their pharmacological effect, orally administered drugs must transverse the intestinal epithelium and be distributed to the active site, which is often located in tissues throughout the body, after which they are usually metabolized and/or excreted. While physico-chemical properties certainly play a significant role in whether a drug is absorbed and distributed throughout the body by passive diffusion, it is now known that membrane transporters are also important determinants of the trans-membrane passage of drugs, including both uptake into cells and efflux out of cells (Fig. 13.1).

Indeed, there has even been some speculation that drug transport, rather than passive diffusion, may play a more important role for molecules to cross cell membranes than has generally been

**Table 13.1** Selected substrates and inhibitors of drug transporters

| Transporter | SAR of substrates | Substrates | Inhibitors | Review article |
|---|---|---|---|---|
| P-gp | Neutral and positively charged bulky (e.g., molecular weight >400)hydrophobic compounds; with a log partition coefficient >1-2; substrate specificity overlaps with CYP3A4 | *Anticancer drugs* (vinblastine, vincristine, paclitaxel, docetaxel doxorubicin, daunorubicin, and epirubicin) *HIV protease inhibitors* (Saquinavir, Ritonavir, Nelfinavir, Indinavir, Lopinavir, Amprenavir) *Others* (fexofenadine, cimetidine, Loperamide, Itraconazole, Ketoconazole, Atorvastatin, Lovastatin, Cyclosporin A, and tacrolimus | Itraconazole, cyclosporine, quinidine, and elacridar | Lin (2003), Leslie et al. (2005), Marchetti et al. (2007), Choudhuri and Klaassen (2006) |
| BCRP | Hydrophilic and hydrophobic compounds including various conjugated compounds | *Anticancer drugs* (daunorubicin, doxorubicin, mitoxantrone, bisantrene, topotecan, irinotecan and it is active metabolite SN-38, methotrexate, *Nucleoside drugs* AZT, Lamivudine *Antibiotics* Ciprofloxacin, Ofloxacin, and Norfloxacin *Others* Cimetidine and rosuvastatin | Estrone GF120918 | Chandra and Brouwer (2004), Leslie et al. (2005) |
| OATP1B1 | Amphipathic organic compounds, e.g., organic anions, some type II cations (bulky molecules with cationic groups located near the ring; e.g., quinidine) and neutral steroids. | *Statins* (atorvastatin, cerivastatin, Fluvastatin Pitavastatin Pravastatin, and rosuvastatin) *Others* Bosentan, fexofenadine, methotrexate ouabain; olmesartan, rifampicin, and valsartan | Saquinovir and Cyclosporin A | Chandra and Brouwer (2004), Kalliokoski and Niemi (2009) |
| OATP1B3 | | *Statins* (Fluvastatin, Pitavastatin, and rosuvastatin) *Others* Amanitin Atrasentan, Bosentan Digoxin, Docetaxel, Enalapril, Fexofenadine Methotrexate Ouabain Paclitaxel Phalloidin Rifampicin Olmesartan Telmisartan Valsartan | Cyclosporin A | Chandra and Brouwer (2004), Kalliokoski and Niemi (2009) |
| OCT2 | Polyspecific, accepts organic cations of different sizes and molecular structures, both hydrophilic (MW < 400) and hydrophobic. | Amantidine, amiloride, acyclovir, cimetidine, metformin, memantine, pindolol, procainamide, ranitidine, oxaliplatin, and varenicline | Amantidine, cimetidine, memantine, and ranitidine | Jonker and Schinkel (2004), Koepsell et al. (2007), Ciarimboli (2008) |
| OAT1 | Monovalent (or selected divalent) organic anions (MW < 500 Da) and some neutral compounds | Acyclovir, adefovir, cidofovir, cefadroxil, cefamandole, cefazolin, and cimetidine, | Probenecid | Shitara et al. (2006) |
| OAT3 | | Benzylpenicillin captopril, cefadroxil, cefamandole, cefazolin, cimetidine, pravastatin, cefoperazone, cefotaxim, ceftriaxone, cephaloridine, and cephalothin | Cimetidine | Shitara et al. (2006) |
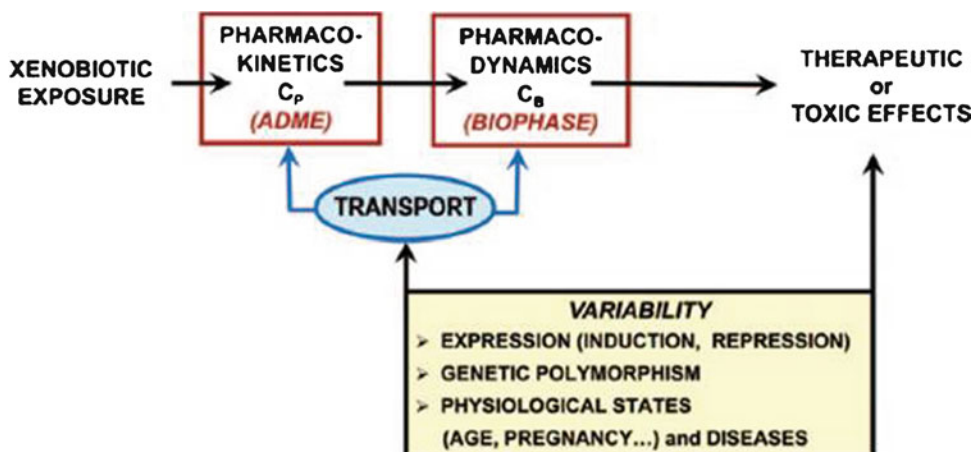
**Fig. 13.1** Impact of transport on pharmacokinetics, pharmacology, toxicology, and the variability to drug response. Reprinted from Scherrmann (2009), Copyright Wiley-VCH Verlag GmbH & Co. KGaA. Reproduced with permission

accepted (Dobson and Kell 2008). The problem with determining which is more important, diffusion or transporters is that selective inhibitors of transporters are not generally available at this time (Giacomini et al. 2010). Nevertheless, evidence from in vitro studies with human transporters, as well as inferences from drug interaction studies and studies with populations of known genetic polymorphisms, it is clear that drug transporters play a significant role in all aspects of drug disposition in humans. Figure 13.2 depicts seven key transporters involved in drug interactions the transporters are currently viewed as having the greatest possibility to contribute to drug interactions and their respective locations in the intestine (Fig. 13.2a), liver (Fig. 13.2b), kidney (Fig. 13.2c) and BBB (Fig. 13.2d). These seven transporters were recommended for study during drug development by the ITC and this recommendation was later endorsed the FDA Advisory Committee for Pharmaceutical Science and Clinical Pharmacology in their meeting of March 17, 2010 (meeting transcript can be found at *www.fda.gov/downloads/AdvisoryCommittees/ CommitteesMeetingMaterials/Drugs/Advisory- CommitteeforPharmaceuticalScienceandClini- calPharmacology/UCM210803.pdf*). Of course, other transporters are located in these tissues and throughout the body and these are mentioned in the legends to Fig. 13.2.

Even though it is difficult to know a priori what the role of transporters may be in the disposition of a given molecule, it is possible to make some reasonable predictions based on a molecule's structure and physicochemical properties. Early attempts to predict mechanisms of absorption were based on a compound's structure and were general in nature. For example, most anionic drugs, some hydrophilic organic cationic and zwitterionic drugs are believed to require transporters for uptake into the liver and kidney cells for their ultimate clearance. More recently, Wu and Benet (2005) have proposed a modification to the Biopharmaceutics and Classification System (BCS, Amidon et al. 1995), which they call the "Biopharmaceutics Drug Distribution and Classification System (BDDCS)" that provides a helpful systematic framework in which to understand the effects of drug transporters on drug disposition and pharmacokinetics (Fig. 13.3). For example, the bioavailability of BCS Class 1 compounds (those with both high permeability and solubility) is not likely to be influenced by transporters because these compounds are highly absorbed by passive diffusion. Moreover, these compounds have free access to intracellular intestinal and hepatic drug metabolizing enzymes (DMEs) which facilitate first pass metabolism, the other major determinant of bioavailability. However, although BCS Class
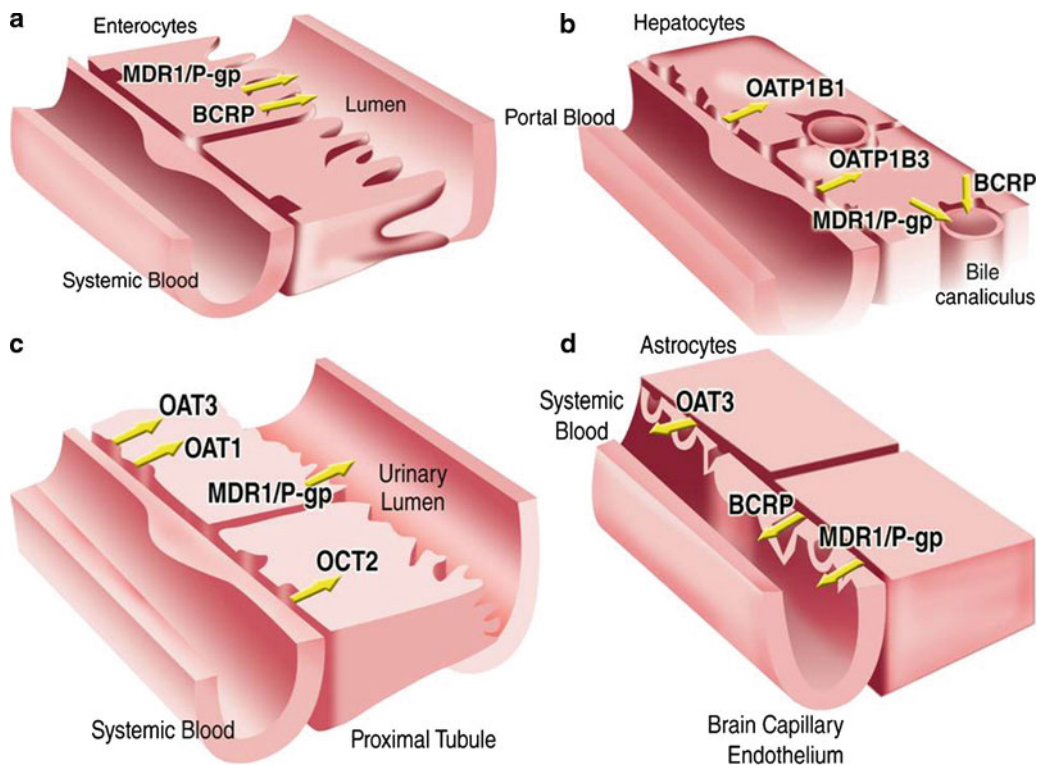
**Fig. 13.2** Key transporters involved in drug interactions and their respective organ locations. These transporters were recommended for study during drug development by the International Transporter Consortium and this recommendation was endorsed the FDA Advisory Committee for Pharmaceutical Science and Clinical Pharmacology. (**a**) Intestine: The efflux transporters P-gp and BCRP are currently viewed as the intestinal transporters having the greatest possibility to contribute to drug interactions. Other intestinal epithelial uptake transporters on the apical (luminal) membrane include one or more members of the organic anion transporting polypeptide (OATP) family; peptide transporter 1 (PEPT1; SLC15A1); ileal apical sodium/bile acid cotransporter (ASBT); and monocarboxylic acid transporter 1 (MCT1). In addition to P-gp and BCRP, another apical ATP-dependent efflux pumps is multidrug resistance protein 2 (MRP2; and ABCC2). The basolateral membrane of intestinal epithelia contains organic cation transporter 1 (OCT1), organic solute transporter (OSTα–OSTβ); and MRP3 (ABCC3) (Giacomini et al. 2010). This illustration is provided courtesy of Optivia Biotechnology (www.optiviabio.com). (**b**) Liver: The uptake transporters OATP1B1 and 1B3, and the efflux transporters MDR1(P-gp) and BCRP are the four hepatic transporters currently viewed as having the greatest possibility to contribute to drug interactions. Other human liver uptake transporters in the basolateral (sinusoidal) membrane include sodium/taurocholate cotransporting peptide (NTCP); OATP2B1, OAT2, OAT7, and OCT1. Efflux pumps in the hepatocyte basolateral membrane include MRP3, MRP4, and MRP6.

Other efflux transporters on the canalicular membrane include bile-salt export pump (BSEP) and MRP2. In addition, multidrug and toxin extrusion protein 1 (MATE1) is located in the apical hepatocyte membrane (Giacomini et al. 2010). This illustration is provided courtesy of Optivia Biotechnology (www.optiviabio.com). (**c**) Kidney proximal tubules: The basolateral uptake transporters OAT1, OAT3, and OCT2 and the apical efflux transporter MDR1/P-gp are the four renal transporters are currently viewed as having the greatest possibility to contribute to drug interactions. Other transporters located on the apical membrane include OAT4; urate transporter 1 (URAT1); PEPT1 and PEPT2; MRP2 and MRP4; MATE1 and MATE2-K (SLC47A2); organic cation/ergothioneine transporter (OCTN1); and organic cation/carnitine transporter (OCTN2). The other basolateral uptake transporters in proximal tubule epithelia is OATP4C1 (Giacomini et al. 2010). This illustration is provided courtesy of Optivia Biotechnology (www.optiviabio.com). (**d**) Blood–brain barrier: The efflux transporters MDR1(P-gp) and BCRP on the apical membrane of the brain capillary endothelium and OAT3 on the astrocyte basolateral membrane are the three transporters in the blood–brain barrier currently viewed as having the greatest possibility to contribute to drug interactions. Other apical (luminal) transport proteins of brain capillary endothelial cells contributing to the function of the blood–brain barrier include the uptake transporters OATP1A2 and OATP2B1; and the efflux pumps MRP4 and MRP5 (Giacomini et al. 2010). This illustration is provided courtesy of Optivia Biotechnology (www.optiviabio.com)

| BDDCS Class | Permeability/Metabolism | Solubility | Effect of drug transporters |
|---|---|---|---|
| 1 | High/Extensive | High | Transporter effects minimal |
| 2 | High/Extensive | Low | Efflux transporter effects predominate in the gut, while absorptive and efflux transporter effects occur the in liver |
| 3 | Low/Poor | High | Absorptive transporter effects predominate (but may be modulated by efflux transporters) |
| 4 | Low/Poor | Low | Absorptive and efflux transporter effects could be important |

**Fig. 13.3** Implications of biopharmaceutics drug disposition classification system (BDDCS) for involvement of drug transporters. Modified from Fig. 5, Shugarts and Benet 2009

2 compounds (high permeability, but low solubility) freely cross the intestinal epithelial cells, their net absorption could still be limited due to the action of efflux transporters. For BCS Class 3 compounds (low permeability, but high solubility), absorptive transporters play an important role in transport across the intestinal epithelia, but like Class 2 compounds, absorption may still be limited by efflux transporters. Finally, for BCS Class 4 compounds (both low permeability and solubility), both absorptive and efflux transporter effects could be important (Wu and Benet 2005, Shugarts and Benet 2009).

With respect to drug clearance, for highly permeable drugs of either Class 1 (high solubility) or Class 2 (low solubility), metabolism dominates the clearance because these compounds have free access to intracellular DMEs. Therefore, transporters would be expected to have minimal effects on clearance for these classes of compounds. However, for poorly permeable drugs of either Class 3 (high solubility) or Class 4 (low solubility), renal and biliary elimination of unchanged drug are the primary routes of clearance and drug transporters would be expected to have a dominant effect on these processes.

## 13.2.1 Absorption

### 13.2.1.1 Uptake

It is has long been known that passive diffusion cannot entirely account for absorption of all drugs, because then absorption should be easily predicted from physicochemical properties alone. Yet it is known that not just lipophilic, unionized drugs are absorbed and the fact that hydrophilic charged or amphoteric molecules are also absorbed implies a role for facilitative absorption by transporters (Thompson 2005). While these transporters most likely evolved to facilitate absorption of essential nutrients such as amino acids, oligopeptides, monosaccharides, monocarboxylic acids, phosphate, bile acids, and several water-soluble vitamins across intestinal apical and basolateral membranes, drugs bearing structural resemblance to these nutrients can also be absorbed by the same carrier systems (Tsuji and Tamai 1996, Kunta and Sinko 2004).

For example, large neutral amino acid transporters are essential for otherwise impermeable drugs such as amino acid-mimetic drugs like baclofen and melphalan. Similarly, antibiotics of the cephalosporin (e.g., cefaclor, cephalexin, cefadroxil, cephradine, cefatrizine, cefroxadine, cephradine) and β-lactam (amoxicillin, ampicillin, cyclacillin, benzylpenicillin, phenoxymethyl-penicillin, and propicillin) class, as well as other diverse drugs such as captopril, bestatin and valacyclovir, are actively transported by the peptide transporter, PEPT1. Monocarboxylic acid transporters (MCT1) are known to play a role in absorption of acids such as pravastatin (Dobson and Kell 2008), while the Na+/bile acid cotransporter ASBT facilitates absorption of acyclovir (ACV). Even drugs with some degree of passive diffusion can be influenced by active uptake. For example, organic ion transporter proteins OATP can contribute to absorption of compounds such as fexofenadine (Cvetkovic et al. 1999).

### 13.2.1.2 Efflux

In addition to active transport in the absorptive (mucosal to serosal) direction, it is now evident active transporters exist to limit absorption by causing the efflux of drugs in the reverse (serosal to mucosal) direction. For example the expression of P-gp or BCRP in the intestinal brush border (apical) membrane of the small intestine leads to net secretion of some drugs in the serosal-to-mucosal direction, serving as part of the absorption barrier in the intestine. Wu and Benet (2005) have postulated efflux transporter effects will predominate for BCS Class 2 compounds because although the high permeability of these compounds allows ready access into the gut membranes, their low solubility will limit the concentrations coming into the enterocytes, thereby preventing saturation of the efflux transporters.

The clinical significance of efflux transporters on absorption can be inferred from the effect of rifampin, a P-gp inducer, on orally administered digoxin, a substrate for P-gp. After concomitant rifampin administration, which results in increased expression of P-gp, digoxin bioavailability is significantly decreased, even though it is known digoxin is not metabolized in humans (Greiner et al. 1999). Similarly, grapefruit juice, a known inhibitor of P-gp and CYP3A4, caused a decrease in the bioavailability of fexofenadine (Banfield et al. 2002) despite the fact that this drug is known to undergo little or no metabolism in humans.

Like P-gp, the clinical significance of BCRP on absorption can be inferred from drug interaction studies. The bioavailability of topotecan, a known substrate for BCRP, but not P-gp, was increased significantly when coadministered with GF120918 which is an inhibitor of both a P-gp and BCRP (Kruijtzer et al. 2002).

### 13.2.2 Distribution

After drugs reach the systemic circulation, they are free to distribute outside the blood compartment to total body water and into tissues. Once thought to be a passive process, it is recognized that transporter-mediated uptake and/or efflux significantly influences tissue distribution. While this is true for all tissues, the two organ systems best studied with respect to transporter influx and efflux are the liver and the brain.

### 13.2.2.1 Distribution to Liver

Distribution of drugs into liver cells is very important to their metabolic and biliary clearance. Moreover, in some cases, the liver itself is the site of therapeutic action. While most lipophilic molecules may move freely from blood and diffuse across the basolateral membrane into the hepatocytes, amphipathic and polar organic compounds often require uptake transporter proteins to gain access (Chandra and Brouwer 2004; Kalliokoski and Niemi 2009). The OATP transporters, OATP1B1, OATP1B3, and OATP2B1, are chiefly responsible for uptake of their substrate drugs into the cytosolic compartment of liver cells (Kalliokoski and Niemi 2009). Once inside the hepatocytes, drug molecules can be metabolized by various drug metabolizing enzymes, or be secreted into bile by transporters such as P-gp, BCRP, MRP2 or BSEP. Alternately, there are examples of drugs

transported in the reverse direction from cytosol back into the blood compartment by efflux transporters such as P-gp or BCRP. In addition to the important role distribution to the liver plays in metabolism and excretion, the liver itself is sometimes the therapeutic target organ, as is the case for the cholesterol lowing class of compounds known as statins. Studies of genetic polymorphism and/or drug interactions have revealed the important role transporter proteins play in both the efficacy and safety of statins.

### 13.2.2.2 Distribution to the Brain

Pharmaceutical scientists have long known that entry into or exclusion from the central nervous system is controlled by the so-called BBB. At one time the BBB was thought to be solely an anatomical barrier, composed of a single layer of endothelial cells lacking fenestrations, and having few pinocytotic vesicles, connected by tight junctions. This barrier effectively excludes any drug either too hydrophilic or bound to plasma proteins. While both these factors are certainly true, it is now known that another crucial component of the BBB is the expression of efflux transporter proteins such as P-gp and BCRP in brain endothelial cells (de Boer et al. 2003; Sun et al. 2003). While most direct evidence for transporter expression comes from animal and in vitro studies, it is interesting to note a survey of marketed drugs revealed 30% were shown to be P-gp substrates (Mahar Doan et al. 2002). Even more significant, however, was the observation that the subset of drugs marketed for CNS indications have a threefold lower incidence of being P-gp substrates.

Examples of the importance of transporters limiting access into the CNS include the case of nonsedating antihistamines, such as cetirizine or fexofenadine, which are excellent substrates for P-gp (Mahar Doan et al. 2002; Cvetkovic et al. 1999). Another example is loperamide, which is a potent opioid agonist with no CNS effects. Similar to the nonsedating antihistamines, the lack of CNS effect of loperamide is likely due to efflux by P-gp (Sadeque et al. 2000). Finally, imatinib, which is an anticancer drug effective for used in treating chronic myelogenous leukemia , gastrointestinal stromal tumors and other cancers, have been found to be effective against glioblastomas in vitro, yet is ineffective clinically. Insofar as imatinib is known to be a BCRP substrate, this lack of efficacy in vivo is most likely due to efflux from the CNS by BCRP.

### 13.2.2.3 Distribution to Other Tissues

Although the role of transporters in the distribution of drugs to the liver and CNS have been the most studied organs, transporters are thought to play important roles in distribution to other tissues and organs as well. For example, efflux transporters such as P-gp and BCRP are also found to be located in other tissues, presumably to protect them from environmental "toxins". Some of these tissues and organs include the lung (Scheffer et al. 2002), the so-called "privileged compartments" in the body, which include the maternal-facing membrane of the syncytiotrophoblasts (placental cells) presumably acting to protect the fetus from xenobiotics (Unadkat et al. 2004), and the blood–testis barrier (Leslie et al. 2005).

In addition, drug distribution to tumors, which in effect are invasive "organs", are known to be influenced by transporters such as P-gp and BCRP. In this case, chemotherapeutic drugs are effluxed out of the cancer cells thereby lowering their intracellular levels and imparting drug resistance. Indeed, it was through research on drug resistance in tumors where P-gp was first discovered (Juliano and Ling 1976).

### 13.2.2.4 Interaction of Drug Transporters with Drug Metabolizing Enzymes

Although drug transporters do not have any function in the metabolic transformation of drugs, they certainly play an important role in metabolic clearance. They exert their influence by (1) controlling intracellular access to drug metabolizing enzymes and (2) completing the elimination of Phase 1 or Phase 2 metabolites by biliary or renal excretion. That transporters could be the rate limiting step of organ clearance can be shown by the following equations (Pang and

Gillette 1978; Yamazaki et al. 1996; Shitara et al. 2006):

$$CL_{int,all} = PS_{u,\,influx} \times \frac{CL_{int}}{CL_{int} + PS_{u,efflux}}.$$

Overall intrinsic clearance by liver or other organs ($CL_{int,\,all}$) is a function not only of the inherent intrinsic clearance of organ's metabolizing enzymes ($CL_{int}$), but also the influx permeability ($PS_{u,\,influx}$). If the $PS_{u,\,influx}$ is very low in comparison to $CL_{int}$, then the equation reduces to

$$CL_{int,all} = PS_{u,\,influx},$$

and $PS_{u,\,influx}$ becomes rate determining for $CL_{int,\,all}$.

Examples of influencing metabolism by controlling intracellular access are provided by several drugs of the statin class, including simvastatin, lovastatin, atorvastatin, and cerivastatin. These drugs are thought to be cleared primarily by hepatic CYP3A4 or in the case of cerivastatin by CYP2C8 metabolism. However, all are substrates for the hepatic uptake transporter OATP1B1, which is essential for their uptake into the hepatocytes, as shown from in vitro studies (e.g., Matsushima et al. 2005) as well as clinical studies. For example, patients who are genetically deficient in OATP1B1 have an increased incidence of rhabdomyolysis from simvastatin (Link et al. 2008). Alternately, patients who received cyclosporine A had a nearly fivefold increase in exposure to cerivastatin (Muck et al. 1999), thought to be due to inhibition of OATP1B1 (Shitara et al. 2003).

It has been suggested that, in some cases, the interaction between transporters and DMEs is not random, but may have evolved purposefully as a coordinated defense against xenobiotics (Zhang and Benet 2001; Benet and Cummins 2001). This is perhaps the best exemplified by the special relationship between P-gp and CYP3A4 in the intestine (Benet and Cummins 2001). Both P-gp and CYP3A4 share similar substrate specificity and both are located in the small intestinal enterocytes. Absorption of drugs or other xenobiotics begins by permeation of the apical membrane.

However, the drugs that happen to be substrates for P-gp are extruded back into the intestine and the process begins again. Alternately, should some drug escape efflux by P-gp, because it is also a substrate for CYP3A4, it may be metabolized. The continual process of diffusion, then efflux has the effect of lengthening the time the drug is exposed to CYP3A4. The net effect is to limit the penetration of the intestinal barrier and thus lower bioavailability. The notion of a coordinated defense between P-gp and CYP3A4 is further strengthened by the observation that both are regulated by the same nuclear receptor, pregnane-X receptor (PXR, Geick et al. 2001). As was noted earlier, the interaction between transporter and enzyme will be most relevant for BDDCS Class 2 compounds as transporters do not figure in the clearance of Class 1 compounds and Class 3 or 4 compounds are eliminated by transporter-based biliary or renal excretion without metabolism (Shugarts and Benet 2009).

## 13.2.3 Excretion

Biliary and renal excretory pathways have been described descriptively for decades, but only since the mid-1990s have the important role of drug transporters in these pathways been known (Giacomini and Sugiyama 2006). This knowledge has enabled us to better understand renal and biliary clearance and appreciate what role genetic polymorphisms and drug interactions may play in drug efficacy and safety with respect to these excretory systems.

### 13.2.3.1 Biliary Excretion

Along with metabolism, biliary excretion is the other pathway of hepatic clearance and transporters play a major role in this process (Ho and Kim 2005; Shitara et al. 2005; Shitara et al. 2006). First, a drug must transverse the sinusoidal membrane from blood into the hepatocytes, a process which is facilitated by OATP1B1 and OATP1B3 and several other SLC transporters. Examples of drugs taken up by OATP1B1 include statins such as atorvastatin, cerivastatin, fluvastatin, pitavastatin, pravastatin, and rosuvastatin as

well as other miscellaneous drugs such as bosentan, fexofenadine, methotrexate, ouabain, olmesartan, rifampicin, and valsartan. Substrates for OATP1B3 include statins such as fluvastatin, pitavastatin, and rosuvastatin as well as diverse drugs such as amantidine, atrasentan, bosentan, digoxin, docetaxel, enalapril, fexofenadine, ouabain, paclitaxel, phalloidin, rifampicin, olmesartan, telmisartan and valsartan (Table 13.1).

Once inside the hepatocytes, one of two things can happen to the drug. First, the drug may be extruded back into the blood by the sinusoidal efflux transporters MRP3, MRP4, or MRP6. However, more likely, the drug may then be susceptible to Phase 1 and Phase 2 metabolism which has the effect of producing more water-soluble metabolites. These more hydrophilic metabolites are often substrates for efflux transporters on the liver canalicular membrane such as P-gp, BCRP, and others, which extrude them into bile. Alternately, sufficiently polar molecules with molecular weights exceeding 400 Da may be substrates for these efflux transporters without prior metabolism and thus are excreted into bile unchanged, e.g., fexofenadine (P-gp) or pravastatin (P-gp or BRCP).

### 13.2.3.2 Renal Excretion

Hydrophilic drugs of low molecular weight (<400 Da) are likely candidates for renal excretion. These drugs are first delivered to the kidney via the renal artery where a portion of the blood is filtered by glomerular filtration, which is a simple diffusion process that does not involve transporters. After drugs are filtered through the glomerulus they pass through the proximal renal tubule, where they may be reabsorbed into bloodstream or be metabolized by renal DMEs. Reabsorption may occur by either passive diffusion across a concentration gradient driven by absorption of water from urine back into blood (Shitara et al. 2006) or actively secreted back into the blood by efflux transporters like PEP1 and OATP1A2.

The remaining portion of renal blood not filtered through the glomerulus is presented to the renal proximal tubule where there are several kinds of transporters located on the sinusoidal membrane. Substrates for these transporters are taken up into the renal proximal tubule cell and excreted into the renal tubule, ultimately being excreted in the urine. Drugs that are organic cations are substrates for uptake by OCT2, and include amantidine, amiloride, cimetidine, metformin, memantine, pindolol, procainamide, ranitidine, oxaliplatin, and varenicline, to name a few. Organic anions are also taken up by OAT1 and include drugs such ACV, adefovir, cidofovir, cefadroxil cefamandole, cefazolin, and cimetidine. Substrates for the other major organic anion transporter OAT3 include β-lactams such as benzylpenicillin, cephalosporins such as cefadroxil, cefamandole, cefazolin, cephaloridine, and other drugs including captopril, cimetidine, methotrexate and pravastatin (Jonker and Schinkel 2004; Shitara et al. 2006; Koepsell et al. 2007; Ciarimboli 2008). Once inside the proximal renal tubule cell they may be actively effluxed into the lumen and ultimately the urine by efflux transporters such as P-gp, MRP2 or MRP4, among others, located on the luminal (brush border) membrane. Hence, transporters in the kidney can, depending on their location in the cell, act to either increase or decrease renal clearance, thereby decreasing or increasing total clearance, respectively.

## 13.3  Effects of Transporters that Influence Drug PK: Clinical Examples

The previous section provided an overview of the role transporters play in drug disposition. This section will provide clinical examples where transporters have been shown to impact drug efficacy or safety. These have been grouped into cases where (1) a drug interaction involving a transporter or (2) a genetic polymorphism of the transporter was responsible for the clinically significant effect.

## 13.3.1 Drug Interactions

The potential for drug interactions resulting from interaction with drug transporters is a rapidly emerging field and has the FDA's full attention (US Food and Drug Administration. Drug Development and Drug Interactions. US FDA website (http://www.fda.gov/Drugs/DevelopmentApprovalProcess/DevelopmentResources/DrugInteractionsLabeling/ucm080499.htm, accessed April 19, 2010) [online]. Transporter-based drug interactions are often complex to sort out as they are confounded by the fact that many transporters are located in multiple tissue sites, and the putative interacting drug may also affect drug metabolizing enzymes, or other transporters. Nevertheless, as our understanding of human drug transporters and their clinical relevance has progressed, more drug interactions involving transporters have been revealed. In many cases, the drug interaction was shown by clinical studies years before the involvement of transporters was sorted out. This topic has been the subject of several recent reviews (Lin 2003; Shitara et al. 2005; Endres et al. 2006; Li et al. 2006; Marchetti et al. 2007; Poirier et al. 2007; Zhang et al. 2008; Kindla et al. 2009). A partial list of clinically significant drug interactions involving transporters is provided in Table 13.2.

Although any of the known transporters could be involved in a drug interaction, the ITC identified the following seven transporters as being of the greatest significance for drug interactions at this time (Giacomini et al. 2010): the efflux transporters P-gp (MDR1) and BCRP located in the intestinal epithelia, canalicular membrane of hepatocytes and the BBB; OCT2, OAT1, and OAT3 located in the kidney proximal tubule, and OATP1B1 and OATP1B3 located on the serosal membrane of the hepatocytes.

Like interactions involving DMEs, transporter-based interactions between drugs can result from either inhibition or induction of a given transporter, and may involve both uptake

**Table 13.2** Selected examples of drug–drug interactions mediated by drug transporters

| Transporter | Interacting drug | Affected drug | Clinical affect | In vivo study |
|---|---|---|---|---|
| Inhibition of intestinal P-gp efflux | Verapamil | Fexofenadine | ↑ Bioavailability by 2.5x | Yasui-Furukori et al. (2005) |
| Inhibition of intestinal P-gp efflux | Quinidine | Digoxin | Increase in the amount of absorbed from this jejunal segment compared with the absorption from the other quinidine-free segment (22.4% vs. 55.8%) | Igel et al. (2007) |
| Inhibition of BCRP efflux | GF120918 | Topotecan | Topotecan AUC ↑143% | Kruijtzer et al. (2002) |
| Inhibition of uptake of renal OAT | Probenecid | Cefaclor and cephadrin | ↑ Cmax and AUC | Welling et al. (1979) |
| Inhibition of uptake of renal OAT | Probenecid | Furosemide | CLr ↓66% | Li et al. (2006) |
| Inhibition of uptake of renal OAT | Probenecid | Cefamandole | CLr ↓75% | Takeda et al. (2002a, b, c) |
| Inhibition of uptake of renal OCT | Cimetidine | Metformin | AUC ↑50% and CLr ↓ 27% | Somogyi et al. (1987) |
| Inhibition of OATP1B1 | Cyclosporin A | Cerivastatin | ↓ Hepatic metabolism by 3A4 and 2C8, ↑AUC by 4-5x | Muck et al. (1999), Shitara et al. (2003) |
| Inhibition of OATP | Cyclosporin A | Pravastatin | AUC ↑890% and Cmax ↑678% and ↓ $CL_{bil}$ | Neuvonen et al. (2006) |

and efflux transporters. Also similar to DME-based interactions, transporter-based interactions first occur at the pharmacokinetic level, meaning they affect the plasma concentration of drug. Such an interaction becomes clinically significant if it results in the plasma concentration falling outside the therapeutic window, resulting in lack of efficacy or adverse effects. While most clinically significant interactions result in noticeable changes in plasma concentrations, there are special cases where a change in plasma concentrations is not evident, as is the case for tissues with a low volume of distribution, e.g., brain, testes, fetus etc. In these instances, a transporter-based interaction could indeed occur, but the resulting effect on tissue concentrations may not be evident from the corresponding plasma concentration.

### 13.3.1.1 Inhibition and Induction of P-gp (MDR1)

P-glycoprotein is without a doubt the best studied transporter to date (Fig. 13.4). Consequently, there are by far more substrates known for P-gp than any other transporter and more drug interactions have been reported (Lin 2003; Schinkel and Jonker 2003; Endres et al. 2006; Marchetti et al. 2007). Many substrates known to be involved in intestinal P-gp drug interactions, including digoxin, loperamide, and fexofenadine (Cvetkovic et al. 1999) just to name a few. Because of its location in the intestinal epithelial cells, drugs or other xenobiotics that inhibit P-gp may block efflux of substrates back into intestine, thereby having the apparent effect of increasing absorption. Conversely, drugs that induce P-gp may have the effect of further limiting absorption (Niemi et al. 2003b). P-gp inhibitors known to cause a clinically significant inhibitory drug interaction on intestinal P-gp include tacrolimus, cyclosporin A, verapamil, and quinidine (Wandel et al. 1999), itraconazole (Fenner et al. 2009), ritonavir (Drewe et al. 1999), while rifampin has been shown to induce intestinal P-gp only (Greiner et al. 1999).

Because P-gp is also located in other tissues, it is sometimes difficult to establish that a P-gp inhibitor affects systemic exposure only by acting on intestinal P-gp and not other tissues. Perhaps the best example of inhibition of only intestinal P-gp is the interaction between digoxin, a P-gp substrate, and quinidine, a P-gp inhibitor. When digoxin was repeatedly administered orally to steady state followed by an intravenous bolus dose of $^3$H-digoxin in the presence of quinidine, a nearly 80% increase in the Cmax and AUC of unlabeled digoxin and a 15% increase in absolute bioavailability was observed compared to controls (Pedersen et al. 1983). Since digoxin is not metabolized, it can be inferred that this effect was due to inhibition of intestinal P-gp by quinidine.

The pharmacokinetics of digoxin (oral and iv) before and after coadministration of rifampin has also been studied (Greiner et al. 1999). The AUC of oral digoxin was significantly lower during rifampin treatment, although the effect was less pronounced after intravenous administration of digoxin. Both digoxin renal clearance and half-life were not altered by rifampin. Duodenal

**Fig. 13.4** Numbers of published papers/patents on major human transporters. Presentation by SM Huang, AAPS ISSX workshop Nov 10, 2007 San Diego CA (http://www.fda.gov/ohrms/dockets/ac/06/slides/2006-4248s1-indes.html, accessed August 2010)
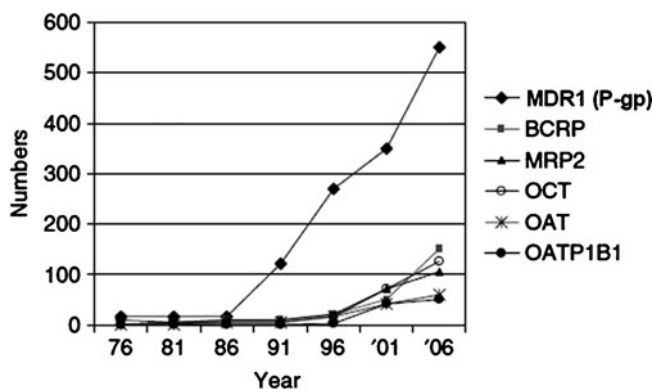
biopsies indicated that P-gp content increased 3.5-fold after rifampin treatment, which correlated with the AUC after oral digoxin but not after intravenous digoxin, indicating that the intestine is the primary site of interaction. Given the fact that rifampin is known to interact with the PXR and PXR regulates expression of P-gp (vide infra), the rifampin–digoxin interaction appears to be mediated by induction of intestinal P-gp.

As previously mentioned, P-gp is also located in several other tissues, leading to other possible sites for drug interactions. For example, P-gp is located on the canalicular membrane of the hepatocytes and is important in biliary excretion. Itraconazole, quinidine, and ritonavir have been shown to inhibit the biliary excretion of digoxin (Endres et al. 2006). For example, quinidine caused a nearly 50% reduction in the steady-state biliary clearance of digoxin (Hedman et al. 1990) and verapamil caused a 43% in biliary clearance of digoxin (Hedman et al. 1991). Subsequent in vitro studies established that quinidine and verapamil were effective P-gp inhibitors (Wandel et al. 1999).

P-gp, also located on the luminal surface of renal proximal kidney cells, is important in the final step of renal secretion. Itraconazole (Jalava et al. 1997), quinidine (Hedman et al. 1990) and ritonavir (Ding et al. 2004) have all been show to decrease renal secretion of digoxin in vivo. Separate in vitro studies established that itraconazole (Wang et al. 2001), quinidine (Wandel et al. 1999), and ritonavir (Drewe et al. 1999) inhibited P-gp. P-gp is also a crucial component of the BBB, so a drug interaction affecting P-gp might serve to affect brain concentrations of a drug. An example of this phenomenon is the interaction between verapamil and CsA in which positron emission tomography (PET) imaging was used to indicate that brain verapamil levels increased upon inhibition of P-gp by CsA. Because the brain has a low volume of distribution, there was no corresponding change in plasma concentrations (Sasongko et al. 2005).

### 13.3.1.2 Inhibition of BCRP

BCRP is another significant efflux transporter located in the intestine, and a clinically significant drug interaction has been observed between topotecan, a BCRP substrate, and GF120918, a BCRP inhibitor (Allen et al. 1999). After oral administration of topotecan (1 mg/m$^2$), with and without of GF120918 (1,000 mg), the AUC of total topotecan increased 2.4-fold, Cmax increased 2.8-fold, and the apparent bioavailability in this cohort increased significantly from 40.0 to 97.1% (Kruijtzer et al. 2002). BCRP may also be involved in the interaction between methotrexate and pantoprazole, both known to be BCRP substrates (Breedveld et al. 2004). Troger et al. 2002 reported that coadministration of pantoprazole with methotrexate resulted in a 70% increase in the plasma levels of the metabolite 7-hydroxy-methotrexate in a cancer patient, as well as a greater incidence of severe myalgia. This effect presumably results from inhibition of renal excretion of methotrexate by pantoprazole, which exposes methotrexate to other routes of clearance such as metabolism to its 7-hydroxy metabolite.

### 13.3.1.3 Inhibition of OATP-Mediated Hepatic Uptake

Inhibition of OATP-mediated hepatic uptake has been demonstrated to be the mechanism for a number of clinically significant drug interactions. OATP1B1 has been shown to actively transport many substrates such as the statins atorvastatin, lovastatin, pravastatin, and rosuvastatin (Schneck et al. 2004; Simonson et al. 2004), as well as valsartan (Yamashiro et al. 2006), and olmesartan (Yamada et al. 2007). Interactions with these OATP1B1 substrates have been reported for OATP1B1 inhibitors, including cyclosporine A (Simonson et al. 2004), gemfibrozil (Schneck et al. 2004), rifampin (Lau et al. 2007), repaglinide (Bachmakov et al. 2008) and ritonavir (Hirano et al. 2006). For example, coadministration of CsA increased atorvastatin AUC by 7.4-fold (Asberg et al. 2001), for lovastatin by 20-fold (Olbricht et al. 1997), and pravastatin by between five- and tenfold (Regazzi et al. 1993; Olbricht et al. 1997 and Hedman et al. 2004). Similarly, coadministration of gemfibrozil increased the AUC of repaglinide by eightfold (Niemi et al. 2003a), and coadministration of

rifampicin increased the AUC of atorvastatin by sevenfold (Lau et al. 2007).

The interaction of CsA and cerivastatin is noteworthy because it is an example the complexity of transporter interactions when inhibition of DMEs is also involved. CsA was shown to cause a nearly fivefold increase of cerivastatin AUC and Cmax (Muck et al. 1999). Later in vitro studies demonstrated that one possible mechanism was that CsA inhibited OATP1B1 (Shitara et al. 2003). However, CsA also inhibits both CYPs 3A4 and 2C8 as well, so this undoubtedly contributes to the overall magnitude of the interaction. Similarly, coadministration of gemfibrozil, another inhibitor of OAT1B1, also causes a 4.4-fold increase in cerivastatin (Backman et al. 2002). However, cerivastatin is metabolized by CYP2C8 (major) and CYP3A4 (minor), and gemfibrozil also inhibits theses DMEs (Wang et al. 2002). Other examples of OATP drug interactions can be found in several recent reviews (Neuvonen et al. 2006; Poirier et al. 2007; Kalliokoski and Niemi 2009; Kindla et al. 2009).

### 13.3.1.4 Inhibition of OAT-Mediated Renal Excretion

There are three organic anion uptake transporters located on the basolateral (serosal) membrane of the kidney proximal tubule, OAT1, OAT2, and OAT3. OAT4 is located on the luminal membrane and is involved in secretion of intracellular drug into urine. Of these, OAT1 and OAT3 have been implicated in drug interactions that result in increased plasma concentrations and/or reduced renal CL. Although a comprehensive list of renal OAT-mediated interactions will not be provided, some of the affected substrates include cefamandole (Takeda et al. 2002a), furosemide (Hosoyamada et al. 1999), methotrexate (Takeda et al. 2002b), ACV, ganciclovir (GCV), and zidovudine (AZT) (Takeda et al. 2002c). Probenecid has been the most widely studied OAT inhibitor, although salicylate, phenylbutazone, indomethacin (Takeda et al. 2002b) have also been established as inhibitors.

In many cases, the clinical drug interactions have been known for years, long before the roles of inhibition of OAT uptake transporters were established. For example, it has been known for years that NSAIDs inhibit renal secretion of methotrexate (Frenia and Long 1992), sometimes resulting in severe adverse events (Thyss et al. 1986). The interaction between probenecid and cephalosporin antibiotics has also been known for some time. For example, oral administration of probenecid before a single intramuscular dose of cefamandole resulted in a nearly twofold increase in serum levels of cefamandole than when cefamandole was given alone (Griffith et al. 1977). Administration of probenecid was shown to increase the AUC of cephadrin and cefaclor by 2.4-fold and 2.1-fold, respectively, and Cmax by 1.9-fold and 1.5-fold, respectively (Welling et al. 1979).

In another study, probenecid was also found to decrease the renal CL of nafcillin by 72% (Waller et al. 1982). Coadministration of probenecid also was shown to interact with AZT, causing a twofold increase in the mean AUC, a corresponding decline in the apparent total clearance, and a prolongation in the mean half-life (de Miranda et al. 1989). Coadministration of probenecid caused famotidine AUC to increase 1.8-fold while both the excretion rate of unchanged famotidine in urine over 24 h and the mean tubular secretion clearance of famotidine was decreased by nearly 90% (Inotsume et al. 1990). More recently, it was demonstrated that probenecid decreased renal CL by 66% for furosemide (Li et al. 2006), and by 68% for of fexofenadine (Yasui-Furukori et al. 2005).

In recent years, the roles of specific OAT transporters in these interactions have begun to be sorted out. Takeda et al. (2002b) demonstrated that NSAIDs (salicylate, ibuprofen, ketoprofen, phenylbutazone, piroxicam, and indomethacin), probenecid, and penicillin G inhibited methotrexate uptake mediated by human-OAT1 (hOAT1), hOAT3, and hOAT4. The same group also established that ACV and GCV were actively taken up by hOAT1, AZT was observed in hOAT1-, hOAT2-, hOAT3-, and hOAT4-expressing cells, and that probenecid could inhibit AZT uptake by hOAT1 (Takeda et al. 2002b). The cephalosporin antibiotics cephalothin, cefoperazone, cefazolin,

ceftriaxone, cephaloridine, cefotaxime, cefadroxil, and cefamandole significantly inhibited organic anion uptake mediated by hOAT1, and to a lesser extent, human-OAT3 and human-OAT4 (Takeda et al. 2002c). In studies using human kidney slices, it was demonstrated that salicylate, indomethacin, phenylbutazone, and probenecid inhibited the uptake of methotrexate at concentrations comparable to plasma concentration observed clinically. In particular, inhibition of renal uptake via OAT3, along with contributions from and efflux processes (via MRP2 and MRP4), is the likely explanation for site of drug–drug interaction for methotrexate with probenecid and some NSAIDs (Nozaki et al. 2007).

However, to put this in perspective, according to a recent review by Ayrton and Morgan (2008), in terms of safety, drug–drug interactions with OATs are generally of limited clinical consequence to drug safety. Obviously this depends on the therapeutic margin of the substrate in question, but concern regarding OAT interactions maybe limited to interactions with the OAT substrate methotrexate and potent OAT inhibitors (Uwai et al. 2000; Nozaki et al. 2007).

### 13.3.1.5 Inhibition of OCT2

In addition to OAT1, OAT2, and OAT3, OCT2 is the other major uptake transporter on located on the basolateral serosal membrane of the kidney proximal tubule cells and undoubtedly contributes to some drug interactions involving renal secretion. Similar to OATs, inhibition of OCT2 would lead to increased systemic exposure and/or decreased renal CL. Drugs known to be substrates of OCT2 include cimetidine, metformin, procainamide, and varenicline (Tsuji 2002; Jonker and Schinkel 2004; Koepsell et al. 2007; Ciarimboli 2008).

Reports of drug interactions involving decreased renal CL have been reported for years prior to investigation of OCT2 and its substrates and inhibitors. For example, coadministration of cimetidine, a known inhibitor of renal tubular secretion of organic bases via the cationic transport system, increased the AUC of metformin by 50% while decreasing renal CL by 27%

(Somogyi et al. 1987). Similarly, coadministration of cimetidine also decreased the renal CL of procainamide by 44% (Somogyi et al. 1983) and AZT by 56% (Fletcher et al. 1995). Coadminstration of trimethoprim decreased the renal CL of AZT by 27%.

More recently, when dofetilide was administered with cimetidine, the plasma AUC of dofetilide increased by as much as 48% while renal CL was reduced by 33% and nonrenal clearance by 21% (Abel et al. 2000). This interaction is important enough to be listed as a black box warning on the package insert for dofetilide (Tikosyn®). Because of overlapping substrate specificity with the OATs, it is difficult to establish to what extent OCT2 is involved in decreased renal secretion. Nevertheless, in vitro studies have established that cimetidine (Motohashi et al. 2004), metformin (Kimura et al. 2005), procainamide (Gorboulev et al. 1997), and varenicline (Feng et al. 2008) are all substrates of OCT2.

### 13.3.2 Clinically Relevant Genetic Polymorphisms of Drug Transporters

As is the case for CYPs and other DMEs, genetic polymorphisms have been identified in many drug transporter proteins. Given the key role transporters play in drug disposition, these variants undoubtedly make a significant contribution to interindividual variation in pharmacokinetics, drug response (Maeda and Sugiyama 2008; DeGorter and Kim 2009), and drug safety (Maeda and Sugiyama 2008; Link et al. 2008). In addition to these, there have also been recent reviews specifically on genetic variation in many of the important transporters, including the ABC transporters P-gp (Cascorbi 2006; Chinn and Kroetz 2007), BCRP (Cascorbi 2006; Maeda and Sugiyama 2008), OATP (Maeda and Sugiyama 2008), OAT (Zair et al. 2008) and OCT (DeGorter and Kim 2009). A comprehensive listing of genetic polymorphisms of drug transporters is beyond the scope of this chapter. Instead, a few key examples will be presented on where the

genetic variants of transporters have influenced the pharmacokinetics of selected drugs, and in so doing affected the efficacy and safety of these drugs.

### 13.3.2.1 P-gp

Because of the importance P-gp in drug disposition, a large body of work has been published linking genetic variants of the gene (ABCB1) for this efflux transporter to pharmacokinetics, pharmacodynamics, and disease susceptibility. These studies have documented at least 100 mutations of this gene (Maeda and Sugiyama 2008). Unfortunately, despite this enormous body of work, the associations of these studies have not been consistently reproducible. For example, using digoxin as a substrate, it has been shown vitro that genetic variants of MDR1 decreased intracellular digoxin accumulation, suggesting that increased P-gp function may be found in such subjects with these variants (Kim et al. 2001).

However, subsequent clinical investigations have failed to establish an unequivocal relationship of P-gp function with common variants such as the G2677T and C3435T polymorphisms. Some studies have shown decreased digoxin exposure, some have shown increased exposure, and others have shown no effect (Chinn and Kroetz 2007). Fexofenadine, another well-characterized P-gp substrate, has also been extensively studied with respect to the influence of the genetic variants G2677T and C3435T on drug exposure. Yet, like digoxin, the clinical results are mixed. Some studies have shown no correlation between the 3435C4T polymorphism and fexofenadine exposure (Drescher et al. 2002), while others have found increased exposure as a result in 2677T/3435T homozygotes (Yi et al. 2004). In a recent review, data for 15 P-gp substrates were summarized for the function of MDR1 by the C3435T variant. As stated above, there were many examples in which P-gp function increased with this variant, but there were also reports of the opposite effect. However, the dominant trend was that there was no difference in P-gp function as a result of this genetic variant (Maeda and Sugiyama 2008).

Clearly, more careful, better controlled clinical studies which control for environmental and other nongenetic as well as genetic factors are still needed to establish a consistent effect between variants of MDR1 and in vivo drug action of P-gp substrates.

### 13.3.2.2 OATP1B1

Genetic variants which decrease the function of the liver uptake transporter OATP1B1 have recently been implicated as an increased risk factor for statin-induced myopathy. In a genome-wide association study, at least one common variant in SLCO1B1 was identified that was strongly associated with an increased risk of simvastatin-induced myopathy. More than 60% of these myopathy cases could be attributed to the C allele of the rs4149056 polymorphism, which is also associated with higher blood concentrations of statins (Link et al. 2008). Similarly, a group of Japanese workers also found that the frequency of OATP-C*15 is significantly higher in patients who experienced myopathy after receiving pravastatin or atorvastatin than in patients without myopathy (Morimoto et al. 2004).

Recently, it has been reported that after administration of irinotecan to patients with non-small cell lung carcinoma , plasma concentration of SN-38, an active metabolite of irinotecan, was significantly higher in those patients withT521C mutation in SLOC1B1 compared with nonholder of this mutation. Moreover, the frequency of Grade 4 neutropenia was significantly higher in this same subset of patients, presumably due to the increased systemic exposure of SN-38 (Han et al. 2008).

### 13.3.2.3 OCT1

OCT1 is known to play an important role in the hepatic uptake of metformin. Thus, it is not surprising that variants of the gene for OCT1 (SLC22A1) have been shown to have a significant effect on metformin pharmacokinetics. Individuals carrying reduced function OCT1 alleles had higher AUC, higher Cmax, and lower oral volume of distribution of metformin (Shu et al. 2008). Given the importance of this transporter to the uptake of metformin into the liver, its

target tissue, this may explain why the effects of metformin in glucose tolerance tests were significantly lower in subjects with reduced function alleles of OCT1 (Shu et al. 2007).

#### 13.3.2.4 OCT2

OCT2-mediated uptake into kidney proximal tubule cells is the first step in the renal excretion of metformin, so the pharmacokinetics of this drug can also be influenced by variants in the gene for OCT2 (SLC22A2). It has been shown that subjects with reduced function genetic variants of SLC22A2 showed significant differences when compared with the reference genotype, with higher metformin Cmax and AUC, and lower renal CL (Song et al. 2008).

## 13.4 Evaluation of Drug Transporters in Drug Discovery and Development

As with CYPs and other DMEs, investigation of the role of that transporters play in the disposition of drugs and as potential mechanisms for drug interactions is now gaining attention in the development of new drugs (Zhang et al. 2010). Of course, like any applied research activity, investigation of transporters can only be justified to the extent that such research improves the safety and efficacy and ultimately reduces attrition of drug candidates (Kohl 2009; Ayrton and Morgan 2008).

This section will describe transporter research activities during the drug discovery stage, as well as during preclinical development and clinical development. Finally, a brief summary will be presented of regulatory issues around drug transporters that may arise during the NDA submission, approval and, ultimately, product labeling process.

### 13.4.1 Discovery Stage

Any activity applied during the Discovery stage must, of necessity, be amenable to high throughput screening (HTS) and rapid turnaround time.

Perhaps the best example of such an evaluation is Caco-2 screening for drug absorption. Using an automated, transwell study design, flux of drug candidates across a monolayer of Caco-2 cells can be measured. Of course, this is only an indirect indication of the involvement of transporters, as Caco-2 cells measure the combined effect of passive diffusion, active uptake by transporters such as PEPT1 or MCT1, and efflux by transporters such as P-gp or BCRP. If a more precise definition of the role of uptake or efflux transporters is needed, other cell lines such as MDCK with a singly expressed transporter are used. For example, MDR1-MDCKII cells with active P-gp are often used as a screening tool in programs for the discovery of CNS compounds. It has been demonstrated that whether a compound is a substrate for P-gp is a critical component in CNS activity in that most marketed CNS drugs are less likely to be substrates (Mahar Doan et al. 2002).

Other high throughput screens for P-gp are the so-called ATPase (Ishikawa et al. 2005) or calcein-AM receptor-based assays (Mahar Doan et al. 2002). Mahar Doan and coworkers (2002) concluded that the interaction with P-gp measured by efflux is a better discriminator between CNS and non-CNS drugs than when measured by calcein-AM. The problem with these assays is that while they are certainly amenable to high throughput, these receptor assays cannot distinguish between whether a compound is a substrate or inhibitor of P-gp.

Increasingly, in silico methods are being developed for predicting transporter interaction (Ekins et al. 2007). For example, it could be very useful to predict based on structure alone whether compounds in a library are substrates for P-gp. In theory, selecting compounds with minimal interaction with this P-gp would tend to facilitate bioavailability and CNS permeability. In silico screening could also be used to develop SAR to increase interaction with PEPT1 in order to enhance absorption of peptide like moieties. In another important application of in silico methods, physiologically based pharmacokinetic modeling combined with in vitro and in vivo animal data has recently been used to examine the effects of

transporter activities on the systemic and liver exposure of pravastatin (Watanabe et al. 2009). This approach could be used at virtually any stage of drug discovery and development, although the reliability increases as more in vivo and in vitro data are available later in development.

## 13.4.2 Preclinical Development Stage

Once a NME becomes a clinical candidate and enters the preclinical development stage, it is essential to begin the process of more fully characterizing the routes of absorption, distribution and clearance, and assessing the potential for drug–drug interactions. As is the case for CYPs and other DMEs, transporter studies at this stage are designed to be more comprehensive and to more fully characterize a drug as an inhibitor and/or substrate of key transporters. There are a multitude of nonclinical studies, both in vitro and in vivo, that can be done to evaluate interaction of the candidate and drug transporters.

### 13.4.2.1 Determination of the Potential for a Transporter-Based Drug Interaction

A major goal in preclinical pharmacokinetics is to predict the likelihood of a drug interaction between the drug in question and other likely concomitant medications. Typically, analogous to the scenario with CYPs, the first question usually investigated is whether the development candidate is an inhibitor (or less likely, inducer) of a transporter and as such, could impact the clearance of another drug. The second question to investigate is whether the development candidate is a transporter substrate to the degree that a transporter inhibitor or inducer could impact its absorption, distribution, or clearance. The timing and extent of these studies vary considerably from compound to compound and also vary with the development group's budget and risk tolerance. A general rule of thumb is that enough information must be known to determine the potential for a drug interaction prior to the first clinical study where concomitant drugs will be administered, typically Phase 2A. The FDA

issued a draft guidance to industry in 2006 that addresses these issues for both CYPs (and other DMEs) as well as transporters. In one of the appendices to this guidance, an outline of an experimental protocol for a "definitive" in vitro transporter-based drug interaction study was provided, along with a decision tree.

Based on the literature on drug interactions available at the time, P-gp was the only transporter mentioned in FDA's guidance on drug interactions for which specific studies were recommended. The decision tree for whether a drug candidate is an inhibitor for P-gp is depicted in Fig. 13.5. The 2006 Guidance recommended that bidirectional transport study design with stably expressed human P-gp (Caco-2 or MDCKII cells) be used because only this type system allows assessment of the true vectorial transport reflective of the in vivo situation.

In order to determine whether a test compound is an inhibitor of P-gp, the compound is added to a system along with a known P-gp substrate such as digoxin. If the net flux ratio, that is, the ratio of flux in the basolateral to apical direction (B→A) divided by the flux in the apical to basolateral (A→B) direction is unaffected by increasing concentrations of the test drug, then the test drug is a not considered to be a P-gp inhibitor and no further action is needed. However, if the net flux ratio is decreased with increasing concentrations of the test drug then the test drug is a probable P-gp inhibitor. At this point, further in vitro studies are warranted to determine the $IC_{50}$ or $K_i$ of P-gp inhibition. If the ratio of the expected unbound plasma concentration of the test drug divided by its the $K_i$ (or $IC_{50}$) for P-gp inhibition is >0.1, a clinical drug interaction study may be warranted.

In addition, if a test drug is determined to be a P-gp inhibitor, then it is quite possible it could also be a substrate for P-gp and vulnerable to interactions with known P-gp inhibitors (or inducers). A decision tree for determining whether a test drug is a P-gp substrate is depicted in Fig. 13.6. The experimental design is similar to the inhibitor decision tree except, in this case, the net flux ratio of the test drug is determined first.
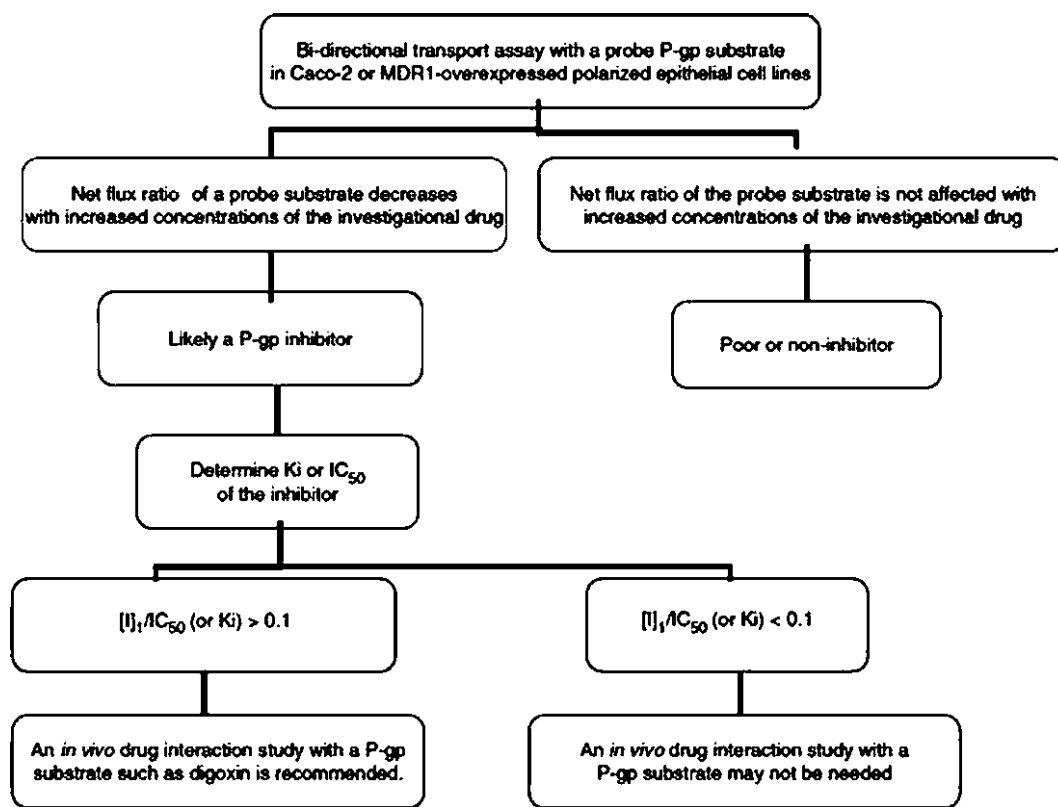
**Fig. 13.5** FDA decision tree to determine if an investigational new drug is a P-gp inhibitor. Slide adapted from FDA's Guidance to Industry: Drug Interactions, 2006 (http://www.fda.gov/downloads/Drugs/GuidanceComplianceRegulatoryInformation/Guidances/ucm072101.pdf, accessed August 2010)

A net flux ratio of <2.0 indicates the test drug is not a P-gp substrate and no further action is warranted. However, if the net flux ratio is >2.0, a follow-up study is undertaken with one or more known P-gp inhibitors such as verapamil, CsA, ketoconazole, or erythromycin. If the net flux ratio is decreased, the test compound is likely to be a P-gp substrate and a follow-up clinical drug interaction study may be warranted.

Although the 2006 draft Drug Interaction Guidance provides a decision tree and recommends studies specifically for P-gp, reports of drug interactions mediated by other transporters continue to accumulate in the literature. Several recent publications have suggested situations for when it may be appropriate to consider similar studies with other transporters. In particular, the 2010 ITC review (Giacomini et al. 2010) depicts

several additional decision trees to test for a compound as an inhibitor or substrate of other transporters, such as OATs, OCTs, and OATPs. For example, renal uptake transporters such as OAT1, OAT3, or OCT2 might be considered if renal CL is greater than 50% of total clearance or if the secretory component of renal CL is more important than glomerular filtration. If so, then bidirectional transport studies with polarized cell lines should be conducted determine if the test drug is an inhibitor and/or substrate for these transporters.

Similarly, studies with biliary uptake transporters such as OATP1B1 or OATP1B3 should be considered if the hepatic elimination of unchanged drug is an important part of overall CL. If hepatic CL is >30% of total CL and if the drug's physicochemical properties suggest poor
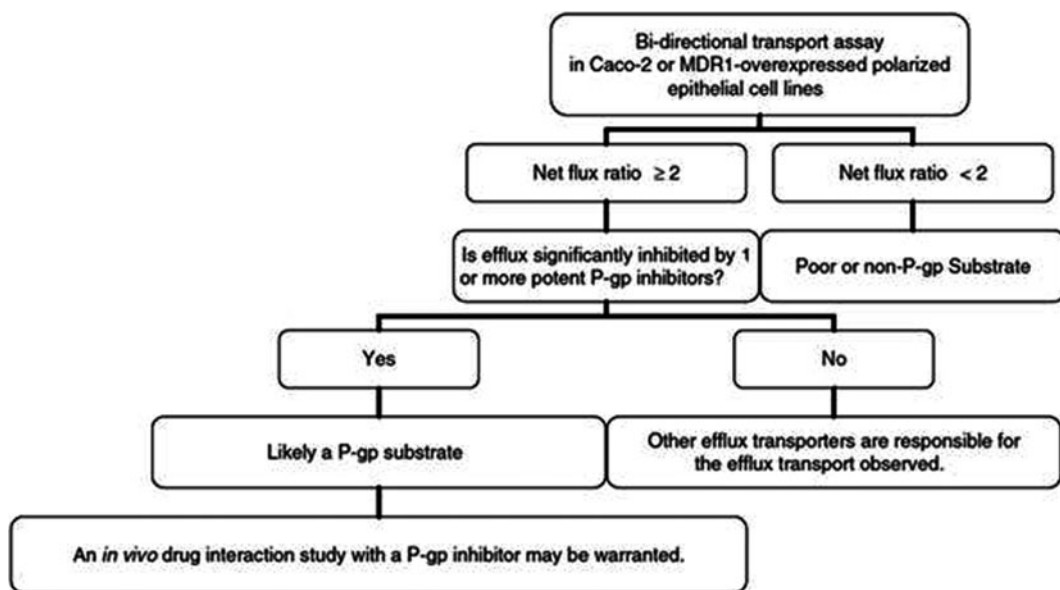
**Fig. 13.6** FDA decision tree to determine if NCE is P-gp substrate. Slide adapted from FDA's Guidance to Industry: Drug Interactions, 2006 (http://www.fda.gov/ downloads/Drugs/GuidanceComplianceRegulatoryInformation/Guidances/ucm072101.pdf, accessed August 2010)

passive perfusion, then bidirectional transport studies with polarized cell lines expressing OATP1B1 or OATP1B3 should be conducted determine if the test drug is an inhibitor and/or substrate for these transporters.

### 13.4.2.2 Other Nonclinical Systems to Understand Mechanism of Transporter Efflux or Uptake

Apart from the use of bidirectional transport studies with Caco-2 or MDR1/MDCKII cell lines just described, there are often situations in which additional information on the mechanism of efflux or uptake by transporters may be desired. While Caco-2 or MDR1/MDCKII cell lines can also be used for mechanism studies, there are also many other experimental techniques to further elucidate the mechanism of drug–transporter interactions. The following information has been compiled from several key review articles (Ghibellini et al. 2006a, b; Ayrton and Morgan 2008; Klaassen and Lu 2008; Giacomini et al. 2010). References to specific techniques can be found within these reviews.

*Hepatocytes*. Fresh or frozen isolated hepatocytes in suspension have proven to be a very useful for hepatic uptake and/or metabolism studies. Of course, like any primary cell, isolated hepatocytes express the full complement of drug transporters and DMEs, which can be both an advantage and a limitation. Hepatocytes are ideal for getting a general overview of hepatic uptake, and to study the interplay between uptake and hepatic metabolism. However, it is difficult to sort out the contribution of a single hepatic transporter using primary hepatocytes. Recently, this limitation has been addressed by knocking down selected transporters by adenoviral vector-mediated RNA interference (RNAi).

Isolated hepatocytes are limited by the lack of normal cell polarity, so canalicular efflux cannot be studied. To address this, sandwich-cultured primary hepatocytes have been developed which express functional and extensive bile canalicular networks. These cells exhibit normal cell polarity, and direct access to the both hepatocyte and adjacent biliary compartment. As such, they are useful to study both basolateral uptake and canalicular efflux transport processes, which make them ideal

for studying the overall process of biliary excretion in vitro.

*Heterologous Expression in Whole Cells*. As stated above, hepatocytes express multiple uptake and efflux transporters, as well as DMEs. In cases where individual transporters need to be studied, other whole cell systems for heterologous expression of individual or specific combinations of transporters are available. An example of one such system is the *Xenopus laevis* (frog) oocyte. When transfected with the transporter of interest, oocytes can be a useful tool for functional studies such as the determining the kinetics of transport, or systematically sorting out the contribution of individual transporters. Many different transporters have been expressed in oocytes, including OATP1B1 and OATP1B3, OCTs, OATs, and PEPT. The main disadvantage with oocytes is that they are a transient expression system and need to be injected individually with cRNA of the transporter protein of interest. This disadvantage is offset, in part, because this system is readily available commercially for certain transporters.

However, for continued use, or for use with a specific transporter or combination of transporters, stably transfected cell lines may be preferred. Many cell types are commonly used for stable transfection of transporter genes, including the aforementioned MDCKII cell lines, as well as human embryonic kidney (HEK 293) or Chinese hamster ovary (CHO) cell lines. These cell lines can be maintained in culture for sustained periods and can be ready for use in a specific experiment within a few days. In addition, these cells can be singly, doubly or even multiply transfected to produce transporter systems of variable complexity, depending on the experimental objective. Even Caco-2 cells, which express multiple transporters, may be useful to study individual transporters when used in combination with the previously mentioned RNAi technique to knockdown transporters not of interest.

*Membrane Vesicles*. There are occasions where subcellular transporter preparations might best meet the experimental objective. In such cases, membrane vesicles isolated from animal hepatocytes or kidney cells can be a useful tool. For example, renal proximal tubule membrane vesicles from either the brush border (luminal) side or the basolateral (serosal) side of the membrane can be isolated from kidney cells. Similarly, hepatocyte membrane vesicles, such as those on the basolateral side, as well as those from the bile canalicular side, can be isolated from hepatocytes. In addition to primary cell lines, membrane vesicles can also be isolated from a wide variety of cultured cell lines, including Caco-2, and Caki-1, a proximal tubule representative cell line, as well as custom transfected and baculovirus-infected cell lines. Many different transporters have been studied using membrane vesicles, including both efflux transporters (e.g., P-gp, and BCRP), as well as uptake transporters (e.g., OCTs and OATs). Although membrane vesicles are an important research tool, there is an inherent limitation in their use. If the membrane vesicles are isolated from kidney or liver cells, or from cell lines expressing multiple transporters (e.g., Caco-2 cells) rather than specific cell lines, they will contain several transporters isolated together. Thus, any interpretation of the results must account for the combined effects of multiple transporters.

*In Vivo Models*. Knockout mouse models are a powerful tool in the determination of whether a drug is a substrate or inhibitor for a given transporter (Klaassen and Lu 2008). A great deal about tissue localization sites have been learned from experiments with transgenic mice. For example, one of the first studies to demonstrate the important role of P-gp in the BBB was carried out in an Mdr1 knockout mouse model (Schinkel et al. 1994). Pharmacokinetic studies in knockout mouse models have been invaluable in determining the role a given transporter plays in the disposition of drugs and xenobiotics. Knockout mouse models are *available for many common transporters*, including Mdr1a or Mdr1a/b (P-gp), Bcrp−/− and Abcg−/− (BCRP), Oct−/−, Oat1−/− and Oat3−/−, Oatp1b2−/−. However, as with all animal studies, the results must be interpreted with caution when attempting to extrapolate results to humans. There are definite species differences in expression levels and tissue

locations and even substrate specificities of drug transporters

Transgenic mice bred to express human transporters are another powerful animal model. PK experiments in transgenic animals may be more directly applicable to humans because the transporters expressed are actually human transporters. A good example of the use of transgenic mice comes from the study of methotrexate pharmacokinetics in transgenic mice with liver-specific expression of human OATP1B1 (van de Steeg et al. 2009).

## 13.4.3 Clinical Development Stage

As described earlier, as recommended by the FDA guidance on drug interactions, bidirectional in vitro transport studies are now routinely conducted to determine whether a development candidate is a P-gp inhibitor or inducer. Soon similar studies may be routine for other transporters. Should the results of such studies be positive, a clinical drug interaction study may be warranted. However, unlike DMEs, the role of individual transporter activity for the PK a given drug is still is poorly understood, in part because of broad substrate specificity the overlaps multiple transporters and DMEs. Further, the lack of selective substrates makes it difficult to study drug transporter-mediated drug interactions in clinical pharmacokinetic setting, although this is an area of ongoing study.

At the present time, P-gp is the only transporter with a (relatively) specific substrate: digoxin. Other potential substrates for P-gp, such as talinolol and fexofenadine, are being investigated, but so far the results are equivocal (Fuhr et al. 2007). Nevertheless, digoxin is a particularly useful substrate for determining P-gp based drug interactions because readily availability in both radiolabeled and nonradiolabeled form and can be administered both orally and intravenously. Furthermore, digoxin is not metabolized and thus it measures only transport and not the interplay of transport and metabolism. On the other hand, while digoxin is a relatively specific substrate for P-gp, there is a high

degree of intersubject variability in digoxin pharmacokinetics, presumably due to genetic polymorphisms of P-gp (Fuhr et al. 2007), especially with Cmax, which confounds interpretation of drug interaction studies. While normally administered alone with the test drug, digoxin is also now being administered as part of a drug interaction "cocktail", e.g., the "Cologne cocktail" (Fuhr et al. 2007). Furthermore, P-gp is expressed in multiple tissues throughout the body, which complicates interpretation of the pharmacokinetic results. The fact that digoxin can also be administered both orally and intravenously, has been used sort out the contribution of intestinal P-gp relative to other tissues where P-gp is located (Rengelshausen et al. 2003; Fenner et al. 2009). Sometimes these studies have been accompanied by intestinal biopsies and direct measurement of P-gp protein to see if the results correlate with the observed pharmacokinetic effect.

As mentioned, P-gp is located in many other tissues, including on the luminal membrane of the renal proximal tubule where it impacts renal excretion and the bile canalicular membrane which impacts biliary excretion. The urine compartment is readily accessible, so P-gp drug interactions at the level of renal excretion can be sorted out by the difference between renal and total body clearance after intravenous administration. However, access to the bile compartment is difficult, making it technically challenging to measure P-gp drug interactions at the level of biliary excretion, at least in the healthy volunteers frequently used in drug interaction studies. Two clinical studies of the interaction between digoxin and P-gp inhibitors quinidine (Hedman et al. 1990) or verapamil (Hedman et al. 1991) are examples of how the relative contributions of P-gp transporter to biliary and renal excretion can be distinguished. In these studies, healthy volunteers were administered digoxin orally with and without quinidine or verapamil. Following treatment, the subjects were catheterized with a duodenal triple-lumen perfusion catheter to give an unambiguous measurement of biliary clearance of digoxin. However, such direct measurements of biliary

excretion remain technically challenging and infrequently utilized.

P-gp is also expressed at the BBB, which is another technically challenging compartment to sample. Recently, a novel noninvasive quantitative imaging technique was used to measure the contribution of P-gp activity at the BBB. In this study, carbon-11-labeled verapamil was used as the P-gp substrate and the effect of the P-gp inhibitor cyclosporine was measured. Brain PET was used to measure brain 11C-labeled verapamil concentrations. Brain uptake of 11C-radioactivity ($AUC_{brain}/AUC_{blood}$) was determined in the presence and absence of cyclosporine (Sasongko et al. 2005).

### 13.4.4 NDA Submission Stage

It is clear from the language in the 2006 draft guidance on drug interactions, the number of presentations and publications originated from FDA authors, as well their participation on the ITC, that the FDA is keenly aware of the pivotal role that transporters play in drug disposition, as well as drug interactions and other adverse effects. Increasingly, information regarding transporters is being included in drug labeling language in new drug applications. For example, OATP1B1 polymorphisms associated with adverse reactions such as liver toxicity with certain statins are mentioned prominently in their warning labels. Also, drug interactions via transporters now more commonly reported in the literature. Accordingly, warnings for interactions on drug labels are also more common, especially for drugs with low therapeutic index such as methotrexate and NSAIDS. Not surprisingly, drugs that are P-gp substrates have received the most attention as exemplified by the fexofenadine label warning of a possible interaction with P-gp inhibitors. Examples of drugs with warnings for other transporters include dofetilide and pramipexole, which are potentially vulnerable to interactions with OCT inhibitors, sitagliptin (Januvia®), which is vulnerable to interaction with OAT-3 inhibitors

and atorvastatin (Lipitor®), which is vulnerable to interactions with OATP1B1 inhibitors.

## 13.5  Conclusion/Summary

Research on the class of proteins known collectively as drug transporters has exploded over the past 30 years. It is now recognized that drug transporters join DMEs in forming a complex gauntlet of proteins that has evolved to control access of xenobiotics to mammalian bodies. Transporters are located in virtually every organ and tissue in the body and are involved in every aspect of drug absorption, distribution, and excretion. In addition, transporters even influence metabolism of xenobiotics by controlling access to the cellular locations of dug metabolizing enzymes. Because of their ubiquity and function, drug transporters profoundly influence drug pharmacokinetics. Moreover, intrinsic and extrinsic factors which influence drug transporter function, such as genetic polymorphisms or transporter-based drug interactions, can have a major impact on drug efficacy and safety.

Because of this significant role in drug safety and efficacy, the importance of transporters is gaining the attention of regulatory agencies. The revised 2006 FDA Guidance on drug interactions included information on transporters for the first time and provided a decision tree for evaluation of drugs as substrates or inhibitors of P-gp. Furthermore, as one activity of the US FDA's Critical Path Initiative, the agency has been active in establishment of the ITC. The recently published report from the ITC workshop held in October 2008 has signaled the increased regulatory interest in understanding the role that transporter-based drug interactions and genetic polymorphisms play in drug safety and efficacy. Indeed, transporter information is becoming increasing more significant in recent NDA submissions. Furthermore, because earlier submissions may have lacked transporter information, in some cases, the FDA has recently asked for postmarketing studies of potential transporter-mediated drug–drug interactions.

Investigation of the role that transporters play in the disposition of drugs and as potential mechanisms for drug interactions is now also gaining the attention of the companies involved in the discovery and development of new drugs. At the present, attention given to transporters in drug development is relatively modest compared to CYPs and other DMEs. However, this research will undoubtedly increase as evidence accumulates that a thorough understanding of transporters can improves the safety and efficacy and ultimately reduces attrition of drug candidates.

Research into drug transporters at the molecular, preclinical, and clinical levels is a vibrant endeavor and undoubtedly will remain well into the future. If the past progress is any indication, continued advancement in the knowledge of how transporters influence drug disposition will certainly lead to discovery and development of safer and more effective new drugs.

# References

Abel S, Nichols DJ, Brearley CJ and Eve MD (2000) Effect of cimetidine and ranitidine on pharmacokinetics and pharmacodynamics of a single dose of dofetilide. Br J Clin Pharmacol 49:64–71.

Allen JD, Brinkhuis RF, Wijnholds J and Schinkel AH (1999) The mouse Bcrp1/Mxr/Abcp gene: amplification and overexpression in cell lines selected for resistance to topotecan, mitoxantrone, or doxorubicin. Cancer Res 59:4237–4241.

Amidon GL, Lennernas H, Shah VP and Crison JR (1995) A theoretical basis for a biopharmaceutic drug classification: the correlation of in vitro drug product dissolution and in vivo bioavailability. Pharm Res 12:413–420.

Asberg A, Hartmann A, Fjeldsa E, Bergan S and Holdaas H (2001) Bilateral pharmacokinetic interaction between cyclosporine A and atorvastatin in renal transplant recipients. Am J Transplant 1:382–386.

Ayrton A and Morgan P (2008) Role of transport proteins in drug discovery and development: a pharmaceutical perspective. Xenobiotica 38:676–708.

Bachmakov I, Glaeser H, Fromm MF and Konig J (2008) Interaction of oral antidiabetic drugs with hepatic uptake transporters: focus on organic anion transporting polypeptides and organic cation transporter 1. Diabetes 57:1463–1469.

Backman JT, Kyrklund C, Neuvonen M and Neuvonen PJ (2002) Gemfibrozil greatly increases plasma concentrations of cerivastatin. Clin Pharmacol Ther 72:685–691.

Banfield C, Gupta S, Marino M, Lim J and Affrime M (2002) Grapefruit juice reduces the oral bioavailability of fexofenadine but not desloratadine. Clin Pharmacokinet 41:311–318.

Benet LZ and Cummins CL (2001) The drug efflux-metabolism alliance: biochemical aspects. Adv Drug Deliv Rev 50 Suppl 1:S3–11.

Breedveld P, Zelcer N, Pluim D, Sonmezer O, Tibben MM, Beijnen JH, Schinkel AH, van Tellingen O, Borst P and Schellens JH (2004) Mechanism of the pharmacokinetic interaction between methotrexate and benzimidazoles: potential role for breast cancer resistance protein in clinical drug-drug interactions. Cancer Res 64:5804–5811.

Cascorbi I (2006) Role of pharmacogenetics of ATP-binding cassette transporters in the pharmacokinetics of drugs. Pharmacol Ther 112:457–473.

Chandra P and Brouwer KL (2004) The complexities of hepatic drug transport: current knowledge and emerging concepts. Pharm Res 21:719–735.

Chinn LW and Kroetz DL (2007) ABCB1 pharmacogenetics: progress, pitfalls, and promise. Clin Pharmacol Ther 81:265–269.

Choudhuri S and Klaassen CD (2006) Structure, function, expression, genomic organization, and single nucleotide polymorphisms of human ABCB1 (MDR1), ABCC (MRP), and ABCG2 (BCRP) efflux transporters. Int J Toxicol 25:231–259.

Ciarimboli G (2008) Organic cation transporters. Xenobiotica 38:936–971.

Cvetkovic M, Leake B, Fromm MF, Wilkinson GR and Kim RB (1999) OATP and P-glycoprotein transporters mediate the cellular uptake and excretion of fexofenadine. Drug Metab Dispos 27:866–871.

de Boer AG, van der Sandt IC and Gaillard PJ (2003) The role of drug transporters at the blood-brain barrier. Annu Rev Pharmacol Toxicol 43:629–656.

de Miranda P, Good SS, Yarchoan R, Thomas RV, Blum MR, Myers CE and Broder S (1989) Alteration of zidovudine pharmacokinetics by probenecid in patients with AIDS or AIDS-related complex. Clin Pharmacol Ther 46:494–500.

Degorter MK and Kim RB (2009) Hepatic drug transporters, old and new: pharmacogenomics, drug response, and clinical relevance. Hepatology 50: 1014–1016.

Ding R, Tayrouz Y, Riedel KD, Burhenne J, Weiss J, Mikus G and Haefeli WE (2004) Substantial pharmacokinetic interaction between digoxin and ritonavir in healthy volunteers. Clin Pharmacol Ther 76:73–84.

Dobson PD and Kell DB (2008) Carrier-mediated cellular uptake of pharmaceutical drugs: an exception or the rule? Nat Rev Drug Discov 7:205–220.

Drescher S, Schaeffeler E, Hitzl M, Hofmann U, Schwab M, Brinkmann U, Eichelbaum M and Fromm MF

(2002) MDR1 gene polymorphisms and disposition of the P-glycoprotein substrate fexofenadine. Br J Clin Pharmacol 53:526–534.

Drewe J, Gutmann H, Fricker G, Torok M, Beglinger C and Huwyler J (1999) HIV protease inhibitor ritonavir: a more potent inhibitor of P-glycoprotein than the cyclosporine analog SDZ PSC 833. Biochem Pharmacol 57:1147–1152.

Ekins S, Ecker GF, Chiba P and Swaan PW (2007) Future directions for drug transporter modelling. Xenobiotica 37:1152–1170.

Endres CJ, Hsiao P, Chung FS and Unadkat JD (2006) The role of transporters in drug interactions. Eur J Pharm Sci 27:501–517.

FDA (2006) Draft guidance for industry: drug interaction studies – study design, data analysis, and implications for dosing and labeling http://www.fda.gov/downloads/Drugs/GuidanceComplianceRegulatoryInformation/Guidances/ucm072101.pdf.

Feng B, Obach RS, Burstein AH, Clark DJ, de Morais SM and Faessel HM (2008) Effect of human renal cationic transporter inhibition on the pharmacokinetics of varenicline, a new therapy for smoking cessation: an in vitro-in vivo study. Clin Pharmacol Ther 83:567–576.

Fenner KS, Troutman MD, Kempshall S, Cook JA, Ware JA, Smith DA and Lee CA (2009) Drug-drug interactions mediated through P-glycoprotein: clinical relevance and in vitro-in vivo correlation using digoxin as a probe drug. Clin Pharmacol Ther 85:173–181.

Fletcher CV, Henry WK, Noormohamed SE, Rhame FS and Balfour HH, Jr. (1995) The effect of cimetidine and ranitidine administration with zidovudine. Pharmacotherapy 15:701–708.

Frenia ML and Long KS (1992) Methotrexate and nonsteroidal antiinflammatory drug interactions. Ann Pharmacother 26:234–237.

Fuhr U, Jetter A and Kirchheiner J (2007) Appropriate phenotyping procedures for drug metabolizing enzymes and transporters in humans and their simultaneous use in the "cocktail" approach. Clin Pharmacol Ther 81:270–283.

Geick A, Eichelbaum M and Burk O (2001) Nuclear receptor response elements mediate induction of intestinal MDR1 by rifampin. J Biol Chem 276:14581–14587.

Ghibellini G, Leslie EM and Brouwer KL (2006a) Methods to evaluate biliary excretion of drugs in humans: an updated review. Mol Pharm 3:198–211.

Ghibellini G, Vasist LS, Hill TE, Heizer WD, Kowalsky RJ and Brouwer KL (2006b) Determination of the biliary excretion of piperacillin in humans using a novel method. Br J Clin Pharmacol 62:304–308.

Giacomini KM, Sugiyama Y (2006) in "Goodman & Gilman's The Pharmacological Basis of Therapeutics" (Brunton LL, Lazo JS, & Parker RL, eds) 41–70. McGraw-Hill, New York.

Giacomini KM, Huang SM, Tweedie DJ, Benet LZ, Brouwer KL, Chu X, Dahlin A, Evers R, Fischer V, Hillgren KM, Hoffmaster KA, Ishikawa T, Keppler D, Kim RB, Lee CA, Niemi M, Polli JW, Sugiyama Y, Swaan PW, Ware JA, Wright SH, Yee SW, Zamek-Gliszczynski MJ and Zhang L (2010) Membrane transporters in drug development. Nat Rev Drug Discov 9:215–236.

Gorboulev V, Ulzheimer JC, Akhoundova A, Ulzheimer-Teuber I, Karbach U, Quester S, Baumann C, Lang F, Busch AE and Koepsell H (1997) Cloning and characterization of two human polyspecific organic cation transporters. DNA Cell Biol 16:871–881.

Greiner B, Eichelbaum M, Fritz P, Kreichgauer HP, von Richter O, Zundler J and Kroemer HK (1999) The role of intestinal P-glycoprotein in the interaction of digoxin and rifampin. J Clin Invest 104:147–153.

Griffith RS, Black HR, Brier GL and Wolny JD (1977) Effect of probenecid on the blood levels and urinary excretion of cefamandole. Antimicrob Agents Chemother 11:809–812.

Hagenbuch B and Gui C (2008) Xenobiotic transporters of the human organic anion transporting polypeptides (OATP) family. Xenobiotica 38:778–801.

Han JY, Lim HS, Shin ES, Yoo YK, Park YH, Lee JE, Kim HT and Lee JS (2008) Influence of the organic anion-transporting polypeptide 1B1 (OATP1B1) polymorphisms on irinotecan-pharmacokinetics and clinical outcome of patients with advanced non-small cell lung cancer. Lung Cancer 59:69-75.

Hedman A, Angelin B, Arvidsson A, Beck O, Dahlqvist R, Nilsson B, Olsson M and Schenck-Gustafsson K (1991) Digoxin-verapamil interaction: reduction of biliary but not renal digoxin clearance in humans. Clin Pharmacol Ther 49:256–262.

Hedman A, Angelin B, Arvidsson A, Dahlqvist R and Nilsson B (1990) Interactions in the renal and biliary elimination of digoxin: stereoselective difference between quinine and quinidine. Clin Pharmacol Ther 47:20–26.

Hedman M, Neuvonen PJ, Neuvonen M, Holmberg C and Antikainen M (2004) Pharmacokinetics and pharmacodynamics of pravastatin in pediatric and adolescent cardiac transplant recipients on a regimen of triple immunosuppression. Clin Pharmacol Ther 75:101–109.

Hirano M, Maeda K, Shitara Y and Sugiyama Y (2006) Drug-drug interaction between pitavastatin and various drugs via OATP1B1. Drug Metab Dispos 34:1229–1236.

Ho RH and Kim RB (2005) Transporters and drug therapy: implications for drug disposition and disease. Clin Pharmacol Ther 78:260–277.

Hosoyamada M, Sekine T, Kanai Y and Endou H (1999) Molecular cloning and functional expression of a multispecific organic anion transporter from human kidney. Am J Physiol 276:F122–128.

Huang SM and Woodcock J (2010) Transporters in drug development: advancing on the Critical Path. Nat Rev Drug Discov 9(3):175–176.

Igel S, Drescher S, Murdter T, Hofmann U, Heinkele G, Tegude H, Glaeser H, Brenner SS, Somogyi AA, Omari T, Schafer C, Eichelbaum M and Fromm MF (2007) Increased absorption of digoxin from the human jejunum due to inhibition of intestinal transporter-mediated efflux. Clin Pharmacokinet 46:777–785.

Inotsume N, Nishimura M, Nakano M, Fujiyama S and Sato T (1990) The inhibitory effect of probenecid on renal excretion of famotidine in young, healthy volunteers. J Clin Pharmacol 30:50–56.

Ishikawa T, Sakurai A, Kanamori Y, Nagakura M, Hirano H, Takarada Y, Yamada K, Fukushima K and Kitajima M (2005) High-speed screening of human ATP-binding cassette transporter function and genetic polymorphisms: new strategies in pharmacogenomics. Methods Enzymol 400:485–510.

Jalava KM, Partanen J and Neuvonen PJ (1997) Itraconazole decreases renal clearance of digoxin. Ther Drug Monit 19:609–613.

Jonker JW and Schinkel AH (2004) Pharmacological and physiological functions of the polyspecific organic cation transporters: OCT1, 2, and 3 (SLC22A1-3). J Pharmacol Exp Ther 308:2–9.

Juliano RL and Ling V (1976) A surface glycoprotein modulating drug permeability in Chinese hamster ovary cell mutants. Biochim Biophys Acta 455:152–162.

Kalliokoski A and Niemi M (2009) Impact of OATP transporters on pharmacokinetics. Br J Pharmacol 158:693–705.

Karjalainen MJ, Neuvonen PJ and Backman JT (2006) Rofecoxib is a potent, metabolism-dependent inhibitor of CYP1A2: implications for in vitro prediction of drug interactions. Drug Metab Dispos 34:2091–2096.

Kim RB, Leake BF, Choo EF, Dresser GK, Kubba SV, Schwarz UI, Taylor A, Xie HG, McKinsey J, Zhou S, Lan LB, Schuetz JD, Schuetz EG and Wilkinson GR (2001) Identification of functionally variant MDR1 alleles among European Americans and African Americans. Clin Pharmacol Ther 70:189–199.

Kimura N, Okuda M and Inui K (2005) Metformin transport by renal basolateral organic cation transporter hOCT2. Pharm Res 22:255–259.

Kindla J, Fromm MF and Konig J (2009) In vitro evidence for the role of OATP and OCT uptake transporters in drug-drug interactions. Expert Opin Drug Metab Toxicol 5:489–500.

Klaassen CD and Lu H (2008) Xenobiotic transporters: ascribing function from gene knockout and mutation studies. Toxicol Sci 101:186–196.

Koepsell H, Lips K and Volk C (2007) Polyspecific organic cation transporters: structure, function, physiological roles, and biopharmaceutical implications. Pharm Res 24:1227–1251.

Kohl C (2009) Transporters – the view from industry. Chem Biodivers 6:1988–1999.

Koshiba S, An R, Saito H, Wakabayashi K, Tamura A and Ishikawa T (2008) Human ABC transporters ABCG2 (BCRP) and ABCG4. Xenobiotica 38:863–888.

Kruijtzer CM, Beijnen JH, Rosing H, ten Bokkel Huinink WW, Schot M, Jewell RC, Paul EM and Schellens JH (2002) Increased oral bioavailability of topotecan in combination with the breast cancer resistance protein and P-glycoprotein inhibitor GF120918. J Clin Oncol 20:2943–2950.

Kunta JR and Sinko PJ (2004) Intestinal drug transporters: in vivo function and clinical importance. Curr Drug Metab 5:109–124.

Lau YY, Huang Y, Frassetto L and Benet LZ (2007) Effect of OATP1B transporter inhibition on the pharmacokinetics of atorvastatin in healthy volunteers. Clin Pharmacol Ther 81:194–204.

Launay O, Sadorge C, Jolly N, Poirier B, Bechet S, van der Vliet D, Seffer V, Fenner N, Dowling K, Giemza R, Johnson J, Ndiaye A, Vray M, Sansonetti P, Morand P, Poyart C, Lewis D and Gougeon ML (2009) Safety and immunogenicity of SC599, an oral live attenuated Shigella dysenteriae type-1 vaccine in healthy volunteers: results of a Phase 2, randomized, double-blind placebo-controlled trial. Vaccine 27:1184–1191.

Leslie EM, Deeley RG and Cole SP (2005) Multidrug resistance proteins: role of P-glycoprotein, MRP1, MRP2, and BCRP (ABCG2) in tissue defense. Toxicol Appl Pharmacol 204:216–237.

Li M, Anderson GD and Wang J (2006) Drug-drug interactions involving membrane transporters in the human kidney. Expert Opin Drug Metab Toxicol 2:505–532.

Lin JH (2003) Drug-drug interaction mediated by inhibition and induction of P-glycoprotein. Adv Drug Deliv Rev 55:53–81.

Link E, Parish S, Armitage J, Bowman L, Heath S, Matsuda F, Gut I, Lathrop M and Collins R (2008) SLCO1B1 variants and statin-induced myopathy – a genomewide study. N Engl J Med 359:789–799.

Maeda K and Sugiyama Y (2008) Impact of genetic polymorphisms of transporters on the pharmacokinetic, pharmacodynamic and toxicological properties of anionic drugs. Drug Metab Pharmacokinet 23:223–235.

Mahar Doan KM, Humphreys JE, Webster LO, Wring SA, Shampine LJ, Serabjit-Singh CJ, Adkison KK and Polli JW (2002) Passive permeability and P-glycoprotein-mediated efflux differentiate central nervous system (CNS) and non-CNS marketed drugs. J Pharmacol Exp Ther 303:1029–1037.

Mao Q and Unadkat JD (2005) Role of the breast cancer resistance protein (ABCG2) in drug transport. AAPS J 7:E118–133.

Marchetti S, Mazzanti R, Beijnen JH and Schellens JH (2007) Concise review: Clinical relevance of drug

drug and herb drug interactions mediated by the ABC transporter ABCB1 (MDR1, P-glycoprotein). Oncologist 12:927–941.

Matsushima S, Maeda K, Kondo C, Hirano M, Sasaki M, Suzuki H and Sugiyama Y (2005) Identification of the hepatic efflux transporters of organic anions using double-transfected Madin-Darby canine kidney II cells expressing human organic anion-transporting polypeptide 1B1 (OATP1B1)/multidrug resistance-associated protein 2, OATP1B1/multidrug resistance 1, and OATP1B1/breast cancer resistance protein. J Pharmacol Exp Ther 314:1059–1067.

Morimoto K, Oishi T, Ueda S, Ueda M, Hosokawa M and Chiba K (2004) A novel variant allele of OATP-C (SLCO1B1) found in a Japanese patient with pravastatin-induced myopathy. Drug Metab Pharmacokinet 19:453–455.

Motohashi H, Uwai Y, Hiramoto K, Okuda M and Inui K (2004) Different transport properties between famotidine and cimetidine by human renal organic ion transporters (SLC22A). Eur J Pharmacol 503:25–30.

Muck W, Mai I, Fritsche L, Ochmann K, Rohde G, Unger S, Johne A, Bauer S, Budde K, Roots I, Neumayer HH and Kuhlmann J (1999) Increase in cerivastatin systemic exposure after single and multiple dosing in cyclosporine-treated kidney transplant recipients. Clin Pharmacol Ther 65:251–261.

Neuvonen PJ, Niemi M and Backman JT (2006) Drug interactions with lipid-lowering drugs: mechanisms and clinical relevance. Clin Pharmacol Ther 80:565–581.

Niemi M, Backman JT, Fromm MF, Neuvonen PJ and Kivisto KT (2003) Pharmacokinetic interactions with rifampicin: clinical relevance. Clin Pharmacokinet 42:819–850.

Niemi M, Backman JT, Neuvonen M and Neuvonen PJ (2003) Effects of gemfibrozil, itraconazole, and their combination on the pharmacokinetics and pharmacodynamics of repaglinide: potentially hazardous interaction between gemfibrozil and repaglinide. Diabetologia 46:347–351.

Nigam SK, Bush KT and Bhatnagar V (2007) Drug and toxicant handling by the OAT organic anion transporters in the kidney and other tissues. Nat Clin Pract Nephrol 3:443–448.

Nozaki Y, Kusuhara H, Kondo T, Iwaki M, Shiroyanagi Y, Nakayama H, Horita S, Nakazawa H, Okano T and Sugiyama Y (2007) Species difference in the inhibitory effect of nonsteroidal anti-inflammatory drugs on the uptake of methotrexate by human kidney slices. J Pharmacol Exp Ther 322:1162–1170.

Olbricht C, Wanner C, Eisenhauer T, Kliem V, Doll R, Boddaert M, O'Grady P, Krekler M, Mangold B and Christians U (1997) Accumulation of lovastatin, but not pravastatin, in the blood of cyclosporine-treated kidney graft patients after multiple doses. Clin Pharmacol Ther 62:311–321.

Pang KS and Gillette JR (1978) Kinetics of metabolite formation and elimination in the perfused rat liver preparation: differences between the elimination of preformed acetaminophen and acetaminophen formed from phenacetin. J Pharmacol Exp Ther 207:178–194.

Pedersen KE, Christiansen BD, Klitgaard NA and Nielsen-Kudsk F (1983) Effect of quinidine on digoxin bioavailability. Eur J Clin Pharmacol 24:41–47.

Poirier A, Funk C, Lave T and Noe J (2007) New strategies to address drug-drug interactions involving OATPs. Curr Opin Drug Discov Devel 10:74–83.

Regazzi MB, Iacona I, Campana C, Raddato V, Lesi C, Perani G, Gavazzi A and Vigano M (1993) Altered disposition of pravastatin following concomitant drug therapy with cyclosporin A in transplant recipients. Transplant Proc 25:2732–2734.

Rengelshausen J, Goggelmann C, Burhenne J, Riedel KD, Ludwig J, Weiss J, Mikus G, Walter-Sack I and Haefeli WE (2003) Contribution of increased oral bioavailability and reduced nonglomerular renal clearance of digoxin to the digoxin-clarithromycin interaction. Br J Clin Pharmacol 56:32–38.

Sadeque AJ, Wandel C, He H, Shah S and Wood AJ (2000) Increased drug delivery to the brain by P-glycoprotein inhibition. Clin Pharmacol Ther 68:231–237.

Sasongko L, Link JM, Muzi M, Mankoff DA, Yang X, Collier AC, Shoner SC and Unadkat JD (2005) Imaging P-glycoprotein transport activity at the human blood-brain barrier with positron emission tomography. Clin Pharmacol Ther 77:503–514.

Scheffer GL, Pijnenborg AC, Smit EF, Muller M, Postma DS, Timens W, van der Valk P, de Vries EG and Scheper RJ (2002) Multidrug resistance related molecules in human and murine lung. J Clin Pathol 55:332–339.

Scherrmann JM (2009) Transporters in absorption, distribution, and elimination. Chem Biodivers 6:1933–1942.

Schinkel AH and Jonker JW (2003) Mammalian drug efflux transporters of the ATP binding cassette (ABC) family: an overview. Adv Drug Deliv Rev 55:3–29.

Schinkel AH, Smit JJ, van Tellingen O, Beijnen JH, Wagenaar E, van Deemter L, Mol CA, van der Valk MA, Robanus-Maandag EC, te Riele HP and et al. (1994) Disruption of the mouse mdr1a P-glycoprotein gene leads to a deficiency in the blood-brain barrier and to increased sensitivity to drugs. Cell 77:491–502.

Schneck DW, Birmingham BK, Zalikowski JA, Mitchell PD, Wang Y, Martin PD, Lasseter KC, Brown CD, Windass AS and Raza A (2004) The effect of gemfibrozil on the pharmacokinetics of rosuvastatin. Clin Pharmacol Ther 75:455–463.

Shitara Y, Horie T and Sugiyama Y (2006) Transporters as a determinant of drug clearance and tissue distribution. Eur J Pharm Sci 27:425–446.

Shitara Y, Itoh T, Sato H, Li AP and Sugiyama Y (2003) Inhibition of transporter-mediated hepatic uptake as a mechanism for drug-drug interaction between cerivastatin and cyclosporin A. J Pharmacol Exp Ther 304:610–616.

Shitara Y, Sato H and Sugiyama Y (2005) Evaluation of drug-drug interaction in the hepatobiliary and renal transport of drugs. Annu Rev Pharmacol Toxicol 45:689–723.

Shu Y, Brown C, Castro RA, Shi RJ, Lin ET, Owen RP, Sheardown SA, Yue L, Burchard EG, Brett CM and Giacomini KM (2008) Effect of genetic variation in the organic cation transporter 1, OCT1, on metformin pharmacokinetics. Clin Pharmacol Ther 83:273–280.

Shu Y, Sheardown SA, Brown C, Owen RP, Zhang S, Castro RA, Ianculescu AG, Yue L, Lo JC, Burchard EG, Brett CM and Giacomini KM (2007) Effect of genetic variation in the organic cation transporter 1 (OCT1) on metformin action. J Clin Invest 117:1422–1431.

Shugarts S and Benet LZ (2009) The role of transporters in the pharmacokinetics of orally administered drugs. Pharm Res 26:2039–2054.

Simonson SG, Raza A, Martin PD, Mitchell PD, Jarcho JA, Brown CD, Windass AS and Schneck DW (2004) Rosuvastatin pharmacokinetics in heart transplant recipients administered an antirejection regimen including cyclosporine. Clin Pharmacol Ther 76:167–177.

Somogyi A, McLean A and Heinzow B (1983) Cimetidine-procainamide pharmacokinetic interaction in man: evidence of competition for tubular secretion of basic drugs. Eur J Clin Pharmacol 25:339-345.

Somogyi A, Stockley C, Keal J, Rolan P and Bochner F (1987) Reduction of metformin renal tubular secretion by cimetidine in man. Br J Clin Pharmacol 23:545–551.

Song IS, Shin HJ, Shim EJ, Jung IS, Kim WY, Shon JH and Shin JG (2008) Genetic variants of the organic cation transporter 2 influence the disposition of metformin. Clin Pharmacol Ther 84:559–562.

Sun H, Dai H, Shaik N and Elmquist WF (2003) Drug efflux transporters in the CNS. Adv Drug Deliv Rev 55:83–105.

Takeda M, Babu E, Narikawa S and Endou H (2002a) Interaction of human organic anion transporters with various cephalosporin antibiotics. Eur J Pharmacol 438:137–142.

Takeda M, Khamdang S, Narikawa S, Kimura H, Hosoyamada M, Cha SH, Sekine T and Endou H (2002b) Characterization of methotrexate transport and its drug interactions with human organic anion transporters. J Pharmacol Exp Ther 302:666–671.

Takeda M, Khamdang S, Narikawa S, Kimura H, Kobayashi Y, Yamamoto T, Cha SH, Sekine T and Endou H (2002c) Human organic anion transporters and human organic cation transporters mediate renal antiviral transport. J Pharmacol Exp Ther 300:918–924.

Thompson TN (2005) Drug metabolism in-vitro and in-vivo results: how do these data support drug discovery? in "Using Mass Spectrometry for Drug Metabolism" (Walter Korfmacher, ed) CRC Press, Boca Raton, FL.

Thyss A, Milano G, Kubar J, Namer M and Schneider M (1986) Clinical and pharmacokinetic evidence of a life-threatening interaction between methotrexate and ketoprofen. Lancet 1:256–258.

Troger U, Stotzel B, Martens-Lobenhoffer J, Gollnick H and Meyer FP (2002) Drug points: Severe myalgia from an interaction between treatments with pantoprazole and methotrexate. BMJ 324:1497.

Tsuji A (2002) Transporter-mediated drug interactions. Drug Metab Pharmacokinet 17:253–274.

Tsuji A and Tamai I (1996) Carrier-mediated intestinal transport of drugs. Pharm Res 13:963–977.

Unadkat JD, Dahlin A and Vijay S (2004) Placental drug transporters. Curr Drug Metab 5:125–131.

Uwai Y, Saito H and Inui K (2000) Interaction between methotrexate and nonsteroidal anti-inflammatory drugs in organic anion transporter. Eur J Pharmacol 409:31–36.

van de Steeg E, van der Kruijssen CM, Wagenaar E, Burggraaff JE, Mesman E, Kenworthy KE and Schinkel AH (2009) Methotrexate pharmacokinetics in transgenic mice with liver-specific expression of human organic anion-transporting polypeptide 1B1 (SLCO1B1). Drug Metab Dispos 37:277–281.

VanWert AL, Gionfriddo MR and Sweet DH (2010) Organic anion transporters: discovery, pharmacology, regulation and roles in pathophysiology. Biopharm Drug Dispos 31:1–71.

Waller ES, Sharanevych MA and Yakatan GJ (1982) The effect of probenecid on nafcillin disposition. J Clin Pharmacol 22:482–489.

Wandel C, Kim RB, Kajiji S, Guengerich P, Wilkinson GR and Wood AJ (1999) P-glycoprotein and cytochrome P-450 3A inhibition: dissociation of inhibitory potencies. Cancer Res 59:3944–3948.

Wang EJ, Casciano CN, Clement RP and Johnson WW (2001) Active transport of fluorescent P-glycoprotein substrates: evaluation as markers and interaction with inhibitors. Biochem Biophys Res Commun 289:580–585.

Wang JS, Neuvonen M, Wen X, Backman JT and Neuvonen PJ (2002) Gemfibrozil inhibits CYP2C8-mediated cerivastatin metabolism in human liver microsomes. Drug Metab Dispos 30:1352–1356

Watanabe T, Kusuhara H, Maeda K, Shitara Y and Sugiyama Y (2009) Physiologically based pharmacokinetic modeling to predict transporter-mediated clearance and distribution of pravastatin in humans. J Pharmacol Exp Ther 328:652–662.

Welling PG, Dean S, Selen A, Kendall MJ and Wise R (1979) Probenecid: an unexplained effect on cephalosporin pharmacology. Br J Clin Pharmacol 8:491–495.

Wright SH (2005) Role of organic cation transporters in the renal handling of therapeutic agents and xenobiotics. Toxicol Appl Pharmacol 204:309–319.

Wu CY and Benet LZ (2005) Predicting drug disposition via application of BCS: transport/absorption/elimination interplay and development of a biopharmaceutics drug disposition classification system. Pharm Res 22:11–23.

Yamada A, Maeda K, Kamiyama E, Sugiyama D, Kondo T, Shiroyanagi Y, Nakazawa H, Okano T, Adachi M, Schuetz JD, Adachi Y, Hu Z, Kusuhara H and Sugiyama Y (2007) Multiple human isoforms of drug transporters contribute to the hepatic and renal transport of olmesartan, a selective antagonist of the angiotensin II AT1-receptor. Drug Metab Dispos 35:2166–2176.

Yamashiro W, Maeda K, Hirouchi M, Adachi Y, Hu Z and Sugiyama Y (2006) Involvement of transporters in the hepatic uptake and biliary excretion of valsartan, a selective antagonist of the angiotensin II AT1-receptor, in humans. Drug Metab Dispos 34:1247–1254.

Yamazaki M, Suzuki H and Sugiyama Y (1996) Recent advances in carrier-mediated hepatic uptake and biliary excretion of xenobiotics. Pharm Res 13: 497–513.

Yasui-Furukori N, Uno T, Sugawara K and Tateishi T (2005) Different effects of three transporting inhibi- tors, verapamil, cimetidine, and probenecid, on fex- ofenadine pharmacokinetics. Clin Pharmacol Ther 77:17–23.

Yi SY, Hong KS, Lim HS, Chung JY, Oh DS, Kim JR, Jung HR, Cho JY, Yu KS, Jang IJ and Shin SG (2004) A variant 2677A allele of the MDR1 gene affects fexofenadine disposition. Clin Pharmacol Ther 76:418–427.

Zair ZM, Eloranta JJ, Stieger B and Kullak-Ublick GA (2008) Pharmacogenetics of OATP (SLC21/SLCO), OAT and OCT (SLC22) and PEPT (SLC15) transpor- ters in the intestine, liver and kidney. Pharmacoge- nomics 9:597–624.

Zhang L, Reynolds KS, Zhao P and Huang SM (2010) Drug interactions evaluation: an integrated part of risk assessment of therapeutics. Toxicol Appl Pharmacol 243:134–145.

Zhang L, Zhang Y, Strong JM, Reynolds KS and Huang S-M (2008) A regulatory viewpoint on transporter- based drug interactions. Xenobiotica 38:709–724.

Zhang Y and Benet LZ (2001) The gut as a barrier to drug absorption: combined role of cytochrome P450 3A and P-glycoprotein. Clin Pharmacokinet 40: 159–168.

Zhou S-F (2008) Structure, function and regulation of P-glycoprotein and its clinical relevance in drug dis- position. Xenobiotica 38:802–832.

# Index